AD-A068 547 ALABAMA UNIV IN HUNTSVILLE SCHOOL OF SCIENCE AND ENG--ETC F/G 20/5
INVESTIGATION OF TRANSIENT FLOW AND HEATING PROBLEMS CHARACTERI--ETC(U)
MAR 79 C C SHIH, G R KARR, J F PERKINS DAAK40-77-C-0161
UNCLASSIFIED UAH-RR-219 DRCPM-HEL-CR-79-8 NL

1 OF 4
AD
A068547

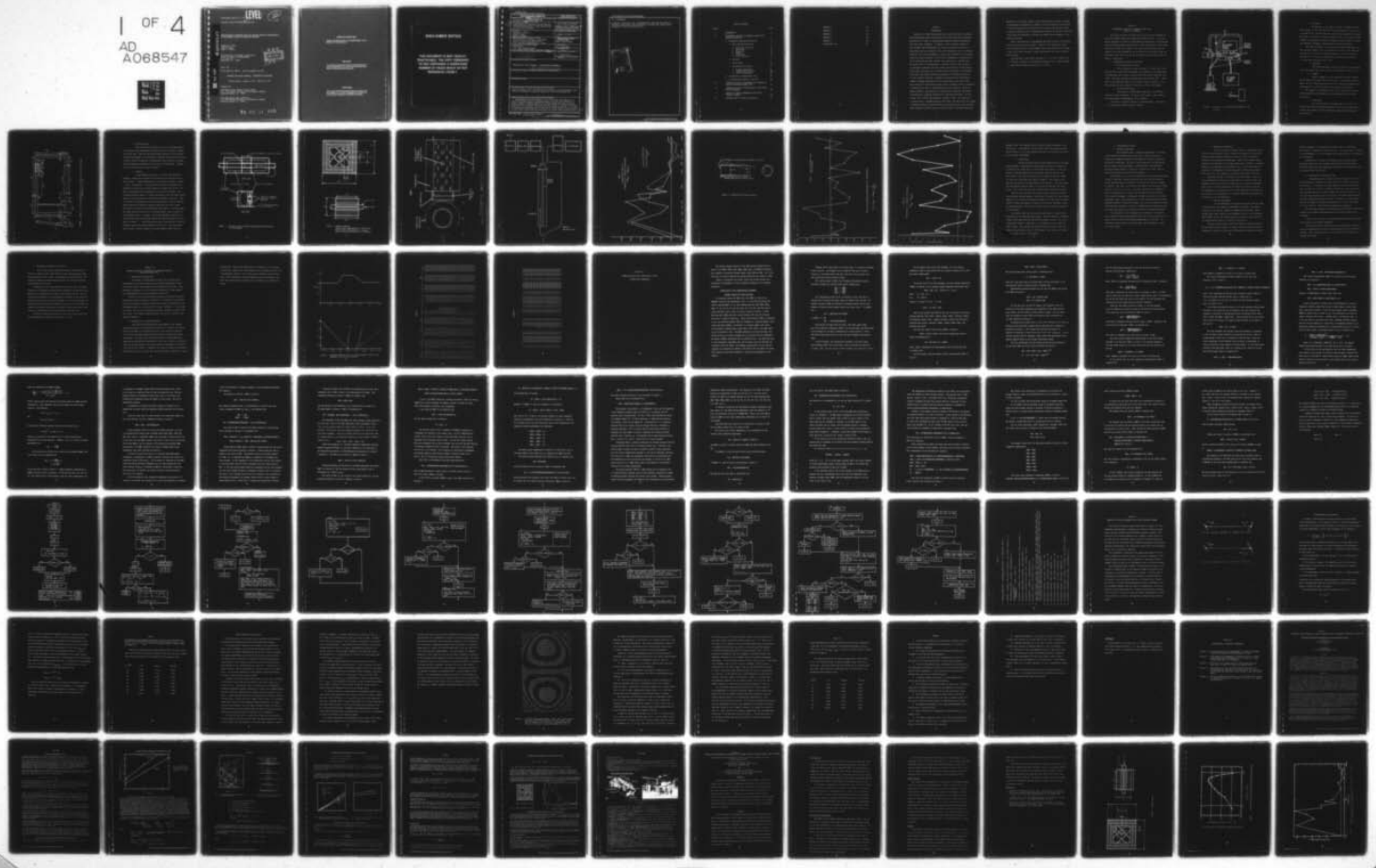

LEVEL II

UAH Research Report No. 219

Technical Report TR-DRCPM-P-HEL-CR-79-8

INVESTIGATION OF TRANSIENT FLOW AND HEATING PROBLEMS CHARACTERISTIC OF HIGH ENERGY LASER GAS CIRCULATION SYSTEMS

Cornelius C. Shih
Gerald R. Karr
James F. Perkins

The University of Alabama in Huntsville
School of Science and Engineering
P. O. Box 1247
Huntsville, AL 35807

March 1979

Final Technical Report: Contract DAAK40-77-C-0161

APPROVED FOR PUBLIC RELEASE: DISTRIBUTION UNLIMITED

Period Covered: August 8, 1977 - March 31, 1979

Prepared for

High Energy Laser Systems Project Office
U. S. Army Missile Research and Development Command
Redstone Arsenal, AL 35809

Army High Energy Laser Laboratory
U. S. Army Missile Research and Development Command
Redstone Arsenal, AL 35809

DISPOSITION INSTRUCTIONS

DESTROY THIS REPORT WHEN IT IS NO LONGER NEEDED. DO NOT RETURN IT TO THE ORIGINATOR.

DISCLAIMER

THE FINDINGS IN THIS REPORT ARE NOT TO BE CONSTRUED AS AN OFFICIAL DEPARTMENT OF THE ARMY POSITION UNLESS SO DESIGNATED BY OTHER AUTHORIZED DOCUMENTS.

TRADE NAMES

USE OF TRADE NAMES OR MANUFACTURERS IN THIS REPORT DOES NOT CONSTITUTE AN OFFICIAL INDORSEMENT OR APPROVAL OF THE USE OF SUCH COMMERCIAL HARDWARE OR SOFTWARE.

DISCLAIMER NOTICE

THIS DOCUMENT IS BEST QUALITY PRACTICABLE. THE COPY FURNISHED TO DDC CONTAINED A SIGNIFICANT NUMBER OF PAGES WHICH DO NOT REPRODUCE LEGIBLY.

(9) Final technical rept. 8 Aug 77 - 31 Mar 79

Unclassified

SECURITY CLASSIFICATION OF THIS PAGE (When Data Entered)

REPORT DOCUMENTATION PAGE	READ INSTRUCTIONS BEFORE COMPLETING FORM
1. REPORT NUMBER (16) DRCPM-P-HEL Technical Report (19) CR-79-8	2. GOVT ACCESSION NO. / 3. RECIPIENT'S CATALOG NUMBER
4. TITLE (and Subtitle) (6) Investigation of Transient Flow and Heating Problems Characteristic of High Energy Laser Gas Circulation Systems	5. TYPE OF REPORT & PERIOD COVERED Final Technical Report August 8, 1977 - March 31, 1979
	6. PERFORMING ORG. REPORT NUMBER UAH Research Report No. 219
7. AUTHOR(s) (10) Cornelius C. Shih, Gerald R. Karr, James F. Perkins	8. CONTRACT OR GRANT NUMBER(s) (15) DAAK40-77-C-0161 new
9. PERFORMING ORGANIZATION NAME AND ADDRESS The University of Alabama in Huntsville, School of Science and Engineering, P. O. Box 1247, Huntsville, AL 35807	10. PROGRAM ELEMENT, PROJECT, TASK AREA & WORK UNIT NUMBERS DA 1X263314D093 AMCSC 623314.0930012
11. CONTROLLING OFFICE NAME AND ADDRESS Headquarters, U. S. Army Missile Command, ATTN: DRSMI-IPBE/Florence, Redstone Arsenal, AL 35809	12. REPORT DATE (11) March 1979
	13. NUMBER OF PAGES 306
14. MONITORING AGENCY NAME & ADDRESS (If different from Controlling Office) (12) 304p.	15. SECURITY CLASS. (of this report) Unclassified
	15a. DECLASSIFICATION/DOWNGRADING SCHEDULE

16. DISTRIBUTION STATEMENT (of this Report)

APPROVED FOR PUBLIC RELEASE: DISTRIBUTION UNLIMITED

(14) UAH-RR-219

17. DISTRIBUTION STATEMENT (of the abstract entered in Block 20, if different from Report)

18. SUPPLEMENTARY NOTES

79 05 11 025

19. KEY WORDS (Continue on reverse side if necessary and identify by block number)

laser circulator, fluid and thermal characteristics of recirculating flows, acoustic attentuators, numerical analysis of the recirculating flow.

20. ABSTRACT (Continue on reverse side if necessary and identify by block number)

Complementing the Army effort on the Closed Cycle Circulator for repetitively pulsed electric discharge lasers, a project was conducted to develop computer programs modeling the recirculating gas flows in pulsed laser operation including steady and unsteady cases; to perform theoretical analysis of the unstable resonator with tilted spherical mirrors; to conduct an experimental investigation of transient fluid and thermal characteristics of the recirculating flow associated with the pulsed laser operation using

DD FORM 1 JAN 73 1473 EDITION OF 1 NOV 65 IS OBSOLETE S/N 0102-014-6601

Unclassified

SECURITY CLASSIFICATION OF THIS PAGE (When Data Entered)

410213

20. (continued)

a subscale circulator; and to experimentally determine the effects of mufflers, screen packs, and honeycombs on acoustic and thermal waves propagated in the recirculating flow.

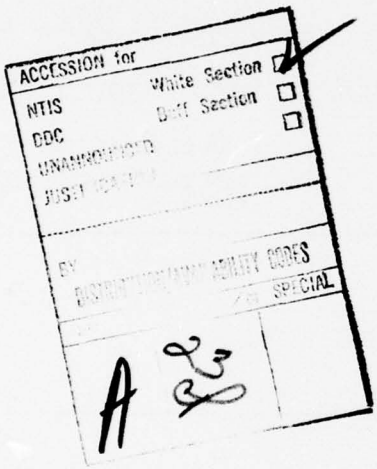

TABLE OF CONTENTS

Chapter I

INTRODUCTION

Operation of a high energy pulsed laser presents problems of acoustics and thermodynamics owing to the generation of shock waves and a heated gas slug which are a result of sudden energy deposition and wave interaction with other laser components. In addition, other transient problems of fluid dynamics and thermodynamics are involved during the start-up of a high energy laser gas circulator from a room temperature, zero flow initial condition until the establishment of steady flow conditions for a sustained repetitive pulsed operation. These start up transients are characteristic of all high energy gas laser systems, both pulsed and cw, and both open and closed cycle to varying degrees. The main purpose of this project is to investigate transient fluid and thermal characteristics of high energy pulsed laser operations and to develop methods of reducing or eliminating the acoustic and thermal problems detrimental to the laser beam quality. In this technical direction, a program was initiated at the Army Missile Command to design, fabricate and test a unique small scale closed cycle gas circulator for repetitively pulsed electric discharge lasers to establish a technology data base for understanding the laser operation. Technical issues relating to operating such a system will be identified and methods of solving these technical problems may be developed and tested. The circulator, with a 28,000 rpm compressor, operates at 200 - 300 ^{o}K and 0.8 - 1.2 atm pressure. Complementing this Army effort, the UAH project was planned: to develope computer programs modeling the recirculating gas flows in pulsed laser operation including steady and unsteady cases; to perform theoretical

analysis of the unstable resonator with tilted spherical mirrors; to conduct an experimental investigation of transient fluid and thermal characteristics of the recirculating flow associated with the pulsed laser operation using a subscale circulator; and to experimentally determine the effects of mufflers, screen packs and honeycombs on acoustic and thermal waves propagated in the recirculating flow.

Some of these efforts are improvements and modifications of the efforts noted in the previous year's report. Results of this project are useful as a technical guide for the development of the Army Closed Cycle Circulator as well as of direct interest to those concerned with all types of pulsed laser systems.

Contributions to this report were made by: G. R. Karr in Chapter IV; J. F. Perkins in Chapter V; David Walker in Chapter III; W. Dahm in Chapter II, under general technical direction of C. C. Shih.

Chapter II

EXPERIMENTAL ANALYSIS OF SUBSCALE CLOSED CYCLE LASER GAS CIRCULATOR

The closed cycle gas circulator used in this study was designed for use with the MICOM single pulse e-beam controlled CO_2 laser. It was originally developed to initiate an experimental investigation on the transient flow and heating problems characteristic of high average power pulsed laser operation in closed cycle systems. The effort reported herein is an extension of the work performed in the year 1976-77 that includes design improvements in the cavity section and two perforation type mufflers and two sizes of screen packs.

A. Experimental Apparatus Description

1. Recirculating Flow System

The recirculation system consisted of a blower, poly vinyl chloride (PVC) piping, mounting flanges for attachment to the e-beam laser, an e-beam mask, and a plastic structure which was mounted inside the laser cavity. The laser was made by Systems Science and Software (S^3). A schematic of the system attached to the S^3 laser is given in Figure 1. The flow through the cavity region is from right to left in that figure.

a. Blower Specifications

The blower is a Dayton Model 4C108 with a 10 5/8" wheel. The inlet is 6½" in diameter. The outlet is 2½" square. The outside of the blower casing is approximately 13" in diameter.

The motor is connected directly to the blower wheel. The motor is a 1 hp Dayton Model 6K232 operated at 3450 rpm.

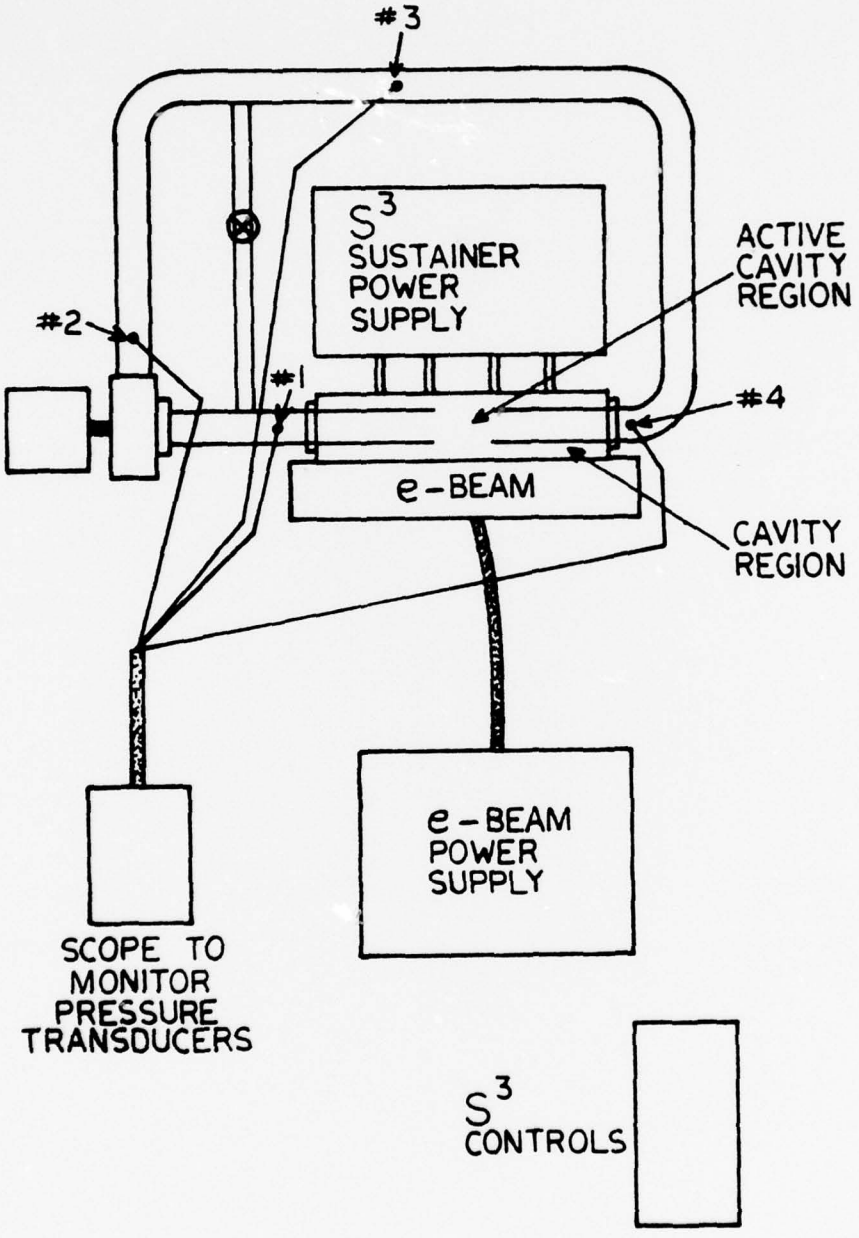

FIGURE 1. TOP VIEW OF PVC SUBSCALE MODEL ATTACHED TO THE S^3 LASER.

b. PVC Piping

The majority of the piping consisted of 3109662 "Certain-Teed Plastics" 4" PVC 1120 Schedule 40 220 psi Astmd-2665. This pipe has 4" ID and 4½" OD. The 90° turns were achieved using standard PVC fittings which have a 4" radius of curvature along the center line of the 90° bend. A number of couplings were employed throughout the path length to accommodate assembly, disassembly, and modification during the testing.

Also shown in Figure 1 is a cross-over or by-pass pipe with valve. This pipe was J24G264 1" PVC 1120 Schedule 80 630 psi at 73°F ASTMD 1785. The pipe was 1" ID and 1¼" OD and was attached to the 4" PVC through a standard 4" to 2" tee with a reducer used to bring the size down to 1". A 1" gate valve was used in the 1" line.

c. Dimensions

The piping dimensions are shown in Figure 2 in centimeters. Total path length around the 4" circuit is approximately 1140 cm (37 ft.).

d. Flanges

Special flanges had to be constructed in order to attach the PVC pipe to the blower and to the S^3 laser. For the blower attachment, a 6" to 4" reducer was used on the inlet side and an aluminum piece was machined to go from the square to the circular cross-section.

The flanges for attachment to the S^3 were constructed from aluminum consisting of 4½" diameter holes with suitable bolt circle and o-ring groove.

e. E-beam Mask

For this test series, an E-beam mask of 45 cm by 10 cm (height) was used with an improved method of base line gas flow and leak control using simple structural changes with taping and caulking with silicone glue.

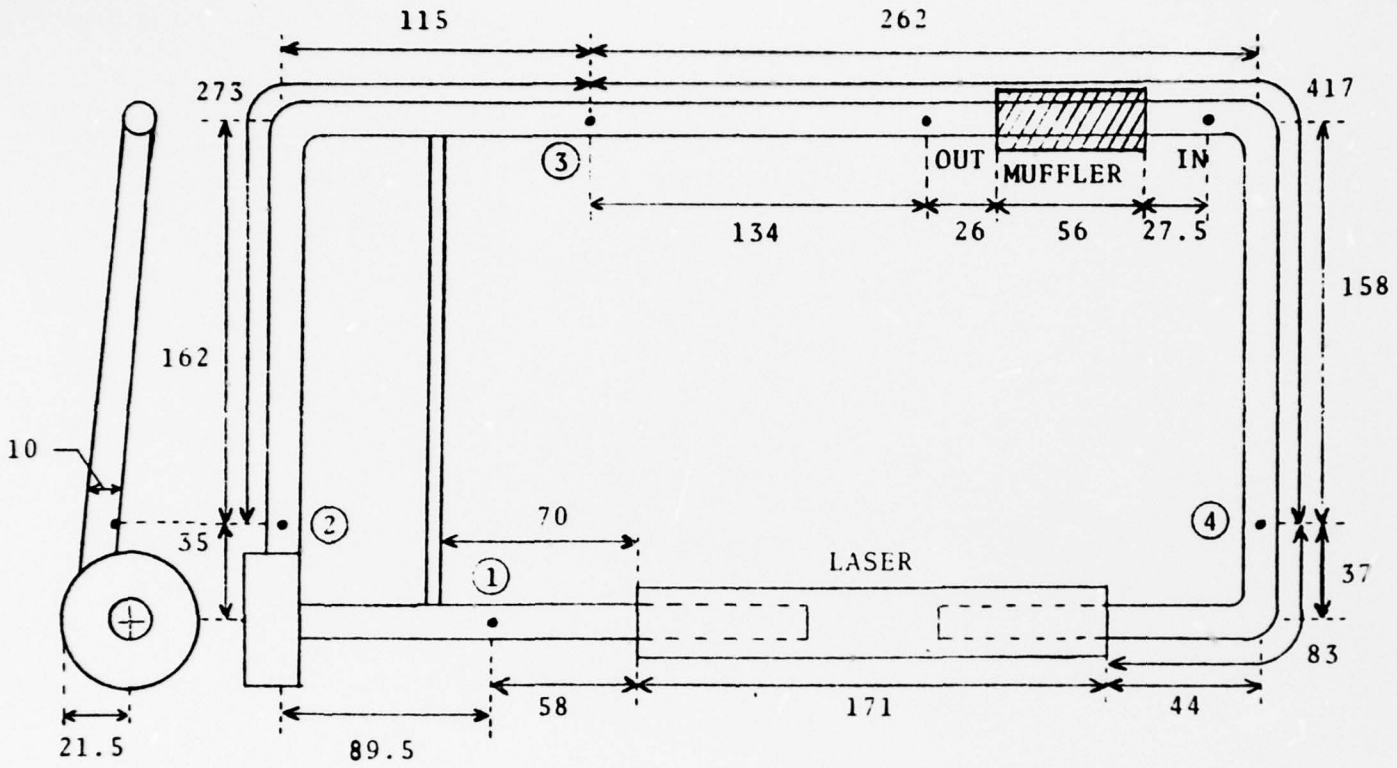

FIGURE 2. PROBE LOCATION MEASUREMENTS ON PVC MODEL WITH MUFFLER ADDED
(Dimensions in cm)

f. Cavity Structure

The cavity structure serves to box in the discharge region in the vertical and longitudinal directions and also to provide a support for the PVC pipe. Since the wave distortions discovered in the previous tests were determined to be attributed to pressure leaks from the structure, a special caution was applied for sealing the cavity structure in contact with the sustainer electrode as well as the 45 cm E-beam mask. A sketch of the cavity structure is shown in Figure 3.

2. Mufflers

A horn-coupled muffler and a cannister type muffler was designed, constructed and tested on the acoustic test bench and then in the circulator. Detailed dimensions of the mufflers are shown in Figures 4 and 5 , respectively. On the acoustic test bench, each muffler was subjected to sound waves of fixed frequencies ranging from 100 HZ to 110 KHZ for determining its effectiveness as an acoustic attenuator. The test setup shown in Figure 6 provides the means of using the same acoustic source for pipe sections with and without the muffler of interest. This will prevent any nonuniformity in wave characteristics from two different sound sources even though the indicator shows that they are the same. This setup also allows for the monitoring of the input to the system since the input wave form is also put on the oscilloscope. Thus, any drift in the amplifiers can be corrected during the experiment. Results of acoustic bench tests for both horn-couples and cannister mufflers are presented in Figure 7 . Both mufflers were found to perform well in the low frequency region with peak d_β difference of 20 to 30. The horn-coupled muffler shows a flatter response in the low frequency region than the

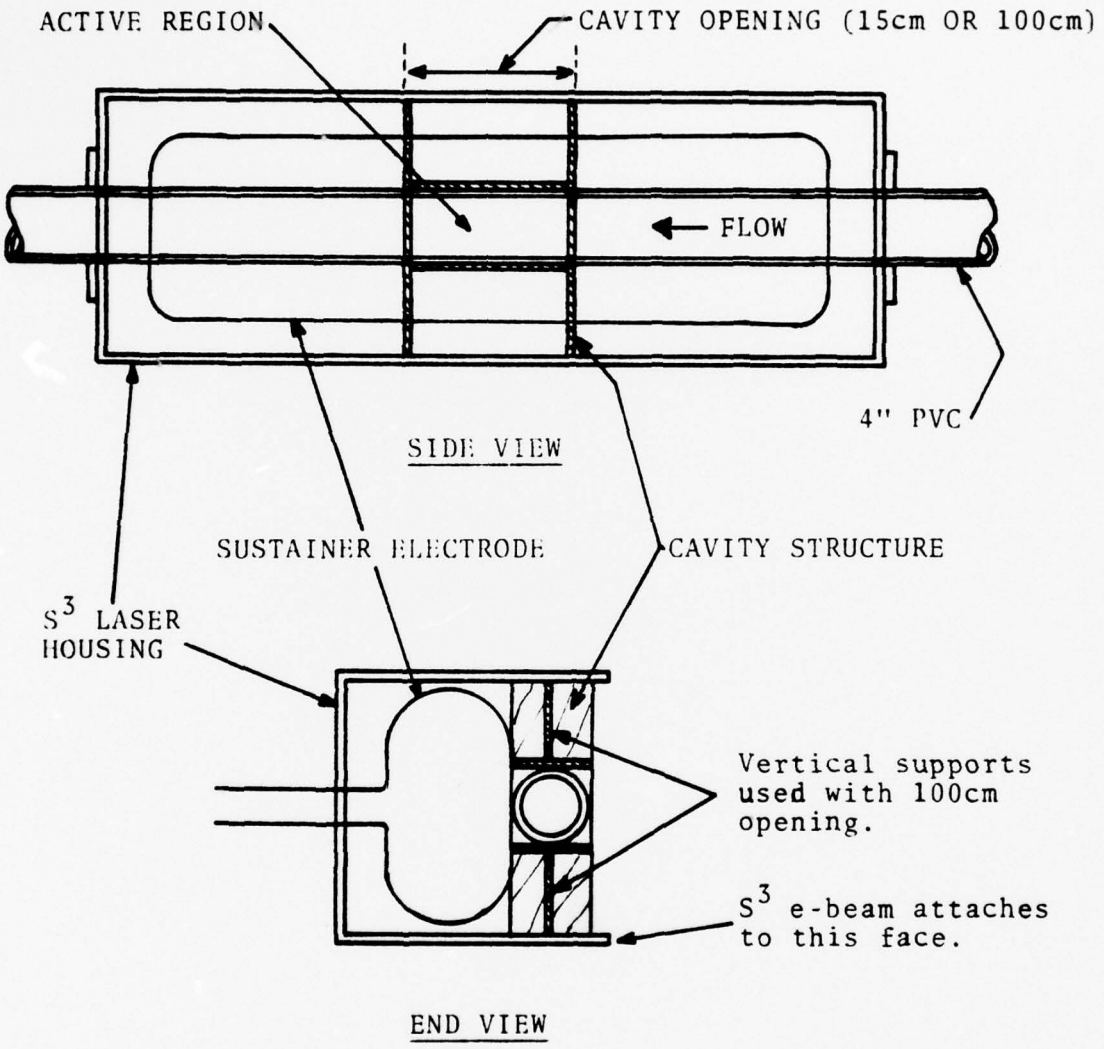

FIGURE 3. SKETCH OF CAVITY STRUCTURE AND INSTALLATION INSIDE THE S^3 LASER HOUSING.

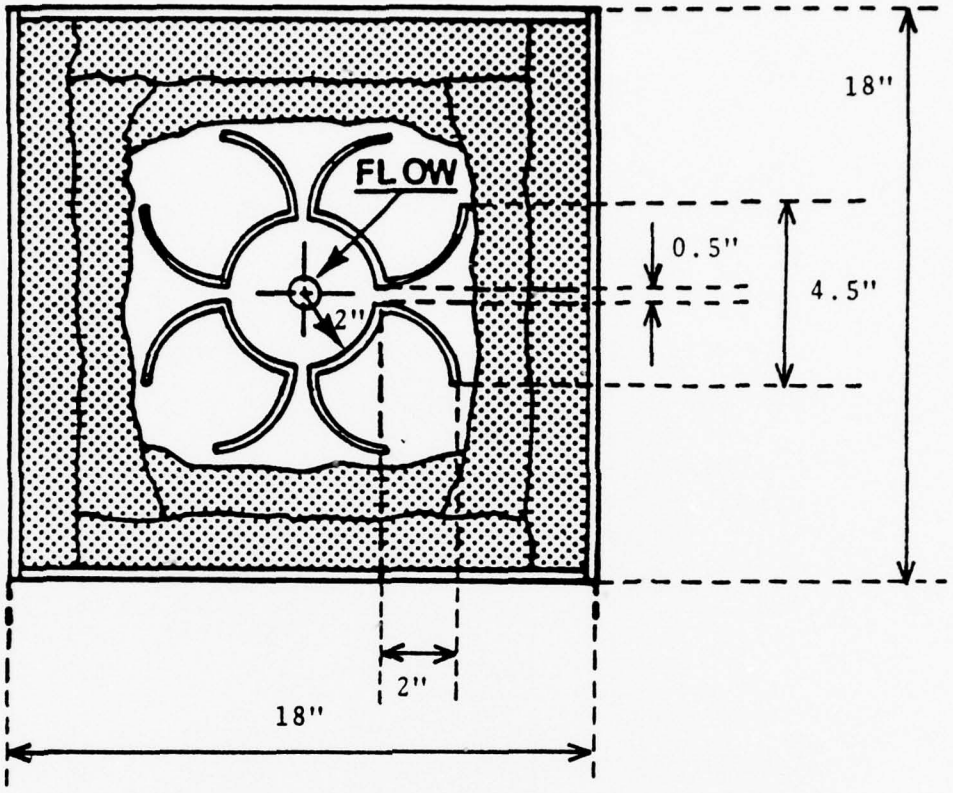

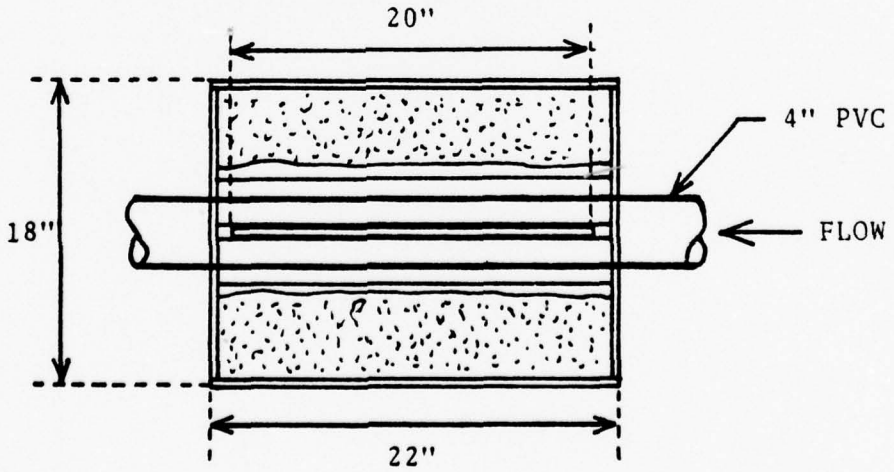

Figure 4. SKETCH OF MUFFLER.
Curved pieces constructed of 4" PVC piping, sides of box constructed of ¼" plywood, and end pieces constructed of ½" plexiglass.

FIGURE 5

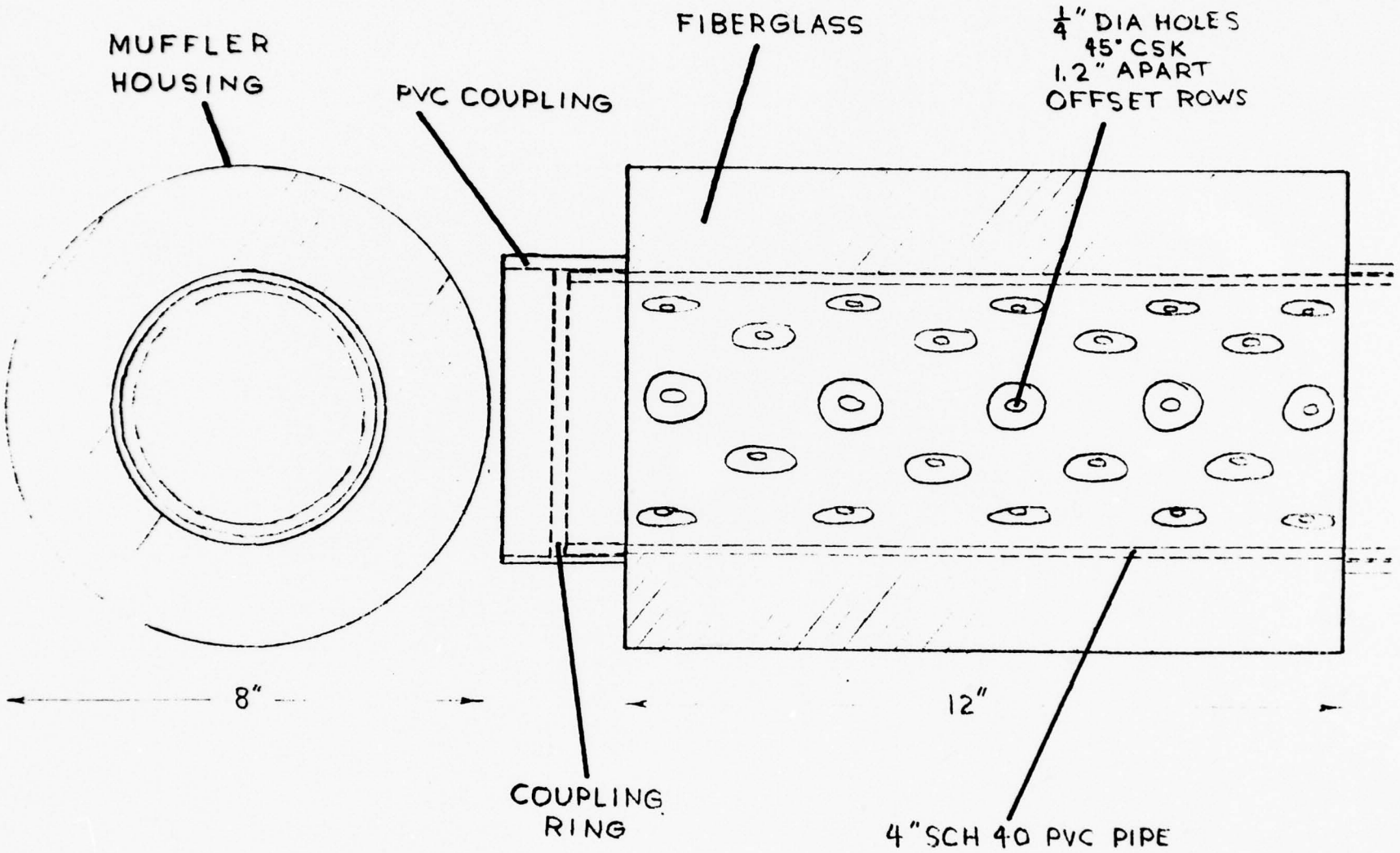

Figure 5. ACOUSTIC MUFFLER

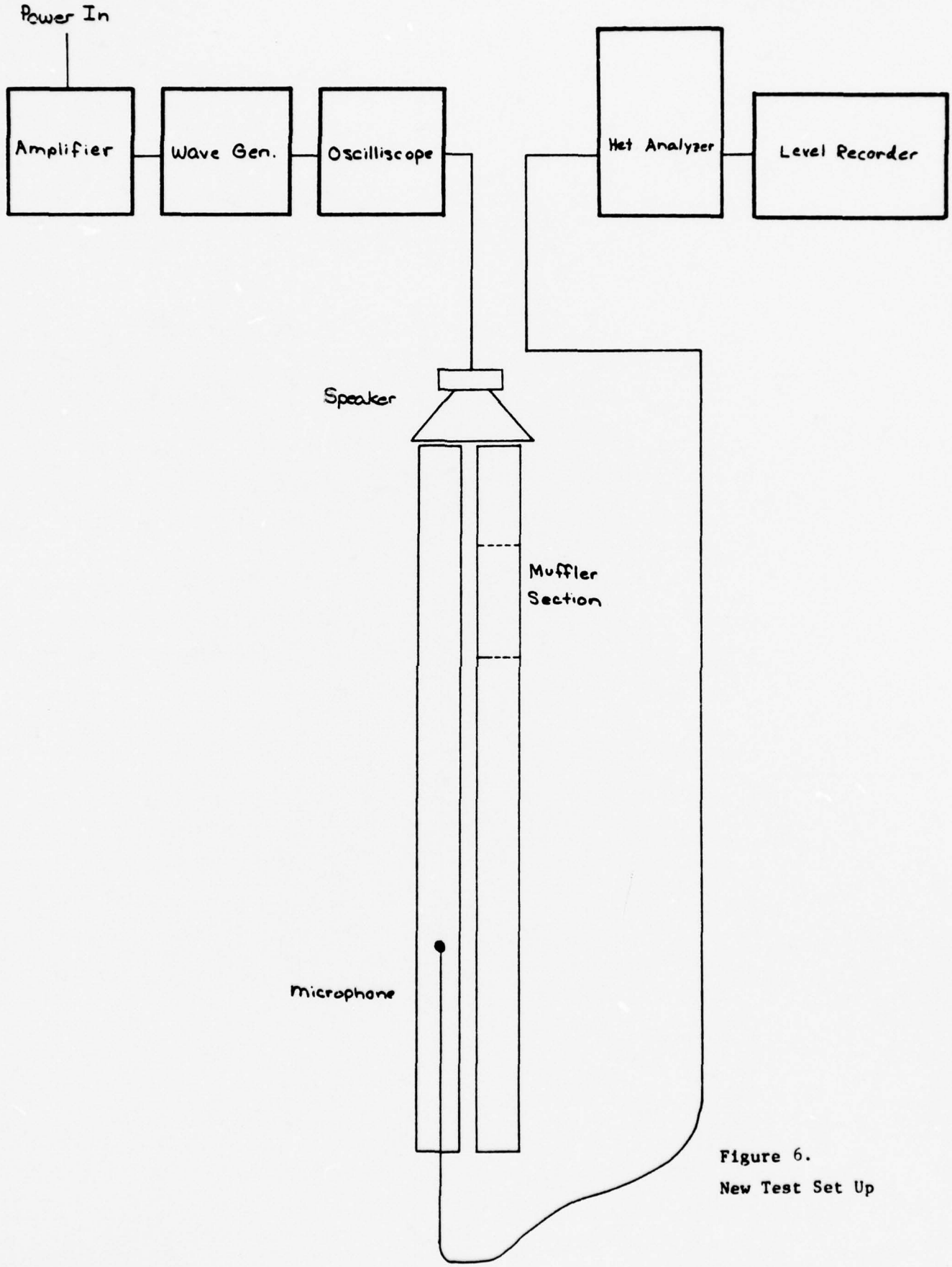

Figure 6.
New Test Set Up

Figure 7.

Comparative Plot of
Frequency vs. Decibel Difference
(dB_{str} - dB_{muff})

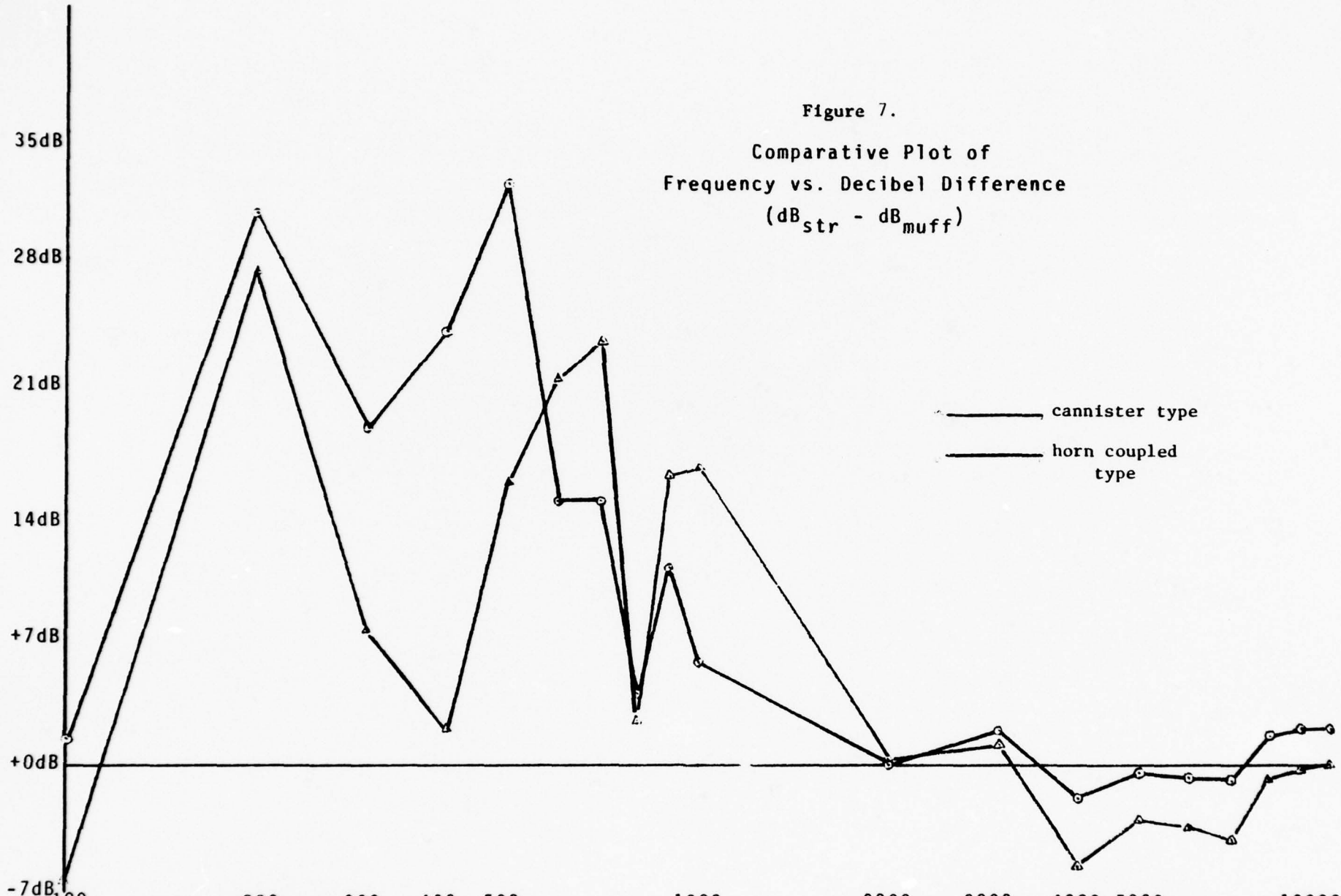

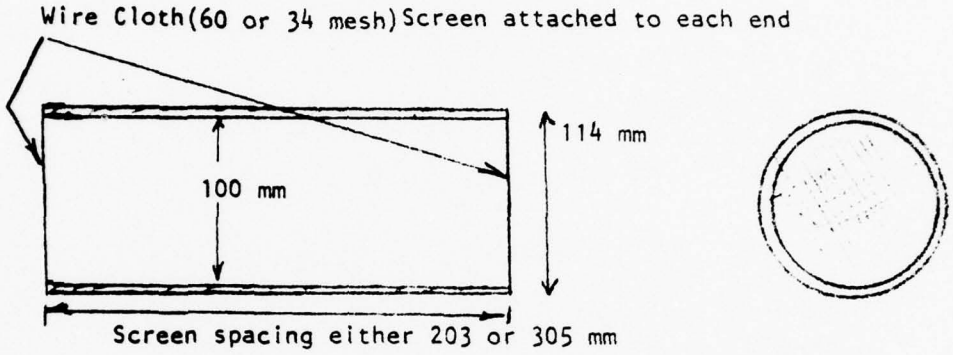

Figure 8. Screen Pack Test Section Design

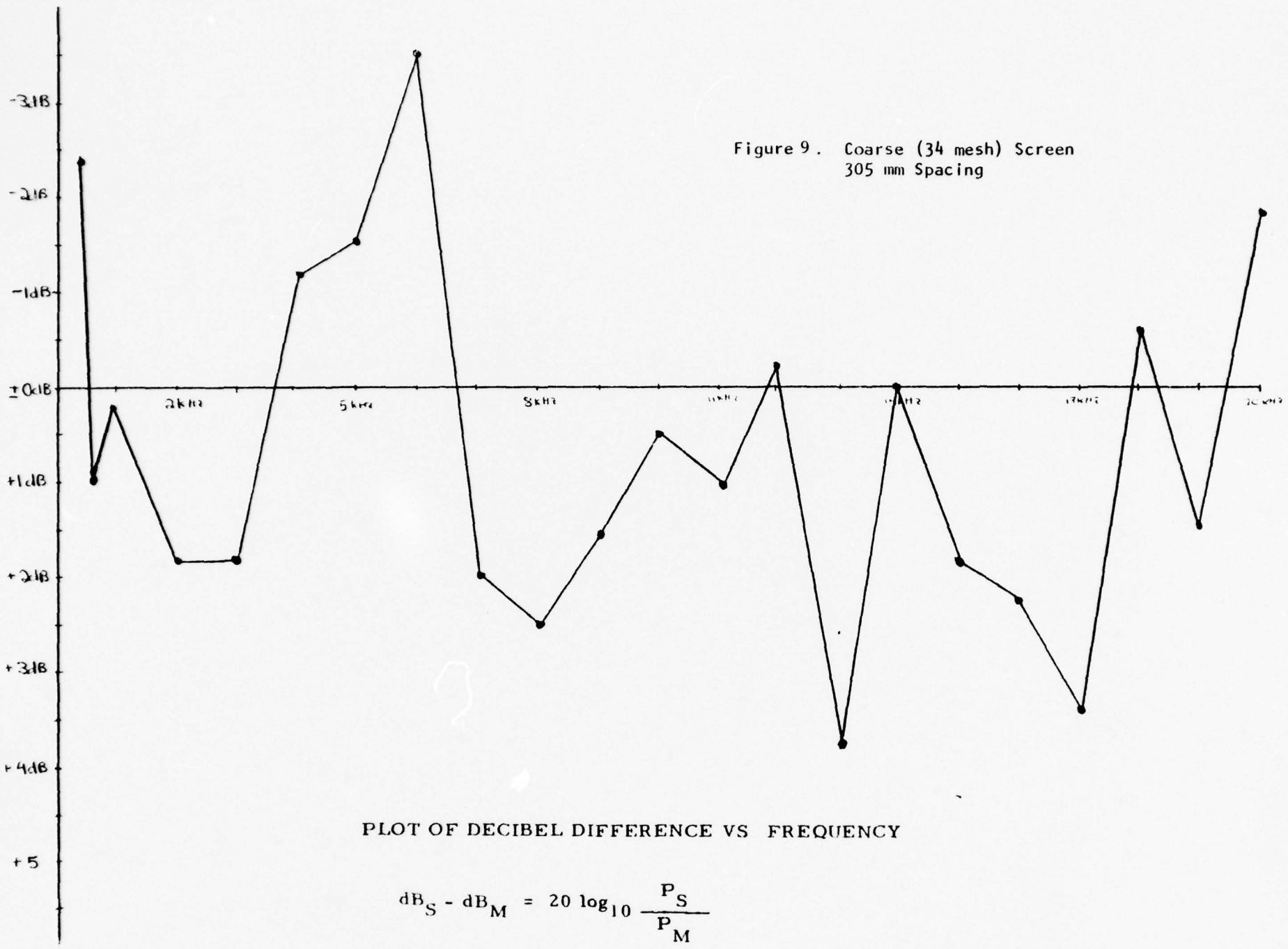

Figure 9. Coarse (34 mesh) Screen
305 mm Spacing

PLOT OF DECIBEL DIFFERENCE VS FREQUENCY

$$dB_S - dB_M = 20 \log_{10} \frac{P_S}{P_M}$$

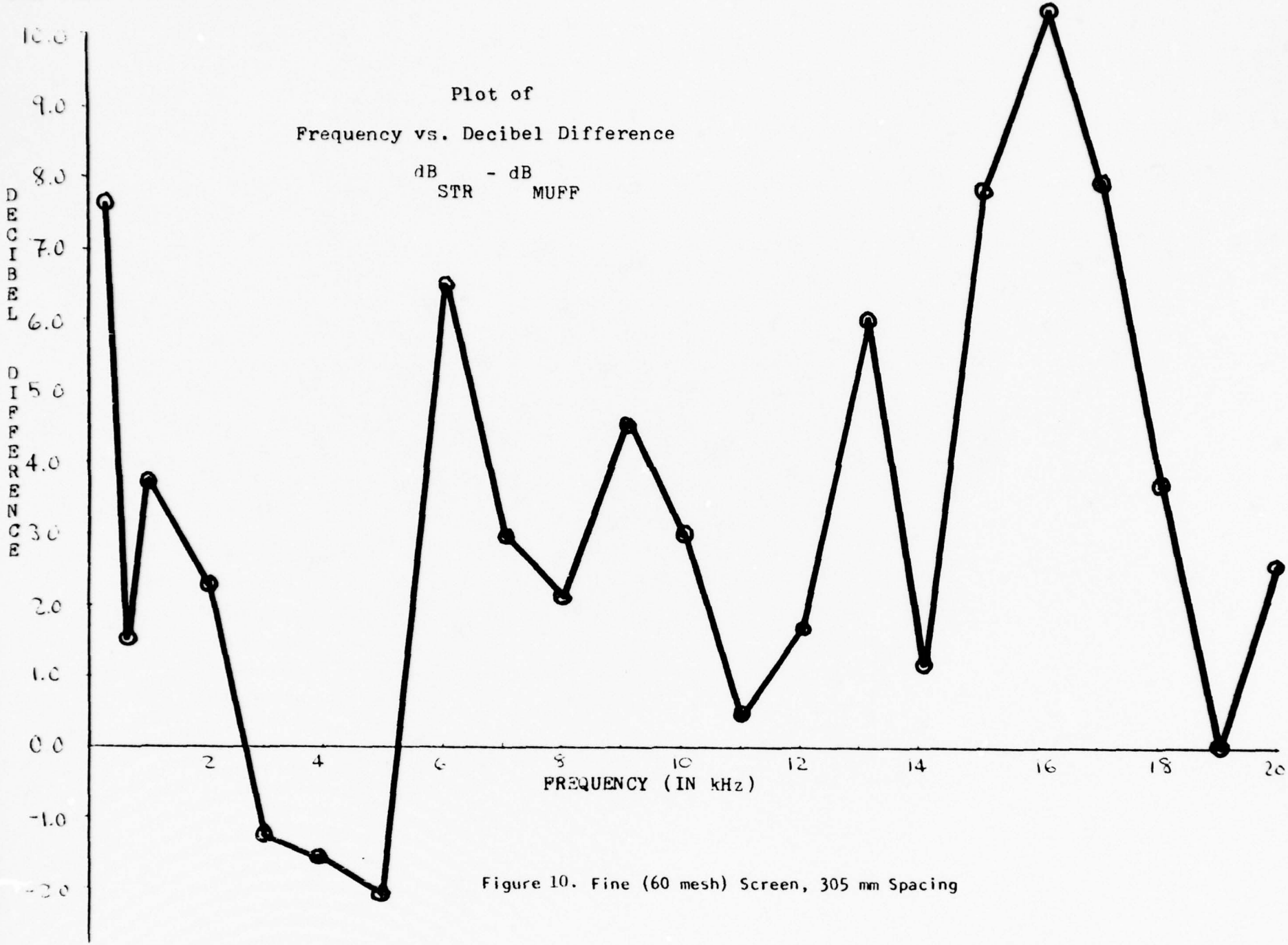

Figure 10. Fine (60 mesh) Screen, 305 mm Spacing

cannister type. The cannister muffler shows an effective damping at the 400 HZ point. Above 2000 HZ, neither muffler shows significant muffling characteristics. B & K test equipment was used on the acoustic test bench for the acoustic measurement.

3. Screen Packs

The use of screen packs has been accepted as one of the most common methods of conditioning or suppressing the level of turbulence in a confined fluid stream such as a wind tunnel test section. At the suggestion of Poseidon Research, two screen mesh sizes (60 mesh per inch with 0.004 in. wire size at 55% open area; 34 mesh per inch with 0.0065 in. wire size at 55% open area) shown in Figure 8 were tested on the acoustic test bench in the same fashion as the mufflers. The screen packs were constructed using two sheets of screen at two spacings, 203 mm and 305 mm. Thus, four test pieces were constructed and tested on the bench.

Both the fine (60 mesh) and coarse (34 mesh) screens were tested using the wide (305 mm) spacing. The results of testing over the frequency range from 1 to 20 KHz are presented in Figure 9 for the coarse (34 mesh) screens on 305 mm spacing and in Figure 10 for the fine (60 mesh) screens on the same spacing. Note that the vertical axis are reversed in sign in the two figures.

The results show that the fine (60 mesh) screen is generally more effective over the frequency range tested. Figure 10 shows a d_β difference between the straight pipe and the pipe with screens of about 4 d_β on the average while Figure 9 shows only a 2 d_β difference for the coarse (34 mesh) screens. Both screens show different peaks at 16 and 13 KHz with a general increase also in the 7 - 10 KHz region. Both screens also show a tive value in the 4 - 6 KHz range.

4. Instrumentation System

a. Pressure Measurement

The instrument used for pressure measurements is a battery of four Piezotron pressure sensing units each of which consists of a piezoelectric pressure transducer (Type 201B5) and a coupler (549B) connected with a 128M cable. The unit is then connected to an oscilloscope for the readout of voltage signals. Specifications of the Piezotron miniature pressure sensor or transducer, the Piezotron coupler, and the Textronix oscilloscope are presented in Appendix A.

The pressure of up to 100 psi was sensed by the mini-gage which gives a direct, high level, voltage signal with less than 100 ohms output impedance and high frequency response of 50 KHz and low frequency response of 0.005 HZ. The sensor then converts the pressure into electrical voltage with bias of up to 11 $\pm$ 2 volts. The power required by the transducer to operate is supplied by the coupler, and the signal from the transducer to the readout equipment is transmitted through the coupler over a single inexpensive cable. This eliminates all of the inherent piezoelectric high impedance problems of electrical leakage, cable noise and signal attenuation and allows the tranducers to be used in contaminated environments and with long and moving cables at low noise and without use of charge amplifiers.

The calibration of the transducers was performed at the factory, and the values of the calibration were noted to be, on the average for all probes, 50 mv per psi for the pressure measurement up to 100 psi. The calibration curve relating the voltage output and the pressure is noted to be quite lenient.

b. Temperature Measurement

Due to the extremely transient nature of temperature variation in the recirculating flow as a result of the pulsed laser operation, a sensor of high frequency response in excess of 1 KHz is considered necessary for the temperature measurement. Search of an adequate sensor resulted in the selection of a hot-wire sensor made of 0.00015 in. diameter tungsten wire coated with platinum powdery film. The hot-wire sensor is connected to the Temperature and Switching Module (Thermo-Systems Model 1040) which is in turn connected to the power supply (Model 1031-10A).

The Module consists of a bridge circuit and amplifier in an open loop configuration so the hot-wire sensor which is ordinarily used as an anemometer probe can be switched to function as a resistance thermometer. Since there is a linear proportionality between the voltage output and the temperature, the calibration can be simply performed by adjusting the zero and gain set potentiometers to a desired temperature range using the calibrate pots of two temperatures.

c. Velocity Measurement

For the measurement of velocities, hot-wire probes the same as those used for the temperature measurement is applied. The probe is connected to the constant temperature anemometer module (Model 1010A). The amplified output signal from the anemometer is sent to the Linearizer (Model 1005B) so that the voltage signal is processed in such a way that it became linearly related to velocity of the gas flow.

The use of these modules ensures the frequency response above 500 KHz with power output as high as 1.5 amps. The noise associated with the anemometer is noted to be less than 0.007% equivalent turbulent intensity.

Frequency response to the Linearizer is found to be up to 400 KHz and the accuracy of linearization can reach $\pm$ 0.2%. With these special features of the instrument, it is able to measure both average velocity and turbulence in one-dimension.

Calibration of the probe is performed by using a Thermo-Systems Calibrator (Model 1125) in accordance with the furnished instructions. The readout system for both temperature and velocity is the Tektronix type oscilloscope (Type 564-3A74-3B3).

B. Presentation of Experimental Data

An experimental run typically involved firing the S^3 laser and recording pressure, temperature, and/or velocity at various locations in the circulator. In addition, the laser discharge current was also monitored for each run in order to determine the power put into the gas flow. Data collected from each run were recorded with two Polaroid photos: one for laser energy deposition and one for fluid and thermal characteristics, along with readings from other indicators. Plates 5381 to 5523 presents the data and complete information regarding the test runs on one figure to a test run basis. These plates are presented in Appendix B.

The tests were designed to investigate the fluid-thermal disturbances produced by the sudden energy deposition in the cavity section of the circulator.

A list of all test runs, with appropriate details, made during this project period is attached as Appendix B.

Based on the previous experience, pure nitrogen gas was found adequate for approximating the laser gas characteristics in the experiment of interest. Thus, nitrogen was used in all test runs for the sake of convenience and economy.

C. Discussion and Analysis of the Data

The S^3 laser without lasing action merely provided the deposition of energy in the cavity section, thereby simulating the energy pulse generated in such a laser. The E-beam was operated at 90 KV, the sustainer voltage was varied between 15-30 KV, and the pulse width was varied between 2 and 3μ sec.

As pertains to the fluid dynamics of the cavity flow, the energy deposition is considered instantaneous and, therefore, the process can be described as an instantaneous constant volume heating process. The gas pressure and temperature are instantaneously increased by the energy deposition while the density remains unchanged. As the flow transports the heated slug of high pressure gas away from the cavity, the frictional resistance and thermal diffusion will take place in the heated slug of gas, causing its deterioration of fluid and thermal characteristics.

Detailed discussion and analysis of the data of some typical test runs are presented in Chapter VI, Sections 2, 3, and 4.

Chapter III

NUMERICAL ANALYSIS OF TRANSIENT FLOW PROBLEMS RESULTING FROM PULSED ENERGY INPUT

A. Theoretical Considerations

As an input of pulsed energy is made into the laser cavity, disturbances in the form of shock waves and thermal changes will travel out from the cavity, overriding the recirculating laser gas flow. These phenomena are modeled by a set of governing equations of fluid dynamics and thermodynamics with the one-dimensional assumption.

Details of the theoretical model including the governing equations, boundary and initial conditions, formulation of the method of characteristics, finite difference schemes and the flow diagram are delineated in the UAH Research Report No. 199 (March 1977), pages 7 through 24. For the sake of brevity, they are not repeated here, and their reference is made to the 1977 report. The computer program modified from the 1977 version is presented in Appendix C.

B. Presentation of Numerical Results

After several modifications and improvements of the computer program pertaining to the transient flow problems of interest, the program has been developed for calculating the flow field quantities including all the flow and thermal properties as functions of temporal and spacial coordinates. The results also include the analysis of shock waves propagating both upstream and downstream from the cavity as well as the heated slug of laser gas bounded by two contact surfaces overriding the recirculating flow in the circulator. Samples of the numerical results are presented graphically and also in tabular form as shown in Figure 11 and Table I and IA,

respectively. These results demonstrate the capability of the program to numerically simulate the flow phenomena with a reasonable accuracy and a considerable flexibility for varying system parameters such as energy input, cavity dimensions, circulator dimensions and gas properties, provided that coefficients associated with the parameters are properly selected.

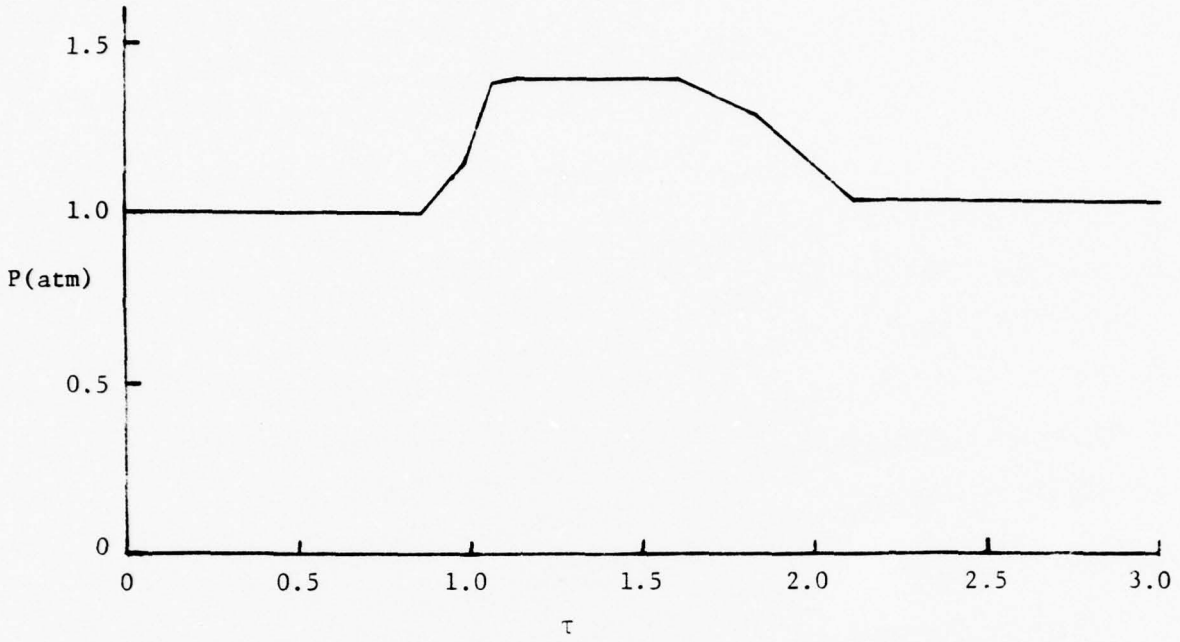

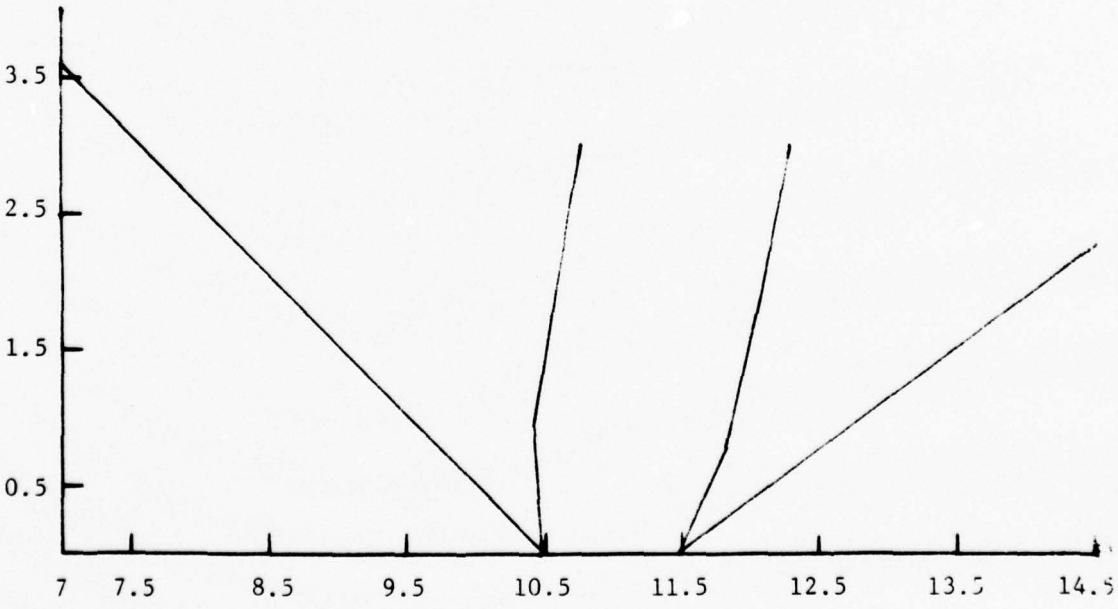

FIGURE 11. GRAPHICAL PRESENTATION OF A TYPICAL NUMERICAL SOLUTION FOR TRANSIENT FLOWS IN THE CIRCULATOR.

TABLE I

ε	τ	U	a	S	D	P	ρ	T
.9025+01	.4286+00	.1749+00	.100+01	.000	.250+00	.212+04	.234-02	.527+03
.9216+01	.4286+00	.1749+00	.100+01	.000	.250+00	.212+04	.234-02	.527+03
.9361+01	.4286+00	.1749+00	.100+01	.000	.250+00	.212+04	.234-02	.527+03
.9504+01	.4286+00	.1749+00	.100+01	.000	.250+00	.212+04	.234-02	.527+03
.9641+01	.4286+00	.1749+00	.100+01	.000	.250+00	.212+04	.234-02	.527+03
.9769+01	.4286+00	.1749+00	.100+01	.000	.250+00	.212+04	.234-02	.527+03
.9889+01	.4286+00	.1749+00	.100+01	.000	.250+00	.212+04	.234-02	.527+03
.1000+02	.4286+00	.1749+00	.100+01	.000	.250+00	.212+04	.234-02	.527+03
.1011+02	.3744+00	-.6440-01	.105+01	.256-02	.250+00	.293+04	.295-02	.579+03
.1021+02	.3802+00	-.6440-01	.105+01	.256-02	.250+00	.293+04	.295-02	.579+03
.1031+02	.3702+00	-.6440-01	.105+01	.256-02	.250+00	.293+04	.295-02	.579+03
.1035+02	.3600+00	-.6440-01	.129+01	.104+01	.250+00	.352+04	.234-02	.877+03
.1071+02	.3603+00	-.6440-01	.129+01	.104+01	.250+00	.352+04	.234-02	.877+03
.1088+02	.3551+00	-.6440-01	.129+01	.104+01	.250+00	.352+04	.234-02	.877+03
.1100+02	.5204+00	.1749+00	.134+01	.104+01	.250+00	.379+04	.234-02	.943+03
.1126+02	.3551+00	.4141+00	.129+01	.104+01	.250+00	.293+04	.195-02	.877+03
.1142+02	.3603+00	.4141+00	.129+01	.104+01	.250+00	.293+04	.195-02	.877+03
.1158+02	.3600+00	.4141+00	.129+01	.104+01	.250+00	.293+04	.195-02	.877+03
.1172+02	.3702+00	.4141+00	.105+01	.256-02	.250+00	.293+04	.295-02	.579+03
.1185+02	.3802+00	.4141+00	.105+01	.256-02	.250+00	.293+04	.295-02	.579+03
.1197+02	.3744+00	.4141+00	.105+01	.256-02	.250+00	.293+04	.295-02	.579+03
.1207+02	.4286+00	.1749+00	.100+01	.000	.250+00	.212+04	.234-02	.527+03
.1222+02	.4286+00	.1749+00	.100+01	.000	.250+00	.212+04	.234-02	.527+03
.1236+02	.4286+00	.1749+00	.100+01	.000	.250+00	.212+04	.234-02	.527+03
.1249+02	.4286+00	.1749+00	.100+01	.000	.250+00	.212+04	.234-02	.527+03
.1261+02	.4286+00	.1749+00	.100+01	.000	.250+00	.212+04	.234-02	.527+03
.1272+02	.4286+00	.1749+00	.100+01	.000	.250+00	.212+04	.234-02	.527+03
.1283+02	.4286+00	.1749+00	.100+01	.000	.250+00	.212+04	.234-02	.527+03
.1293+02	.4286+00	.1749+00	.100+01	.000	.250+00	.212+04	.234-02	.527+03
.1303+02	.4286+00	.1749+00	.100+01	.000	.250+00	.212+04	.234-02	.527+03
.1312+02	.4286+00	.1749+00	.100+01	.000	.250+00	.212+04	.234-02	.527+03

TABLE IA

E=	11.200	TO=	.000	U=	.175	P=	3787.146	RO=	.002340	T=	943.060
E=	11.200	TO=	.107	U=	.175	P=	3787.146	RO=	.002340	T=	943.060
E=	11.200	TO=	.225	U=	.200	P=	3697.910	RO=	.002299	T=	936.123
E=	11.200	TO=	.338	U=	.340	P=	3199.650	RO=	.002071	T=	897.389
E=	11.200	TO=	.506	U=	.292	P=	2815.866	RO=	.001943	T=	844.155
E=	11.200	TO=	.675	U=	.175	P=	2702.214	RO=	.001937	T=	812.928
E=	11.200	TO=	.815	U=	.175	P=	2702.213	RO=	.001937	T=	812.928
E=	11.200	TO=	.955	U=	.175	P=	2702.213	RO=	.001937	T=	812.928
E=	11.200	TO=	1.093	U=	.175	P=	2702.212	RO=	.001937	T=	812.928
E=	11.200	TO=	1.232	U=	.173	P=	2700.199	RO=	.001937	T=	812.322
E=	11.200	TO=	1.373	U=	.169	P=	2623.712	RO=	.001907	T=	801.520
E=	11.200	TO=	1.514	U=	.175	P=	2606.748	RO=	.001899	T=	800.061
E=	11.200	TO=	1.628	U=	.287	P=	2703.347	RO=	.001899	T=	829.388
E=	11.200	TO=	1.737	U=	.175	P=	2833.300	RO=	.001986	T=	829.375
E=	11.200	TO=	1.877	U=	.175	P=	3005.033	RO=	.002052	T=	851.632
E=	11.200	TO=	2.017	U=	.175	P=	2655.971	RO=	.001918	T=	806.424
E=	11.200	TO=	2.159	U=	.175	P=	3137.161	RO=	.002103	T=	868.744
E=	11.200	TO=	2.300	U=	.172	P=	2705.597	RO=	.001938	T=	812.469
E=	11.200	TO=	2.441	U=	.172	P=	3037.197	RO=	.002066	T=	855.415
E=	11.200	TO=	2.582	U=	.180	P=	2849.794	RO=	.001990	T=	832.207
E=	11.200	TO=	2.719	U=	.181	P=	2821.645	RO=	.001979	T=	828.679
E=	11.200	TO=	2.861	U=	.184	P=	2995.425	RO=	.002045	T=	851.762
E=	11.200	TO=	3.001	U=	.175	P=	2625.695	RO=	.001906	T=	802.416

Chapter IV

NUMERICAL ANALYSIS OF STEADY FLOWS IN THE CLOSED CYCLE CIRCULATOR

The overall program consists of the MAIN calling program which is aided by the ENPUT, GASP, AIRP, MACH, SIMQ, LIQP, and OUTPUT subroutines. Data transfer is conducted through common blocks VAR and IVAR. All of the real data is stored in VAR and the integer quantities are stored in IVAR.

Figure 1 illustrates the overall tunnel and coolant system, and identifies the assignment of station numbers referenced in the computer simulation.

DESCRIPTION OF THE COMPUTATIONAL PROCEDURE -

PRIMARY EMPHASIS ON MAIN AND ENPUT

At statement number two MAIN calls upon ENPUT to read in the NAMELIST case data and alphanumeric title. In the UAH simulations the control variable NTAM = 0, so that temperatures TA1, TIG, TØ2G, TØ6G, TØ7G, T1, T2, T3, T4, T6, T8, T10, T14, T16, T18, T20, and TA2 receive either specified input values or built-in values by default. Blower pressure ratio (BPR) and cavity inlet velocity (VI) are also obtained from input or default conditions. Cavity inlet pressure (PIG) is converted to psi, air relative humidity (RH) is converted to a decimal number, laser output efficiency (EFFL) is converted to a decimal number, and cavity inlet hydraulic diameter (DC), height (HI), width (WT1), and length (CL1) are all converted to feet. The AIRP subroutine is called with TA1, PAT, and RH so that air molecular weight will be available for the subsequent air density (RØA1) calculation for the radiator inlet. Air mass flow rate is next determined using RØA1, TA1, and the input value of corrected air volumetric flow rate (CWA). Fin thermal conductivities for all heat exchangers are converted into BTU/sec.-ft^2-($^\circ$F/ft) and the number of coolant fluid passes in each heat exchanger is converted from integers to real numbers.

Although cavity inlet area is a routine input, it is again calculated from H1 and CL1. An estimate of the volumetric flow rate at tunnel station 6 is obtained from VI and A(1). The input list and case title are printed and control returns to MAIN.

With control again in MAIN, the following relationships provide starting estimates for certain tunnel static temperatures:

$$T2G = T\emptyset 2G$$
$$T5G = T\emptyset 2G$$
$$T6G = T\emptyset 6G$$
$$T10G = T\emptyset 7G$$

The loop counters JV and II are initialized at zero, and GASP is entered with TIG and FN providing values for GAMIG, CPIG, and GMU. The decision variable JCPRØ is consulted to determine whether cavity inlet pressure or density should remain fixed at its input value. If JCPRØ ≥ 0, then

$$PIG = R\emptyset 1*TIG/(.093178*GMU)$$

if JCPRØ < 0, then

$$R\emptyset 1 = .093178*PIG*GMU/TIG$$

Calculations for mass flow rate (WG), inlet Mach number (FM1), and inlet stagnation temperature (TØ1G) are now performed; and TØ1G serves as an estimate for the static temperature at tunnel station 11 (T11G). The AMT and BMT arrays are set to zero and heat exchanger calculations begin.

In the following, only calculations related to the first tunnel heat exchanger (HX1) will be outlined, since the calculation pertinent to (HX2), (HX3), and the outside radiator assembly are essentially similar.

On the coolant side of the heat exchanger, the bulk average temperature (TMI) is determined from the arithmetic average of the inlet and outlet temperatures:

$$TMI = .5*(T2 + T4)$$

On the gas side of the heat exchanger, the bulk average temperature (TGMI) is defined as the log-mean average temperature determined from:

$$TGMI = TMI + (Z1 - Z2)/(\ln Z1 - \ln Z2)$$

where $Z1 = T5G - T4$

and $Z2 = T6G-T2$

However, if either Z1 or Z2 0., then

$$TGMI = .5* (T5G + T6G)$$

GASP is now entered with TGMI and FN, and it provides the constant pressure specific heat (CPGI), Prandtl Number (PRGI), viscosity (GIMU), and molecular weight (GMU). LIQP is similarly called with TMI and FG, providing the coolant viscosity (ZIMU), Prandtl Number (PRI), and specific heat (CPI).

The gas side overall frontal area (AFRGI) is given by

AFRGI = DL(1) * DH(1), and the gas stream mass velocity (GGI) is determined from

$$GGI = WG/(DSIG (1) * AFRGI)$$

where DSIG(1) represents the dimensionless ratio of free-flow area to frontal area.

For the coolant side,the overall frontal area per pass (AFRI) is given by

$$AFRI = DW(1) * DH(1)/DNP(1)$$

The coolant stream mass velocity (GI) is determined from

$$GI = WI/(DSI(1) * AFRI)$$

where WI is the input value of coolant mass flow rate and DSI(1) is the dimensionless ratio of free-flow area to frontal area.

Representative Reynolds Numbers for the gas side (REGI) and coolant side (REI) are given by

$$REGI = GGI * DDHG(1)/GIMU$$

$$REI = GI * DDH(1)/ZIMU$$

For the gas side, the data on Figure 2 was employed in the construction of functions expressing the dependence of the mean friction factor (GFI), and the Colburn J factor (GJI), on REGI. For the liquid side, the Colburn J factor (ZJI) was related to REI on the basis of the data presented in Figure 3.

It should also be noted that the three heat exchangers have identical plate-fin core structures, whereas the gas side data for a radiator is presented in Figure 4. The coolant side plate-fin structure of a radiator is identical to that of the three tunnel heat exchangers. Coolant friction factors were not computed, since current UAH simulations do not examine pressure drops in the coolant circulation system.

The unit conductances for the thermal convection heat transfer on the gas side (HGI) and on the liquid side (HI) are given by

$$HGI = GGI * CPGI * GJI * (PRGI)^{-2/3}$$

$$HI = GI * CPI * ZJI * (PRI)^{-2/3}$$

The fin effectiveness parameters on the gas and coolant sides are denoted by GMI and GM1, respectively.

$$GMI = \frac{2 * HGI}{DK(1) * DDEL(1)}$$

where DDEL (1) represents the gas side fin thickness in feet. Similarly,

$$GM1 = \frac{2 * HI}{DK(1) * DA(1)}$$

where DA(1) represents the liquid side fin thickness in feet. It should also be noted that the identical thermal conductivities used in the expressions for GMI and GM1 imply that fins on both sides of the heat exchanger are constructed from the same material (currently aluminum).

Since the fins extend from wall-to-wall, it has been assumed that the effective fin length is given by one half of the wall spacing. On the gas side, the fin efficiency (ATFI) is given by

$$ATFI = \frac{TANH[GMI*DSL(1)]}{GMI * DSL(1)}$$

where DSL(1) represents the gas side fin length in feet. Similarly, the liquid side fin efficiency (ATF1L) is computed from

$$ATF1L = \frac{TANH[GMI*DSLL(1)]}{GM1 * DSLL(1)}$$

where DSLL(1) represents the liquid side fin length in feet.

The total surface temperature effectiveness of the heat transfer surfaces on the gas side (ATØ1) is given by the weighted average of the 100% effectiveness of the prime surface and the less effective fin surface.

$$ATØI = 1.-DAFØA(1) * (1.-ATFI)$$

where DAFØA(1) represents the ratio of fin area to surface area.

On the liquid side, the total temperature effectiveness (ATØ1) is computed from

$$AT\emptyset 1 = 1.- DAFAL(1) * (1.-ATF1L)$$

where DAFAL(1) represents the ratio of fin area to surface area.

The overall conductance for heat transfer for the first heat exchanger (UI) is given by

$$UI = 1./(1./(AT\emptyset I*HGI)+AB(1)/DK(1)*(1.-DAF\emptyset A(1)))+ DALG(1)/(DALF(1)*HI*AT\emptyset 1))$$

where AB(1) represents the parting plate thickness in feet, DALG(1) is the gas side heat transfer surface area to volume ratio in 1/ft., and DALF(1) is the ratio of liquid side heat transfer surface area to volume in 1/ft.

In the final calculations related to the heat exchanger effectiveness estimation, the coolant and hot gas capacity rates are evaluated and compared to establish the appropriate minimum and maximum values identified by CMINI and CMAXI, respectively. Having defined AGI as the surface area on which UI is based, the number of heat transfer units (TUNI) is now given by

$$TUNI = AGI * UI/CMINI$$

The heat exchangers and radiators have been assumed to correspond to the multipass overall-counterflow configuration; and the number of coolant passes in each unit is contained in the DNP array. Kays and London (Reference 1) have observed that the effect on performance of fluid mixing, either within passes or between passes, is not significantly different from cases where there is no mixing at all, hence the single-pass effectiveness (ESSI) is computed from

$$ESSI = 1.-EXP - T\emptyset WI*CMAXI/CMINI$$

where

$$T\emptyset WI = 1.-EXP\ \ -TUNI*CMINI/(CMAXI*DNP(1))$$

The overall effectiveness (EPSI) is now given by the following sequence of calculations

$$EPSI = ((1.-ESSI*CMINI/CMAXI)/(1.-ESSI))**NP(1)$$

$$EPSI = (EPSI-1.)/(EPSI-CMINI/CMAXI)$$

However, if CMINI/CMAXI is greater than .9999, then

$$EPSI = DNP(1)*ESSI/(1.+ESSI*(DNP(1)-1.))$$

Tunnel calculations continue with the determination of station 1 stagnation pressure using known values for Mach number, specific heat ratio, and static pressure. Since the cavity design control parameter NDSGN was always set at a value of two, the calculations are forced to assume a constant area cavity. Although A(2) is an external input, it is now set equal to the cavity inlet area. Assuming constant specific heat for the gas flowing in a heated duct, the temporary variable Z1 representing stagnation temperature for a choked/heated cavity at a station where the Mach number is postualted equal to one, is obtained from

$$Z1 = \frac{T\emptyset 1G*(1.+GAMIG*FM1^2)^2}{2*(GAMIG+1.)*FM1^2*\ \ 1.+\frac{GAMIG-1.}{2.}\ \ *FM1^2} \equiv T_o^*$$

Next, Z1 is redefined as $T\emptyset 2G/T_o^*$; and if Z1>1 the message "Choked Cavity-Read New Data" is printed and the case is aborted.

If the test on Z1 was satisfactory, then the static temperature loop counter is initialized at a value of zero and GASP is entered with known values of T2G and FN. GASP returns values for GAM2G, CP2G and GMU (which is fixed for the case since it only depends upon the gas mixture specified initially).

Under the assumption that GAMIG $\approx$ GAM2G

$$\frac{T\emptyset 2G}{T_o^*} = \frac{2\,(\gamma_2+1)\,M_2^{\,2}\,(1+\frac{\gamma_2-1}{2}\,M_2^{\,2})}{(1+\gamma_2\,M_2^{\,2})^{\,2}} = Z1$$

where γ_2 and M_2 have been employed as shorthand forms for GAM2G and FM2, respectively. This convention will also be adopted for other tunnel stations. Upon defining

$$Z2 \equiv 2\,\gamma_2\,Z1 - 2\,\gamma_2 - 2$$

and

$$Z3 \equiv \gamma_2^{\,2}\,(Z1-1) + 1$$

we obtain the following equation that must be satisfied by M_2

$$Z3\,(M_2^{\,2})^{\,2} + Z2\,M_2^{\,2} + Z1 = 0$$

Finally, M_2 is given by the square root of a positive solution $\leq$ 1 determined for the above equation. However, if Z3 = 0, then M_2 is simply determined from

$$M_2 = \frac{-\,Z1}{Z2}$$

The current value of T2G is now stored as the variable T2GØLD, and a new value of T2G is computed from

$$T2G = \frac{T\emptyset 2G}{1 + M_2^2\,\frac{\gamma_2-1}{2}}$$

If the new value of T2G is within a .5 degree (Rankine) neighborhood of T2GØLD, then the solution continues. If T2G does not pass this test but the loop counter has not been exceeded, then the static temperature loop

is reentered at statement number 12000 using the current value of T2G. If the above two conditions have not been satisfactorily met, then the message "Failure to Converge in Static Temp. Loop 1" is printed, also recording the temperature error and number of loop cycles. The run is subsequently aborted.

A successful pass through the above criteria is followed by the computation of static (P2G) and stagnation (PØ2G) pressures at the cavity exit.

Using the fixed value of total pressure loss coefficient (CF23) for the first diffuser, the exit stagnation pressure is given by

$$PØ3G = PØ2G - CF23*(PØ2G-P2G)$$

Using estimated values of γ_3 and M_3 the MACH subroutine is called in conjunction with known values for DELM, NLIM, PØ3G, TØ3G = TØ2G, WG, GMU, A(3), and FN. Internally, MACH calls upon GASP to provide values for C_p (T) and γ (T); and MACH iterates on M_3 until a value of M_3 is found that lies within DELM of the M_3 computed on the previous pass through MACH. By-products of the MACH subroutine are values of GAM3G, CP3G, static temperature, and static pressure at station 3.

It should be noted that since γ_3 is computed after MACH number convergence, "convergence" in MACH is actually obtained with slightly inconsistent values of T3G and γ_3. If the number of iterations in the MACH subroutine equals NLIM and convergence has not been obtained then the error message, "Failure to Converge in MACH No. Subroutine", along with the error value, is printed; and control returns to the main program (the run is not aborted).

With the assumption that stagnation temperature from station 2 to station 5 is constant, the calculations for gas flow properties at stations

4 and 5 are obtained in a manner analogous to the calculations performed for station 3.

The density at station 5 (RØ5) is given by

$$RØ5 = .093178 * P5G * GMU/T5G$$

The counter for Density Loop 1 is initialized at a value of zero and initial estimates for RØ6, M_6, and γ_6 are obtained from

$$RØ6 = RØ5$$
$$GAM6G = GAM5G$$

$$FM6 = WG*DSQRT(TØ6G/GAM5G/GMU) / (20.7774*PØ5G*A(6))$$

The value of RØ6 is stored in the dummy variable Z1 and the stagnation pressure at station 6 is predicted from

$$PØ6G = PØ5G-GGI^2 * ((1.+DSIG(1)^2) * (RØ5/RØ6-1)+GFI*DALG(1)*DW(1)*$$
$$RØ5/(.5*DSIG(1) * (RØ6 + RØ5)))/9266.11*RØ5)$$

Having TØ6G and PØ6G, MACH is called to provide values for the static temperature and static pressure at station 6. These values are used to compute a new value for RØ6. The absolute value of the dummy variable Z3 = RØ6 - Z1 is compared with RØLIM, to determine if convergence has been attained. If the comparison is not satisfactory and the loop counter is less than NLIM, then the loop is reentered with the current value of RØ6. If the loop counter equals NLIM and convergence has not been obtained, then the error message "Failure to Converge in Density Loop 1" is printed. The error is also recorded and the run is not aborted. For situations of satisfactory convergence, the message "Density Loop 1-cycles (number of passes through loop) - error (Z3)" is printed and calculations continue.

Using the current value of TØ7G as an approximation for T7G, and a subsequent call to GASP, results in an approximation for GAM7G. The stagnation pressure at station 7 (PØ7G) is computed from

$$PØ7G = PØ6G * BPR$$

and the counter for the pressure loop is initialized at a value of 0. The MACH number at station 7 (FM7) is estimated from

$$FM7 = WG*DSQRT\ \ TØ7G/(GAM7G*GMU)\ \ /(20.7774*PØ7G*A(7))$$

The estimates of FM7 and GAM7G plus other currently known quantities are used with a call to the MACH subroutine, whose convergence yields a value for the static pressure at tunnel station 7 (P7G). To go from station 7 to station 8, the heat exchanger equations are solved for the third heat exchanger. Since the diffuser pressure loss coefficient CF89 is a known quantity, the stagnation pressure at tunnel station 9 (PØ9G) is computed from

$$PØ9G = PØ8G - CF89 * (PØ8G - P8G)$$

Under the assumption of a constant stagnation temperature existing between stations 8 through 11, the above technique is also exploited in the successive evaluation of corresponding flow properties for stations 9 through 10. The density for station 10 (RØ10) is given by

$$RØ10 = .093178 * P10G * GMU/T10G$$

Starting estimates are obtained for the MACH number FM11 and density (RØ11) at station 11; and the counter for the second density loop is initialized at a value of zero.

The value for RØ11 is also stored in the dummy variable Z1, and the stagnation pressure at station 11 (PØ11G) is given by

$$P\emptyset 11G = P\emptyset 10G - GGII^2*((1.+DSIG(2)^2)*(R\emptyset 10/R\emptyset 11-1.)+GFI*DALG(2)*DW(2)*$$

$$R\emptyset 10/(.5*DSIG(2)*(R\emptyset 10+R\emptyset 11)))/(9266.11*R\emptyset 10)$$

A call to the MACH subroutine, assuming that T∅11G = T∅1G and letting GAM10G be an initial estimate for GAM11G, results in values for T11G, P11G, FM11, GAM11G, and CP11G, upon convergence.

A new value for R∅11 is now computed from

$$R\emptyset 11 = .093178*P11G*GMU/T11G$$

and the dummy variable Z3 is defined by

$$Z3 = R\emptyset 11 - Z1$$

The absolute value of Z3 is compared with RØLIM to determine if convergence has occurred in the density loop. If $|Z3| > R\emptyset LIM$ and the current value of the loop counter is less than NLIM, then the loop is reentered with the present value of R∅11. If the loop counter equals NLIM and convergence has not been attained, then the error message "Failure to Converge in Density Loop-2" is printed. The error is also recorded and the run is not aborted. For situations of satisfactory convergence, the message "Density Loop-2-Cycles (number of passes through loop) - Error = (Z3)" is printed and system calculations resume.

Next, FM11 is reestimated from other known quantities:

$$FM11 = WG*DSQRT(T\emptyset 1G/(GAMIG*GMU))/(20.7774*P\emptyset 11G*A(11))$$

and the MACH subroutine is again called to provide refined values of T11G, P11G, FM11, GAM11G, and CP11G.

If the decision variable JCPR∅ ≥ 0, then a new dummy variable Z1 is defined by

$$Z1 = R\emptyset1*TIG/(.093178*GMU)*(1.+(GAMIG-1.)*FM1^2/2)**(GAMIG/(GAMIG-1.))$$

and subsequently, Z1 becomes

$$Z1 = P\emptyset11G - CF111*(P\emptyset11G-P11G) - Z1$$

However, if JCPR$\emptyset$ < 0, then the variable Z1 is defined by

$$Z1 = P\emptyset11G - CF111* (P\emptyset11G - P11G) - P\emptyset1G$$

Note that if Z1 > 0 there is an implied overshoot of inlet stagnation pressure as determined by the flow conditions at station 11. Since Z1 will probably never turn out identically zero in the computations, flow stagnation pressure adjustments are necessary:

$$P\emptyset11G = P\emptyset11G - Z1$$
$$P\emptyset10G = P\emptyset10G - Z1$$
$$P\emptyset9G = P\emptyset9G - Z1$$
$$P\emptyset8G = P\emptyset8G - Z1$$
$$P\emptyset7G = P\emptyset7G - Z1$$

The known static temperature at station 6 is used with a call to subroutine GASP so that values will be available for GAM6G and CP6G.

The desired blower pressure ratio (BPR) can now be computed from

$$BPR = P\emptyset7G/P\emptyset6G$$

and the volumetric flow at station 6 (Q6G) is determined from

$$Q6G = 60.*A(6)*FM6*DSQRT(GAM6G*T6G*32.174*1545.43/GMU)$$

Having specified the volumetric flow rate, the number of blower sets, and the blower rpm, the blower polytropic efficiency (ATAB) is given by

```
ATAB = .73-7.09843*(DABS(Q6G/BRPM/NBS-.5355))**2.08014
```

The above efficiency function is also presented in Figure 5.

Hence, TØ7G can be recomputed from

```
TØ7G = TØ6G*(BPR**((GAM6G-1.)/(ATAB*GAM6G)))
```

The pressure loop counter J is incremented by one, and the magnitude of the stagnation pressure error at station 11 is compared with the pressure error tolerance PLIM. If $|Z1| < PLIM$, then calculations resume at statement number 85. If $|Z1| \geq PLIM$ and $J < NLIM$, then the pressure loop repeats itself from statement 80. Alternatively, if J = NLIM and a pressure error still exists, then the message "Failure to Converge in Pressure Loop-Error = Z1" is written and the calculations continue at statement 85, where AIRP is called to determine the constant pressure specific heat of ambient air. The message "Total Passes Through Pressure Loop = (value of J) - Error = (value of Z1)" is next recorded.

Subroutine AIRP is called to determine the constant pressure specific heat and specific heat ratio for radiator exhaust air. Similarly, subroutine LIQP is called 11 times to establish specific heats associated with the coolant temperatures existing at the various reference locations. Until the call to SIMQ, all subsequent calculations are associated with the determination of the values for the elements of the 18 by 18 [AMT] matrix and the 18 x 1 [BMT] matrix used in performing the simultaneous solution of all system temperatures.

The matrix equation $[AMT]\ \bar{X} = [BMT]$ denotes the 18 equations used to establish energy balances across system components expressing a change in enthalpy between entering and leaving fluid streams. Energy balances across the heat exchangers and radiators are supplemented by effectiveness/

temperature change relationships. The elements of the [AMT] and [BMT] matrices are identified in Table II, and the 18 x 1 solution vector returned by SIMQ is an updated estimate for the following temperatures: TØ1G, TØ2G, TØ6G, TØ7G, T1, T2, T3, T4, T6, T8, T10, T14, T16, T18, T20, TA2, TØ8G, and T7.

It should be noted that the equivalence statement preceeding statement number 2 in the MAIN program immediately loads the elements of $\overline{X}$ into the appropriate locations of COMMON VAR. Hence, each time SIMQ is called by MAIN all the sytem temperatures represented in the vector $\overline{X}$ are updated.

The Final Mach Loop counter JJ is initialized at a value of zero and the dummy variable Z2 is set equal to FM1.

The cavity inlet static temperature is now determined from the revised inlet stagnation temperature

$$TIG = BMT(1)/(1.+(GAMIG-1.)*FM1^2/2.)$$

and GASP is called to provide values for GAMIG and CPIG consistent with TIG.

If JCPRØ $\geq$ 0, then the cavity inlet static pressure becomes

$$PIG = RØ1*TIG/(.093178*GMU)$$

If JCPRØ < 0, then the cavity inlet density is given by

$$RØ1 = .093178*PIG*GMU/TIG$$

The gas mass flow rate (WG) is determined from

$$WG = RØ1*VI*A(1)$$

and a new cavity inlet MACH number is given by

FM1 = WG*DSQRT(TIG/(GAMIG*GMU))/(20.7774*PIG*A(1))

The counter JJ is incremented by one and the dummy variable Z3 is defined by

Z3 = Z2 - FM1

If the absolute value of Z3 is less than DELM then calculations resume at statement 7. If MACH number convergence has not been attained and JJ < NLIM, then the current value of FM1 is used in reentry of the Final Mach Loop at statement 6. However, if the MACH number is not within tolerance and JJ = NLIM, then the message "Failed to Converge in Final Mach Loop - Error = (value of Z3)" is written and calculations again reach statement 7. Statement 7 writes the message "Total Passes in Final Mach Loop = (value of JJ) - Error = (value of Z3)".

If the value of the error indicator KS defined in SIMQ is one, the program goes to statement 91 and writes the error message "Singular Matrix" and aborts the case.

The eighteen elements in the array NN are set equal to -1, and

TDIF(KS) = SVR(KS) - BMT(KS)

where KS = 1, 2, ...16 is a new dummy variable, SVR is the array composed of system temperatures before calling SIMQ, and BMT is the system temperature array provided by the call to SIMQ.

If the absolute value of any of the elements in the TDIF array is greater than the corresponding value input into the temperature convergence tolerance array CØNV, then the appropriate element in the NN array is set equal to one.

The temperature differences recorded in array TDIF are now presented under the heading of "State Variable Errors." The message "End of SIMQ Pass No. (value of II)" is recorded; and if II > NLIM then computations resume at statement 92 where the warning "Failure to Converge in State Variable Loop" is printed, and the solution continues at statement 90 without having guaranteed convergence on temperatures.

However, if II $\leq$ NLIM, then each element of the NN array is examined to determine whether it is zero or positive. If any element of NN satisfies this test then calculations resume at statement 95, where the SVR array is reset with corresponding values from the BMT array, and the case repeats from statement 10. If all elements of NN fail this test, then the case continues at statement 90 where FM6 is estimated from

```
FM6 = WG*DSQRT(TØ6G/(GAM6G*GMU))/(20.7774*PØ6G*A(6))
```

This calculation is followed by a call to MACH so that convergence on FM6 can be obtained.

After converting the number of blower sets and the number of blowers per set from integers to real numbers, the cavity inlet velocity correction GC is determined via the following six equations

```
DPSS = ((PØ7G-PØ6G)*TØ6G*28.966)/(PØ6G*BRPM*BRPM*518.7*GMU*FNBPS)
DPSB = .8396-3.2323*(DABS(Q6G/(BRPM*FNBS)-.46875))**/.42327
DPSB = DPSB * 1. E-9
ERR  = DPSB - DPSS
GC   = 11.661 E-7/(BRPM*FNBS) + 11.589 E-5*VIM**.667/(BRPM*BRPM*FNBPS)
GC   = ERR/GC
```

Note that the calculation of DPSB is derived from the empirical blower pressure data presented on Figure 5.

The velocity loop counter JV is incremented by one before the message "Pass No (value of JV) Through Velocity Loop, Correction = (value of GC)" is printed.

If $|GC| \leq VLIM$, then calculations resume at statement number 502.

If $JV \geq NLIM$, then calculations resume at statement number 503, where the error message "Failure to Converge in Velocity Loop-Error = (value of GC)" is recorded before calculations resume at statement number 502.

If GC < 0 and Q6G/(BRPM*FNBS) < .46875, then the message "Blowers are Choked - Process Next Case" is printed and the run is aborted.

For all other situations, before repeating at statement number 501, the cavity inlet velocity is updated in the following manner

VIM = VIM + GC

VIM = VIM * 3.281

At statement number 502, the following revisions are made to chosen stagnation temperatures:

TØ3G = TØ2G

TØ4G = TØ2G

TØ5G = TØ2G

TØ8G = TØ7G

TØ9G = TØ7G

TØ10G = TØ7G

TØ11G = TØ1G

The blower power required in horsepower (BLPR) is given by

BLPR=WG*.5(CP6G+CP7G)*TØ6G*(BPR**((1.-2./(GAM6G+GAM7G))/ATAB)-1.)*778./550.

whose kilowatt equivalent (BLPRM) becomes

$$BLPRM = BLPR * .7457$$

It should also be noted that since this investigation centered on the recirculating laser gas flow in the wind tunnel, the coolant friction factors and pressure drops were not computed.

The radiator inlet air density (RØA1 is computed from

$$RØA1 = 144.*PAT*AML/(1545.32*TA1)$$

The radiator exit air density (RØA2) is initially assumed the same as the inlet air density and the radiator density loop counter (LL) is initialized at a value of zero. After setting the dummy variable Z1=RØA2 the exit air static pressure (PA2) is computed from

```
PA2 = PAT-GA*GA*((1.+DSIG(3)**2)*(RØA1/RØA2-1.)  +
      AF*DALG(3)*DW(3)*RØA1/(.5*DSIG(3)*(RØA1+RØA2)))/
      (RØA1*2.*32.174*144.)
```

The outlet air density is now recomputed from

$$RØA2 = 144.*PA2*AML/(1545.32*TA2)$$

The loop counter is subsequently incremented by one and the dummy variable Z3 is defined by

$$Z3 = RØA2 - Z1$$

If $|Z3| < RØLIM$, then density convergence has been attained and the calculations resume at statement number 38. If $|Z3| \geq RØLIM$ and $LL \leq NLIM$ then the density loop is repeated at statement 37, using the

current value of RØA2 as the initial guess in the loop. However, if LL = NLIM, then the error message "Failure to Converge in Aux. Density Loop - Error = (value of Z3)" is recorded before resuming at statement number 39. The run is not aborted.

When convergence on density has been attained, the message "Total Passes Through Aux. Density Loop = (value of LL) - Error = (value of Z3)" is printed before resuming calculations at statement number 39.

The fan power required in horsepower (PF) is given by

```
PF = WA*CPA2*TA2*((PAT/PA2)**((1.1./GAM2A)/ATAP)-1.)*778./550.
```

whose kilowatt equivalent (PFM) becomes

```
PFM = PF * .7457
```

Tunnel gas density at station 6 (RØ6G) is determined from

```
RØ6G = .093178 * P6G * GMU/T6G
```

and the corrected volumetric flow rate at this station (QCØRR) is given by

```
QCØRR = 60.*WG*DSQRT(1.4*GMU*518.7/(GAM6G*28.97*TØ6G))/RØ6G
```

The elements of the SVR array are given values matching values in corresponding elements of the BMT array and the total heat transfer rate in BTU/HR for the first heat exchange (QDI) is computed from

```
QDI = WI * 1800.*(CP2 + CP4) * (T4-T2)
```

The heat transfer rates for the second and third heat exchanger and radiator system are given, respectively, by

QDII = WII * 1800 . * (CP2+CP6)*(T6-T2)

QDIII = WIII * 1800 . * (CP2+CP7)*(T7-T2)

QDA = W3 * 1800 . * (CP3+CP1)*(T3-T1)

The complete program flow charts are presented in Table II. An Input List for a typical example and the corresponding Output Results are presented in Table III. Appendix D presents the Program Listing.

Appendix E presents some sample results obtained for flow variables around the system for the case of three heat exchangers. We show the results for static temperature (Figure E1), total temperature (Figure E2), density (Figure E3), static pressure (Figure E4), total pressure (Figure E5), velocity (Figure E6), and Mach number (Figure E7). The results are for the following:

PLKW = 50 PIGA = 1

TA1F = -50

TABLE II

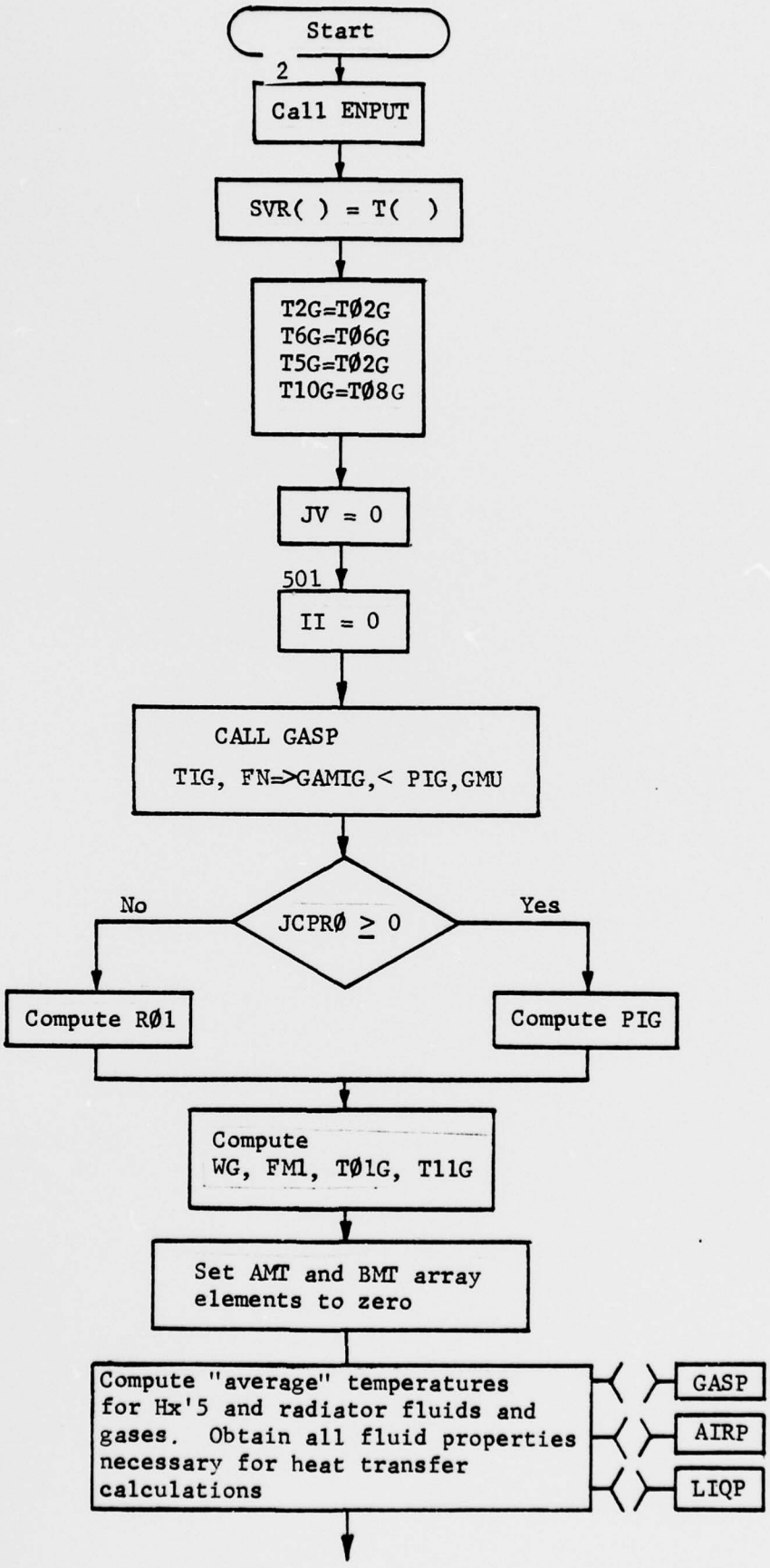
Start
2
Call ENPUT
SVR( ) = T( )
T2G=TØ2G
T6G=TØ6G
T5G=TØ2G
T10G=TØ8G
JV = 0
501
II = 0
CALL GASP
TIG, FN=>GAMIG,< PIG,GMU
No
JCPRØ ≥ 0
Yes
Compute RØ1
Compute PIG
Compute
WG, FM1, TØ1G, T11G
Set AMT and BMT array
elements to zero
Compute "average" temperatures
for Hx'5 and radiator fluids and
gases. Obtain all fluid properties
necessary for heat transfer
calculations
GASP
AIRP
LIQP

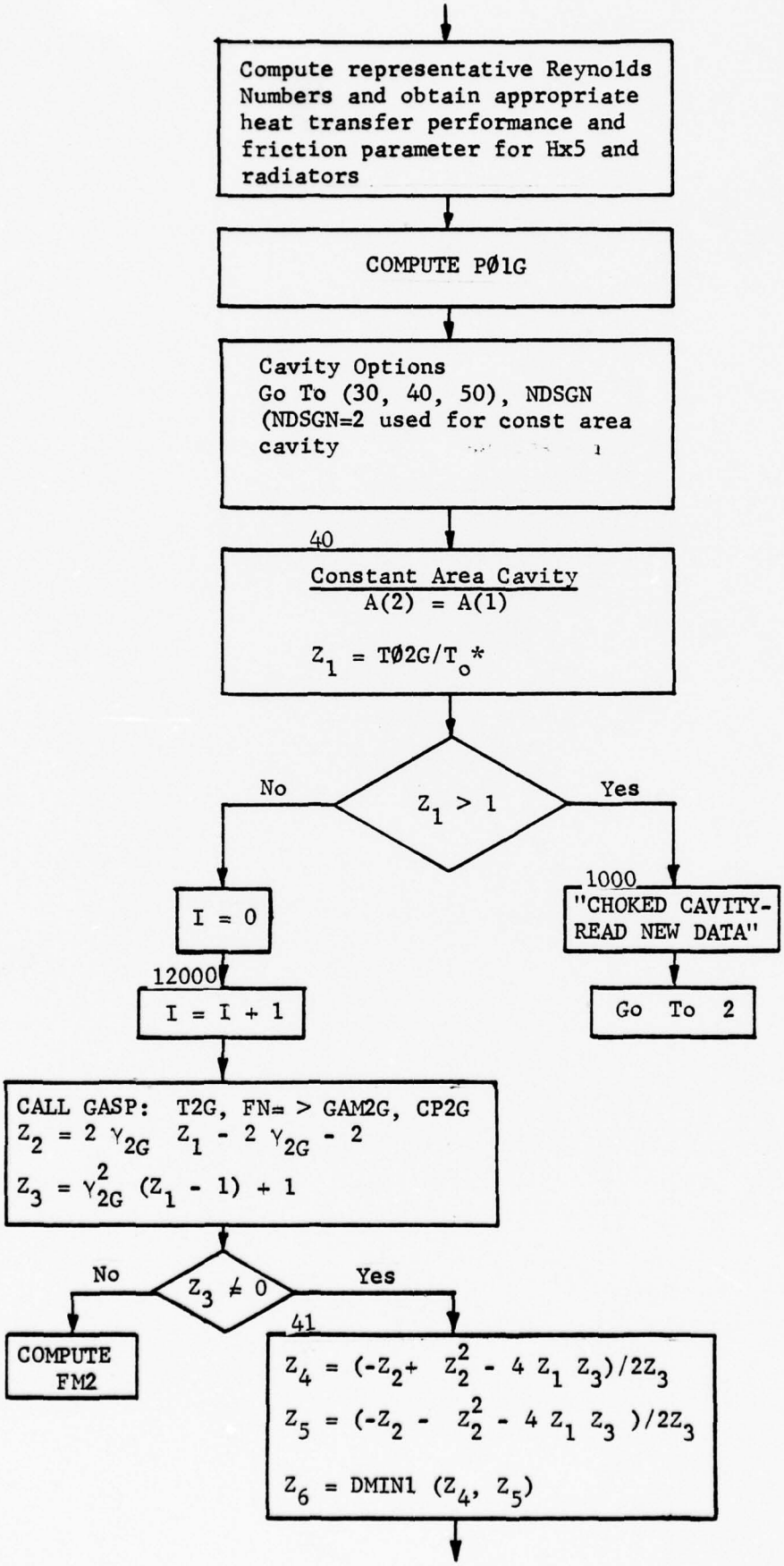
Compute representative Reynolds Numbers and obtain appropriate heat transfer performance and friction parameter for Hx5 and radiators
COMPUTE PØ1G
Cavity Options
Go To (30, 40, 50), NDSGN
(NDSGN=2 used for const area cavity
40
Constant Area Cavity
A(2) = A(1)
Z_1 = TØ2G/T_o*
Z_1 > 1
No
Yes
I = 0
12000
I = I + 1
1000
"CHOKED CAVITY-READ NEW DATA"
Go To 2
CALL GASP: T2G, FN= > GAM2G, CP2G
$Z_2 = 2\gamma_{2G}$ $Z_1 - 2\gamma_{2G} - 2$
$Z_3 = \gamma_{2G}^2 (Z_1 - 1) + 1$
$Z_3 \neq 0$
No
Yes
COMPUTE FM2
41
$Z_4 = (-Z_2 + \sqrt{Z_2^2 - 4 Z_1 Z_3})/2Z_3$
$Z_5 = (-Z_2 - \sqrt{Z_2^2 - 4 Z_1 Z_3})/2Z_3$
Z_6 = DMIN1 (Z_4, Z_5)

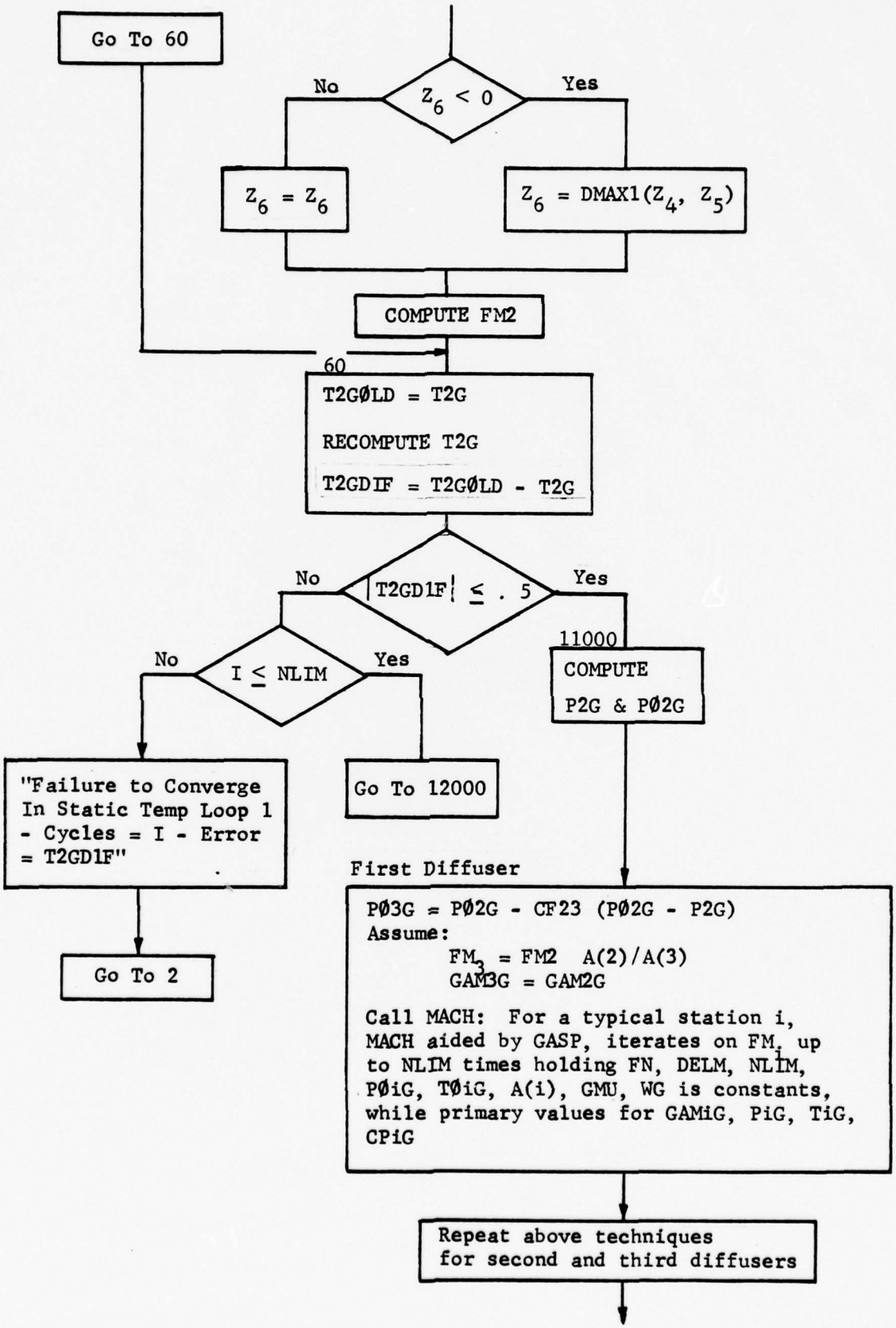
Go To 60
No
$Z_6 < 0$
Yes
$Z_6 = Z_6$
$Z_6 = DMAX1(Z_4, Z_5)$
COMPUTE FM2
60
T2GØLD = T2G
RECOMPUTE T2G
T2GDIF = T2GØLD - T2G
No
|T2GD1F| ≤ .5
Yes
11000
COMPUTE
P2G & PØ2G
No
I ≤ NLIM
Yes
"Failure to Converge In Static Temp Loop 1 - Cycles = I - Error = T2GD1F"
Go To 12000
Go To 2
First Diffuser
PØ3G = PØ2G - CF23 (PØ2G - P2G)
Assume:
FM3 = FM2 A(2)/A(3)
GAM3G = GAM2G
Call MACH: For a typical station i, MACH aided by GASP, iterates on FMi up to NLIM times holding FN, DELM, NLIM, PØiG, TØiG, A(i), GMU, WG is constants, while primary values for GAMiG, PiG, TiG, CPiG
Repeat above techniques for second and third diffusers

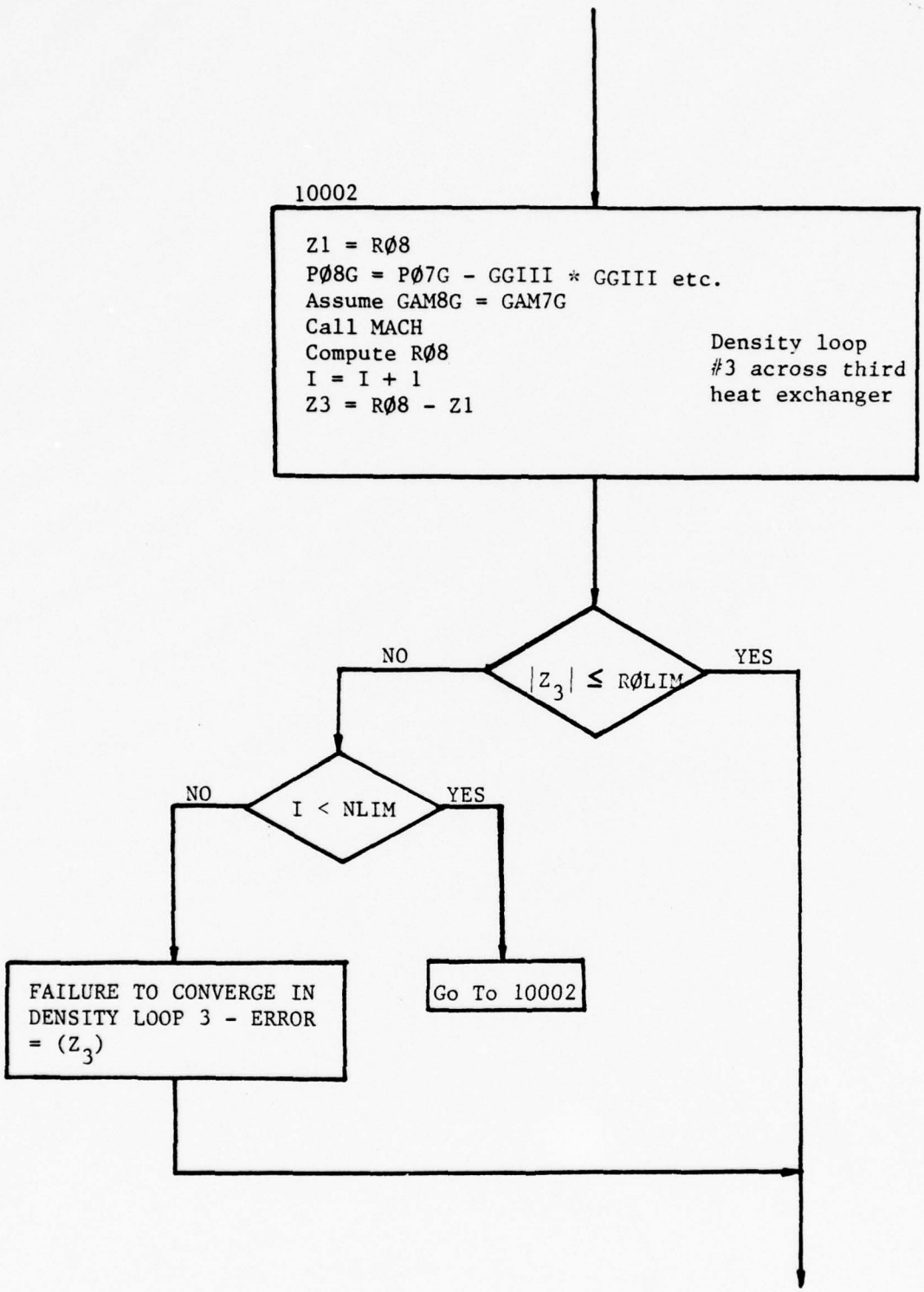
10002
Z1 = RØ8
PØ8G = PØ7G - GGIII * GGIII etc.
Assume GAM8G = GAM7G
Call MACH
Compute RØ8
I = I + 1
Z3 = RØ8 - Z1
Density loop #3 across third heat exchanger
NO
$|Z_3| \leq$ RØLIM
YES
NO
I < NLIM
YES
FAILURE TO CONVERGE IN DENSITY LOOP 3 - ERROR = (Z_3)
Go To 10002

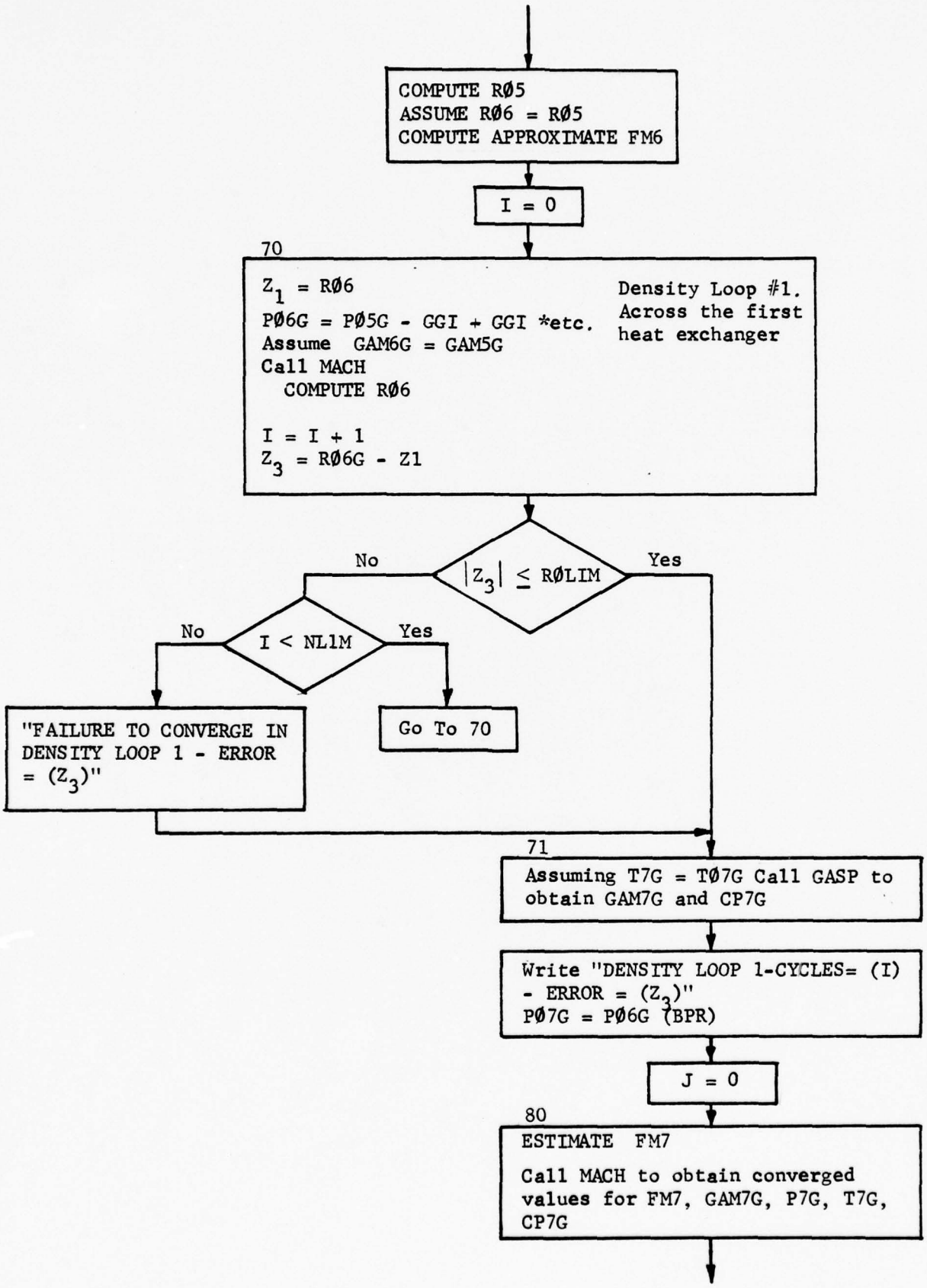
COMPUTE RØ5
ASSUME RØ6 = RØ5
COMPUTE APPROXIMATE FM6
I = 0
70
Z1 = RØ6
PØ6G = PØ5G - GGI + GGI *etc.
Assume GAM6G = GAM5G
Call MACH
COMPUTE RØ6
I = I + 1
Z3 = RØ6G - Z1
Density Loop #1. Across the first heat exchanger
|Z3| ≤ RØLIM
No
Yes
I < NL1M
No
Yes
"FAILURE TO CONVERGE IN DENSITY LOOP 1 - ERROR = (Z3)"
Go To 70
71
Assuming T7G = TØ7G Call GASP to obtain GAM7G and CP7G
Write "DENSITY LOOP 1-CYCLES= (I) - ERROR = (Z3)"
PØ7G = PØ6G (BPR)
J = 0
80
ESTIMATE FM7
Call MACH to obtain converged values for FM7, GAM7G, P7G, T7G, CP7G

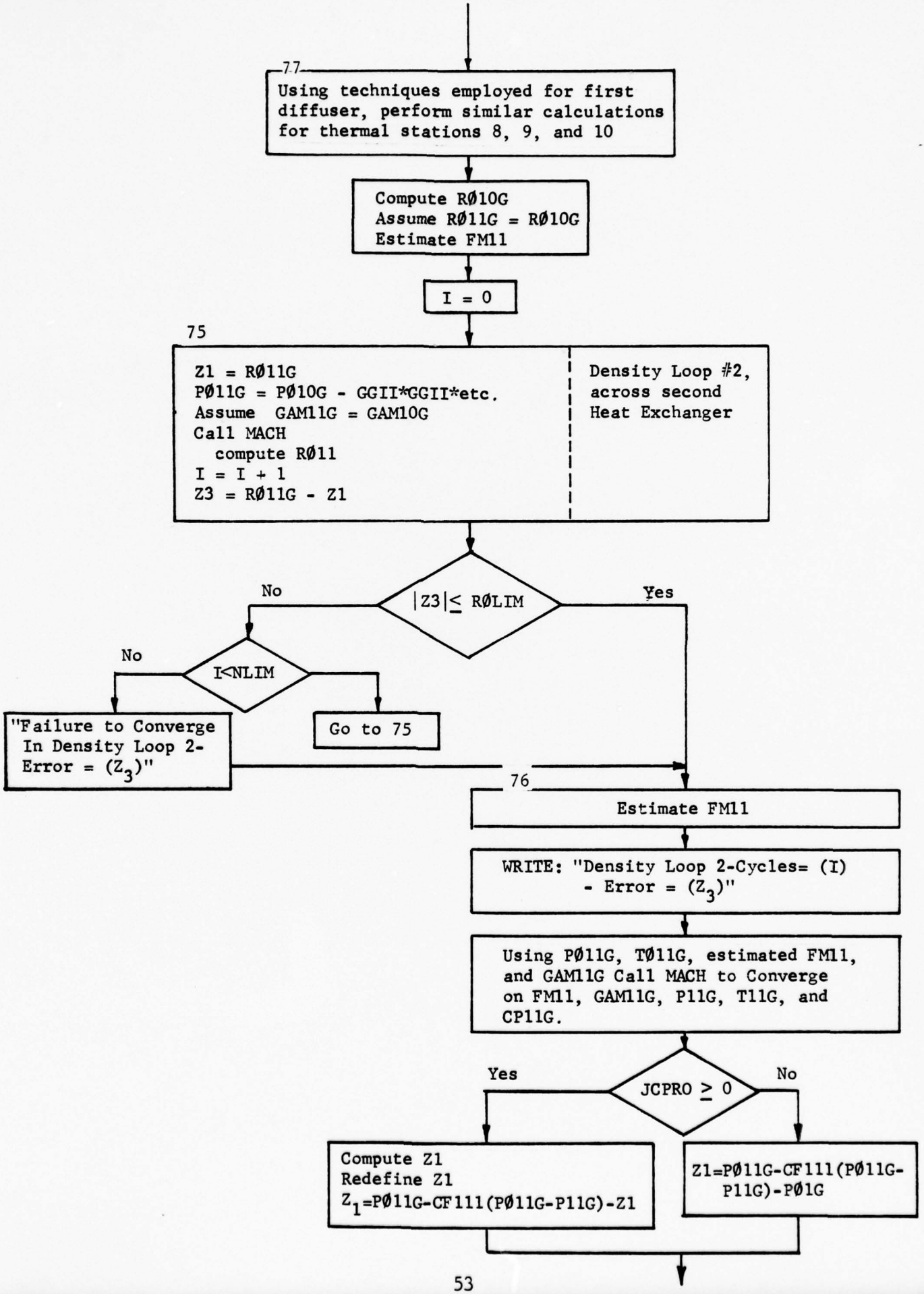
77
Using techniques employed for first diffuser, perform similar calculations for thermal stations 8, 9, and 10
Compute RØ10G
Assume RØ11G = RØ10G
Estimate FM11
I = 0
75
Z1 = RØ11G
PØ11G = PØ10G - GGII*GGII*etc.
Assume GAM11G = GAM10G
Call MACH
compute RØ11
I = I + 1
Z3 = RØ11G - Z1
Density Loop #2, across second Heat Exchanger
|Z3| ≤ RØLIM
No
Yes
I<NLIM
No
Go to 75
"Failure to Converge In Density Loop 2- Error = (Z3)"
76
Estimate FM11
WRITE: "Density Loop 2-Cycles= (I) - Error = (Z3)"
Using PØ11G, TØ11G, estimated FM11, and GAM11G Call MACH to Converge on FM11, GAM11G, P11G, T11G, and CP11G.
JCPRO ≥ 0
Yes
No
Compute Z1
Redefine Z1
Z1=PØ11G-CF111(PØ11G-P11G)-Z1
Z1=PØ11G-CF111(PØ11G-P11G)-PØ1G

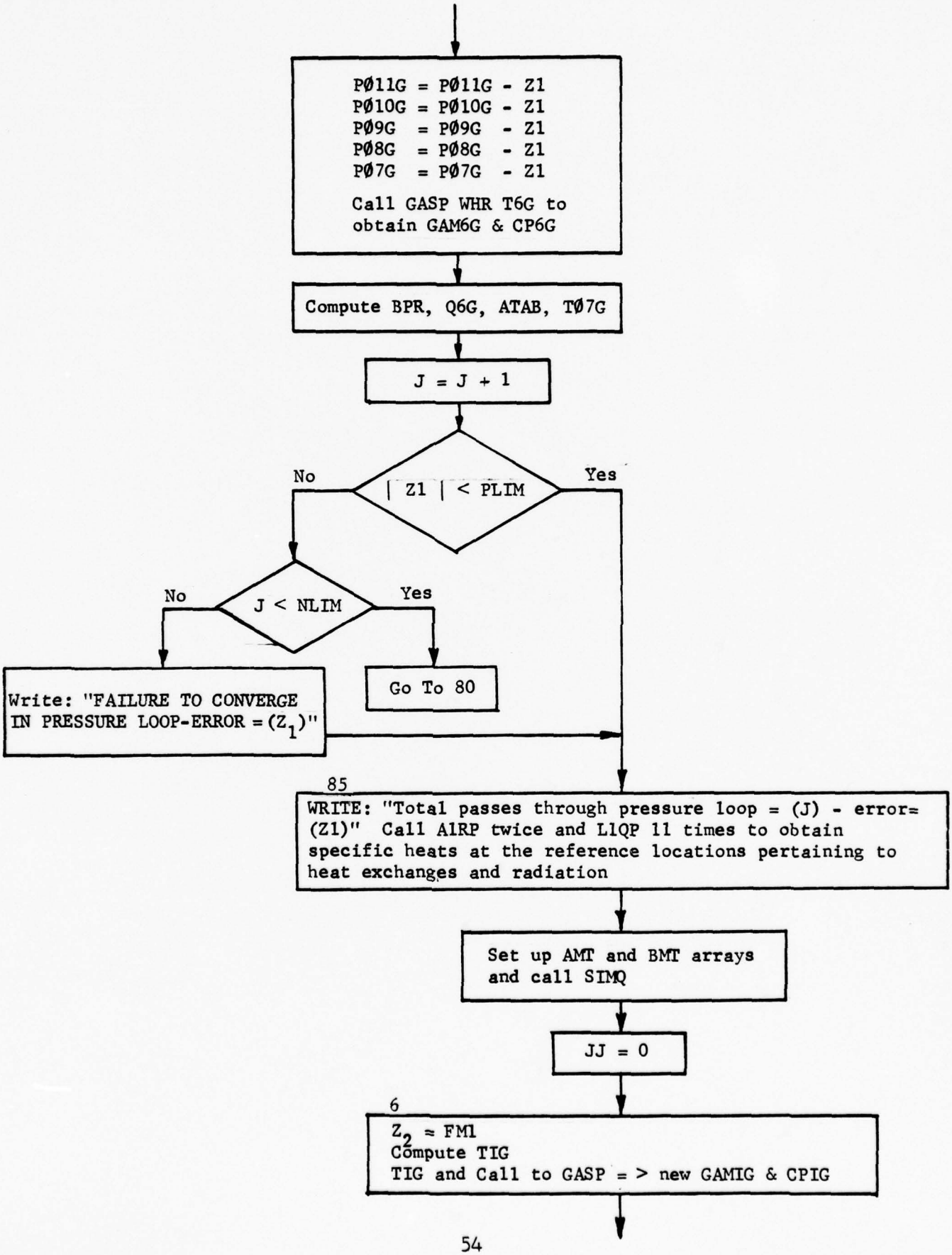
P011G = P011G - Z1
P010G = P010G - Z1
P09G = P09G - Z1
P08G = P08G - Z1
P07G = P07G - Z1
Call GASP WHR T6G to obtain GAM6G & CP6G
Compute BPR, Q6G, ATAB, T07G
J = J + 1
No
| Z1 | < PLIM
Yes
No
J < NLIM
Yes
Write: "FAILURE TO CONVERGE IN PRESSURE LOOP-ERROR = (Z1)"
Go To 80
85
WRITE: "Total passes through pressure loop = (J) - error= (Z1)" Call AIRP twice and LIQP 11 times to obtain specific heats at the reference locations pertaining to heat exchanges and radiation
Set up AMT and BMT arrays and call SIMQ
JJ = 0
6
Z2 = FM1
Compute TIG
TIG and Call to GASP = > new GAMIG & CPIG

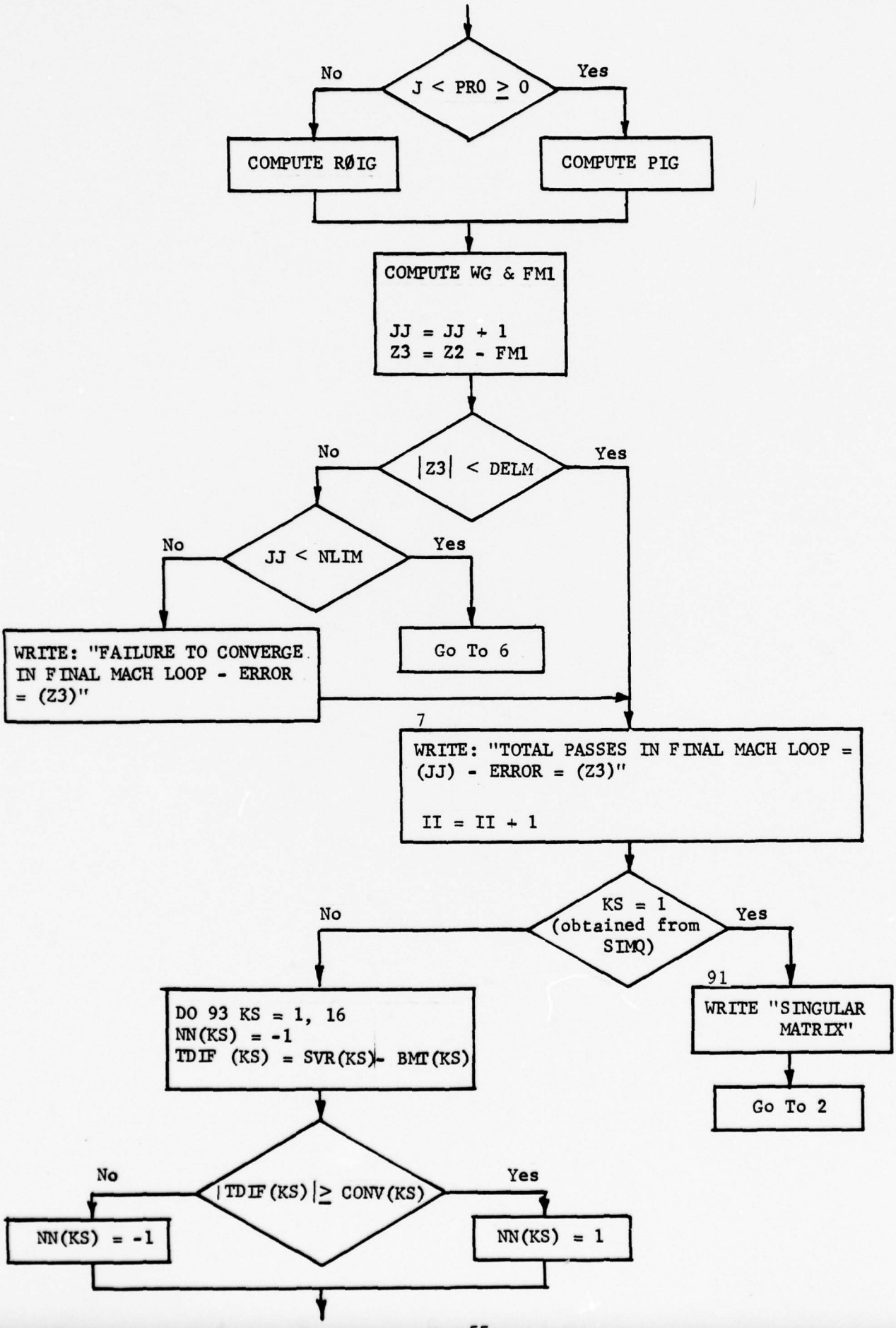
No
J < PRO ≥ 0
Yes
COMPUTE RØIG
COMPUTE PIG
COMPUTE WG & FM1
JJ = JJ + 1
Z3 = Z2 - FM1
No
|Z3| < DELM
Yes
No
JJ < NLIM
Yes
WRITE: "FAILURE TO CONVERGE IN FINAL MACH LOOP - ERROR = (Z3)"
Go To 6
7
WRITE: "TOTAL PASSES IN FINAL MACH LOOP = (JJ) - ERROR = (Z3)"
II = II + 1
No
KS = 1 (obtained from SIMQ)
Yes
91
WRITE "SINGULAR MATRIX"
Go To 2
DO 93 KS = 1, 16
NN(KS) = -1
TDIF (KS) = SVR(KS) - BMT(KS)
No
|TDIF(KS)| ≥ CONV(KS)
Yes
NN(KS) = -1
NN(KS) = 1

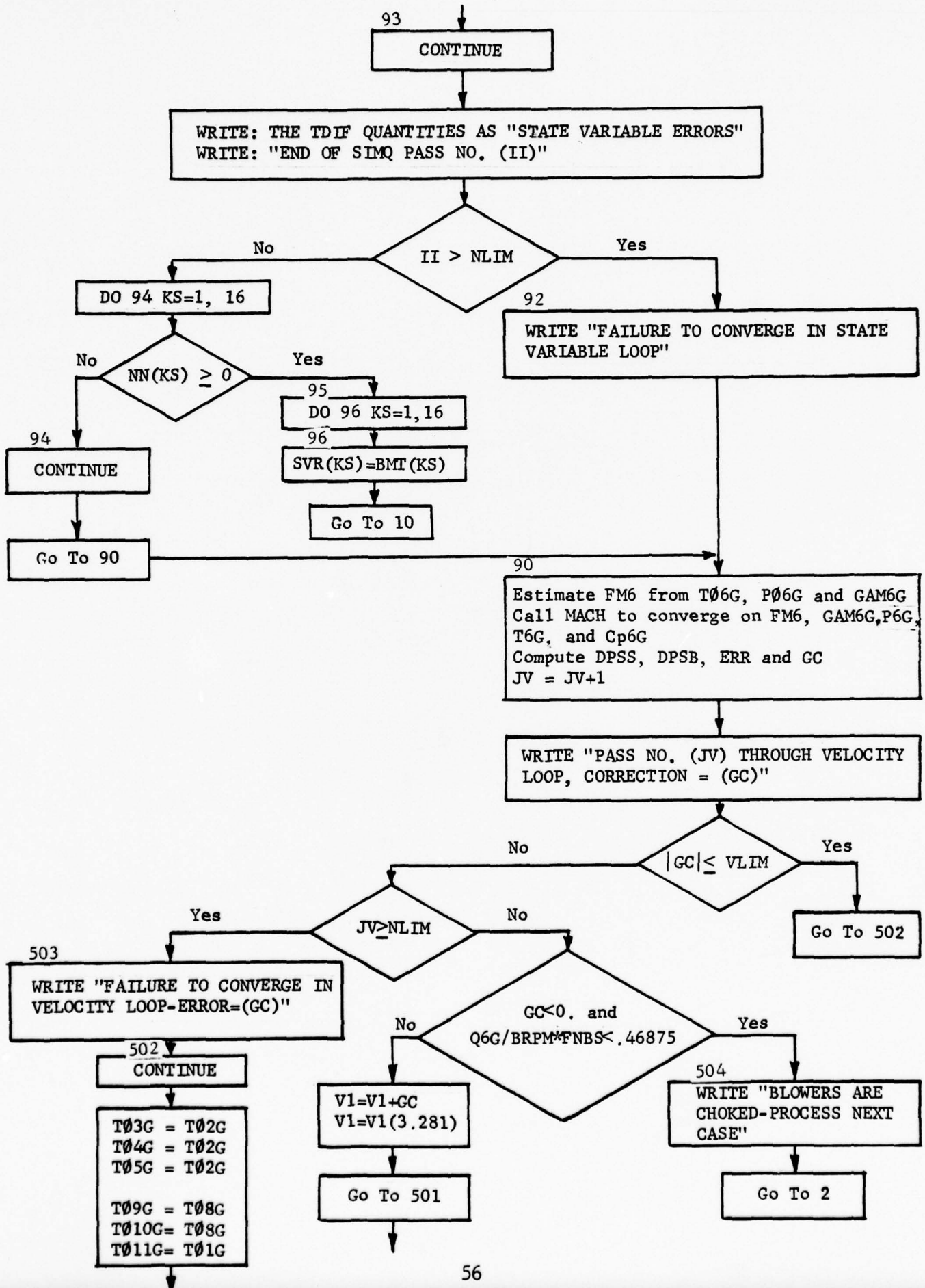
93
CONTINUE
WRITE: THE TDIF QUANTITIES AS "STATE VARIABLE ERRORS"
WRITE: "END OF SIMQ PASS NO. (II)"
II > NLIM
No
Yes
DO 94 KS=1, 16
92
WRITE "FAILURE TO CONVERGE IN STATE VARIABLE LOOP"
NN(KS) ≥ 0
No
Yes
95
DO 96 KS=1,16
96
SVR(KS)=BMT(KS)
94
CONTINUE
Go To 10
Go To 90
90
Estimate FM6 from TØ6G, PØ6G and GAM6G
Call MACH to converge on FM6, GAM6G, P6G, T6G, and Cp6G
Compute DPSS, DPSB, ERR and GC
JV = JV+1
WRITE "PASS NO. (JV) THROUGH VELOCITY LOOP, CORRECTION = (GC)"
|GC| ≤ VLIM
No
Yes
Go To 502
JV≥NLIM
Yes
No
503
WRITE "FAILURE TO CONVERGE IN VELOCITY LOOP-ERROR=(GC)"
GC<0. and Q6G/BRPM*FNBS<.46875
No
Yes
502
CONTINUE
V1=V1+GC
V1=V1(3.281)
504
WRITE "BLOWERS ARE CHOKED-PROCESS NEXT CASE"
TØ3G = TØ2G
TØ4G = TØ2G
TØ5G = TØ2G
TØ9G = TØ8G
TØ10G= TØ8G
TØ11G= TØ1G
Go To 501
Go To 2

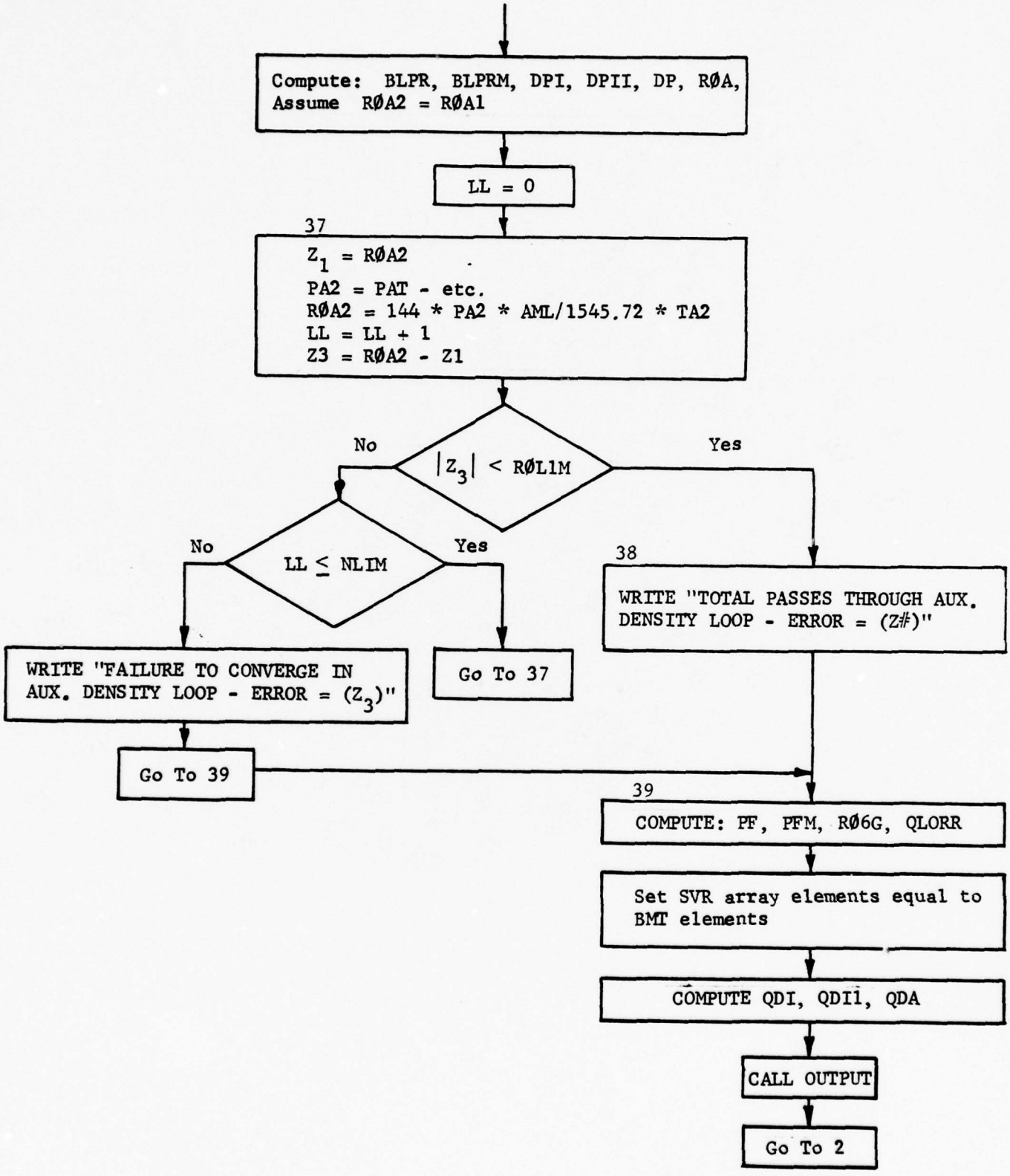
Compute: BLPR, BLPRM, DPI, DPII, DP, RØA,
Assume RØA2 = RØA1
LL = 0
37
Z_1 = RØA2
PA2 = PAT - etc.
RØA2 = 144 * PA2 * AML/1545.72 * TA2
LL = LL + 1
Z3 = RØA2 - Z1
No
$|Z_3|$ < RØL1M
Yes
No
LL ≤ NL1M
Yes
38
WRITE "TOTAL PASSES THROUGH AUX. DENSITY LOOP - ERROR = (Z#)"
WRITE "FAILURE TO CONVERGE IN AUX. DENSITY LOOP - ERROR = (Z_3)"
Go To 37
Go To 39
39
COMPUTE: PF, PFM, RØ6G, QLORR
Set SVR array elements equal to BMT elements
COMPUTE QDI, QDII, QDA
CALL OUTPUT
Go To 2

TABLE III

1. $WG\left(\frac{CPIG + CP2G}{2}\right)(TO1G) + \left(-WG\left(\frac{CPIG + CP2G}{2}\right)\right)(TO2G) = QS-.948(PLKW)(1./EFFL-1.)$

2. $CGI(TO2G) - CGI(TO6G) + (WI(.5)(CP2 + CP4))(T2) + (-WI(.5)(CP2 + CP4))(T4) = 0$

3. $(EPSI(CMIMI)-CG1)(TO2G) + CGI(TO6G) - (EPSI(CMIMI)(T2)) = 0$

4. $\frac{-(PO7G/PO6G)^{GAM6G-1.}}{ATAB(GAM6G)}\ (TO6G) + 1.(TO7G) = 0$

5. $-CGII(TO1G) + CGII(TO8G) + (WII(.5)(CP2 + CP6))(T2) - (WII(.5)(CP2 + CP6))(T6) = 0$

6. $CGII(TO1G) + (EPSII(CMIMII)-CGII)(TO8G) - EPSII(CMINII)(T2) = 0$

7. $-W3(.5)(CP1 + CP3)(T1) + W3(.5)(CP1 + CP3) - (CA(TA2)) = -CA(TA1$

8. $EPSA(CMIN)(T3) - (CA(TA2)) = (EPSA(CMIN)-CA)(TA1)$

9. $W3(.5)(CP1 + CP2)(T1) - W3(.5)(CP1 + CP2)(T2) = -QP$

10. $-WB(.5)(CP2 + CP3)(T2) + \{WI(.5)(CP4 + CP3) + WII(.5)(CP6 + CP3) + WM(.5)(CP16 + CP3) + WB(.5)(CP2 + CP3) + WV1(.5)(CP8 + CP3) + WV2(.5)(CP10 + CP3) + WE(.5)(CP18 + CP3) + WS(.5)(CP20 + CP3)\}(T3) - WI(.5)(CP4 + CP3)(T4) - WII(.5)(CP6 + CP3)(T6) - WV1(.5)(CP8 + CP3)(T8) - WV2(.5)(CP10 + CP3)(T10) - WM(.5)(CP16 + CP3)(T16) - WE(.5)(CP18 + CP3)(T18) - WS(.5)(CP20 + CP3)(T20) = 0$

11. $WM(.5)(CP2 + CP14)(T2) - WM(.5)(CP2 + CP14)(T14) = -QCM$

12. $WM(.5)(CP14 + CP16)(T14) - WM(.5)(CP14 + CP16)(T16) = -QM$

13. $WV1(.5)(CP2 + CP8)(T2) - WV1(.5)(CP2 + CP8)(T8) = -QV1$

14. $WV2(.5)(CP2 + CP10)(T2) - WV2(.5)(CP2 + CP10)(T10) = -QV2$

15. $WE(.5)(CP2 + CP18)(T2) - WE(.5)(CP2 + CP18)(T18) = -QE$

16. $WS(.5)(CP2 + CP20)(T2) - WS(.5)(CP2 + CP20)(T20) = -QS$

17. $CGIII(TO7G) + WIII(.5)(CP7 + CP8)(T2) - CGIII(TO8G) - WIII(.5)(CP7 + CP8)(T7) = 0$

18. $CGIII(TO8G) + (EPS3(CMIN3)-CGIII)(TO7G) - EPS3(CMIN3)(T7) = 0$

Chapter V

ANALYSIS OF OPTICAL RESONATORS WITH TILTED SPHERICAL MIRRORS

This study has employed closed-form analytical studies (of a two-dimensional approximation), extensions of previously existing computer codes, and newly prepared three-dimensional computer programs. This report will be concerned primarily with a summary of major aspects of the study and its conclusions; details have been furnished separately. The work has been coordinated with a MIRADCOM experimental investigation employing interferometry; the theoretical-computational and experimental results are in satisfactory agreement.

The development of theoretical and computational methods not only affords insight into observed trends, but provides a capability for determining expected optical quality properties of additional detailed designs without the need for an experimental study for each such design.

The investigations were primarily concerned with the effect, on an initially collimated beam, of one complete passage from convex to concave mirror, as indicated schematically in Figure 1. The two types of configurations, distinguished by the difference in relative signs of tilt angles of the two spherical mirrors, are referred to as "U-type" and "Z-type." The basic design equations, as given in Reference 1, do not distinguish between these two types of configurations. One of the purposes of the present study was to compare optical-quality properties of the two types. It turns out that the Z-type configuration is clearly to be preferred to the U-type configuration as regards output optical quality.

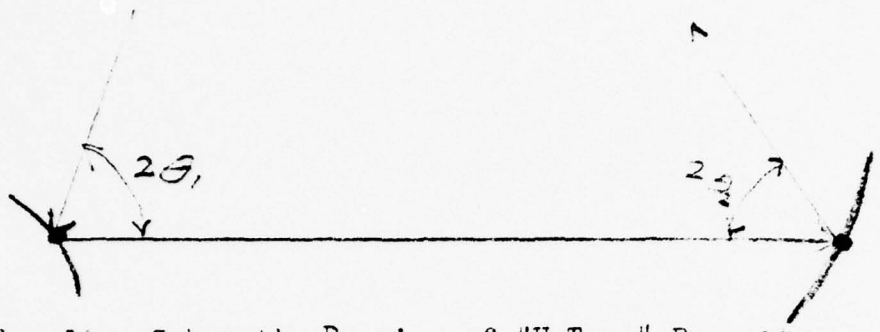

Fig. 1A. Schematic Drawing of "U-Type" Resonator.

Fig. 1B . Schematic Drawing of "Z-Type" Resonator.

Two-Dimensional Approximation

By using a local wave front curvature approach in the two-dimensional approximation, it was possible to derive a closed form approximate expression for the optical path difference, here labelled z, as a function of lateral displacement y, and of other parameters of the resonator:

$$z = \frac{1}{R_2^3 \cos^3 \theta_2} \left[- |R_1| \sin \theta_1 \pm R_2 \sin \theta_2 \right] y^3 \quad .$$

The above expression is perhaps deceptively simple in appearance, since the value of θ_2 which appears in it must be determined from additional equations, which are given in Reference 1. The points to which attention are here drawn are:

(1) The z-dependence is of the form $C_{03}\, y^3$, i.e. of third power in transverse position y.

(2) The choice of signs in the numerator is such that the Z-type configuration is clearly better, as regards optical quality, than the U-type configuration.

(3) The dependence on mirror radii of curvature is, roughly speaking, of inverse-square type.

In addition to the closed-form analysis leading to the equation given above, two-dimensional numerical calculations were carried out, which tended to confirm the above conclusions.

The equation given above could be rewritten in the form

$$z_{cp} = C_{03}\, Y^3$$

where Y is used to represent the maximum value of y, measured from center to edge, and the subscripts cp refer to the center-to-peak deviation. The optical quality is essentially determined by root-mean-square values of the optical-path deviations; these depend, of course, on the reference plane with respect to which they are measured. We will use $z_{rms,nt}$ to refer to rms values with no tilt of the reference plane, i.e., the reference plane is chosen as strictly perpendicular to the output central ray. The actual optical properties will be determined by the rms deviations with respect to a reference plane whose tilt is optimized; the corresponding value of z will be labelled as $z_{rms,opt}$. It was found that in the two-dimensional approximation, the following equations apply:

$$z_{rms,nt} = 0.378 \; z_{cp},$$

$$z_{rms,opt} = 0.4 \; z_{rms,nt}.$$

Specific numerical predictions of the above two-dimensional equations are listed in Table I for a situation corresponding to an experimental study, for a range of values of convex-mirror tilt angles θ_1. Three-dimensional predictions for the same cases will be given below for comparison.

Table I.

Two-Dimensional Approximate Predictions of Optical Path Differences in Microns, for a Z-Configuration Travelling Wave Resonator with R_1 = -290 cm, R_2 = 675 cm, Y = y_{max} = 7.62 cm, for Various Values of Convex Mirror Tilt Angle θ_1.

The second column gives the center-to-edge values, the third column gives the rms OPD for an untilted reference plane, while the fourth column gives the rms OPD relative to an optimally-tilted reference plane.

θ_1 (deg)	z_{cp}	$z_{rms,nt}$	$z_{rms,opt}$
10	0.393	0.149	0.059
20	0.855	0.323	0.129
30	1.481	0.560	0.224
45	3.168	1.198	0.479
50	4.165	1.574	0.630
55	5.614	2.122	0.849
60	7.866	2.973	1.189
70	19.233	7.270	2.908

Three-Dimensional Calculations

The major portion of this study has been concerned with developing and applying three-dimensional ray-tracing computational methods.

A collimated beam is assumed to be incident on the convex mirror. Given x and y coordinates of an incident ray measured relative to the central ray, the computer program calculates the path of the ray through the system and determines (a) direction cosines after reflection from the concave mirror, measured in a coordinate system with the positive z-axis parallel to the central ray and (b) the optical path difference (OPD) between the ray considered and the central ray. The OPD's are of primary interest, and are calculated for a position close to the concave mirror. It was found necessary to utilize double precision arithmetic in order to obtain reliable values of OPD's.

Included in the input data are half-widths, in the x and y directions, of the desired output beam and the number of mesh points along x and y (usually 9 x 9). Coordinates x and y of incident rays are obtained by dividing corresponding desired coordinates of output rays by magnifications M_x and M_y, which are computed by the program from input values of R_1, R_2, and θ_1. Unless otherwise specified, the program uses the values of mirror spacing L and of concave mirror tilt angle θ_2 which result in a collimated output beam, values of these parameters being determined by an initial portion of the program. The first page of computer output is a table of calculated OPD's over the specified mesh; the OPD's are given in microns, while mirror spacing and radii of curvature are in centimeters.

It was found that there is a good deal of order in the calculated OPD's as might be expected, and that their functional dependence on x and y can be rather well represented by a relatively small number of terms of

a Taylor's expansion. Of primary importance are terms $C_{03}\ y^3$ and $C_{21}\ x^2y$; values of the coefficients C_{03} and C_{21} are not the same. The quadratic terms $C_{20}\ x^2$ and $C_{02}\ y^2$ can, of course, be important if the system is not properly adjusted. These terms have been included in the function fitting process in order to be able to investigate the effects of adjusting L and θ_2 to values slightly different from their ideal values. Also allowed for is a cross-term $C_{22}\ x^2\ y^2$ as well as fourth-order terms of the form $C_{40}\ x^4$ and $C_{04}\ y^4$.

The computer program evaluates the series coefficients from the table of calculated OPD's and prints these. It also calculates and prints a table of residuals showing the difference between the directly calculated OPD's and values obtained from the truncated series expansion; these seem typically to be of the order of one percent or less of the OPD's themselves. The coefficient C_{tilt} corresponding to a reference plane defined by $z = C_{tilt}\ y$, which minimizes the rms OPd, is also determined and printed. Also a table is printed of the rms values of OPD for various values of reference beam tilt measured in units of the optimal value.

If L and/or θ_2 are set to values which are incremented slightly from their proper values there will be wave-front curvature in either or usually both the x and y directions, i.e., C_{20} and/or C_{02} will differ appreciably from zero. Expected values of these coefficients can be derived analytically and compared with results of the function fitting process applied to the ray tracing OPD calculations. Agreement noted between analytically predicted and "function-fitting" calculated values is felt to be a confirmation of proper functioning of the computer program.

The primary experimental data regarding optical quality from tilted-spherical mirror resonator are in the form of interferograms. While

providing very previse and detailed information about the optical systems, interferograms do not immediately (without an intervening measurement and data-reduction process) lead to quantities predicted by the calculations. For the purpose of comparing experiment and calculations, it, therefore, seemed useful to convert the calculated OPD results into the form of computer simulated quasi-interferograms. For this purpose, the computer generates a fairly large (49 x 49) array of OPD's obtained by evaluation of the truncated series expansion at each of the array points. The array of numerical values is then converted to an array of alphabetic characters or blanks and used to generate a one-page printer plot whose general appearance simulates that of an interferogram. Successive characters of the alphabet correspond to incremental OPD's of one wavelength (0.6328 micron). The interspersing of blanks with letters of the alphabet has the result that (at least in the central portion of the plot) light areas are interspersed with dark areas, and hence, simulate an interferogram. An example of a computer generated quasi-interferogram is given in Figure 2.

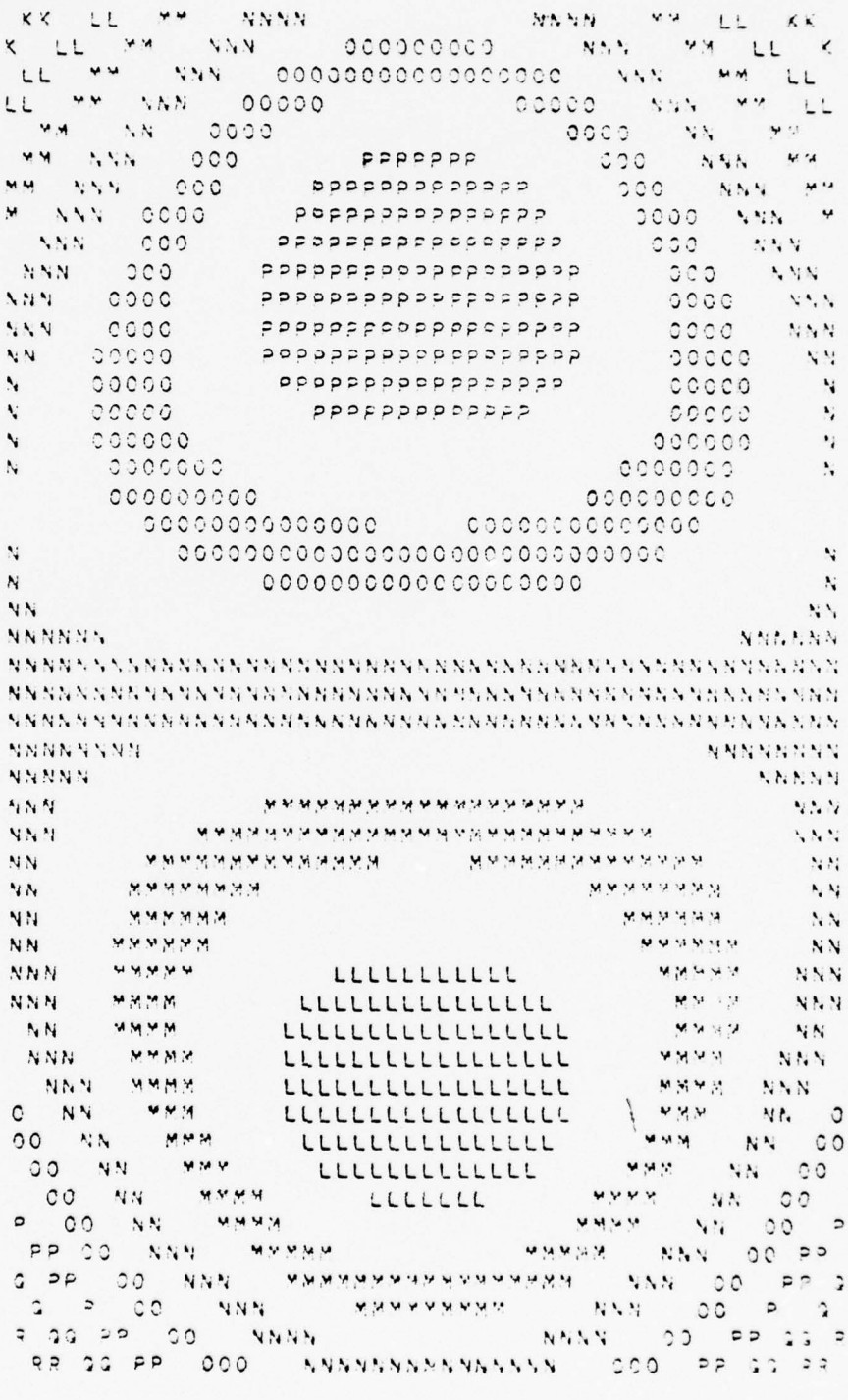

Figure 2. A Typical Quasi-interferogram. Here L and θ_2 are properly adjusted and reference beam tilt has its optical value. Note the symmetry of the pattern, a property which was found to be typical of proper adjustment of L and θ_2.

The computer program will optionally produce multiple quasi-interferograms, corresponding to a specified set of reference beam tilts, from a single set of OPD calculations. The observed progression of shapes as tilt is systematically varied has proven interesting and useful since, of course, reference beam tilt can also be varied experimentally.

Inspection of quasi-interferograms leads to some interesting observations for a properly-aligned system (which was treated computationally prior to investigating effects of incremented values of L and θ_2):

(1) There is symmetry in x, as would be expected since the entire optical system is assumed to have such symmetry.

(2) For Z-type configurations, the pattern is symmetric in y to a fairly high degree of approximation (the OPD's are approximately anti-symmetric).

(3) For Z-type configurations there is a regular progression of shapes as reference beam tilt is increased from zero to its optimal value and beyond. Specifically, the pattern changes from a single central oval to a pair of ovals, symmetrically spaced about y = 0, which move further apart and are separated by an increasing number of fringes.

The properties just noted should be useful in experimental adjustment of L and θ_2, since the symmetry in y seems to be a rather good "signature." Calculations made with values of L and/or θ_2 which are incremented from their ideal values produce quasi-interferograms which are quite noticeably lacking in the y-symmetry property.

A number of calculations were made for $\theta_1 = 45^o$, for various values of ΔL and $\Delta\theta_2$ (as well as reference beam tilts). One can reduce to zero the coefficient of either the x^2 or y^2 term by suitable choice of one of the increments,(i.e., ΔL or $\Delta\theta_2$), when the other is specified. Reduction

to zero of the $C_{20}\ x^2$ term shows up most clearly; one notes from the plot that there is very little OPD variation along x for y = 0. When the coefficient of y^2 is reduced to zero, the corresponding quasi-interferogram is somewhat more involved, since there is still an appreciable amount of aberration present associated with other expansion terms. What is especially noticeable is that the y-symmetry is decidedly absent; this emphasizes usefulness of the y-symmetry property in making experimental adjustments. If one reverses the signs of both ΔL and $\Delta\theta_2$, the y^2 coefficient still vanishes, there is still a lack of y-symmetry, and the plot is essentially just the mirror image of the plot obtained without reversal of signs. This mirror image property applies for any pair of magnitudes of ΔL and $\Delta\theta_2$. In the special case of zero magnitudes of both these increments, the mirror image of the pattern is simply (to a rather good approximation) identical with the pattern itself; that is to say, the y-symmetry property is characteristic of proper adjustment of L and θ_2.

For cases where comparisons have been made, it appears that the three-dimensional ray tracing calculations predict optical quality parameters which are not greatly different from those obtained by the much simpler approach based on the two-dimensional approximation. Some specifics will be given for one case. For the mirror parameters associated with the experimental studies, three dimensional ray tracing calculations have been carried out for a range of values of θ_1; results are listed in Table II. These results may be directly compared with the two-dimensional predictions of the same case as given in Table I. The 3D predictions of the optimized rms OPD range from only some 25% to some 50% larger than the 2D predictions.

Table II.

Three-Dimensional Ray Tracing Predictions of Optical Path Differences, in Microns, for a Z-configuration Travelling Wave Resonator with R_1 = -290 cm, R_2 = 675 cm, $x_{max} = y_{max}$ = 7.62 cm, for Various Values of Convex Mirror Tilt Angle θ_1.

The second column gives the center-to-edge values (taken along y for x = 0); center-to-corner values are somewhat larger but are not listed here. The third column gives the rms OPD for an ultilted reference plane, while the fourth column gives the rms OPD relative to an optimally-tilted reference plane.

θ_1(deg)	z_{cp}	$z_{rms,nt}$	$z_{rms,opt}$
10	0.393	0.230	0.091
20	0.855	0.496	0.194
30	1.481	0.848	0.330
45	3.171	1.764	0.678
50	4.171	2.287	0.876
55	5.626	3.031	1.157
60	7.892	4.159	1.582
70	19.450	9.529	3.667

Summary

1. A closed form expression was derived and confirmed for optical path difference in a two-dimensional approximation as a function of various resonator parameters.

2. The closed form expression was confirmed by numerical calculations in both two and three dimensions.

3. It was found that the Z-type configuration is clearly to be preferred to the U-type configuration as regards optical quality.

4. For the two-dimensional case, expressions were derived for the root-mean-square optical path difference, which is the proper measure of optical quality degradation. It was found that the rms deviation is substantially less than the maximum deviation.

5. A computer program was prepared for three-dimensional ray tracing calculations of optical path differences.

6. The 3D computer program was checked in various ways, including comparison to separate 2D calculations, and comparison to analytical predictions for effects of varying L and θ_2 from their proper values.

7. The 3D program was extended to extract Taylor's series expansion coefficients for OPD's and to use these to generate large (49 x 49) arrays of OPD's for various values of reference beam tilt angle.

8. The program was arranged to plot quasi-interferograms from the large arrays of calculated OPD's.

9. Various effects were investigated by performing series of 3D computer runs.

10. For properly adjusted L and θ_2, the quasi-interferograms were found to range from a central oval to a symmetrically arranged pair of ovals as the reference beam tilt is increased.

11. Improper adjustment of L was found to result in introduction of wave front curvature of the same sign in both x and y coordinates.

12. Improper adjustment of θ_2 was found to result in introduction of wave front curvature of opposite signs for x and y coordinates.

13. Reversal of sign of incremental values of L and θ_2 was found to result in inverting the quasi-interferogram along the y dimension.

14. Proper adjustment of L and θ_2 was found to lead to quasi-interferograms which are symmetric in y (as well as x). The y-symmetry property seems to be a useful "signature" for use in experimental adjustments.

15. Numerical predictions were made for rms OPD variations for selected cases. It was found that the full 3D rms OPD's were typically some tens of percent larger than the 2D values.

REFERENCES

1. Charles Cason, R. W. Jones, and J. F. Perkins, "Optical Resonators with Tilted Spherical Mirrors," U. S. Army MIRADCOM Technical Report H-77-9, Sept. 1977. Also published in Optic Letters, 2, Page 145-147, June 1978.

Chapter VI

CONTRIBUTIONS TO TECHNICAL CONFERENCES

Section 1 -- Gas Dynamic and Acoustic Management for Visible Wavelength Lasers by Cornelius C. Shih and Charles M. Cason

Section 2 -- Investigation and Management of Acoustical Waves in Closed Cycle High Energy Pulsed Lasers by G. R. Karr, C. C. Shih, Charles Cason and A. H. Werkheiser

Section 3 -- Non-Linear Wave Propagations in a Pulsed High Energy Gas Laser by C. C. Shih, G. R. Karr, and Charles Cason

Section 4 -- Measurements of Fluid and Thermal Characteristics of Re-circulating Laser Gas Flows in a Closed Cycle Circulator for Pulsed Lasers by Cornelius C. Shih, Gerald R. Karr and Charles Cason

Section 5 -- Fluid and Thermal Characteristics of Closed Cycle Flow Systems for High Power Lasers by G. R. Karr, C. C. Shih, C. M. Cason, and Vernon Ayre

Section 1

Presented at SPIE Advances in Laser Technology 1978, Bellingham, Washington, March 1978.

GAS DYNAMIC AND ACOUSTIC MANAGEMENT FOR VISIBLE WAVELENGTH LASERS

Cornelius C. Shih
The University of Alabama in Huntsville
Huntsville, Alabama

and

Charles M. Cason
U.S. Army Missile Research and Development Command
Redstone Arsenal, Alabama

Abstract

Criteria for fluid and thermal properties delineating the baseline flow homogeneity, such as those for $\Delta T/T$, $\Delta P/P$, $\Delta\rho/\rho$, and $\Delta U/U$ will be established. These are based on medium optical characteristics and requirements in terms of wavelength, pressure, and temperature of the gas medium associated with visible wavelength lasers. To meet these criteria, various methods for conditioning the baseline flow from the standpoint of gas dynamic and acoustic technologies will be presented and discussed. The merits of open and closed cycles for the baseline flow will be evaluated through consideration of gas utilization efficiency and component requirements. These criteria become acoustic dominated for pulsed lasers. The pulse repetition frequency required for a given laser defines the clearing time allowed to restore the original baseline flow. A parallel consideration becomes necessary to account for the pulse input perturbation. Solutions to acoustic management problems must be obtained by considering all sources of reflection, acoustic characteristics of open and closed cycles in terms of wave propagation, attenuation, and dissipation.

Introduction

In recent years, visible wavelength lasers of KrF, XeF, and HgCl have wide-spread interest in the field of high energy laser technology because of the potential applications. These visible lasers with wavelengths ranging from 0.25 to one micron are generally known to attain lasing conditions suitably at the temperatures of $500^{o}k$ - $500^{o}k$. The concept of repetitively pulsed energy input through the use of an electron beam or self-sustained discharge into the laser cavity has been shown to be an efficient and compact means of achieving high power levels in Argon and Helium at one to five atmospheric pressures. In such a system, the E-beam, through secondaries, supplies direct pumping energy to Argon and also produces a plasma in the laser cavity. Across the plasma, a sustainer voltage is applied at an adjusted field streneth to excite the laser states with optimum pumping. If the lasing pulse duration is approximately equal to the relaxation time of the lower lasing state, the optimum lasing output is achieved. On the other hand, shorter pulses will cause a premature self-termination of lasing process, and longer pulses will result in gas heating and reduction of the lower state capacity. The pulse duration is considered to be approximately one μ second for the gas composition and temperature of interest.

In the operation of electrically pulsed lasers, the abrupt deposition of energy in the laser media causes the development of pressure and temperature variations. The resulting pressure and temperature gradients are responsible for producing acoustical perturbations. Optical beam quality is known to be degraded by acoustically produced density fluctuations as noted by previous investigations particularly for CO_2 lasers [1],[2], [3], [4], [5]. To avoid these defects, the heating of laser gases must be accommodated by both applying a pulsed duty cycle of sufficient duration and imposing a flow of the gases through the cavity. Therefore, efficient operation of the visible wavelength pulsed lasers requires serious attention to gas dynamic and acoustic management of the laser media in the flow systems. The flow systems under consideration are either open (blow-down) or closed cycle (circulator) type. The power input for these lasers of interest is limited practically at about 100 Joules per liter of cavity volume under various operational constraines, while the length of laser cavity along the optical axis is chosen at 100 cm for present study.

This paper is intended to focus attention on technical issues pertinent to the gas dynamic and acoustic management for the flow systems of the high power visible wavelength laser with repetitively pulsed modes of operation under the above mentioned constrains on the laser parameters. Specifically, issues to be discussed are as follows: medium homogeneity criteria; methodology of gas dynamic and acoustic management of the baseline flow; merits of open and closed cycle flow systems.

In this study, the energy deposition in the laser gas cavity is assumed to be for the duration of one μ second as the pumping boundary condition representative of desirable e-beam, e-beam plus discharge, or externally initiated TEA approaches. However, problems of electric pumping, arcing limits, and kinetic details for specific electric discharge laser gas systems are not considered in the paper.

Baseline Flow Homogeneity Criteria

Fluid and thermal properties governing the baseline flow homogeneity of high power lasers are closely associated with the radiation intensity ratio in defining the beam quality. The intensity ratio, I/I_o in the far field where I_o refers to the diffraction limited far field central spot intensity and I denotes the reduced intensity due to induced aberrations. For small r and down fluctuation, it is directly related to the square of the rms fractional density fluctuation, $\Delta\rho/\rho$. Systematic, large-scale ordered variations in the density, ρ, cause the optical pathlengths along the ray paths to vary, while smooth ordered ρ variations produced in the flow that causes a spatial tilt plane error in the phase front which is a fundamental loss. Linear plane errors in the spatial phase, ϕ, can be corrected by careful resonator mirror alignment to require the optical pathlengths along the rays to be the same.

Relatively small randomized density fluctuations in the flow field can cause spatial phase, ϕ, fluctuations that have no simple temporal and spatial order. A qualitative estimate of the allowable $(\Delta\rho/\rho)_{rms}$ can be made for small phase aberrations by use of the Strehl criterion,

$$I/I_o = \exp(-\phi^2_{rms}) \sim 1 - \phi^2_{rms}, \tag{1}$$

at the point that errors become significant because higher order terms are neglected in Eq. 1, $I/I_o \sim 0.8$. Specifying this optimizational point requires $1 - \phi^2_{rms} \geq 0.8$. The spatial phase front criteria becomes $\phi \leq .071\lambda_{rms}$ where λ is the optical wavelength. Using this criteria to determine the maximum allowable rms pathlength gives a useful medium quality parameter in terms of gas density variation:

$$L(\Delta\rho/\rho)_{rms} \leq .071\lambda_{rms}\,\rho_{ref}/\rho\beta \tag{2}$$

where L is the optical pathlength, for resonators with large out-coupling, $\frac{\partial\rho}{\partial\rho_{ref.}} = n - 1$ where n is the index of refraction, β the Gladstone-Dale constant, ρ the gas density, ρ_{ref} the density at STP conditions. Using the given requirement for the medium quality for 2 atm typical visible laser mixtures gives $L(\Delta\rho/\rho)_{rms}$ to be 3.2×10^{-3}cm, 1.5×10^{-3}cm and 1.2×10^{-2}cm of KrF, XeF, and HgCl, respectively in Argon at 2 atm. Values of $(\Delta\rho/\rho)_{rms}$ for most E-beam pumped A_r mixtures are therefore approximately 10^{-5} and for TEA discharges in He $(\Delta\rho/\rho)_{rms}$ is approximately 10^{-4} for L = 100 cm.

Reducing the scale of the density fluctuations further reaches a point wherein the far field intensity is degraded by scattering[6], [7] a portion of the optical beam from the resonator. This portion of the output laser energy will appear as a very broad flattened background in the far field to be added to the proportionally reduced Fraunhoffer pattern.

The approximations used to determine the allowed $(\Delta\rho/\rho)_{rms}$ for specified values of L provide little beyond a qualitative feel for high gain systems having large output coupling. Real cases may impose more stringent $(\Delta\rho/\rho)_{rms}$ requirements. Numerical calculations to correctly determine the phase-perturbed cavity properties would be expensive and should be very carefully planned[6]. However, the very important systems advantage of the Helium diluent over Argon presents a flow medium quality of $\Delta\rho/\rho = 10^{-4}$ may be obtainable for 100 cm He mixtures.

The medium homogeneity is expressed in acoustic terms for the two laser gases, Helium and Argon at two ATM under the normal laser conditions. The $(\Delta\rho/\rho)_{rms}$ for the two gases are expressed graphically in terms of the driving sound pressure level in Figure 1. It shows that acoustical energy in Helium will produce a lower $(\Delta\rho/\rho)_{rms}$ than the same level in ARgon laser.

The criteria established in terms of $\Delta\rho/\rho$ for various visible wavelength lasers (VWL) are based on the beam quality requirements, and they are considerably restrictive, about two orders of magnitude higher than those applied to the pulsed chemical lasers. This unfavorable situation is amplified by the fact that the flow Mach numbers of about 0.5 for the VWL are noted to be larger than for most other pulsed UDL. This study considers the issues concerning the sources of medium inhomogeneity in the baseline flow due to the pulsing as well as the gas dynamic and acoustic management of the perturbations has been given in this study.

Gas-Dynamic and Acoustic Phenomena in the Pulsed Laser Operation

The gas density response to rapid volumetric heating takes place after lasing because the acoustic time constant is relatively long, 30 to 100 μsec.

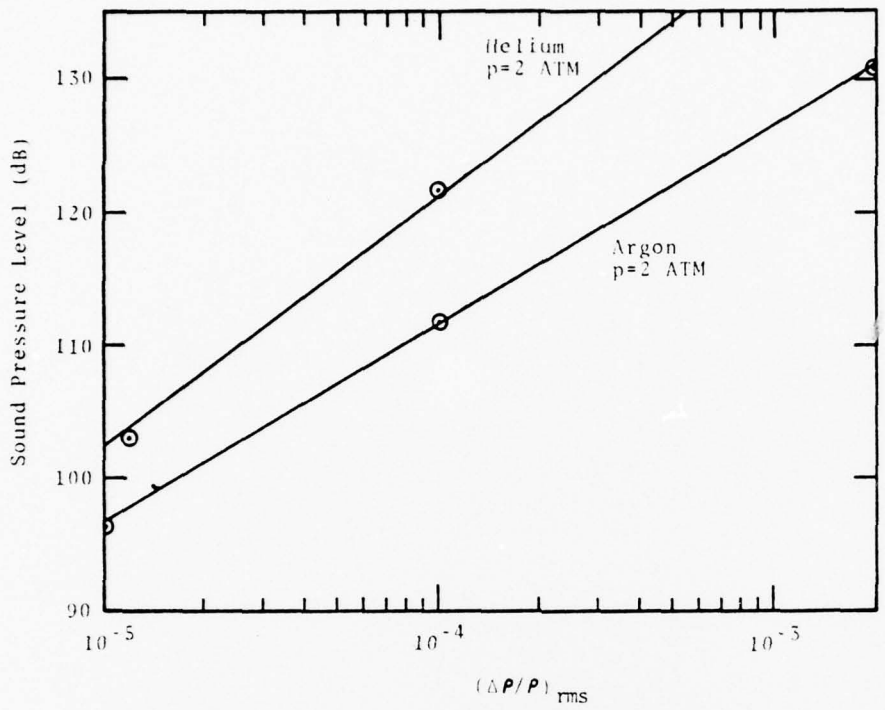

Fig. 1: Sound Pressure Level Versus $(\Delta\rho/\rho)_{rms}$ for Helium and Argon at 2 atm.

Although it has been determined that this acoustically significant temperature rise occurs on a relatively long time comparing with the pulse duration of about 1μ sec, but it is short for significant changes in the liter size flow system at the cavity. Thus, the assumption of constant volume heating of the gas in the cavity is reasonably justified for the gas dynamic analysis of the flow systems under the pulsed operation. The temperature rise coupled with pressure surge in the slug of laser gas in the cavity generates the formation of shock waves and expansion waves which lead to the issuance of an interface or so-called contact surface between them. Propagations and reflections of these pressure waves complicated by the existence of the interface separating the heated gas from the cold in the flow system contribute the main source of thermo-acoustical problems in subsequent pulses. Qualitative descriptions of these thermo-acoustic phenomena are presented graphically in space vs. time plane in Figure 2 and in space vs. thermodynamic properties for various time frames in Figure 3. These graphical presentations were developed from numerical results of computer modeling of the laser gas flow system under pulsed operation based on the method of characteristics. The computer code devises a simultaneous approximate solution of the coupled state, continuity, momentum and energy equations including the effect of friction for the time-dependent one-dimensional flow of the pulsed laser gas system centered around the laser cavity[8].

Sources of random medium inhomogeneity accumulatively contributes additive rms elements that degrades the beam quality. It is expressed in terms of $\Delta\rho/\rho$ as follows:

$$\text{Total } \left(\frac{\Delta\rho}{\rho}\right)_{rms} = \left\{ \underbrace{\left(\frac{\Delta\rho}{\rho}\right)^2_{rms}}_{\text{Thermodynamics}} + \underbrace{\left(\frac{\Delta\rho}{\rho}\right)^2_{rms}}_{\text{Turbulence}} + \underbrace{\left(\frac{\Delta\rho}{\rho}\right)^2_{rms}}_{\text{Acoustics}} \right\}^{1/2} \tag{3}$$

where

$$\underbrace{\left(\frac{\Delta\rho}{\rho}\right)^2_{rms}}_{\text{Thermodynamics}} \approx \left(\frac{\Delta T}{T}\right)^2_{rms} \quad \text{for temperature fluctuations in boundary layers, interfaces and other flow components.} \tag{4}$$

$$\underbrace{\left(\frac{\Delta\rho}{\rho}\right)_{rms}}_{\text{Turbulence}} \approx \frac{1}{2} M_\infty^2 \left(\frac{\Delta u}{u_\infty}\right)^2_{rms} \quad \text{for free stream turbulence} \tag{5}$$

$$\approx C_f M_\infty^2 \frac{\delta^*}{\ell} \quad \text{for boundary layer turbulence} \tag{6}$$

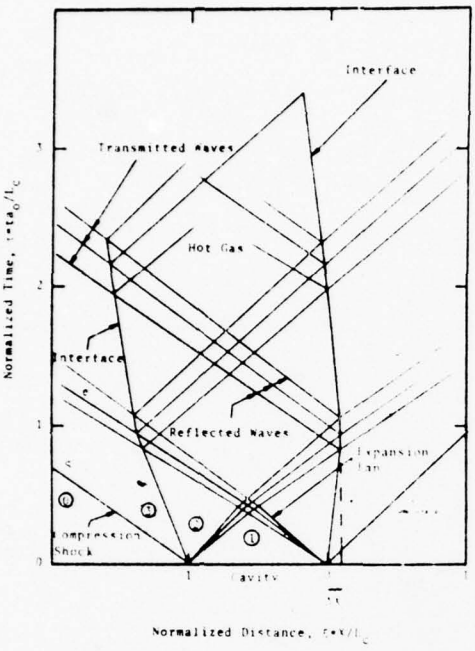

Fig. 2: Wave Propagation and Interaction Due to Pulsed Energy Input

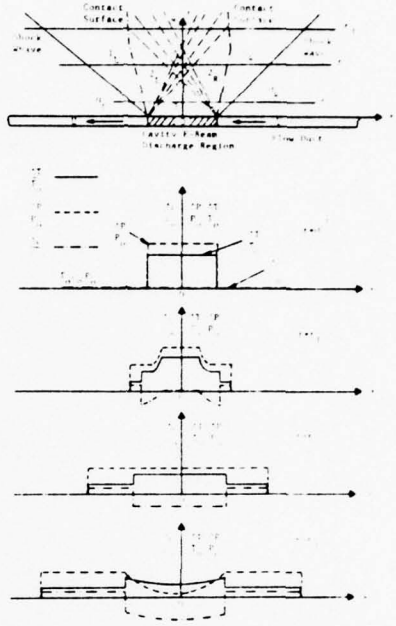

Fig. 3: Thermodynamic Property Variations Versus Space for Various Time Frames

δ^*: boundary layer displacement thickness

ℓ: boundary layer characteristic length

C_f: skin-friction coefficient

u_∞: average flow velocity in the cavity

M_∞: Mach number in the cavity

Δu_∞: rms longitudinal turbulent velocity fluctuation

$$\left(\frac{\Delta\rho}{\rho}\right)_{\substack{\text{rms}\\ \text{Acoustics}}} \sim \frac{1}{\gamma}\left(\frac{\Delta p}{p}\right) \frac{\gamma+1}{2+M_s^2(\gamma-1)} \quad \text{for shock waves} \tag{7}$$

$$\sim \frac{1}{\gamma}\left(\frac{\Delta p}{p}\right) \text{ for acoustic waves where } M_s = 1 \tag{8}$$

In order to attain the beam quality required, the total $(\Delta\rho/\rho)_{\text{rms}}$ must meet the criteria of 10^{-5} for KrF and XeF in Argon and 10^{-4} for TEA discharges in Helium and HgCl in Argon, respectively. Technical challenges are evident in the methodology for gas dynamic and acoustic management of these medium homogeneity problems.

From the quantitative viewpoint of excessive energies remaining in the flow system to be managed, they can be represented by the following equation derived from the energy balance and thermodynamic relationships of the flow system:

$$A_e = [(1 + R_e) - (1 + R_e)^{1/\gamma}] \quad : \text{Acoustic Energy Ratio} \tag{9}$$

where

$$A_e = \frac{E_a}{E_o}, \qquad R_e = \frac{E_{in} - E_L}{E_o} \quad : \text{Remaining Energy Ratio}$$

E_a: Acoustic energy to be managed

E_o: Energy of the baseline flow, $E_o = C_v T_o$

E_{in}: Pulsed energy input

E_L: Lasing energy output

γ: Specific heat ratio

The above relationship is graphically presented in Figure 4 for various γ. For the VWL of interest, the above Equation 4 is modified in dimensional form with the given γ of 1.67 and presented in Figure 5 with energy input in Joule/litre versus acoustic energy efficiency, E_a/E_{in} in percent for a range of energy input peculiar to the VWL[9].

Magnitudes of the remaining energies which must be managed are known to be about 90% of the total energy input while about 10% of the energy becomes lased energy output from the cavity. Figure 5 shows that the acoustic energy is about 40% of the input energy. The remaining is the thermal energy which must be removed by heat exchangers.

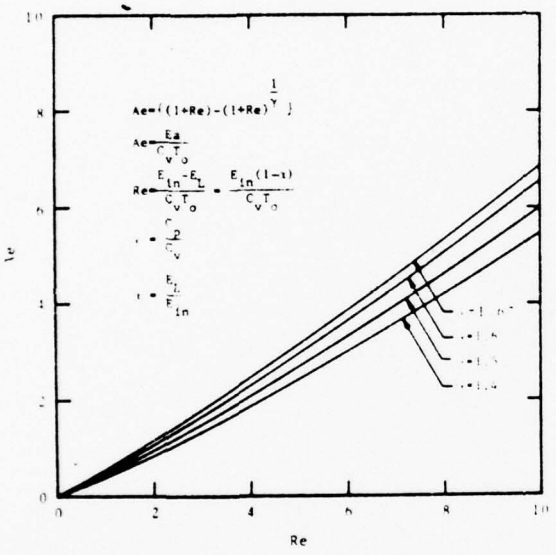

Fig. 4: Acoustic Energy Ratio Versus Remaining Energy Ratio for Various Specific Heat Ratios

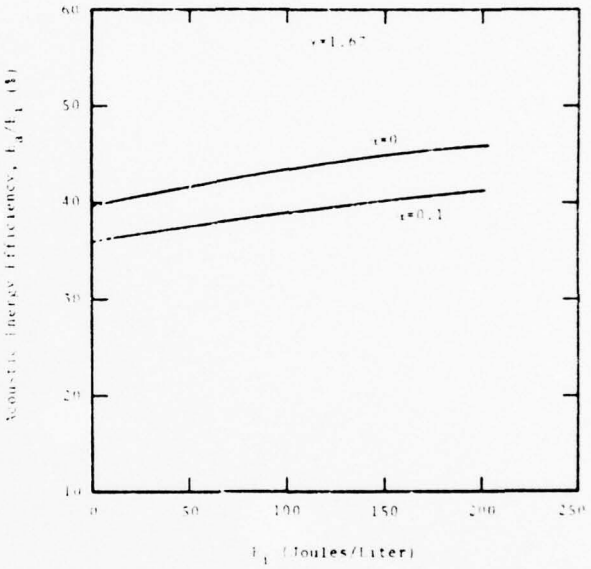

Fig. 5: Acoustic Energy Efficiency Versus Input Energy for VWL Gases

Methodology of Gas Dynamics and Acoustic Management

Since the main sources of inhomogeneity are originated from the turbulence, temperature fluctuation, and pressure waves, consideration of respective solution approaches to various sources will be given as follows:

Turbulence

Effects of free stream turbulence on $\Delta p/p$ may be approximated by Equation 5:

$$\frac{\Delta p}{p} \approx \tfrac{1}{2} M_\infty^2 \left(\frac{\Delta u}{u_\infty}\right)^2_{rms}$$

The velocity fluctuation, $\left(\frac{\Delta u}{u_\infty}\right)_{rms}$, can be considerably reduced by suppressing turbulence upstream of the laser cavity. The technique to suppress the turbulence has been well developed and proven effective particularly in the wind tunnel practice. Use of damping screens suggested by Dryden [10] has been accepted as an effective method of turbulence suppression. Without application of any turbulence management system,

velocity fluctuations in a closed cycle circulator could be at least 10% at a Mach number around 0.5. With the use of properly designed contracting entrance to the cavity, and correctly sized screen packs, a sophisticated turbulence management system could suppress the turbulence down to the level below 0.1%. For $M_\infty = 0.5$, $\Delta\rho/\rho$ can be lowered to 0.125×10^{-8} with some moderate effort in this problem area.

Another source of turbulence exists in the boundary layers on the mirrors, their protective windows and cavity walls. Since the Reynolds number of the flow in the cavity region is determined to be above 10^7, using $M_\infty = 0.5$, the boundary layer is definitely turbulent. Numerous experiments on turbulent boundary layers have confirmed that density fluctuations caused by boundary layer turbulence or eddies are larger than those due to freestream turbulence. A simplified expression of the relationship is given by Equation 6:

$$\frac{\Delta\rho}{\rho} \approx C_f M_\infty^2 \frac{\delta^*}{\ell}$$

Since $C_f\delta^* = f(N_{RX}, X)$ where N_{RX} denotes the Reynolds number along the boundary layer, $N_{RX} = \frac{UX}{\gamma}$, X the space coordinate along the flow direction. A coarse estimate of $\Delta\rho/\rho$ based on the value of C_f from Schlichting[11] for $M_\infty = 0.5$ and $N_{RX} = 10^7$ becomes

$$\frac{\Delta\rho}{\rho} \approx 0.5 \times 10^{-5} \frac{X}{\ell} \tag{10}$$

Equation 10 indicates that if the distance X from the virtual origin of the boundary layer is less than twice the boundary layer characteristic length which is comparable to the layer thickness, the fractional density fluctuation can be kept under control even for Argon flows. In practice, this can be accomplished by careful design of the cavity entrance or the application of boundary bleed along the cavity walls.

Temperature Fluctuations

The temperature rise in the heated slug of gas in the laser cavity after the pulsed energy input is expected to be about 30% of the original temperature for 100 Joules per liter of Ei and about 50% for Ei = 200 Joules per litre. Since the temperature of the baseline flow, T_o, is expected to be about 300^oK, the thermal energy added into the slug of gas does not exceed 200 Joules per litre. This amount of heat in the baseline flow even at $M_\infty = 0.5$ is easily manageable with efficient light weight heat exchangers.

As for the temperature fluctuations in the boundary layers at the mirrors, their protective windows, and the cavity walls, a preliminary study shows that the temperature at the boundary surface could rise not more than 10% for the boundary layer flow previously defined if $\Delta\rho/\rho$ is to be limited under 10^{-5}. Again cooling the boundary surfaces can be accomplished with the existing means. Detailed analysis of boundary layers should be deferred unless found necessary from the experimental measurements. The removal of input energy is a problem for the closed cycle type but is no concern for the open cycle flow system.

Pressure Waves

Pressure waves generated due to the pulsed energy input at the cavity in the flow system include shock waves and expansion waves. Realizing that propagation, reflection, transmission, and attenuation of these waves must be treated at least with nonlinear acoustic theory for the energy input range of 100 to 300 Joules per litre[9]; the concept and materials for the attenuator design should be based on the nonlinear acoustic consideration rather than the available linear acoustic theory and data.

First $\Delta\rho/\rho$ due to the shock wave is represented with the following equation for $\gamma = 1.67$, a typical diluent gas, and $M_s = 1.15$ for Ei = 200 Joules per liter and $\Delta\rho/\rho = 0.403$:

$$\frac{\Delta\rho}{\rho} = \frac{2(M_s^2 - 1)}{2 + M_s^2(\gamma - 1)} \tag{11}$$

Thus $\frac{\Delta\rho}{\rho}$ becomes 0.224 and obviously requires attenuation of a strong measure.

On the other hand, $\Delta\rho/\rho$ for acoustic waves under the isentropic process must be

$$\frac{\Delta P}{P} < k \frac{\Delta \rho}{\rho} \quad \text{required.}$$

Thus $\frac{\Delta P}{P}$ must be less than 1.67×10^{-5} in order that the medium homogeneity is acceptable.

Under these stringent requirements for acoustic management, an effort is currently in progress at the University of Alabama in Huntsville to develop reactive attenuators such as a muffler with exponential horns as shown in Figure 6. Attenuation characteristics of the muffler is presented in Figure 7 for frequency versus attenuated dB. It shows that this particular type of muffler design will be effective in the frequency range up to 1 KHZ and most effective in the 200 ~ 500 HZ.

There are many other reactive attenuators and sound absorbing materials for pressure damping or attenuation as reported in numerous literatures (12), (13), (14), (15), (16), and (17), however it is important that the attenuation characteristics with respect to the wave frequency must be carefully matched with the pressure waves generated in the laser flow systems so that the attenuation will be effective.

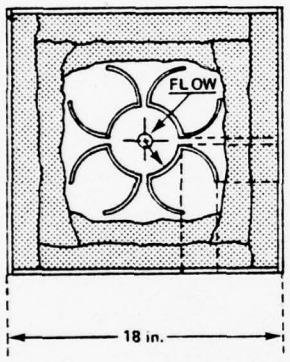

Fig. 6: Reactive Attenuator (Muffler)

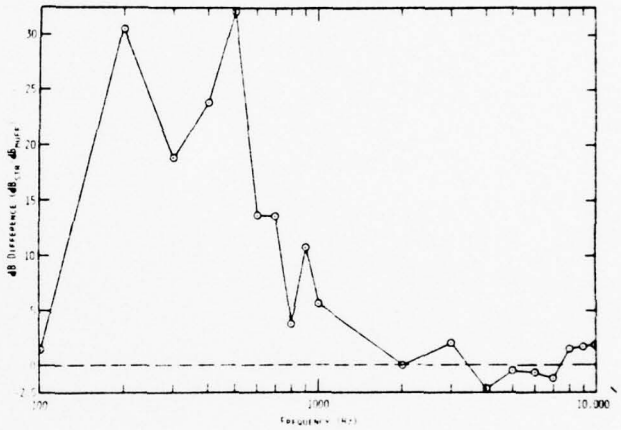

Fig. 7: Attenuation Characteristics in dB Versus Frequency of the Muffler

Consideration of Open Cycle and Closed Cycle Flow Systems

For delivering the laser gas suitably conditioned to meet homogeneity criteria at the cavity, a necessary flow system could be the open cycle or the closed cycle type. Choice of a system depends on various factors such as size and weight limitations, sources of gas supply, capabilities of gas dynamic and acoustic management, lasing energy output, and pulse rate restriction.

High energy laser technology has gained considerable advances in terms of experience, knowledge, design, and fabrication so far in the open cycle flow system for pulsed lasers through numerous projects such as ABEL, Humdinger, CCEBL, etc.; however, the closed cycle flow system or circulator has not been applied to high power pulse lasers extensively to the authors' knowledge, except the one being developed by the Army and being tested currently at Rocketdyne. Technical illustration and general view of the Army closed cycle gas recirculator are presented in Figures 8 and 9.

Comparative evaluation of the two systems is rather premature at this time due to its lack of sufficient data for analytical comparison; however, some of the significant comparative features of the two systems are noteworthy for system development considerations.

Open Cycle Flow System

a) No heat exchanger is required at downstream side of the cavity since the heated gas will be blown down into the ambient.

b) In the acoustic management, aside from proper application of resistive and reactive attenuators around the cavity, serious attention be given to the possible wave reflection of nonlinear nature at the system exit, which may be a serious management problem.

c) The weight and size of the total system including the gas supply may be less flexible for optimization.

d) The duration of operation may be limited by the size of gas supply.

e) The potential for higher repetitive pulse rate exists.

f) Reconditioning or repurification of the gas is not required.

Closed Cycle Flow System

a) Economy in gas consumption and supply is evident.
b) Gas dynamic management of the laser gas in terms of reconditioning to desirable temperature, pressure, velocity, and turbulence is a challenging task requiring additional heat exchangers.
c) Repurification of the gas may be required in some system depending on the rate of degradation and thermal environment.
d) Acoustic management of the pressure waves is as difficult as that of the open cycle type, but it lacks the concern for the wave reflection from the exit.
e) Optimization of the system weight and size is more promising.
f) The pulse rate may be less flexible for increase.

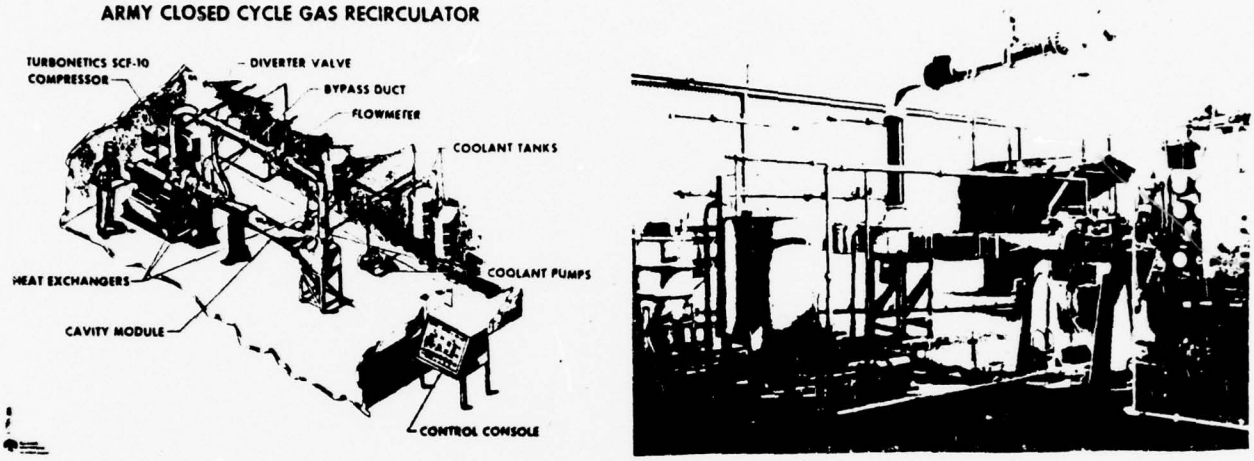

Fig. 8 and 9: Technical Illustration and General View

References

1. Pugh, E. R.; Wallace, J.; Jacob, J. H.; Northam, D. B.; and Daugherty, J. D.: "Optical Quality of Pulsed Electron-Beam Sustained Lasers. Appl. Optics, Vol. 13, 1974, p. 251.

2. McAllister, G. L.; Draggoo, V. G.; and Eguchi, R. G.: "Acoustical Wave Effects on the Beam Quality of a High Energy CO Electric Discharge Laser. Appl. Optics, Vol. 14, 1975, p. 1290.

3. Culick, F. E. C.; Shen, P. I.; and Griffins, W. S.: "Acoustical Waves Formed in an Electric Discharge Co Laser Cavity. AIAA Paper No. 75-851, 1975.

4. Kast, S. and Cason, C.: "Performance Comparison of Pulsed Discharge and E-Beam Controlled CO_2 Lasers J. Appl. Phys., Vol. 44, 1973, p. 1631.

5. Basov, N. G.; Danilychev, V. A.; et al.: "Maximum Output Energy of an Electron-Beam-Controlled CO_2 Laser. Sov. J. Quantum Electronics, Vol. 4, 1975, p. 1414.

6. Holmes, D. A. and Avizonis, P. V.: "Approximate Optical Systems Model," Appl. Opt., Vol. 15, No. 4, pp. 1075-1082, 1976.

7. Siegman, A. E., "Effects of Small-Scale Phase Perturbations on Laser Oscillator Beam Quality," IEEE J. Quantum Electron, Vol. QE-13, No. 5, pp. 334-337, 1977.

8. Shih, C. C. and Karr, G. R.: "Investigation of Transient Flow and Heating Problems Characteristic of High Energy Laser Gas Circulation Systems," UAH Research Report No. 199 (H-CR-77-9), March, 1977.

9. Cason, C. and Horton, T. E.: "Thermal-Acoustical Phenomena in Pulsed High Energy Lasers," ASME (78-HT-61), to be presented in May, 1978, at 2nd. AIAA/ASME Thermophysics and Heat Transfer Conference.

10. Dryden, H. L. and Schubauer, G. B.: "The Use of Damping Screens for the Reduction of Wind-Tunnel Turbulence," J. Aero. Sciences, pp. 221, Vol. 14, No. 4, April, 1947.

11. Schlichting, H.: Boundary Layer Theory, McGraw-Hill Co., 1968.

12. Kesselring, R. C. and Nestlerode, J. A.: "Pressure Damping for Pulsed Electric Discharge Laser," Final Report, AFWL-TR-75-170, Air Force Weapons Lab., Kirtland, AFB, New Mexico, July, 1975.

13. Horton, T. E., and Wylie, K. E.: "Acoustical Problems in High Energy E-Beam Lasers," pp. 963-975, Advances in Eng. Sciences, Vol. 3, NASA CP-2001, Nov., 1976.

14. McMillion, R. L. and Nestlerode, J. A.: "Design Criterion for Acoustic Absorbers," 8th JANNAF Combustion Meeting CPIA Publication, Nov.,1971.

15. Ingard, U. and Bolt, R. H., "Absorption Characteristics of Acoustic Material with Perforated Facings," J. Acoust. Soc. Amer. 23, 5, pp. 533-540, Sept., 1951.

16. Rice, E. J., "Propagation of Waves in an Acoustically Lined Duct with a Mean Flow," NASA SP 207, p. 345.

17. Mechel, F. and Schilz, W: "Research on Sound Propagation in Sound-Absorbent Ducts with Superimposed Air Streams," Tech. Report AMRL-TDR-62-140 (I-IV), Dec.,1962, Air Force Systems Command, Wright-Patterson AFB, Ohio.

Section 2
Presented at International Symposium on Nonlinear Acoustics, Paris, France, July 3-6,1978

INVESTIGATION AND MANAGEMENT OF ACOUSTICAL WAVES IN CLOSED CYCLE HIGH ENERGY PULSED LASERS

G. R. Karr and C. C. Shih
The University of Alabama in Huntsville
Huntsville, Alabama 35807

and

Charles Cason and A. H. Werkheiser
U. S. Army Missile Research and Development Command
Redstone Arsenal, Alabama 35809

Abstract

To investigate the acoustic problems in high energy, closed cycle, pulsed lasers, a closed cycle system was fabricated and attached to an existing E-beam controlled single pulse laser system. Electrical energy was input to one atm. flowing gas mixture typical of that required by CO_2 and excimer lasers. A frequency power spectrum of the produced acoustic pulse was measured and compared with the frequency power spectrum of acoustic energy transmitted and reflected by the muffler. The results showed the muffler attenuated the input wave nearly 40 db at near 500 Hz and 12 db at 5000 Hz.

Resumé

En vue d'étudier les problémes acoustiques dans les lasers pulsés à haute energie opérant en cycle fermé, un system à cycle fermé a été construit et rattaché à un laser opérant en pulse unique et contrôlé par un faisceau électronique. L'énergie électrique a été appliquée à un flow de mélange gazeux typique de celui exigé par les lasers CO_2 et excimer. Le spectre de puissance de l'impulsion acoustique produite a été mesuré et comparé avec le spectre de puissance de l'énergie acoustique transmise et réfléchie par le déflecteur. Les résultats montrent que le déflecteur atténue l'onde d'entrée par prés de 40 db autour de 500 Hz et par prés de 12 db autour de 5000 Hz.

Introduction

The energy input into the cavity of a pulsed high energy gas laser causes shock waves and expansion waves which propagate away from the cavity and interact with system components.[1,2,3] This acoustical energy, if unmanaged, will interact with gas in the cavity, thereby seriously degrading the output laser beam quality. The work reported here describes experiments which identify the nature of the acoustic environment and the effectiveness of acoustic control devices in managing acoustic waves.

The sequence of operation of a pulsed high energy gas laser consists of (1) the laser gas media flows into the cavity region; (2) energy is deposited in the gas at a magnitude of 10^2 - 10^3 J/ℓ in a total time of magnitude 10^{-6}s; (3) shock waves and expansion waves travel throughout the system at speeds of magnitude 10^3 m/s; (4) the process is repeated as soon as new gas lasing media flows into the cavity. An experimental program was initiated to investigate the nature of the acoustic energy put into the laser gas and devices were tested which were designed to remove these disturbances from the system.

Description of Experiment

Experiments were performed employing a high energy laser of the e-beam electric discharge type having the capability of depositing energy of the order 100-1000 J/ℓ in a single pulse of order 10^{-6} s duration. No attempt was made to extract laser power from the system and net power input to the gas was assumed to equal the electrical input to the cavity.

A closed cycle recirculating system was attached to the laser to move gas through the cavity region at a speed of about 3 m/s. Pressure transducers capable of following the pressure rise associated with shock waves were placed at four locations in the recirculation system. The simultaneous output of all four transducers were recorded on photographs of the four traces made on an oscilloscope.[1]

The recirculating system had provision for introducing acoustic management devices into the recirculator flow. Devices employed included honeycomb structures, screens, and a muffler designed to extract the acoustic energy without introducing a pressure drop in the flow. Since only the muffler proved effective in the tests performed, the muffler design and test results will be discussed in the following section.

Muffler Design

The acoustic wave produced by the laser input is represented approximately as a square wave pressure pulse. Since the square wave can be approximated by an infinite series of sine and cosine waves, a muffler must be able to attenuate waves over a wide band in frequency in order to be effective. An additional requirement for the muffler is that it present a low pressure loss to the flow of gas since energy must be expended to counter any pressure drop. In order to satisfy the two major requirements of the muffler, a horn coupled resonator was designed and built. The resonator volume is placed outside the flow field so that interference with the main flow is avoided. An exponential horn is used to couple the resonator volume to the flow since this horn design has the potential to act as a high pass filter. The muffler design is shown in Figure 1.

Results

The pressure records were analyzed to find the nature of the acoustic energy produced by the laser pulse and to determine the effectiveness of the muffler in removing the acoustic disturbance. By analyzing the record from two probes mounted a known distance apart, the traveling acoustic wave could be accurately determined. This wave was examined for its frequency content and the results of the power spectral analysis of the laser produced acoustic wave is shown in Figure 2. The results show

that the energy peaks in the 5000 Hz range with a sharp drop off on both sides.

The pressure records were examined to find the effectiveness of the muffler by examining the power spectrum of the wave leaving the muffler. The results of the muffler effectiveness is given in Figure 3 which shows that the muffler attenuated the input wave nearly 40 db at near 500 Hz and 12 db at 5000 Hz. The muffler is found to be effective and to present no measurable pressure drop for the main flow due to the straight pipe design.

References

1. Cornelius C. Shih and Gerald R. Karr, "Investigation of Transient Flow and Heating Problems Characteristic of High Energy Laser Gas Circulation Systems," UAH Research Report No. 199, March 1977.
2. C. Cason and T. E. Horton, "Thermal-Acoustical Phenomena in Pulsed High Energy Lasers," AIAA/ASME (78-HT-61), May 1978.
3. Cornelius C. Shih and Charles M. Cason, "Gas Dynamic and Acoustic Management for Visible Wavelength Lasers," SPIE Technical Symposium East '78, Washington, D. C., March 1978.

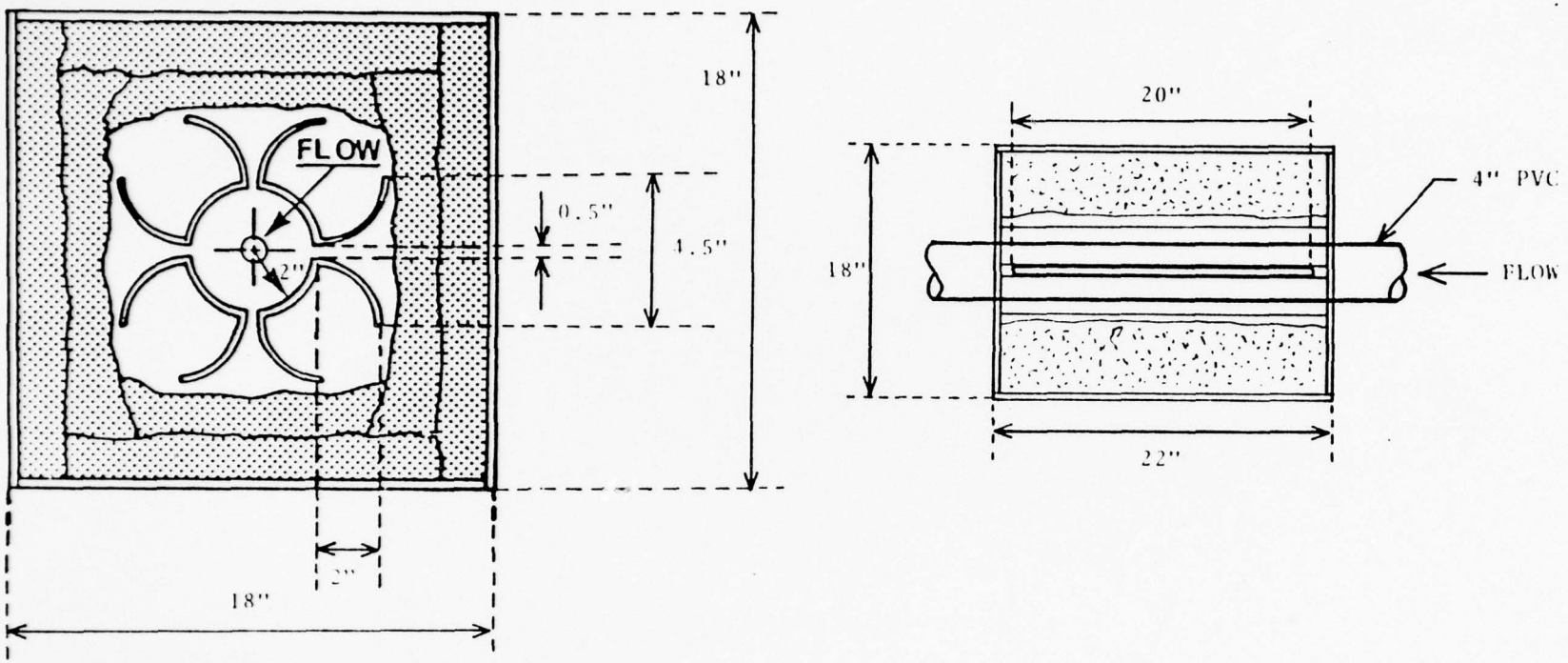

FIGURE 1. MUFFLER DESIGN

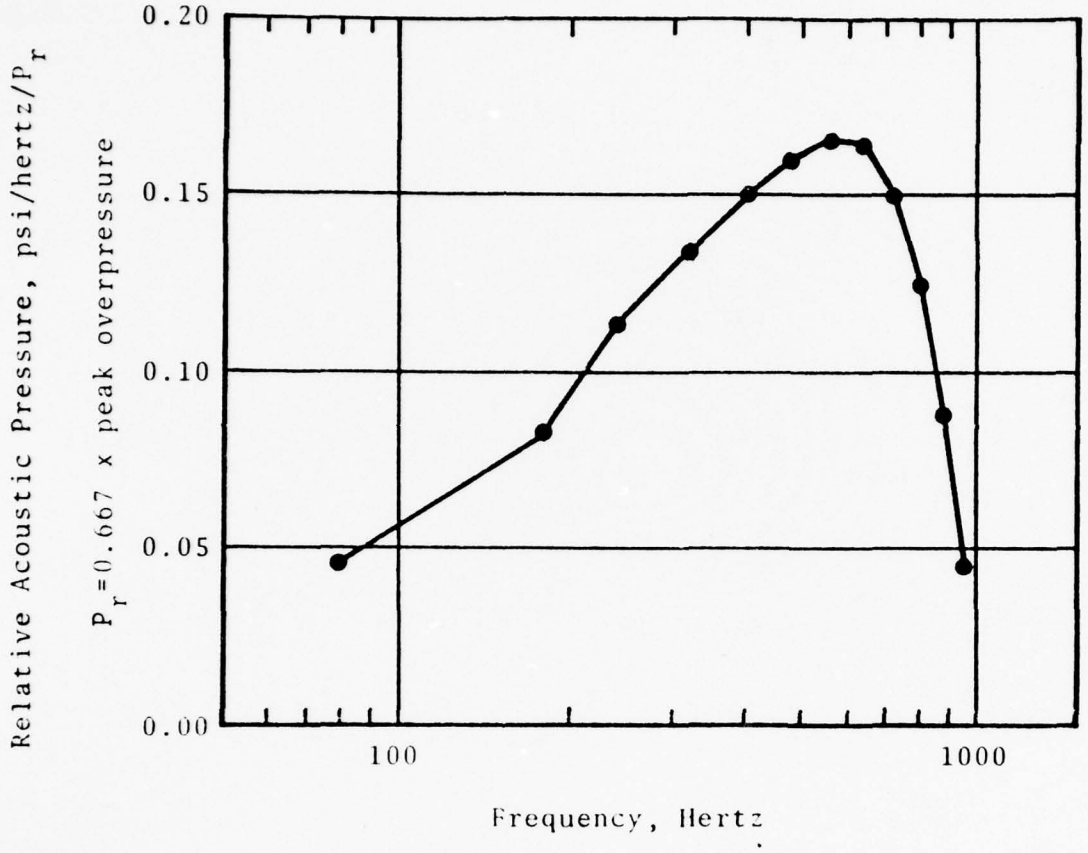

FIGURE 2. ACOUSTIC PRESSURE SPECTRUM RESULTING FROM LASER FIRINGS.

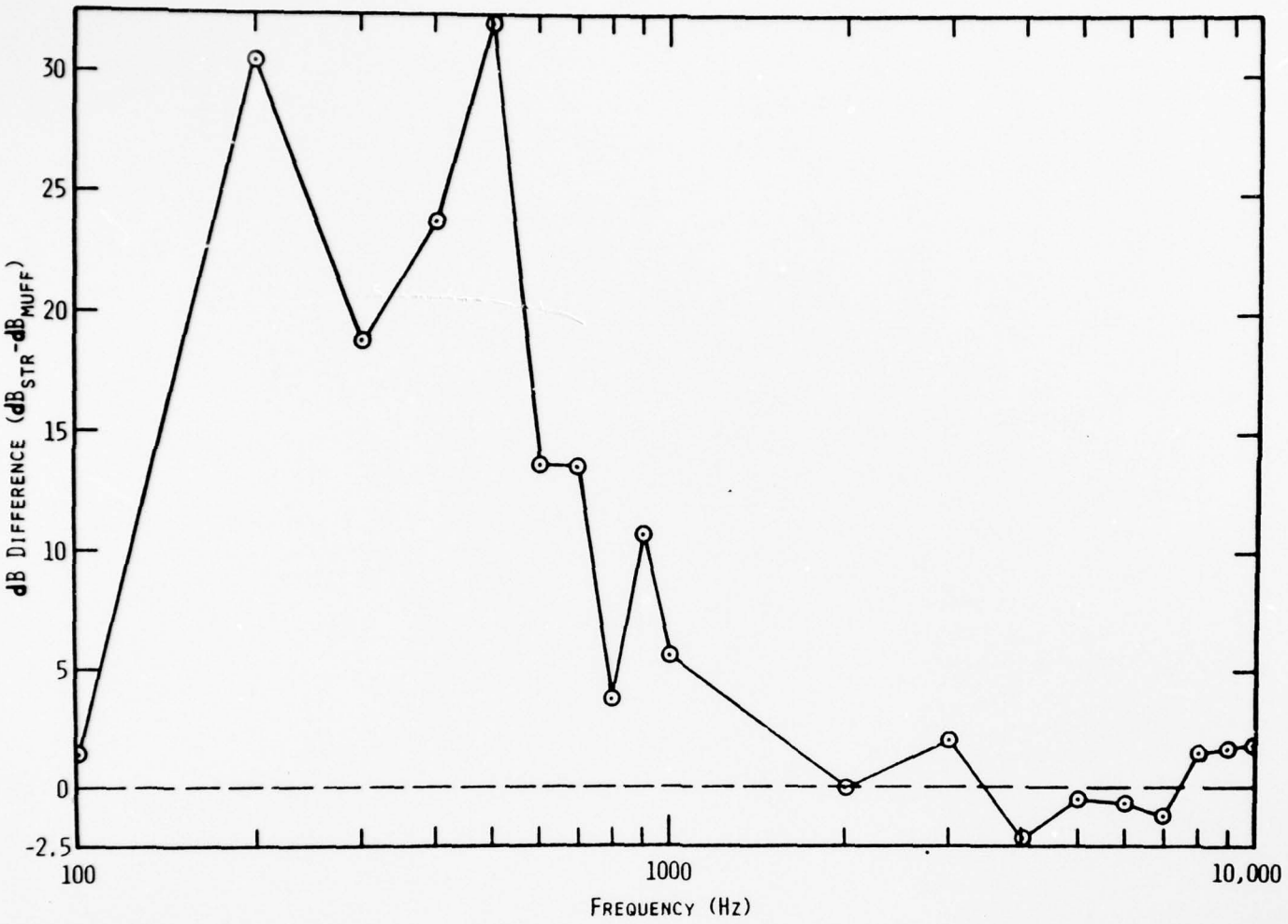

Figure 3. Results of Muffler Attenuation Showing Input Wave at 40 db near 500 Hz and 12 db at 5000 Hz.

AD-A068 547 ALABAMA UNIV IN HUNTSVILLE SCHOOL OF SCIENCE AND ENG--ETC F/G 20/5
INVESTIGATION OF TRANSIENT FLOW AND HEATING PROBLEMS CHARACTERI--ETC(U)
MAR 79 C C SHIH, G R KARR, J F PERKINS DAAK40-77-C-0161
UNCLASSIFIED UAH-RR-219 DRCPM-HEL-CR-79-8 NL

2 OF 4
AD
A068547

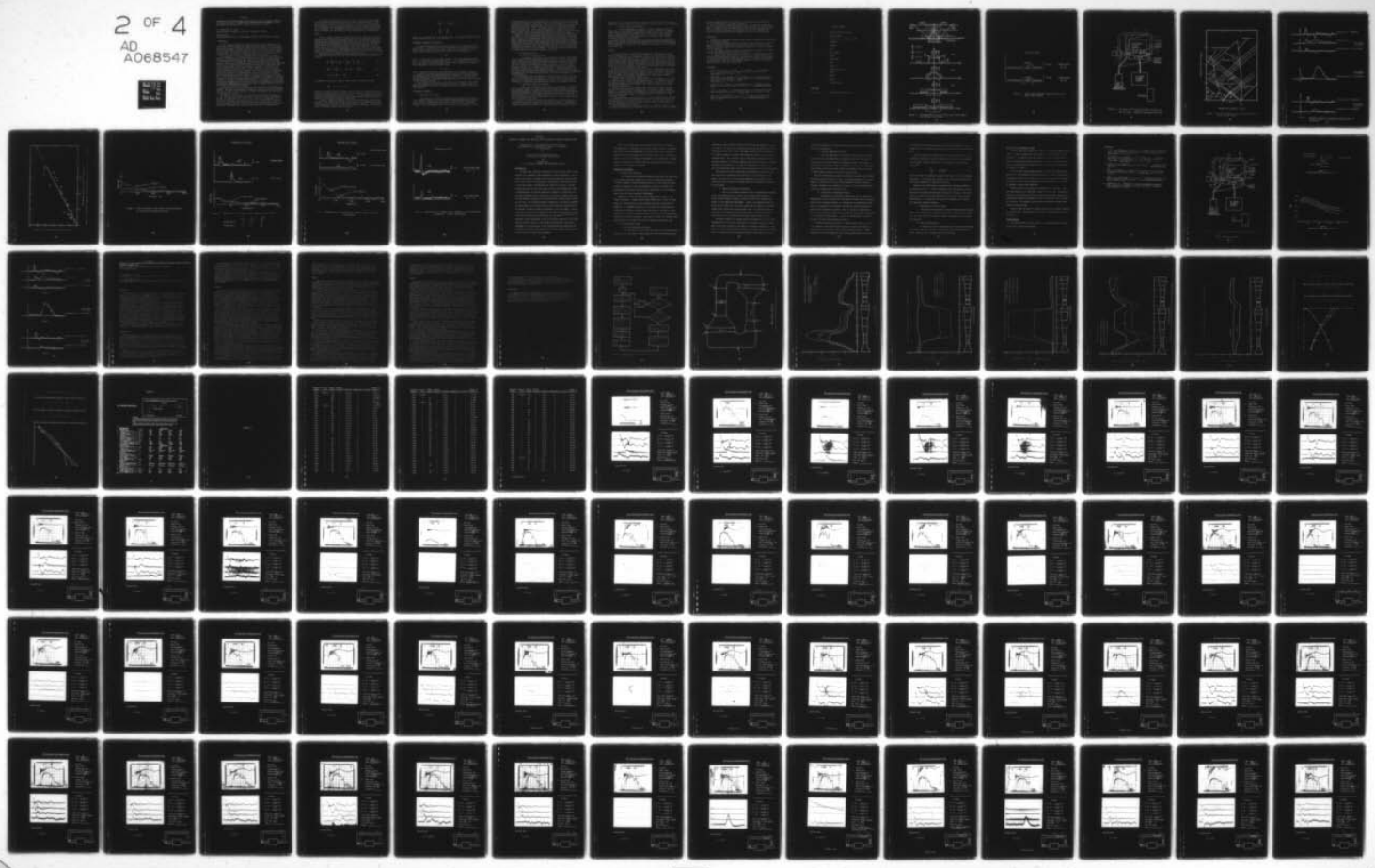

Section 3

Presented at the Joint Meeting of the Acoustical Society of America (ASA) and the Acoustical Society of Japan (ASJ) in Honolulu Nov. 28-December 1, 1978

NON-LINEAR WAVE PROPAGATIONS IN A PULSED HIGH ENERGY GAS LASER

C. C. SHIH AND G. R. KARR
The University of Alabama in Huntsville, Huntsville, Alabama

CHARLES CASON
US Army Missile Research and Development Command, Redstone Arsenal, Alabama

INTRODUCTION

In the recent development of pulsed high energy lasers, problems of non-linear waves of both acoustic and thermal nature propagating in the laser gas media have attracted considerable research interest because of their effects on the fractional density gradient which, in turn, relates to the optical quality of laser beams. One of these lasers uses a closed cycle circulator to provide an acoustically and thermally conditioned flow of the laser gas suitable for lasing at the laser cavity on a continuous basis of operation.

The closed cycle circulator consists of a compressor, heat exchangers, acoustic attenuators, flow regulator and diverter, ducting, control and instrumentation systems along with a laser cavity for the purpose of maintaining a recirculating flow of the laser gas. Reconditioning the laser gas with gas dynamic, acoustic and thermodynamic means is necessitated by the abrupt deposition of energy at a repetitive rate in the recirculating flow of laser gas at the cavity, causing severe spacial and temporal variations of fluid and thermal characteristics throughout the flow. These variations are results of shock waves and expansion waves which propagate away from the cavity, following the e-beam controlled pulsed energy discharge. The transient pressure, temperature, and velocity gradients are responsible for producing acoustical and thermal perturbations which are directly related to density fluctuations of the laser media. Optical beam quality is known to be degraded by the density fluctuations as noted by previous investigations particularly for CO_2 lasers[1-5]. Efficient operation of the laser requires serious attention to gas dynamic, thermodynamic, and acoustic management of the laser media in the recirculating flow system based on meaningful measurements and analysis of fluid and thermal characteristics of the flow in the pulsed laser operation.

A study has been made to determine the characteristics and propagation of the waves generated by the input power pulse characteristic of high energy laser systems. The study has consisted of an analytic prediction based on one-dimensional flow theory and are also used to study the propagation and interaction of the waves with the system.

The sequence of operation of a pulsed high energy gas laser consists of (1) the laser gas media flows in the cavity region; (2) energy is deposited in the gas at a magnitude of 10^2 - 10^3 J/ℓ in a total time of magnitude 10^{-5} s; (3) lasing action and laser power extraction occur in total time of magnitude 10^{-6} s; (4) shock waves and expansion waves travel throughout the system at speeds of magnitude 10^3 m/s; (5) the process is repeated by the pulse repetition rate which is governed by the flow rate and time needed to dissipate waves.

The quality and magnitude of the laser output is governed by the quality of the flow present in the cavity just prior to the energy deposition. Thus, waves which were generated by the previous laser pulse must be dissipated so that the quality of the flow is not disturbed. The work reported here examines the initial shape of waves generated by the pulse and the changes of this wave as it propagates. This information will find application to the design of devices to dissipate the wave energy by linear and nonlinear wave interactions.

THEORY

Since the energy deposition in high energy lasers in much faster than the rate at which acoustic signals can travel typical cavity dimensions, the gas is considered to be stationary during the energy input. The net energy into the gas (total input energy minus the laser energy extracted) is then assumed to be represented by an instaneaneous, constant volume heating process. The energy deposition causes an instantaneous rise in pressure and temperature in the cavity region. The pressure discontinuity causes shock waves to propagate both upstream and downstream and corresponding expansion waves in towards the cavity center. The expansion waves pass through the cavity and interact with each other and with the hot cold gas interface left by the energy pulse.

These phenomena of nonlinear wave propagations imposed on the laser gas flow are approximately modeled with a set of one-dimensional unsteady equations as follows:

$$\frac{1}{\rho}\frac{\partial \rho}{\partial t} + \frac{u}{\rho}\frac{\partial \rho}{\partial x} + \frac{\partial u}{\partial x} + \frac{u}{A}\frac{\partial A}{\partial x} = 0 \qquad (1)$$

$$\frac{\partial u}{\partial t} + u\frac{\partial u}{\partial x} = -\frac{1}{\rho}\frac{\partial P}{\partial x} - \frac{f u|u|}{2D} \qquad (2)$$

$$ds = Cv\frac{dT}{T} - R\frac{d\rho}{\rho} \qquad (3)$$

and implicitly the rate of change of entropy may be a function as shown,

$$\frac{ds}{dt} = f(x, t, A, u, s) \qquad (4)$$

Numerically solving the above equations with the method of characteristics has yielded a one-dimensional description of the wave formation structure as shown on a time versus displacement plot given in Figure 1. One-dimensional unsteady gas dynamics is successfully employed to predict the pressures, temperatures, and velocities in the various regions of interaction.

A computer program was prepared to solve the one-dimensional unsteady flow equations. The program requires the initial pressure, P_0, temperature T_0, and velocity, U_0, of the gas and the net energy input to the gas, Q. This is sufficient information to find the pressure and temperature resulting for the energy input for constant volume heating as given by

$$\frac{P_1}{P_0} = \frac{Q}{\rho c_v T_o} + 1$$

$$\frac{T_1}{T_0} = \frac{P_1}{P_0}$$

where ρ is the density and c_v the specific heat. The computer program then obtains solutions for P_2, T_2, P_3, T_3, etc.

FUNDAMENTAL FREQUENCY DETERMINATION

The flow axis mode pressure waves are propagated from the generating excitation cavity. Fundamental flow axis mode frequencies of the waves are estimated to first order by the given cavity dimensions and propagation speed as shown in the following equation for an organ pipe open at both ends:

$$f = \frac{C}{2\ell}$$

where f fenotes the flow axial mode frequency, C the wave propagation speed, and ℓ the excitation dimension along the flow. The fundamental flow axis frequency can also be found approximately from the wave pressure trace recorded in one experiment, using the equation below,

$$f = \frac{1}{2\tau}$$

where τ represents the period of overall pressure rise as shown in Figure 2.

In order to perform a detailed frequency spectrum analysis of the waves, the method of Fourier Transform Analysis may be employed. A computer program for performing the Fourier Transform Analysis coupled with a A-D converter capable of providing a sufficiently high sampling rate, has been used to analyze the wave frequency spectrum.

Since the gas flow velocity in relatively small circulators is not negligible when compared to the acoustic wave speed, and the pressure probes are mounted stationary in the flow, a Doppler correction is required to the organ pipe equation,

EXPERIMENTAL APPARATUS

1. Closed Cycle Circulator

The closed cycle circulator designed and fabricated for this study is a 1-D simulation having a full scale flow axis dimension and a mirror optical axis. It uses a controlled pulsed discharge that is capable of delivering pulsed energy up to 500 Joules per liter in a single pulse of order 10^{-5} s duration. The instrumentation system for transient flow measurements of flow

axis characteristics may be determined at the preliminary level of the full size circulator development. Transverse frequency mode components will be very high in comparison to the flow axis modes. There was no attempt made to extract laser power from the system. Net power input to the gas was assumed to equal the electrical input to the cavity. The cavity region was tightly sealed in all but the flow direction. The cavity had dimensions of 11 cm x 11 cm in the planes perpendicular to the flow direction and a foil length of 45 cm in the flow direction, but e-beam spreading added an additional 10 cm to this length.

Components of this circulator shown schematically in Figure 3 are listed as follows: a blower (Dayton Model 4C108) with a 10 5/8 in. wheel driven by a electric motor of one horsepower operated at 3450 RPM; PVC piping of 4 in. diameter including 1 in. by-pass pipe; e-beam masks for containing the e-beam to within a specified region of the casity; cavity structures to box in the discharge region in the vertical and longitudinal directions; mufflers; reflectors, The blower is capable of producing flows with velocities up to about 100 ft/sec by adjusting the by-pass pipe. Figure 3 also shows the relative locations of instrumentation probes in section numbers. The e-beam system was manufactured by Systems Science and Software of Hayward, California.

2. Instrumentation System

a) Pressure Measuring Instrument

The pressure transient of up to 10 psi was sensed by the minigage (Kistler Quartz Pressure Sensor Model 201B5) which gives a direct, high level, voltage signal with less than 100 ohms output impedance and high frequency response of 50 KHz and low frequency response of 0.005 Hz. The sensor then converts the pressure into electrical voltage with bias of up to 11 $\pm$ 2 volts. The power required by the transducer to the readout equipment is transmitted through the coupler over a single inexpensive cable. This eliminates all of the inherent piezoelectric high impedance problems of electrical leakage, cable noise and signal attentuation and allows the transducers to be used in contaminated environments and with long and moving cables at low noise and without use of charge amplifiers.

The calibration of the transducers was performed at the factory, and the values of the calibration were noted to be, on the average for all probes, 50 mv per psi for the pressure measurement up to 10 psi. The calibration curve relating the voltage output and the pressure is noted to be linear to $\pm$ 0.5%.

b) Temperature Measuring Instrument

Due to the extremely transient nature of temperature variation in the recirculating flow as a result of the pulsed laser operation, a sensor of high frequency response in excess of 500 Hz is considered necessary for the temperature measurement. Search of an adequate sensor resulted in the selection of a hot-wire sensor made of 0.00015 in. diameter tungsten wire coated with platinum powdery film. The hot-wire sensor is connected to the Temperature and Switching Module (Thermo-Systems Model 1040) which is, in turn, connected to the power supply (Model 1031-10A).

The Module consists of a bridge circuit and amplifier in an open loop configuration so the hot-wire sensor which is ordinarily used as an anemometer probe can be switched to function as a resistance thermometer. Since there is a linear proportionality between the voltage output and the temperature, the

calibration can be simply performed by adjusting the zero and gain set potentiometers to a desired temperature range using the calibrate pots of two temperatures.

c) Velocity Measuring Instrument

For the measurement of velocities, hot-wire probes the same as those used for the temperature measurement is applied. The probe is connected to the constant temperature anemometer module (Model 1010A). The amplified output signal from the anemometer is sent to the Linearizer (Model 1005B) so that the voltage signal is processed in such a way that it became linearly related to velocity of the gas flow.

The use of these modules ensures the frequency response above 500 KHz with power output as high as 1.5 amps. The noise associated with the anemometer is noted to be less than 0.007% equivalent turbulent intensity. Frequency response to the Linearizer is found to be up to 400 KHz and the accuracy of linearization can reach $\pm$ 0.2%.

RESULTS

The wave structure expected from one-dimensional unsteady flow theory is shown in Figures 1 and 4. The shock wave travels at a Mach number of between 1.1 to 1.5 causing pressure, temperature, density, and velocity rises which are a function of the input energy level. The quantities remain constant until reduced by the expansion wave which has traveled from the outer edge of the cavity. They then again remain constant until reduced by other expansion waves which criss-cross the cavity region. The quantities and the times at which the waves arrive at a point are predicted based on the one-dimensional theory, dimensions of the davity, and the location of the probe.

Figure 5 shows the recorded outputs of pressure, temperature, and velocity probes at various sections in the circulator for a typical firing. The first gauge which is closest to the cavity region is seen to record the expected wave form with sharply defined shock and expansion wave signals. The output of the other two probes show, however, that the wave structure changes to simply a sharp pressure rise followed by a smooth decay.

Figure 6 shows a plot of the results obtained for the pressure rise across the shock wave as a function of input energy density. Also shown is a plot of the results obtained from the one-dimensional computer program. The results show general agreement with the theory. One source of error is due to non-uniform energy deposition.

Figure 7 shows traces of pressure waves measured at position 7, Figure 3, for two levels of power input, 54 and 34 J/ℓ, respectively. Wave frequency spectra of the two waves are also presented as a result of Fourier Transform Analysis. A slight increase in the frequency at higher harmonics was noted due to the decrease in power input. Nonlinear effects are not apparent at the fundamental frequency.

Figure 8 presents pressure wave traces of a wave passing through a 90^{o} bend in the circulator. The wave forms before and after the bend are distinctively altered mostly in the frequency spectra. The wave after the bend seems to reduce its fundamental frequency from about 280 Hz to 230 Hz. No effects are noted at the fundamental frequency.

Figure 9 delineates the attenuation effects of a muffler. Results of the frequency spectrum analysis demonstrate that the muffler is effective in reducing

the wave pressure amplitude by 19 dB in 5.5 flow diameters and changing the frequency distribution at the higher harmonics.

Figure 10 presents temperature traces of the thermal pulse passing (see Figure 1) through a resistive attenuator (Ceramic honeycomb) of 10 cm in thickness. It shows the heat absorbing nature of the honeycomb, signifying that the resistive acoustic attenuator may be used as a heat sink at the same time. Forty cm of material was found to eliminate all traces of the thermal wave.

CONCLUSIONS

Based on the preliminary results of this study, some qualitative conclusions may be deduced as follows:

a) Nonlinear characteristics of the acoustic waves for excimer levels of input energy are best seen in the frequency distribution of acoustic energy changes in the high harmonics due to the wave propagation in the duct, through bends and mufflers.

b) Only minor changes are found in the fundamental frequency due to form changes and propagation effects in the circulator.

c) Most of the energy is found to be stored in the fundamental frequency.

d) Design of the attenuators for closed cycle circulators should be effective and conservatively based when the fundamental flow axis mode frequency is used and linear acoustic methods are applied. Low pressure loss structures providing about a 40 dB one way attenuation should be effective at relatively high repetitively pulse rate applications.

REFERENCES

1. Pugh, E. R.; Wallace, J.; Jacob, J. II.; Northam, D. B.; and Daugherty, J. D.: "Optical Quality of pulsed Electron Beam Sustained Lasers." Appl. Optics, Vol. 13, 1974, p. 251.

2. McAllister, G. L.; Draggoo, V. G.; and Egushi, R. G.: "Acoustical Wave Effects on the Beam Quality of a High Energy CO Electric Discharge Laser." Appl. Optics, Vol. 14, 1975, p. 1290.

3. Culick, E. E. C.; Shen, P. I.; and Griffins, W. S.: "Acoustical Waves Formed in an Electric Discharge CO Laser Cavity," AIAA Paper No. 75-851, 1975.

4. Kast, S. and Cason, C.: "Performance Comparison of Pulsed Discharge and E-beam Controlled CO_2 Lasers." J. Appl. Phys., Vol. 44, 1973, p. 1631.

5. Basov, N. G.; Danilychev, V. A.; et al.: "Maximum Output Energy of an Electron-Beam-Controlled CO_2 Laser." Sov. J. Quantum Electronics, Vol. 4, 1975, p. 1414.

LIST OF SYMBOLS

A	area of flow cross section
C	speed of sound
Cv	specific heat at constant volume
f	frequency
P	pressure
Q	heat
R	gas constant
s	entropy
T	temperature
t	time
u	velocity
x	length in flow axis
ℓ	length
ρ	density
τ	period
δ	friction factor

Subscripts

0, 1, 2, 3 ...	regions in the flow field

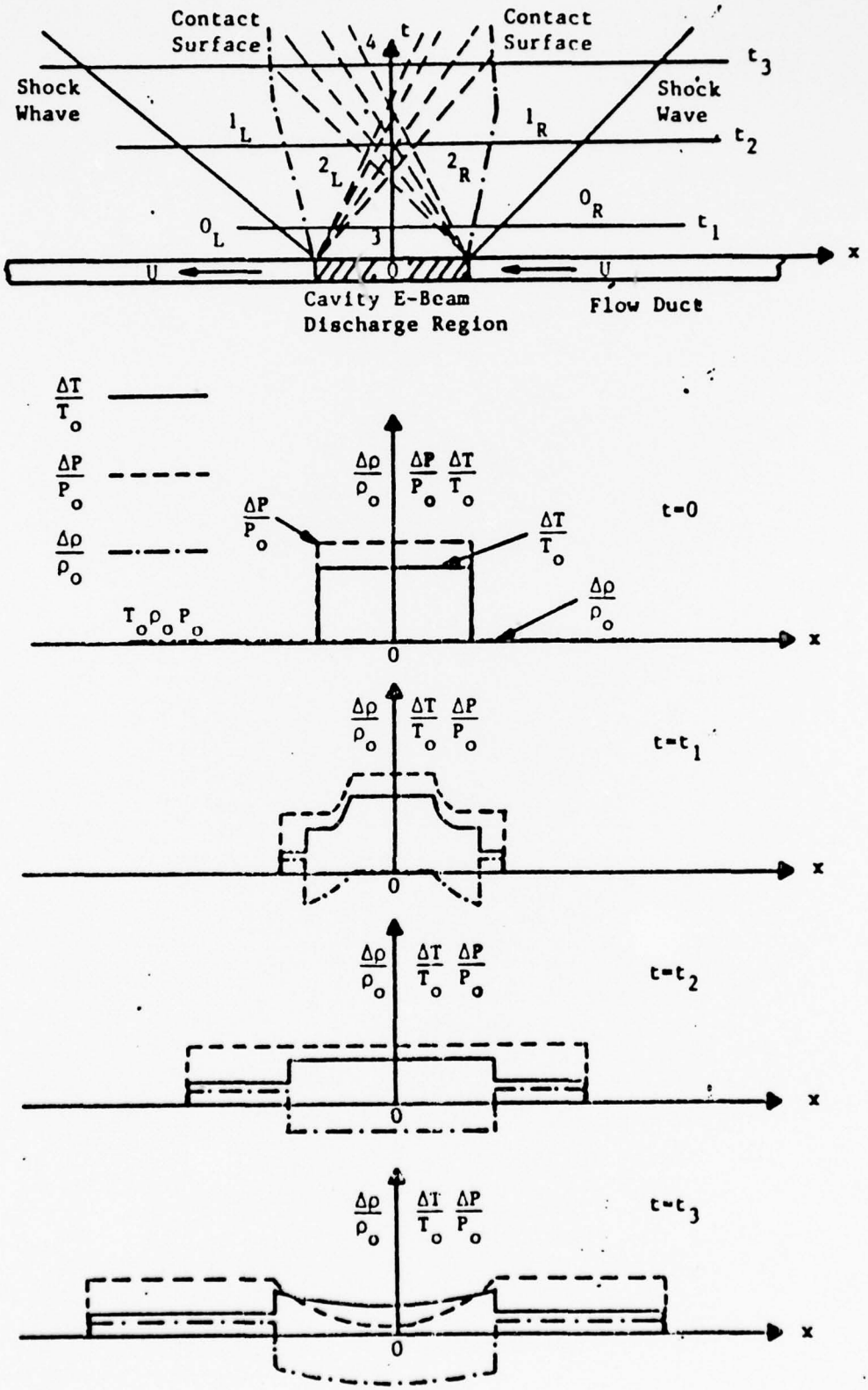

Figure 1. Thermodynamic Property Variations Versus Space for Various Time Frames.

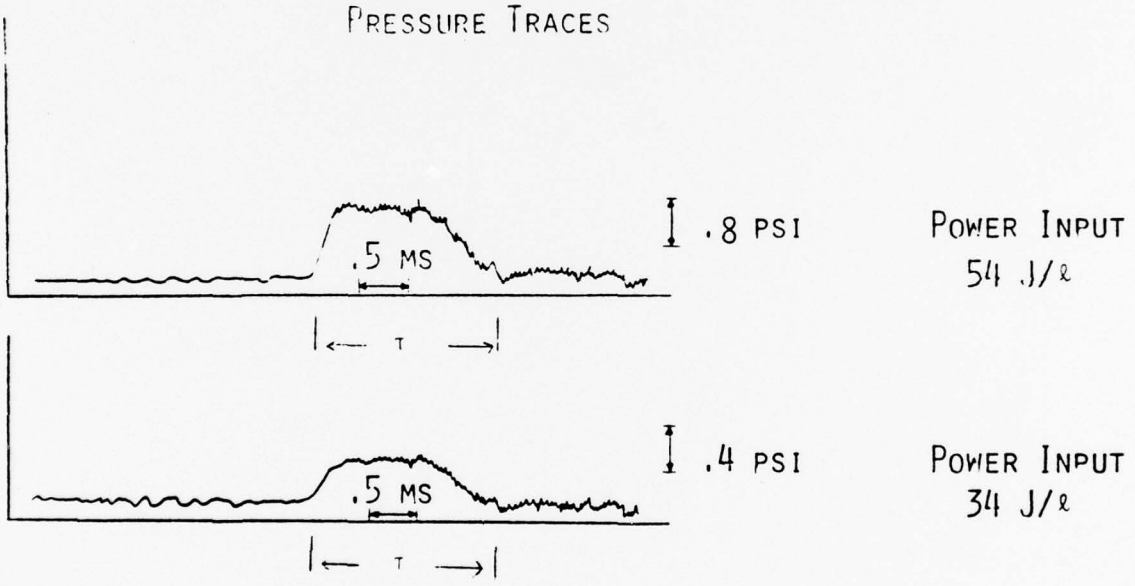

Figure 2. SHOCK WAVE PRESSURE TRACE FOR TWO CAVITY POWER INPUT LEVELS.

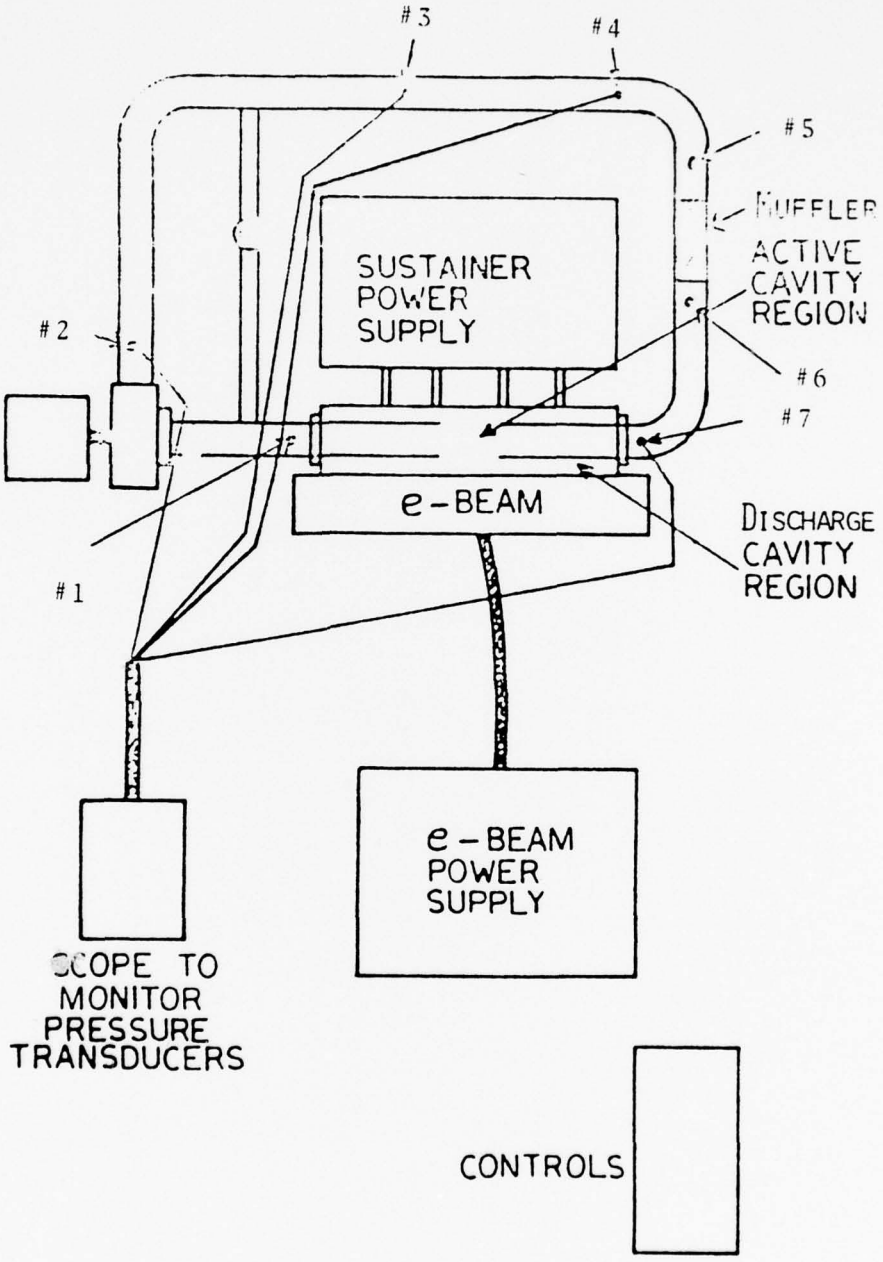

FIGURE 3. TOP VIEW OF PVC SUBSCALE MODEL ATTACHED TO THE S^3 LASER. SYMBOL # INDICATES SECTIONS.

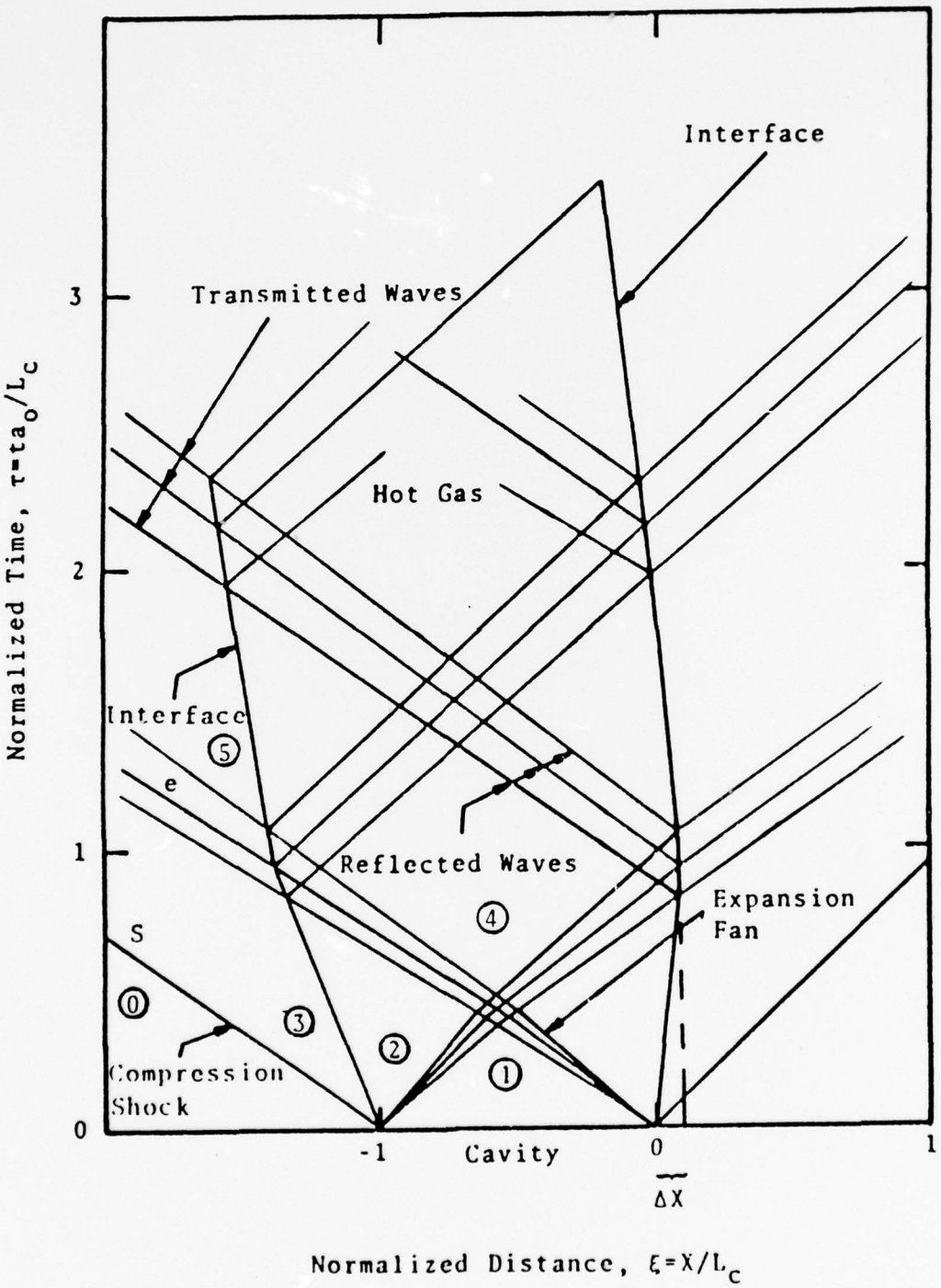

Figure 4. Weight Propagation and Interaction Due to Pulsed Energy Input.

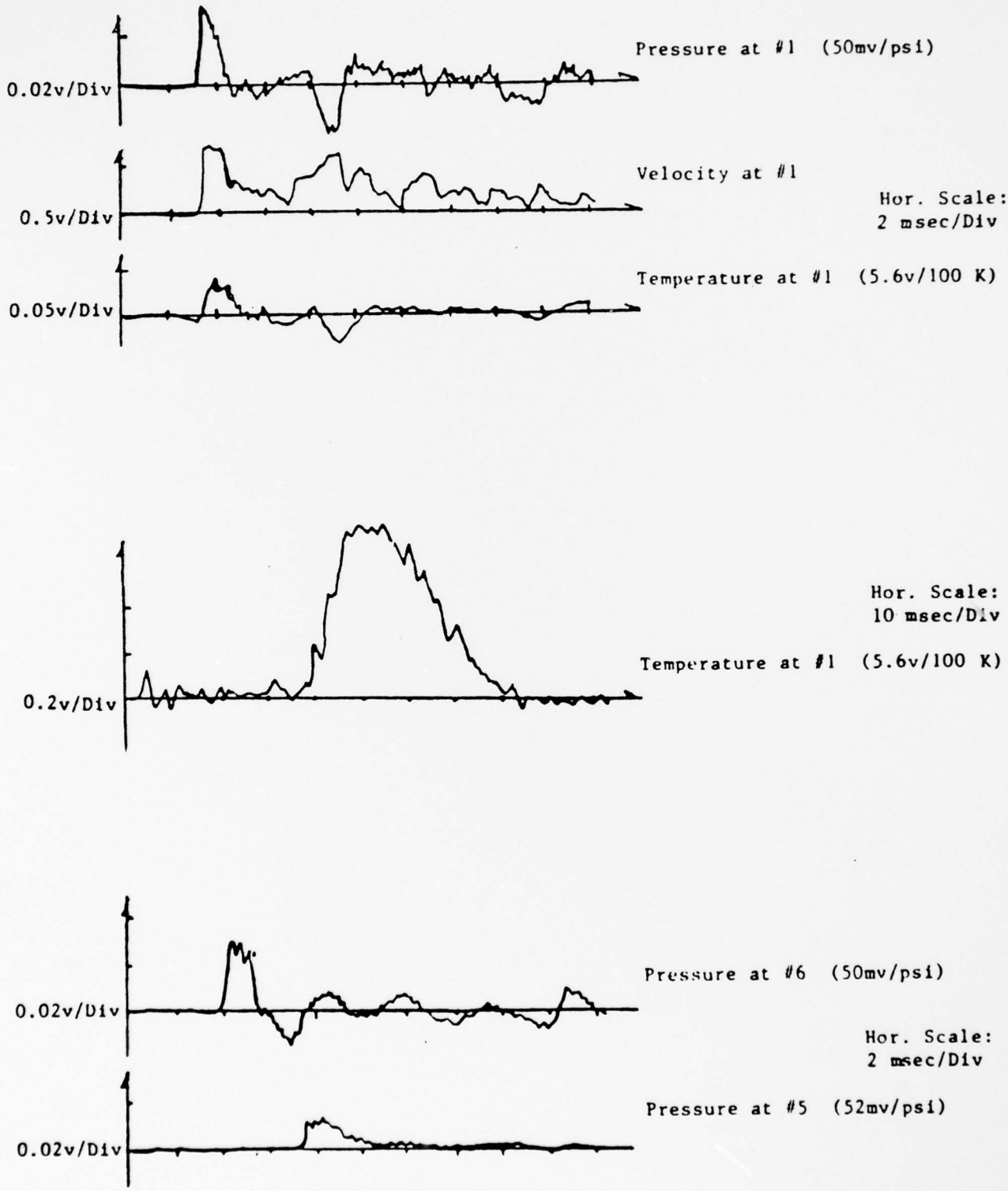

FIGURE 5. RECORDED OUTPUTS OF PRESSURE, TEMPERATURE, AND VELOCITY PROBES AT VARIOUS SECTIONS IN THE CIRCULATOR.

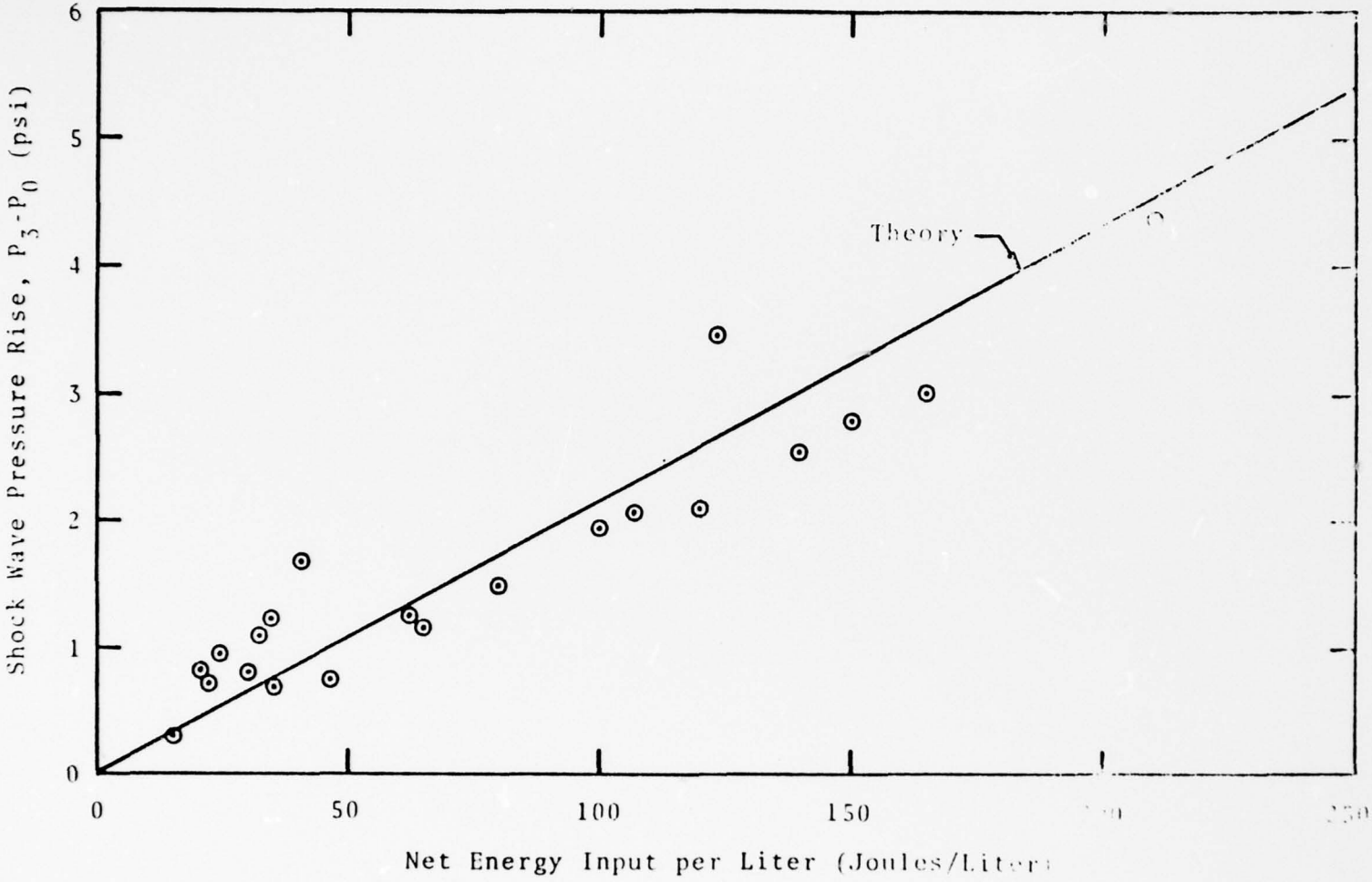

Figure 6. Comparison of Experiment and Theory for Shock Pressure as Function of Input Energy.

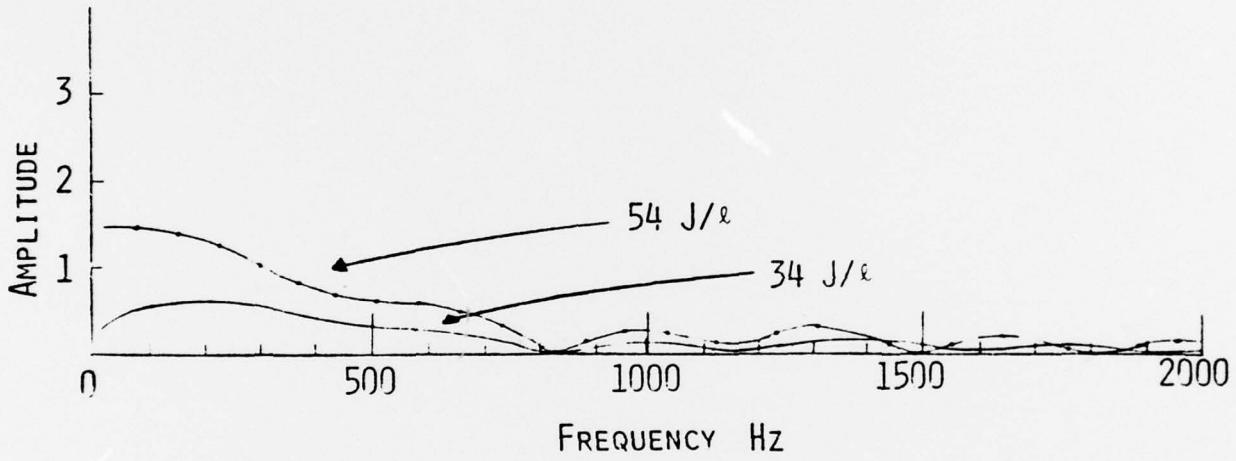

FIGURE 7. WAVE SPECTRUM AT TWO POWER LEVELS DETERMINED BY THE FOURIER TRANSFORM METHOD.

PRESSURE WAVE TRACES

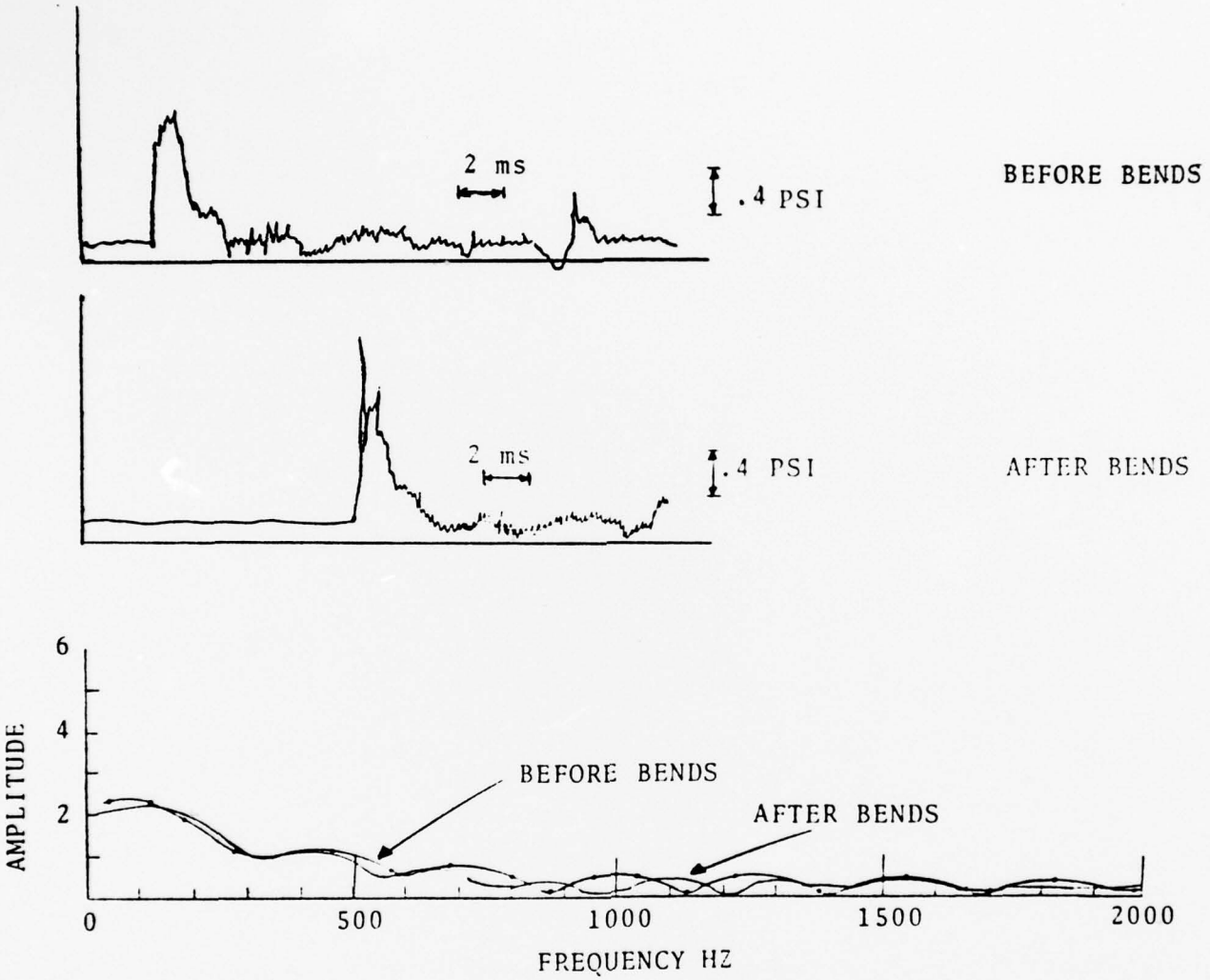

Figure 8. PROPAGATION OF PRESSURE WAVES THROUGH TWO 90° BENDS

	f (Hz)	f_τ (Hz)	f_{FFT} (Hz)
BEFORE BENDS	273	312	280
AFTER BENDS	273	277	230

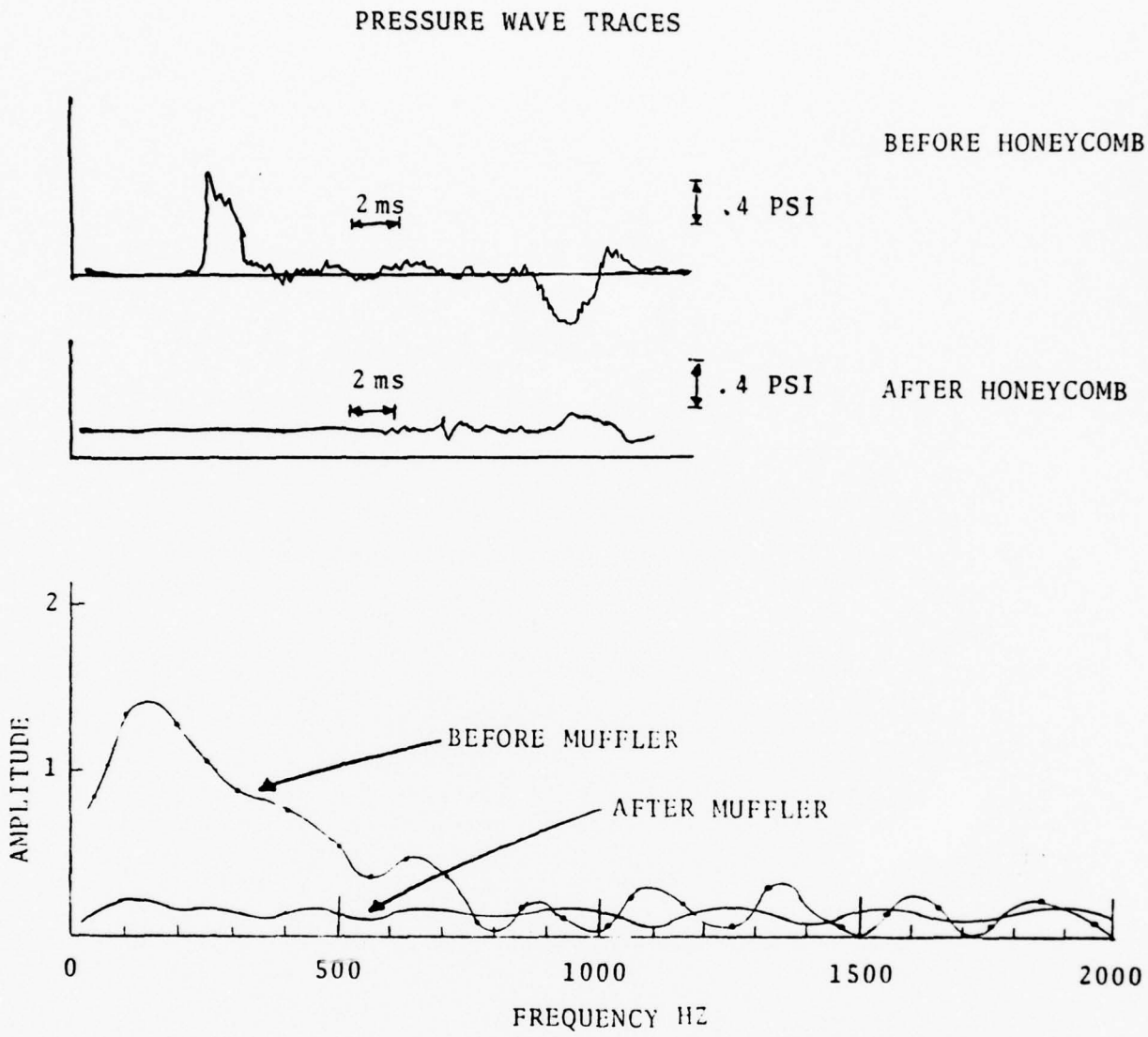

FIG. 9. PROPAGATION OF PRESSURE WAVE THROUGH HORN RESONATOR TYPE MUFFLER

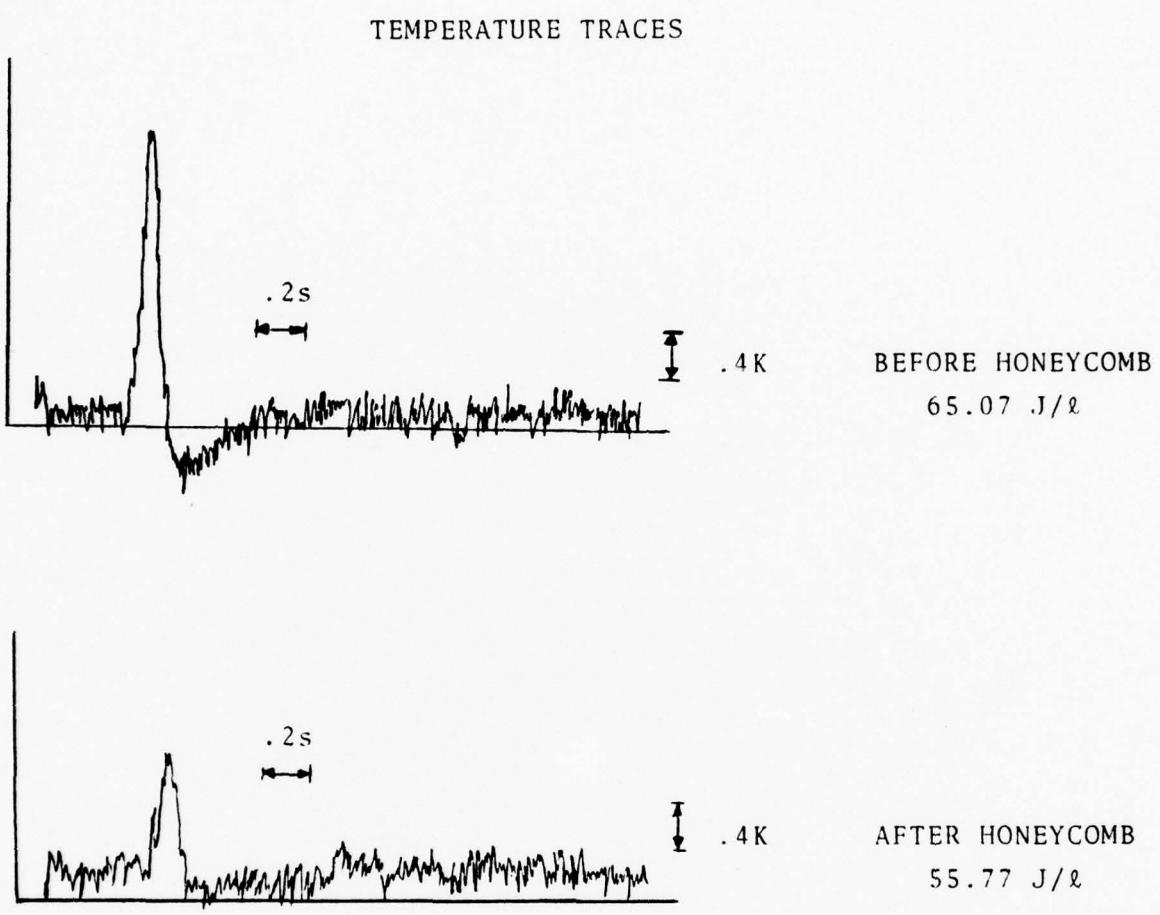

FIG. 10. PROPAGATION OF THERMAL PULSE THROUGH 10 CM OF RESISTIVE ATTENUATOR (CERAMIC HONEYCOMB)

Section 4

Presented at Dynamic Flow Conference 1978 in Baltimore, Maryland, September 1978

Measurements of Fluid and Thermal Characteristics of Recirculating Laser Gas Flows in a Closed Cycle Circulator for Pulsed Lasers

by

Cornelius C. Shih and Gerald R. Karr
The University of Alabama in Huntsville

and

Charles Cason
U. S. Army Missile Research and Development Command

Introduction

A closed cycle circulator associated with electrically pulsed lasers consists of a compressor, heat exchangers, acoustic attenuators, flow regulator and diverter, ducting, control and instrumentation systems along with a laser cavity for the purpose of maintaining a recirculating flow of laser gas suitably reconditioned for lasing at the cavity. Reconditioning the laser gas with gas dynamic, acoustic and thermodynamic means is necessitated by the abrupt deposition of energy at a repetitive rate in the recirculating flow of laser gas at the cavity, causing severe spacial and temporal variations of fluid and thermal characteristics throughout the flow. The resulting pressure, temperature, and velocity gradients are responsible for producing acoustical and thermal perturbations which are directly related to density fluctuations of the laser media. Optical beam quality is known to be degraded by the density fluctuations as noted by previous investigations particularly for CO_2 lasers[1],[2],[3],[4],[5]. Therefore, design improvement as well as efficient operation of the lasers requires serious attention to gas dynamic, thermodynamic, and acoustic management of the laser media in the recirculating flow system based on meaningful measurements and analysis of fluid and thermal characteristics of the flow in the pulsed laser operation.

This paper presents some of the efforts and findings pertaining to the measurements of unsteady flow quantities, namely pressure, temperature and velocity of the recirculating flow in the closed cycle circulator at various locations for several levels of pulsed energy input. Special emphasis is made on the technique development for the measurement of temperature fluctuations in the highly transient flow where high frequency response of the instrument is required.

Experimental Apparatus

1) Closed Cycle Circulator

The closed cycle circulator designed and fabricated for this study is of subscale size and intended for use with a single pulse generator (S^3 laser) capable of delivering pulse energy up to 500 Joules per litre, so that the adequacy of the instrumentation system for transient flow measurements of particular interest may be determined at the preliminary level of the full size circulator development.

Components of this circulator shown schematically in Fig. 1, are listed as follows: a blower (Dayton Model 4C108) with a 10 5/8 in. wheel driven by a electric motor of one horsepower operated at 3450 RPM; PVC piping of 4 in. diameter including 1 in. by-pass pipe; E-beam masks for containing the E-beam to within a specified region of the cavity; cavity structures to box-in the discharge region in the vertical and longitudinal directions; mufflers; reflectors. The blower is capable of producing flows with velocities up to about 100 ft/sec by adjusting the by-pass pipe.

2) Instrumentation System

a) Pressure Measuring Instrument

The pressure of up to 100 psi was sensed by the mini-gage which gives a direct, high level, voltage signal with less than 100 ohms output

impedance and high frequency response of 50 KHZ and low frequency response of 0.005 HZ. The sensor then converts the pressure into electrical voltage with bias of up to 11 $\pm$ 2 volts. The power required by the transducer to the readout equipment is transmitted through the coupler over a single inexpensive cable. This eliminates all of the inherent piezoelectric high impedance problems of electrical leakage, cable noise and signal attenuation and allows the transducers to be used in contaminated environments and with long and moving cables at low noise and without use of charge amplifiers.

The calibration of the transducers was performed at the factory, and the values of the calibration were noted to be, on the average for all probes, 50 mv per psi for the pressure measurement up to 100 psi. The calibration curve relating the voltage output and the pressure is noted to be quite linear.

b) Temperature Measuring Instrument

Due to the extremely transient nature of temperature variation in the recirculating flow as a result of the pulsed laser operation, a sensor of high frequency response in excess of 500 HZ is considered necessary for the temperature measurement. Search of an adequate sensor resulted in the selection of a hot-wire sensor made of 0.00015 in. diameter tungsten wire coated with platinum powdery film. The hot-wire sensor is connected to the Temperature and Switching Module (Thermo-Systems Model 1040) which is in turn connected to the power supply (Model 1031-10A).

The Module consists of a bridge circuit and amplifier in an open loop configuration so the hot-wire sensor which is ordinarily used as an anemometer probe can be switched to function as a resistance thermometer. Since there is a linear proportionality between the voltage output and the temperature, the calibration can be simply performed by adjusting the zero and

gain set potentiometers to a desired temperature range using the calibrate pots of two temperatures.

c) Velocity Measuring Instrument

For the measurement of velocities, hot-wire probes the same as those used for the temperature measurement is applied. The probe is connected to the constant temperature anemometer module (Model 1010A). The amplified output signal from the anemometer is sent to the Linearizer (Model 1005B) so that the voltage signal is processed in such a way that it became linearly related to velocity of the gas flow.

The use of these modules ensures the frequency response above 500 KHZ with power output as high as 1.5 amps. The noise associated with the anemometer is noted to be less that 0.007% equivalent turbulent intensity. Frequency response to the Linearizer is found to be up to 400 KHZ and the accuracy of linearization can reach $\pm$ 0.2%.

d) Calibration of Temperature Probes

Examination of preliminary experimental data of temperature measurements of the flow laden with shock waves, thermal waves and acoustic waves in the circulator resulted in a finding that the temperature probes were not as sensitive as the pressure and velocity probes responding to waves of high frequency or gradient. Thus, an extensive calibration of the probes to relate the probe characteristics and environmental temperature to the frequency response became necessary for establishing a corrective procedure to ensure the measurement accuracy.

A calibration device consisting of a circular disc with two 1 in. by 1 in. windows at the opposite sides rotating at various fixed speeds, a heated gas flow source and a probe support as shown in Fig. 2. Proper adjustment of the flow temperature and rotation speed enabled the device

to similate the thermal environments surrounding the probe for a given duration due to the thermal waves and shock waves laden on the recirculating flow.

Based on theoretical consideration of the probe characteristics, instrumental principles and thermal conditions of the flow, it was deduced that the probe frequency response may be delineated by the following equation[6]:

$$\frac{T_s}{T_e} = \frac{1}{1 + K\,\omega} \qquad (1)$$

where T_s denotes the temperature sensed by the probe, T_e the environmental temperature, ω the thermal wave frequency, and K the probe characteristic coefficient expressed as a function of T_e and ω.

Results of the calibration are presented with the above parameters and variables in Fig. 3. These calibration curves for various T_e can be applied for correcting the temperature measured by the probe. The coefficient K was found to be highly dependent on T_e and ω for a given probe. Theoretically, it is known that the smaller the diameter of the probe, the higher the frequency response.

e) Calibration of Velocity Probes

The probes were calibrated by using a Thermo-Systems Calibrator (Model 1125) following the furnished instructions. Results of the calibration were analyzed with the aid of a computer programmed for the standard data analysis.

f) Data Recording System

To amplify and record experimental data from these measurements with proper time sweep, Tektronix oscilloscope (Type 564-3A74-3B3) with memory, equipped with a Polaroid camera, was employed.

Presentation of Experimental Data

A typical test run involved the S^3 laser and recording temporal variations of pressure, temperature and velocity at various locations in the circulator. In addition, the laser discharge current was monitored in order to determine the energy put into the laser media. For brevity, few typical recorded data are traced from the oscillograph photos presented in Figures 4, 5, and 6.

Figure 4 shows time-dependent pressure, velocity and temperature at Section 1 in the circulator recorded at Channels 1, 2 and 3, respectively. The sweeping time of 2 m sec per div. in the oscilloscope was fast enough to capture the shock wave propagating at the Mach number of 1.1 in terms of pressure, velocity and temperature.

Figure 5 depicts the passing of a thermal wave at Section 1. The wave was measured to be traveling at about 100 ft. per sec. Diffusion of the wave at the section was noted to be rather significant, resulting in a considerable decrease in temperature ($24^{o}C$) from the one ($74^{o}C$) initiated at the cavity. The volume of the heat gas was diffused to almost three times the initial volume.

Figure 6 shows the decay of pressure waves across a muffler installed in the circulator. More than 19 db in acoustic attenuation was noted for this case.

Acknowledgement

The research effort of Werner Dahm, Jr. contributed greatly to this project and is hereby acknowledged.

References

1. Pugh, E. R.; Wallace, J.; Jacob, J. II.; Northam, D. B.; and Daugherty, J. D.: "Optical Quality of Pulsed Electron Beam Sustained Lasers." Appl. Optics, Vol. 13, 1974, p. 251.

2. McAllister, G. L.; Draggoo, V. G.; and Eguchi, R. G.: "Acoustical Wave Effects on the Beam Quality of a High Energy CO Electric Discharge Laser." Appl. Optics, Vol. 14, 1975, p. 1290.

3. Culick, E. E. C.; Shen, P. I.; and Griffins, W. S.: "Acoustical Waves Formed in an Electric Discharge CO Laser Cavity." AIAA Paper No. 75-851, 1975.

4. Kast, S. and Cason, C.: "Performance Comparison of Pulsed Discharge and E-Beam Controlled CO_2 Lasers." J. Appl. Phys., Vol. 44, 1973, p. 1631.

5. Basov, N. G.; Danilychev, V. A.; et al.: "Maximum Output Energy of an Electron-Beam-Controlled CO_2 Laser." Sov. J. Quantum Electronics, Vol. 4, 1975, p. 1414.

6. Fingerson, L. M.: "Parameter for Comparing Anemometer Response." Proc. Symposium of Turbulence in Liquids, University of Missouri, Rolla, Missouri, Oct. 1971.

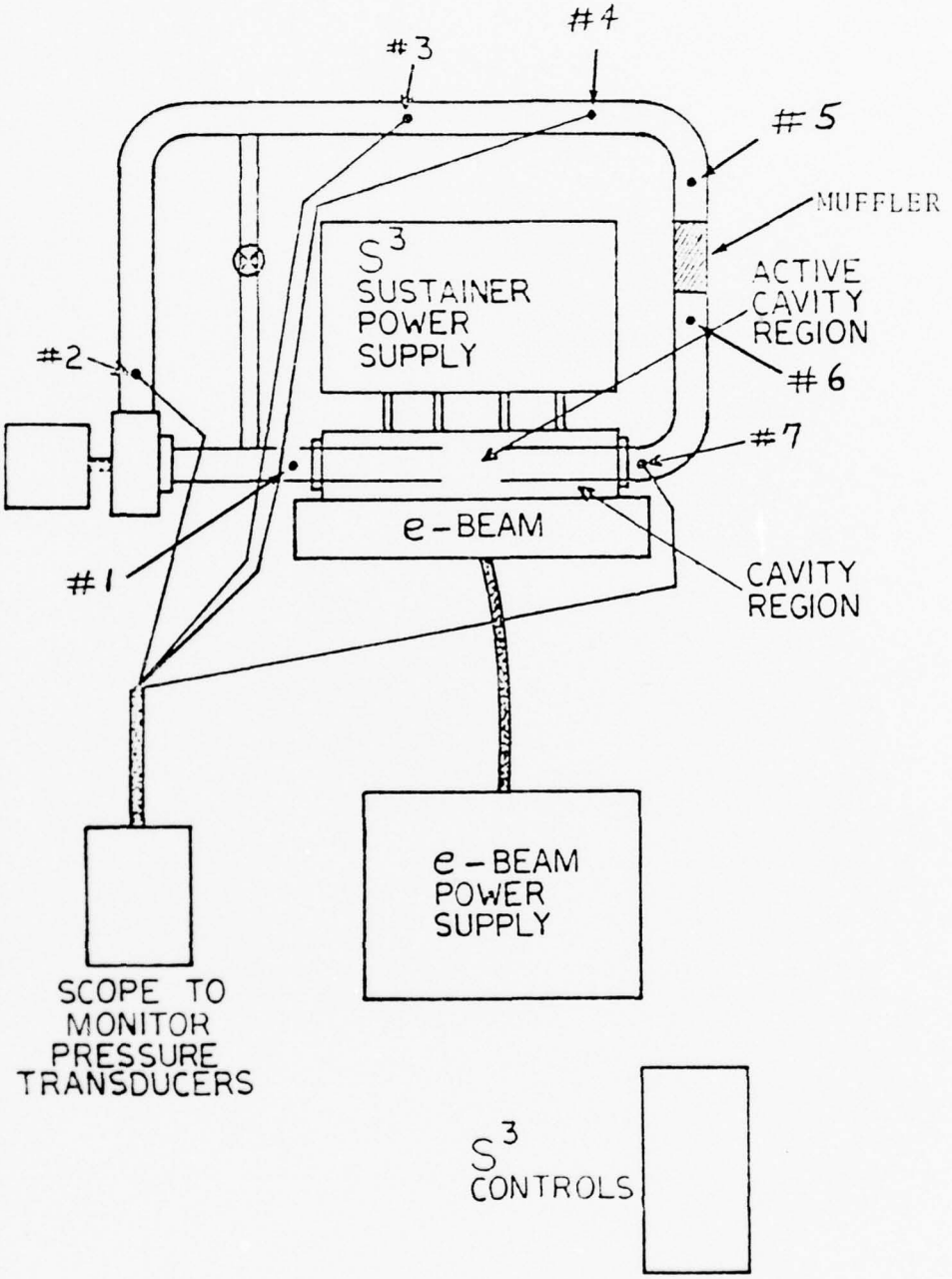

FIGURE 1. TOP VIEW OF PVC SUBSCALE MODEL ATTACHED TO THE S^3 LASER.

Symbol # indicates Sections.

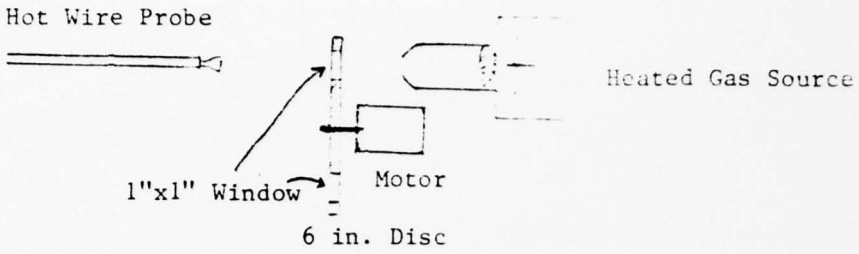

Figure 2
Temperature Probe Calibration Device

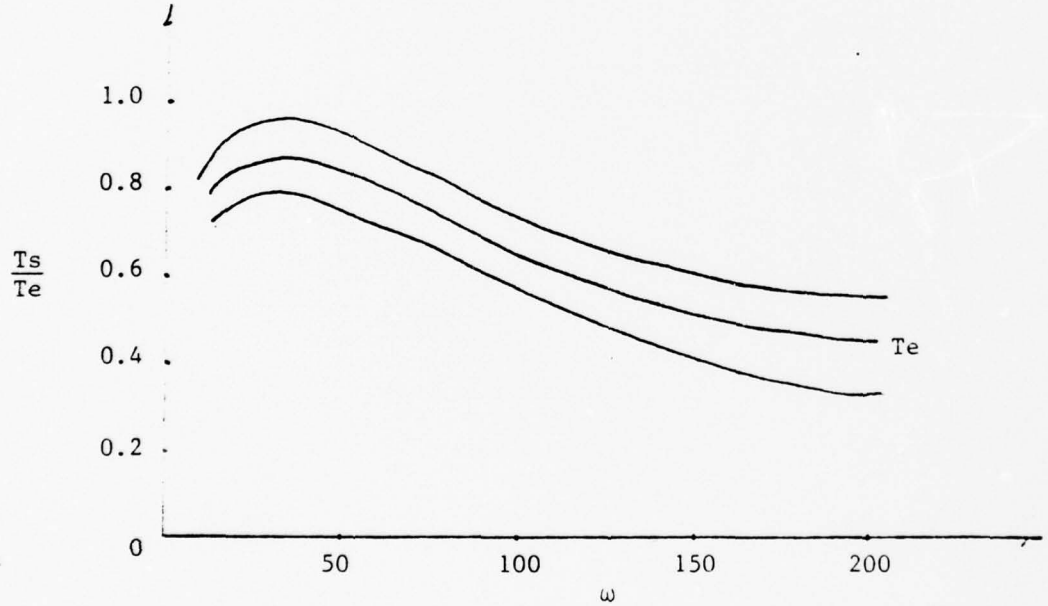

Figure 3
Temperature Probe Calibration Curves

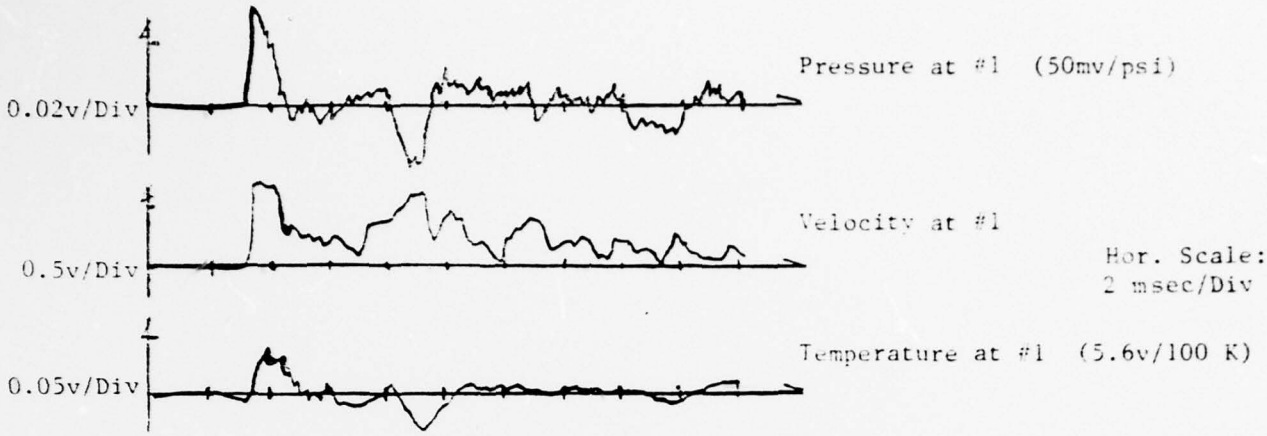

Figure 4

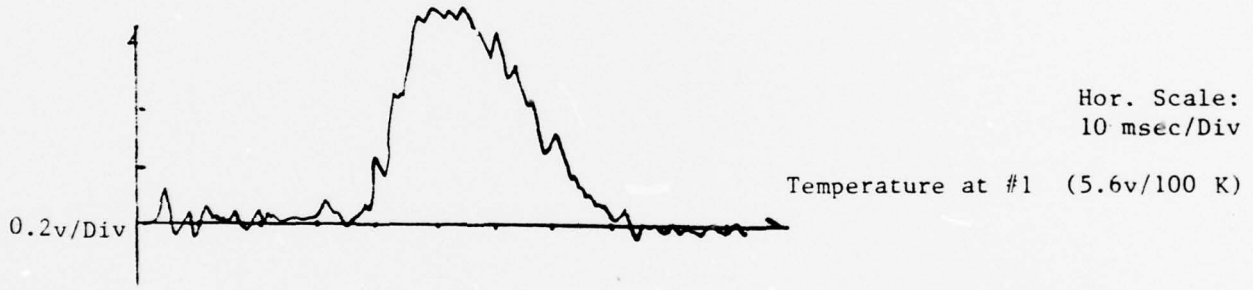

Figure 5

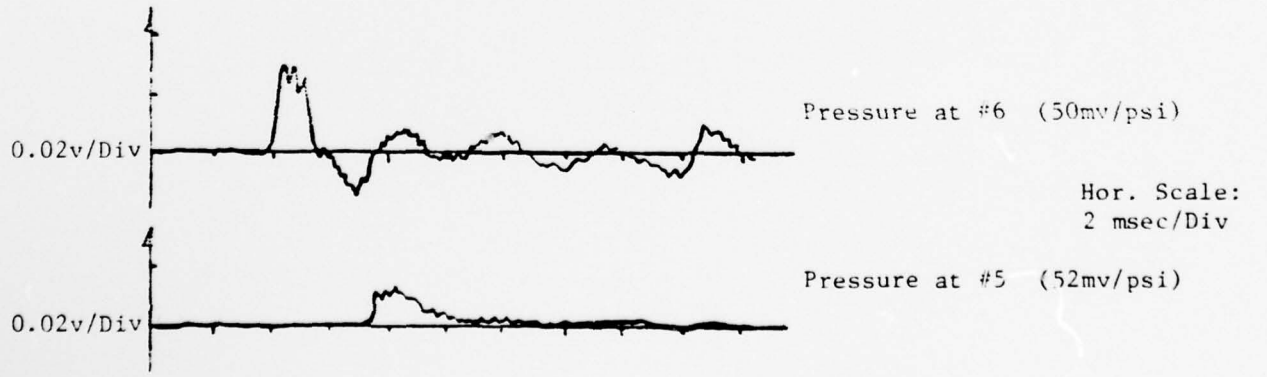

Figure 6

Section 5

Presented at Second International Symposium on Gas-Flow and Chemical Lasers, Brussels, Belgium, September 1978

FLUID AND THERMAL CHARACTERISTICS OF CLOSED CYCLE FLOW SYSTEMS FOR HIGH POWER LASERS

G. R. KARR AND C. C. SHIH
The University of Alabama in Huntsville, Huntsville, Alabama

C. M. CASON AND VERNON AYRE
U. S. Army Missile Research and Development Command, Redstone Arsenal, Alabama

ABSTRACT

In high power lasers of electric discharge type, the laser gas is recirculated in a closed cycle flow system similar to a subsonic wind tunnel including a laser cavity and heat exchangers. Due to the high heat input at the cavity during the laser operation, peculiar fluid and thermal characteristics have been noted in the closed cycle flow system.

This paper presents a study of these characteristics under steady state operating conditions for various heat input levels and flow parameters, using computer calculation of a one-dimensional model. The computer program has incorporated the characteristics of a specific blower and heat exchanger design and he gas properties of a typical CO_2 laser gas mixture. Thus, the steady state operating conditions for a given heat input, a given inlet operating pressure and given ambient conditions for the heat exchangers have been determined with the program. Also analyzed are the operating characteristics of the system for off-design conditions. Results of the analysis are presented in terms of velocity, density, temperature, and pressure distributions throughout the system, comparing with a set of standard, nominal operating conditions. This comparison enables an understanding of the changing trends of fluid and thermal characteristics due to the changes of heat input.

Results of this study provide a design tool for the development of a high power laser with optimum efficiency. They also serve as a basis for the investigation of unsteady phenomena using a quasi-steady method of analysis.

INTRODUCTION

The high power laser of electric discharge type under this study has the laser gas recirculating in a closed cycle flow system including a laser cavity and heat exchangers. In the laser cavity section, the electric discharge increases the temperature of the laser gas mixture. This increase in temperature will have the detrimental effect of filling the lower energy levels of the CO_2 and resulting in breakdown of the laser gain unless the gas is cooled or refreshed. Recirculating flow is necessary for sustaining a continuous performance of the laser at high power levels without the need to provide large volumes of gas.

Cooling of the laser gas at a pressure below atmospheric is primarily managed in this system by flow convection which replenish the cavity with cooled gas which has been recycled through the heat exchangers. This method of cooling is superior to the blow-down type or open cycle system from the standpoint of gas economy and other engineering considerations.

The closed cycle flow system is basically similar to a subsonic wind tunnel, but differs from it because of the severe heating and cooling of the recirculating gas under the low operating pressure. Main features of the system are the heating that occurs in the cavity region, the cooling that occurs in the heat exchangers, and the blowers which maintain the flow.

The objectives of this study are: to develop a computer model which is capable of calculating fluid and thermal conditions of the recirculating flow at various stations in the closed cycle and which is capable of simulating major element arrangements and ranges of input parameters; to verify the model with experimental data collected from a limited experiment to evaluate feasibility of the recycling concept; and to estimate the limit of the operating range of such a system.

METHOD

Coupling the one-dimensional equations of continuity, motion, energy, heat transfer for heat exchangers, compressor performance, and gas kinetics at the laser cavity, a computer program was developed to perform calculations converging on a steady-state operation solution for a closed cycle flow system defined in terms of laser output power and efficiency, gas composition, tunnel heat exchangers, and external radiators, tunnel dimensions, diffuser pressure loss coefficients, blower performance data, coolant flow rates, and a definition of the external heat sources couples to the coolant flow. The steady state solution is obtained for a fixed inlet density or pressure at the cavity entrance. A simplified flow chart of the computer program is presented in Figure 1 to describe the flow of calculations.

With reference to the flow chart in Figure 1, the calculation is started by inputs of initial assumed values throughout the system. Since the steady state operating characteristics are dependent upon the system performance, only one flow variable can be specified at one location in the system. In many high energy systems, the cavity inlet pressure or density is used to control the system and that is why one of these properties is chosen as specified to begin the calculation. Based on the assumed input flow parameters, the gas thermodynamic and physical properties are calculated and all heat exchanger friction factors and heat transfer coefficients are computed.

The gas enters the cavity region and is subjected to the severe heating characteristic of high energy laser system. The cavity area change in the flow direction may be of arbitrary shape or one which provides for constant Mach number through the cavity region. The duct flow losses and heat exchanger induced changes in pressure and temperature are calculated. Performance curves of the blower then provides values for the outlet pressure and temperature for assumed mass flow rate. Additional duct flow and heat exchanger losses are calculated to give flow properties at the cavity inlet. If the calculated and assumed inlet properties differ, a new flow rate and inlet temperature is chosen and the process repeated until convergence is reached. Computation of system energy balance and blower total pressure matching with the system resistance are included. Specific heats, viscosity, and heat transfer coefficients are recalculated as the computation proceeds.

With the ambient air temperature, pressure, and relative humidity given, convergence of the calculations is attained when changes in 16 system temperatures and supplementary pressure, density, temperature, velocity, and Mach number loops fall within prespecified tolerances. The closed cycle flow system under study is shown schematically in Figure 2, with the identification numbers representing the stations where computer calculations are performed.

In the numerical scheme of solving the set of heat-balance and flow equations representing the laser gas flow recirculating with a heat input at the cavity, the Wegstein method of iteration was employed along with the initial forcing

condition that inlet parameters are equal to outlet parameters in the closed loop. When the inlet flow conditions are fixed, the laser power output and efficiency, liquid coolant flow rate, gas properties and system geometry are determined, then a solution for the required heat exchanger effectiveness as well as the number of heat transfer units, and for the blower pressure ratio can be deduced.

RESULTS

Simulation of a high energy CO_2 electric discharge laser with an e-beam was employed to illustrate the steady state operation of such a system. The results are presented in Figures 3 through 7 for the system velocity, density, total temperatures, static pressure, and total pressure, respectively. The inlet static pressure is kept the same in these results.

Figure 3 shows the velocity values obtained from the steady state program for 3 ranges of heat deposited in the cavity region (zero, nominal, and twice nominal). The velocity at the cavity inlet for the nominal case is used to non-dimensionalize the results which are plotted relative to the location around the recirculation system. At the bottom of the figure is a drawing of the one-dimensional cross section of the system used in the computation. The cavity cross section was taken as constant for the results presented here. The heat addition at the cavity is seen to cause increased velocity in the system up to the first heat exchanger. The high velocity/high temperature gas encounters increased resistance at the first heat exchanger as the heat input to the system is increased.

Figure 4 shows the values of density throughout the system with the density at the cavity inlet for the nominal-heat case used to non-dimensionalize the results. The results show that the total integrated mass in the system decreases as the heat input to the cavity is increased. During start up of the system from a zero heat input to the cavity, the results show that gas will have to be taken from the system if constant inlet pressure is used as a control for the system.

Figure 5 shows a plot of the total temperature throughout the system using a format similar to Figures 3 and 4. As expected, heat deposited in the cavity causes an increase in the total temperature of the gas. The first heat exchanger removes the majority of the heat in the example considered here. The blower is seen to increase the total temperature of the gas. This temperature rise is removed by the second heat exchanger.

Figure 6 shows a plot of the static pressure throughout the system for the three heating cases. The pressure at Station 1 is the same for all the cases. Limited experimental data was available from the system under simulation and the results are shown on this figure by the dark circles. The results show good agreement for the zero heat case except near Station 3 which is the region of the 180^{o} turning of the flow.

Figure 7 shows the results of the computer simulation for total pressure for the zero and nominal heating case only. The major losses in the system with no heating are seen to be at the two heat exchangers. The losses in the ducts and turning regions are seen to be small. For the nominal heating case, there is an added significant loss of total pressure in the cavity region which the blower must overcome. The heating in the cavity acts as a load on the system which requires added blower power.

Figures 8 and 9 are results of the investigation of the effect on operating conditions for off nominal heating and inlet pressure, respectively. In Figure 8, the inlet pressure is held constant as the heat input is varied. The resulting changes in inlet velocity, temperature, and mass flow rate are plotted as a function of the variation in heating. The results of Figure 8 show that the velocity and mass flow rate decrease while the temperature of the inlet

condition that inlet parameters are equal to outlet parameters in the closed loop. When the inlet flow conditions are fixed, the laser power output and efficiency, liquid coolant flow rate, gas properties and system geometry are determined, then a solution for the required heat exchanger effectiveness as well as the number of heat transfer units, and for the blower pressure ratio can be deduced.

RESULTS

Simulation of a high energy CO_2 electric discharge laser with an e-beam was employed to illustrate the steady state operation of such a system. The results are presented in Figures 3 through 7 for the system velocity, density, total temperatures, static pressure, and total pressure, respectively. The inlet static pressure is kept the same in these results.

Figure 3 shows the velocity values obtained from the steady state program for 3 ranges of heat deposited in the cavity region (zero, nominal, and twice nominal). The velocity at the cavity inlet for the nominal case is used to non-dimensionalize the results which are plotted relative to the location around the recirculation system. At the bottom of the figure is a drawing of the one-dimensional cross section of the system used in the computation. The cavity cross section was taken as constant for the results presented here. The heat addition at the cavity is seen to cause increased velocity in the system up to the first heat exchanger. The high velocity/high temperature gas encounters increased resistance at the first heat exchanger as the heat input to the system is increased.

Figure 4 shows the values of density throughout the system with the density at the cavity inlet for the nominal-heat case used to non-dimensionalize the results. The results show that the total integrated mass in the system decreases as the heat input to the cavity is increased. During start up of the system from a zero heat input to the cavity, the results show that gas will have to be taken from the system if constant inlet pressure is used as a control for the system.

Figure 5 shows a plot of the total temperature throughout the system using a format similar to Figures 3 and 4. As expected, heat deposited in the cavity causes an increase in the total temperature of the gas. The first heat exchanger removes the majority of the heat in the example considered here. The blower is seen to increase the total temperature of the gas. This temperature rise is removed by the second heat exchanger.

Figure 6 shows a plot of the static pressure throughout the system for the three heating cases. The pressure at Station 1 is the same for all the cases. Limited experimental data was available from the system under simulation and the results are shown on this figure by the dark circles. The results show good agreement for the zero heat case except near Station 3 which is the region of the 180^{o} turning of the flow.

Figure 7 shows the results of the computer simulation for total pressure for the zero and nominal heating case only. The major losses in the system with no heating are seen to be at the two heat exchangers. The losses in the ducts and turning regions are seen to be small. For the nominal heating case, there is an added significant loss of total pressure in the cavity region which the blower must overcome. The heating in the cavity acts as a load on the system which requires added blower power.

Figures 8 and 9 are results of the investigation of the effect on operating conditions for off nominal heating and inlet pressure, respectively. In Figure 8, the inlet pressure is held constant as the heat input is varied. The resulting changes in inlet velocity, temperature, and mass flow rate are plotted as a function of the variation in heating. The results of Figure 8 show that the velocity and mass flow rate decrease while the temperature of the inlet

gas increases as the heat input to the cavity is increased.

Figure 9 shows the results on velocity, temperature, and mass flow rate (for constant cavity heating at the nominal value) as the inlet pressure varies. The results show that all three quantities increase as the pressure at the cavity inlet is allowed to increase.

CONCLUSIONS

The results presented in dimensionless form for general application serve as an important tool in the engineering design of high energy laser system. The results also provide an understanding of the means for controlling inlet conditions which, in turn, control the laser output performance. For example, Figures 8 and 9 reveal that inlet temperature control requires pressure and heat input variation of opposite sign for stable control.

COMPUTER PROGRAM FLOW CHART

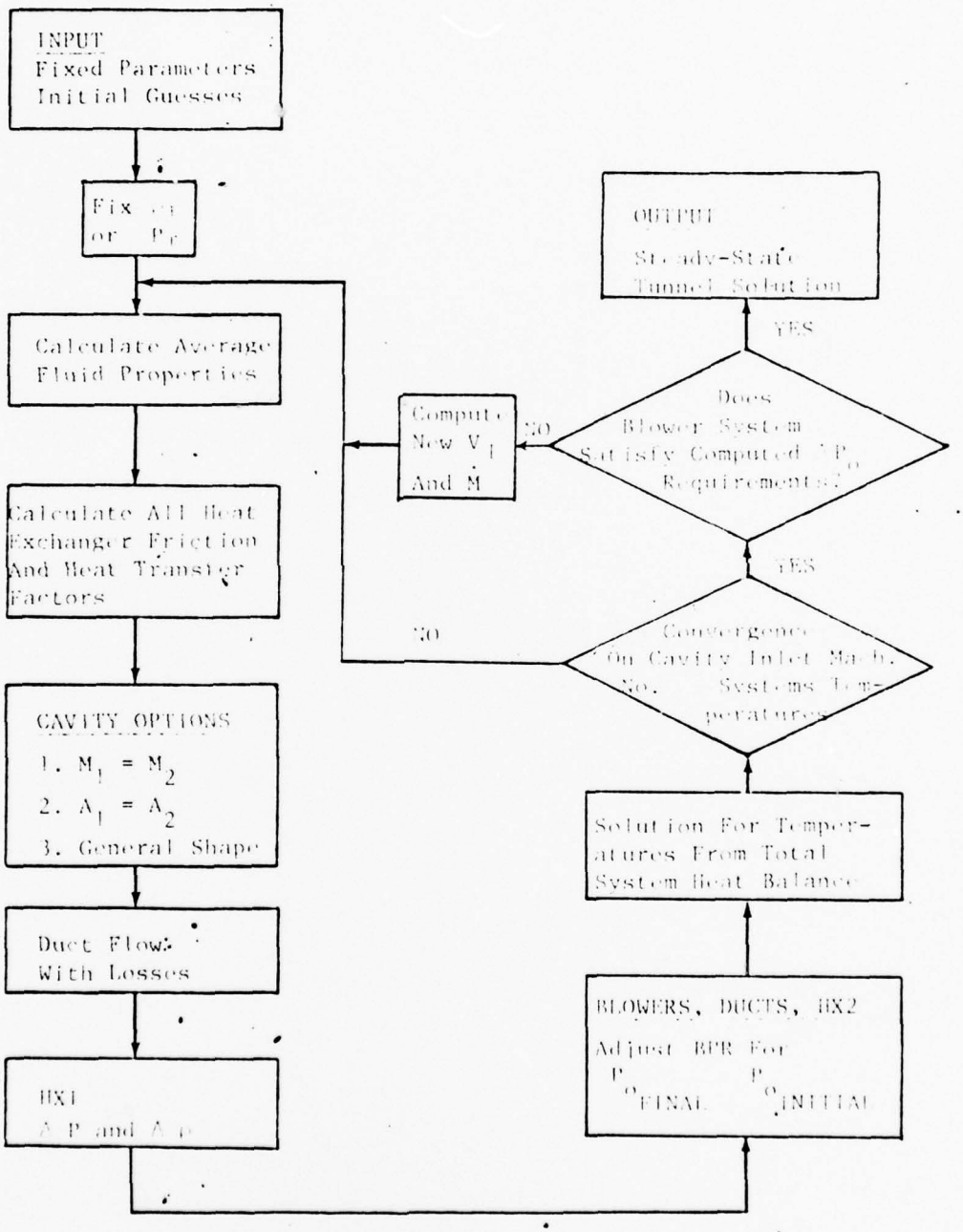

Figure 1. Flow Chart of Computations for Steady State Operation of Recirculator.

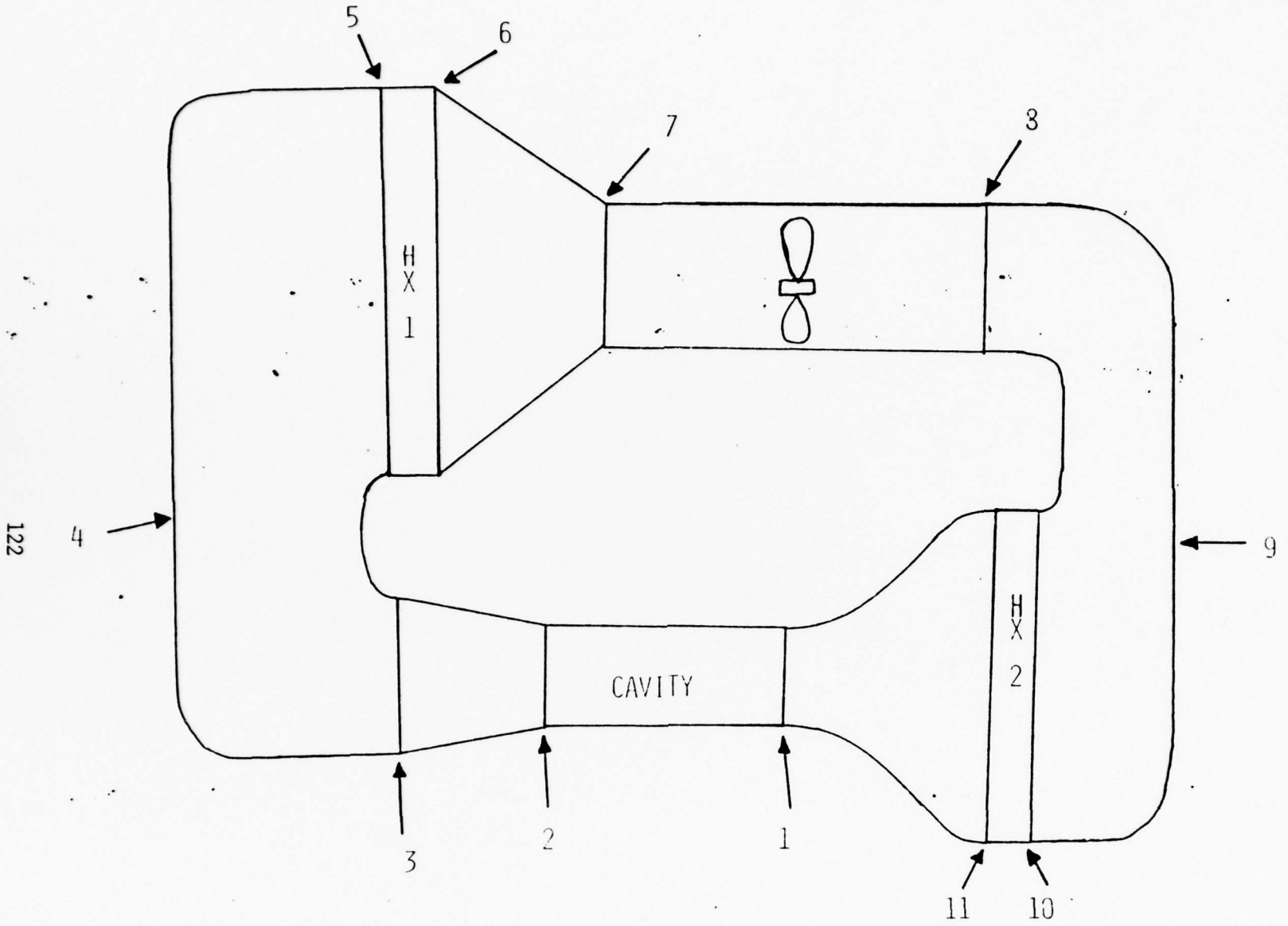

WIND TUNNEL SCHEMATIC

Figure 2. Recirculating System Section Numbering.

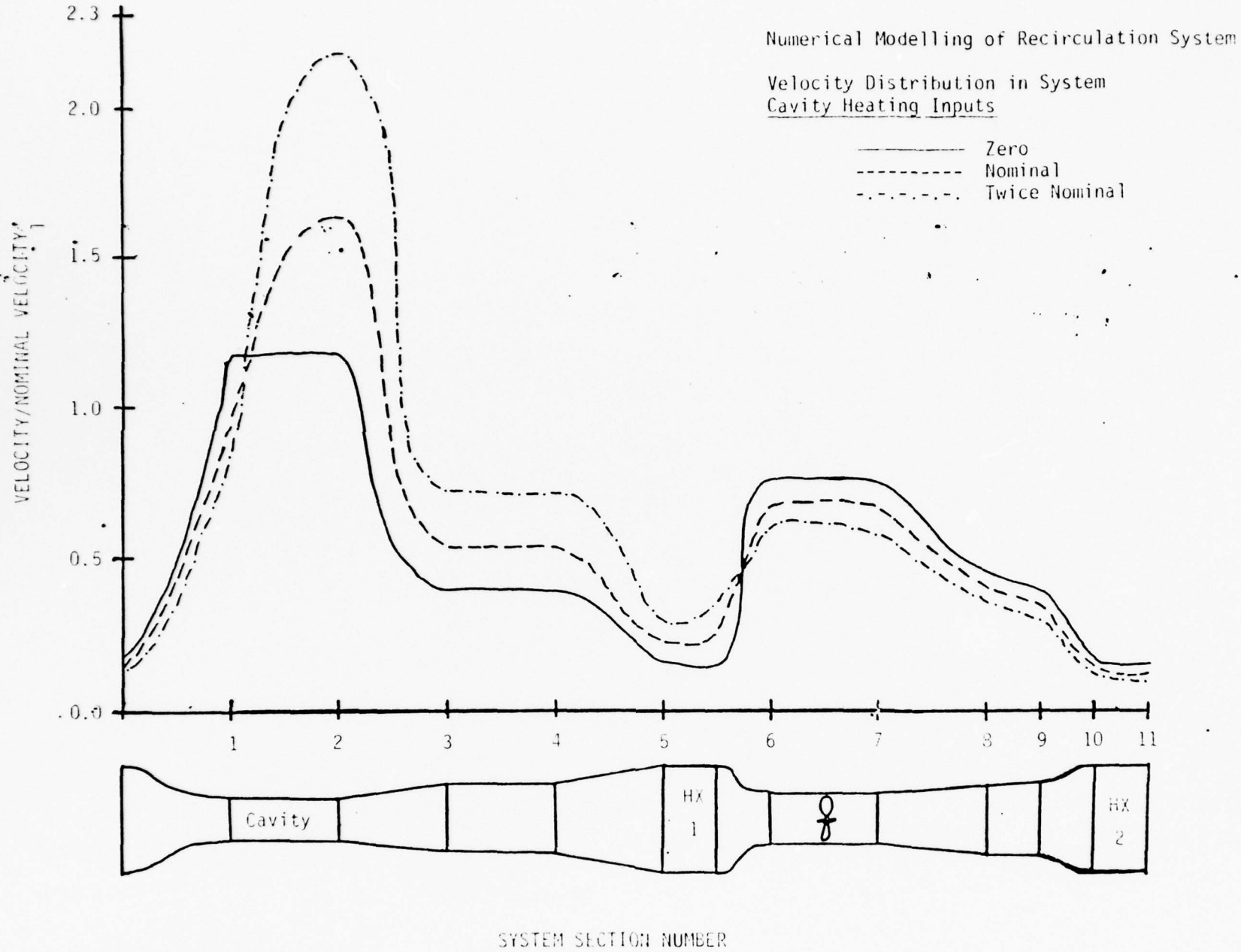

Figure 3. Velocity Throughout System for Three Heating Values.

Figure 4. Density Throughout System for Three Heating Values.

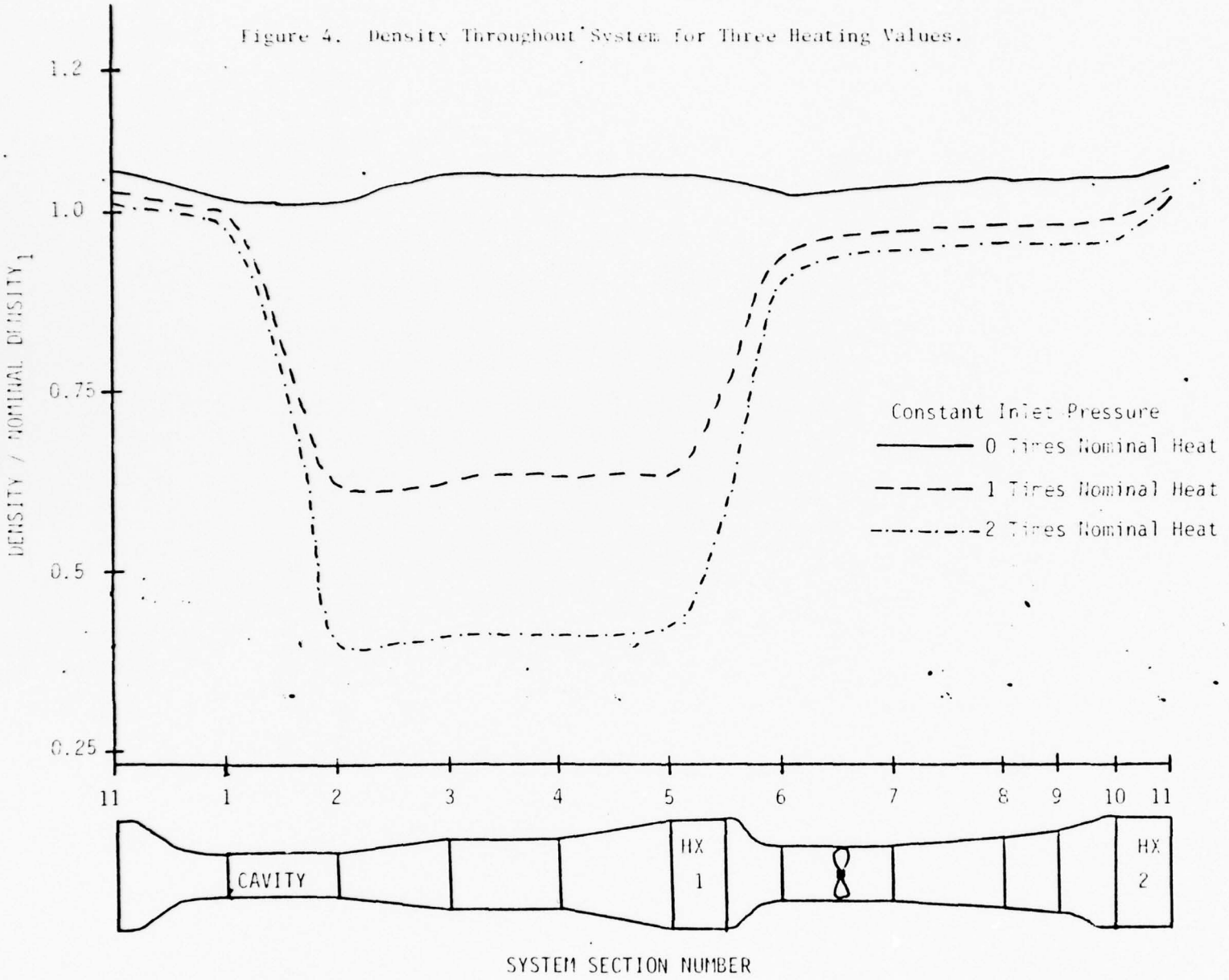

Figure 5. Total Temperature Throughout System for Three Heating Values.

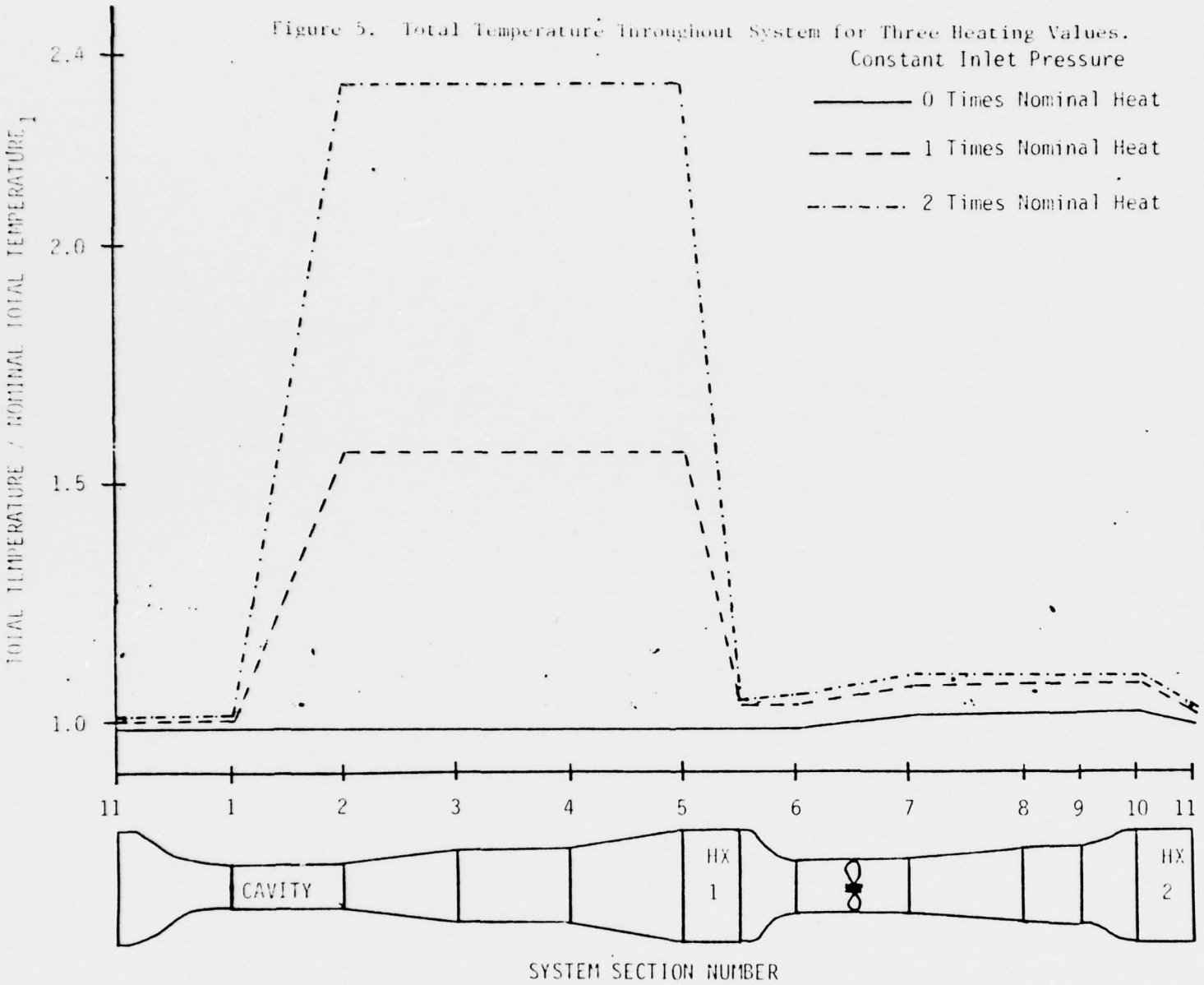

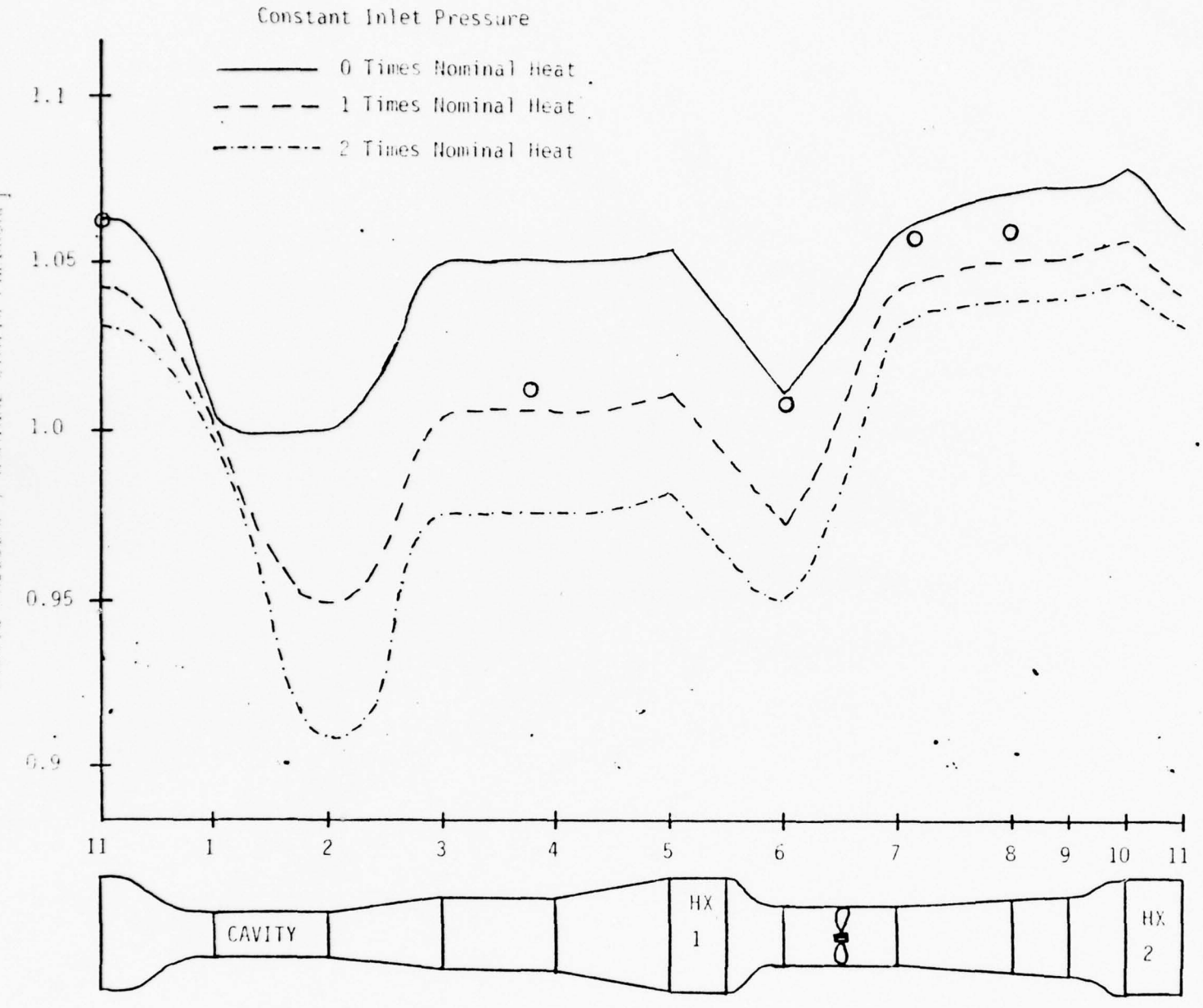

Figure 6. Static Pressure Throughout System for Three Heating Values.

Figure 7. Total Pressure Throughout System for Two Heating Values.

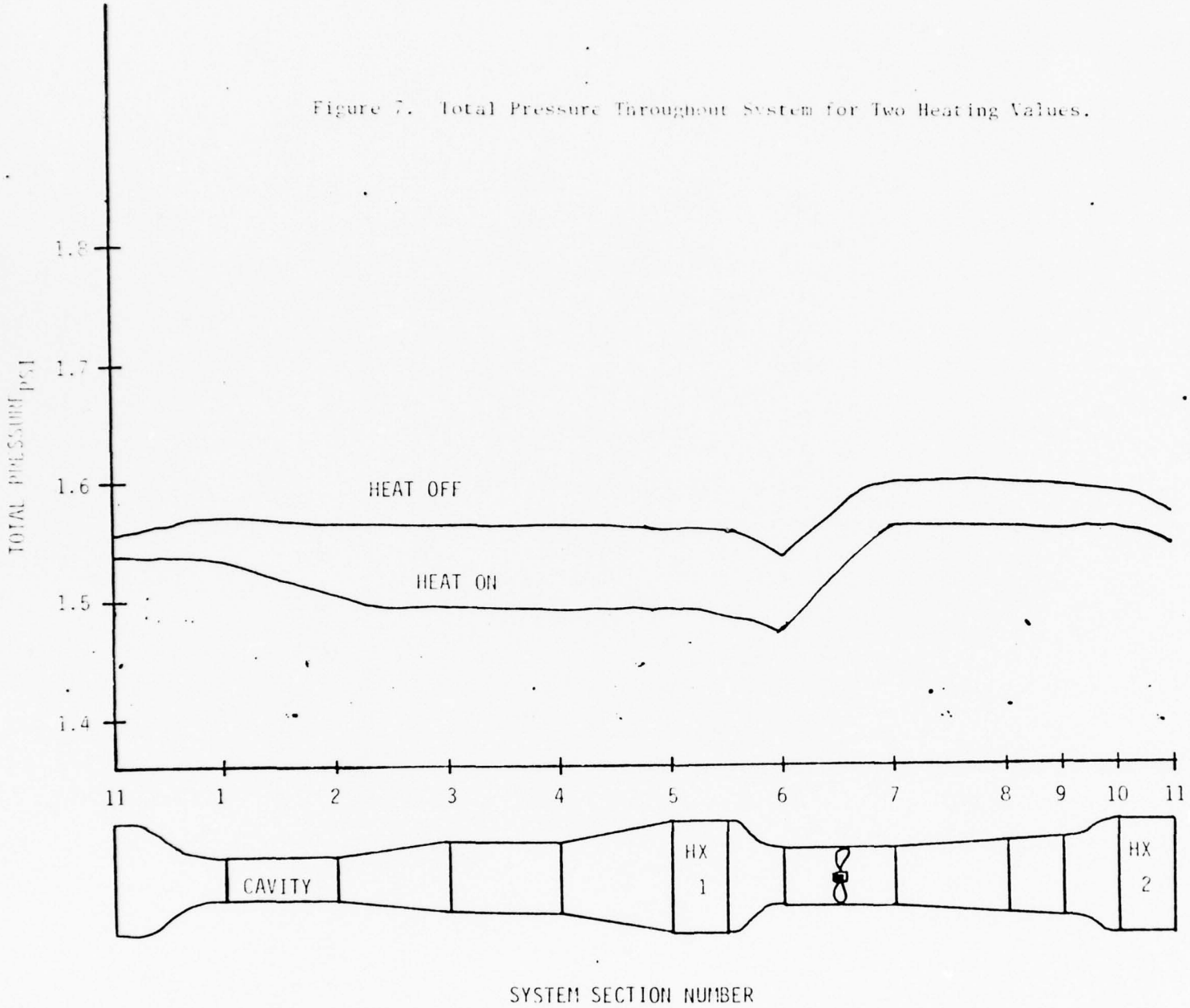

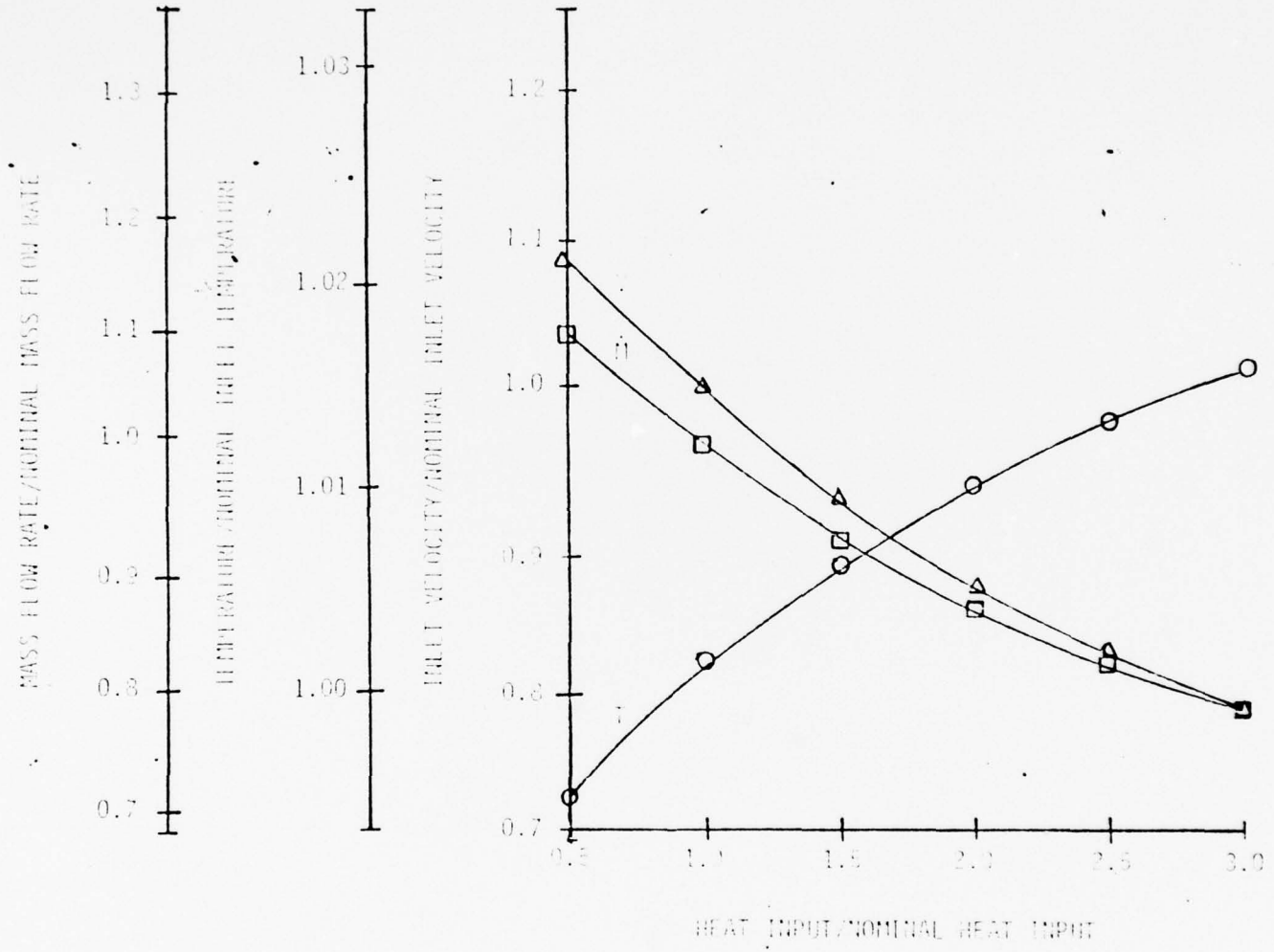

Figure 8. Variation in Inlet Velocity, Temperature, and Mass Flow Rate Versus Heating Values.

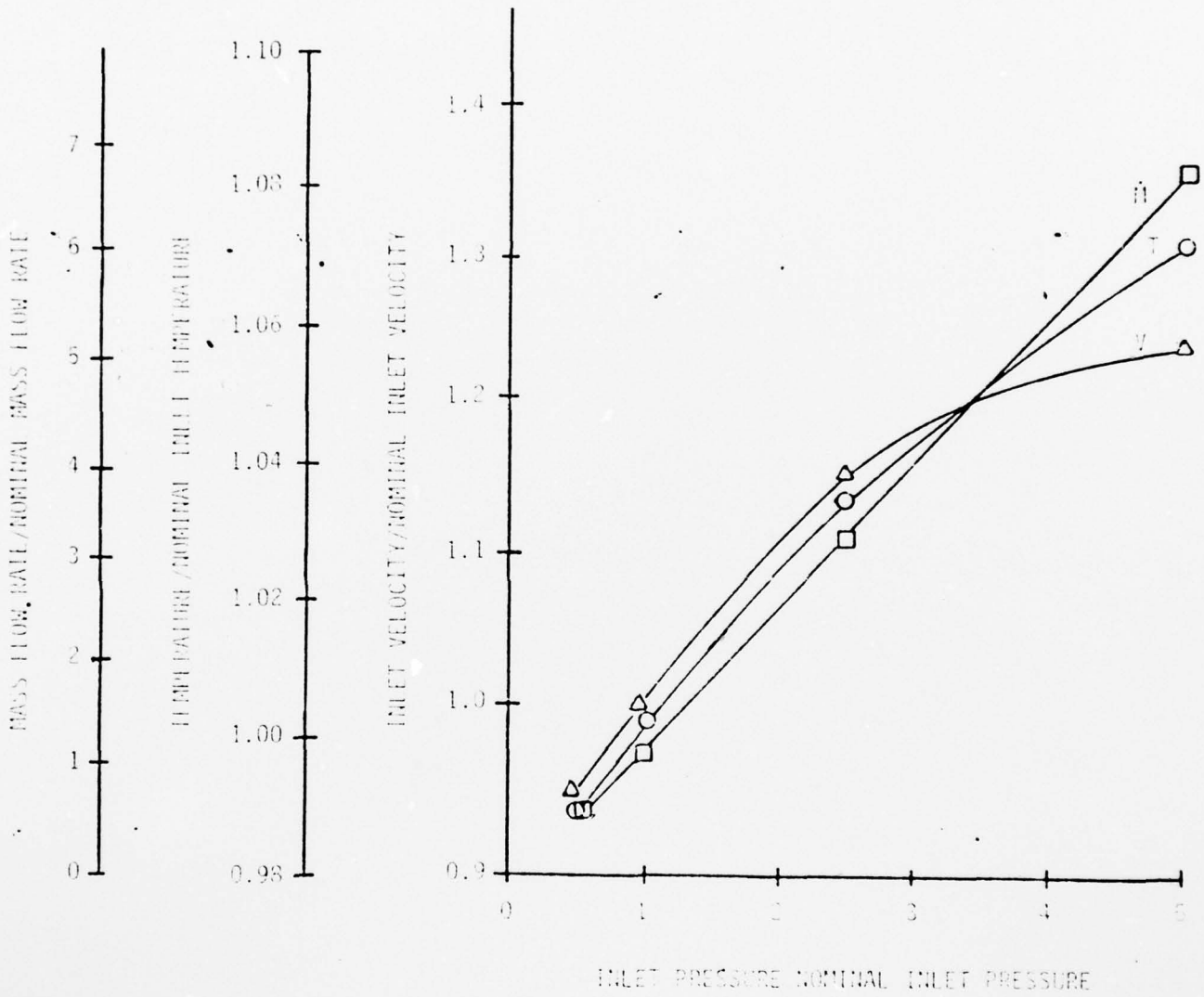

Figure 9. Variation in Inlet Velocity, Temperature, and Mass Flow Rate Versus Heating Values.

201 SERIES MINI-GAGE

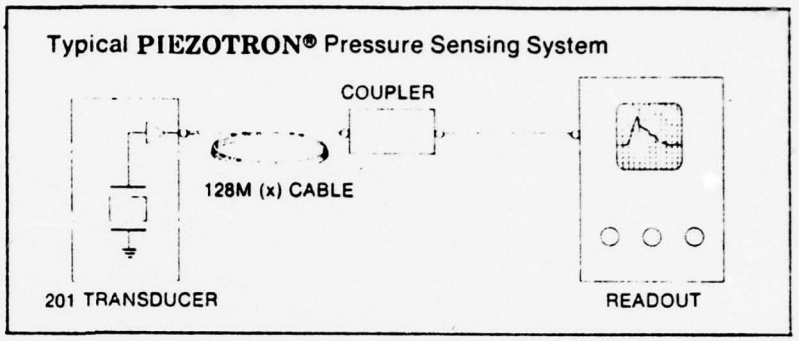

Couplers

To complete the system a wide choice of couplers is offered in the 548 and 549 series. Optional filters and several types of power inputs are available. Model 587D Coupler provides increased capability. Please refer to our Coupler Data Sheet for details.

In addition Models 583, 503D and 504D Laboratory Amplifiers are offered with extensive versatility and many options for more complete pressure studies.

Specifications

		Model Variation			
PERFORMANCE	UNITS	201B1	201B2	201B4	201B5
Pressure Range, 5V out	psi	5,000	500	200	100
Overrange	psi	7,500	750	300	150
Resolution (noise)	psi rms	0.05	0.005	0.002	0.001
Maximum Pressure	psi	15,000	5,000	2,000	1,000
Sensitivity	mV/psi	1	10	25	50
Linearity, B.F.S.L.	%	±1	±1	±1	±1
Resonant Frequency, nom.	kHz	500	500	500	250
Rise Time, 10-90%	μ sec	1	1	1	2
Time Constant, R.T.	sec	1,500	400	200	100
Low Frequency Response, −5%	Hz	0.0003	0.001	0.0025	0.005
High Frequency Response, +5%	Hz	100,000	100,000	100,000	50,000
ENVIRONMENTAL			Common Specs		
Vibration Sensitivity, max.	psi/g	0.002	0.002	0.002	0.002
Shock, 1 ms	g	5,000	5,000	5,000	5,000
Vibration Limit	g	500	500	500	500
Temperature Range	°F	−65 to 280	−65 to 280	−65 to 280	−65 to 280
Temperature Sensitivity Shift	/°F	0.03%	0.03%	0.03%	0.03%
ELECTRICAL					
Output Current, min.	mA	2	2	2	2
Polarity, pressure increase		Negative	Negative	Negative	Negative
Bias Voltage	V	11 ±2	11 ±2	11 ±2	11 ±2
Circuit Return		Case	Case	Case	Case
Output Impedance, max.	ohms	100	100	100	100
MECHANICAL					
Weight	gms	< 10	< 10	< 10	< 10
Case and Diaphragm Material		Stainless St.	Stainless St.	Stainless St.	Stainless St.
Mounting Torque	in-lb	24	24	24	24
Sealing		All Welded	All Welded	All Welded	All Welded
POWER SUPPLY					
Constant Current Source	mA	4 ±1	4 ±1	4 ±1	4 ±1
Supply Ripple, max.	mV rms	25	25	25	25
Supply Voltage, no load	VDC	20-30	20-30	20-30	20-30
Source Impedance, nom.	ohms	250 k	250 k	250 k	250 k

APPENDIX B

Reference Number	Date of Test	Blower Status	Muffler Location	Pressure	Temperature	Velocity	Energy of Pulse, J
5381	6/26/78	Off	2	1,6,5A	7	-	33.80
5382	"	Off	"	1,6,5.5	7	-	106.4045
5400		Off	"	1,6,5A	7	-	56.59535
5402		Off	"	1,6,5A	1	-	49.01
5403		On	"	1,6,5A	1	-	34.06202
5408	7/11/78	On	"	1,5A,6	1	-	71.70709
5410	"	Off	"	1,5.5,6	2	-	64.22
5411	"	On	"	1,6,5.5	2	-	72.67
5412	"	Off	"	1,6,5.5	2	-	67.6
5413	"	Off	"	1,6,5.5	7	-	67.6
5414	"	Off	"	1,6,5.5	3	-	60.84
5415	"	On	"	1,6,5.5	3	-	57.46
5416	"	On	"	1,6,5.5	3	-	72.67
5420	"	Off	"	1,6,5A	7	-	23.66
5421	"	Off	"	1,6,5A	7	-	57.46
5422	"	On	"	1,6,5A	7	-	60.84
5423	"	On	"	6,5A,4	7	-	60.84
5424	"		"	1,6,5.5	3	-	64.22
5425	"	Off	"	1,6,5	5	-	62.53
5426	"	On	"	1,6,5	5	-	64.22
5427	"	Off	-	1,6,5	5	-	62.53
5428	"	On	-	1,6,5	5	-	67.60
5430	"	On	-	1,6,5	5	-	37.18
5431	"	Off	-	1,6,5	4	-	54.08
5433	"	On	-	1,6,5	4	-	59.15
5435	"	Off	-	1,6,5.5	3	-	59.15
5436	"	On	-	1,6,5.5	3	-	65.91
5437	"	On	-	1,6,5.5	3	-	65.91
5438	"	Off	-	1,6,5	2	-	60.84*
5439	"	On	-	1,6,5	2	-	64.22*
5441	"	On	-	1,6,5	2	-	72.67*
5443	"	Off	-	1,6,5	1	-	67.60*

Reference Number	Date of Test	Blower Status	Muffler Location	Pressure	Temperature	Velocity	Energy of Pulse, J
5444	7/11/78		-	1,6,5	1	-	77.74*
5445	"	On	-	1,6,5	1	-	77.74*
5446	"	On	-	1,6,5	1	-	67.60*
5448	7/12/78	On	2	1,5,6	1	-	60.84
5449	"	Off	2	1,6,5	2	-	55.77
5450	"	Off	-	1,5,6	2	-	64.22
5451	"	On	-	1,5,6	2	-	59.15
5452	"	Off	-	1,5,6	3	-	64.22
5453	"	On	-	1,5,6	3	-	67.60
5454	"	On	-	1,5,6	3	-	74.93643
5456	"	Off	-	1,5,6	4	-	67.60
5457	"	On	-	1,5,6	4	-	64.22
5459	"	On	1,2	1,5,6	4	-	72.67
5460	"	Off	"	4,6,5	5	-	60.84*
5461	"	Off	"	4,6,5	5	-	62.53*
5462	"	On	"	4,6,5	4	-	64.22*
5463	"	On	"	4,6,5	5	-	57.46
5464	"	Off	"	4,6,5	6	-	57.46
5466	"	On	"	4,6,5	6	-	57.46
5467	"	On	"	4,6,5	6	-	57.46
5468	"	Off	"	4,6,5	1	-	60.84
5469	"	On	"	4,6,5	1	-	60.84
5470	"	On	"	1,6,5A	1	-	55.77
5471	"	On	"	4,6,5	1	-	64.22
5472	"	On	"	4,6,5	1	-	67.60
5473	"		1	4,6,5	1	-	60.84
5474	"		1	4,6,5	1	-	67.60
5475	"	On	1	4,6,5	1	-	62.53
5476	"	On	1	4,6,5	1	-	64.22
5477	"		1	4,6,5	2	-	46.475
5478	"	On	1	4,6,5	2	-	60.84
5479	"	On	1	4,6,5	2	-	59.15

Reference Number	Date of Test	Blower Status	Muffler Location	Pressure	Temperature	Velocity	Energy of Pulse, J
5480	7/12/78	Off	1	4,6,5	3	-	59.15
5481	"	Off	1	4,6,5	3	-	55.77
5482	"	On	1	4,6,5	3	-	59.15
5483	"	On	1	4,6,5	3	-	66.755
5484	"	On	1	4,6,5	4	-	65.91
5485	"		1	4,6,5	5	-	60.84
5486	"	Off	1	4,6,5	5	-	64.22
5491	"	Off	1	4,6,5	4	-	62.53
5492	"	On	1	4,6,5	4	-	54.08
5493	"		1	4,7,5	7	-	64.22
5494	"	On	1	4,7,5	7	-	64.22
5496	"	Off	1	4,7,5	7	-	33.80
5497	"	Off	1	4,7,5	7	-	54.08
5498	"	Off	1	4,7,5	7	-	50.70
5500	"	Off	1	4,7,5	4	-	54.08
5501	"	Off	1	4,7,5	4	-	54.08
5502	"	On	1	4,7,5	4	-	62.53
5503	"	On	1	4,7,5	4	-	69.29
5504	"	On	1	4,7,5	4	-	70.135
5505	"	On	1	4,7,5	5	-	67.60
5506	"	On	1	4,7,5	5	-	65.065
5507	"	On	1	4,7,5	5	-	70.135
5508	"	Off	1	4,7,5	5	-	65.91
5509	"	Off	1	4,7,5	5	-	54.08
5512	"	On	1	4,7,5	4	-	64.22
5517	7/14/78	On	1	4,5	4	1	65.065
5518	"	On	1	4,5	5	1	55.77
5519	"	On	1	4,5	5	4	87.035
5521	"	On	1	4,5	5	4	67.60
5522	"	On	1	4,5	5	4	80.275
5523	"	On	1	4,5	4	5	67.60

* Assumed Value

PVC Circulator Experimental Data

Page 135
No. 5381
Date 26 June 1978

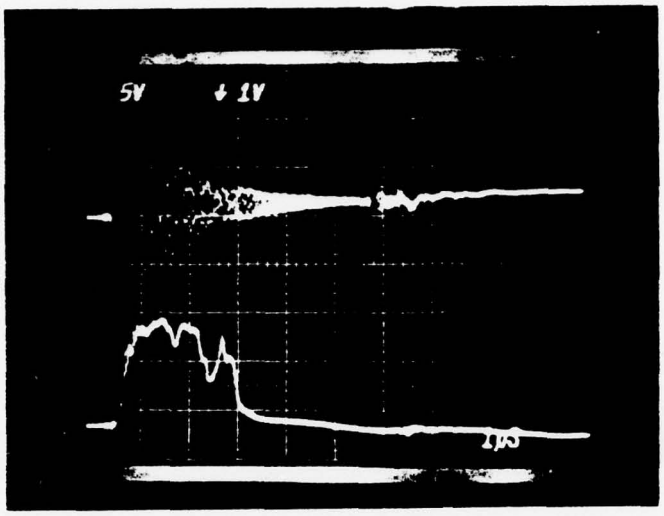

Gun Data

1. Upper Trace
   Voltage 1μsec/div
   Time Scale 1V /div
   Inverted? (Yes) No
2. Lower Trace
   Voltage 5V /div
   Time Scale 1μsec /div
   Inverted? Yes (No)
   Attenuation _____

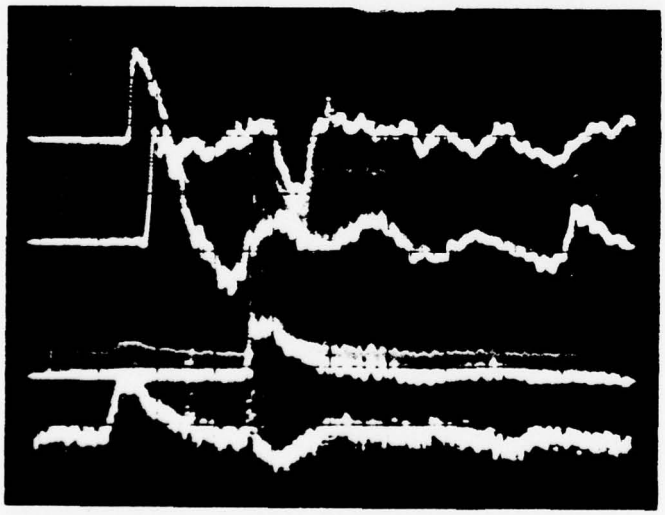

Voltages

P_1 Ch. 1 0.02V /div
P_6 Ch. 2 0.02V /div
P_{5A} Ch. 3 0.02V /div
T_7 Ch. 4 0.05V /div

Time Scale 2msec /div
Sustainer Voltage 25.9kV
Flow? On (Off)
Gas Type N_2
Notes: 1 muffler only

Analyzed Data:

E = 33.80

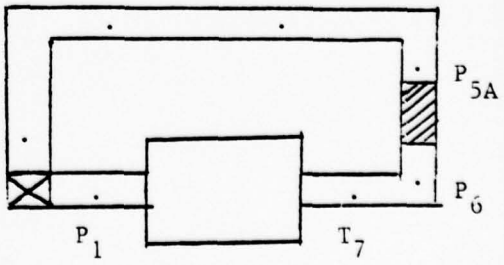

PVC Circulator Experimental Data

Page 136
No. 5382
Date 26 June 1978

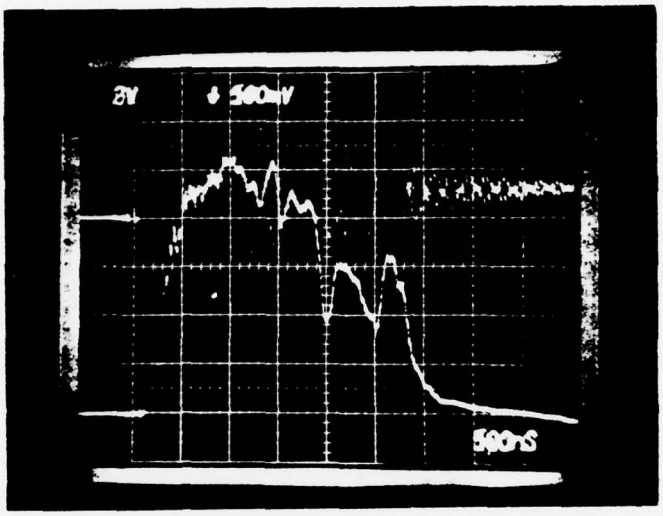

Gun Data

1. Upper Trace
   Voltage 500mV/div
   Time Scale 500nsec/div
   Inverted? (Yes) No
2. Lower Trace
   Voltage 2V /div
   Time Scale 500nsec/div
   Inverted? Yes (No)
   Attenuation _____

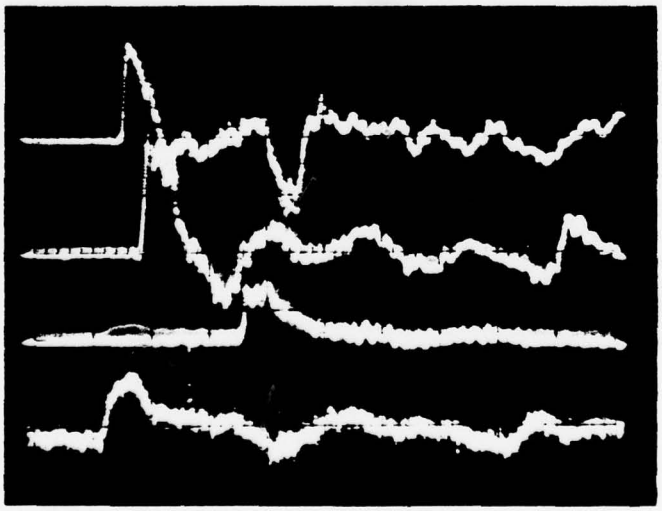

Voltages

P_1 Ch. 1 0.02V /div

P_6 Ch. 2 0.02V /div

$P_{5.5}$ Ch. 3 0.02V /div

T_7 Ch. 4 0.05V /div

Time Scale 2msec /div
Sustainer Voltage 26.2kV
Flow? On (Off)
Gas Type N_2
Notes: _____

Analyzed Data:

E = 106.4045

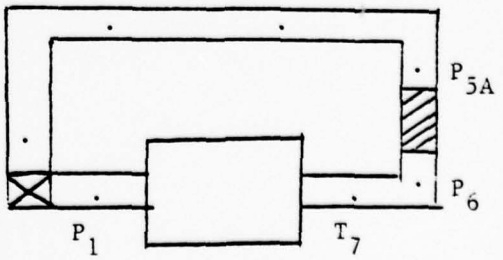

PVC Circulator Experimental Data

Page 137
No. 5400
Date _____

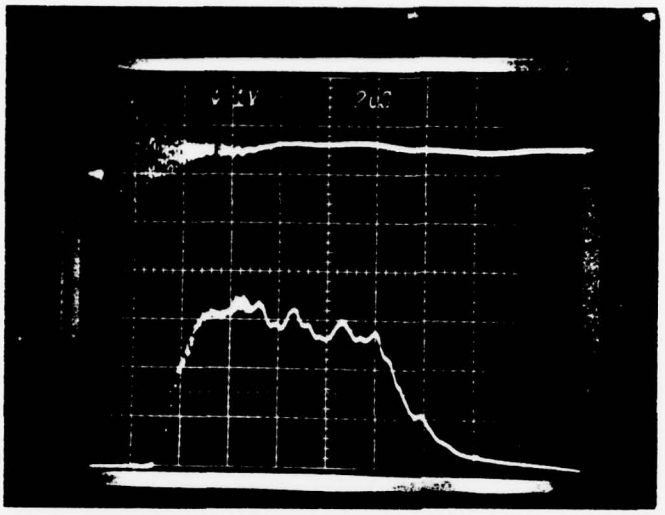

Gun Data

1. Upper Trace
   Voltage 1V /div
   Time Scale 2μsec/div
   Inverted? (Yes) No
2. Lower Trace
   Voltage 5V /div
   Time Scale 500nsec/div
   Inverted? Yes (No)
   Attenuation _____

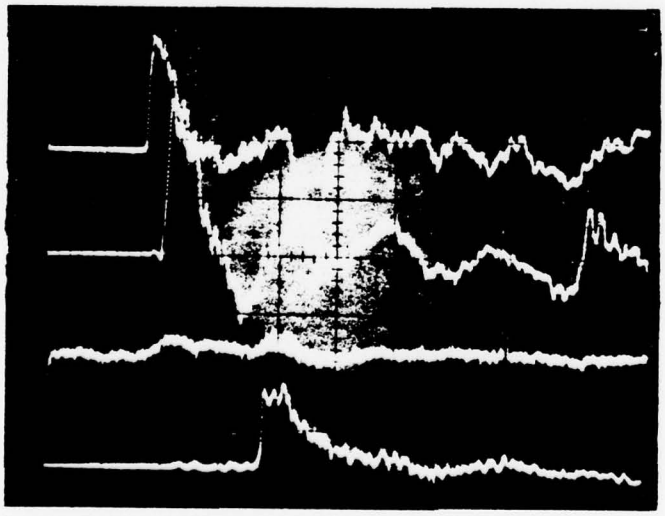

Voltages

P_1 Ch. 1 0.02V /div
P_6 Ch. 2 0.02V /div
T_7 Ch. 3 0.10V /div
P_{5A} Ch. 4 0.02V /div

Time Scale 2msec /div
Sustainer Voltage 28.8kV
Flow? On (Off)
Gas Type N_2
Notes: _____

Analyzed Data:

E = 56.59535

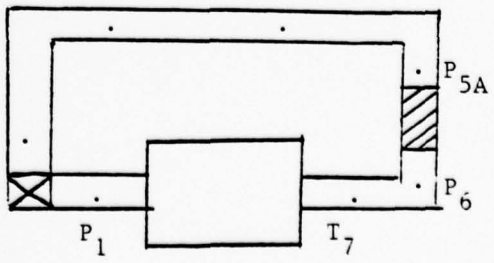

PVC Circulator Experimental Data

Page 138
No. 5402
Date _____

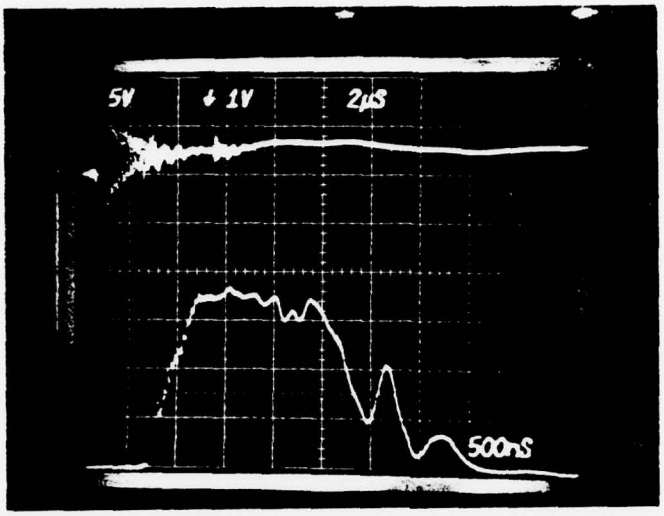

Gun Data

1. Upper Trace
   Voltage 1V /div
   Time Scale 2usec/div
   Inverted? (Yes) No
2. Lower Trace
   Voltage 5V /div
   Time Scale 500nsec/div
   Inverted? Yes (No)
   Attenuation _____

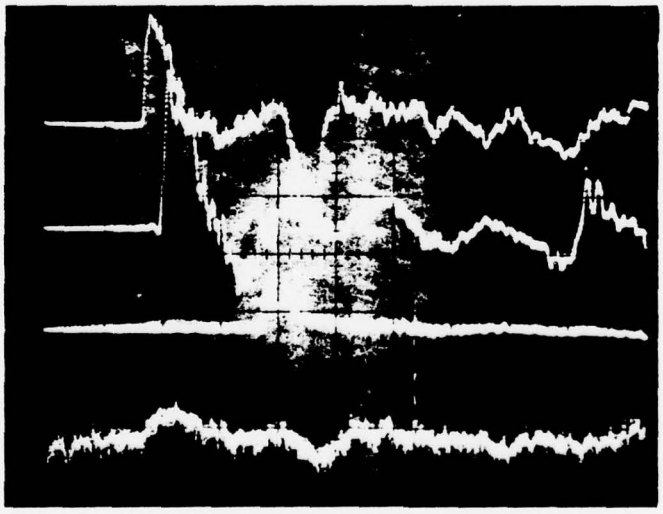

Voltages

P_1 Ch. 1 0.02V /div

P_6 Ch. 2 0.02V /div

P_{5A} Ch. 3 0.05V /div

T_1 Ch. 4 0.05V /div

Time Scale 2msec /div
Sustainer Voltage 25.9kV
Flow? On (Off)
Gas Type N_2
Notes: _____

Analyzed Data:

E = 49.01

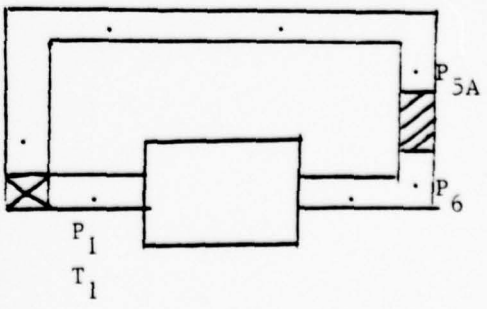

PVC Circulator Experimental Data

Page 139
No. 5403
Date _____

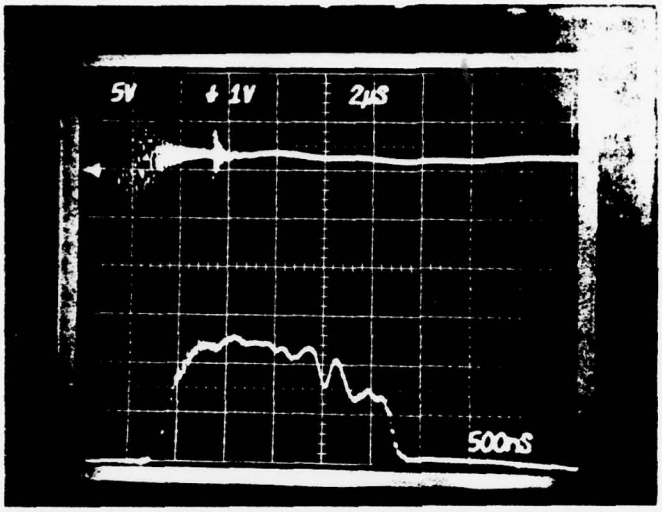

Gun Data

1. Upper Trace
   Voltage 1V /div
   Time Scale 2μsec /div
   Inverted? (Yes) No
2. Lower Trace
   Voltage 5V /div
   Time Scale 500nsec/div
   Inverted? Yes (No)
   Attenuation _____

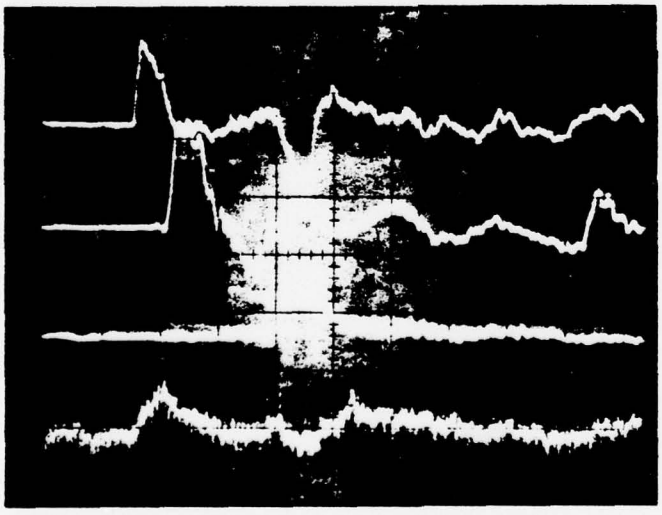

Voltages

P_1 Ch. 1 0.02V /div
P_6 Ch. 2 0.02V /div
P_{5A} Ch. 3 0.02V /div
T_1 Ch. 4 0.05V /div

Time Scale 2msec /div
Sustainer Voltage 26.0kV
Flow? (On) Off
Gas Type N_2
Notes: _____

Analyzed Data:

E = 34.06202

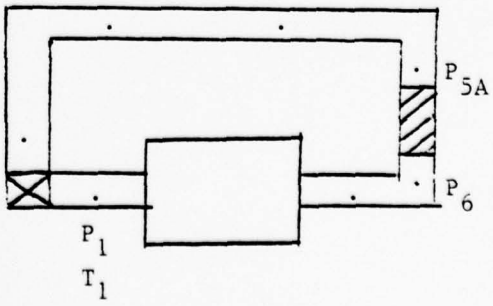

PVC Circulator Experimental Data

Page 140
No. 5408
Date 11 July 1978

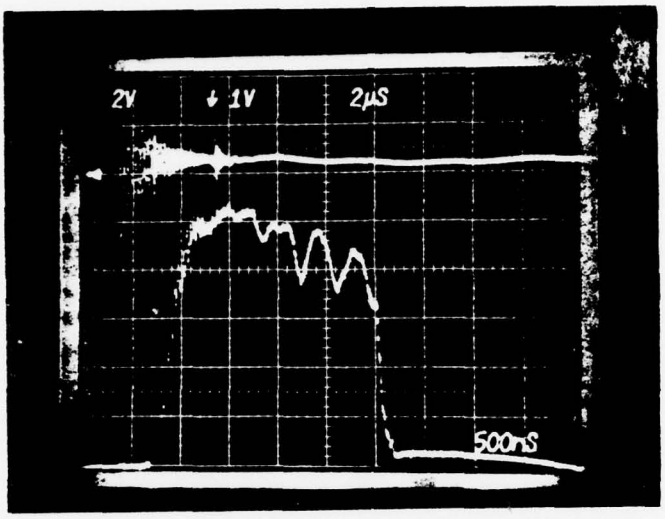

Gun Data

1. Upper Trace
   Voltage 1V /div
   Time Scale 2μsec /div
   Inverted? (Yes) No
2. Lower Trace
   Voltage 2V /div
   Time Scale 500nsec/div
   Inverted? Yes (No)
   Attenuation _____

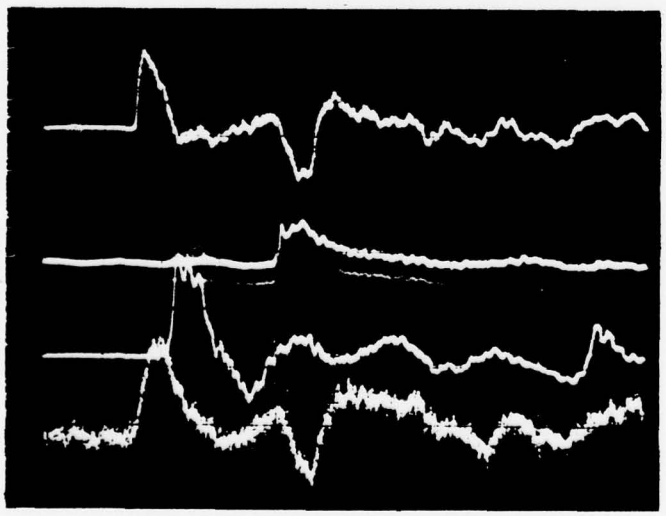

Voltages

P_1 Ch. 1 0.02V /div
P_{5A} Ch. 2 0.02V /div
P_6 Ch. 3 0.02V /div
T_1 Ch. 4 0.05V /div

Time Scale 2msec /div
Sustainer Voltage 26.7kV
Flow? (On) Off
Gas Type N_2
Notes: _____

Analyzed Data:

E = 71.70709

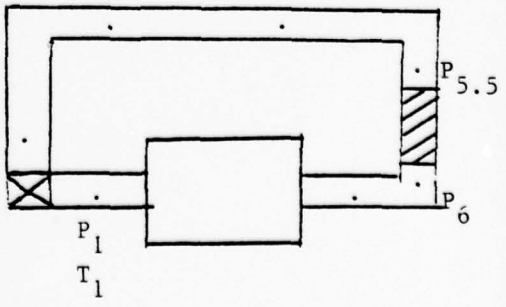

PVC Circulator Experimental Data

Page 141
No. 5410
Date 11 July 1978

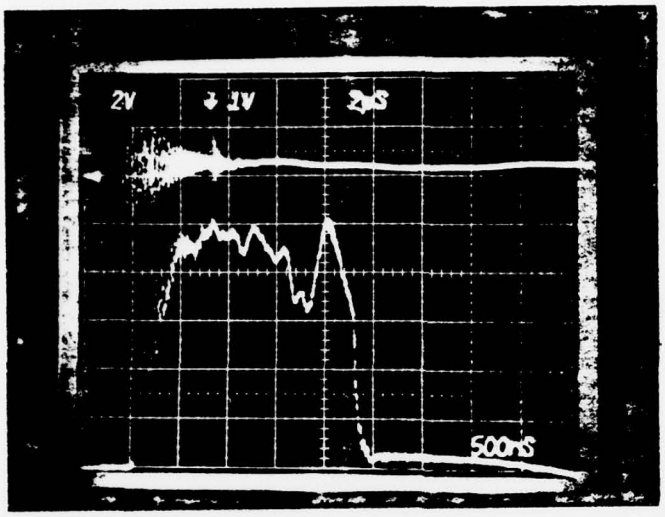

Gun Data

1. Upper Trace
   Voltage 1V /div
   Time Scale 2μsec/div
   Inverted? (Yes) No
2. Lower Trace
   Voltage 2V /div
   Time Scale 500nsec/div
   Inverted? Yes (No)
   Attenuation _____

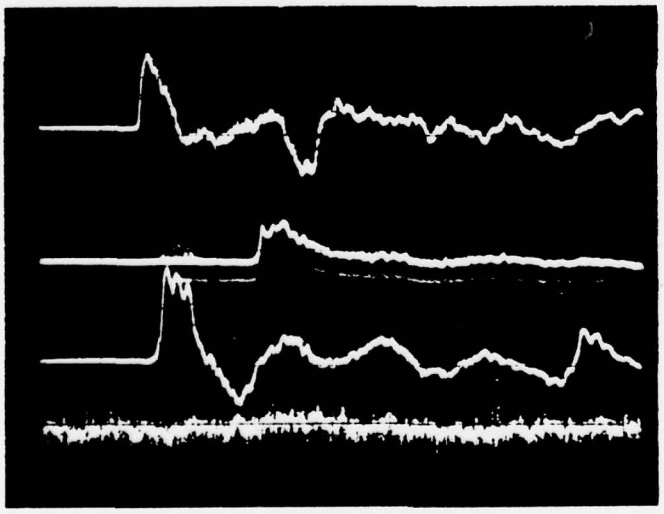

Voltages

P_1 Ch. 1 0.02V /div
$P_{5.5}$ Ch. 2 0.02V /div
P_6 Ch. 3 0.02V /div
T_2 Ch. 4 0.05V /div

Time Scale 2msec /div
Sustainer Voltage 25.8kV
Flow? On (Off)
Gas Type N_2
Notes: _____

Analyzed Data:

E = 64.22

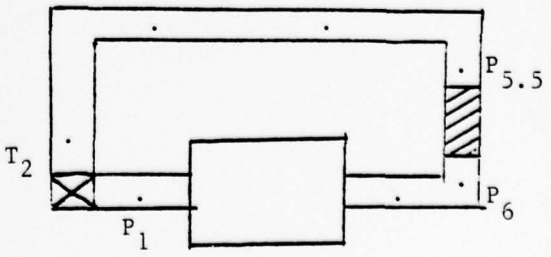

PVC Circulator Experimental Data

Page 143
No. 5412
Date 11 July 1978

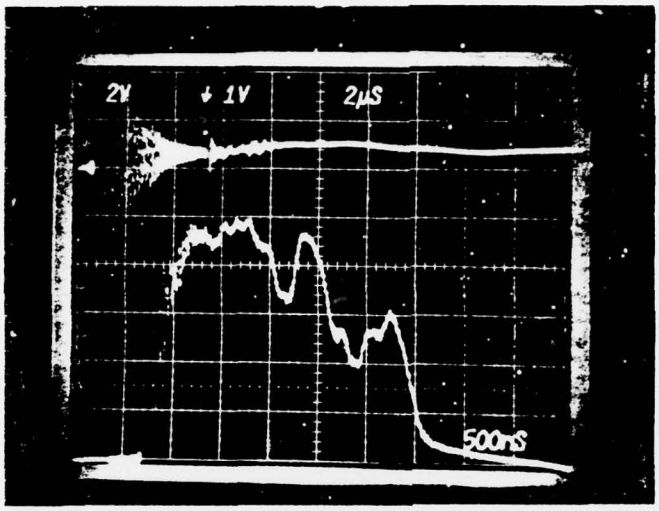

Gun Data

1. Upper Trace
   Voltage 1V /div
   Time Scale 2μsec /div
   Inverted? (Yes) No
2. Lower Trace
   Voltage 2V /div
   Time Scale 500nsec/div
   Inverted? Yes (No)
   Attenuation _____

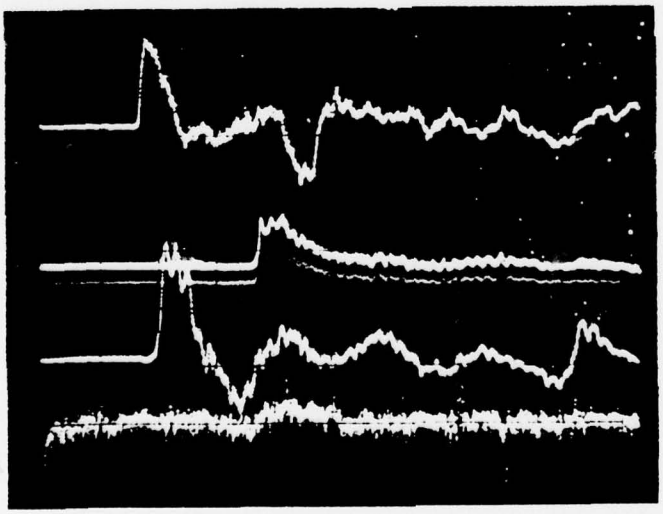

Voltages

P_1 Ch. 1 0.02V /div

P_6 Ch. 2 0.02V /div

$P_{5.5}$ Ch. 3 0.02V /div

T_2 Ch. 4 0.05V /div

Time Scale 2msec /div
Sustainer Voltage 25.8
Flow? On (Off)
Gas Type N_2
Notes: _____

Analyzed Data:

E = 67.6

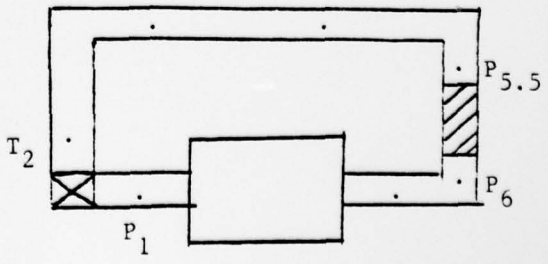

PVC Circulator Experimental Data

Page 144
No. 5413
Date 11 July 1978

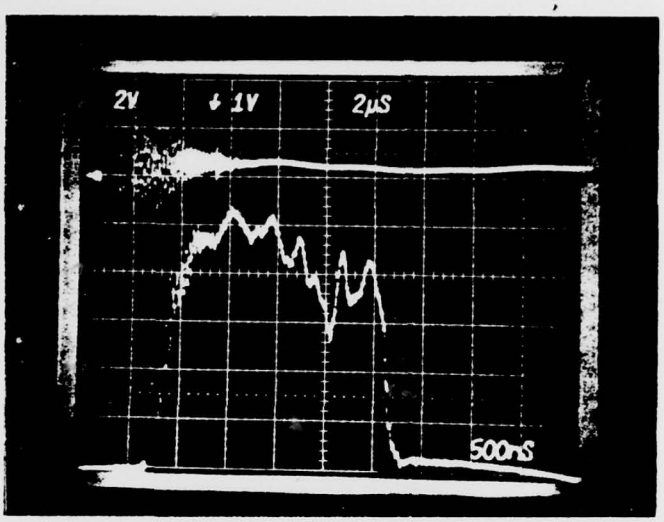

Gun Data

1. Upper Trace
   Voltage 1V /div
   Time Scale 2μsec /div
   Inverted? (Yes) No
2. Lower Trace
   Voltage 2V /div
   Time Scale 500nsec/div
   Inverted? Yes (No)
   Attenuation _____

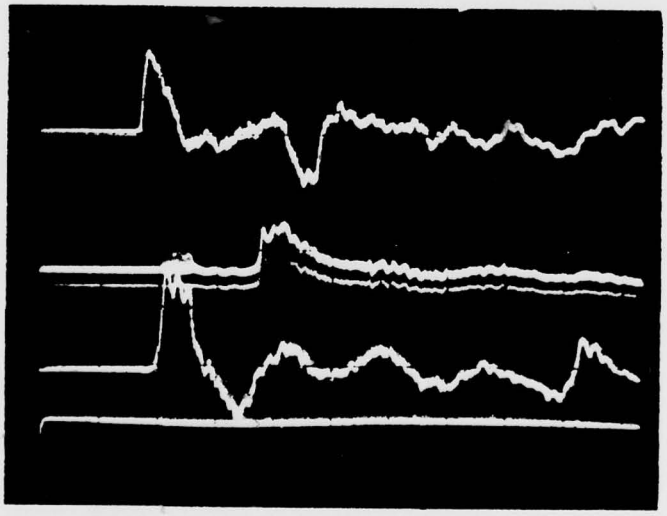

Voltages

P_1 Ch. 1 0.02V /div
P_6 Ch. 2 0.02V /div
$P_{5.5}$ Ch. 3 0.02V /div
T_7 Ch. 4 0.05V /div

Time Scale 2msec /div
Sustainer Voltage 25.8
Flow? On (Off)
Gas Type N_2
Notes: temp. unit off

Analyzed Data:

E = 67.6

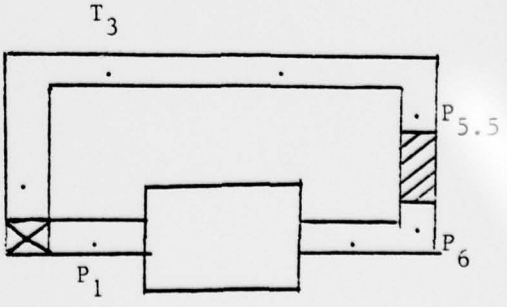

PVC Circulator Experimental Data

Page 145
No. 5414
Date 11 July 1978

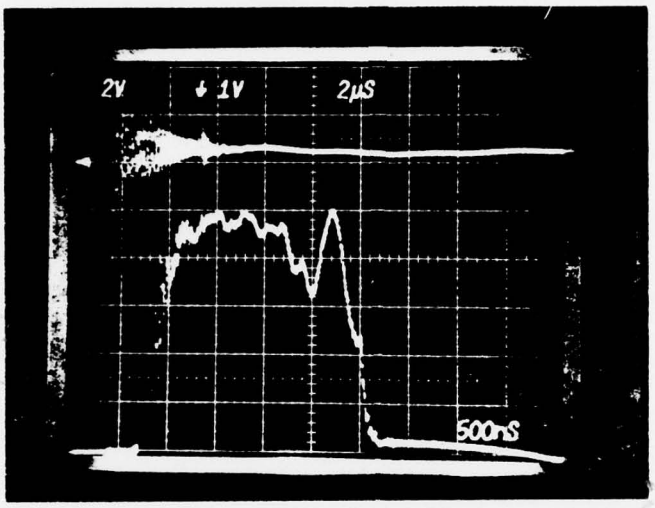

Gun Data

1. Upper Trace
   Voltage 1V /div
   Time Scale 2μsec/div
   Inverted? (Yes) No
2. Lower Trace
   Voltage 2V /div
   Time Scale 500nsec/div
   Inverted? Yes (No)
   Attenuation _____

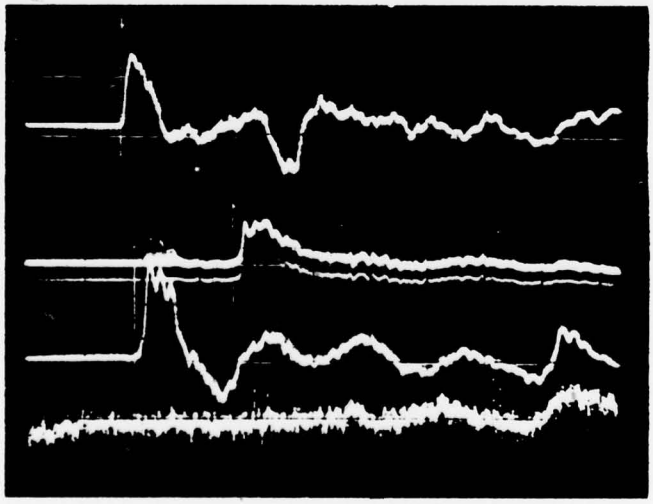

Voltages

P_1 Ch. 1 0.02V /div

P_6 Ch. 2 0.02V /div

$P_{5.5}$ Ch. 3 0.02V /div

T_3 Ch. 4 0.05V /div

Time Scale 2msec /div
Sustainer Voltage 25.8
Flow? On (Off)
Gas Type N_2
Notes: _____

Analyzed Data:

E = 60.84

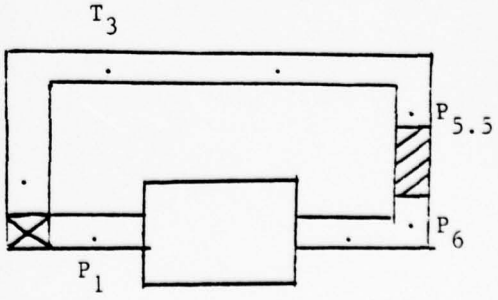

PVC Circulator Experimental Data

Page 146
No. 5415
Date 11 July 1978

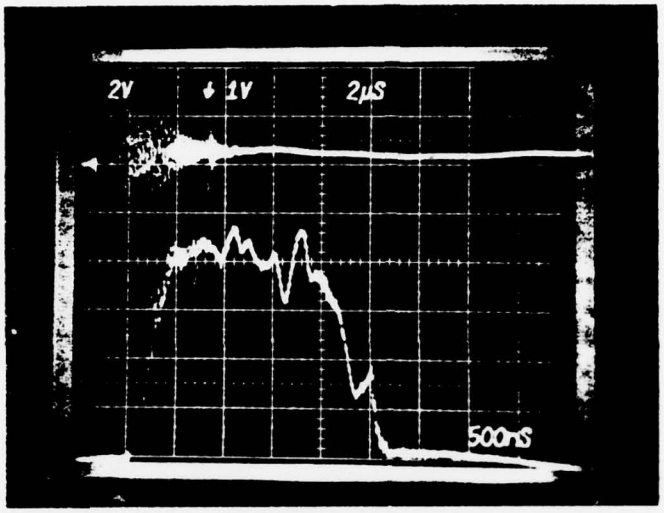

Gun Data

1. Upper Trace
   Voltage 1V /div
   Time Scale 2μsec/div
   Inverted? (Yes) No
2. Lower Trace
   Voltage 2V /div
   Time Scale 500nsec/div
   Inverted? Yes (No)
   Attenuation _____

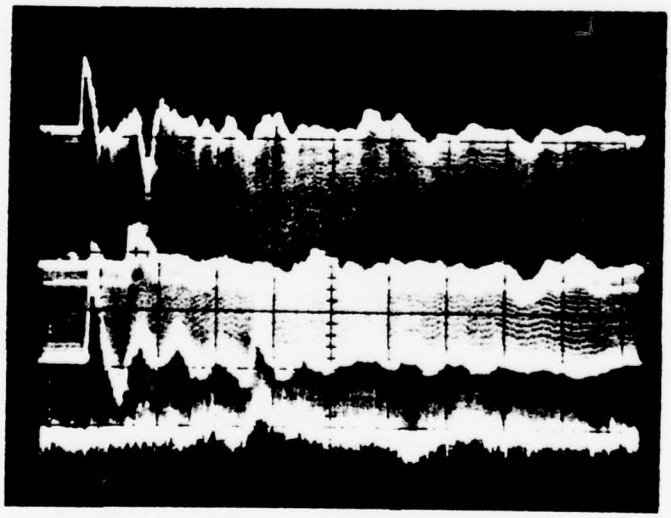

Voltages

P_1 Ch. 1 0.02V /div

P_6 Ch. 2 0.02V /div

$P_{5.5}$ Ch. 3 0.02V /div

T_3 Ch. 4 0.05V /div

Time Scale 5msec /div
Sustainer Voltage 25.8
Flow? (On) Off
Gas Type N_2
Notes: _____

Analyzed Data:

E = 57.46

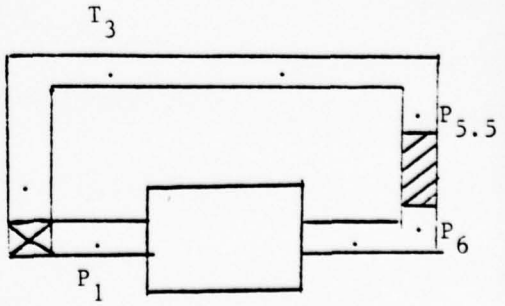

PVC Circulator Experimental Data

Page 147
No. 5416
Date 30 June 1978

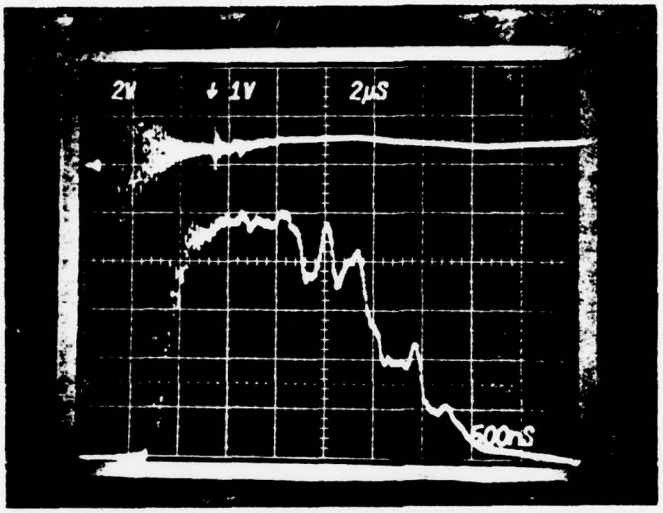

Gun Data

1. Upper Trace
   Voltage 1V /div
   Time Scale 2μsec/div
   Inverted? (Yes) No
2. Lower Trace
   Voltage 2V /div
   Time Scale 500nsec/div
   Inverted? Yes (No)
   Attenuation _____

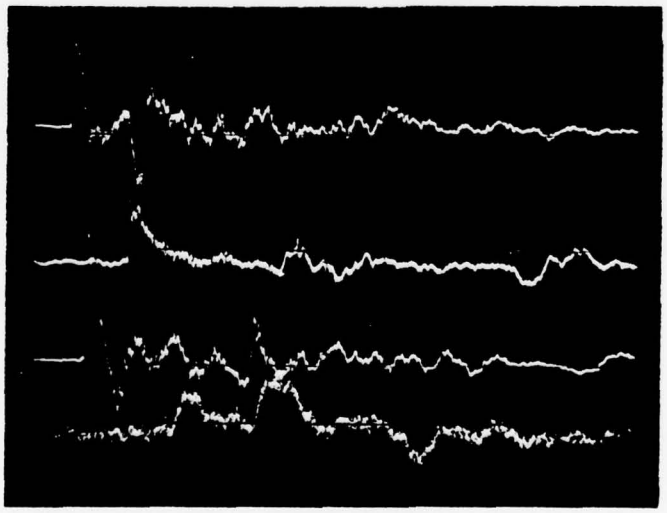

Voltages

P_1 Ch. 1 0.02V /div
P_6 Ch. 2 0.02V /div
$P_{5.5}$ Ch. 3 0.02V /div
T_3 Ch. 4 0.05V /div

Time Scale 5msec /div
Sustainer Voltage 25.8
Flow? (On) Off
Gas Type N_2
Notes: _____

Analyzed Data:

E = 72.67

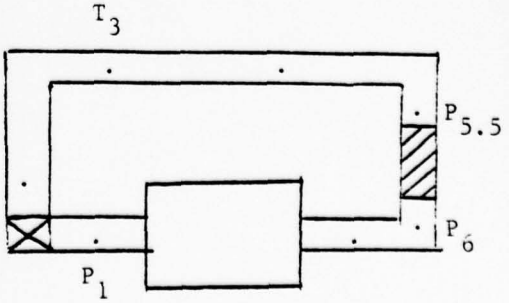

PVC Circulator Experimental Data

Page 148
No. 5420
Date 11 July 1978

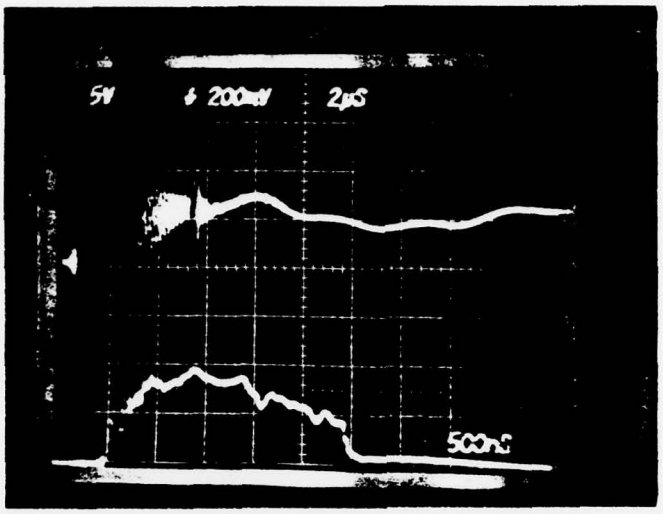

Gun Data

1. Upper Trace
   Voltage 200mV/div
   Time Scale 2msec/div
   Inverted? (Yes) No
2. Lower Trace
   Voltage 5V /div
   Time Scale 500nsec/div
   Inverted? Yes (No)
   Attenuation _____

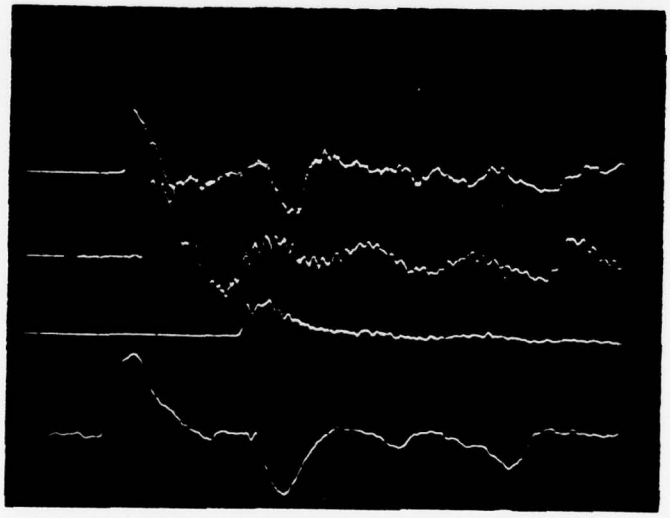

Voltages

P_1 Ch. 1 0.02V /div

P_6 Ch. 2 0.02V /div

P_{5A} Ch. 3 0.02V /div

T_7 Ch. 4 0.05V /div

Time Scale 2msec /div
Sustainer Voltage 25.8kV
Flow? On (Off)
Gas Type N_2
Notes: Muffler (II)

Analyzed Data:

E = 23.66

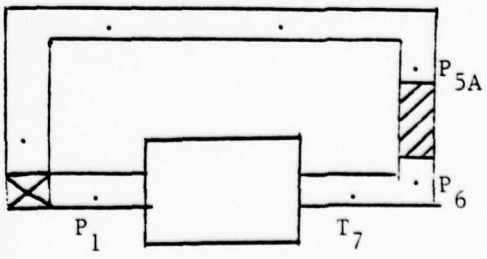

PVC Circulator Experimental Data

Page 149
No. 5421
Date 11 July 1978

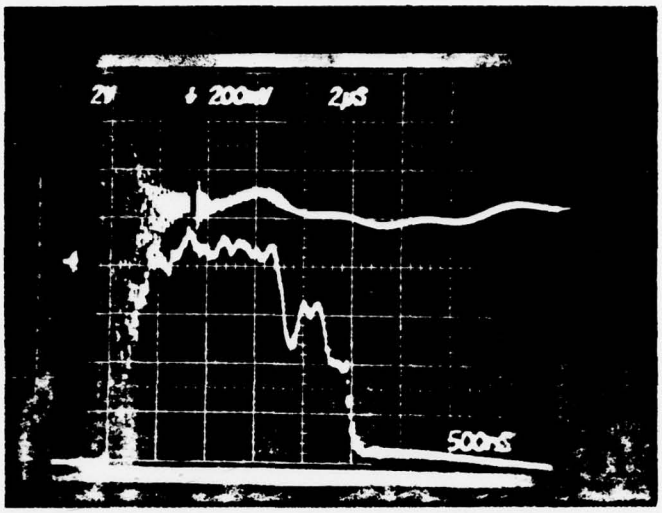

Gun Data

1. Upper Trace
   Voltage 200mV/div
   Time Scale 2msec /div
   Inverted? (Yes) No
2. Lower Trace
   Voltage 2V /div
   Time Scale 500nsec/div
   Inverted? Yes (No)
   Attenuation _____

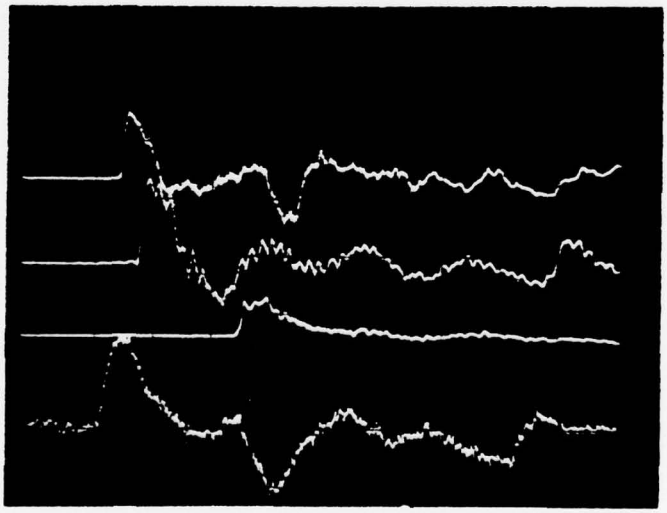

Voltages

P_1 Ch. 1 0.02V /div
P_6 Ch. 2 0.02V /div
P_{5A} Ch. 3 0.02V /div
T_7 Ch. 4 0.05V /div

Time Scale 2msec /div
Sustainer Voltage 25.8kV
Flow? On (Off)
Gas Type N_2
Notes: _____

Analyzed Data:

E = 57.46

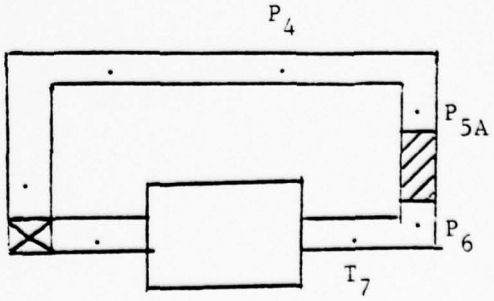

PVC Circulator Experimental Data

Page 150
No. 5422
Date 11 July 1978

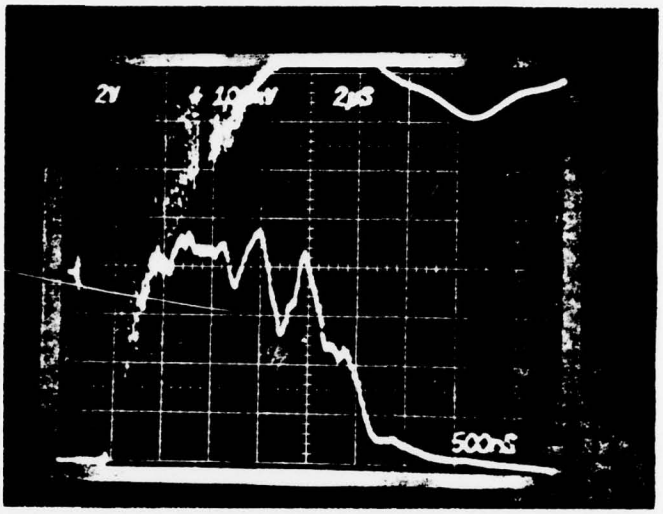

Gun Data

1. Upper Trace
   Voltage 100mV/div
   Time Scale 2msec/div
   Inverted? (Yes) No
2. Lower Trace
   Voltage 2V /div
   Time Scale 500nsec/div
   Inverted? Yes (No)
   Attenuation _____

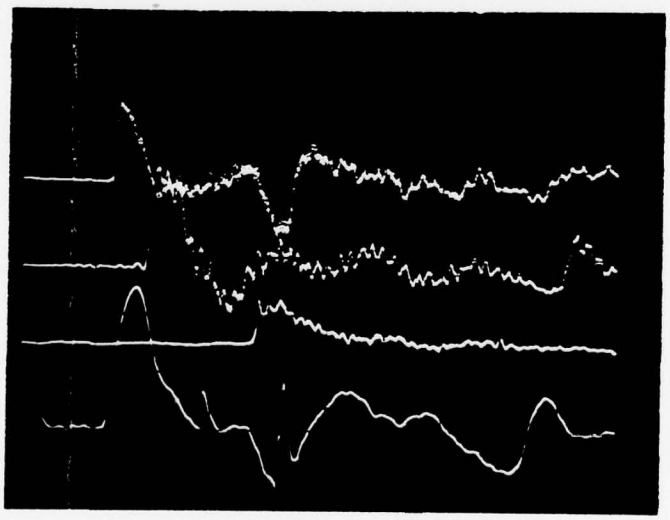

Voltages

P_1 Ch. 1 0.02V/div

P_6 Ch. 2 0.02V/div

P_{5A} Ch. 3 0.02V/div

T_7 Ch. 4 0.05V/div

Time Scale 2msec /div
Sustainer Voltage 25.8kV
Flow? (On) Off
Gas Type N_2
Notes: Muffler (II)

Analyzed Data:

E = 60.84

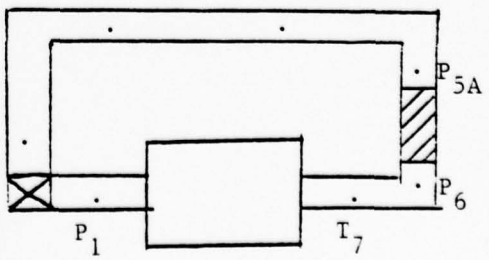

PVC Circulator Experimental Data

Page 151
No. 5423
Date 11 July 1978

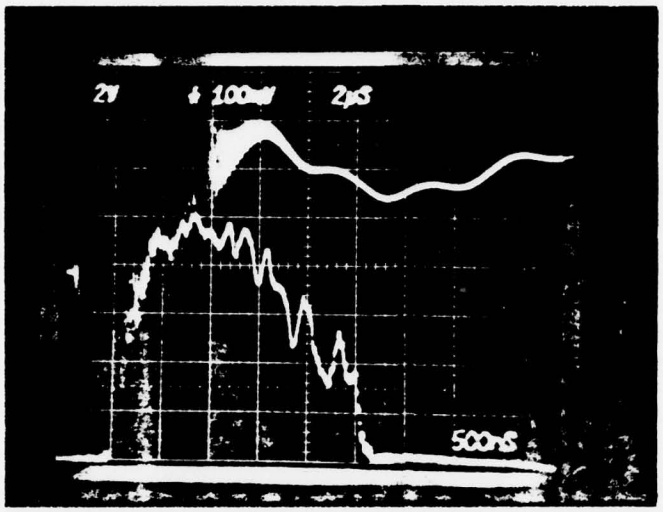

Gun Data

1. Upper Trace
   Voltage 100mV/div
   Time Scale 2msec/div
   Inverted? (Yes) No
2. Lower Trace
   Voltage 2V /div
   Time Scale 500nsec/div
   Inverted? Yes (No)
   Attenuation _____

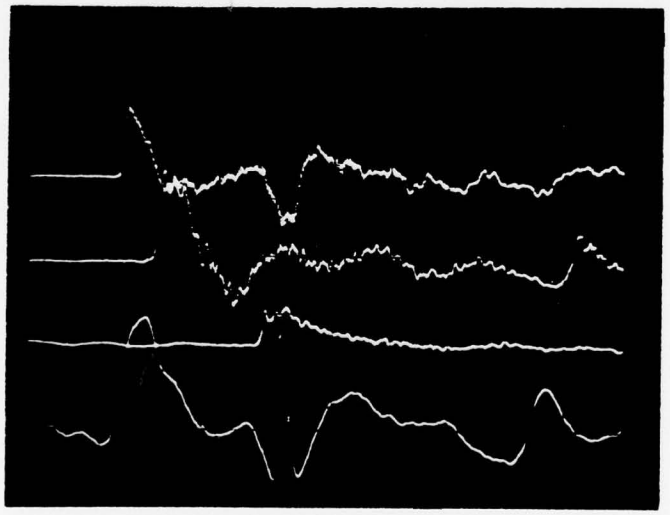

Voltages

P_6 Ch. 1 0.02V/div

P_{5A} Ch. 2 0.02V/div

P_4 Ch. 3 0.02V/div

T_7 Ch. 4 0.05V/div

Time Scale 2msec/div
Sustainer Voltage 25.8kV
Flow? (On) Off
Gas Type N_2
Notes: Muffler

Analyzed Data:

E = 60.84

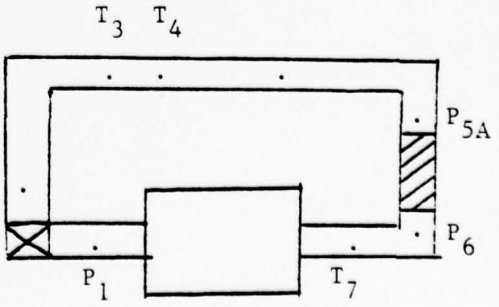

PVC Circulator Experimental Data

Page 152
No. 5424
Date 11 July 1978

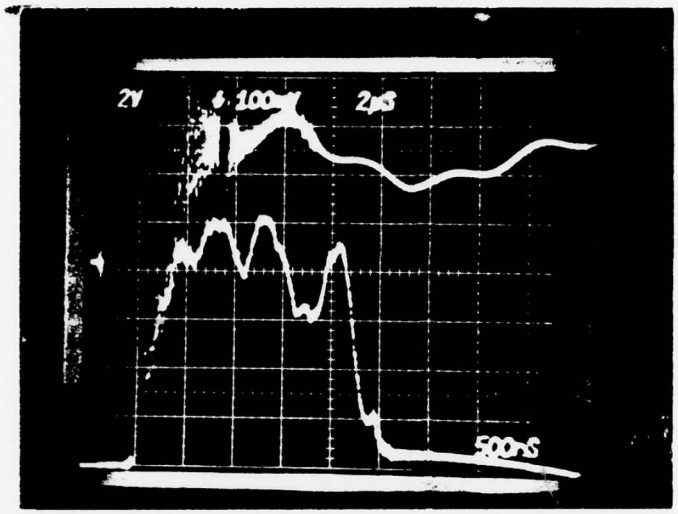

Gun Data

1. Upper Trace
   Voltage 100mV/div
   Time Scale 2μsec/div
   Inverted? (Yes) No
2. Lower Trace
   Voltage 2V /div
   Time Scale 500nsec/div
   Inverted? Yes (No)
   Attenuation _____

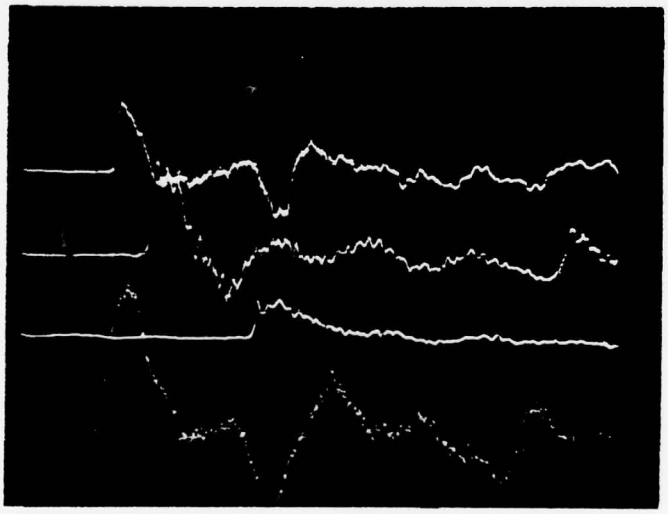

Voltages

P_1 Ch. 1 0.02V/div

P_6 Ch. 2 0.02V/div

$P_{5.5}$ Ch. 3 0.02V/div

T_3 Ch. 4 0.05V/div

Time Scale 2msec/div
Sustainer Voltage 25.8
Flow? On Off
Gas Type N_2
Notes: amp out

Analyzed Data:

E = 64.22

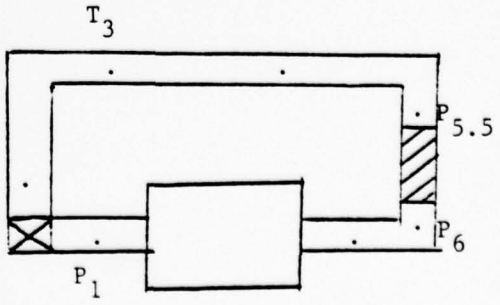

PVC Circulator Experimental Data

Page 153
No. 5425
Date 11 July 1978

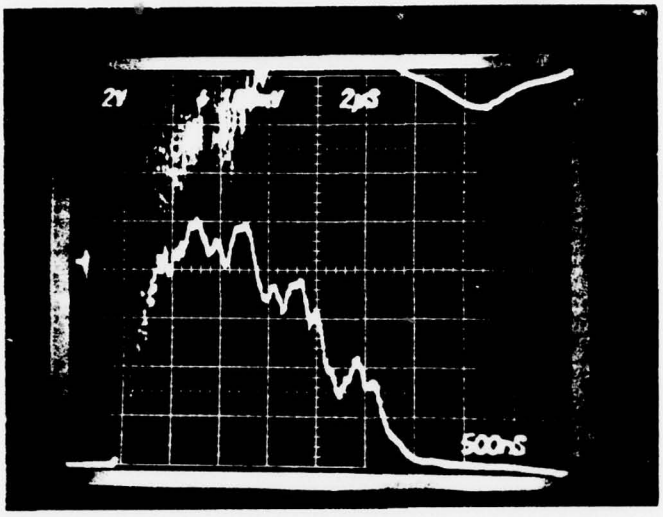

Gun Data

1. Upper Trace
   Voltage 100mV/div
   Time Scale 2msec /div
   Inverted? (Yes) No
2. Lower Trace
   Voltage 2V /div
   Time Scale 500nsec/div
   Inverted? Yes (No)
   Attenuation _____

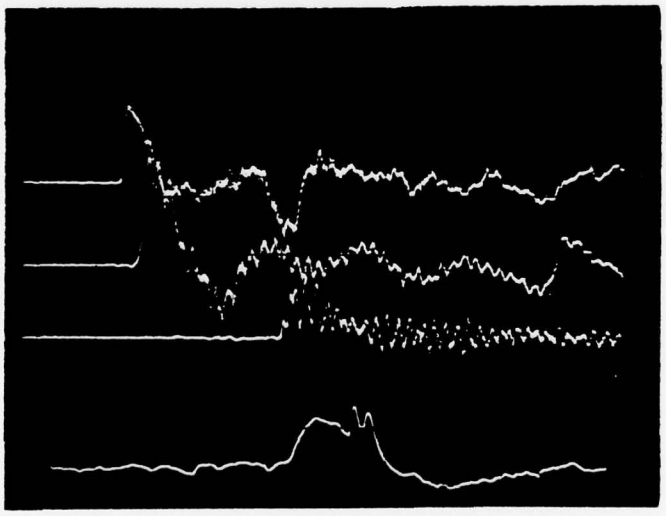

Voltages

P_1 Ch. 1 0.02V /div

P_6 Ch. 2 0.02V /div

P_5 Ch. 3 0.02V /div

T_5 Ch. 4 0.05V /div

Time Scale 2msec /div
Sustainer Voltage 25.8kV
Flow? On (Off)
Gas Type N_2
Notes: Muffler (II)

Analyzed Data:

E = 62.53

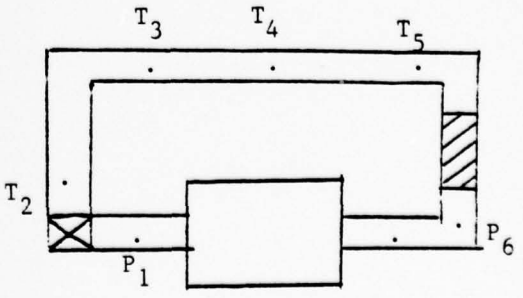

PVC Circulator Experimental Data

Page 154
No. 5426
Date 11 July 1978

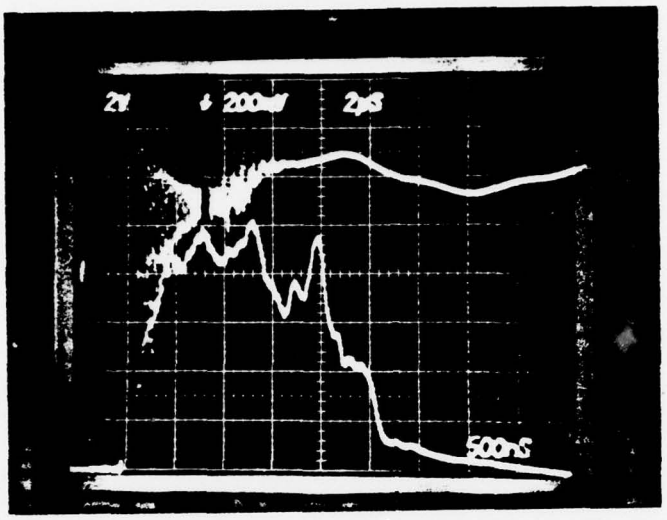

Gun Data

1. Upper Trace
   Voltage 200mV/div
   Time Scale 2msec/div
   Inverted? (Yes) No
2. Lower Trace
   Voltage 2V /div
   Time Scale 500nsec/div
   Inverted? Yes (No)
   Attenuation _____

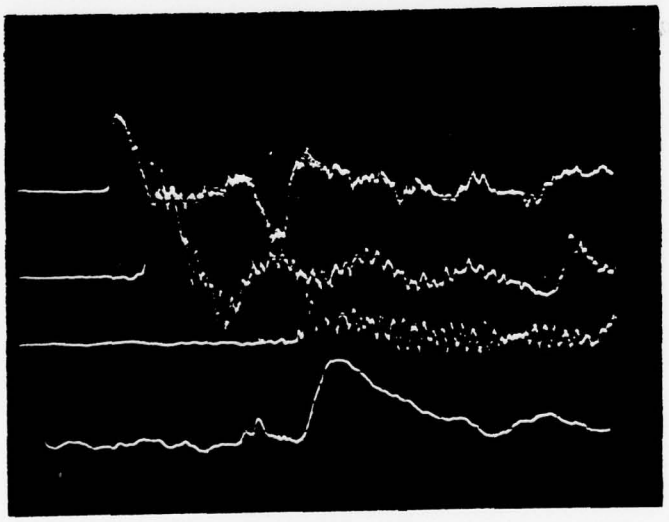

Voltages

P_1 Ch. 1 0.02V /div

P_6 Ch. 2 0.02V /div

P_5 Ch. 3 0.02V /div

T_5 Ch. 4 0.05V /div

Time Scale 2msec /div
Sustainer Voltage 25.8kV
Flow? (On) Off
Gas Type N_2
Notes: _____

Analyzed Data:

E = 64.22

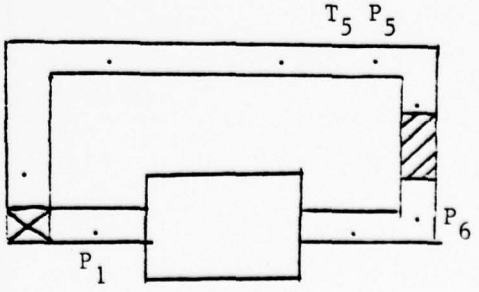

PVC Circulator Experimental Data

Page 155
No. 5427
Date 11 July 1978

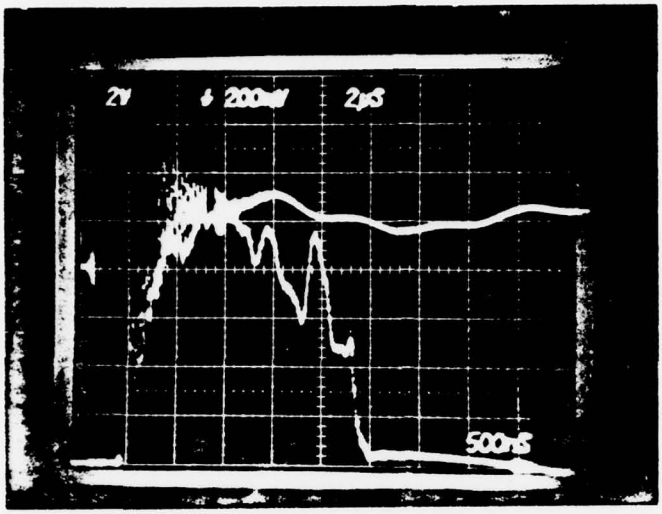

Gun Data

1. Upper Trace
   Voltage 200mV/div
   Time Scale 2msec/div
   Inverted? (Yes) No
2. Lower Trace
   Voltage 2V /div
   Time Scale 500nsec/div
   Inverted? Yes (No)
   Attenuation _____

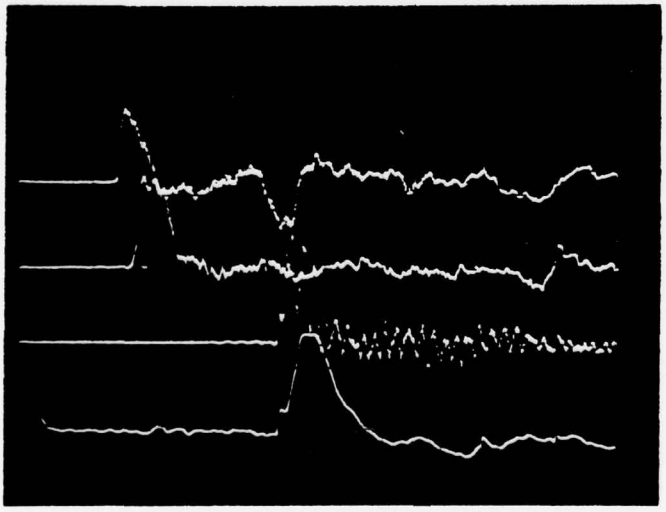

Voltages

P_1 Ch. 1 0.02V/div

P_6 Ch. 2 0.02V/div

P_5 Ch. 3 0.02V/div

T_5 Ch. 4 0.05V/div

Time Scale 2msec/div
Sustainer Voltage 25.8kV
Flow? On (Off)
Gas Type N_2
Notes: No Muffler

Analyzed Data:

E = 62.53

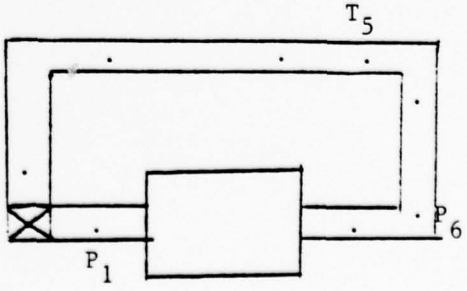

PVC Circulator Experimental Data

Page 156
No. 5428
Date 11 July 1978

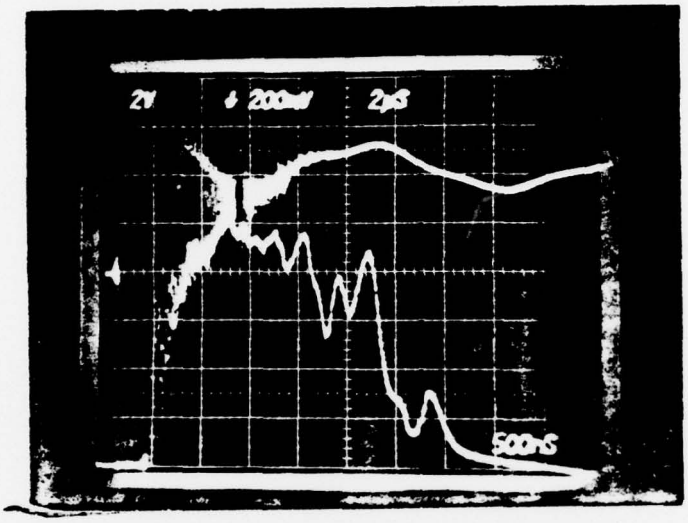

Gun Data

1. Upper Trace
   Voltage 200mV/div
   Time Scale 2msec/div
   Inverted? (Yes) No
2. Lower Trace
   Voltage 2V /div
   Time Scale 500nsec/div
   Inverted? Yes (No)
   Attenuation _____

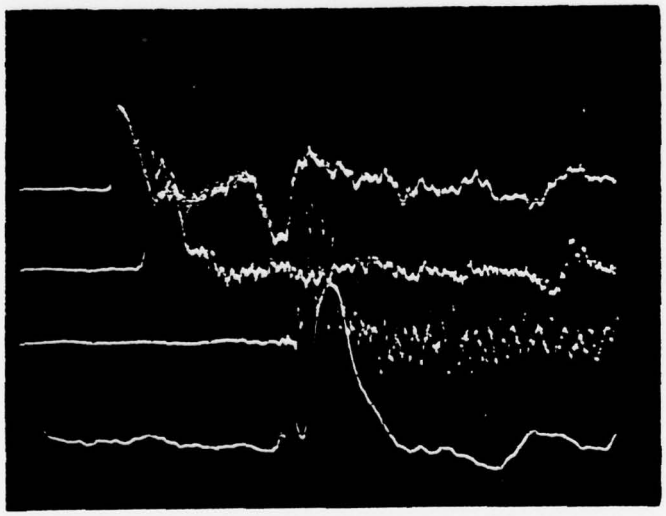

Voltages

P_1 Ch. 1 0.02V /div
P_6 Ch. 2 0.02V /div
P_5 Ch. 3 0.02V /div
T_5 Ch. 4 0.05V /div

Time Scale 2msec /div
Sustainer Voltage 25.8kV
Flow? (On) Off
Gas Type N_2
Notes: _____

Analyzed Data:

E = 67.6

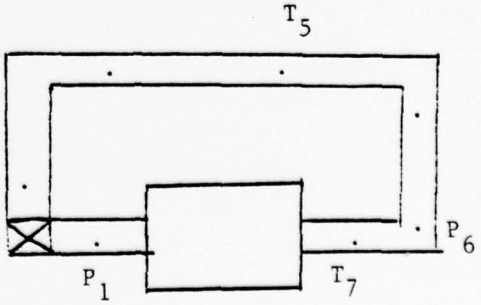

PVC Circulator Experimental Data

Page 157
No. 5430
Date 11 July 1978

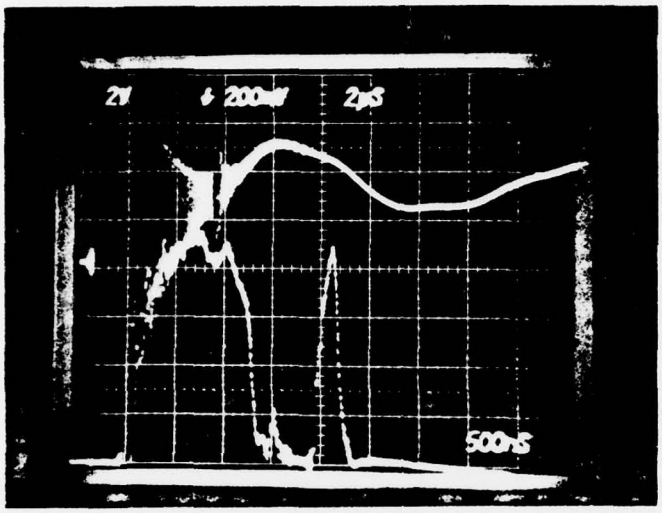

Gun Data

1. Upper Trace
   Voltage 200mV/div
   Time Scale 2msec/div
   Inverted? (Yes) No
2. Lower Trace
   Voltage 2V /div
   Time Scale 500nsec/div
   Inverted? Yes (No)
   Attenuation _____

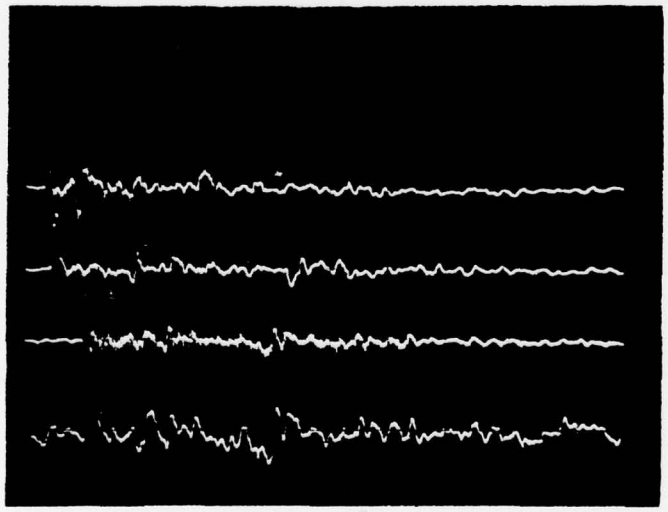

Voltages

P_1 Ch. 1 0.02V /div

P_6 Ch. 2 0.02V /div

P_5 Ch. 3 0.02V /div

T_5 Ch. 4 0.05V /div

Time Scale 10msec /div
Sustainer Voltage 25.8kV
Flow? (On) Off
Gas Type N_2
Notes: _____

Analyzed Data:

E = 37.18

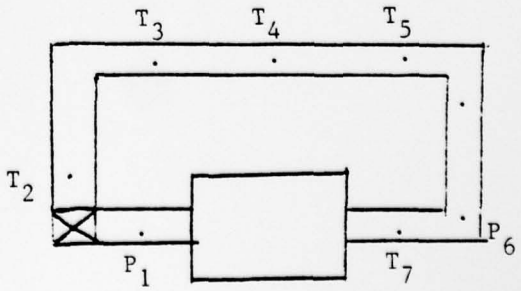

PVC Circulator Experimental Data

Page 158
No. 5431
Date 11 July 1978

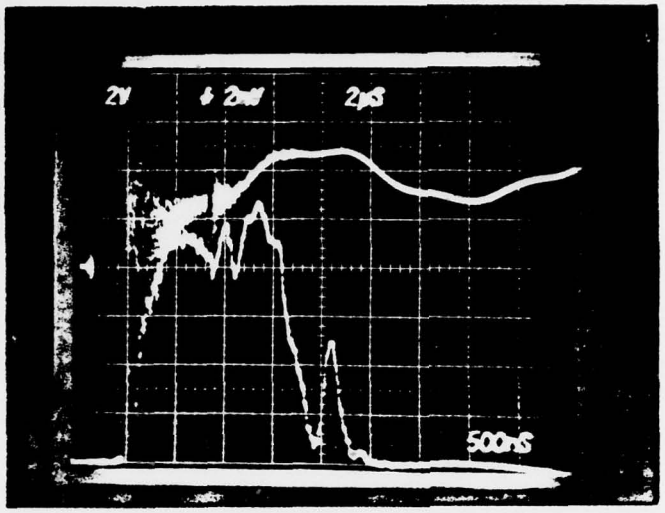

Gun Data

1. Upper Trace
   Voltage 2mV /div
   Time Scale 2msec/div
   Inverted? (Yes) No
2. Lower Trace
   Voltage 2V /div
   Time Scale 500nsec/div
   Inverted? Yes (No)
   Attenuation _____

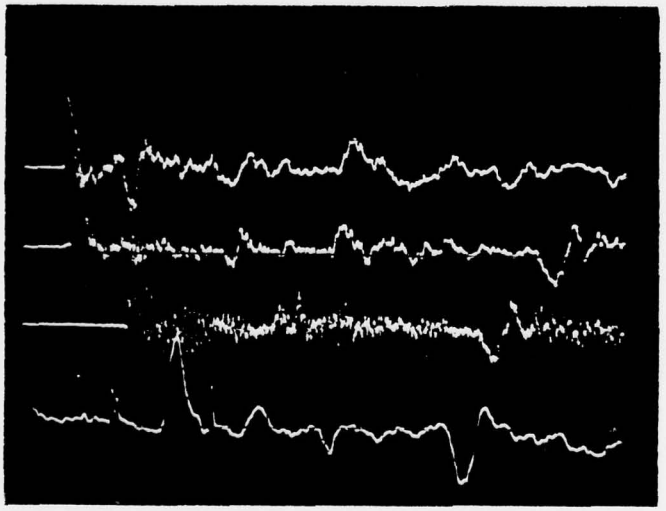

Voltages

P_1 Ch. 1 0.02V /div
P_6 Ch. 2 0.02V /div
P_5 Ch. 3 0.02V /div
T_4 Ch. 4 0.05V /div

Time Scale 5msec /div
Sustainer Voltage 25.8kV
Flow? On (Off)
Gas Type N_2
Notes: _____

Analyzed Data:

E = 54.08

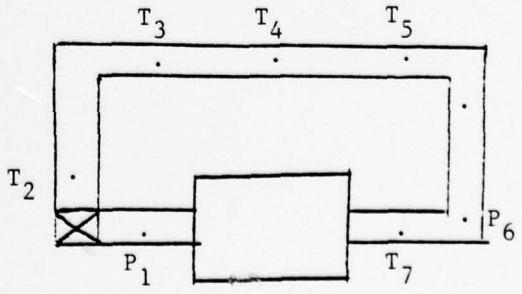

PVC Circulator Experimental Data

Page 159
No. 5433
Date 11 July 1978

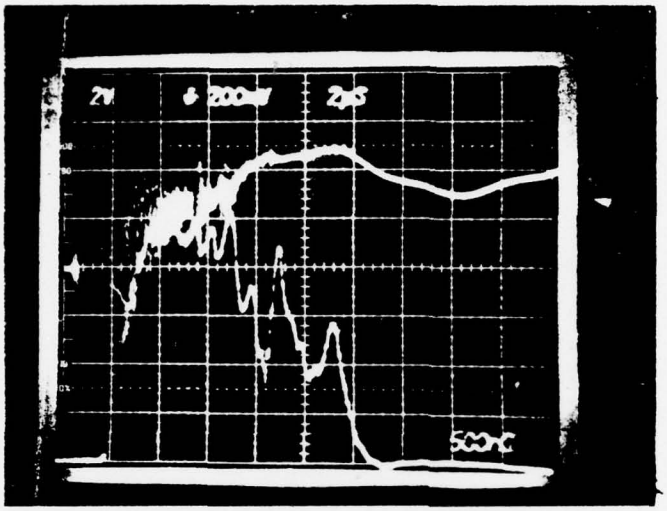

Gun Data

1. Upper Trace
   Voltage 200mV/div
   Time Scale 2msec/div
   Inverted? (Yes) No
2. Lower Trace
   Voltage 2V /div
   Time Scale 500nsec/div
   Inverted? Yes (No)
   Attenuation _____

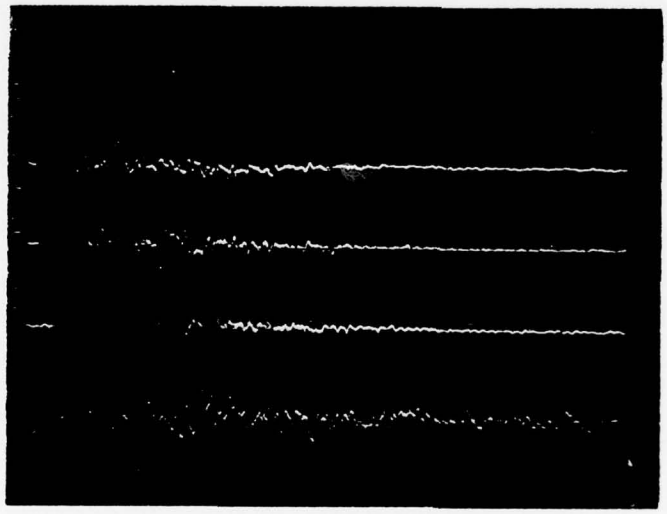

Voltages

P_1 Ch. 1 0.02V /div

P_6 Ch. 2 0.02V /div

P_5 Ch. 3 0.02V /div

T_4 Ch. 4 0.05V /div

Time Scale 20msec /div
Sustainer Voltage 25.8kV
Flow? (On) Off
Gas Type N_2
Notes: _____

Analyzed Data:

E = 59.15

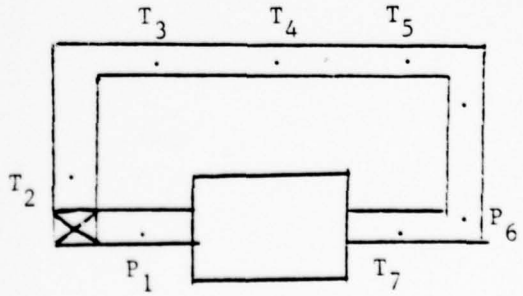

PVC Circulator Experimental Data

Page 160
No. 5435
Date 11 July 1978

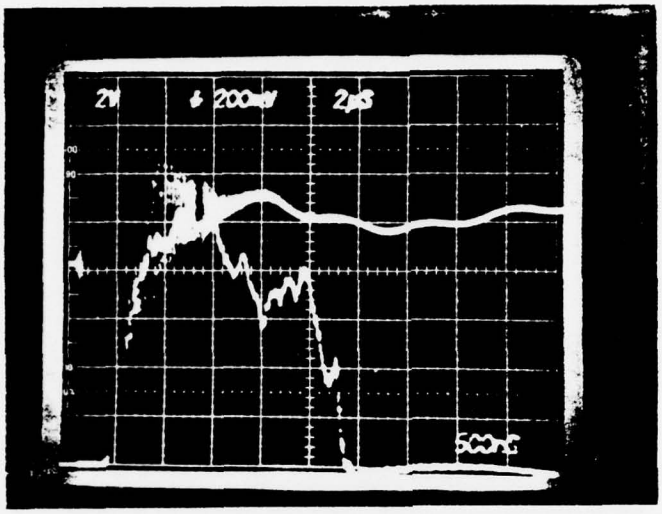

Gun Data

1. Upper Trace
   Voltage 200mV/div
   Time Scale 2μsec/div
   Inverted? (Yes) No
2. Lower Trace
   Voltage 2V /div
   Time Scale 500nsec/div
   Inverted? Yes (No)
   Attenuation _____

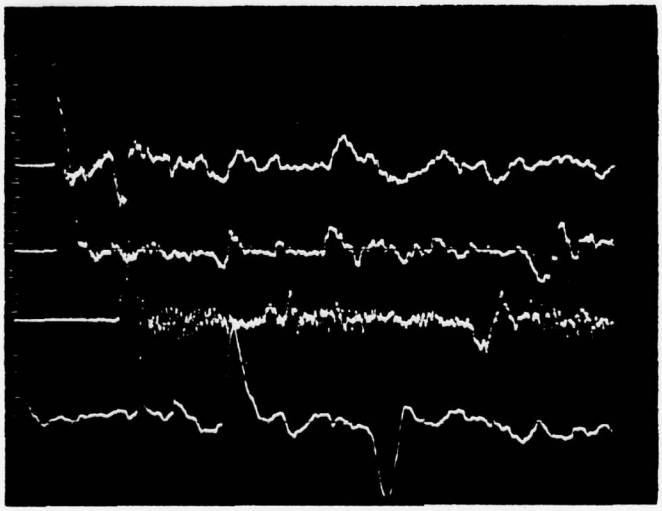

Voltages

P_1 Ch. 1 0.02V /div

P_6 Ch. 2 0.02V /div

$P_{5.5}$ Ch. 3 0.02V /div

T_3 Ch. 4 0.05V /div

Time Scale 5msec /div
Sustainer Voltage 25.8kV
Flow? On (Off)
Gas Type N_2
Notes: No muffler

Analyzed Data:

E = 59.15

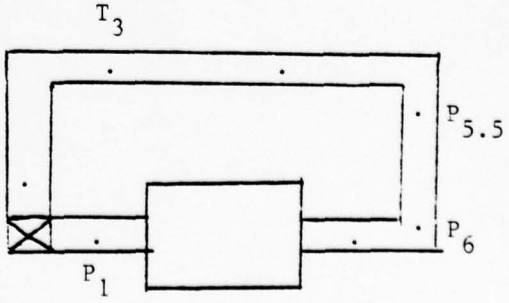

PVC Circulator Experimental Data

Page 161
No. 5436
Date 11 July 1978

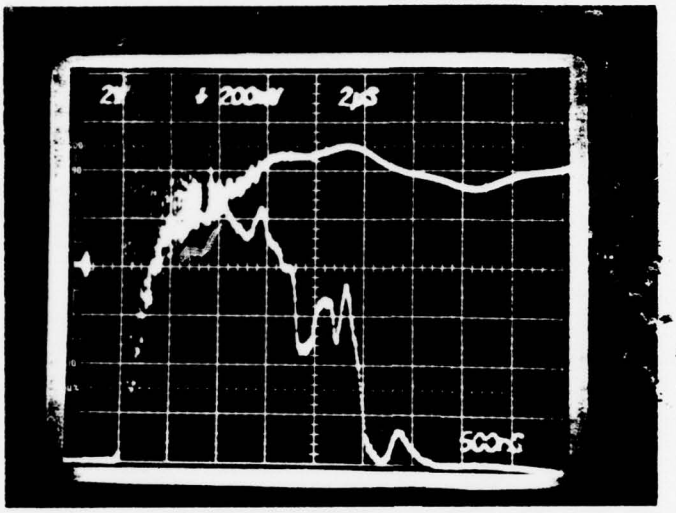

Gun Data

1. Upper Trace
   Voltage 200mV/div
   Time Scale 2μsec/div
   Inverted? (Yes) No
2. Lower Trace
   Voltage 2V /div
   Time Scale 500nsec/div
   Inverted? Yes (No)
   Attenuation _____

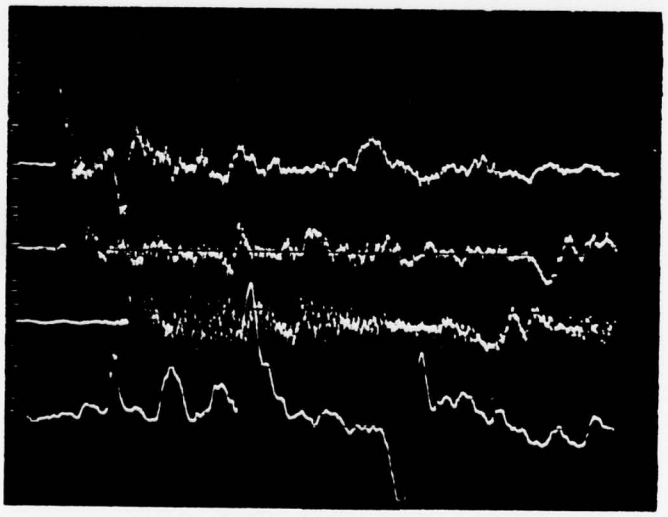

Voltages

P_1 Ch. 1 0.02V /div

P_6 Ch. 2 0.02V /div

$P_{5.5}$ Ch. 3 0.02V /div

T_3 Ch. 4 0.05V /div

Time Scale 5msec /div
Sustainer Voltage 25.8kV
Flow? (On) Off
Gas Type N_2
Notes: No muffler

Analyzed Data:

E = 65.91

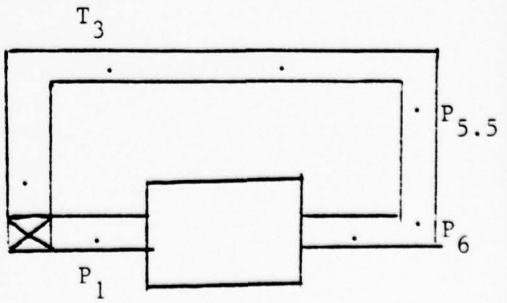

PVC Circulator Experimental Data

Page 162
No. 5437
Date 11 July 1978

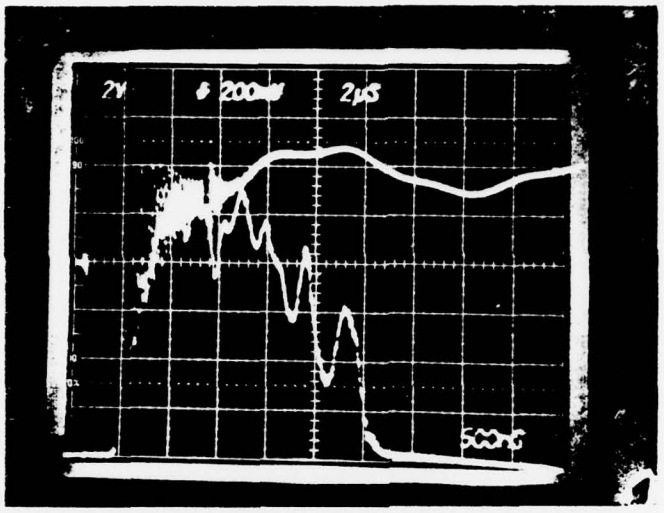

Gun Data

1. Upper Trace
   Voltage 200mV/div
   Time Scale 2usec/div
   Inverted? (Yes) No
2. Lower Trace
   Voltage 2V /div
   Time Scale 500nsec/div
   Inverted? Yes (No)
   Attenuation _____

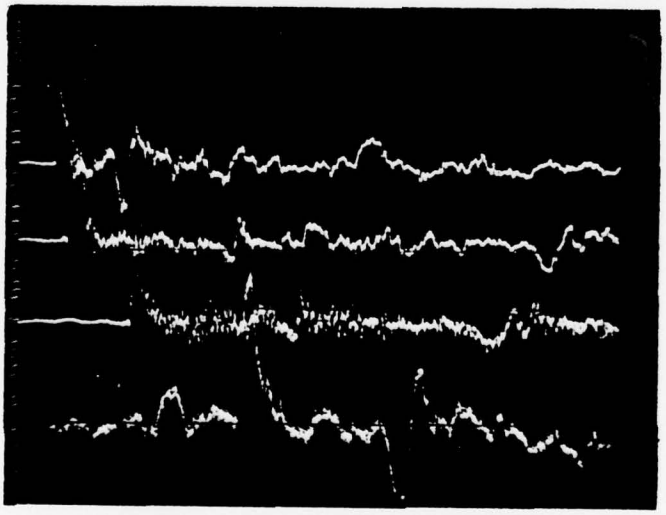

Voltages

P_1 Ch. 1 0.02V /div

P_6 Ch. 2 0.02V /div

$P_{5.5}$ Ch. 3 0.02V /div

T_3 Ch. 4 0.05V /div

Time Scale 5msec /div

Sustainer Voltage 25.8kV

Flow? (On) Off

Gas Type N_2

Notes: amp. not in circuit, no muffler

Analyzed Data:

E = 65.91

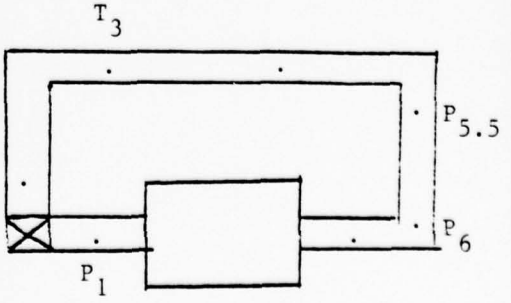

PVC Circulator Experimental Data

Page 163
No. 5438
Date 11 July 1978

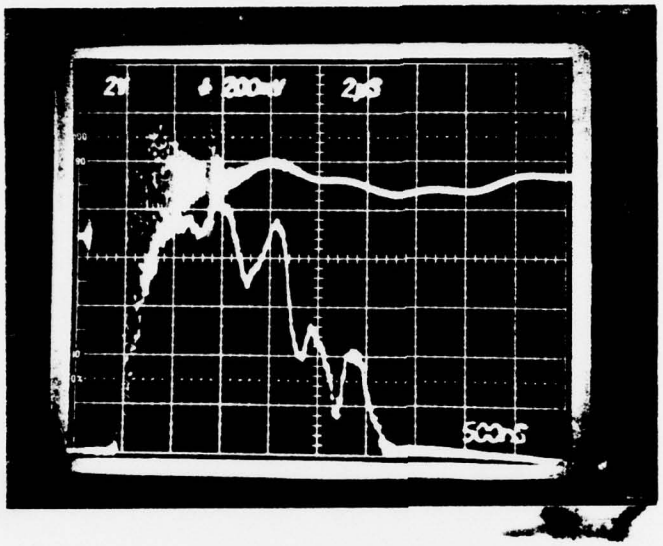

Gun Data

1. Upper Trace
   Voltage 200mV/div
   Time Scale 2μsec/div
   Inverted? (Yes) No
2. Lower Trace
   Voltage 2V /div
   Time Scale 500nsec/div
   Inverted? Yes (No)
   Attenuation _____

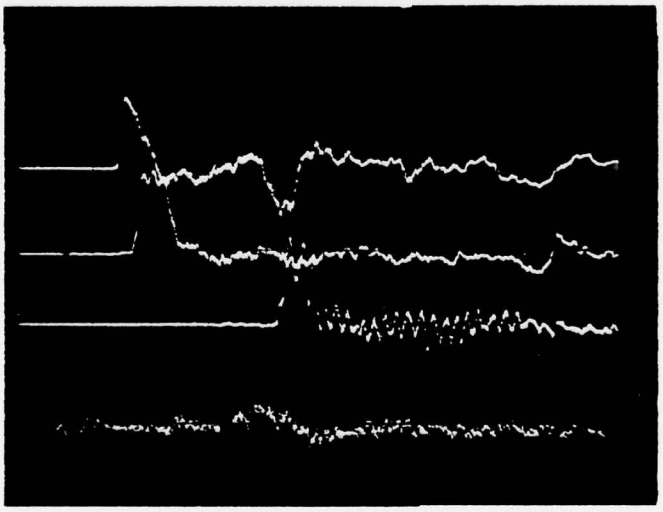

Voltages

P_1 Ch. 1 0.02V /div

P_6 Ch. 2 0.02V /div

P_5 Ch. 3 0.02V /div

T_2 Ch. 4 0.05V /div

Time Scale 2msec /div
Sustainer Voltage 25.8kV*
Flow? On (Off)
Gas Type N_2
Notes: no muffler

Analyzed Data:

E = 60.84*

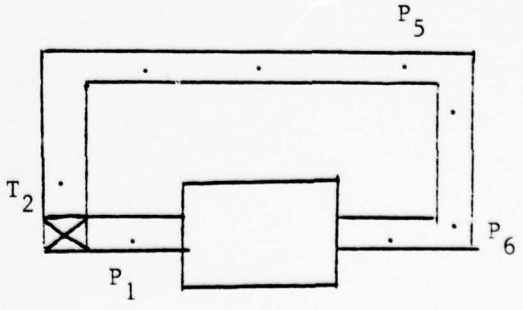

*Assumed value

PVC Circulator Experimental Data

Page 164
No. 5439
Date 11 July 1978

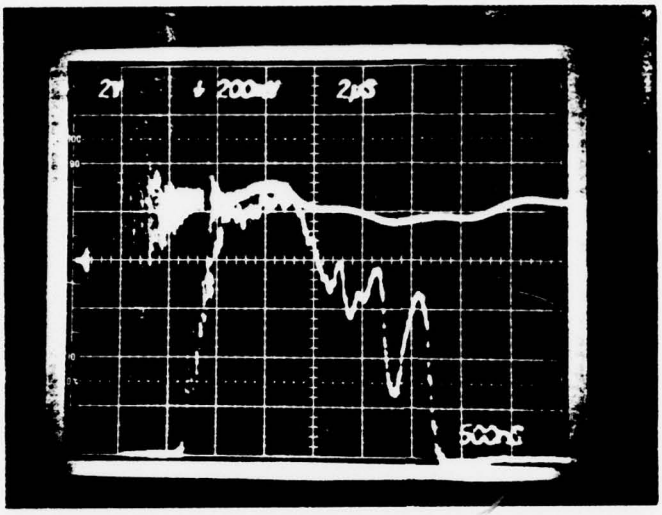

Gun Data

1. Upper Trace
   Voltage 200mV/div
   Time Scale 2usec/div
   Inverted? (Yes) No
2. Lower Trace
   Voltage 2V /div
   Time Scale 500msec/div
   Inverted? Yes (No)
   Attenuation _____

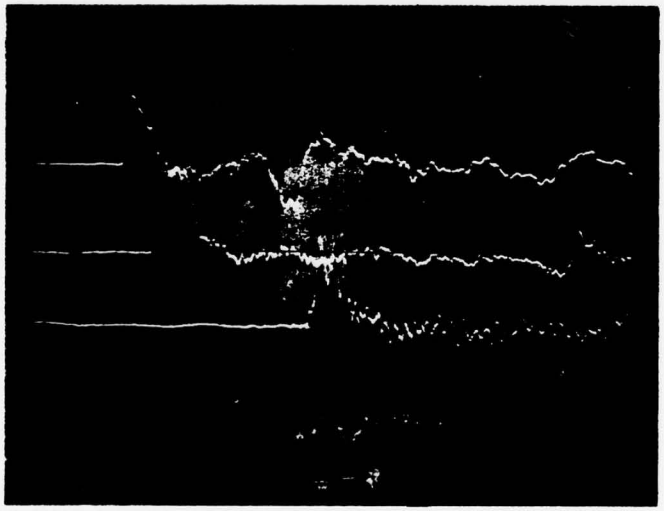

Voltages

P_1 Ch. 1 0.02V/div

P_6 Ch. 2 0.02V/div

P_5 Ch. 3 0.02V/div

T_2 Ch. 4 0.05V/div

Time Scale 2msec/div
Sustainer Voltage 25.8kV*
Flow? (On) Off
Gas Type N_2
Notes: no muffler

Analyzed Data:

E = 64.22*

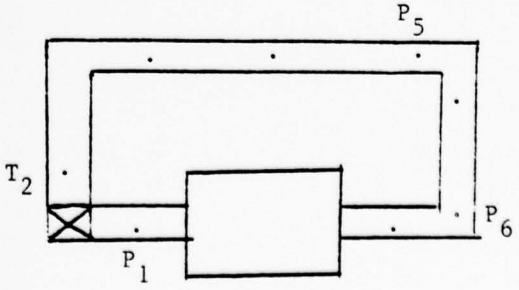

*Assumed value

PVC Circulator Experimental Data

Page 165
No. 5441
Date 11 July 1978

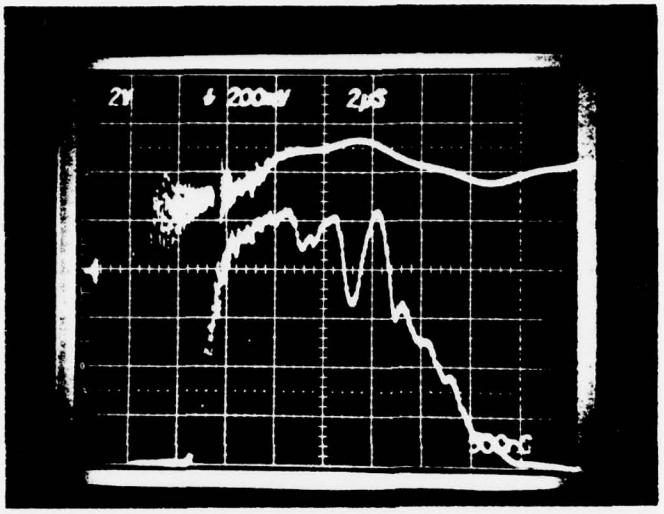

Gun Data

1. Upper Trace
   Voltage 200mV/div
   Time Scale 2μsec /div
   Inverted? (Yes) No
2. Lower Trace
   Voltage 2V /div
   Time Scale 500nsec/div
   Inverted? Yes (No)
   Attenuation _____

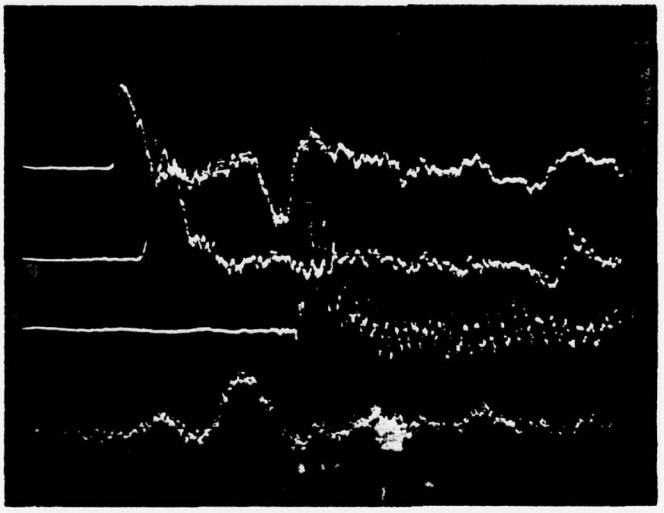

Voltages

P_1 Ch. 1 0.02V /div
P_6 Ch. 2 0.02V /div
P_5 Ch. 3 0.02V /div
T_2 Ch. 4 0.02V /div

Time Scale 2msec /div
Sustainer Voltage 25.8kV*
Flow? (On) Off
Gas Type N_2
Notes: no muffler

Analyzed Data:

$E = 72.67^*$

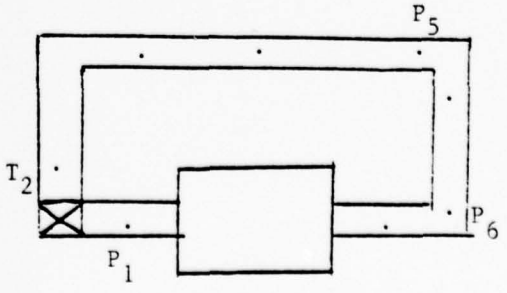

*Assumed value

PVC Circulator Experimental Data

Page 166
No. 5443
Date 11 July 1978

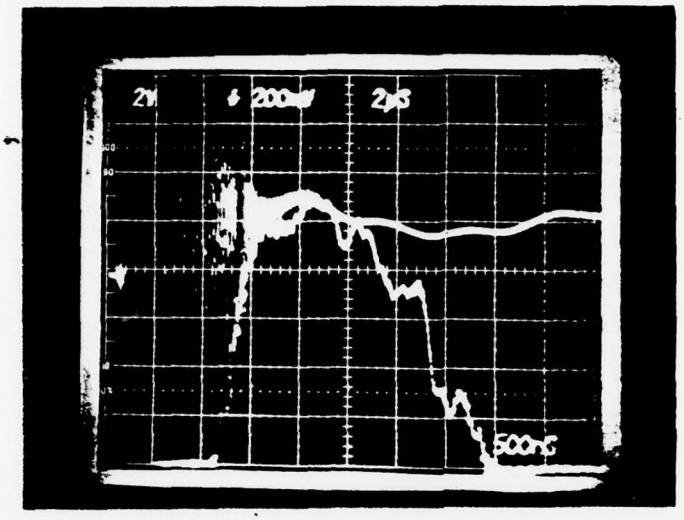

Gun Data

1. Upper Trace
   Voltage 200mV/div
   Time Scale 2µsec/div
   Inverted? (Yes) No
2. Lower Trace
   Voltage 2V /div
   Time Scale 500nsec/div
   Inverted? Yes (No)
   Attenuation _____

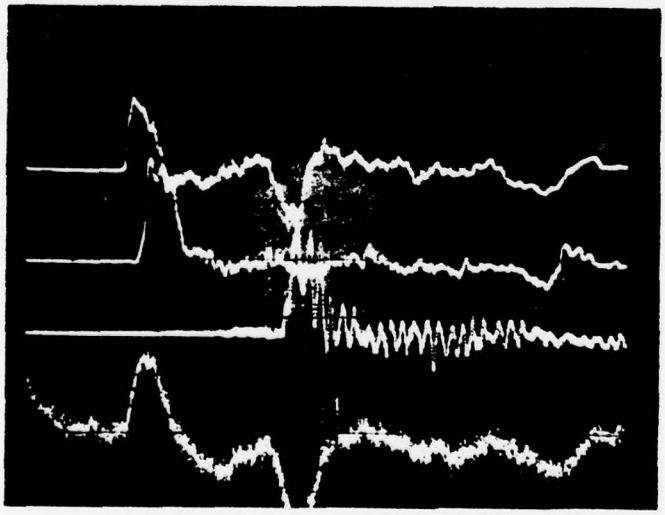

Voltages

P_1 Ch. 1 0.02V /div
P_6 Ch. 2 0.02V /div
P_5 Ch. 3 0.02V /div
T_1 Ch. 4 0.05V /div

Time Scale 2msec /div
Sustainer Voltage 25.8kV*
Flow? On (Off)
Gas Type N_2
Notes: no muffler

Analyzed Data:

E = 67.60*

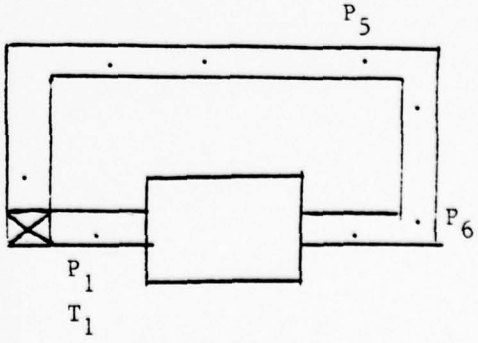

*Assumed value

PVC Circulator Experimental Data

Page 167
No. 5444
Date 11 July 1978

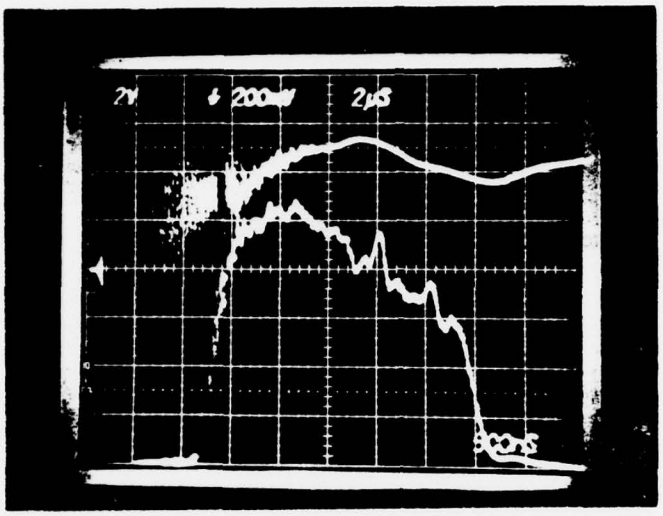

Gun Data

1. Upper Trace
   Voltage 200mV/div
   Time Scale 2μsec/div
   Inverted? (Yes) No
2. Lower Trace
   Voltage 2V /div
   Time Scale 500nsec/div
   Inverted? Yes (No)
   Attenuation _____

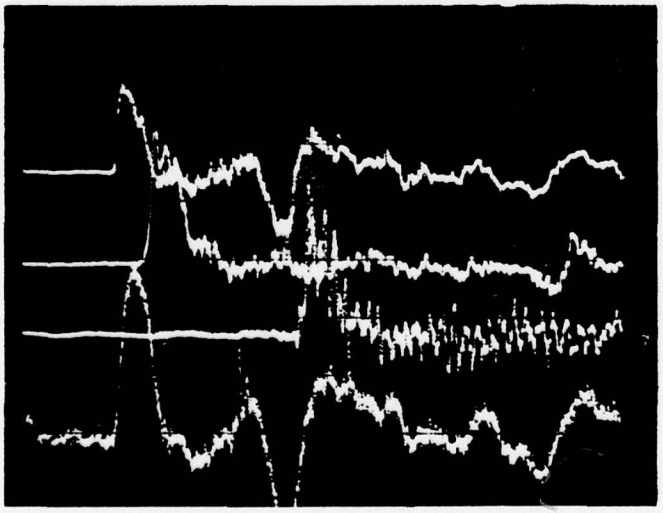

Voltages

P_1 Ch. 1 0.02V /div

P_6 Ch. 2 0.02V /div

P_5 Ch. 3 0.02V /div

T_1 Ch. 4 0.05V /div

Time Scale 2msec /div
Sustainer Voltage 25.8kV*
Flow? On Off
Gas Type N_2
Notes: no muffler

Analyzed Data:

$E = 77.74^*$

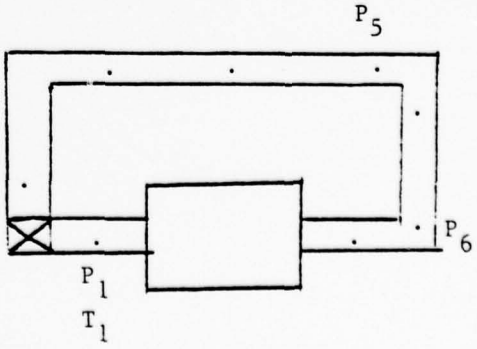

*Assumed value

PVC Circulator Experimental Data

Page 168
No. 5445
Date 11 July 1978

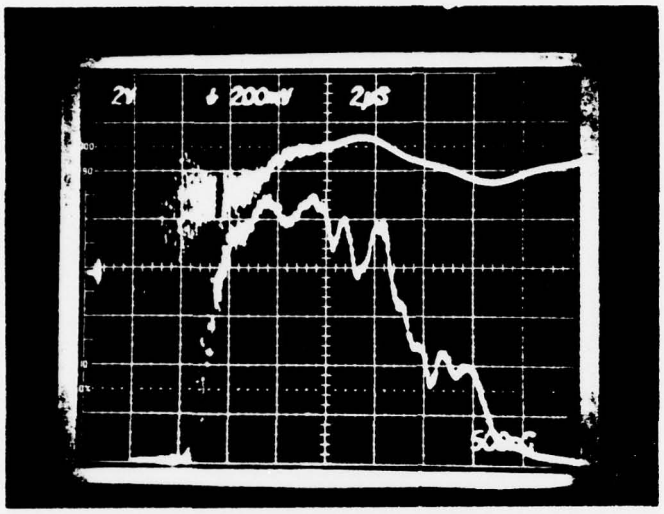

Gun Data

1. Upper Trace
   Voltage 200mV/div
   Time Scale 2μsec /div
   Inverted? (Yes) No
2. Lower Trace
   Voltage 2V /div
   Time Scale 500nsec/div
   Inverted? Yes (No)
   Attenuation _____

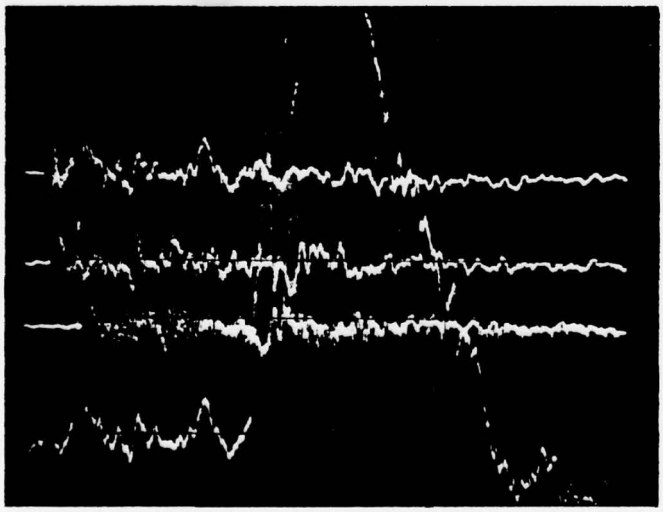

Voltages

P_1 Ch. 1 0.02V /div
P_6 Ch. 2 0.02V /div
P_5 Ch. 3 0.02V /div
T_1 Ch. 4 0.10V /div

Time Scale 10msec /div
Sustainer Voltage 25.8kV*
Flow? (On) Off
Gas Type N_2
Notes: no muffler

Analyzed Data:

E = 77.74*

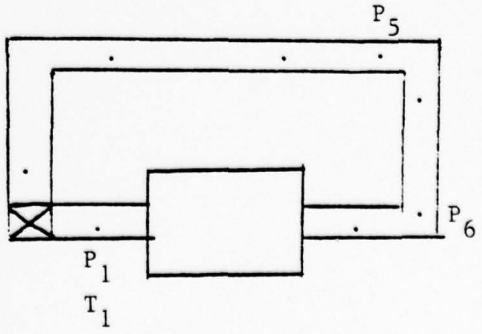

* Assumed value

PVC Circulator Experimental Data

Page 169
No. 5446
Date 11 July 1978

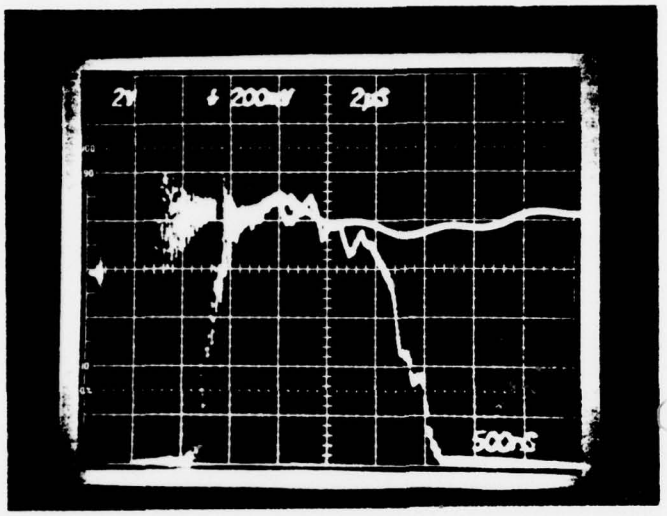

Gun Data

1. Upper Trace
   Voltage 200mV/div
   Time Scale 2μsec/div
   Inverted? (Yes) No
2. Lower Trace
   Voltage 2V /div
   Time Scale 500nsec/div
   Inverted? Yes (No)
   Attenuation _____

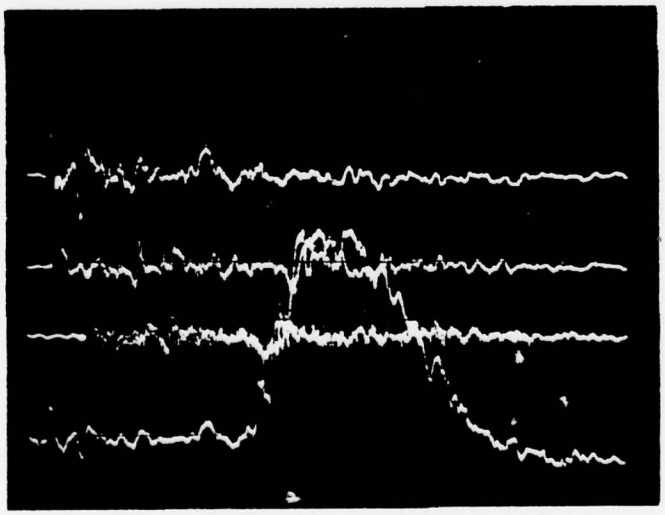

Voltages

P_1 Ch. 1 0.02V/div
P_6 Ch. 2 0.02V/div
P_5 Ch. 3 0.02V/div
T_1 Ch. 4 0.20V/div

Time Scale 10msec/div
Sustainer Voltage 25.8kV*
Flow? (On) Off
Gas Type N_2
Notes: no muffler

Analyzed Data:

$E = 67.60^*$

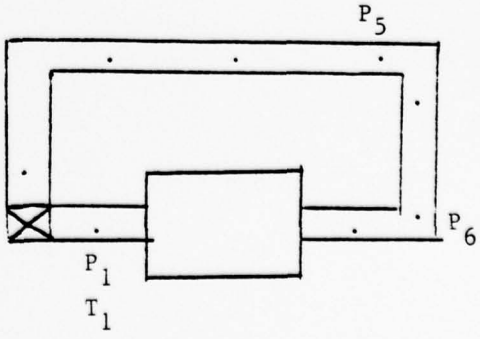

*Assumed value

PVC Circulator Experimental Data

Page 170
No. 5448
Date 12 July 1978

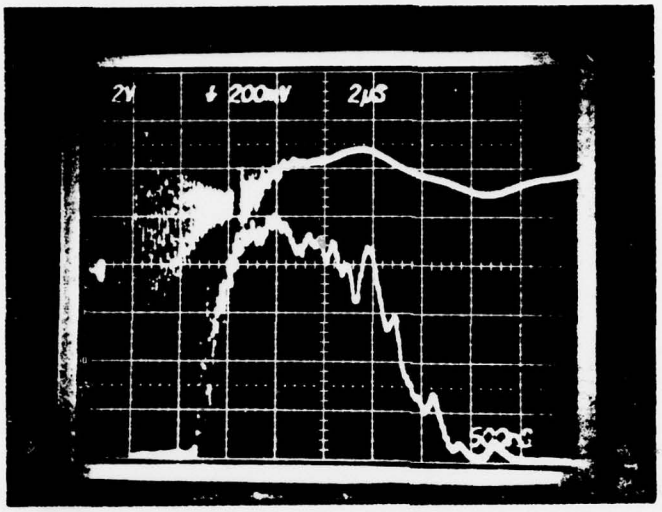

Gun Data

1. Upper Trace
   Voltage 200mV/div
   Time Scale 2μsec/div
   Inverted? (Yes) No
2. Lower Trace
   Voltage 2V /div
   Time Scale 500nsec/div
   Inverted? Yes (No)
   Attenuation _____

Voltages

P_1 Ch. 1 0.02V/div
P_5 Ch. 2 0.02V/div
P_6 Ch. 3 0.02V/div
T_1 Ch. 4 0.05V/div

Time Scale 2msec/div
Sustainer Voltage 25.8kV
Flow? (On) Off
Gas Type N_2
Notes: _____

Analyzed Data:

E = 60.84

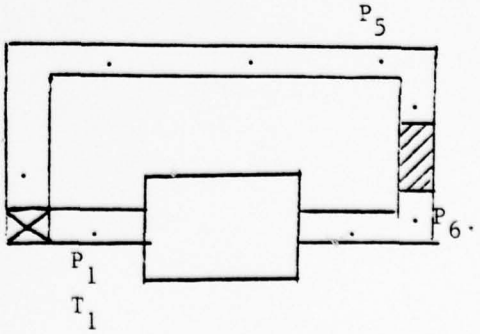

PVC Circulator Experimental Data

Page 171
No. 5449
Date 12 July 1978

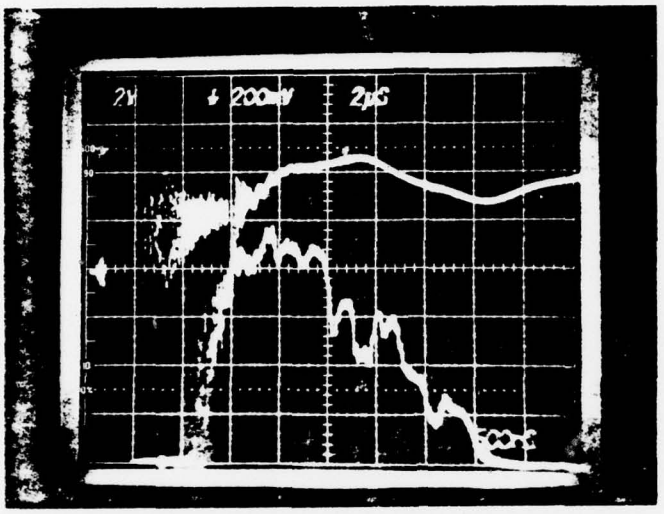

Gun Data

1. Upper Trace
   Voltage 200mV/div
   Time Scale 2µsec /div
   Inverted? (Yes) No
2. Lower Trace
   Voltage 2V /div
   Time Scale 500nsec/div
   Inverted? Yes (No)
   Attenuation _____

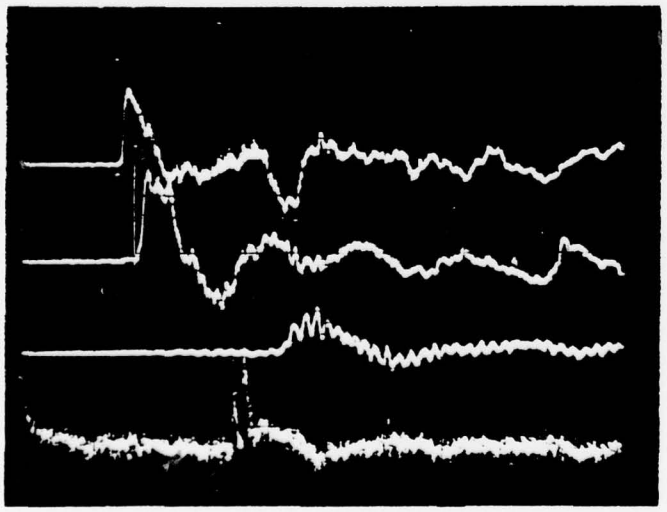

Voltages

P_1 Ch. 1 0.02V /div

P_6 Ch. 2 0.02V /div

P_5 Ch. 3 0.02V /div

T_2 Ch. 4 0.05V /div

Time Scale 2msec /div
Sustainer Voltage 25.8kV
Flow? On (Off)
Gas Type N_2
Notes: _____

Analyzed Data:

E = 55.77

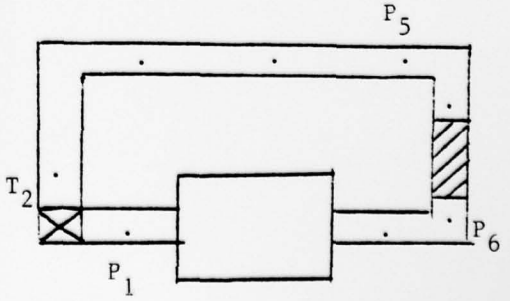

PVC Circulator Experimental Data

Page 172
No. 5450
Date 12 July 1978

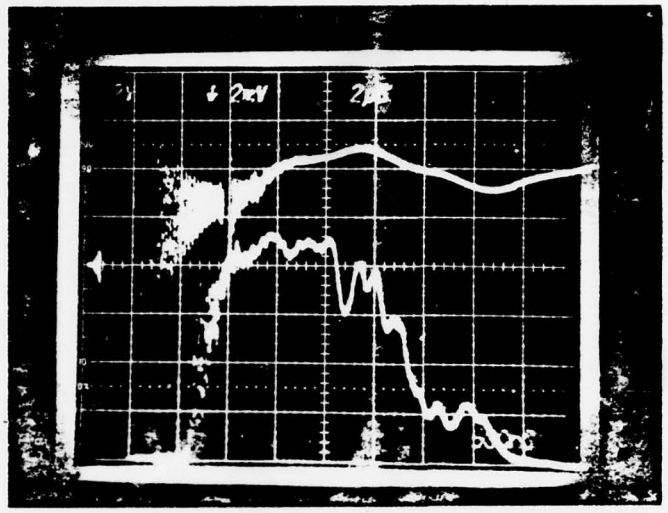

Gun Data

1. Upper Trace
   Voltage 2mV /div
   Time Scale 2μsec/div
   Inverted? (Yes) No
2. Lower Trace
   Voltage 2V /div
   Time Scale 500nsec/div
   Inverted? Yes (No)
   Attenuation _____

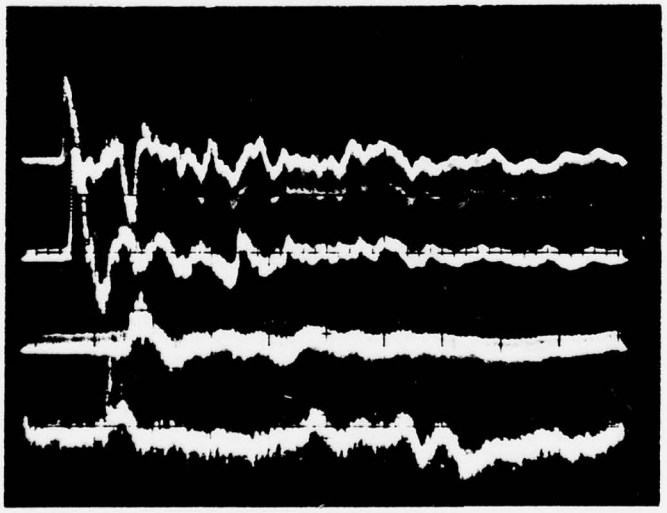

Voltages

P_1 Ch. 1 0.02V /div
P_5 Ch. 2 0.02V /div
P_6 Ch. 3 0.02V /div
T_2 Ch. 4 0.05V /div

Time Scale 5msec /div
Sustainer Voltage 25.8kV
Flow? On (Off)
Gas Type N_2
Notes: _____

Analyzed Data:

E = 64.22

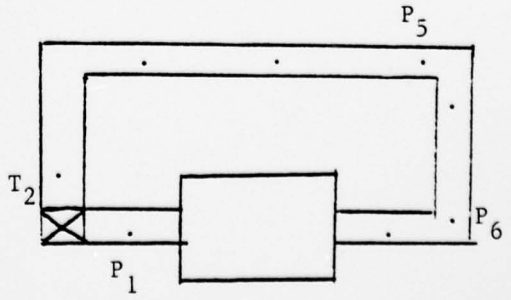

PVC Circulator Experimental Data

Page 173
No. 5451
Date 12 July 1978

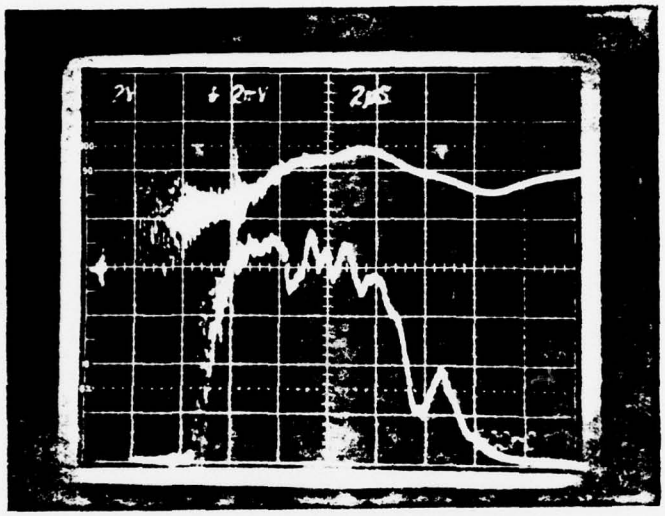

Gun Data

1. Upper Trace
   Voltage 2mV /div
   Time Scale 2μsec/div
   Inverted? (Yes) No
2. Lower Trace
   Voltage 2V /div
   Time Scale 500nsec/div
   Inverted? Yes (No)
   Attenuation _____

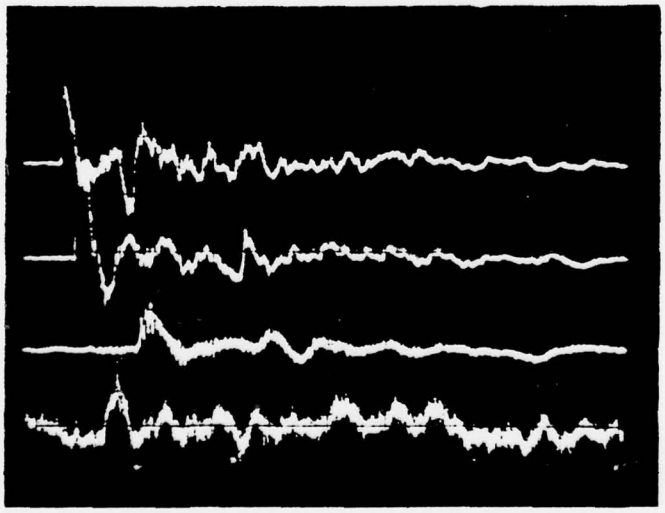

Voltages

P_1 Ch. 1 0.02V /div
P_5 Ch. 2 0.02V /div
P_6 Ch. 3 0.02V /div
T_2 Ch. 4 0.05V /div

Time Scale 5msec /div
Sustainer Voltage 25.8kV
Flow? (On) Off
Gas Type N_2
Notes: _____

Analyzed Data:

E = 59.15

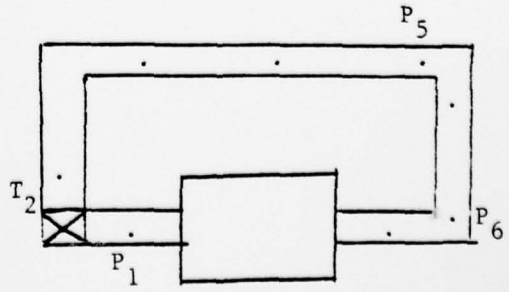

PVC Circulator Experimental Data

Page 174
No. 5452
Date 12 July 1978

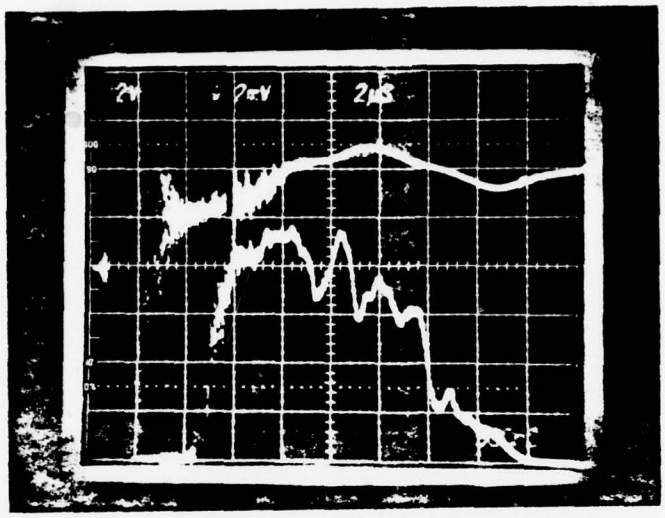

Gun Data

1. Upper Trace
   Voltage 2mV /div
   Time Scale 2μsec /div
   Inverted? (Yes) No
2. Lower Trace
   Voltage 2V /div
   Time Scale 500nsec/div
   Inverted? Yes (No)
   Attenuation _____

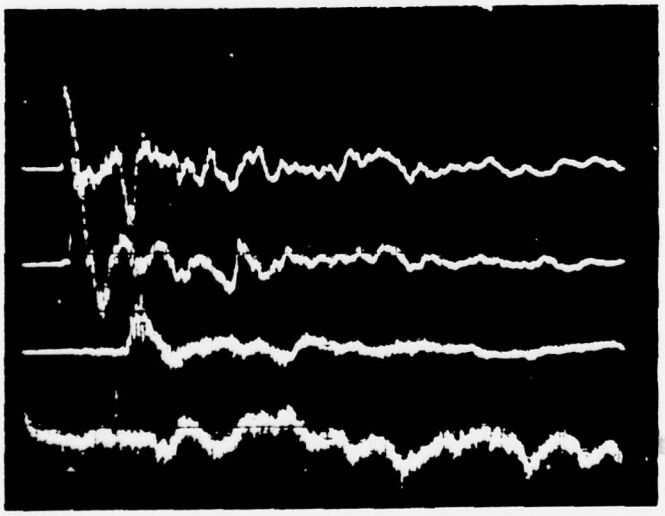

Voltages

P_1 Ch. 1 0.02V /div

P_5 Ch. 2 0.02V /div

P_6 Ch. 3 0.02V /div

T_3 Ch. 4 0.05V /div

Time Scale 5msec /div
Sustainer Voltage 25.8kV
Flow? On (Off)
Gas Type N_2
Notes: _____

Analyzed Data:

E = 64.22

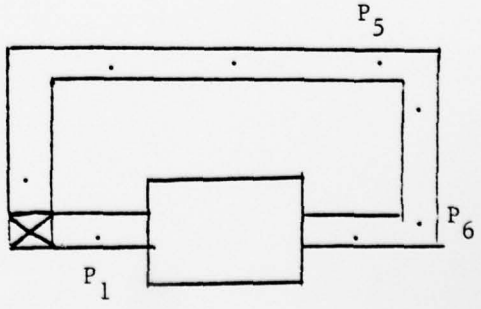

PVC Circulator Experimental Data

Page 175
No. 5453
Date 12 July 1978

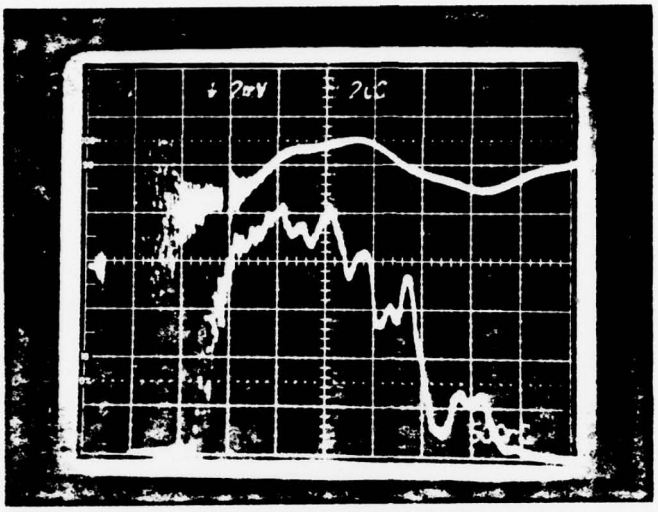

Gun Data

1. Upper Trace
   Voltage 2mV /div
   Time Scale 2μsec /div
   Inverted? (Yes) No
2. Lower Trace
   Voltage 2V /div
   Time Scale 500nsec/div
   Inverted? Yes (No)
   Attenuation _____

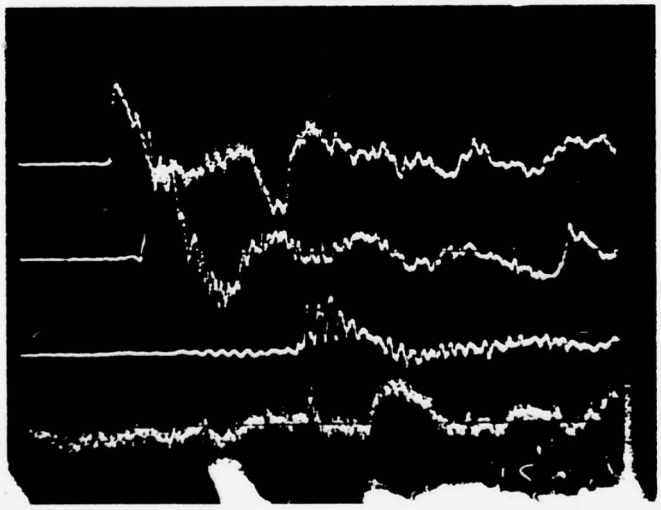

Voltages

P_1 Ch. 1 0.02V /div

P_5 Ch. 2 0.02V /div

P_6 Ch. 3 0.02V /div

T_3 Ch. 4 0.05V /div

Time Scale 2msec /div
Sustainer Voltage 25.8kV
Flow? (On) Off
Gas Type N_2
Notes: _____

Analyzed Data:

E = 67.6

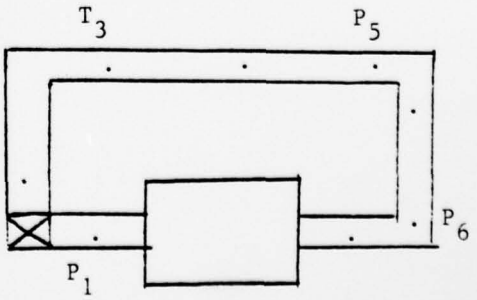

PVC Circulator Experimental Data

Page 176
No. 5454
Date 12 July 1978

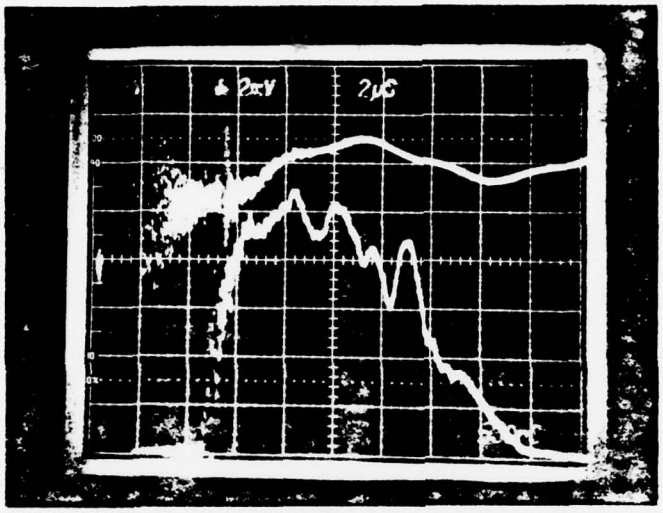

Gun Data

1. Upper Trace
   Voltage 2mV /div
   Time Scale 2μsec/div
   Inverted? (Yes) No
2. Lower Trace
   Voltage 2V /div
   Time Scale 500nsec/div
   Inverted? Yes (No)
   Attenuation _____

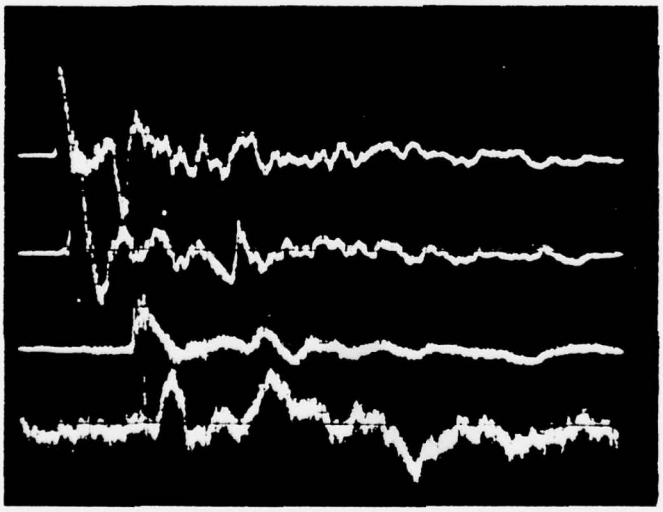

Voltages

P_1 Ch. 1 0.02V /div
P_5 Ch. 2 0.02V /div
P_6 Ch. 3 0.02V /div
T_3 Ch. 4 0.05V /div

Time Scale 5msec /div
Sustainer Voltage 26.0kV
Flow? (On) Off
Gas Type N_2
Notes: _____

Analyzed Data:

E = 74.93643

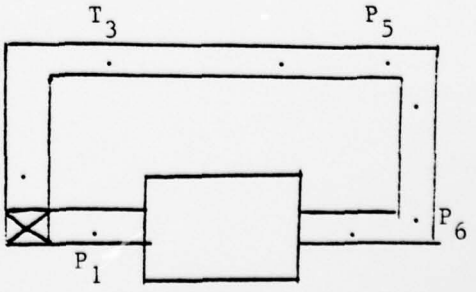

PVC Circulator Experimental Data

Page 177
No. 5456
Date 12 July 1978

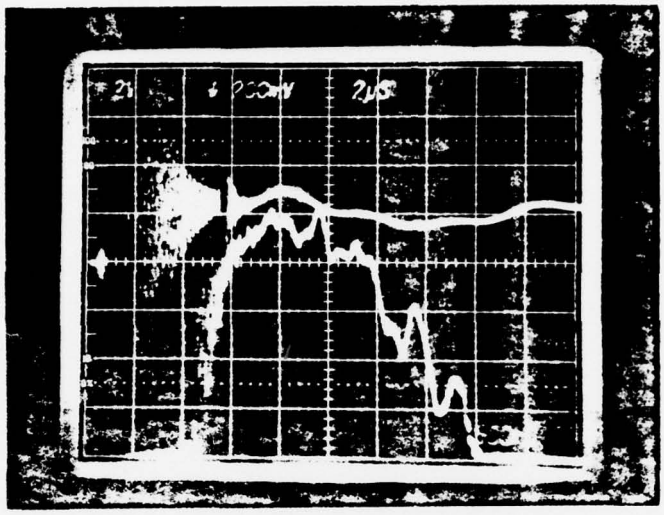

Gun Data

1. Upper Trace
   Voltage 200mV/div
   Time Scale 2μsec/div
   Inverted? (Yes) No
2. Lower Trace
   Voltage 2V /div
   Time Scale 500nsec/div
   Inverted? Yes (No)
   Attenuation _____

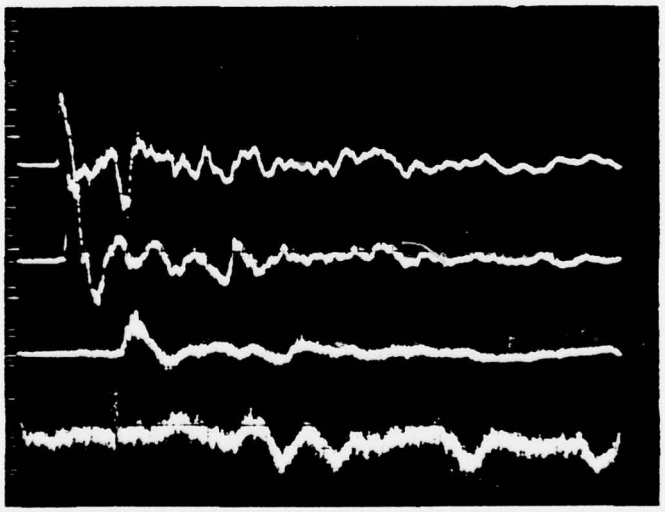

Voltages

P_1 Ch. 1 0.02V/div
P_5 Ch. 2 0.02V/div
P_6 Ch. 3 0.02V/div
T_4 Ch. 4 0.02V/div

Time Scale 5msec /div
Sustainer Voltage 25.8kV
Flow? On (Off)
Gas Type N_2
Notes: _____

Analyzed Data:

E = 67.6

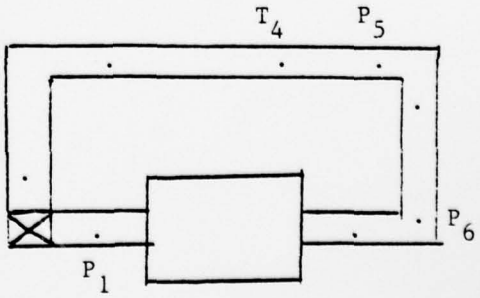

PVC Circulator Experimental Data

Page 178
No. 5457
Date 12 July 1978

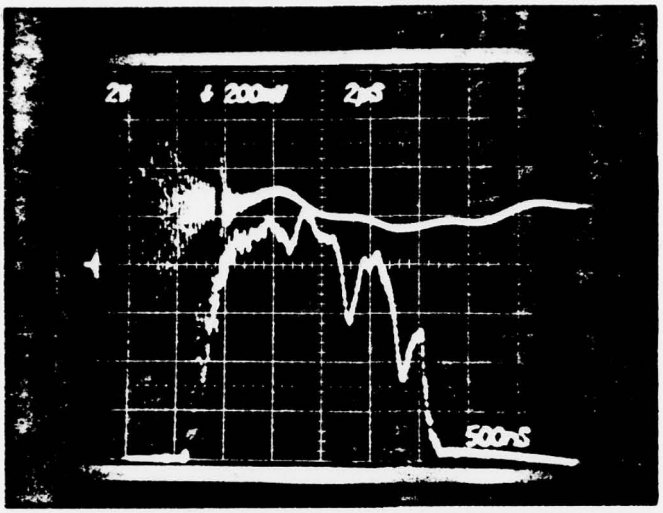

Gun Data

1. Upper Trace
   Voltage 200mV/div
   Time Scale 2μsec/div
   Inverted? (Yes) No
2. Lower Trace
   Voltage 2V /div
   Time Scale 500nsec/div
   Inverted? Yes (No)
   Attenuation _____

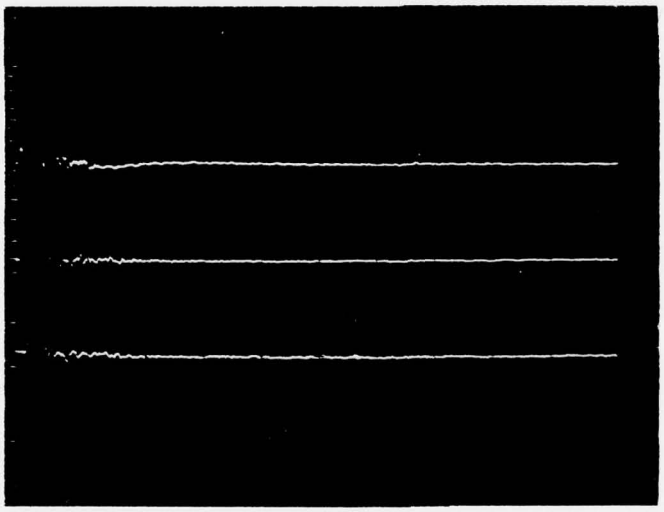

Voltages

P_1 Ch. 1 0.02V /div

P_5 Ch. 2 0.02V /div

P_6 Ch. 3 0.02V /div

T_4 Ch. 4 0.05V /div

Time Scale 50msec /div
Sustainer Voltage 25.8kV
Flow? (On) Off
Gas Type N_2
Notes: _____

Analyzed Data:

E = 64.22

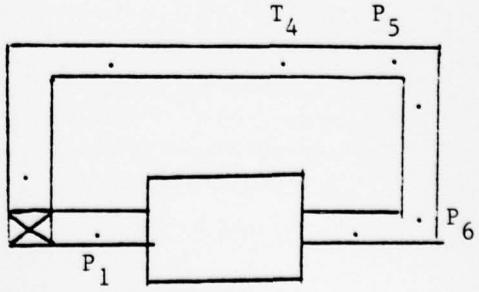

PVC Circulator Experimental Data

Page 179
No. 5459
Date 12 July 1978

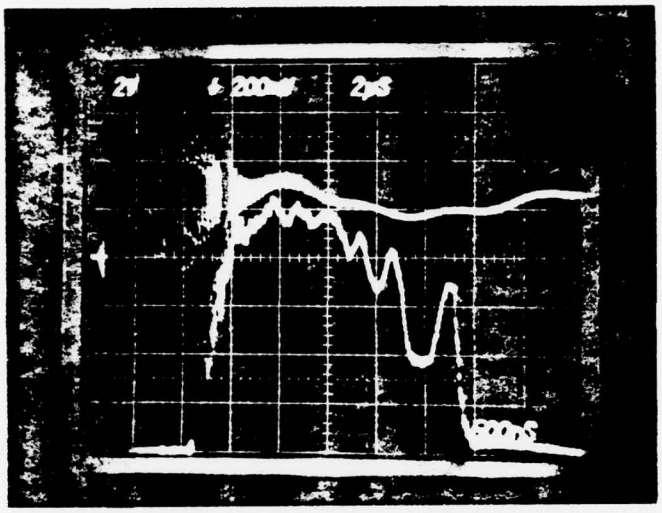

Gun Data

1. Upper Trace
   Voltage 200mV/div
   Time Scale 2μsec/div
   Inverted? (Yes) No
2. Lower Trace
   Voltage 2V /div
   Time Scale 500nsec/div
   Inverted? Yes (No)
   Attenuation _____

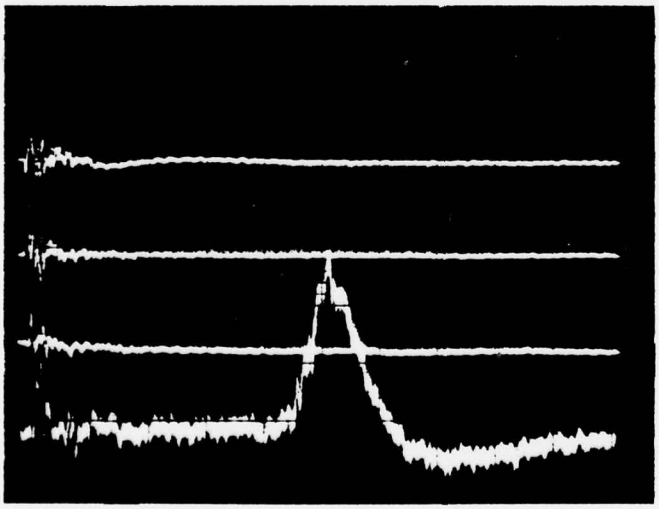

Voltages

P_1 Ch. 1 0.02V/div

P_5 Ch. 2 0.02V/div

P_6 Ch. 3 0.02V/div

T_4 Ch. 4 0.05V/div

Time Scale 50msec/div
Sustainer Voltage 25.8kV
Flow? (On) Off
Gas Type N_2
Notes: both mufflers in

Analyzed Data:

E = 72.67

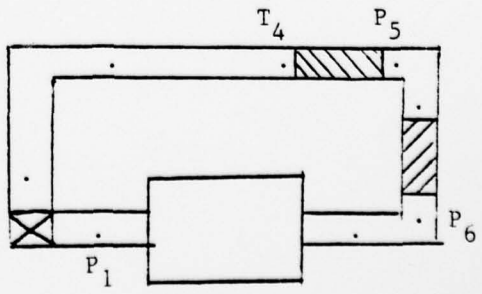

PVC Circulator Experimental Data

Page 180
No. 5460
Date 12 July 1978

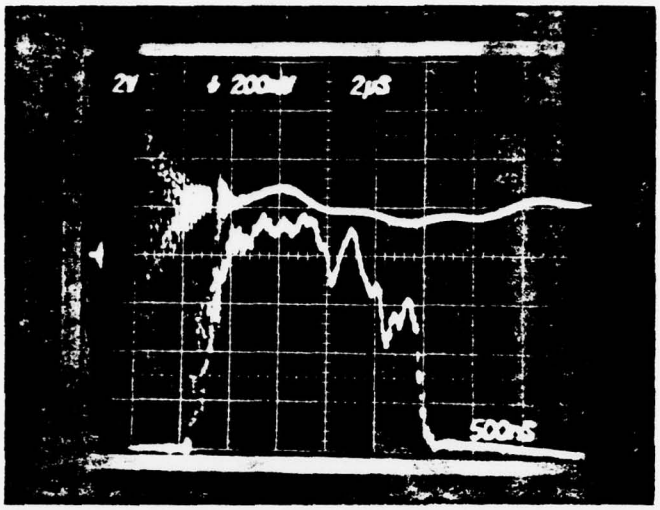

Gun Data

1. Upper Trace
   Voltage 200mV/div
   Time Scale 2μsec /div
   Inverted? (Yes) No
2. Lower Trace
   Voltage 2V /div
   Time Scale 500nsec/div
   Inverted? Yes (No)
   Attenuation _____

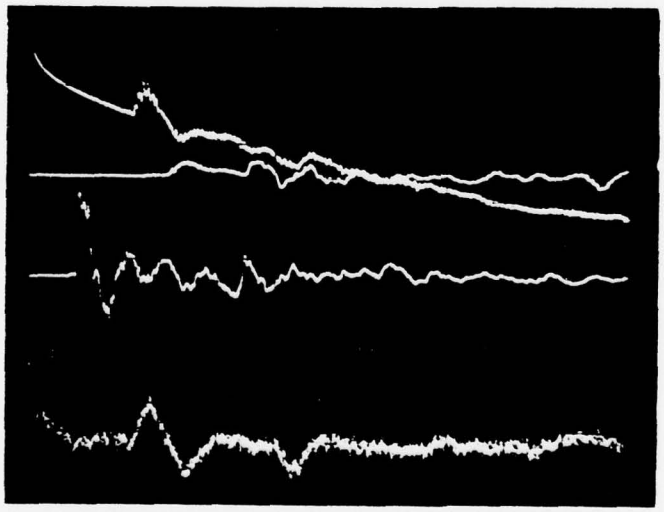

Voltages

P_4 Ch. 1 0.02V /div

P_6 Ch. 2 0.02V /div

P_5 Ch. 3 0.02V /div

T_5 Ch. 4 0.05V /div

Time Scale 5msec /div

Sustainer Voltage 25.8kV*

Flow? On (Off)

Gas Type N_2

Notes: both mufflers in
Channel 3 was hit by pulse at trigering time

Analyzed Data:

E = 60.84*

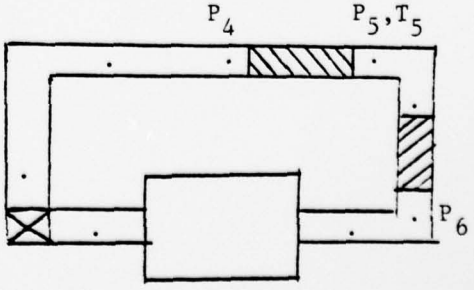

*Assumed value

PVC Circulator Experimental Data

Page 181
No. 5461
Date 12 July 1978

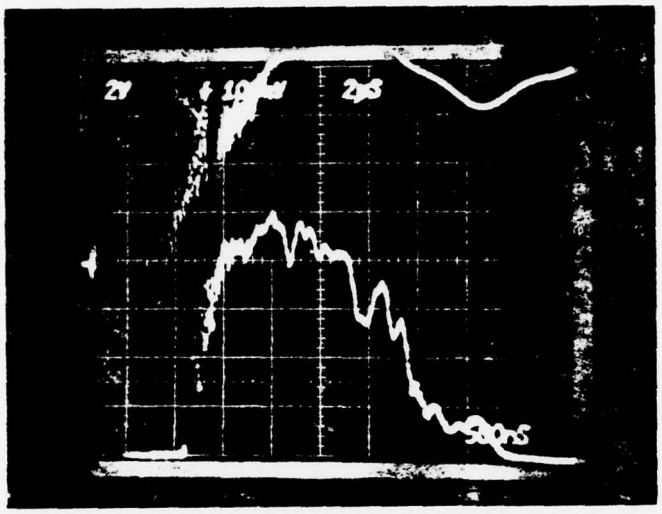

Gun Data

1. Upper Trace
   Voltage 100mV/div
   Time Scale 2μsec/div
   Inverted? (Yes) No
2. Lower Trace
   Voltage 2V /div
   Time Scale 500nsec/div
   Inverted? Yes (No)
   Attenuation _____

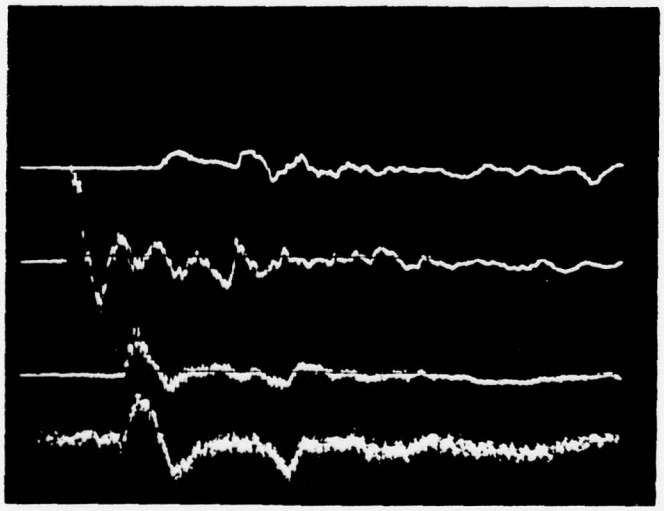

Voltages

P_4 Ch. 1 0.02V /div

P_6 Ch. 2 0.02V /div

P_5 Ch. 3 0.02V /div

T_5 Ch. 4 0.05V /div

Time Scale 5msec /div
Sustainer Voltage 25.8kV*
Flow? On (Off)
Gas Type N_2
Notes: same as 5460 with stable channel 3

Analyzed Data:

E = 62.53*

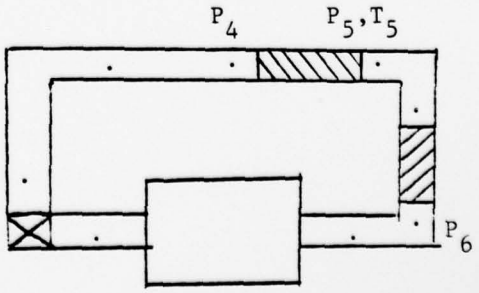

*Assumed value

PVC Circulator Experimental Data

Page 182
No. 5462
Date 12 July 1978

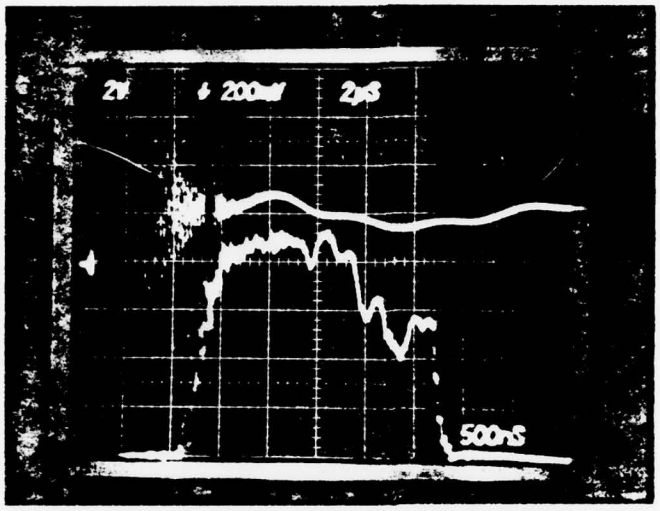

Gun Data

1. Upper Trace
   Voltage 200mV/div
   Time Scale 2μsec/div
   Inverted? (Yes) No
2. Lower Trace
   Voltage 2V /div
   Time Scale 500nsec/div
   Inverted? Yes (No)
   Attenuation _____

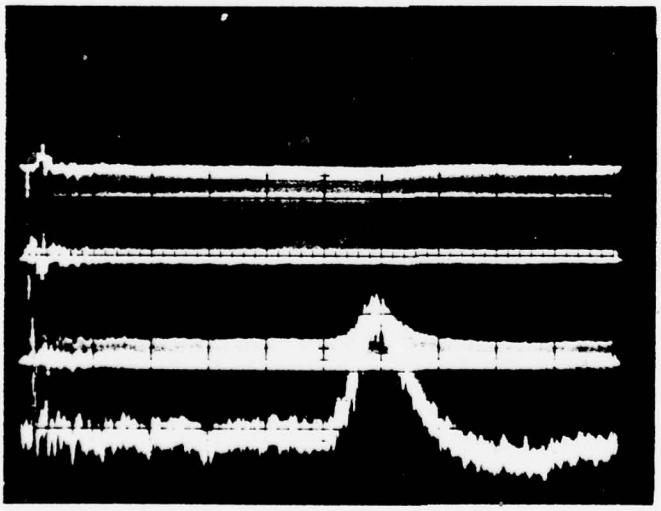

Voltages

P_4 Ch. 1 0.02V/div
P_6 Ch. 2 0.02V/div
P_5 Ch. 3 0.02V/div
T_4 Ch. 4 0.05V/div

Time Scale 50msec/div
Sustainer Voltage 25.8kV*
Flow? (On) Off
Gas Type N_2
Notes: _____

Analyzed Data:

E = 64.22*

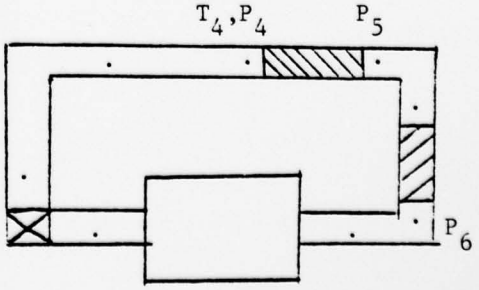

*Assumed value

PVC Circulator Experimental Data

Page 183
No. 5463
Date 12 July 1978

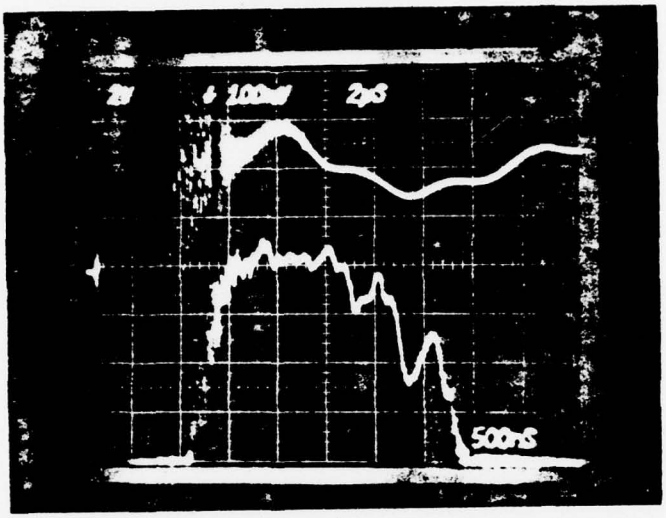

Gun Data

1. Upper Trace
   Voltage 100mV/div
   Time Scale 2µsec /div
   Inverted? (Yes) No
2. Lower Trace
   Voltage 2V /div
   Time Scale 500nsec/div
   Inverted? Yes (No)
   Attenuation _____

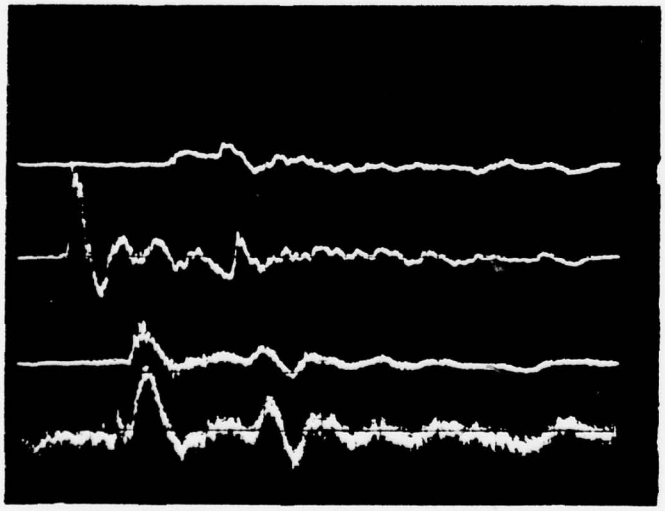

Voltages

P_4 Ch. 1 0.02V /div
P_6 Ch. 2 0.02V /div
P_5 Ch. 3 0.02V /div
T_5 Ch. 4 0.05V /div

Time Scale 5msec/div
Sustainer Voltage 25.8kV
Flow? (On) Off
Gas Type N_2
Notes: _____

Analyzed Data:

E = 57.46

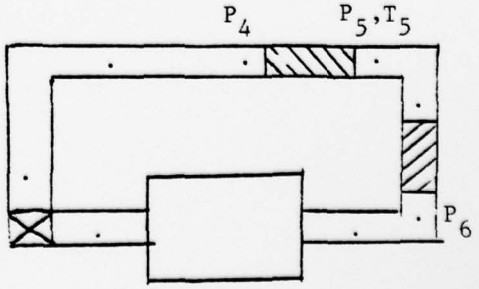

PVC Circulator Experimental Data

Page 184
No. 5464
Date 12 July 1978

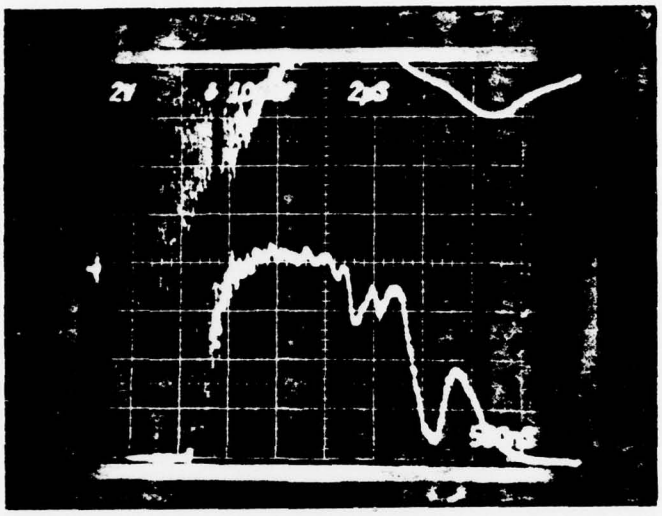

Gun Data

1. Upper Trace
   Voltage 100mV/div
   Time Scale 2μsec /div
   Inverted? (Yes) No
2. Lower Trace
   Voltage 2V /div
   Time Scale 500nsec/div
   Inverted? Yes (No)
   Attenuation _____

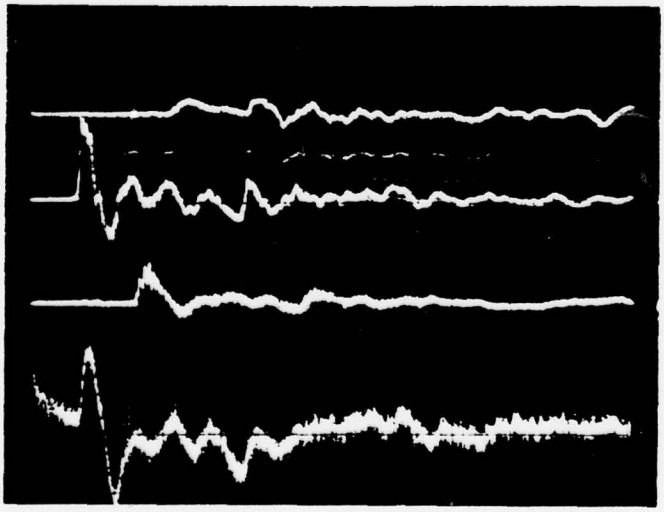

Voltages

P_4 Ch. 1 0.02V /div

P_6 Ch. 2 0.02V /div

P_5 Ch. 3 0.02V /div

T_6 Ch. 4 0.05V /div

Time Scale 5msec /div
Sustainer Voltage 25.8kV
Flow? On (Off)
Gas Type N_2
Notes: _____

Analyzed Data:

E = 57.46

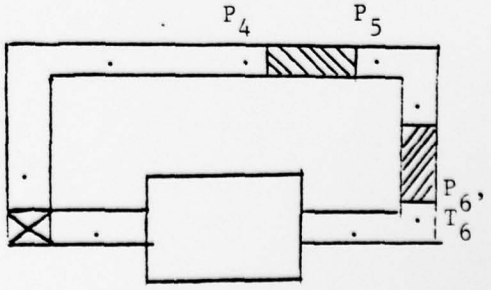

PVC Circulator Experimental Data

Page 185
No. 5466
Date 12 July 1978

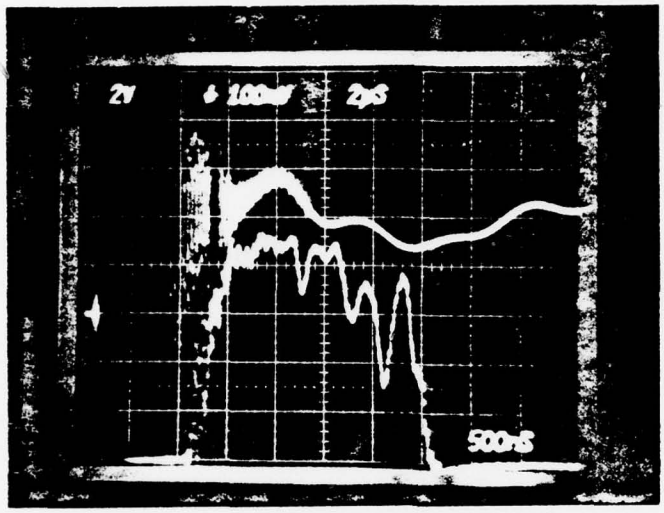

Gun Data

1. Upper Trace
   Voltage 100mV/div
   Time Scale 2µsec/div
   Inverted? (Yes) No
2. Lower Trace
   Voltage 2V /div
   Time Scale 500nsec/div
   Inverted? Yes (No)
   Attenuation _____

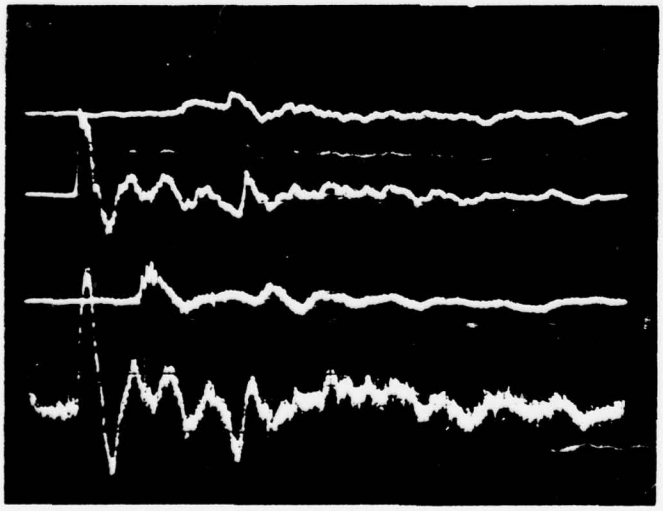

Voltages

P_4 Ch. 1 0.02V /div

P_6 Ch. 2 0.02V /div

P_5 Ch. 3 0.02V /div

T_6 Ch. 4 0.05V /div

Time Scale 5msec/div
Sustainer Voltage 25.8kV
Flow? (On) Off
Gas Type N_2
Notes: _____

Analyzed Data:

E = 57.46

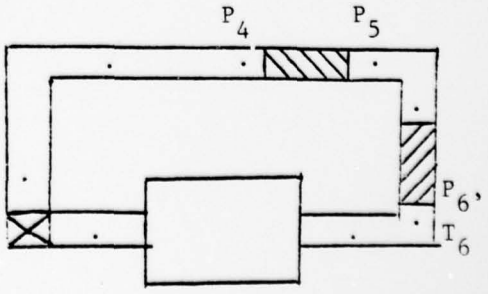

AD-A068 547 ALABAMA UNIV IN HUNTSVILLE SCHOOL OF SCIENCE AND ENG--ETC F/G 20/5
INVESTIGATION OF TRANSIENT FLOW AND HEATING PROBLEMS CHARACTERI--ETC(U)
MAR 79 C C SHIH, G R KARR, J F PERKINS DAAK40-77-C-0161
UNCLASSIFIED UAH-RR-219 DRCPM-HEL-CR-79-8 NL

3 OF 4
AD
A068547

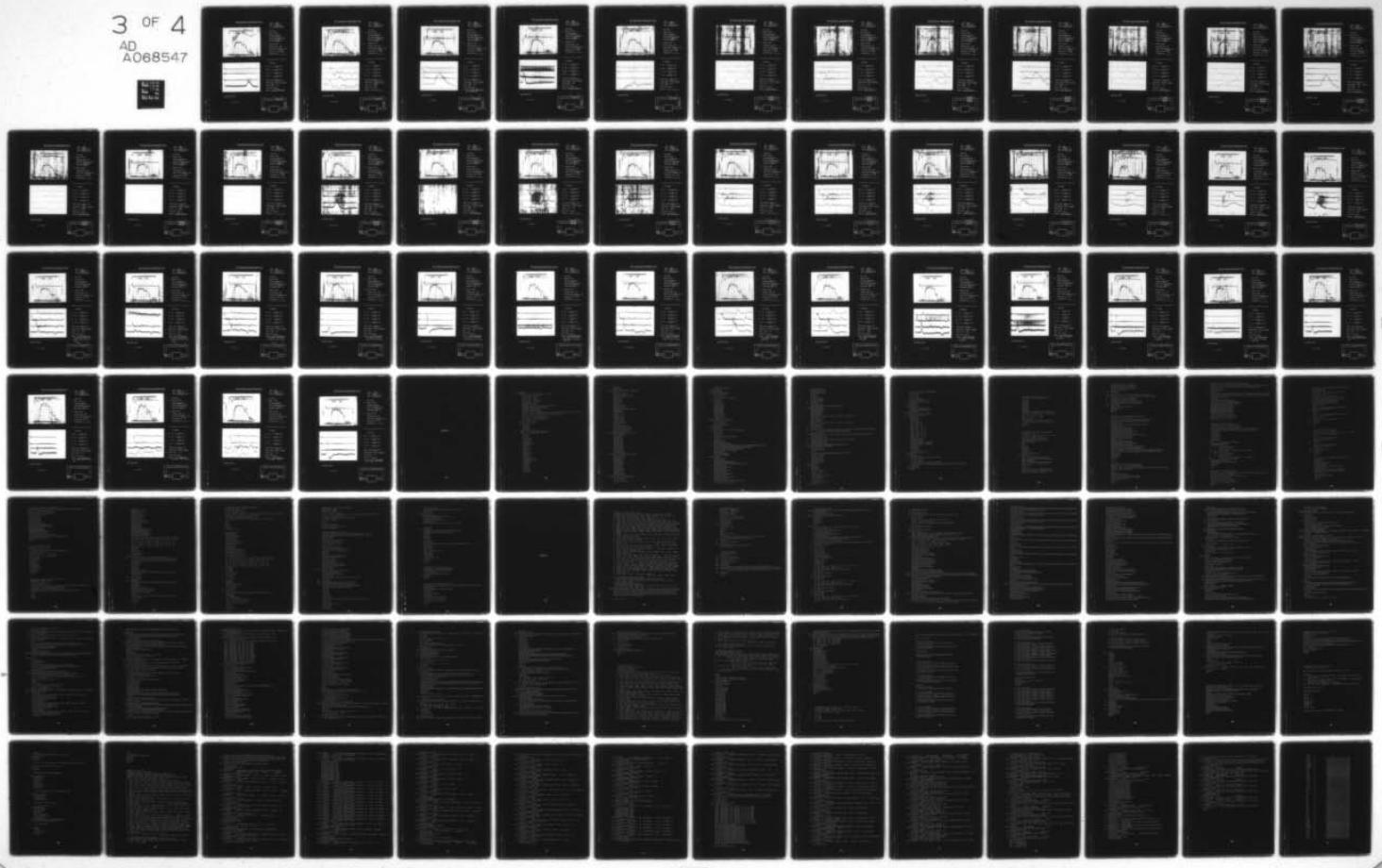

PVC Circulator Experimental Data

Page 186
No. 5467
Date 12 July 1978

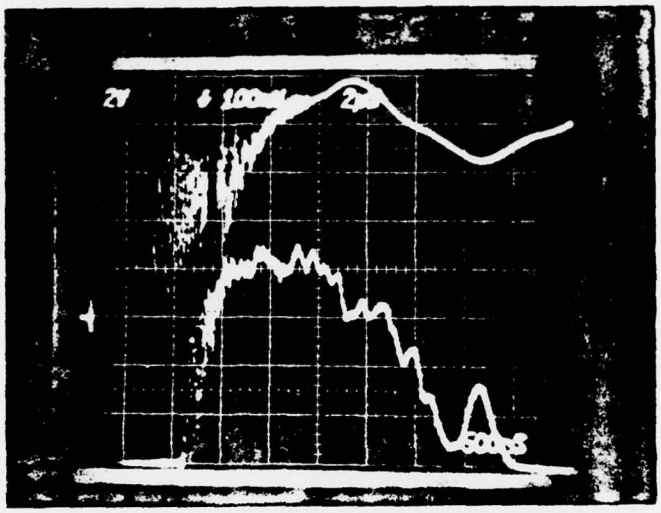

Gun Data

1. Upper Trace
   Voltage 100mV/div
   Time Scale 2μsec /div
   Inverted? (Yes) No
2. Lower Trace
   Voltage 2V /div
   Time Scale 500nsec/div
   Inverted? Yes (No)
   Attenuation _____

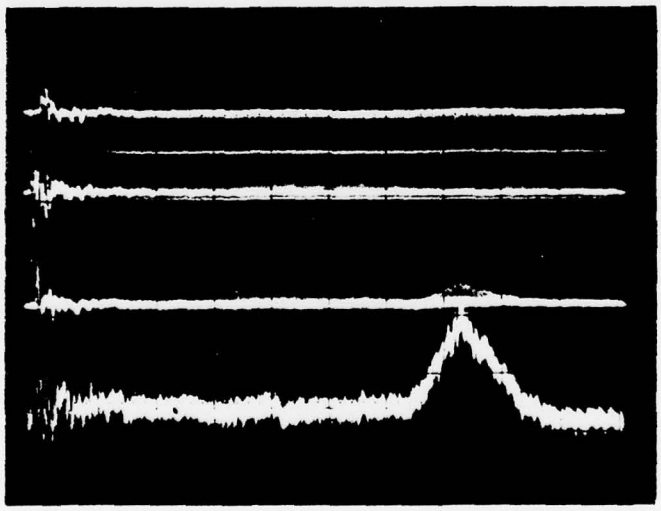

Voltages

P_4 Ch. 1 0.02V /div

P_6 Ch. 2 0.02V /div

P_5 Ch. 3 0.02V /div

T_6 Ch. 4 0.05V /div

Time Scale 50msec /div
Sustainer Voltage 25.8kV
Flow? (On) Off
Gas Type N_2
Notes: heat pulse test

Analyzed Data:

E = 57.46

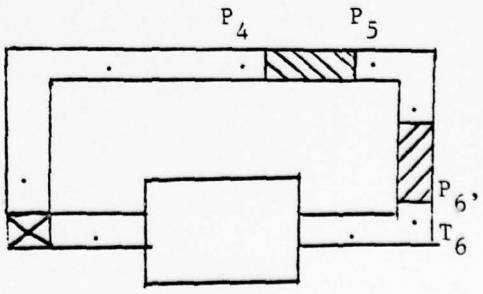

PVC Circulator Experimental Data

Page 187
No. 5468
Date 12 July 1978

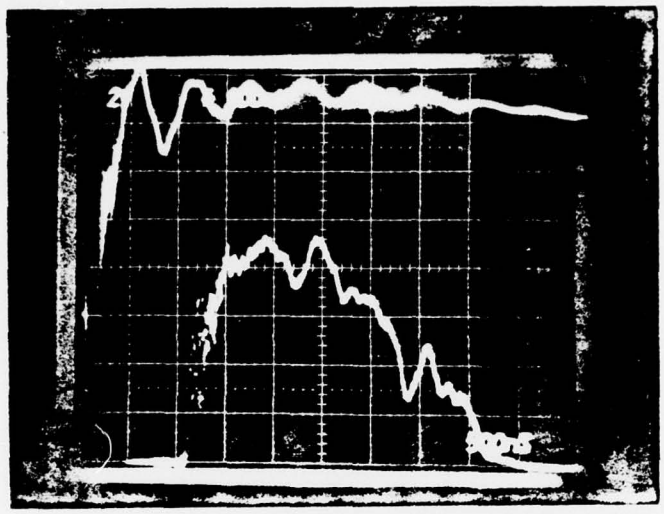

Gun Data

1. Upper Trace
   Voltage 100mV/div
   Time Scale 10μsec/div
   Inverted? (Yes) No
2. Lower Trace
   Voltage 2V /div
   Time Scale 500nsec/div
   Inverted? Yes (No)
   Attenuation _____

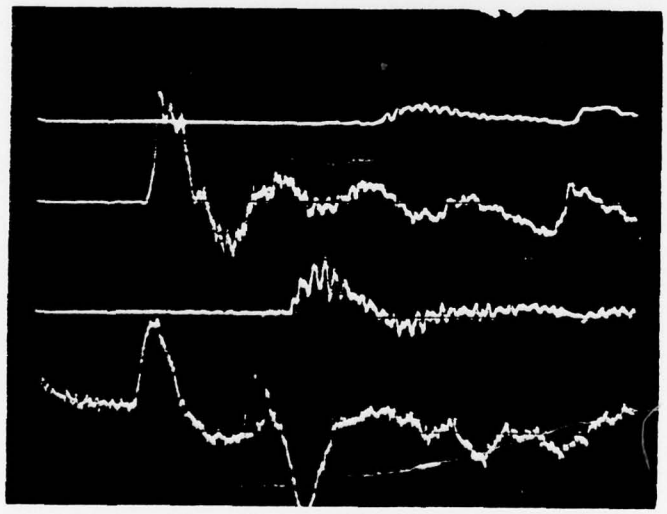

Voltages

P_4 Ch. 1 0.02V /div

P_6 Ch. 2 0.02V /div

P_5 Ch. 3 0.02V /div

T_1 Ch. 4 0.05V /div

Time Scale 2msec /div
Sustainer Voltage 25.8kV
Flow? On (Off)
Gas Type N_2
Notes: _____

Analyzed Data:

E = 60.84

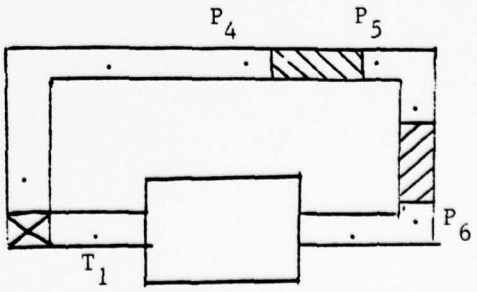

PVC Circulator Experimental Data

Page 188
No. 5469
Date 12 July 1978

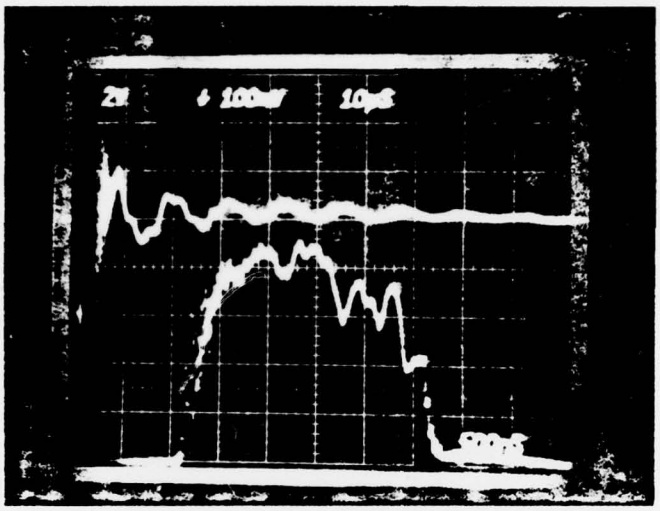

Gun Data

1. Upper Trace
   Voltage 100mV/div
   Time Scale 10μsec/div
   Inverted? (Yes) No
2. Lower Trace
   Voltage 2V /div
   Time Scale 500nsec/div
   Inverted? Yes (No)
   Attenuation _____

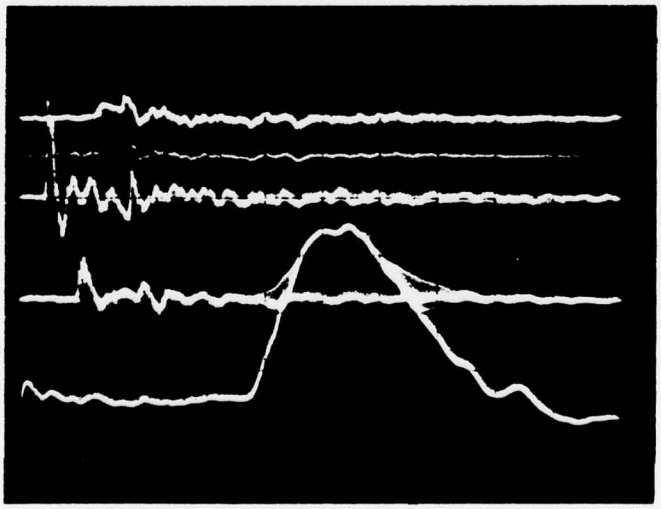

Voltages

P_4 Ch. 1 0.02V /div

P_6 Ch. 2 0.02V /div

P_5 Ch. 3 0.02V /div

T_1 Ch. 4 0.20V /div

Time Scale 10msec /div
Sustainer Voltage 25.8kV
Flow? (On) Off
Gas Type N_2
Notes: Preston amp set on 100Hz bandwidth

Analyzed Data:

E = 60.84

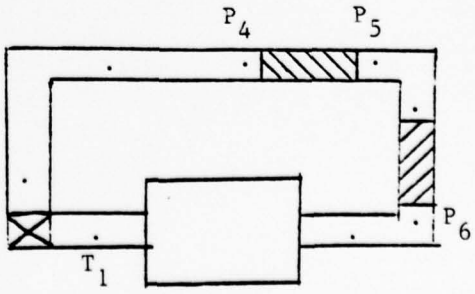

PVC Circulator Experimental Data

Page 189
No. 5470
Date 12 July 1978

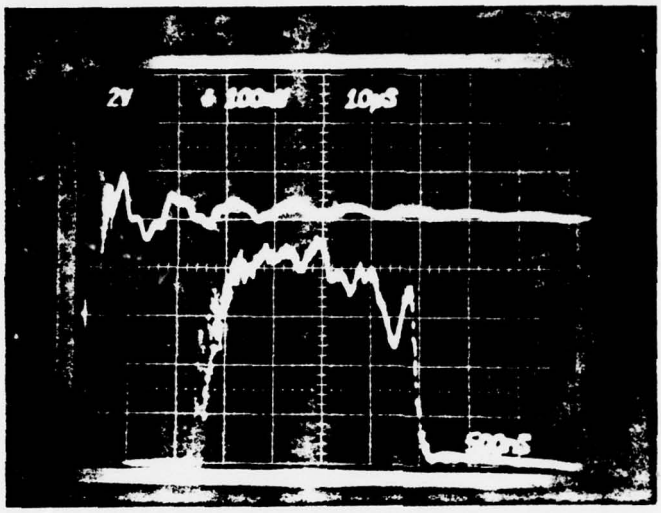

Gun Data

1. Upper Trace
   Voltage 100mV/div
   Time Scale 10µsec/div
   Inverted? (Yes) No
2. Lower Trace
   Voltage 2V /div
   Time Scale 500nsec/div
   Inverted? Yes (No)
   Attenuation _____

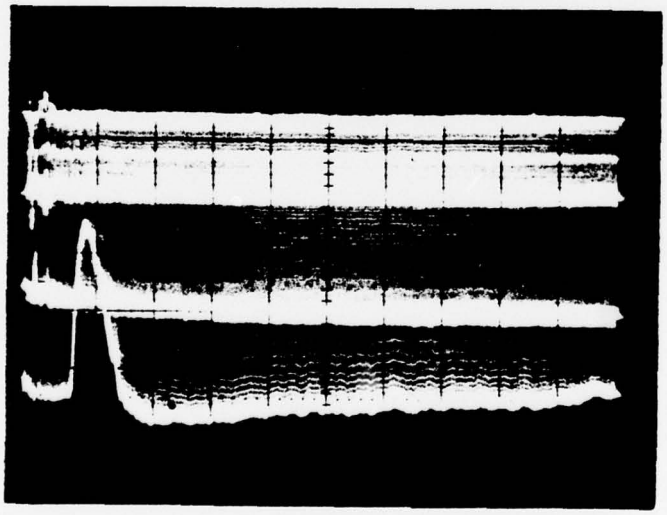

Voltages

P_1 Ch. 1 0.02V/div

P_6 Ch. 2 0.02V/div

P_{5A} Ch. 3 0.02V/div

T_1 Ch. 4 0.20V/div

Time Scale 50msec/div
Sustainer Voltage 25.8kV
Flow? (On) Off
Gas Type N_2
Notes: Preston amp on

Analyzed Data:

E = 55.77

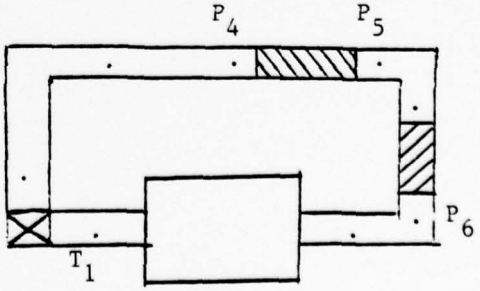

PVC Circulator Experimental Data

Page 191
No. 5472
Date 12 July 1978

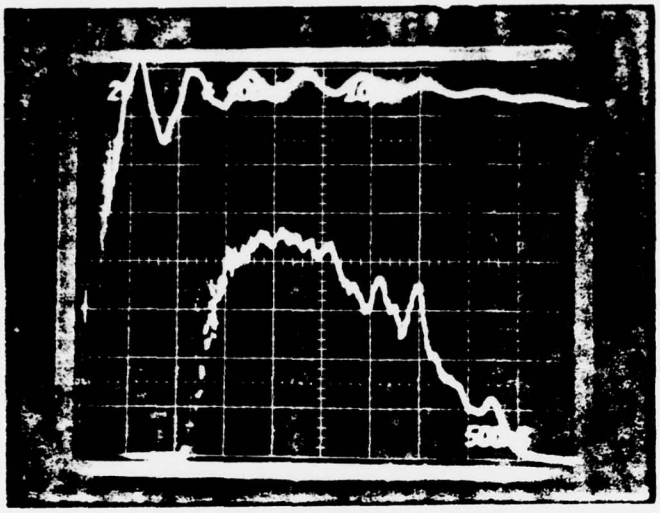

Gun Data

1. Upper Trace
   Voltage 100mV/div
   Time Scale 10μsec/div
   Inverted? (Yes) No
2. Lower Trace
   Voltage 2V /div
   Time Scale 500nsec/div
   Inverted? Yes (No)
   Attenuation _____

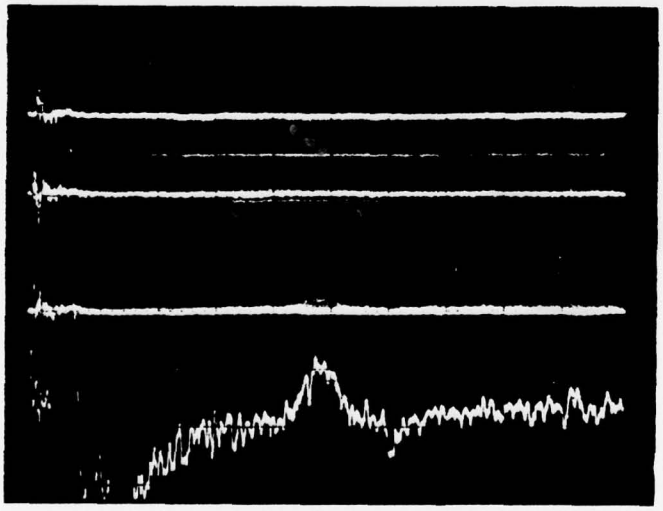

Voltages

P Ch. 1 0.02V /div
P_6 Ch. 2 0.02V /div
P_5 Ch. 3 0.02V /div
T Ch. 4 0.05V /div

Time Scale .1sec /div
Sustainer Voltage 25.8kV
Flow? (On) Off
Gas Type N_2
Notes: _____

Analyzed Data:

E = 67.6

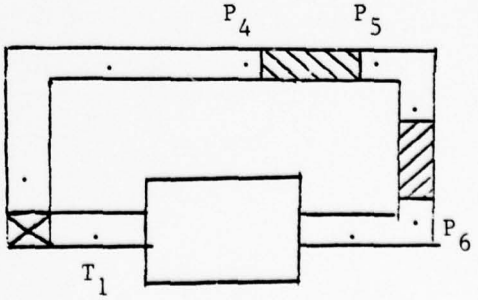

PVC Circulator Experimental Data

Page 192
No. 5473
Date 12 July 1978

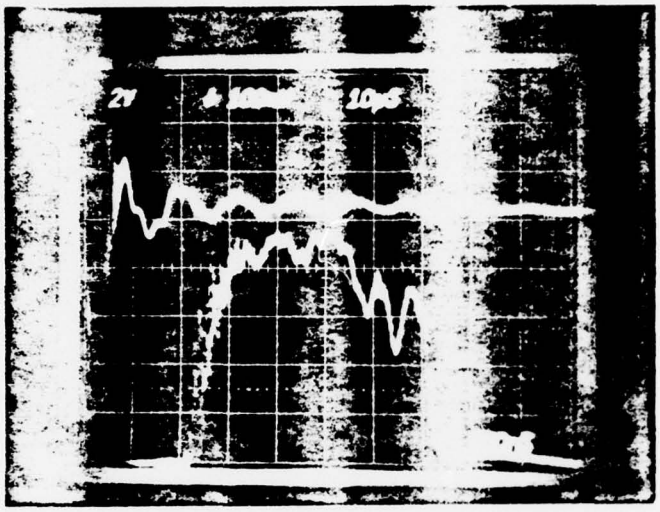

Gun Data

1. Upper Trace
   Voltage 100mV/div
   Time Scale 10μsec/div
   Inverted? (Yes) No
2. Lower Trace
   Voltage 2V/div
   Time Scale 500nsec/div
   Inverted? Yes (No)
   Attenuation _____

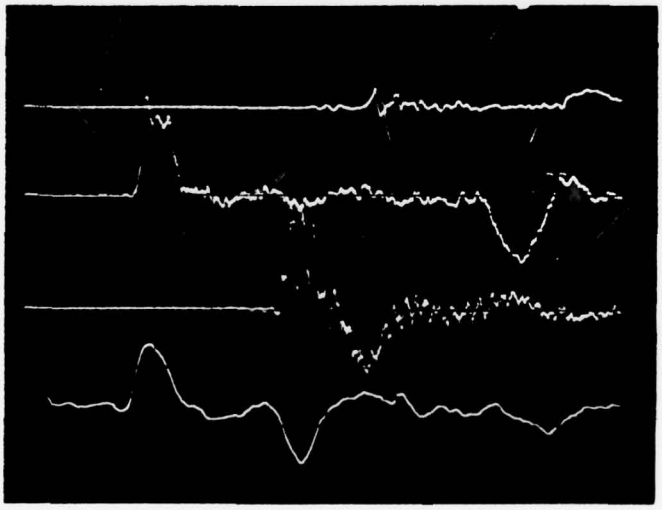

Voltages

P_4 Ch. 1 0.02V/div

P_6 Ch. 2 0.02V/div

P_5 Ch. 3 0.02V/div

T_1 Ch. 4 0.05V/div

Time Scale 2msec/div
Sustainer Voltage 25.8kV
Flow? On Off
Gas Type N_2
Notes: Horn muffler

Analyzed Data:

E = 60.84

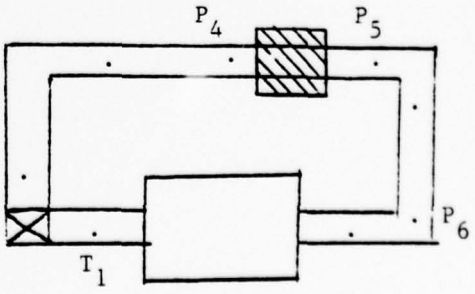

PVC Circulator Experimental Data

Page 193
No. 5474
Date 12 July 1978

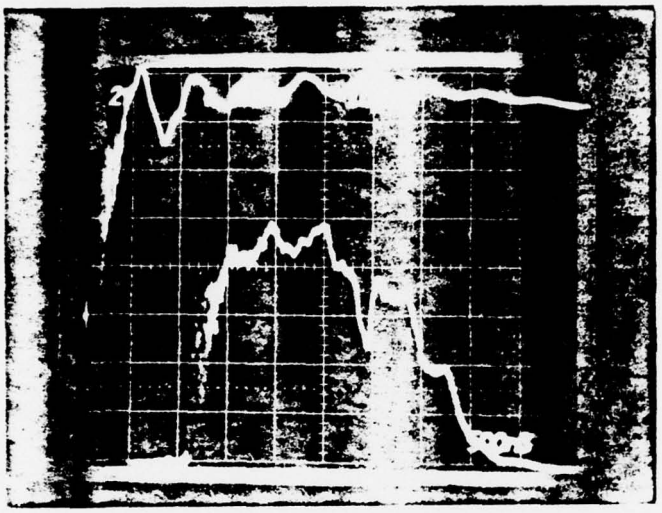

Gun Data

1. Upper Trace
   Voltage 100mV/div
   Time Scale 10μsec/div
   Inverted? (Yes) No
2. Lower Trace
   Voltage 2V /div
   Time Scale 500nsec/div
   Inverted? Yes (No)
   Attenuation _____

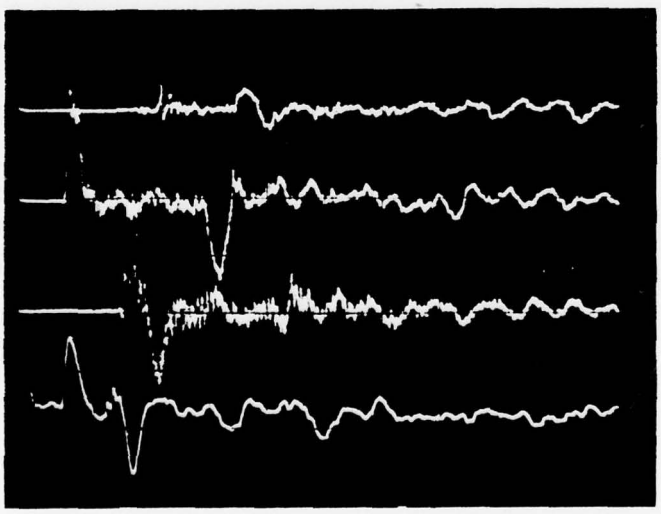

Voltages

P_4 Ch. 1 0.02V /div

P_6 Ch. 2 0.02V /div

P_5 Ch. 3 0.02V /div

T_1 Ch. 4 0.05V /div

Time Scale 5msec /div
Sustainer Voltage 25.8kV
Flow? On Off
Gas Type N_2
Notes: Horn muffler

Analyzed Data:

E = 67.6

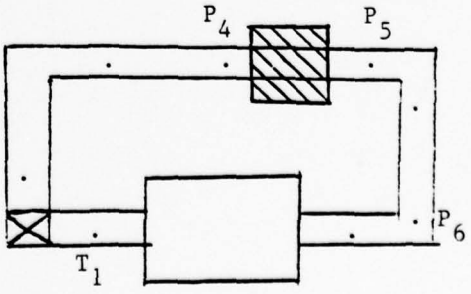

PVC Circulator Experimental Data

Page 194
No. 5475
Date 12 July 1978

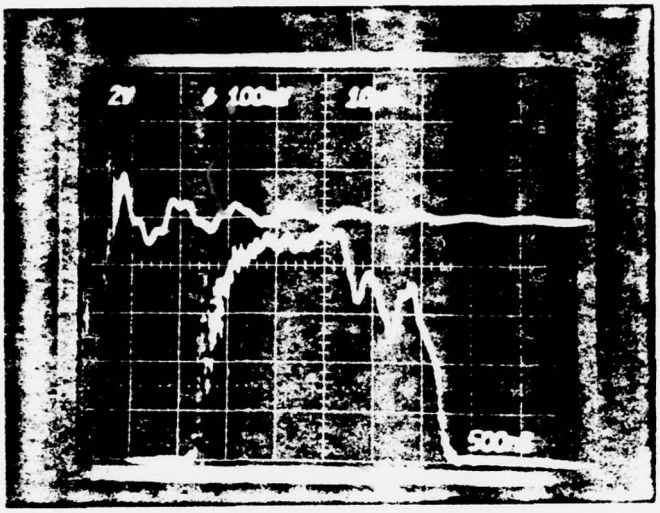

Gun Data

1. Upper Trace
   Voltage 100mV/div
   Time Scale 10μsec/div
   Inverted? (Yes) No
2. Lower Trace
   Voltage 2V /div
   Time Scale 500nsec/div
   Inverted? Yes (No)
   Attenuation _____

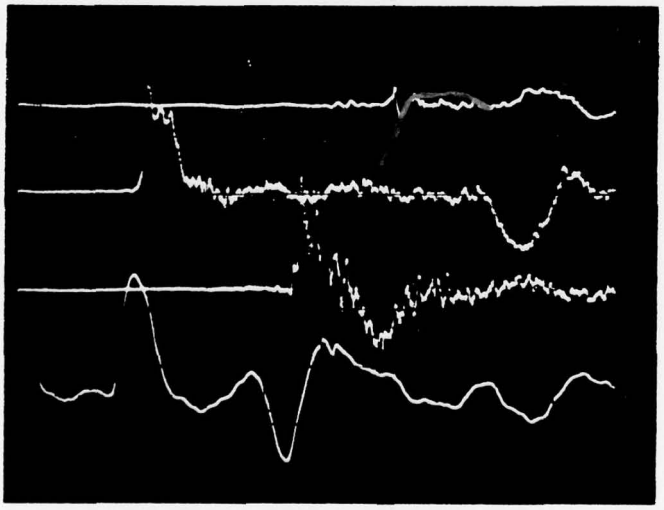

Voltages

P_4 Ch. 1 0.02V /div

P_6 Ch. 2 0.02V /div

P_5 Ch. 3 0.02V /div

T_1 Ch. 4 0.05V /div

Time Scale 2msec /div
Sustainer Voltage 25.8kV
Flow? (On) Off
Gas Type N_2
Notes: Horn muffler

Analyzed Data:

E = 62.53

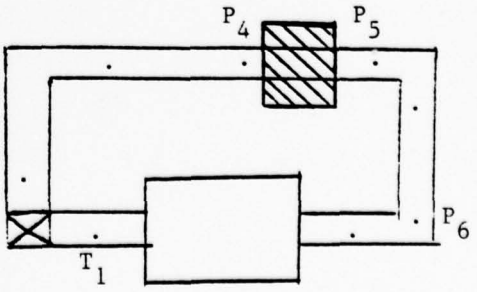

PVC Circulator Experimental Data

Page 195
No. 5476
Date 12 July 1978

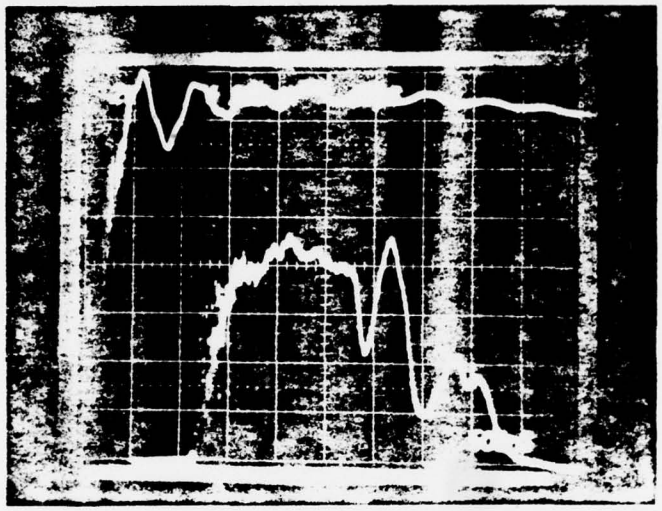

Gun Data

1. Upper Trace
   Voltage 100mV/div
   Time Scale 10μsec/div
   Inverted? (Yes) No
2. Lower Trace
   Voltage 2V /div
   Time Scale 500nsec/div
   Inverted? Yes (No)
   Attenuation _____

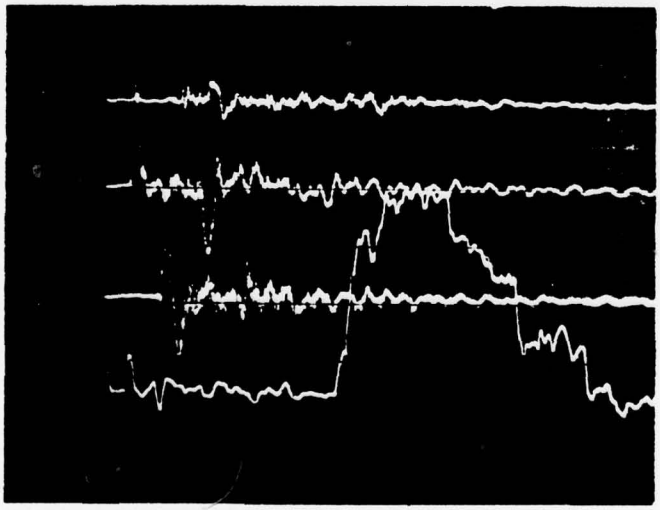

Voltages

P_4 Ch. 1 0.02V /div

P_6 Ch. 2 0.02V /div

P_5 Ch. 3 0.02V /div

T_1 Ch. 4 0.20V /div

Time Scale 10msec /div
Sustainer Voltage 25.8kV
Flow? (On) Off
Gas Type N_2
Notes: Horn muffler

Analyzed Data:

E = 64.22

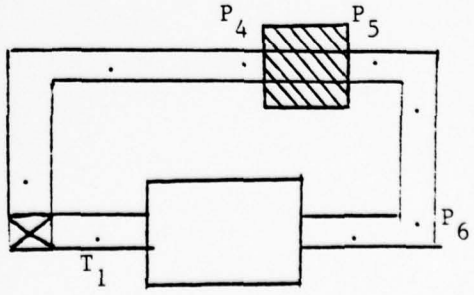

PVC Circulator Experimental Data

Page 196
No. 5477
Date 12 July 1978

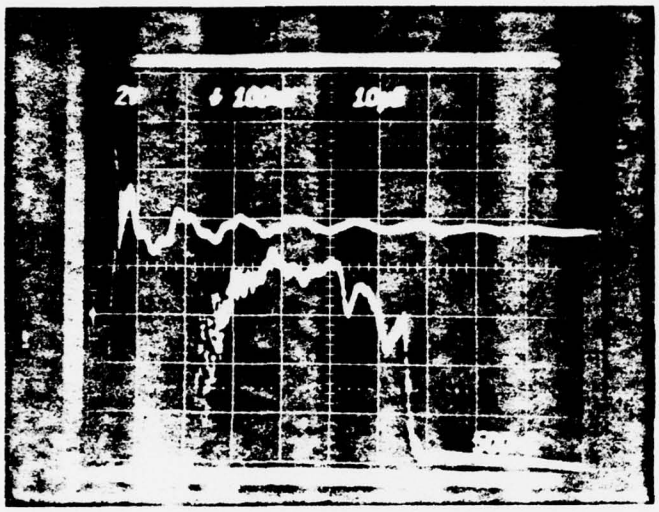

Gun Data

1. Upper Trace
   Voltage 100mV/div
   Time Scale 10μsec/div
   Inverted? (Yes) No
2. Lower Trace
   Voltage 2V /div
   Time Scale 500nsec/div
   Inverted? Yes (No)
   Attenuation _____

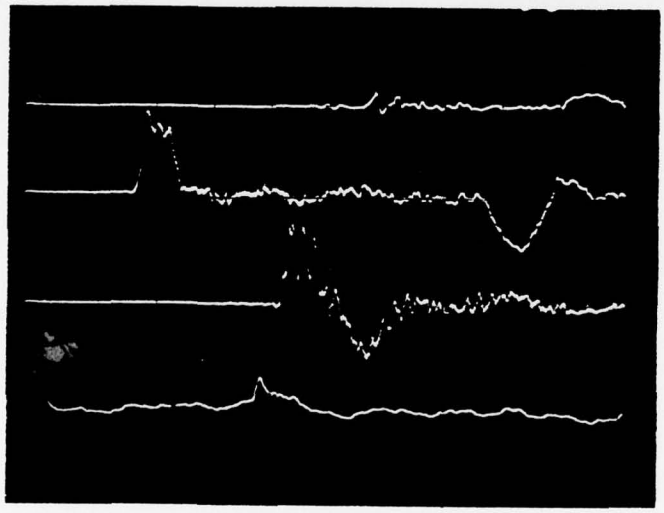

Voltages

P_4 Ch. 1 0.02V/div

P_6 Ch. 2 0.02V/div

P_5 Ch. 3 0.02V/div

T_2 Ch. 4 0.05V/div

Time Scale 2msec/div
Sustainer Voltage 25.8kV
Flow? On Off
Gas Type N_2
Notes: Horn muffler

Analyzed Data:

E = 46.475

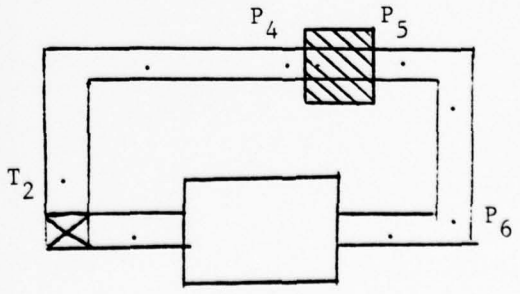

PVC Circulator Experimental Data

Page 197
No. 5478
Date 12 July 1978

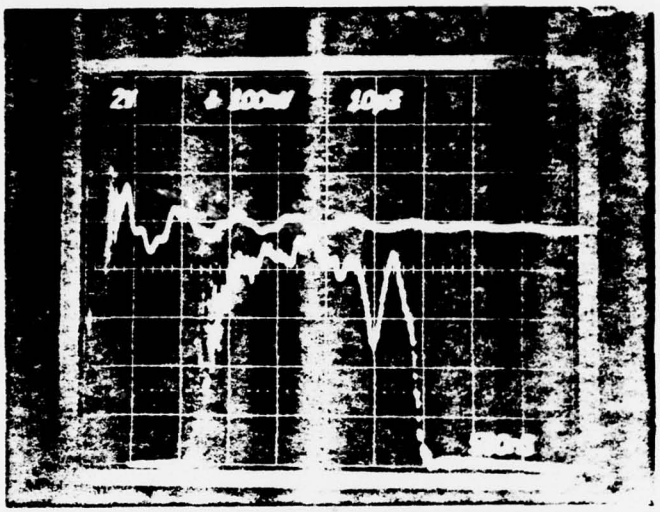

Gun Data

1. Upper Trace
   Voltage 100mV/div
   Time Scale 10μsec/div
   Inverted? (Yes) No
2. Lower Trace
   Voltage 2V /div
   Time Scale 500nsec/div
   Inverted? Yes (No)
   Attenuation _____

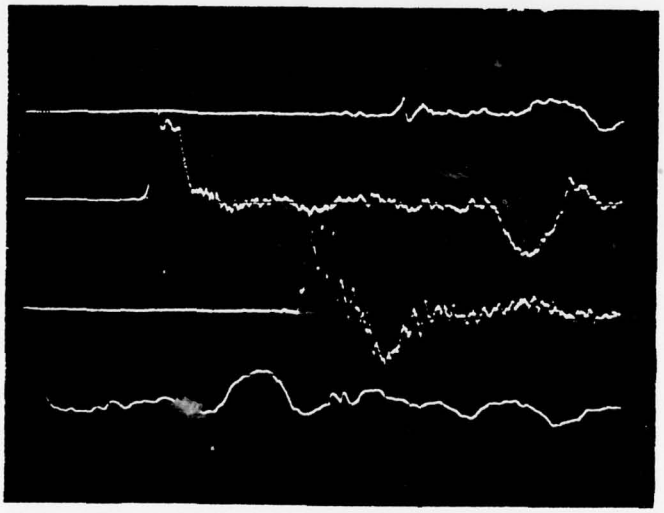

Voltages

P_4 Ch. 1 0.02V /div

P_6 Ch. 2 0.02V /div

P_5 Ch. 3 0.02V /div

T_2 Ch. 4 0.05V /div

Time Scale 2msec /div
Sustainer Voltage 25.8kV
Flow? (On) Off
Gas Type N_2
Notes: Horn muffler

Analyzed Data:

E = 60.84

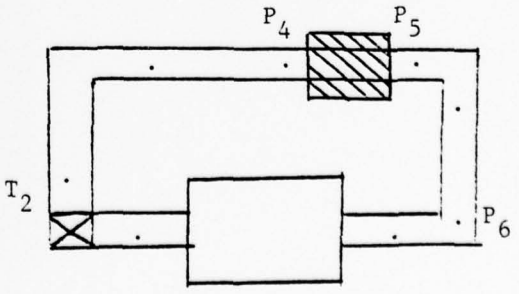

PVC Circulator Experimental Data

Page 198
No. 5479
Date 12 July 1978

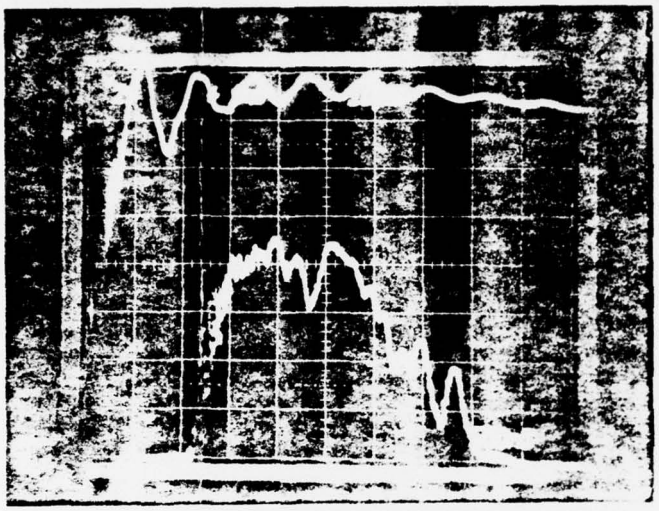

Gun Data

1. Upper Trace
   Voltage 1mV /div
   Time Scale 10μsec/div
   Inverted? (Yes) No
2. Lower Trace
   Voltage 2V /div
   Time Scale 500nsec/div
   Inverted? Yes (No)
   Attenuation _____

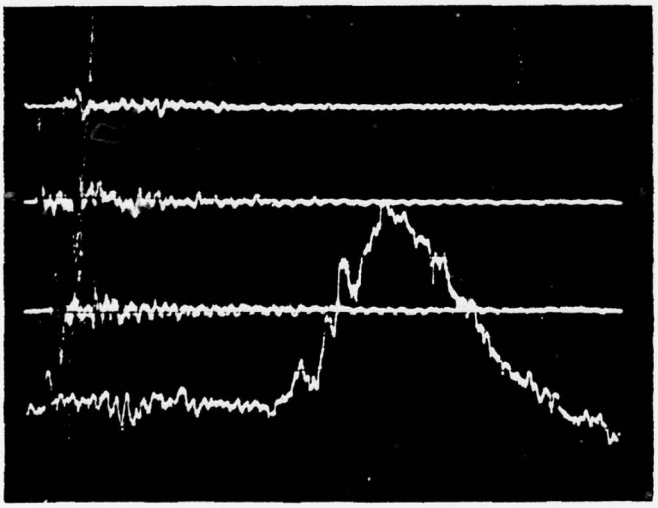

Voltages

P_4 Ch. 1 0.02V /div

P_6 Ch. 2 0.02V /div

P_5 Ch. 3 0.02V /div

T_2 Ch. 4 0.05V /div

Time Scale 20msec /div
Sustainer Voltage 25.8kV
Flow? (On) Off
Gas Type N_2
Notes: Horn muffler

Analyzed Data:

E = 59.15

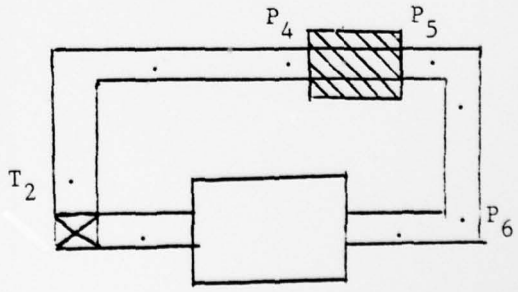

PVC Circulator Experimental Data

Page 199
No. 5480
Date 12 July 1978

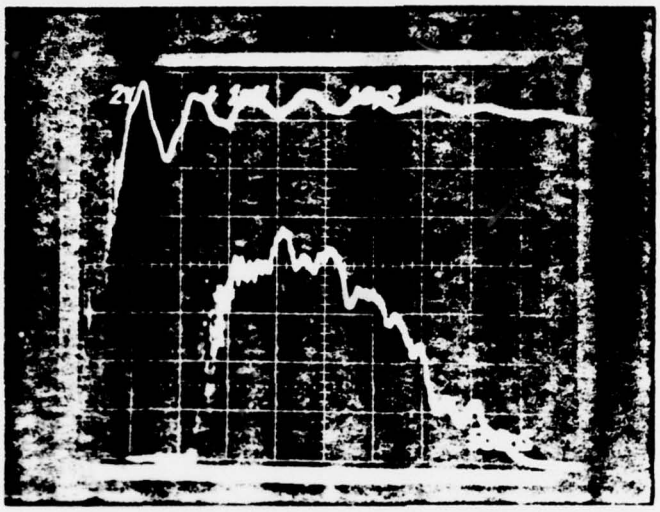

Gun Data

1. Upper Trace
   Voltage 1mV /div
   Time Scale 10μsec/div
   Inverted? (Yes) No
2. Lower Trace
   Voltage 2V /div
   Time Scale 500nsec/div
   Inverted? Yes (No)
   Attenuation _____

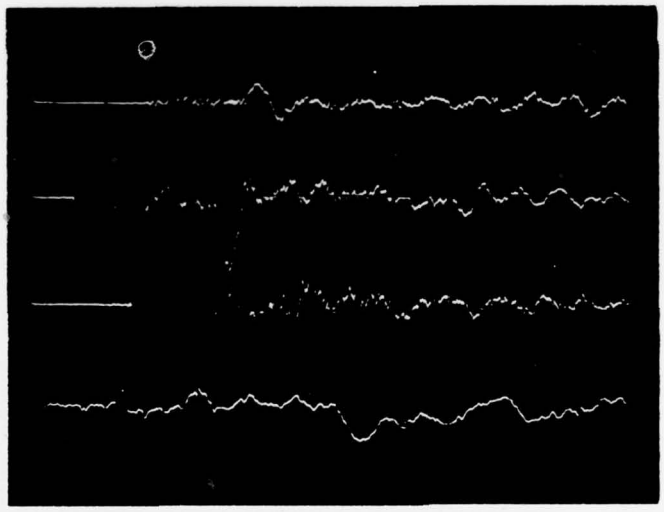

Voltages

P_4 Ch. 1 0.02V /div

P_6 Ch. 2 0.02V /div

P_5 Ch. 3 0.02V /div

T_3 Ch. 4 0.05V /div

Time Scale 5msec /div
Sustainer Voltage 25.8kV
Flow? On (Off)
Gas Type N_2
Notes: Horn muffler

Analyzed Data:

E = 59.15

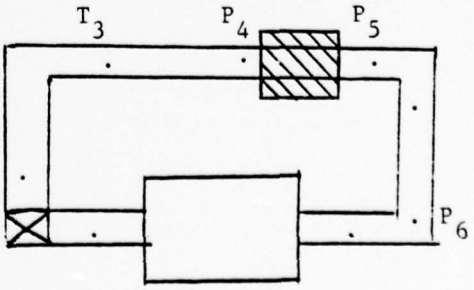

PVC Circulator Experimental Data

Page 200
No. 5481
Date 12 July 1978

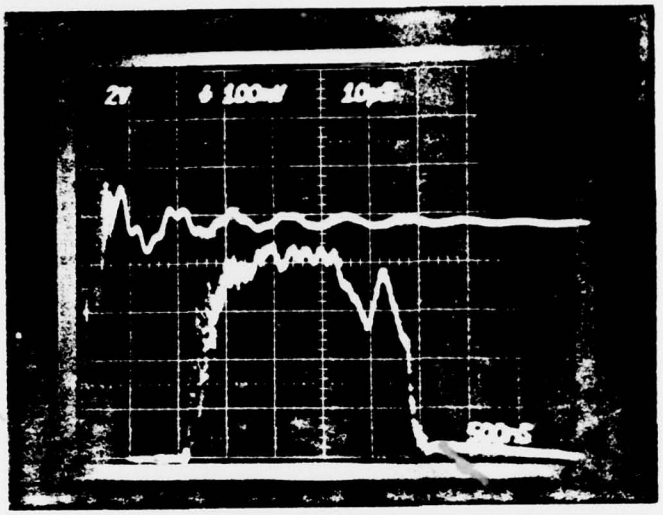

Gun Data

1. Upper Trace
   Voltage 100mV/div
   Time Scale 10μsec/div
   Inverted? (Yes) No
2. Lower Trace
   Voltage 2V /div
   Time Scale 500nsec/div
   Inverted? Yes (No)
   Attenuation _____

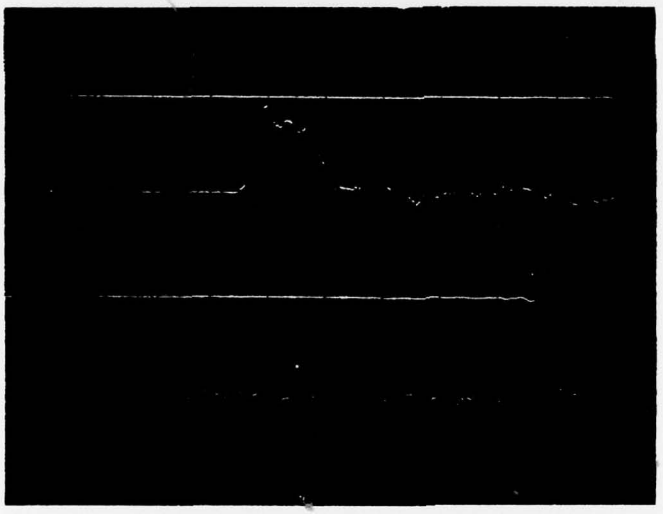

Voltages

P_4 Ch. 1 0.02V /div

P_6 Ch. 2 0.02V /div

P_5 Ch. 3 0.02V /div

T_3 Ch. 4 0.05V /div

Time Scale .1msec/div
Sustainer Voltage 25.8kV
Flow? On (Off)
Gas Type N_2
Notes: Horn muffler

Analyzed Data:

E = 55.77

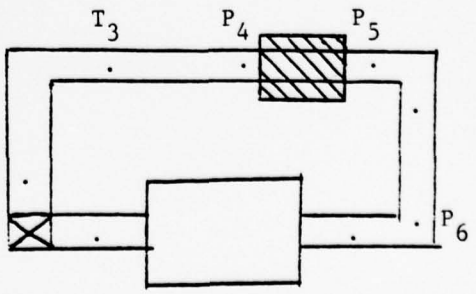

PVC Circulator Experimental Data

Page 201
No. 5482
Date 12 July 1978

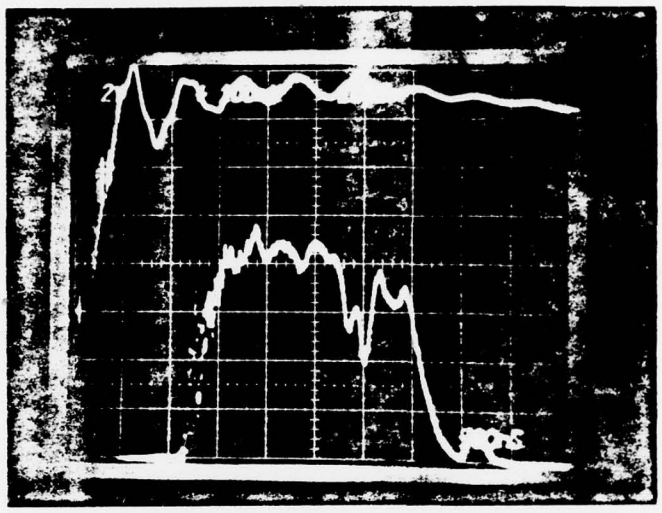

Gun Data

1. Upper Trace
   Voltage 100mV/div
   Time Scale 10μsec/div
   Inverted? (Yes) No
2. Lower Trace
   Voltage 2V /div
   Time Scale 500nsec/div
   Inverted? Yes (No)
   Attenuation _____

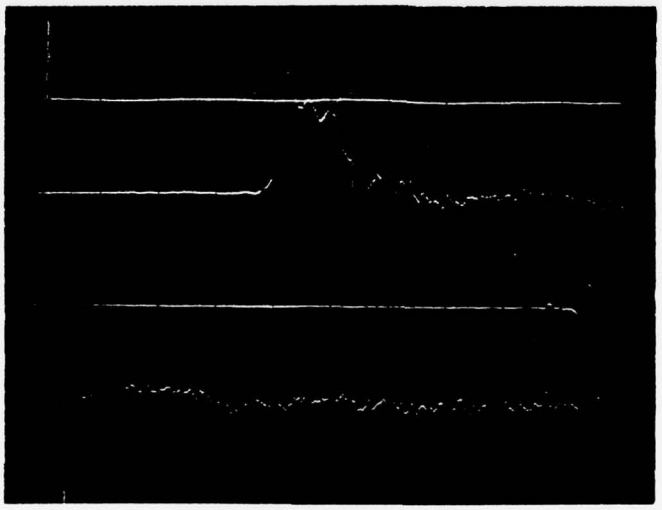

Voltages

P_4 Ch. 1 0.02V /div

P_6 Ch. 2 0.02V /div

P_5 Ch. 3 0.02V /div

T_3 Ch. 4 0.05V /div

Time Scale 1msec/div
Sustainer Voltage 25.8kV
Flow? (On) Off
Gas Type N_2
Notes: _____

Analyzed Data:

E = 59.15

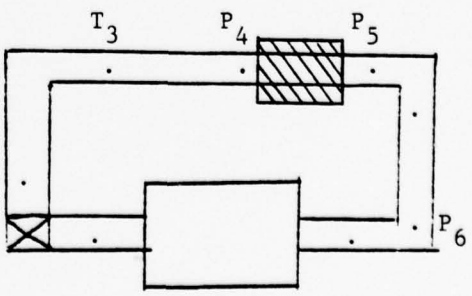

PVC Circulator Experimental Data

Page 202
No. 5483
Date 12 July 1978

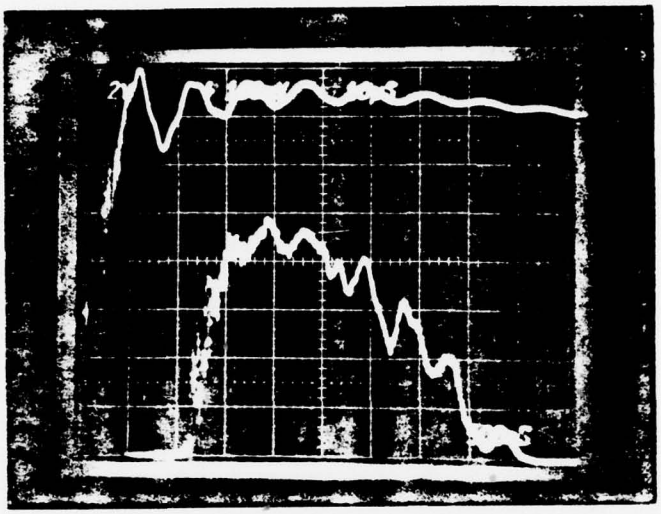

Gun Data

1. Upper Trace
   Voltage 100mV/div
   Time Scale 10used/div
   Inverted? (Yes) No
2. Lower Trace
   Voltage 2V /div
   Time Scale 500nsec/div
   Inverted? Yes (No)
   Attenuation _____

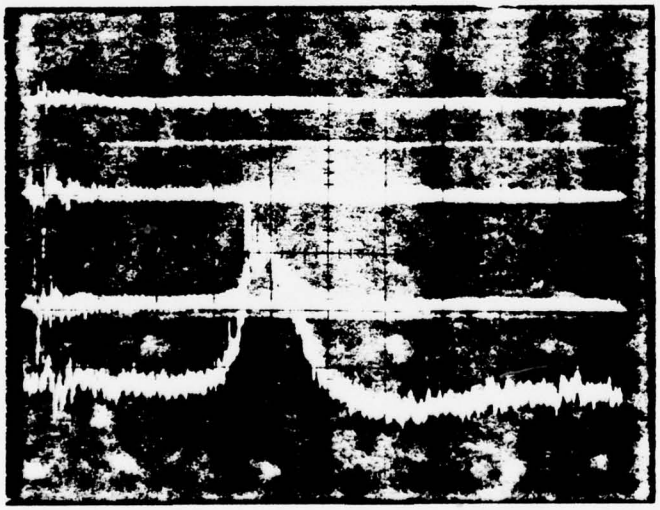

Voltages

P_4 Ch. 1 0.02V/div

P_6 Ch. 2 0.02V/div

P_5 Ch. 3 0.02V/div

T_3 Ch. 4 0.05V/div

Time Scale 50msec/div
Sustainer Voltage 25.8kV
Flow? (On) Off
Gas Type N_2
Notes: Horn muffler

Analyzed Data:

E = 66.755

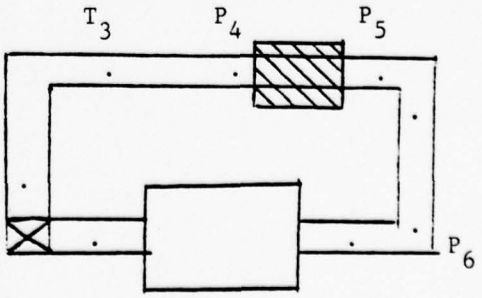

PVC Circulator Experimental Data

Page 203
No. 5484
Date 12 July 1978

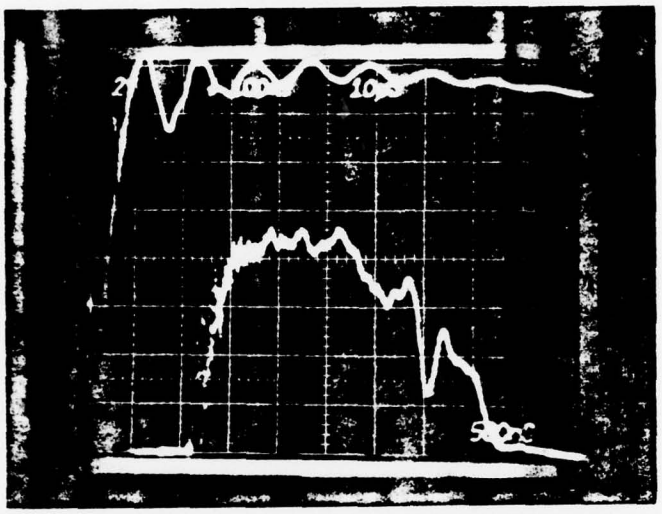

Gun Data

1. Upper Trace
   Voltage 100mV/div
   Time Scale 10μsec/div
   Inverted? (Yes) No
2. Lower Trace
   Voltage 2V /div
   Time Scale 500nsec/div
   Inverted? Yes (No)
   Attenuation _____

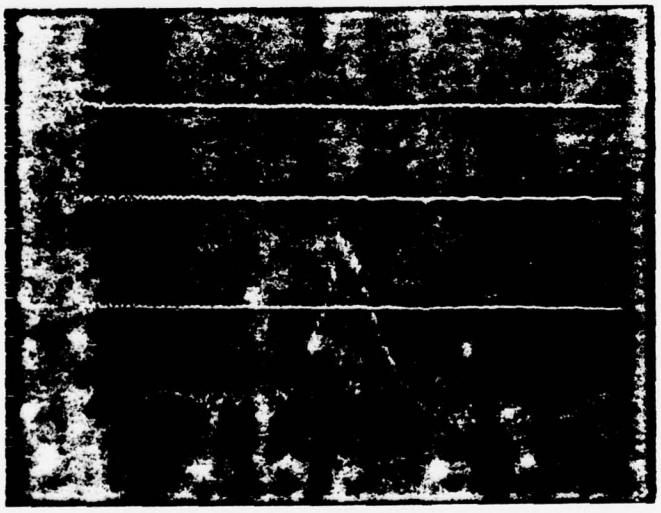

Voltages

P_4 Ch. 1 0.02V /div

P_6 Ch. 2 0.02V /div

P_5 Ch. 3 0.02V /div

T_4 Ch. 4 0.05V /div

Time Scale 50msec/div
Sustainer Voltage 25.8kV
Flow? (On) Off
Gas Type N_2
Notes: Horn muffler

Analyzed Data:

E = 65.91

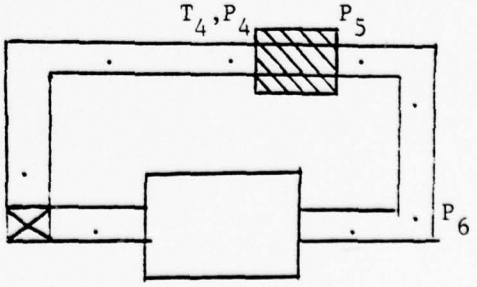

PVC Circulator Experimental Data

Page 204
No. 5485
Date 12 July 1978

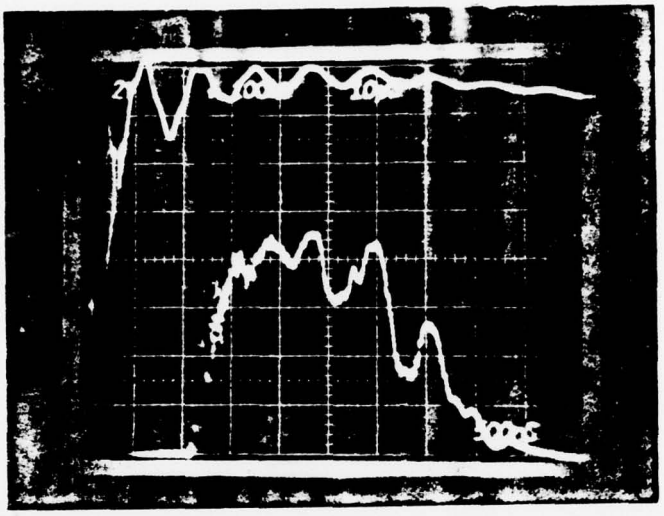

Gun Data

1. Upper Trace
   Voltage 100mV/div
   Time Scale 10used/div
   Inverted? (Yes) No
2. Lower Trace
   Voltage 2V /div
   Time Scale 500nsec/div
   Inverted? Yes (No)
   Attenuation _____

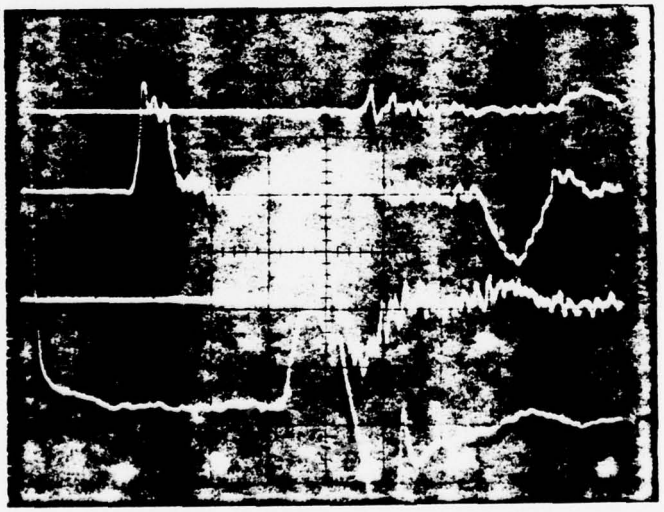

Voltages

P_4 Ch. 1 0.02V/div

P_6 Ch. 2 0.02V/div

P_5 Ch. 3 0.02V/div

T_5 Ch. 4 0.02V/div

Time Scale 2msec /div
Sustainer Voltage 25.8kV
Flow? On Off
Gas Type N_2
Notes: _____

Analyzed Data:

E = 60.84

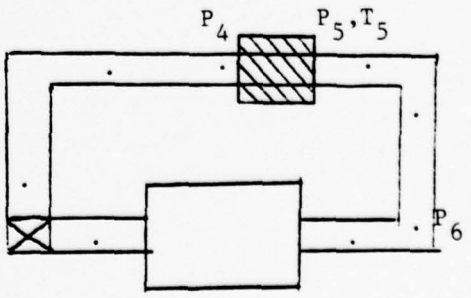

PVC Circulator Experimental Data

Page 205
No. 5486
Date 12 July 1978

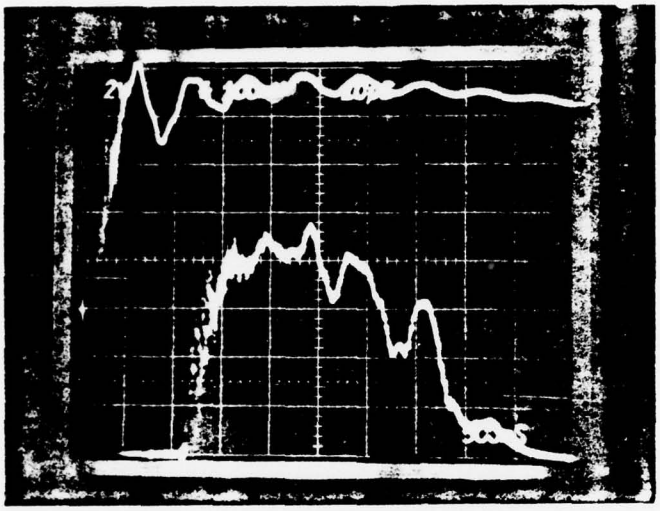

Gun Data

1. Upper Trace
   Voltage 100mV/div
   Time Scale 10μsec/div
   Inverted? (Yes) No
2. Lower Trace
   Voltage 2V /div
   Time Scale 500nsec/div
   Inverted? Yes (No)
   Attenuation _____

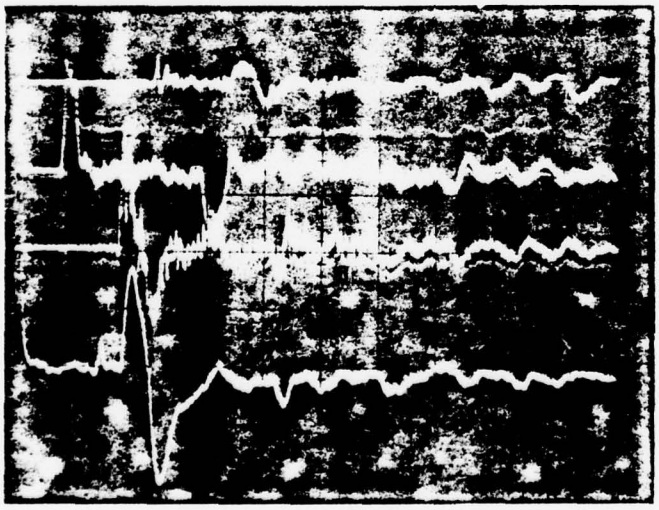

Voltages

P_4 Ch. 1 0.02V /div

P_6 Ch. 2 0.02V /div

P_5 Ch. 3 0.02V /div

T_5 Ch. 4 0.05V /div

Time Scale 5msec /div
Sustainer Voltage 25.8kV
Flow? On (Off)
Gas Type N_2
Notes: Horn muffler

Analyzed Data:

E = 64.22

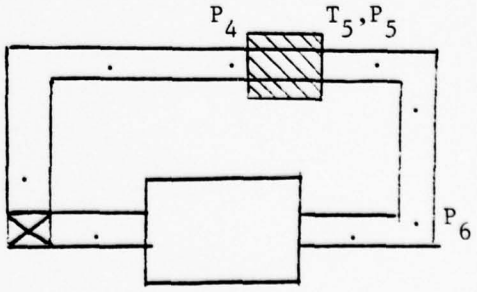

PVC Circulator Experimental Data

Page 206
No. 5491
Date 12 July 1978

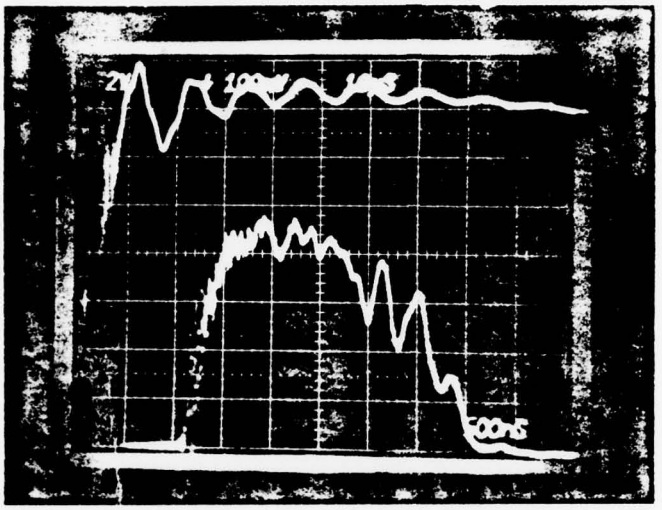

Gun Data

1. Upper Trace
   Voltage 100mV/div
   Time Scale 10μsec/div
   Inverted? (Yes) No
2. Lower Trace
   Voltage 2V /div
   Time Scale 500nsec/div
   Inverted? Yes (No)
   Attenuation _____

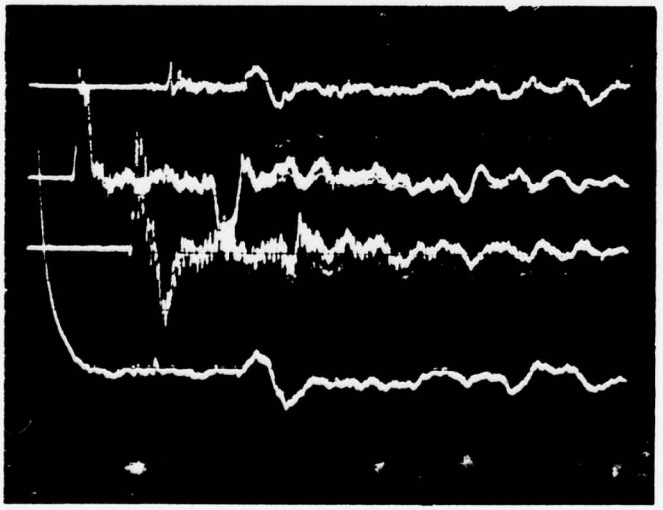

Voltages

P_4 Ch. 1 0.02V/div

P_6 Ch. 2 0.02V/div

P_5 Ch. 3 0.02V/div

T_4 Ch. 4 0.05V/div

Time Scale 5msec /div
Sustainer Voltage 25.8kV
Flow? On (Off)
Gas Type N_2
Notes: _____

Analyzed Data:

E = 62.53

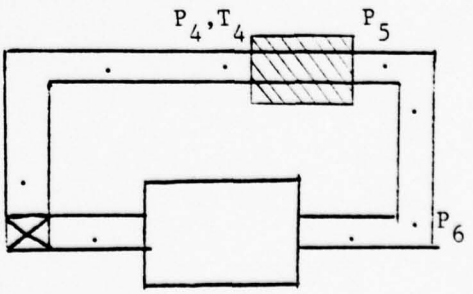

PVC Circulator Experimental Data

Page 207
No. 5492
Date 12 July 1978

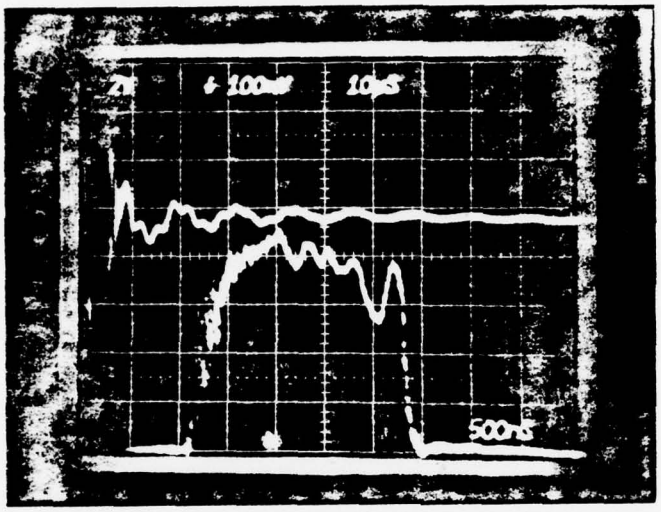

Gun Data

1. Upper Trace
   Voltage 100mV/div
   Time Scale 10µsec/div
   Inverted? (Yes) No
2. Lower Trace
   Voltage 2V /div
   Time Scale 500nsec/div
   Inverted? Yes (No)
   Attenuation _____

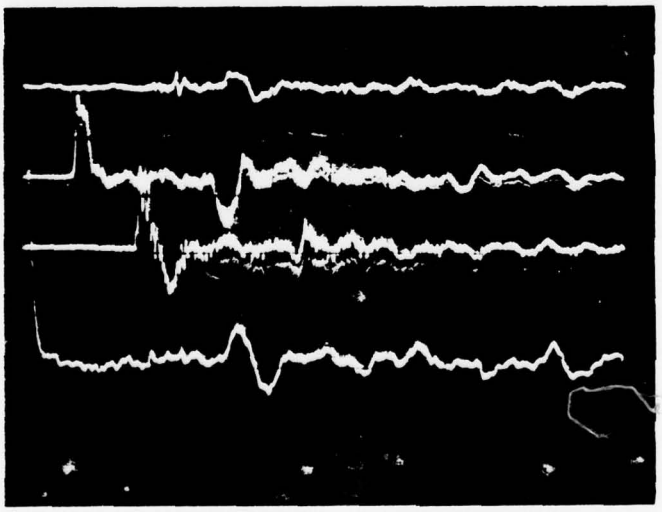

Voltages

P_4 Ch. 1 0.02V /div

P_6 Ch. 2 0.02V /div

P_5 Ch. 3 0.02V/div

T_4 Ch. 4 0.05V /div

Time Scale 5msec/div
Sustainer Voltage 25.8kV
Flow? (On) Off
Gas Type N_2
Notes: Horn muffler

Analyzed Data:

E = 54.08

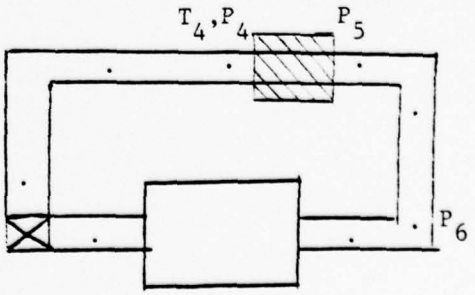

PVC Circulator Experimental Data

Page 208
No. 5493
Date 12 July 1978

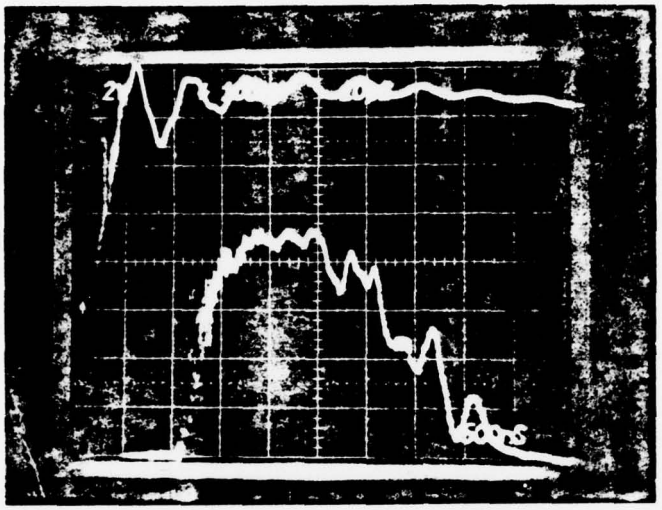

Gun Data

1. Upper Trace
   Voltage 100mV/div
   Time Scale 10μsec/div
   Inverted? (Yes) No
2. Lower Trace
   Voltage 2V /div
   Time Scale 500nsec/div
   Inverted? Yes (No)
   Attenuation _____

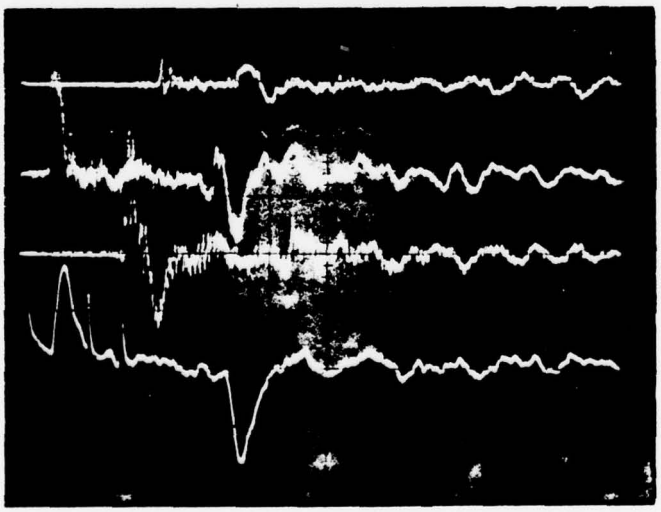

Voltages

P_4 Ch. 1 0.02V /div

P_7 Ch. 2 0.02V /div

P_5 Ch. 3 0.02V/div

T_7 Ch. 4 0.05V /div

Time Scale 5msec /div
Sustainer Voltage 25.8kV
Flow? (On) Off
Gas Type N_2
Notes: Horn muffler

Analyzed Data:

E = 64.22

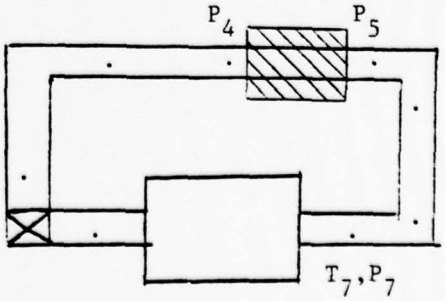

PVC Circulator Experimental Data

Page 209
No. 5494
Date 12 July 1978

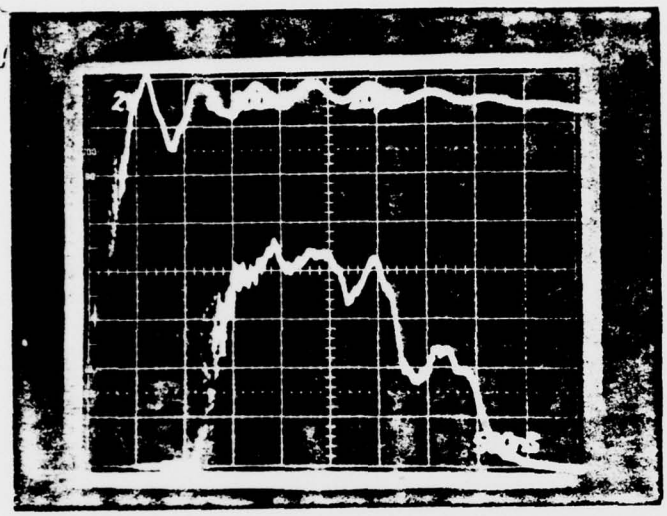

Gun Data

1. Upper Trace
   Voltage 100mV/div
   Time Scale 10μsec/div
   Inverted? (Yes) No
2. Lower Trace
   Voltage 2V /div
   Time Scale 500nsec/div
   Inverted? Yes (No)
   Attenuation _____

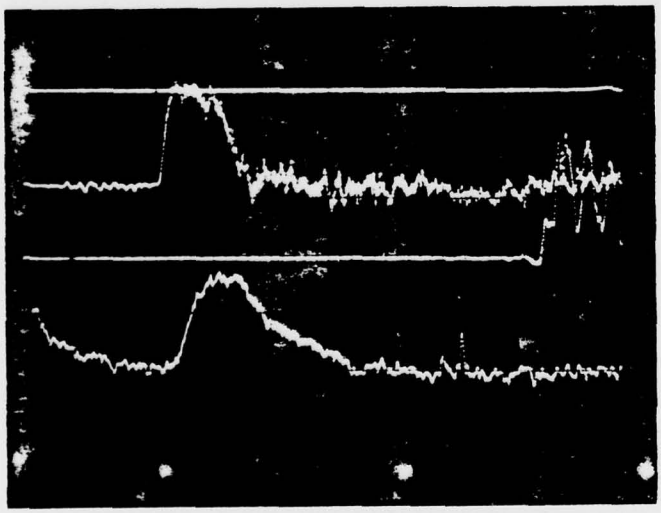

Voltages

P_4 Ch. 1 0.02V /div

P_7 Ch. 2 0.02V /div

P_5 Ch. 3 0.02V/div

T_7 Ch. 4 0.05V /div

Time Scale 1msec /div
Sustainer Voltage 25.8kV
Flow? (On) Off
Gas Type N_2
Notes: Horn muffler

Analyzed Data:

E = 64.22

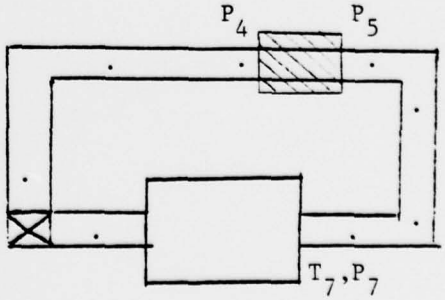

PVC Circulator Experimental Data

Page 210
No. 5496
Date 12 July 1978

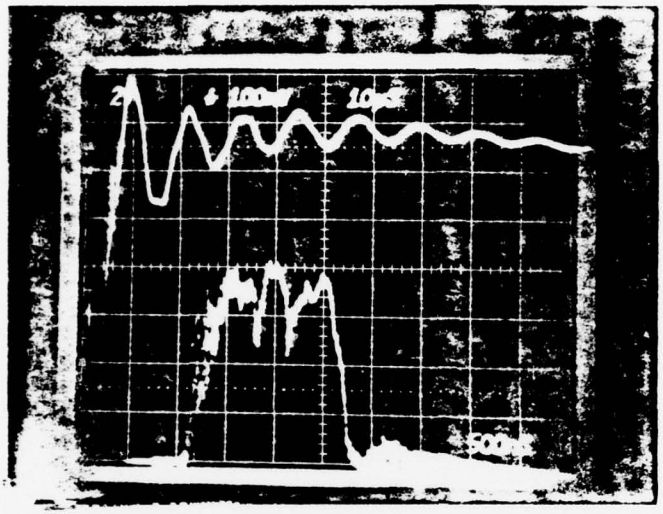

Gun Data

1. Upper Trace
   Voltage 100mV/div
   Time Scale 10used/div
   Inverted? (Yes) No
2. Lower Trace
   Voltage 2V /div
   Time Scale 500nsec/div
   Inverted? Yes (No)
   Attenuation _____

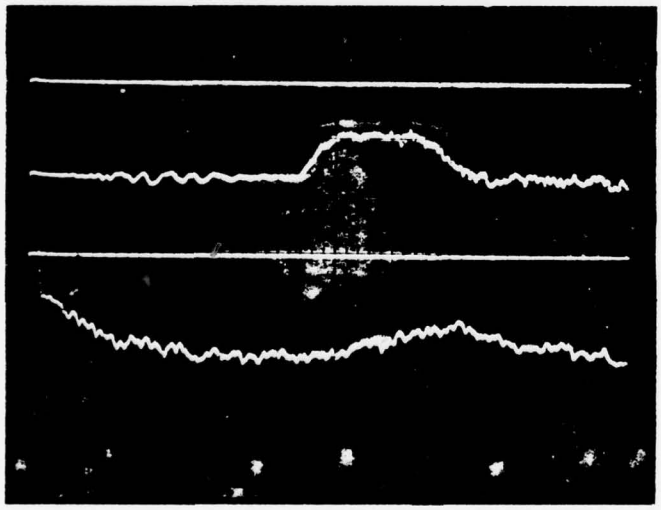

Voltages

P_4 Ch. 1 0.02V /div

P_7 Ch. 2 0.02V /div

P_5 Ch. 3 0.02V/div

T_7 Ch. 4 0.05V /div

Time Scale .5msec/div
Sustainer Voltage 25.8kV
Flow? On (Off)
Gas Type N_2
Notes: _____

Analyzed Data:

E = 33.80

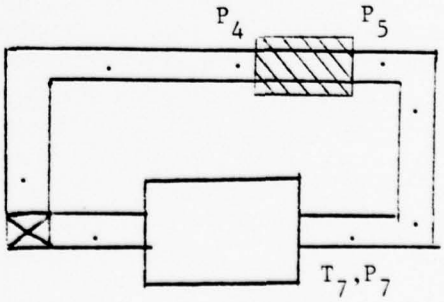

PVC Circulator Experimental Data

Page 211
No. 5497
Date 12 July 1978

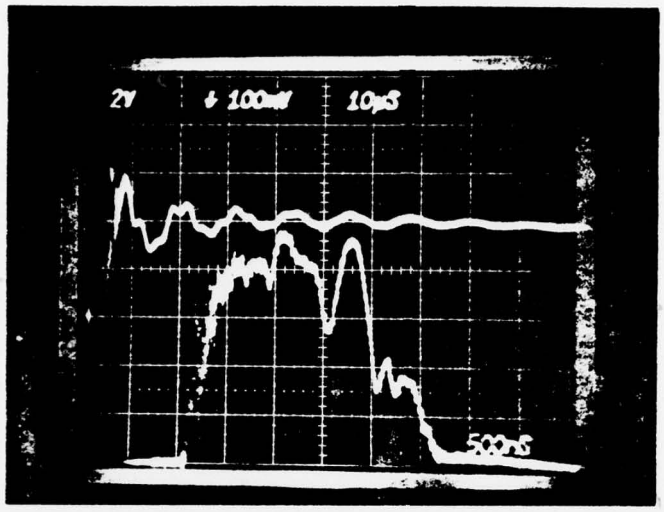

Gun Data

1. Upper Trace
   Voltage 100mV/div
   Time Scale 10µsec/div
   Inverted? (Yes) No
2. Lower Trace
   Voltage 2V /div
   Time Scale 500nsec/div
   Inverted? Yes (No)
   Attenuation _____

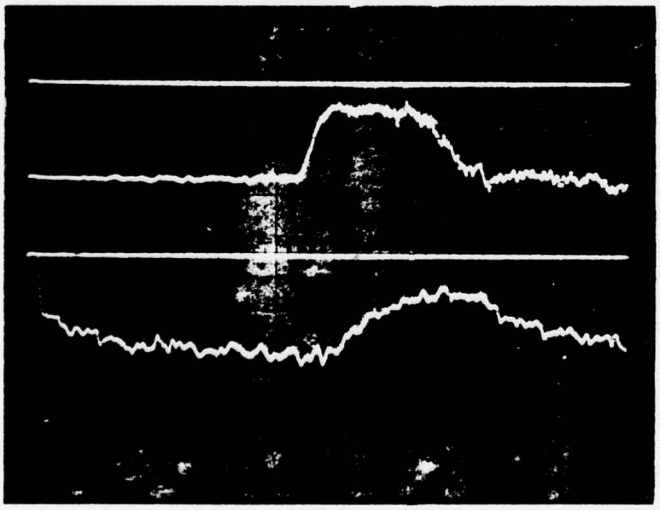

Voltages

P_4 Ch. 1 0.02V /div

P_7 Ch. 2 0.02V /div

P_5 Ch. 3 0.02V/div

T_7 Ch. 4 0.05V /div

Time Scale .5msec/div
Sustainer Voltage 25.8kV
Flow? On (Off)
Gas Type N_2
Notes: Horn muffler

Analyzed Data:

E = 54.08

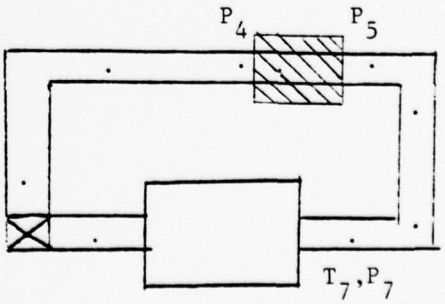

PVC Circulator Experimental Data

Page 212
No. 5498
Date 12 July 1978

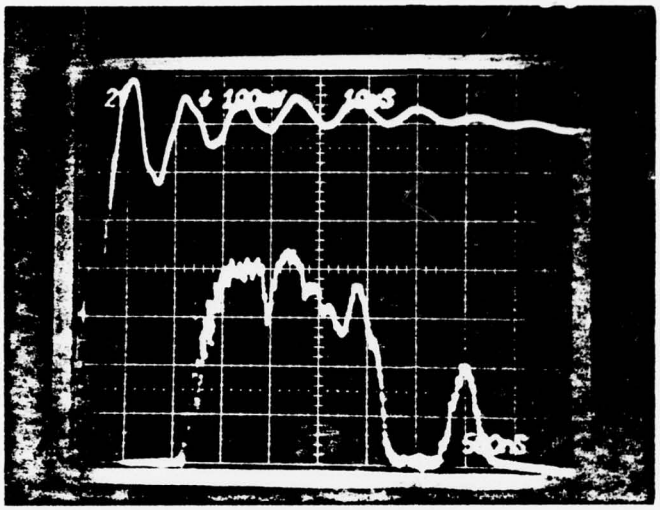

Gun Data

1. Upper Trace
   Voltage 100mV/div
   Time Scale 10μsec/div
   Inverted? (Yes) No
2. Lower Trace
   Voltage 2V /div
   Time Scale 500nsec/div
   Inverted? Yes (No)
   Attenuation _____

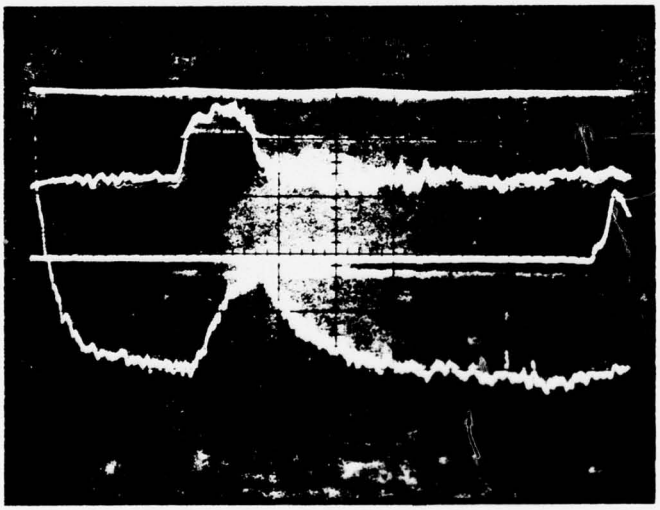

Voltages

P_4 Ch. 1 0.02V /div

P_7 Ch. 2 0.02V /div

P_5 Ch. 3 0.02V /div

T_7 Ch. 4 0.05V /div

Time Scale 1msec /div
Sustainer Voltage 25.8kV
Flow? On (Off)
Gas Type N_2
Notes: Horn muffler

Analyzed Data:

E = 50.70

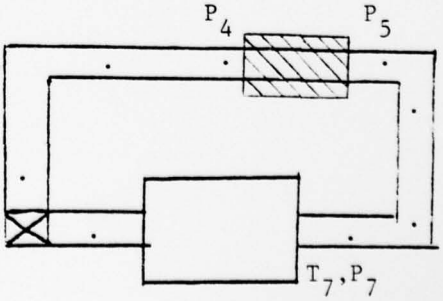

PVC Circulator Experimental Data

Page 213
No. 5500
Date 12 July 1978

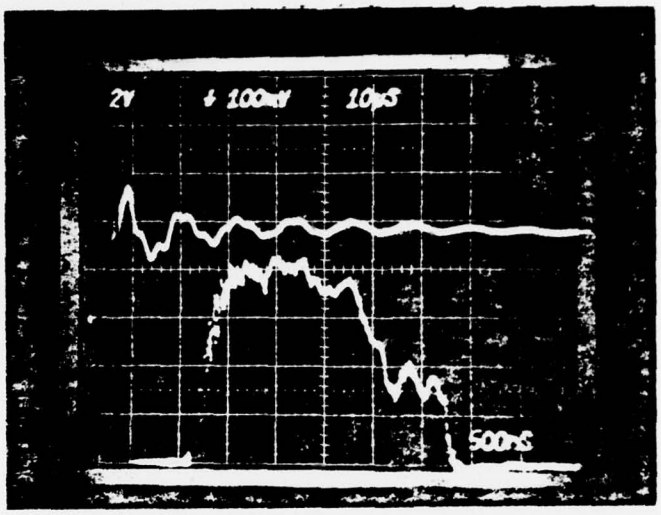

Gun Data

1. Upper Trace
   Voltage 100mV/div
   Time Scale 10μsec/div
   Inverted? (Yes) No
2. Lower Trace
   Voltage 2V /div
   Time Scale 500nsec/div
   Inverted? Yes (No)
   Attenuation _____

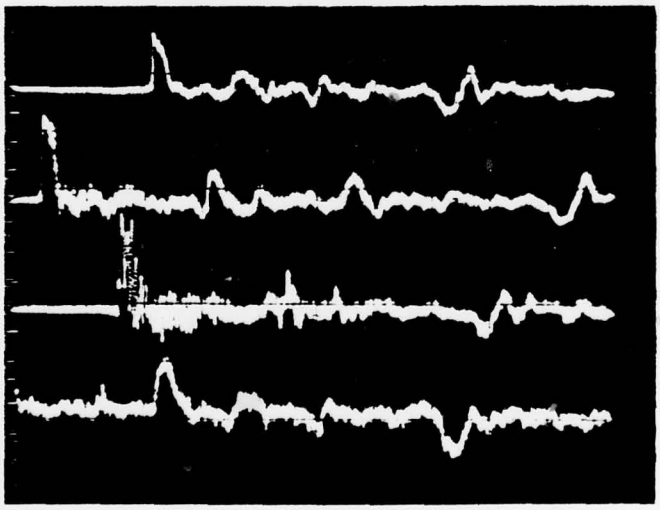

Voltages

P_4 Ch. 1 0.02V /div

P_7 Ch. 2 0.02V /div

P_5 Ch. 3 0.02V/div

T_4 Ch. 4 0.05V /div

Time Scale 5msec /div

Sustainer Voltage 25.8kV

Flow? On (Off)

Gas Type N_2

Notes: 12-1" honeycomb sections(6 coarse + 6 fine) 1 KHz low pass filter

Analyzed Data:

E = 54.08

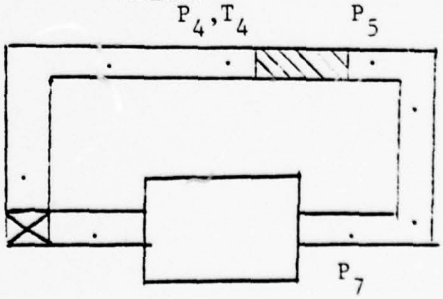

PVC Circulator Experimental Data

Page 214
No. 5501
Date 12 July 1978

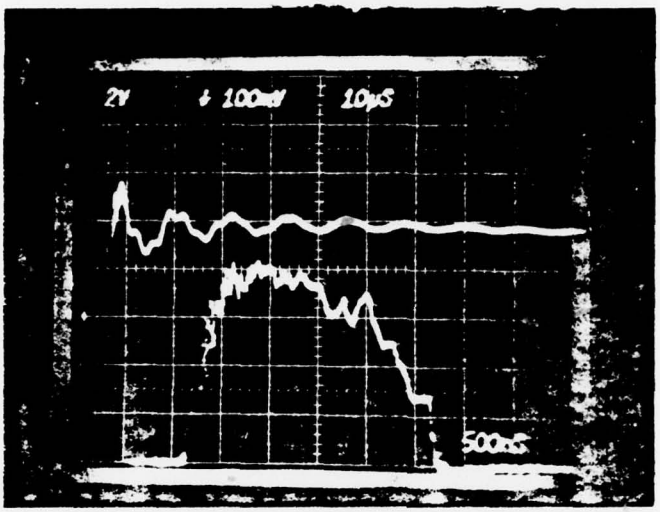

Gun Data

1. Upper Trace
   Voltage 100mV/div
   Time Scale 10μsec/div
   Inverted? (Yes) No
2. Lower Trace
   Voltage 2V /div
   Time Scale 500nsec/div
   Inverted? Yes (No)
   Attenuation _____

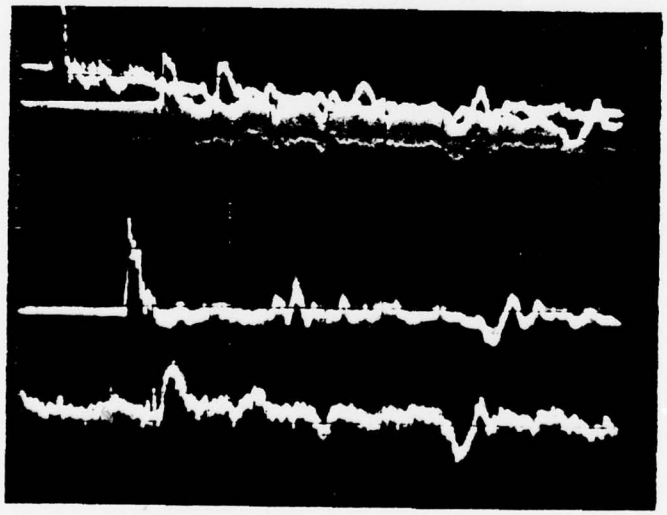

Voltages

P_4 Ch. 1 0.02V /div

P_7 Ch. 2 0.02V /div

P_5 Ch. 3 0.02V /div

T_4 Ch. 4 0.05V /div

Time Scale 5msec /div

Sustainer Voltage 25.8kV

Flow? On (Off)

Gas Type N_2

Notes: 12-1" honeycomb sections (6 coarse + 6 fine) 1 KH2 low pass filter

Analyzed Data:

E = 54.08

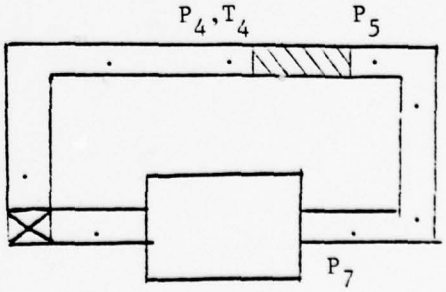

PVC Circulator Experimental Data

Page 215
No. 5502
Date 12 July 1978

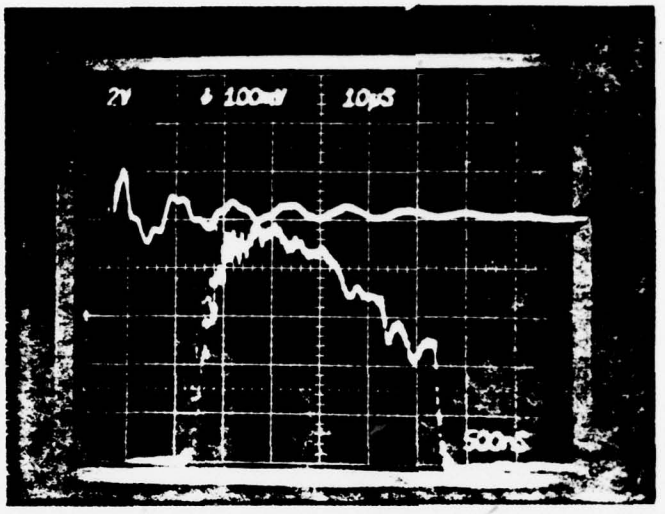

Gun Data

1. Upper Trace
   Voltage 100mV/div
   Time Scale 10μsec/div
   Inverted? (Yes) No
2. Lower Trace
   Voltage 2V /div
   Time Scale 500nsec/div
   Inverted? Yes (No)
   Attenuation _____

Voltages

P_4 Ch. 1 0.02V /div

P_7 Ch. 2 0.02V /div

P_5 Ch. 3 0.02V/div

T_4 Ch. 4 0.05V /div

Time Scale 5msec /div

Sustainer Voltage 25.8kV

Flow? (On) Off

Gas Type N_2

Notes: 12-1" honeycomb
(6 coarse + 6 fine)
1 KHz low pass filter

Analyzed Data:

E = 62.53

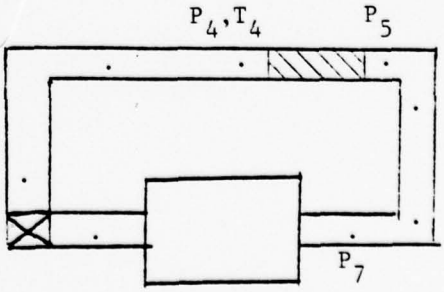

PVC Circulator Experimental Data

Page 216
No. 5503
Date 12 July 1978

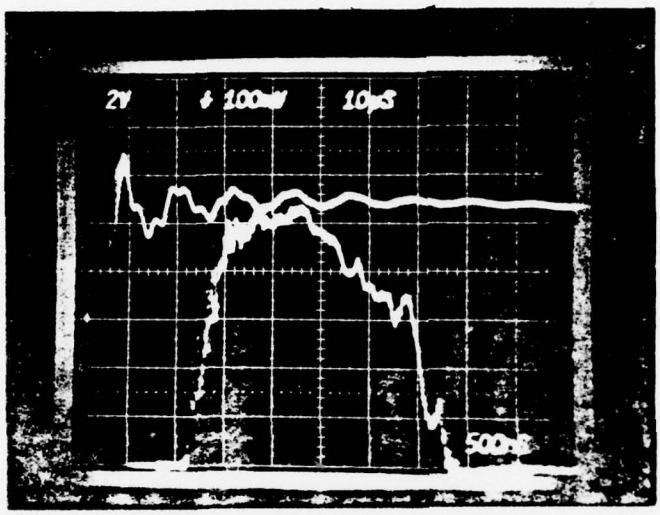

Gun Data

1. Upper Trace
   Voltage 100mV/div
   Time Scale 10usec/div
   Inverted? (Yes) No
2. Lower Trace
   Voltage 2V /div
   Time Scale 500nsec/div
   Inverted? Yes (No)
   Attenuation _____

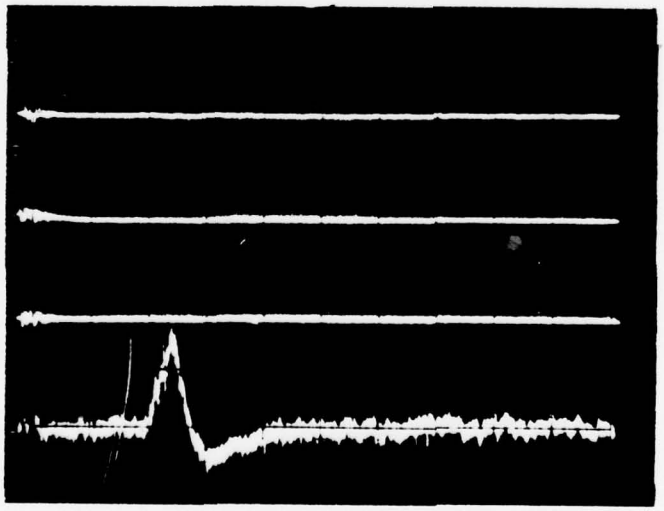

Voltages

P_4 Ch. 1 0.02V /div

P_7 Ch. 2 0.02V /div

P_5 Ch. 3 0.02V /div

T_4 Ch. 4 0.05V /div

Time Scale 0.2sec/div

Sustainer Voltage 25.8kV

Flow? (On) Off

Gas Type N_2

Notes: 12-1" honeycomb
(6 coarse + 6 fine)
1 KHz low pass filter

Analyzed Data:

E = 69.29

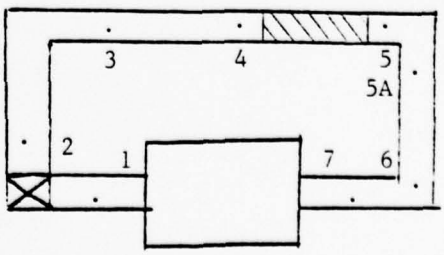

PVC Circulator Experimental Data

Page 217
No. 5504
Date 12 July 1978

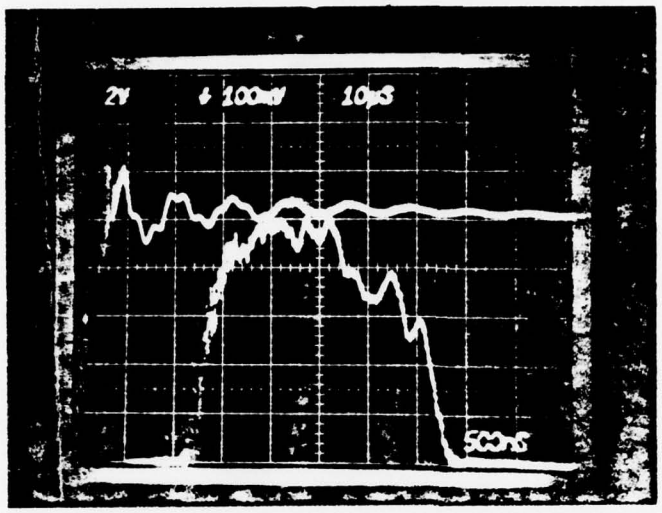

Gun Data

1. Upper Trace
   Voltage 100mV/div
   Time Scale 10μsec/div
   Inverted? (Yes) No
2. Lower Trace
   Voltage 2V /div
   Time Scale 500nsec/div
   Inverted? Yes (No)
   Attenuation _____

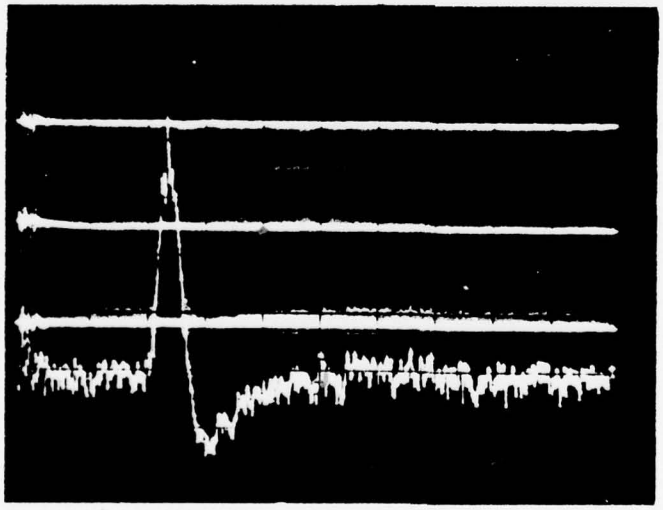

Voltages

P_4 Ch. 1 0.02V /div

P_7 Ch. 2 0.02V /div

P_5 Ch. 3 0.02V /div

T_4 Ch. 4 0.02V /div

Time Scale 0.2sec/div
Sustainer Voltage 25.8kV
Flow? (On) Off
Gas Type N_2
Notes: 12-1" honeycomb
(6 coarse + 6 fine)
100 Hz low pass filter

Analyzed Data:

E = 70.135

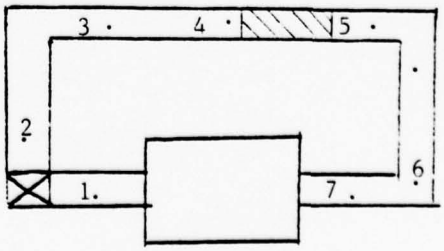

PVC Circulator Experimental Data

Page 218
No. 5505
Date 12 July 1978

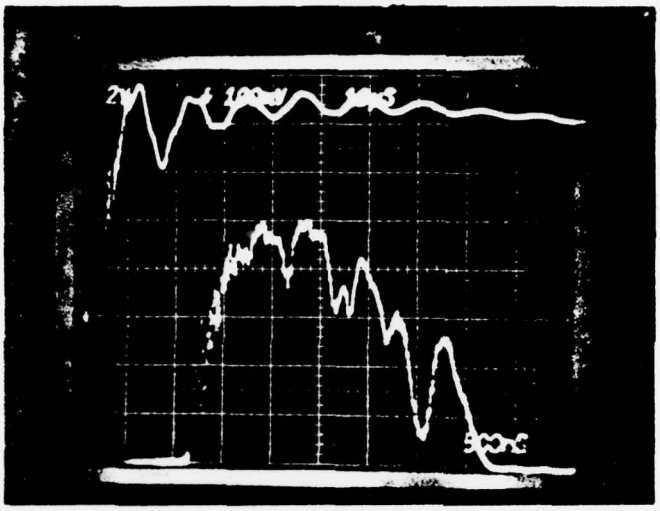

Gun Data

1. Upper Trace
   Voltage 100mV/div
   Time Scale 10μsec/div
   Inverted? (Yes) No
2. Lower Trace
   Voltage 2V /div
   Time Scale 500nsec/div
   Inverted? Yes (No)
   Attenuation _____

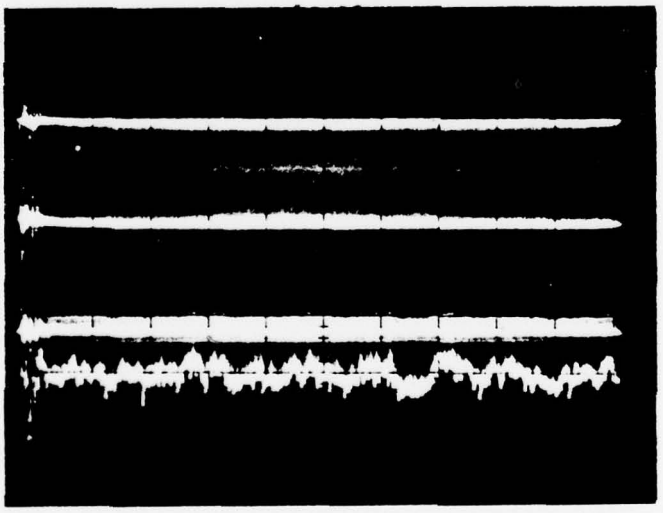

Voltages

P_4 Ch. 1 0.02V /div

P_7 Ch. 2 0.02V /div

P_5 Ch. 3 0.02V /div

T_5 Ch. 4 0.02V /div

Time Scale 0.2sec /div
Sustainer Voltage 25.8kV
Flow? (On) Off
Gas Type N_2
Notes: 100 Hz bandwidth
low pass filter 12-1"
honeycomb (6 coarse +
6 fine)

Analyzed Data:

E = 67.60

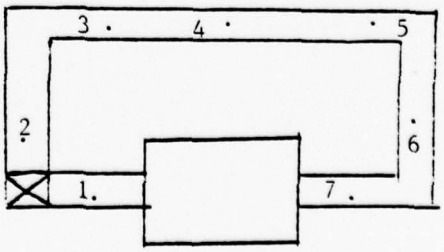

PVC Circulator Experimental Data

Page 219
No. 5506
Date 12 July 1978

Gun Data

1. Upper Trace

   Voltage 100mV/div

   Time Scale 10usec/div

   Inverted? (Yes) No

2. Lower Trace

   Voltage 2V /div

   Time Scale 500nsec/div

   Inverted? Yes (No)

   Attenuation _____

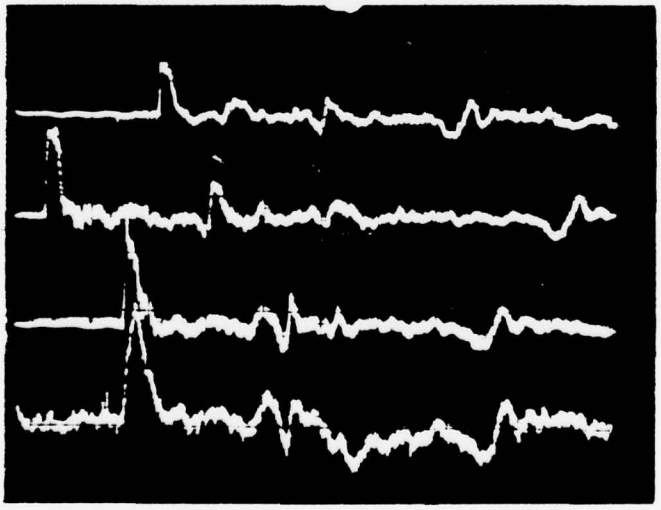

Voltages

P_4 Ch. 1 0.02V /div

P_7 Ch. 2 0.02V /div

P_5 Ch. 3 0.02V /div

T_5 Ch. 4 0.05V /div

Time Scale 5msec /div

Sustainer Voltage 25.8kV

Flow? (On) Off

Gas Type N_2

Notes: 12-1" honeycomb
(6 coarse + 6 fine)
1 KHz low pass filter

Analyzed Data:

E = 65.065

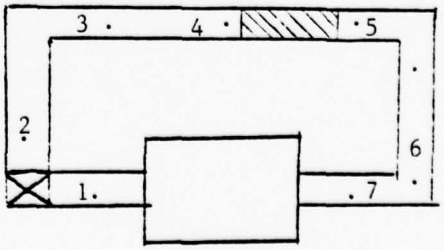

PVC Circulator Experimental Data

Page 220
No. 5507
Date 12 July 1978

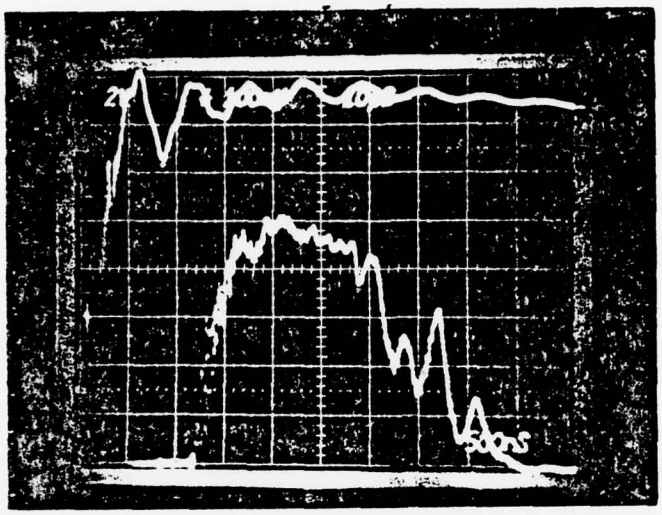

Gun Data

1. Upper Trace
   Voltage 100mV/div
   Time Scale 10usec/div
   Inverted? (Yes) No
2. Lower Trace
   Voltage 2V /div
   Time Scale 500nsec/div
   Inverted? Yes (No)
   Attenuation _____

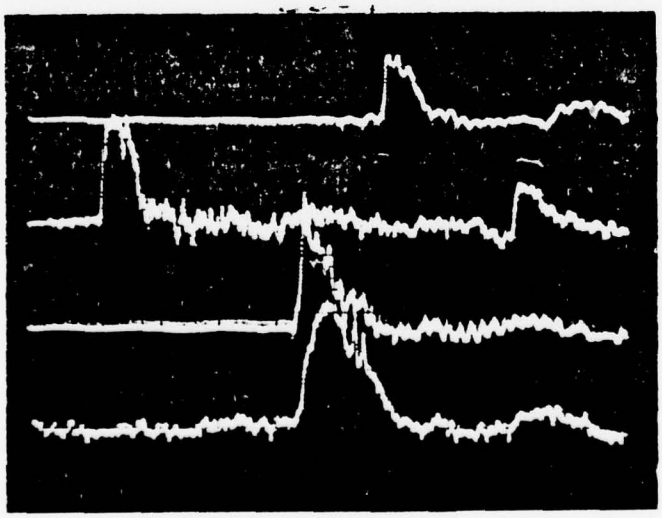

Voltages

P_4 Ch. 1 0.02V /div

P_7 Ch. 2 0.02V /div

P_5 Ch. 3 0.02V /div

T_5 Ch. 4 0.05V /div

Time Scale 2msec /div

Sustainer Voltage 25.8kV

Flow? (On) Off

Gas Type N_2

Notes: 12-1" honeycomb
(6 coarse + 6 fine)
1 KHz LPF

Analyzed Data:

E = 70.135

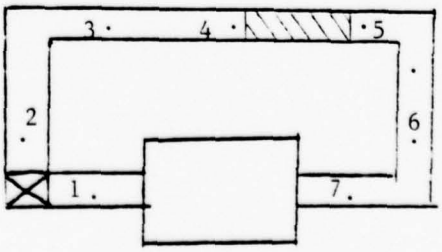

PVC Circulator Experimental Data

Page 221
No. 5508
Date 12 July 1978

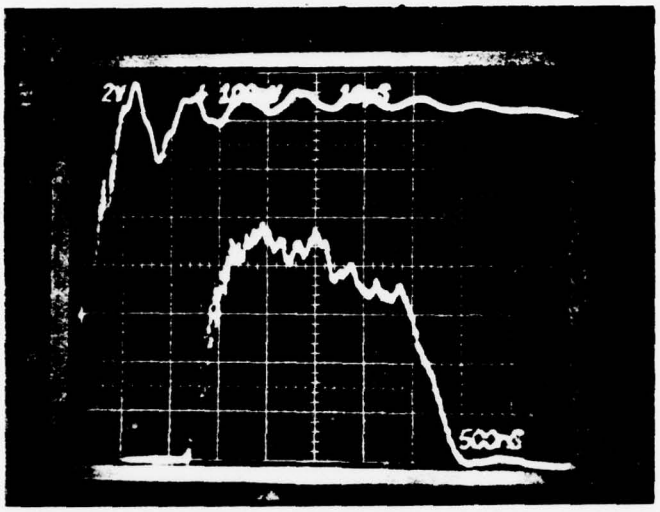

Gun Data

1. Upper Trace
   Voltage 100mV/div
   Time Scale 10μsec/div
   Inverted? (Yes) No
2. Lower Trace
   Voltage 2V /div
   Time Scale 500nsec/div
   Inverted? Yes (No)
   Attenuation _____

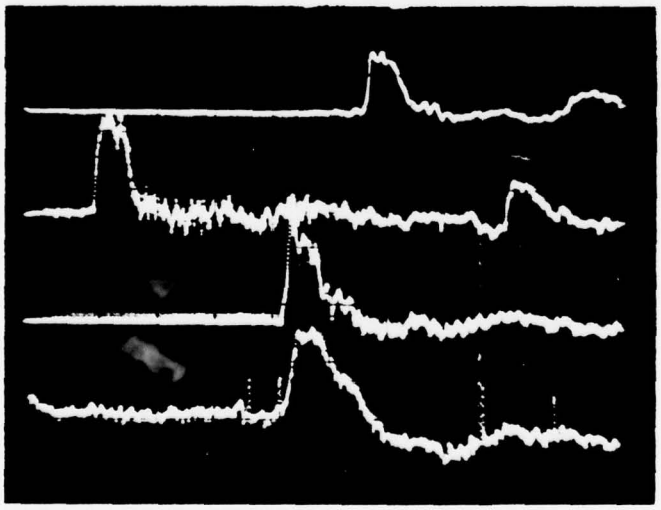

Voltages

P_4 Ch. 1 0.02V /div

P_7 Ch. 2 0.02V /div

P_5 Ch. 3 0.02V /div

T_5 Ch. 4 0.05V /div

Time Scale 2msec /div
Sustainer Voltage 25.8kV
Flow? On (Off)
Gas Type N_2
Notes: 12-1" honeycomb
(6 coarse + 6 fine)
1 KHz LPF

Analyzed Data:

E = 65.91

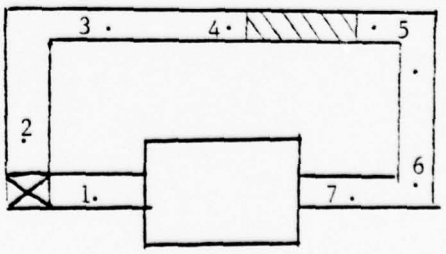

PVC Circulator Experimental Data

Page 222
No. 5509
Date 12 July 1978

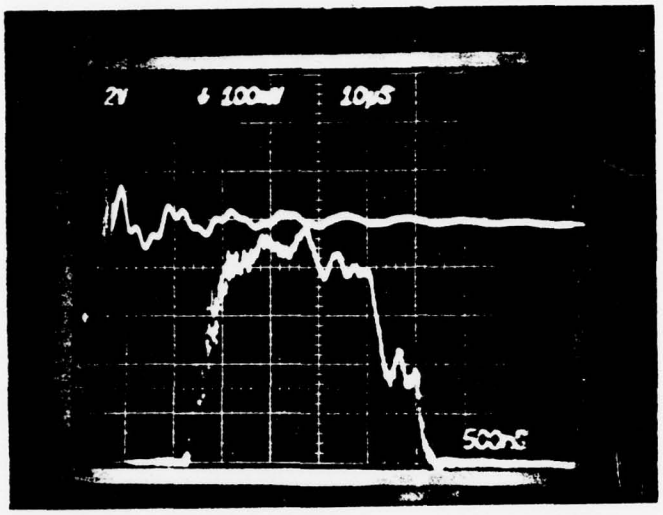

Gun Data

1. Upper Trace

   Voltage 100mV/div

   Time Scale 10μsec/div

   Inverted? (Yes) No

2. Lower Trace

   Voltage 2V /div

   Time Scale 500nsec/div

   Inverted? Yes (No)

   Attenuation _____

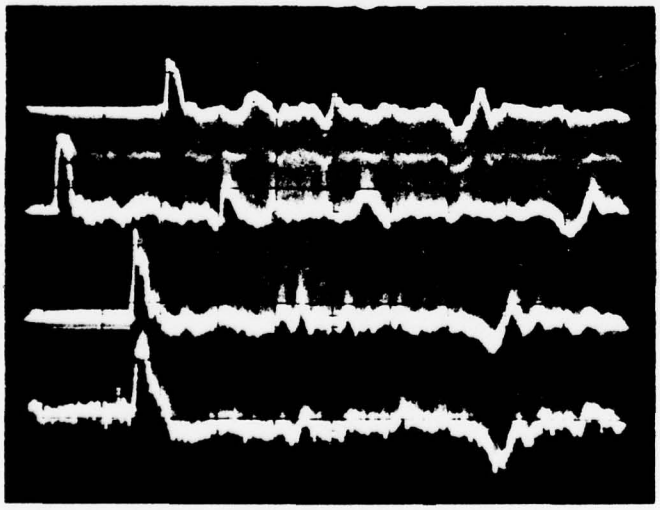

Voltages

P_4 Ch. 1 0.02V /div

P_7 Ch. 2 0.02V /div

P_5 Ch. 3 0.02V /div

T_5 Ch. 4 0.05V /div

Time Scale 5msec /div

Sustainer Voltage 25.8kV

Flow? On (Off)

Gas Type N_2

Notes: 12-1" honeycomb
(6 coarse + 6 fine)
1 KHz LPF

Analyzed Data:

E = 54.08

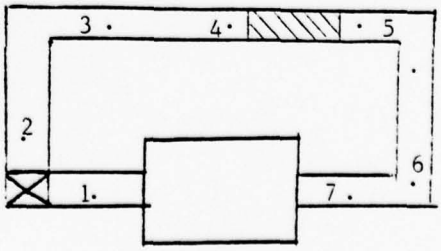

PVC Circulator Experimental Data

Page 223
No. 5512
Date 12 July 1978

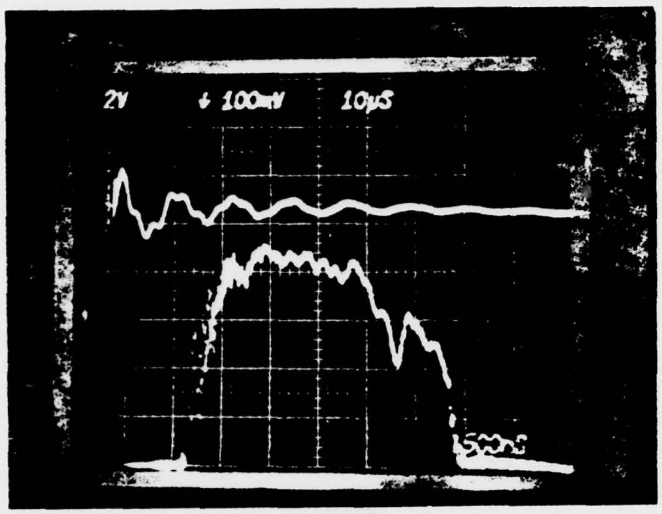

Gun Data

1. Upper Trace
   Voltage 100mV/div
   Time Scale 10μsec/div
   Inverted? (Yes) No
2. Lower Trace
   Voltage 2V /div
   Time Scale 500nsec/div
   Inverted? Yes (No)
   Attenuation _____

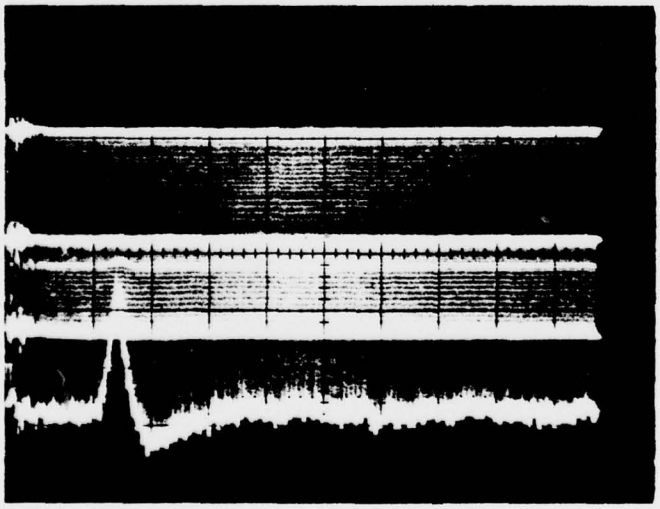

Voltages

P_4 Ch. 1 0.02V /div

P_7 Ch. 2 0.02V /div

P_5 Ch. 3 0.02V/div

T_4 Ch. 4 0.05V /div

Time Scale 0.2sec/div
Sustainer Voltage 25.8kV
Flow? (On) Off
Gas Type N_2
Notes: 4-1" honeycomb
(2 coarse + 2 fine)
1 KHz LPF

Analyzed Data:

E = 64.22

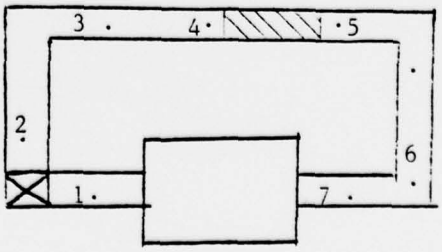

PVC Circulator Experimental Data

Page 224
No. 5517
Date 14 July 1978

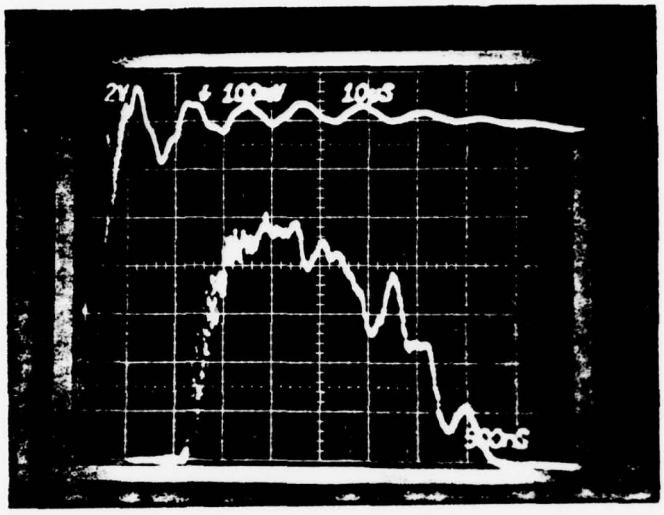

Gun Data

1. Upper Trace
   Voltage 100mV/div
   Time Scale 10µsec/div
   Inverted? (Yes) No
2. Lower Trace
   Voltage 2V /div
   Time Scale 500nsec/div
   Inverted? Yes (No)
   Attenuation _____

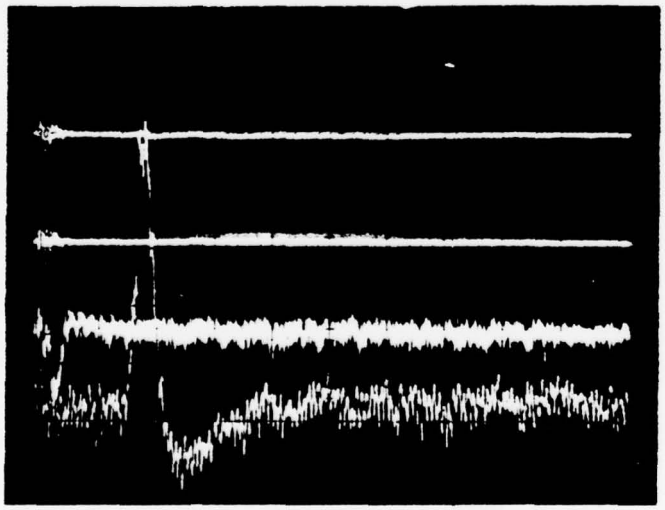

Voltages

P_4 Ch. 1 0.02V /div

P_5 Ch. 2 0.02V /div

V_1 Ch. 3 0.20V /div

T_4 Ch. 4 0.02V /div

Time Scale 0.2sec/div
Sustainer Voltage 25.8kV
Flow? (On) Off
Gas Type N_2
Notes: 4-1" honeycomb
(2 coarse + 2 fine)
1 KHz LPF

Analyzed Data:

E = 65.065

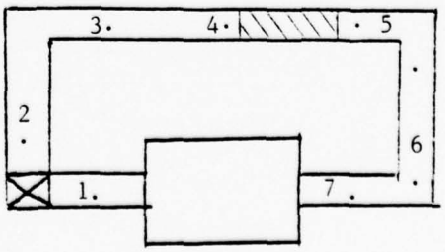

PVC Circulator Experimental Data

Page 225
No. 5518
Date 14 July 1978

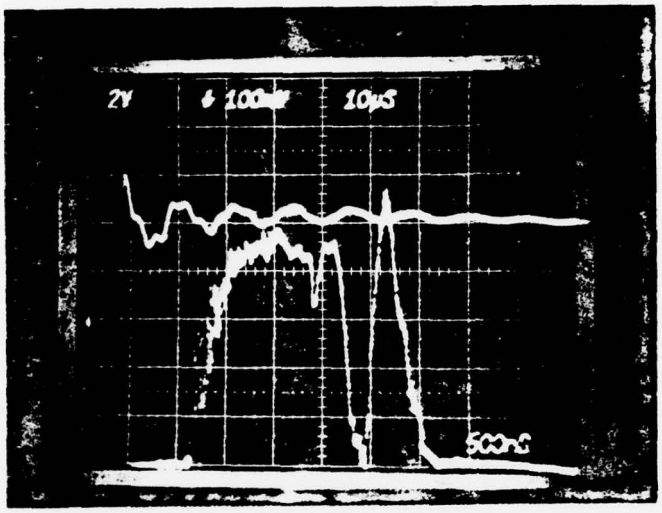

Gun Data

1. Upper Trace
   Voltage 100mV/div
   Time Scale 10μsec/div
   Inverted? (Yes) No
2. Lower Trace
   Voltage 2V /div
   Time Scale 500nsec/div
   Inverted? Yes (No)
   Attenuation _____

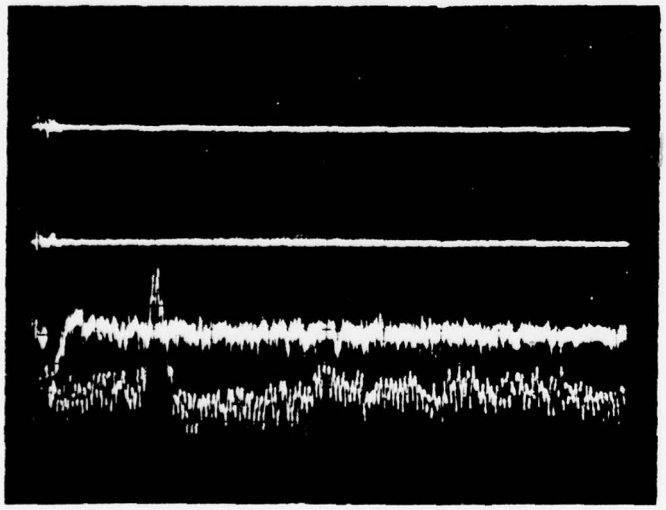

Voltages

P_4 Ch. 1 0.02V /div

P_5 Ch. 2 0.02V /div

V_1 Ch. 3 0.20V /div

T_5 Ch. 4 0.02V /div

Time Scale 0.2sec /div
Sustainer Voltage 25.8kV
Flow? (On) Off
Gas Type N_2
Notes: 4-1" honeycomb
(2 coarse + 2 fine)
1 KHz LPF

Analyzed Data:

E = 55.77

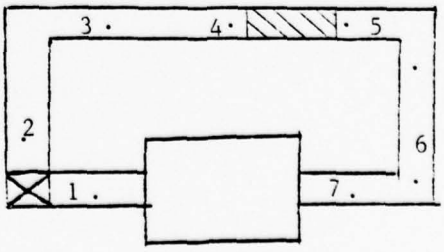

PVC Circulator Experimental Data

Page 226
No. 5519
Date 14 July 1978

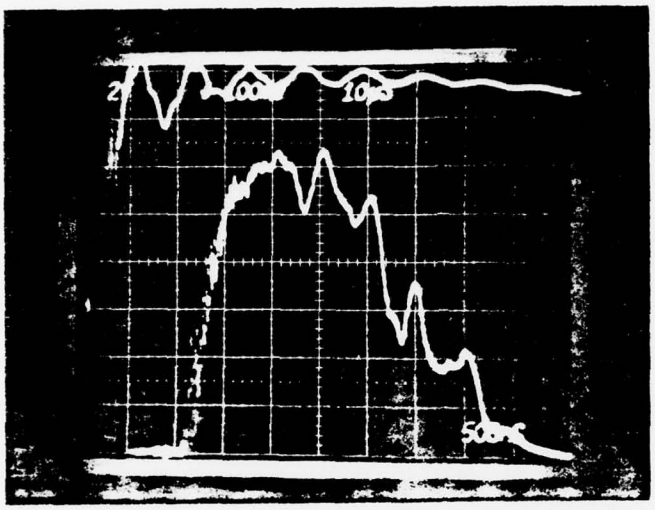

Gun Data

1. Upper Trace
   Voltage 100mV/div
   Time Scale 10μsec/div
   Inverted? (Yes) No
2. Lower Trace
   Voltage 2V /div
   Time Scale 500nsec/div
   Inverted? Yes (No)
   Attenuation _____

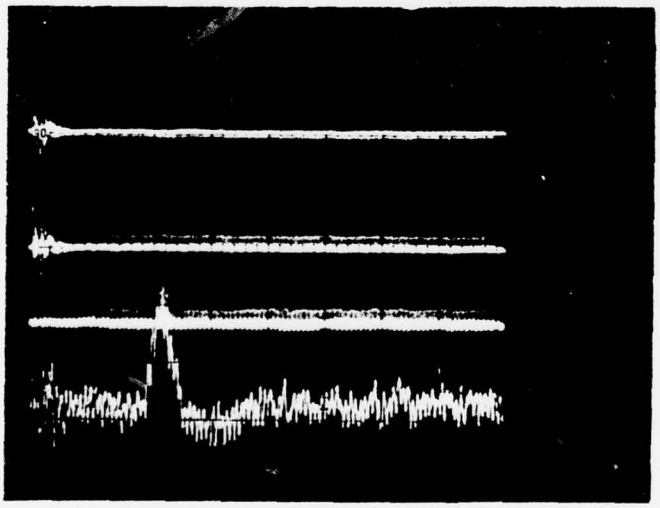

Voltages

P_4 Ch. 1 0.02V /div

P_5 Ch. 2 0.02V /div

V_4 Ch. 3 0.10V /div

T_5 Ch. 4 0.02V /div

Time Scale 0.2sec/div
Sustainer Voltage 25.8kV
Flow? (On) Off
Gas Type N_2
Notes: 4-1" honeycomb
all small (fine) 1 KHz LPF

Analyzed Data:

E = 87.035

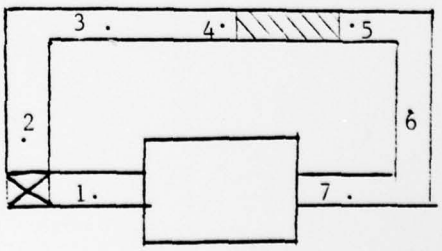

PVC Circulator Experimental Data

Page 226
No. 5519
Date 14 July 1978

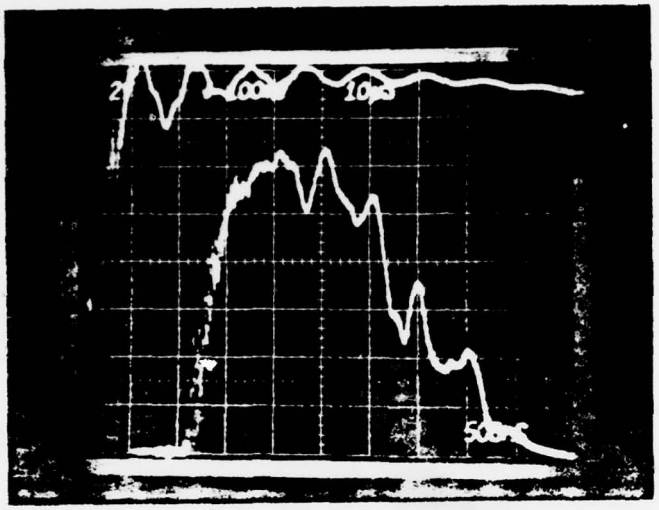

Gun Data

1. Upper Trace
   Voltage 100mV/div
   Time Scale 10μsec/div
   Inverted? (Yes) No
2. Lower Trace
   Voltage 2V /div
   Time Scale 500nsec/div
   Inverted? Yes (No)
   Attenuation _____

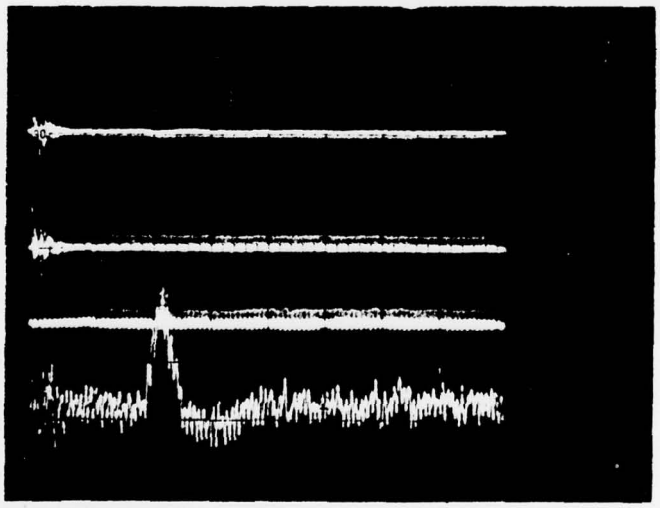

Voltages

P_4 Ch. 1 0.02V /div

P_5 Ch. 2 0.02V /div

V_4 Ch. 3 0.10V /div

T_5 Ch. 4 0.02V /div

Time Scale 0.2sec/div
Sustainer Voltage 25.8kV
Flow? (On) Off
Gas Type N_2
Notes: 4-1" honeycomb
all small (fine) 1 KHz
LPF

Analyzed Data:

E = 87.035

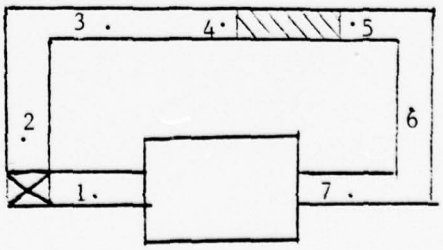

PVC Circulator Experimental Data

Page 227
No. 5521
Date 14 July 1978

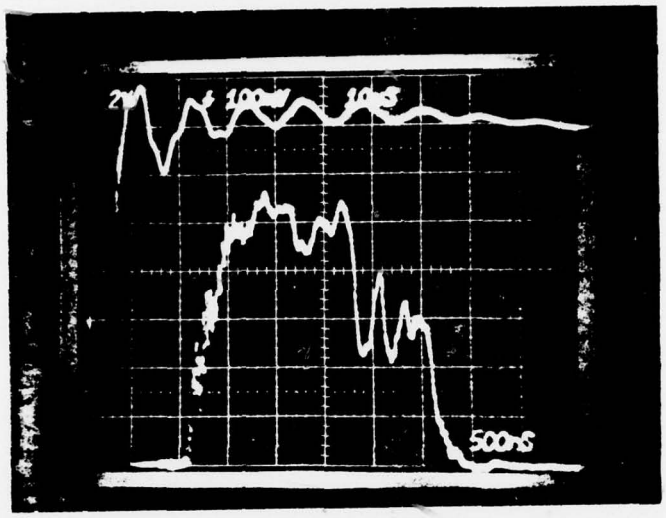

Gun Data

1. Upper Trace
   Voltage 100mV/div
   Time Scale 10μsec/div
   Inverted? (Yes) No
2. Lower Trace
   Voltage 2V /div
   Time Scale 500nsec/div
   Inverted? Yes (No)
   Attenuation _____

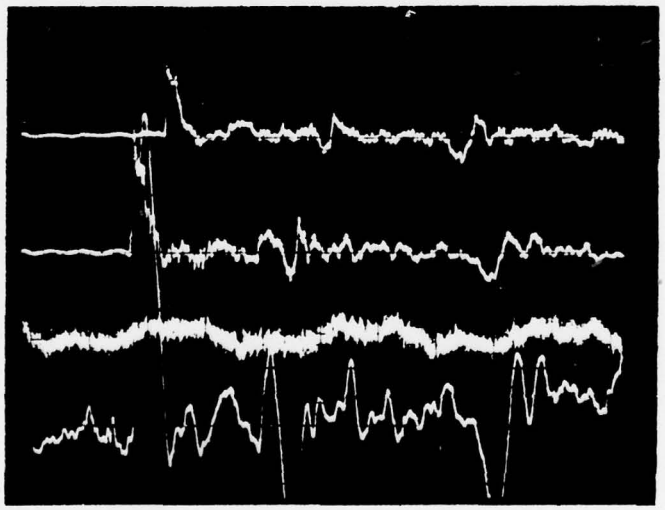

Voltages

P_4 Ch. 1 0.02V /div

P_5 Ch. 2 0.02V /div

V_4 Ch. 3 0.02V/div

T_5 Ch. 4 0.02V /div

Time Scale 5msec /div
Sustainer Voltage 25.8kV
Flow? (On) Off
Gas Type N_2
Notes: 4-1" honeycomb
1 KHz LPF small (fine)

Analyzed Data:

E = 67.60

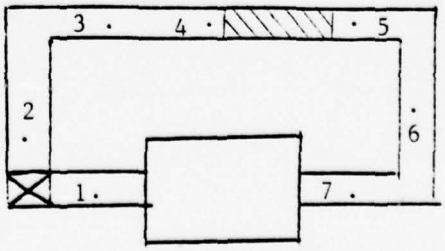

PVC Circulator Experimental Data

Page 228
No. 5522
Date 14 July 1978

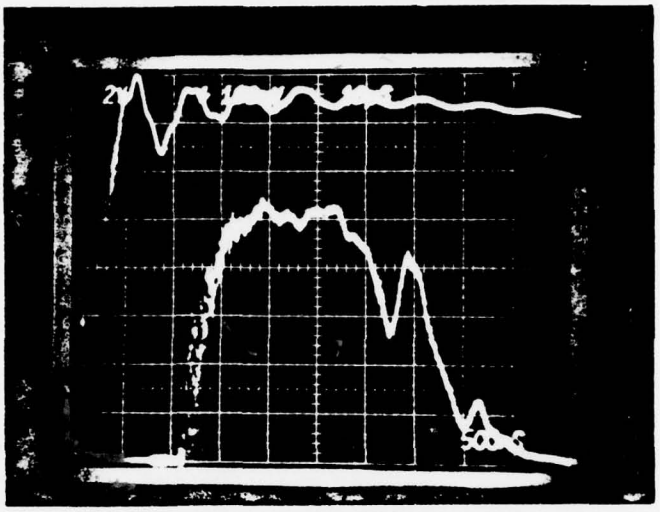

Gun Data

1. Upper Trace
   Voltage 100mV/div
   Time Scale 10usec/div
   Inverted? (Yes) No
2. Lower Trace
   Voltage 2V /div
   Time Scale 500nsec/div
   Inverted? Yes (No)
   Attenuation _____

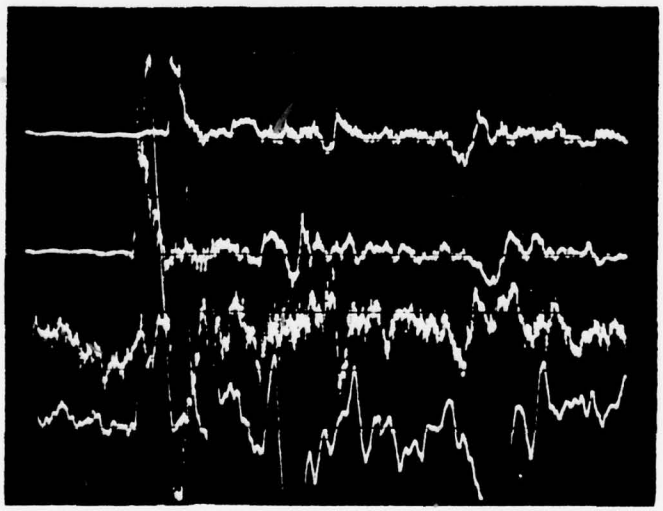

Voltages

P_4 Ch. 1 0.02V /div

P_5 Ch. 2 0.02V /div

V_4 Ch. 3 0.1V /div

T_5 Ch. 4 0.02V /div

Time Scale 5msec /div
Sustainer Voltage 25.8kV
Flow? (On) Off
Gas Type N_2
Notes: 4-1" honeycomb
1 KHz LPF small

Analyzed Data:

E = 80.275

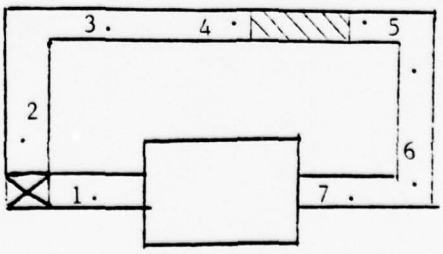

PVC Circulator Experimental Data

Page 229
No. 5523
Date 14 July 1978

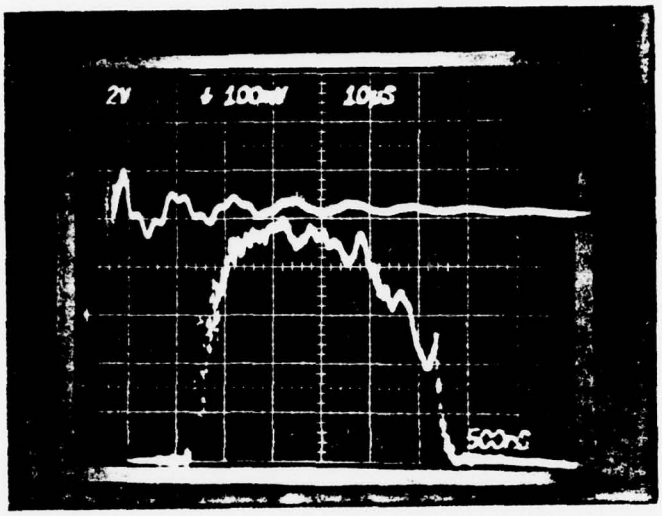

Gun Data

1. Upper Trace
   Voltage 100mV/div
   Time Scale 10usec/div
   Inverted? (Yes) No
2. Lower Trace
   Voltage 2V /div
   Time Scale 500nsec/div
   Inverted? Yes (No)
   Attenuation _____

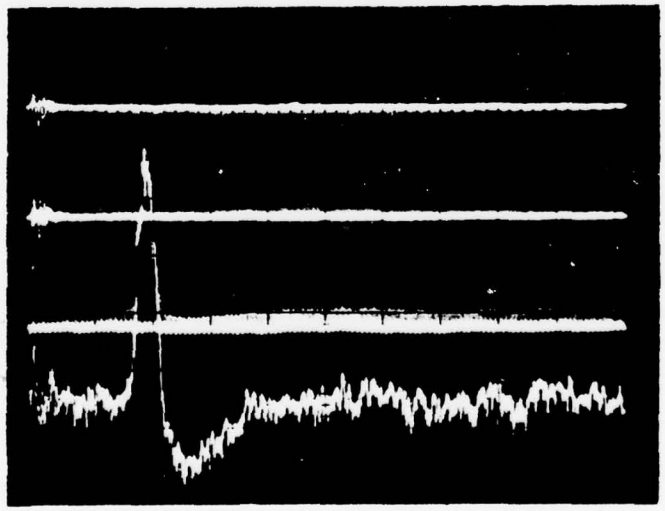

Voltages

P_4 Ch. 1 0.02V /div

P_5 Ch. 2 0.02V /div

V_5 Ch. 3 0.10V /div

T_4 Ch. 4 0.02V /div

Time Scale 0.2sec /div
Sustainer Voltage 25.8kV
Flow? (On) Off
Gas Type N_2
Notes: 4-1" honeycomb
all fine 1 Kz LPF

Analyzed Data:

E = 67.60

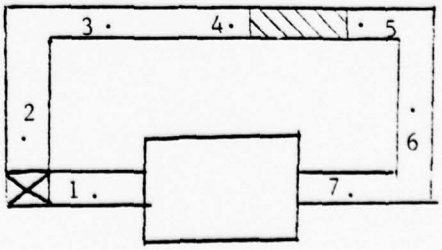

APPENDIX C

```
C   PROGRAM B
C   COMPARE WITH AVCO-EVERETT  (P55)
        PARAMETER ISEG=154
        PARAMETER JJ=23
        PARAMETER  M=12
        PARAMETER  II=ISEG+1
        PARAMETER N=15
        PARAMETER  NZ=4
        COMMON /ABC/ XT,G,DT,EI,EO,TI,TO
        COMMON /ASPT/ AZ,SZ,PZ,TZ
        COMMON /B/ BIC(M)
        COMMON /CONST/ XD,XF
        COMMON /DDD/ G,CP,CV,PF,R,RR,U,A,CA,CE,CC,HX,AZ,ZERO,F,XL
        COMMON /DLL/ CSL(NZ),CSR(NZ),SL(N),SR(N)
        COMMON /P/  P(M,II,JJ)
        DIMENSION X1(M),X2(M),X3(M)
        DIMENSION BC1(M),BC2(M)
        DIMENSION SW(N)
C DEFINE CONSTANTS
        SEG=ISEG
        IC=II-1
        MI=II-2
        MJ=JJ-1
C   START OF INDEPENDENT VARIABLES
C    (SEE THE PARAMETERS ALSO)
        CP=0.24
        G=1.4
        XBC11=0.0
        RF=53.34
        XP=2116.8
        XRO=0.00234
        XU=196.8
        XL=1.0
        XXST=0.0
        XXD=0.25
        XF=0.0
        FLAG=-10.0
        XTZ=0.0
        XES=0.0
        GG=5.3683
        DTIME=30.0E-06
        XMF=0.0
        XTI=0.0
        XTO=0.0
        TD=3.5
        SEP=0.5
        XIN=0.1
        XVA=-1.0
```

```
      XVB=-3.0
      XVC=-5.0
C  END OF INDEPENDENT VARIABLES
      F=XF
      BC11=XBC11/XL
      BC21=SEP*SEG/TD+BC11
      X=BC21-BC11
      DX=X/SEG
      DIS=TD*DX
      HX=2.0*DX
      CV=CP/G
      RR=RF/778.161
      R=RF*32.1739
      XST=(XXST/G/RR)/(A/XL)
      XD=XXD/XL
      TZ=A*XTZ/XL
      AZ=TZ
      ES=XES/G/RR
      TI=A*XTI/XL
      TO=A*XTO/XL
      XT=XP/XPO/R
      A=SQRT(G*R*XT)
      U=(XU/A)
      DT=A*DTIME/XL
      CA=(G-1.0)/(2.0*G)
      CE=(G+1.0)/(2.0*G)
      CC=2.0/(G+1.0)
C BOUNDARY CONDITIONS (LEFT)
      BC1(1)=BC11
      BC1(2)=FLAG
      BC1(3)=U
      BC1(4)=A/A
      BC1(5)=ES
      BC1(6)=XST
      BC1(7)=XD
      BC1(8)=XP
      BC1(9)=XRO
      BC1(10)=XT
      BC1(11)=XF
      BC1(12)=XNF
C BOUNDARY CONDITIONS (RIGHT)
      BC2(1)=BC21
      BC2(2)=FLAG
      BC2(3)=U
      BC2(4)=A/A
      BC2(5)=ES
      BC2(6)=XST
      BC2(7)=XD
      BC2(8)=XP
      BC2(9)=XRO
      BC2(10)=XT
      BC2(11)=XF
      BC2(12)=XNF
C LOAD BOUNDARY CONDITIONS
      DO 15 J=1,JJ
      DO 14 K=1,M
      P(K,1,J)=BC1(K)
```

```
      P(K,II,J)=BC2(K)
   14 CONTINUE
   15 CONTINUE
C INITIAL CONDITIONS
      DO 18 I=2,IC
      IM1 = I-1
      P(1,I,1)=P(1,IM1,1)+DX
   18 CONTINUE
      BIC(2)=T2
      BIC(3)=U
      BIC(4)=A/A
      BIC(5)=ES
      BIC(6)=XST
      BIC(7)=XD
      BIC(8)=XP
      BIC(9)=XRO
      BIC(10)=XT
      BIC(11)=XE
      BIC(12)=XMF
C LOAD INITIAL CONDITIONS
      DO 17 I=2,IC
      DO 16 K=2,M
      P(K,I,1)=BIC(K)
   16 CONTINUE
   17 CONTINUE
C    CAVITY HEATING  (LUMPED ANALYSIS)
      D1=BIC(9)
      S1=BIC(5)
      T1=BIC(10)
      G=(QQ/D1)*(1.0/32.1739)
      DS=Q/T1
      T2=Q/CV+T1
      P2=D1*R*T2
      A2=SQRT(G*R*T2)/A
      S2=(2.0/(G-1.0))*ALOG(A2)-(1.0/G)*ALOG(P2/BIC(3))+S1
      CALL XPRES(P2,BIC(8),A2,BIC(4),G,PRES)
      XA=1.0+((G+1.0)/(G-1.0))*PRES
      XB=(G+1.0)/(G-1.0)+PRES
      DENS=XA/XB
      TEMP=PRES/DENS
      SPEED=SQRT(TEMP)
C SHOCK WAVE
      SW(1)=X/2.0
      SW(2)=BIC(2)
      SW(3)=SQRT(CA+CB*PRES)
      SW(4)=CC*(SW(3)-1.0/SW(3))+BIC(3)
      SW(5)=BIC(3)
      SW(6)=PRES*BIC(8)
      SW(7)=BIC(8)
      SW(8)=DENS*BIC(9)
      SW(9)=BIC(9)
      SW(10)=TEMP*BIC(10)
      SW(11)=BIC(10)
      SW(12)=SPEED*BIC(4)
      SW(13)=BIC(4)
      SH=CP*ALOG(TEMP)-RR*ALOG(PRES)
      SW(14)=SH/G/RR+BIC(5)
```

```
      SW(15)=BIC(5)
      SL(1)=SW(1)-DIS
      SR(1)=SW(1)+DIS
      EI=SL(1)
      EO=SR(1)
      DO 32 IK=2,N
      SL(IK)=SW(IK)
      SR(IK)=SW(IK)
 32   CONTINUE
      SL(3)=-SW(3)
      SL(4)=BIC(3)-CC*(SW(3)-1.0/SW(3))
C  CONTACT SURFACE
      P22=PRES*BIC(3)
      CSL(1)=SL(1)
      CSL(2)=SL(2)
      CSL(4)=-1.0
      CALL CONT( CSL(4) , P22 , BIC(8) , CSL(3) )
      CSR(1)=SR(1)
      CSR(2)=SR(2)
      CSR(4)=+1.0
      CALL CONT( CSR(4) , P22 , BIC(8) , CSR(3) )
      WRITE(6,299)
 299  FORMAT(1H1)
      WRITE(6,300)
 300  FORMAT(3X,'LOCATION',3X,'TIME',3X,'MACH',10X,'U2',10X,'U1',10X,
     1      'P2',10X,'P1',9X,'RO2',9X,'RO1')
      WRITE(6,301)
 301  FORMAT(14X,'T2',10X,'T1',10X,'A2',10X,'A1',10X,'S2',10X,'S1')
      WRITE(6,109) SL
      WRITE(6,109) SR
 109  FORMAT((1X,'SW=',2X,9(2X,E10.4),2X,'MAIN')/)
      WRITE(6,201) CSL
      WRITE(6,201) CSR
 201  FORMAT(2X,'INTERFACE',5X,4(2X,E10.4) )
C  SET UP CAVITY CONDITIONS
      DO 33 IK=1,II
      HHX=P(1,IK,1)
      KK=0
      IF(HHX.GE.SL(1).AND.HHX.LE.SR(1)) KK=1
      IF(KK) 33,33,34
 34   P(4,IK,1)=A2
      P(5,IK,1)=S2
      P(8,IK,1)=P2
      P(10,IK,1)=T2
 33   CONTINUE
C SOLUTION
      IS=ISEG/2
      IW=IS+1
      DO 13 J=1,MJ
      DO 12  IZ=1,MI
      I=IW-IZ
      IF(IZ.GE.IW) I=IZ
      DO 10 K=1,M
      X1(K)=P(K,I,J)
      IP2 = I+2
      X2(K)=P(K,IP2,J)
   10 CONTINUE
```

```
      CALL FIC(M,X1,X2,X3,SL,SR)
      DO 11 K=1,M
      IP1 = I+1
      JP1 = J+1
      P(K,I,J)=X1(K)
      P(K,IP2,J)=X2(K)
      P(K,IP1,JP1) = X3(K)
   11 CONTINUE
   12 CONTINUE
   13 CONTINUE
      P(2,1,JJ)=P(2,2,JJ)
      P(2,II,JJ)=P(2,IC,JJ)
C END SOLUTION
C  PRINT OUT SPECIAL RESULTS
C   PRINTOUT LOCATIONS
      VA=EI+XVA
      VB=EI+XVB
      VC=EI+XVC
      VV=0.25*BC21
      VH=0.75*BC21
      CALL PLT(  VA  )
      CALL PLT(  VB  )
      CALL PLT(  VC  )
      CALL PLT(  VV  )
      CALL PLT(  EI  )
      CALL PLT( SW(1))
      CALL PLT(  EO  )
      CALL PLT(  VH  )
      PI=EI-2.0*DIS
      PE=EO+2.0*DIS
      IF(PI.LT.BC11) PI=BC11
      IF(PE.GT.BC21) PE=BC21
      DA=PI-XIN
 3    CONTINUE
      DA=DA+XIN
      CALL PLT(  DA  )
      IF(DA.LE.PE) GO TO 3
C PRINTOUT
      WRITE(6,1)
    1 FORMAT(1H1,6X,'ARRAY P(K,I,J)')
      DO 20 J=1,JJ
      DO 19 I=1,II
      WRITE(6,2) I,J,(P(K,I,J),K=1,M)
 2    FORMAT(2(2X,I3),2(2X,E9.4),2X,E10.4,8(2X,G8.3),2X,F4.1)
   19 CONTINUE
   20 CONTINUE
      END
```

```
      SUBROUTINE RADIUS(N,X,Y,Z,LD)
      DIMENSION X(N),Y(N),Z(N)
      R=0.01
      EX=X(1)
      TX=X(2)
      EY=Y(1)
      TY=Y(2)
      EZ=Z(1)
      TZ=Z(2)
      DA=SQRT( (EZ-EX)**2+ (TZ-TX)**2 )
      DB=SQRT( (EZ-EY)**2 + (TZ-TY)**2 )
      IF( DA .LE. R )  LD=1
      IF( DB .LE. R )  LD=1
      IF(LD)2,2,1
 1    WRITE(6,3) R,EX,TX,EY,TY,EZ,TZ
 3    FORMAT(2X,'RADIUS',2X,7(F12.5,2X) )
 2    CONTINUE
      RETURN
      END
```

```
      SUBROUTINE SSS(NN,AA1,AA2,AA3)
      PARAMETER M=12
      DIMENSION AA1(NN),AA2(NN),AA3(NN)
      DIMENSION AA4(M),HH3(M)
      AA3(3)=(AA1(3)+AA2(3))/2.0
      AA3(4)=(AA1(4)+AA2(4))/2.0
      AA4(3)=AA3(3)
      LL=0
      LD=0
 101  CONTINUE
      LL=LL+1
      LMAX=5
      LN=LL-LMAX
      IF(LN) 103,103,105
 103  CONTINUE
      CALL GEO(NN,AA1,AA2,AA3,AA4)
      CALL SOL(NN,AA1,AA2,AA3,AA4,HH3)
C     TEST ROUTINE
      CALL RADIUS(NN,AA1,AA2,AA3,LD)
      IF( LD .GT. 0 ) GO TO 104
      TX=0.001
      II=0
      IF(AA3(3).EQ.0.0) AA3(3)=1.0E-6
      IF(AA3(4).EQ.0.0) AA3(4)=1.0E-6
      RV=(AA3(3)-HH3(3))/AA3(3)
```

```
      RA=(AA3(4)-HH3(4))/AA3(4)
      IF(ABS(RV).GT.TX) II=II+1
      IF(ABS(RA).GT.TX) II=II+1
      IF(II) 102,102,101
102   CONTINUE
      GO TO 104
105   WRITE(6,106) TX,RV,RA,AA3(1),AA3(2),LMAX
106   FORMAT(1X,5(2X,E10.4),3X,'LMAX=',I5,2X,'SSS')
      WRITE(6,1)(AA1(IM),IM=1,M)
      WRITE(6,2)(AA2(IM),IM=1,M)
1     FORMAT(1X,12(2X,E9.3),2X,'AA1')
2     FORMAT(1X,12(2X,E8.3),2X,'AA2')
104   CONTINUE
      CALL PPP(NN,AA1,AA3)
      AA3(12)=LL
      RETURN
      END
```

```
      SUBROUTINE GEO(NN,AA1,AA2,AA3,AA4)
      COMMON /CONST/ XD,XF
      DIMENSION AA1(NN),AA2(NN),AA3(NN),AA4(NN)
      R13=(AA1(3)+AA1(4)+AA3(3)+AA3(4))/2.0
      S13=1.0/R13
      R23=(AA2(3)-AA2(4)+AA3(3)-AA3(4))/2.0
      S23=1.0/R23
      B13=AA1(2)-S13*AA1(1)
      B23=AA2(2)-S23*AA2(1)
      AA3(1)=(B23-B13)/(S13-S23)
      AA3(2)=S13*AA3(1)+B13
      S12=(AA1(2)-AA2(2))/(AA1(1)-AA2(1))
      B12=AA1(2)-S12*AA1(1)
      R34=(AA3(3)+AA4(3))/2.0
      S34=1.0/R34
      B34=AA3(2)-S34*AA3(1)
      AA4(1)=(B12-B34)/(S34-S12)
      AA4(2)=S34*AA4(1)+B34
      PF=(AA2(1)-AA4(1))/(AA2(1)-AA1(1))
      AA4(5)=(1.0-PF)*AA2(5)+PF*AA1(5)
      CALL HEAT(AA3(1),AA3(2),AA3(3),AA3(4),AA3(5),AA3(6))
      CALL HEAT(AA4(1),AA4(2),AA4(3),AA4(4),AA4(5),AA4(6))
      AA3(7)=XD
      AA3(11)=XF
      AA4(7)=XD
      RETURN
      END
```

```
      SUBROUTINE HEAT(E,T,UU,AA,S,H)
      COMMON /ABC/ XT,Q,DT,EI,EO,TI,TO
      COMMON /DDD/ G,CP,CV,RF,R,RR,U,A,CA,CB,CC,HX,AZ,ZERO,F,XL
      TE=(AA*AA/1.0/1.0)*XT
      I=0
      H=0.0
      XH=Q/(TE*DT*G*RR)
      IF(E.GT.EI.AND.E.LT.EO) I=I+1
      IF(T.GT.TI.AND.T.LT.TO) I=I+1
      IF(I.EQ.2) H=XH
      RETURN
      END
```

```
      SUBROUTINE SUL(NN,AA1,AA2,AA3,AA4,HH3)
      COMMON /DDD/ G,CP,CV,RF,R,RR,U,A,CA,CB,CC,HX,AZ,ZERO,F,XL
      DIMENSION AA1(NN),AA2(NN),AA3(NN),AA4(NN),HH3(NN)
      DO 10 I=1,NN
      HH3(I)=AA3(I)
   10 CONTINUE
      FU=((AA2(1)-AA4(1))/(AA2(1)-AA1(1)))*(AA1(3)-AA2(3))+AA2(3)
      SU=((AA2(2)-AA4(2))/(AA2(2)-AA1(2)))*(AA1(3)-AA2(3))+AA2(3)
      AA4(3)=0.5*(FU+SU)
      S4=AA4(5)
      DS43=(AA4(6)+HH3(6))/2.0
      P1=(2.0/(G-1.0))*AA1(4)+AA1(3)
      Q2=(2.0/(G-1.0))*AA2(4)-AA2(3)
      A13=(AA1(4)+HH3(4))/2.0
      A23=(AA2(4)+HH3(4))/2.0
      U13=(AA1(3)+HH3(3))/2.0
      U23=(AA2(3)+HH3(3))/2.0
      DS13=(AA1(6)+HH3(6))/2.0
      DS23=(AA2(6)+HH3(6))/2.0
      F13=(AA1(11)+HH3(11))/2.0
      F23=(AA2(11)+HH3(11))/2.0
      D13=(AA1(7)+HH3(7))/2.0

      D23=(AA2(7)+HH3(7))/2.0
      DD13=(AA1(7)**2+HH3(7)**2)/2.0
      DD23=(AA2(7)**2+HH3(7)**2)/2.0
      DA31=(AA3(7)**2-AA1(7)**2)/DD13/(AA3(1)-AA1(1))
      DA32=(AA3(7)**2-AA2(7)**2)/DD23/(AA3(1)-AA2(1))
      T1=AA1(2)
      T2=AA2(2)
      T3=HH3(2)
      T4=AA4(2)
      S1=AA1(5)
      S2=AA2(5)
C     START      GOVERNING EQUATIONS
      S3=S4+DS43*(T3-T4)
      P3=P1+A13*(S3-S1)
     1    +(   (G-1.0)*A13*DS13
     1    -    A13*U13*DA31
     1    -    F13*U13*ABS(U13)/2.0/D13   )*(T3-T1)
      Q3=Q2+A23*(S3-S2)
     1    +(   (G-1.0)*A23*DS23
     1    -    A23*U23*DA32
     1    -    F23*U23*ABS(U23)/2.0/D23   )*(T3-T2)
C     END        GOVERNING EQUATIONS
      AA3(3)=(P3-Q3)/2.0
      AA3(4)=(G-1.0)*(P3+Q3)/4.0
      AA3(5)=S3
      RETURN
      END

      SUBROUTINE PPP(NN,AA1,AA3)
      COMMON /DDD/ G,CP,CV,RF,R,RR,U,A,CA,CB,CC,HX,AZ,ZERO,F,XL
      DIMENSION AA1(NN),AA3(NN)
      C1=(2.0/(G-1.0))*ALOG(AA3(4)/AA1(4))
      C2=G*(AA3(5)-AA1(5))
      AA3(9)=AA1(9)*EXP(C1-C2)
      AA3(10)=A*A*AA3(4)*AA3(4)/G/R
      AA3(8)=AA3(9)*R*AA3(10)
      RETURN
      END
```

```
      SUBROUTINE FIG(NX,AA1,AA2,AA3,SWL,SWR)
      PARAMETER M=12
      PARAMETER N=15
      DIMENSION AA1(NX),AA2(NX),AA3(NX)
      DIMENSION AA4(M)
      DIMENSION SWL(N),SWR(N)
      IF(AA1(2).LT.(0.0)) AA1(2)=AA2(2)
      IF(AA2(2).LT.(0.0)) AA2(2)=AA1(2)
      AA3(3)=(AA1(3)+AA2(3))/2.0
      AA3(4)=(AA1(4)+AA2(4))/2.0
      AA4(3)=AA3(3)
      NM=0
      CALL CHKR(NX,AA1,AA2,AA3,AA4,SWR,NM)
      IF(NM) 109,109,107
  109 CONTINUE
      MM=0
      CALL CHKL(NX,AA1,AA2,AA3,AA4,SWL,MM)
      IF(MM) 110,110,107
  110 CONTINUE
      CALL SUB(NX,AA1,AA2,AA3)
  107 CONTINUE
      RETURN
      END
```

```
      SUBROUTINE SUB(N,A,B,C)
      PARAMETER  NZ=4,  NA=15
      COMMON /DLL/ CSL(NZ),CSR(NZ),SL(NA),SR(NA)
      DIMENSION A(N),B(N),C(N)
      NM=0
      CALL CCS(N,A,B,C,CSL,NM)
      IF(NM) 109,109,107
  109 CONTINUE
      MM=0
      CALL CCS(N,A,B,C,CSR,MM)
      IF(MM) 110,110,107
  110 CONTINUE
      CALL SSS(N,A,B,C)
  107 CONTINUE
      RETURN
      END
```

```
      SUBROUTINE XPRES(P4,P1,A4,A1,G,PRES)
      XX=0.001
      PRES=1.0-XX
      EX=-2.0*G/(G-1.0)
    1 PRES=PRES+XX
      XA=(G-1.0)*(A1/A4)*(PRES-1.0)
      XB=SQRT(2.0*G)
      XC=SQRT(2.0*G+(G+1.0)*(PRES-1.0))
      PP=P1*PRES*((1.0-XA/XB/XC)**EX)
      TF=0.005
      Y=ABS((P4-PP)/P4)
      IF(Y.GT.TF) GO TO 1
      RETURN
      END
```

```
      SUBROUTINE RAN(NN,BB1,BB2,PR,XX)
      COMMON /DDD/ G,CP,CV,RF,R,RR,U,A,CA,CB,CC,HX,AZ,ZERO,F,XL
      DIMENSION BB1(NN),BB2(NN)
      XA=1.0+((G+1.0)/(G-1.0))*PR
      XB=(G+1.0)/(G-1.0)+PR
      BB2(1)=BB1(1)
      BB2(2)=BB1(2)
      BB2(6)=BB1(6)
      BB2(7)=BB1(7)
      BB2(8)=PR*BB1(8)
      BB2(9)=BB1(9)*(XA/XB)
      BB2(10)=BB1(10)*PR*(XB/XA)
      BB2(11)=BB1(11)
      V1=SQRT(CA+CB*PR)
      V2=V1*(BB1(9)/BB2(9))
      BB2(3)=U+XX*(V1-V2)
      BB2(4)=SQRT(G*R*BB2(10))/A
      BH=CP*ALOG(BB2(10)/BB1(10))-RR*ALOG(PR)
      BB2(5)=BH/G/RR+BB1(5)
      RETURN
      END

      SUBROUTINE SZ(NN,XN,Z)
      PARAMETER  NZ=4,   N=15
      COMMON /CONST/ XD,XF
      COMMON /DLL/ CSL(NZ),CSR(NZ),SL(N),SR(N)
      DIMENSION Z(NN)
      IF(XN .LT. 0.0 ) Z(3)=SL(4)
      IF(XN .GT. 0.0 ) Z(3)=SR(4)
      Z(4)=SL(12)
      Z(5)=SL(14)
      Z(6)=0.0
      Z(7)=XD
      Z(8)=SL(6)
      Z(9)=SL(8)
      Z(10)=SL(10)
      Z(11)=XF
      Z(12)=-7.0
      RETURN
      END


      SUBROUTINE CHKL(NN,X,Y,Z,AB,SW,ID)
      PARAMETER M=12,  N=15
      COMMON /B/ BIC(M)
      COMMON /CONST/ XD,XF
      COMMON /DDD/ G,CP,CV,RF,R,RR,U,A,CA,CB,CC,HX,AZ,ZERO,F,XL
      DIMENSION X(NN),Y(NN),Z(NN),AB(NN)
      DIMENSION SW(N),XP(M),XQ(M),YP(M)
   50 FORMAT(2X,'SW LEFT',5X,'E=',F12.5,5X,'TO=',F12.5)
      ID=0
      IZ=0
      IL=IZ
      IR=IZ
```

```
      XN=-1.0
      PR=SW(6)/BIC(8)
      RSL=X(3)+X(4)
      SL=1.0/RSL
      BL=X(2)-SL*X(1)
      RSR=Y(3)-Y(4)
      SR=1.0/RSR
      BR=Y(2)-SR*Y(1)
      PE=(BL-BR)/(SR-SL)
      PT=SL*PE+BL
      RSS=U+SW(3)
      SS=1.0/RSS
      BS=SW(2)-SS*SW(1)
      YP(1)=(BR-BS)/(SS-SR)
      YP(2)=SS*YP(1)+BS
      XP(1)=(BL-BS)/(SS-SL)
      XP(2)=SS*XP(1)+BS
      IF( YP(1) .GE. PE .AND. YP(1) .LE. Y(1) ) IR=10
      IF(XP(1) .GE. X(1) .AND. XP(1) .LT. PE ) IL=100
      IF( IL .EQ. IZ .AND. IR .EQ. IZ ) GO TO 100
      IF( IL .EQ. IZ .AND. IR .GT. IZ ) GO TO  70
      IF( IL .GT. IZ .AND. IR .GT. IZ ) GO TO  80
      IF( IL .GT. IZ  .AND. IR .EQ. IZ ) GO TO  90
70    CONTINUE
      Z(1)=PE
      Z(2)=PT
      DO 71 I=3,4
      Z(I)=BIC(I)
71    CONTINUE
201   FORMAT(2X,'CHKL',4(2X,E10.4),3(2X,I5) )
5     FORMAT(2(2X,E9.4),2X,E10.4,5(2X,E9.3),2X,F4.1)
      WRITE(6,201) YP(1),YP(2),XP(1),XP(2),IZ,IL,IR
      WRITE(6,5) Z
      GO TO 100
80    CONTINUE
      Z(1)=PE
      Z(2)=PT
      CALL SZ(NN,XN,Z)
      WRITE(6,201) YP(1),YP(2),XP(1),XP(2),IZ,IL,IR
      WRITE(6,5) Z
      GO TO 100
90    DO 91 I=3,N
      XP(I)=X(I)
91    CONTINUE
      CALL HEAT(XP(1),XP(2),XP(3),XP(4),XP(5),XP(6) )
      XP(7)=XD
      XP(11)=XF
      XP(12)=BIC(12)
      CALL RAN(NN,XP,XQ,PR,XN)
      WRITE(6,50) XQ(1),XQ(2)
      CALL SUB(NN,XQ,Y,Z)
      ID=90
      WRITE(6,201) YP(1),YP(2),XP(1),XP(2),IZ,IL,IR
      WRITE(6,5) Z
      GO TO 100
100   CONTINUE
      RETURN

      END
```

```
      SUBROUTINE CHKR(NN,X,Y,Z,AB,SW,ID)
      PARAMETER M=12,  N=15
      COMMON /B/ BIC(M)
      COMMON /CONST/ XD,XF
      COMMON /DDD/ G,CP,CV,RF,R,RR,U,A,CA,CB,CC,HX,AI,ZERO,F,XL
      DIMENSION X(NN),Y(NN),Z(NN),AB(NN)
      DIMENSION SW(N),XP(M),YP(M),YG(M)
50    FORMAT(2X,'Sw RIG-T',5X,'E=',F12.5,5X,'TO=',F12.5)
      ID=0
      IZ=0
      IL=IZ
      IR=IZ
      XN=+1.0
      PR=SW(5)/BIC(5)

      RSL=X(3)+X(4)
      SL=1.0/RSL
      BL=X(2)-SL*X(1)
      RSR=Y(3)-Y(4)
      SR=1.0/RSR
      BR=Y(2)-SR*Y(1)
      PE=(BL-BR)/(SR-SL)
      PT=SL*PE+BL
      RSS=U+SW(3)
      SS=1.0/RSS
      BS=SW(2)-SS*SW(1)
      YP(1)=(BR-BS)/(SS-SR)
      YP(2)=SS*YP(1)+BS
      XP(1)=(BL-BS)/(SS-SL)
      XP(2)=SS*XP(1)+BS
      IF( XP(1) .GE. X(1) .AND. XP(1) .LE. PE ) IL=10
      IF( YP(1) .GT. PE .AND. YP(1) .LE. Y(1) ) IR=100
      IF( IL .EQ. IZ .AND. IR .EQ. IZ ) GO TO 100
      IF( IL .GT. IZ .AND. IR .EQ. IZ ) GO TO  70
      IF( IL .GT. IZ .AND. IR .GT. IZ ) GO TO  80
      IF( IL .EQ. IZ .AND. IR .GT. IZ ) GO TO  90
70    CONTINUE
      Z(1)=PE
      Z(2)=PT
      DO 71 I=3,M
      Z(I)=BIC(I)
71    CONTINUE
      GO TO 100
80    CONTINUE
      Z(1)=PE
      Z(2)=PT
      CALL SZ(NN,XN,Z)
      GO TO 100
90    DO 91 I=3,M
      YP(I)=Y(I)
91    CONTINUE
      CALL HEAT(YP(1),YP(2),YP(3),YP(4),YP(5),YP(6) )
      YP(7)=XD
      YP(11)=XF
      YP(12)=BIC(12)
      CALL RAN(NN,YP,YG,PP,YN)
      WRITE(6,50) YG(1),YG(2)
      CALL SUB(NN,X,YG,Z)
      ID=90
      GO TO 100
100   CONTINUE
      RETURN
      END
```

```
      SUBROUTINE CCS(M,X,Y,Z,FACE,IN)
      PARAMETER  NZ=4
      PARAMETER  NX=12
      COMMON /CONST/ XD,XF
      COMMON /DDD/ G,CP,CV,PF,R,RR,U,A,CA,CB,CC,HX,AZ,ZERO,E,XL
      DIMENSION X(M),Y(M),Z(M)
      DIMENSION FACE(NZ),AB(NX),YY(NX)
      DIMENSION XX(NX)
      IN=0
      XHX=4.0
      XXL=X(1)-FACE(1)
      IF(XXL.GT.XHX) GO TO 200
      YYL=FACE(1)-Y(1)

      IF(YYL.GT.XHX) GO TO 200
      IF(X(1).EQ.FACE(1).AND.X(2).EQ.FACE(2)) GO TO 200
      IF(Y(1).EQ.FACE(1).AND.Y(2).EQ.FACE(2)) GO TO 200
      RCS=FACE(3)
      SCS=1.0/RCS
      BCS=FACE(2)-SCS*FACE(1)
      Z(3)=(X(3)+Y(3))/2.0
      Z(4)=(X(4)+Y(4))/2.0
      AB(3)=Z(3)
      CALL GEO(M,X,Y,Z,AB)
      PL=(2.0/(G-1.0))*X(4)+X(3)
      QR=(2.0/(G-1.0))*Y(4)-Y(3)
      SL=X(5)
      SR=Y(5)
      CAL=0.25*(G-1.0)*(SL-SR)
      QL=(PL+QR)*TANH(CAL)+QR
      PR=(QR-QL)+PL
      VL=(PL-QL)/2.0
      VR=(PR-QR)/2.0
      CL=0.25*(G-1.0)*(PL+QL)
      CR=0.25*(G-1.0)*(PR+QR)
      V=0.5*(VL+VR)
C   RIGHT LEG ONLY
      S23=(Z(2)-Y(2))/(Z(1)-Y(1))
      B23=Y(2)-S23*Y(1)
      E=(BCS-B23)/(S23-SCS)
      T=S23*E+B23
      IF(E.GE.Z(1).AND.E.LE.Y(1)) GO TO 101
      GO TO 102
  101 CONTINUE
   98 FORMAT(2X,6(2X,F12.4),5X,'CCS 1')
   99 FORMAT(2X,6(2X,F12.4),5X,'CCS 2')
      WRITE(6,98) X(3),X(4),Y(3),Y(4),SL,SR
      WRITE(6,99) QL,PR,VL,VR,V,CAL
      IN=101
      YY(1)=E
      YY(2)=T
      YY(3)=V
      YY(4)=CL
      YY(5)=X(5)
      CALL HEAT(YY(1),YY(2),YY(3),YY(4),YY(5),YY(6))
      YY(7)=XD
      YY(11)=XF
      CALL CCS(M,X,YY,Z)
      FACE(1)=E
      FACE(2)=T
      FACE(3)=V
```

```
      WRITE(6,1) FACE
    1 FORMAT(2X,'INTERFACE',5X,4(2X,E10.4) )
      GO TO 200
  102 CONTINUE
C   LEFT LEG ONLY
      S12=(Z(2)-X(2))/(Z(1)-X(1))
      B12=X(2)-S12*X(1)
      E=(BCS-B12)/(S12-SCS)
      T=S12*E+B12
      IF(E.GE.X(1).AND.E.LE.Z(1)) GO TO 103

      GO TO 200
  103 CONTINUE
      WRITE(6,98) X(3),X(4),Y(3),Y(4),SL,SR
      WRITE(6,99) GL,PR,VL,VR,V,CAL
      IN=103
      XX(1)=E
      XX(2)=T
      XX(3)=V
      XX(4)=CR
      XX(5)=Y(5)
      CALL HEAT(XX(1),XX(2),XX(3),XX(4),XX(5),XX(6))
      XX(7)=X9
      XX(8)=Y(8)
      XX(11)=XF
      CALL SSS(M,XX,Y,Z)
      FACE(1)=E
      FACE(2)=T
      FACE(3)=V
      WRITE(6,1) FACE
  200 CONTINUE
      RETURN
      END


      SUBROUTINE COM(NN,C1,C2,C3)
      DIMENSION C1(NN),C2(NN),C3(NN)
      P=(C2(1)-C1(1))/(C3(1)-C1(1))
      DO 10 I=3,NN
      C2(I)=P*C3(I)+(1.0-P)*C1(I)
   10 CONTINUE
      RETURN
      END


      SUBROUTINE CONT(XN,P2,P1,YG)
      COMMON /DDD/ G,CP,CV,RF,R,RR,U,A,CA,CB,CC,HX,AZ,ZERO,F,XL
      PRES=P2/P1
      IF(PRES.LT.1.0) PRES=1.0/PRES
      YA=PRES-1.0
      YB=2.0/G
      YC=(G+1.0)*PRES
      YD=G-1.0
      YF=YA*SQRT(YB/(YC+YD))
      IF(XN.LT.0.0) YG=U-YF
      IF(XN.GT.0.0) YG=U+YF
      RETURN
      END
```

APPENDIX D

```
      IMPLICIT REAL*8 (A-H,O-Z)
      DIMENSION AMT(13,10), NN(13), SVR(19), TDIF(19), BMT(13)
      COMMON /VAR/ TO1G, TO2G, TO6G, TO7G, T1, T2, T3, T4, T6, T8,
     A  T10, T14, T16, T18, T20, TA2, TO8G, T7,
     B  TO3G, TO4G, TO5G, TO9G, TO10G, TO11G, T5, T9, T11,
     C  T12, T13, T15, T17, T19, TIG, T2G, T3G, T4G, T5G, T6G, T7G,
     D  T8G, T9G, T10G, T11G, TA1, EFFL, PO1G, PO2G, PO3G, PO4G, PO5G,
     E  PO6G, PO7G, PO8G, PO9G, PO10G, PO11G, PIG, P2G, P3G, P4G, P5G,
     F  P6G, P7G, P8G, P9G, P10G, P11G, P(20), AC(20), VC(20), FM1,
     G  FM2, FM3, FM4, FM5, FM6, FM7, FM8, FM9, FM10, FM11, A(11),
     H  GAMIG, GAM2G, GAM3G, GAM4G, GAM5G, GAM6G, GAM7G, GAM8G, GAM9G,
     I  GAM10G, GAM11G, TGMI, TGMII, TGM3, TMA, GIMU, GIIMU, GIMU, AMU,
     1  PRGI,
     J  PRGII, PRG3, PRA, CPGI, CPGII, CPG3, CPA, TMI, TMII, TMIII, TM,
     1  ZIMU, ZIIMU, ZIMU, ZMU,
     K  PRI, PRII, PRIII, PR, CPI, CPII, CPIII, CP, GGI, GGII, GGIII,
     1GA, GI, GII, GIII, G, REGI,
     L  REGII, REGI, REA, REI, REII, REIII, RE, GFI, GFII, GFIII,
      COMMON/VARB/                                    AF, FI, FII, F, GJI,
     M  GJII, GJIII, AJ, ZJI, ZJII, ZJIII, ZJ, HGI, HGII, HGIII, HA,
     1  HI, HII, HIII, H, CCI, CGII, CGIII,
     N  CA, CI, CII, CIII, C, UI, UII, UIII, U, AGI, AGII, AGIII, AA,
     1  TUNI, TUNII, TUNIII, TUN,
     O  TOWI, TOWII, TOW3, TOW, EPSI, EPSII, EPS3, EPSA, ESSI, ESSII,
     1  ESS3, ESS, WG,
     P  Q6G, QCORR, BPR, ALT, PAT, PA2, RH, FN(4),     EFFLP, VI, VIM,
     Q  PICA, H1M, CL1M, WT1M, DCM, BLPR, BLPRM, CPP, CPPM, PF, PFM,
     R  RO1, PLKW, WI, WII, WIII, WB, WM, WV1, WV2, WE, WS, WA, QP, QCM,
     S  QM, QV1, QV2, QE, QS, CF23, CF34, CF45, CF78, CF89, CF910
      COMMON /VARC/CF111,     ATAP, H1, CL1, WT1, ACN(20), DC, DL(4),
     A  DH(4), DW(4), DDHG(4), DALG(4), DAFOA(4), DSIG(4), DDEL(4),
     B  DA(4), DK(3), DSL(4), DSI(4), DALF(4), DDH(4), CONV(16), DELM,
     C  ROLIM, PLIM, FG, TITLE(28), DP,  DPI, DPII, DPIII, PPR, PPRM,
     D  TA1F, RHP, TIGM, DKH(4), ETIG,  ET02G, ET06G, ET07G, ET1,
     E  ET2, ET3, ET4, ET6, ET8, ET10, ET14, ET16, ET18, ET20, ETA2,
     1  ET08G,ET7,
     F  EBPR, CWA, DNP(3), GDI, GDII, GDIII,
     1                                GDA, EVIM, BRPM, VLIM, ROA1,
     G  ROA2,DAFAL(4),DSLL(4),AB(4)
      COMMON/VARD/GC,GCG,CP2,CP6,W3,CP3,CP1,FIII,TUN3
      COMMON /IVAR/ NTAM, NDSGN, NCS, KI, KO, NLIM, NP(4), NFULL,
     1  NBS, NBPS, JCPRO
      EQUIVALENCE (SVR( 1),TO1G)
      WRITE(6,10021)TO1G, TO2G, TO6G, TO7G, T1, T2, T3, T4, T6, T8,
     1T10, T14, T16, T18, T20, TA2
10021 FORMAT(1HO,3X,'TO1G=',E15.7,5X, 'TO2G=',E15.7, 5X,'TO6G=',E15.7,
     15X,'TO7G=',E15.7,/3X,'T1=',E15.7,5X,'T2=',E15.7,5X,'T3=',E15.7,
     25X,'T8=',E15.7,5X,'T6=',E15.7,5X,//3X,'T8=',E15.7,5X,'T10=',
     3E15.7,5X,'T14=',E15.7,5X,'T16=',E15.7,5X,//3X,'T18=',E15.7,5X,
     4'T20=',E15.7,5X,'TA2=',E15.7)
C
   2  CALL ENPUT
```

```
      SUBROUTINE PLT( XX )
      PARAMETER ISEG=154
      PARAMETER II=ISEG+1
      PARAMETER JJ=23
      PARAMETER M=12
      COMMON /P/  P(M,II,JJ)
      DIMENSION A(M),B(M),C(M)
      ZZZ=1.0E-06
      WRITE(6,459)
  459 FORMAT(1H1)
      IM0=II-1
      DO 450 J=1,JJ
      B(1)=XX
      IL=0
      IX=0
      DO 451 I=1,IM0
      IP1=I+1
      IF(XX.GT.P(1,I,J).AND.XX.LT.P(1,IP1,J)) IL=I
      IF(ABS(XX-P(1,I,J)).LE.ZZZ) IX=I
  451 CONTINUE
      IF(IL) 452,452,453
  453 ILP=IL+1
      B(2)=0.5*(P(2,IL,J)+P(2,ILP,J))
      DO 456 LX=1,M


      A(LX)=P(LX,IL,J)
      C(LX)=P(LX,ILP,J)
  456 CONTINUE
      CALL CON(M,A,B,C)
  452 IF(IX) 454,454,455
  455 DO 457 LX=1,M
      B(LX)=P(LX,IX,J)
  457 CONTINUE
  454 CONTINUE
      WRITE(6,458) B(1),B(2),B(3),B(8),B(9),B(10),IL,IX
  458 FORMAT(2X,'E=',F9.3,2X,'TO=',F9.3,2X,'U=',F9.3,2X,'P=',F9.3,
     1       2X,'RO=',F9.6,2X,'T=',F9.3,4X,'IL=',I4,2X,'IX=',I4)
  450 CONTINUE
      RETURN
      END
```

```
      WRITE(6,10022)T08G
10022 FORMAT(1H0,3X,'T08G=',E15.7,3X,'AFTER SUBROUTINE ENPUT')
      DNP(2)=DNP(1)
      WRITE(6,10012)DNP(2)
10012 FORMAT(1H0,3X,'DNP(2)='E12.6)
      T2G=T02G
      T6G=T06G
      T5G=T02G
      T10G=T08G
      JV=0
  501 II=0
      CALL GASP(TIG, PN, GAMIG, CPIG, Z1, Z1, GMU)
      IF (JCPRO .GE. 0)
     1  PIG=R01*TIG/(.093178*GMU)
      IF (JCPRO .LT. 0)
     1  R01=.093178*PIG*GMU/TIG
      WG=R01*VI*A(1)
      FM1=WG*DSQRT(TIG/(GAMIG*GMU))/(20.7774*PIG*A(1))
      T01G=TIG*(1.+FM1*FM1*(GAMIG-1.)/2.)
      WRITE(6,198)R01,GMU,PIG,TIG
  198 FORMAT(1H0,3X,'R01=',E15.7,5X,'GMU=',E15.7,5X,'PIG=',E15.7,
     1 5X,'TIG=',E15.7)
      T11G=T01G
   10 DO 3 I=1,18
      DO 4 J=1,18
    4 AMT(I,J)=0.
    3 BMT(I)=0.0
      TMI=.5*(T2+T4)
      TMII=.5*(T2+T6)
      TMIII = .5*(T2+T7)
      WIII = WII
      TM=.5*(T3+T1)
      Z1=T5G-T4
      Z2=T6G-T2
      IF (Z1 .LE. 0.  .OR.  Z2 .LE. 0.)  GO TO 11
      IF (Z1 .EQ. Z2)  GO TO 12
      TGMI=TMI+(Z1-Z2)/(DLOG(Z1)-DLOG(Z2))
      GO TO 13
   11 TGMI=.5*(T5G+T6G)
      GO TO 13
   12 TGMI=.5*(T5G+T6G)
   13 Z1=T10G-T6
      Z2=T11G-T2
      IF (Z1 .LE. 0.  .OR.  Z2 .LE. 0.)  GO TO 14
      IF (Z1 .EQ. Z2)  GO TO 15
      TGMII=TMII+(Z1-Z2)/(DLOG(Z1)-DLOG(Z2))
      GO TO 16
   14 TGMII=.5*(T10G+T11G)
      GO TO 16
   15 TGMII=.5*(T10G+T11G)
   16 Z1= T1-TA1
      Z2=T3-TA2
      IF (Z1 .LE. 0.  .OR.  Z2 .LE. 0.)  GO TO 17
      IF (Z1 .EQ. Z2)  GO TO 18
      TMA=TM-(Z1-Z2)/(DLOG(Z1)-DLOG(Z2))
      GO TO 19
```

```
   17 TMA=.5*(TA1+TA2)
      GO TO 19
   18 TMA=.5*(TA1+TA2)
   19 CALL GASP(TGMI, FN, Z1, CPGI, PRGI, GIMU, GMU)
      Z1 = T7G-T7
      Z2 = T8G-T2
      IF(Z1 .LE. 0 .OR. Z2 .LE. 0) GO TO 20
      IF(Z1 .EQ. Z2) GO TO 21
      TGM3 = TMIII + (Z1-Z2)/(DLOG(Z1)-DLOG(Z2))
      GO TO 22
   20 TGM3 = .5*(T7G+T8G)
      GO TO 22
   21 TGM3 = .5*(T7G+T8G)
   22 CONTINUE
      CALL GASP(TGMII, FN, Z1, CPGII, PRGII, GIIMU, GMU)
      CALL GASP(TGM3, FN, Z1, CPG3, PRG3, G3MU, GMU)
      WRITE(6,199)GIMU,GIIMU,VI
  199 FORMAT(1HO,3X,'GIMU=',E15.7,5X,'GIIMU=',E15.7,5X,'VI=',E15.7)
      CALL AIRP(TA1, PAT, TMA, RH, PRA, AMU, CPA, Z1, AML)
      CALL LIQP(TMI, FG, ZIMU, PRI, CPI)
      CALL LIQP(TMII, FG, ZIIMU, PRII, CPII)
      CALL LIQP(TMIII, FG, Z3MU, PRIII, CPIII)
      CALL LIQP(TM, FG, ZMU, PR, CP)
      AFRGI=DL(1)*DH(1)
      AFRGII=DL(2)*DH(2)
      AFRA=DL(4)*DH(4)
      GGI=WG/(DSIG(1)*AFRGI)
      GGII=WG/(DSIG(2)*AFRGII)
      GGIII=GGII
      GA=WA/(DSIG(4)*AFRA)
      AFRI=DW(1)*DH(1)/DNP(1)
      AFRII=DW(2)*DH(2)/DNP(2)
      AFR=DW(4)*DH(4)/DNP(3)
      GI=WI/(DSI(1)*AFRI)
      GII=WII/(DSI(2)*AFRII)
      GIII=GII
      WRITE(6,10009)WII,DSI(2),AFRII
      WRITE(6,10010)DW(2),DH(2),DNP(2)
10009 FORMAT(1HO,3X,'WII=',E12.6,5X,'DSI(2)=',E12.6,5X,'AFRII=',E12.6)
10010 FORMAT(1HO,3X,'DW(2)=',E12.6,5X,'DH(2)=',E12.6,5X,'DNP(2)=',E12.6)
      W3=WI+WII+WB+WM+WV1+WV2+WE+WS
      G=W3/(DSI(4)*AFR)
      REGI=GGI*DDHG(1)/GIMU
      REGII=GGII*DDHG(2)/GIIMU
      REG3=REGII
      REA=GA*DDHG(4)/AMU
      REI=GI*DDH(1)/ZIMU
      REII=GII*DDH(2)/ZIIMU
      REIII=REII
      WRITE(6,10006)GI,GII,REI,REII
10006 FORMAT(1HO,3X,'GI=',E15.7,5X,'GII=',E15.7,5X,'REI=',E15.7,5X,
     1'REII=',E15.7)
      RE=G*DDH(4)/ZMU
      WRITE(6,197)REGI,REGII,REA,REI,REII,RE
  197 FORMAT(1HO,3X,'REGI=',E13.6,4X,'REGII=',E13.6,4X,'REA=',E13.6,4X,
     1 'REI=',E13.6,4X,'REII=',E13.6,4X,'RE=',E13.6)
```

```
      Z1=DLOG(REGI)
      Z2=-750.2946+629.2028*Z1-219.5279*Z1**2+40.7569*Z1**3-4.253034*Z1*
     1*4+.236432*Z1**5-.0054e6298*Z1**6
      GFI=DEXP(Z2)
      Z1=-360.4224+335.276*Z1-129.1436*Z1**2+26.20469*Z1**3-2.961196*Z1*
     1*4+.1766745*Z1**5-.00434543*Z1**6
      GJI=DEXP(Z1)
      Z1=DLOG(REGII)
      Z2=-750.2946+629.2028*Z1-219.5279*Z1**2+40.7569*Z1**3-4.253034*Z1*
     1*4+.236432*Z1**5-.0054e6298*Z1**6
      GFII=DEXP(Z2)
      GFIII=GFII
      Z1=-360.4224+335.276*Z1-129.1436*Z1**2+26.20469*Z1**3-2.961196*Z1*
     1*4+.1766745*Z1**5-.00434543*Z1**6
      GJII=DEXP(Z1)
      GJIII=GJII
      Z1=DLOG(REA)
      Z2=-7.6524e2+6.206772*Z1-1.715187*Z1**2+.1756196*Z1**3-.00620780e*
     1Z1**4
      AF=DEXP(Z2)
      Z1=2.123751-1.083736*Z1-.05205297*Z1**2+.0164666*Z1**3-.000782202
     11*Z1**4
      AJ=DEXP(Z1)
      Z1=DLOG(REI)
      Z1=-22.04452+12.84988*Z1-3.122052*Z1**2+.3159152*Z1**3-.01161237*Z
     11**4
      ZJI=DEXP(Z1)
      Z1=DLOG(REII)
      Z1=-22.04452+12.84988*Z1-3.122052*Z1**2+.3159152*Z1**3-.01161237*Z
     11**4
      ZJII=DEXP(Z1)
      ZJIII=ZJII
      Z1=DLOG(RE)
      Z1=-22.04452+12.84988*Z1-3.122052*Z1**2+.3159152*Z1**3-.01161237*Z
     11**4
      ZJ=DEXP(Z1)
      TO3=-2./3.
      HGI=GGI*CPGI*GJI*PRGI**TO3
      HGII=GGII*CPGII*GJII*PRGII**TO3
      HGIII=HGII
      HA=GA*CPA*AJ*PRA**TO3
      HI=GI*CPI*ZJI*PRI**TO3
      HII=GII*CPII*ZJII*PRII**TO3
      HIII=HII
      WRITE(6,10007)ZJII,CPII,PRII
10007 FORMAT(1HO,3X,'ZJII=',E15.7,5X,'CPII=',E15.7,5X,'PRII=',E15.7)
      H=G*CP*ZJ*PR**TO3
      GMI=DSQRT(2.*HGI/(DK(1)*DDEL(1)))
      GMII=DSQRT(2.*HGII/(DK(2)*DDEL(2)))
      AM=DSQRT(2.*HA/(DK(3)*DDEL(4)))
      TO3=GMI*DSL(1)
      ATFI=DTANH(TO3)/TO3
      TO3=GMII*DSL(2)
      ATFII=DTANH(TO3)/TO3
      TO3=AM*DSL(4)
```

```
      ATFA=DTANH(TO3)/TO3
      ATOI=1.-DAFOA(1)*(1.-ATFI)
      ATOII=1.-DAFOA(2)*(1.-ATFII)
      ATO=1.-DAFOA(4)*(1.-ATFA)
      GM1=DSQRT(2.*HI/(DK(1)*DA(1)))
      GM2=DSQRT(2.*HII/(DK(2)*DA(2)))
      AMN=DSQRT(2.*H/(DK(3)*DA(4)))
      TO3=GM1*DSLL(1)
      ATF1L=DTANH(TO3)/TO3
      TO3=GM2*DSLL(2)
      ATF2L=DTANH(TO3)/TO3
      TO3=AMN*DSLL(4)
      ATFAL=DTANH(TO3)/TO3
      ATO1=1.-DAFAL(1)*(1.-ATF1L)
      ATO2=1.-DAFAL(2)*(1.-ATF2L)
      ATOL=1.-DAFAL(4)*(1.-ATFAL)
      UI=1./(1./(ATOI*HGI) +AB(1)/(DK(1)*(1.-DAFOA(1))) +DALG(1)/(DALF(1
     1)*HI*ATO1))
      UII=1./(1./(ATOII*HGII)+AB(2)/(DK(2)*(1.-DAFOA(2)))+DALG(2)/(DALF(
     12)*HI*ATO2))
      UIII=UII
      U=1./(1./(ATO*HA)+AB(4)/(DK(3)*(1.-DAFOA(3)))+DALG(4)/(DALF(4)*HI*
     1ATOL))
      CGI=WG*CPGI
      CGII=WG*CPGII
      CGIII=CGII
      CA=WA*CPA
      CI=WI*CPI
      CII=WII*CPII
      CIII=CII
      C=W3*CP
      CMINI=DMIN1(CGI,CI)
      CMAXI=DMAX1(CGI,CI)
      CMINII=DMIN1(CGII,CII)
      CMAXII=DMAX1(CGII,CII)
      CMIN=DMIN1(CA,C)
      CMAX=DMAX1(CA,C)
      AGI=DL(1)*DH(1)*DW(1)*DALG(1)
      AGII=DL(2)*DH(2)*DW(2)*DALG(2)
      AGIII=AGII
      AA=DL(4)*DH(4)*DW(4)*DALG(4)
      TUNI=AGI*UI/CMINI
      TUNII=AGII*UII/CMINII
      TUN3=TUNII
      TUN=AA*U/CMIN
      TOWI=1.-DEXP(-TUNI*CMINI/(CMAXI*DNP(1)))
      TOWII=1.-DEXP(-TUNII*CMINII/(CMAXII*DNP(2)))
      TOW3=TOWII
      TOW=1.-DEXP(-TUN*CMIN/(CMAX*DNP(3)))
      ESSI=1.-DEXP(-TOWI*CMAXI/CMINI)
      ESSII=1.-DEXP(-TOWII*CMAXII/CMINII)
      ESS3=ESSII
      ESS=1.-DEXP(-TOW*CMAX/CMIN)
      IF (CMINI/CMAXI .GT. .9999) GO TO 31
      EPSI=((1.-ESSI*CMINI/CMAXI)/(1.-ESSI))**NP(1)
      EPSI=(EPSI-1.)/(EPSI-CMINI/CMAXI)
```

```
      GO TO 32
   31 EPSI=DNP(1)*ESSI/(1.+ESSI*(DNP(1)-1.))
   32 IF (CMINII/CMAXII .GT. .9999)  GO TO 33
      EPSII=((1.-ESSII*CMINII/CMAXII)/(1.-ESSII))**NP(2)
      EPSII=(EPSII-1.)/(EPSII-CMINII/CMAXII)
      EPS3=EPSII
      GO TO 34
   33 EPSII=DNP(2)*ESSII/(1.+ESSII*(DNP(2)-1.))
      EPS3=EPSII
   34 IF (CMIN/CMAX .GT. .9999)  GO TO 35
      EPSA=((1.-ESS*CMIN/CMAX)/(1.-ESS))**NP(4)
      EPSA=(EPSA-1.)/(EPSA-CMIN/CMAX)
      GO TO 36
   35 EPSA=DNP(4)*ESS/(1.+ESS*(DNP(4)-1.))
   36 CONTINUE
      T03=FM1*FM1
      P01G=PIG*(1.+T03*(GAMIG-1.)/2.)**(GAMIG/(GAMIG-1.))
      GO TO (30, 40, 50), NDSGN
C    CAVITY OPTION 1  CONST. MACH NUMBER
   30 FM2=FM1
      A(2)=A(1)*(T02G/T01G)**((1.+GAMIG*T03)/2.)
      GO TO 60
C    CAVITY OPTION 2  CONST. AREA
   40 A(2)=A(1)
      Z1=T01G*(1.+GAMIG*T03)**2/(2.*(GAMIG+1.)*T03*
     1  (1.+T03*(GAMIG-1.)/2.))
      Z1=T02G/Z1
      IF (Z1 .GT. 1.)  GO TO 10000
      I=0
12000 I=I+1
      CALL CASP(T2G , FN, GAM2G, CP2G, T03, T03, GMU)
      Z2 = 2.*GAM2G*Z1-2.*GAM2G-2.
      Z3=GAM2G*GAM2G*(Z1-1.)+1.
      IF (Z3 .NE. 0.)  GO TO 41
      FM2=DSQRT(-Z1/Z2)
      GO TO 60
   41 Z4=(-Z2+DSQRT(Z2*Z2-4.*Z1*Z3))/(2.*Z3)
      Z5=(-Z2-DSQRT(Z2*Z2-4.*Z1*Z3))/(2.*Z3)
      Z6=DMIN1(Z4, Z5)
      IF (Z6 .LT. 0.)  Z6=DMAX1(Z4, Z5)
      WRITE(6,174)T02G,T03,PR
  174 FORMAT(1H0,3X,'T02G=',E15.7,5X,'T03=',E15.7,5X,'PR=',E15.7)
      WRITE(6,173)Z1,Z2,Z3,Z4,Z5,Z6
  173 FORMAT(1H0,3X,'Z1=',E15.7,5X,'Z2=',E15.7,5X,'Z3=',E15.7,5X,
     1/,4X,'Z4=',E15.7,5X,'Z5=',E15.7,5X,'Z6=',E15.7)
      FM2=DSQRT(Z6)
      GO TO 60
C    CAVITY OPTION 3  GENERAL SHAPE
   50 Z5=(GAMIG+GAM2G)/2.
      Z6=FM1*FM1
      N=NCS-1
      DO 51 J=1,N
      Z1=-2.*(1.+Z6*(Z5-1.)/2.)/(1.-Z6)
      Z2=(1.+Z5*Z6)*(-.5*Z1)
      Z3=(ACN(J+1)-ACN(J))/(2.*(ACN(J+1)+ACN(J)))
      Z4=(T02G-T01G)/((NCS-1.)*T01G-(J-.5)*(T02G-T01G))
```

```
      Z6=Z6*(1.+Z3*Z1+Z2*Z4)
      IF (Z6 .LE. 1.) GO TO 51
10000 WRITE(KO,105)
  105 FORMAT(41H**** CHOKED CAVITY - READ NEW DATA ******)
      GO TO 2
   51 CONTINUE
      FM2=DSQRT(Z6)
      A(2)=ACN(NCS)
   60 T2GOLD=T2G
      T2G=T02G/(1.+FM2*FM2*(GAM2G-1.)/2.)
      T2GDIF=T2GOLD-T2G
      IF(DABS(T2GDIF).LE..500) GO TO 11000
      IF(I.LE.NLIM) GO TO 12000
      PRINT 13000,I,T2GDIF
13000 FORMAT(58H****FAILURE TO CONVERGE IN STATIC TEMP. LOOP 1 - CYCLES
     '= ,I3,' - ERROR=',E12.5)
      GO TO 2
11000 WRITE(6,10050)GAM2G, GMU,T2G
10050 FORMAT (1HO,5X,'GAM2G = ', E15.7,3X,'GMU = ',E15.7,3X,'T2G = '
     1,E15.7,3X,'RIGHT BEFORE 11000',//)
      P2G=WG*DSQRT(T2G/(GAM2G*GMU))/(20.7774*A(2)*FM2)
      P02G=P2G*(1.+FM2*FM2*(GAM2G-1.)/2.)**(GAM2G/(GAM2G-1.))
C     FIRST DIFFUSER
      P03G=P02G-CF23*(P02G-P2G)
      FM3=FM2*A(2)/A(3)
      GAM3G=GAM2G
      CALL MACH(DELM, NLIM, P03G, GAM3G, FM3, T02G, WG, GMU,
     1  A(3), P3G, T3G,FN,CP3G)
C     SECOND DIFFUSER
      P04G=P03G-CF34*(P03G-P3G)
      FM4=FM3*A(3)/A(4)
      GAM4G=GAM3G
      CALL MACH(DELM, NLIM, P04G, GAM4G, FM4, T02G, WG, GMU,
     1  A(4), P4G, T4G,FN,CP4G)
C     THIRD DIFFUSER
      P05G=P04G-CF45*(P04G-P4G)
      FM5=FM4*A(4)/A(5)
      GAM5G=GAM4G
      CALL MACH(DELM, NLIM, P05G, GAM5G, FM5, T02G, WG, GMU,
     1  A(5), P5G, T5G,FN,CP5G)
      R05=.093178*P5G*GMU/T5G
      R06=R05
      FM6=WG*DSQRT(T06G/GAM5G/GMU)/(20.7774*P05G*A(6))
      I=0
   70 Z1=R06
      P06G=P05G-GGI*GGI*((1.+DSIG(1)*DSIG(1))*(R05/R06-1.)+
     1  GFI*DALG(1)*DW(1)*R05/(.5*DSIG(1)*(P06+R05)))/
     2  (9266.11*R05)
      GAM6G=GAM5G
      CALL MACH(DELM,NLIM,P06G,GAM6G,FM6,T06G,WG,GMU,A(6),P6G,T6G,FN,
     *  CP6G)
      R06=.093178*P6G*GMU/T6G
      I=I+1
      Z3=R06-Z1
      IF (DABS(Z3) .LE. ROLIM) GO TO 71
```

```
      IF (I .LT. NLIM)  GO TO 70
      WRITE(KO,101) Z3
  101 FORMAT(53H**** FAILURE TO CONVERGE IN DENSITY LOOP 1 - ERROR = ,
     1  E12.5,6H******)
   71 CALL GASP(T07G, FN, GAM7G, CP7G, T03, T03, GMU)
      WRITE(KO,150) I, Z3
  150 FORMAT(10X,'DENSITY LOOP 1 - CYCLES =',I3,' - ERROR =',E12.5)
      P07G=P06G*BPR
      J=0
   60 FM7=WG*DSQRT(T07G/(GAM7G*GMU))/(20.7774*P07G*A(7))
      CALL MACH(DELM, NLIM, P07G, GAM7G, FM7, T07G, WG, GMU,
     1  A(7), P7G, T7G,FN,CP7G)
      R07=.093178*P7G*GMU/T7G
      R08=R07
      WRITE(6,10023)T08G
10023 FORMAT(1H0,3X,'T08G=',E15.7,3X,'FIRST USED IN A CALCULATION')
      FM8=WG*DSQRT(T08G/GAM7G/GMU)/(20.7774*P07G*A(8))
      I=0
10002 Z1=R08
      DW(4)=DW(1)
      DALG(4)=DALG(1)
      GGIII=GGI
      P08G=P07G-GGIII*GGIII*((1.+DSIG(1)*DSIG(1))*
     1(R07/R08-1.)+GFIII*DALG(3)*DW(3)*R07/(.5*DSIG(3)*
     2(R07+R08)))/(9266.11*R07)
      GAM8G=GAM7G
      WRITE(6,10001)P08G,GAM8G,FM8,T01G,WG
10001 FORMAT(1H0,3X,'P08G=',E15.7,5X,'GAM8G=',E15.7,5X,
     1'FM8=',E15.7,5X,'T01G=',E15.7,5X,'WG=',E15.7)
      CALL MACH (DELM,NLIM,P08G,GAM8G,FM8,T08G,WG,GMU,A(8),
     1P8G,T8G,FN,CP8G)
      R08=.093178*P8G*GMU/T8G
      I=I+1
      Z3=R08-Z1
      IF (DABS(Z3) .LE. ROLIM) GO TO 77
      IF (I .LT. NLIM) GO TO 10002
      WRITE (KO,10003)Z3
10003 FORMAT (53H****FAILURE TO CONVERGE IN DENSITY LOOP 3 - ERROR=,
     1E12.5,6H******)
77    CONTINUE
      CALL MACH(DELM, NLIM, P08G, GAM8G, FM8, T08G, WG, GMU,
     1  A(8), P8G, T8G,FN,CP8G)
      P09G=P08G-CF89*(P08G-P8G)
      FM9=FM8*A(8)/A(9)
      GAM9G=GAM8G
      CALL MACH(DELM, NLIM, P09G, GAM9G, FM9, T08G, WG, GMU,
     1  A(9), P9G, T9G,FN,CP9G)
      P010G=P09G-CF910*(P09G-P9G)
      FM10=FM9*A(9)/A(10)
      GAM10G=GAM9G
      CALL MACH(DELM, NLIM, P010G, GAM10G, FM10, T08G, WG, GMU,
     1  A(10), P10G, T10G,FN,CP10G)
      R010=.093178*P10G*GMU/T10G
      R011=R010
```

```
      FM11=WG*DSQRT(T011G/GAM10G/GMU)/(20.7774*P010G*A(10))
      I=0
   75 Z1=R011
      P011G=P010G-GGII*GGII*((1.+DSIG(2)*DSIG(2))*(R010/R011-1.)+
     1  GFII*DALG(2)*DW(2)*R010/(.5*DSIG(2)*(R010+R011)))/
     2  (9266.11*R010)
      GAM11G=GAM10G
      WRITE(6,183)P011G,GAM11G,FM11,T01G,WG
  183 FORMAT(1H0,3X,'P011G=',E15.7,5X,'GAM11G=',E15.7,5X,'FM11=',
     1E15.7,5X,'T01G=',E15.7,5X,'WG=',E15.7)
      CALL MACH(DELM,NLIM,P011G,GAM11G,FM11,T01G,WG,GMU,A(10),P11G,
     * T11G,FN,CP11G)
      R011=.093178*P11G*GMU/T11G
      I=I+1
      Z3=R011-Z1
      IF (DABS(Z3) .LE. ROLIM)  GO TO 76
      IF (I .LT. NLIM)  GO TO 75
      WRITE(KO,120) Z3
  120 FORMAT(53H**** FAILURE TO CONVERGE IN DENSITY LOOP 2 - ERROR = ,
     1  E12.5,6H******)
   76 FM11=WG*DSQRT(T01G/(GAM1G*GMU))/(20.7774*P011G*A(11))
      WRITE(KO,151) I, Z3
  151 FORMAT(10X,'DENSITY LOOP 2 - CYCLES =',I3,' - ERROR =',E12.5)
      CALL MACH(DELM, NLIM, P011G,GAM11G ,FM11, T01G, WG, GMU,
     1  A(11), P11G, T11G,FN,CP11G)
      IF (JCPRO .GE. 0)
     1  Z1=R01*TIG/(.093178*GMU)*(1.+(GAM1G-1.)*FM1*FM1/2.)
     2     **(GAM1G/(GAM1G-1.))
      Z1=P011G-CF111*(P011G-P11G)-Z1
      IF (JCPRO .LT. 0)
     1  Z1=P011G-CF111*(P011G-P11G)-P01G
      P011G=P011G-Z1
      P010G=P010G-Z1
      P09G=P09G-Z1
      P08G=P08G-Z1
      P07G=P07G-Z1
      CALL GASP(T6G,FN, GAM6G, CP6G,Z2,Z2,GMU)
      BPR=P07G/P06G
      Q6G=60.*A(6)*FM6*DSQRT(GAM6G*T6G*32.174*1545.43/GMU)
      ATAB=.730-7.09843*(DABS(Q6G/BRPM/NBS-.5355))**2.08014
      ATAB=0.6
      WRITE(6,186)Z1,P07G,P06G,Q6G
  186 FORMAT(1H0,3X,'Z1=',E15.7,5X,'P07G=',E15.7,5X,'P06G=',E15.7,5X,
     1'Q6G=',E15.7)
      WRITE(6,187) T06G,BPR,GAM6G,ATAB
  187 FORMAT(1H0,3X,'T06G=',E15.7,5X,'BPR=',E15.7,5X,'GAM6G=',E15.7,5X,
     1 'ATAB=',E15.7)
      T07G=T06G*(BPR**((GAM6G-1.)/(ATAB*GAM6G)))
      WRITE(6,180) T06G,BPR,GAM6G,ATAB,T07G
  180 FORMAT(1H0,3X,'T06G=',E15.7,5X,'BPR=',E15.7,5X,'GAM6G=',E15.7,5X,
     1 'ATAB=',E15.7,5X,'T07G=',E15.7)
      J=J+1
      IF (DABS(Z1) .LT. PLIM)  GO TO 85
      IF (J .LT. NLIM)  GO TO 50
```

```
      WRITE(KO,103) Z1
  103 FORMAT(52H**** FAILURE TO CONVERGE IN PRESSURE LOOP - ERROR = ,
     1  E12.5,6H******)
   85 CALL AIRP(TA1, PAT, TA1, RH, Z2, Z2, CPA1, Z2, AML)
      WRITE(KO,152) J, Z1
  152 FORMAT(10X,'TOTAL PASSES THROUGH PRESSURE LOOP =',I3,
     1  ' - ERROR =',E12.5)
      CALL AIRP(TA1, PAT, TA2, RH, Z1,Z1, CPA2, GAM2A, AML)
      CALL LIQP(T1, FG, Z1, Z1, CP1)
      CALL LIQP(T2, FG, Z1, Z1, CP2)
      CALL LIQP(T3, FG, Z1, Z1, CP3)
      CALL LIQP(T4, FG, Z1, Z1, CP4)
      CALL LIQP(T6, FG, Z1, Z1, CP6)
      CALL LIQP(T7, FG, Z1, Z1, CP7)
      CALL LIQP(T8, FG, Z1, Z1, CP8)
      CALL LIQP(T10, FG,Z1, Z1, CP10)
      CALL LIQP(T14, FG,Z1, Z1, CP14)
      CALL LIQP(T16, FG,Z1, Z1, CP16)
      CALL LIQP(T18, FG,Z1, Z1, CP18)
      CALL LIQP(T20, FG,Z1, Z1, CP20)
      WRITE(6,20000) CP2,CP6,FG,T2,T6
20000 FORMAT (1H0,3X,5F20.10)
      CMIN3=CMINII
      AMT( 1, 1)=WG*(CPIG+CPZG)/2.
      AMT( 1, 2)=-AMT(1,1)
      BMT( 1)=GS-.948*PLKW*(1./EFFL-1.)
      AMT(2,2)=CGI
      AMT(2,3)=-AMT(2,2)
      AMT(2,6)=WI*.5*(CP2+CP4)
      AMT(2,8)=-AMT(2,6)
      AMT(3,2)=EPSI*CMINI-CGI
      AMT(3,6)=-EPSI*CMINI
      AMT(3,3)= CGI
      AMT(4,4)=1.
      AMT(4,3)=-(P07G/P06G)**((GAM6G-1.)/(ATAB*GAM6G))
      AMT(5,17) = CGII
      AMT(5,1)=-AMT(5,4)
      AMT(5,6)=WII*.5*(CP2+CP6)
      AMT(5,9)=-AMT(5,6)
      AMT(6,17)=EPSII*CMINII-CGII
      AMT( 6, 6)=-EPSII*CMINII
      AMT(6,1)=CGII
      AMT(7,7)=W3*.5*(CP1+CP3)
      AMT(7,5)=-AMT(7,7)
      AMT(7,16)=-CA
      BMT(7)=AMT(7,16)*TA1
      AMT( 8, 7)=EPSA*CMIN
      AMT(8,16)=-CA
      BMT(8)=(EPSA*CMIN-CA)*TA1
      AMT(9,5)=W3*.5*(CP1+CP2)
      AMT(9,6)=-AMT(9,5)
      BMT(9)=-GP
      AMT(10,8)=-WI*.5*(CP4+CP3)
      AMT(10,9)=-WII*.5*(CP6+CP3)
```

```
      AMT(10,13)=-WM*.5*(CP16+CP3)
      AMT(10,6)=-WB*.5*(CP2+CP3)
      AMT(10,10)=-WV1*.5*(CP8+CP3)
      AMT(10,11)=-WV2*.5*(CP10+CP3)
      AMT(10,14)=-WE*.5*(CP18+CP3)
      AMT(10,15)=-WS*.5*(CP20+CP3)
      AMT(10,7)=-AMT(10,8)-AMT(10,9)-AMT(10,13)-AMT(10,6)-AMT(10,10)-
     * AMT(10,11)-AMT(10,14)-AMT(10,15)
      AMT(11,6)=WM*.5*(CP2+CP14)
      AMT(11,12)=-AMT(11,6)
      BMT(11)=-QCM
      AMT(12,12)=WM*.5*(CP14+CP16)
      AMT(12,13)=-AMT(12,12)
      BMT(12)=-QM
      AMT(13,6)=WV1*.5*(CP2+CP8)
      AMT(13,10)=-AMT(13,6)
      BMT(13)=-QV1
      AMT(14,6)=WV2*.5*(CP2+CP10)
      AMT(14,11)=-AMT(14,6)
      BMT(14)=-QV2
      AMT(15,6)=WE*.5*(CP2+CP18)
      AMT(15,14)=-AMT(15,6)
      BMT(15)=-QE
      AMT(16,6)=WS*.5*(CP2+CP20)
      AMT(16,15)=-AMT(16,6)
      BMT(16)=-QS
      AMT(17,4)=CGIII
      AMT(17,6) =WIII*.5*(CP7+CP2)
      AMT(17,17)=CGIII
      AMT(17,17)=-CGIII
      AMT(17,18)=-WIII*.5*(CP7+CP2)
      AMT(18,4) =EPS3  *(CMIN3)-CGIII
      AMT(18,18)=-EPS3  *(CMIN3)
      CALL SIMQ(AMT, BMT, 18, KS)
      JJ=0
    6 Z2=FM1
      TIG=BMT(1)/(1.+(GAMIG-1.)*FM1*FM1/2.)
      CALL GASP(TIG, FN, GAMIG, CPIG, Z1, Z1, GMU)
      IF (JCPRO .GE. 0)
     1  PIG=RO1*TIG/(.093178*GMU)
      IF (JCPRO .LT. 0)
     1  RO1=.093178*PIG*GMU/TIG
      WG=RO1*VI*A(1)
      WRITE (6,10051) TIG, GAMIG, GMU
10051 FORMAT(1HO,5X,'TIG = ',E15.7,3X,'GAMIG = ',E15.7,3X,'GMU = ',E15.7
     1,3X,'RIGHT AFTER WG=',//)
      FM1=WG*DSQRT(TIG/(GAMIG*GMU))/(20.7774*PIG*A(1))
      JJ=JJ+1
      Z3=Z2-FM1
      IF (DABS(Z3) .LT. DELM)  GO TO 7
      IF (JJ .LT.NLIM)  GO TO 6
      WRITE(6,400) Z3
  400 FORMAT(54H**** FAILURE TO CONVERGE IN FINAL MACH LOOP - ERROR = ,
     1  E12.5,6H******)
```

```
  7 WRITE(KO,301) JJ, ZZ
301 FORMAT(10X,'TOTAL PASSES IN FINAL MACH LOOP =',I3,' - ERROR =',
   1  E12.5)
    II=II+1
    IF (KS .EG. 1)  GO TO 91
    DO 93 KS=1,16
    NN(KS)=-1
    TDIF(KS)=SVR(KS)-BMT(KS)
    IF  (DABS(TDIF(KS)) .GT. CONV(KS))  NN(KS)=1
 93 CONTINUE
    WRITE(KO,201)
201 FORMAT(10X,'STATE VARIABLE ERRORS')
    WRITE(KO,300) TDIF
300 FORMAT(10X,10E12.4)
    WRITE(KO,153) II
153 FORMAT(10X,'END OF SIMG PASS NO.',I3/)
    CALL OUTPUT
    IF (II .GT. NLIM)  GO TO 92
    DO 94 KS=1,16
    IF (NN(KS) .GE. 0)  GO TO 95
 94 CONTINUE
    GO TO 90
 92 WRITE(KO,104)
104 FORMAT(46H**** FAILURE TO CONVERGE IN STATE VARIABLE LOOP*,
   1 6H******)
 90 FM6=WG*DSQRT(T06G/(GAM6G*GMU))/(20.7774*P06G*A(6))
    CALL MACH(DELM, NLIM, P06G, GAM6G, FM6, T06G, WG, GMU,
   1  A(6), P6G, T6G,FN,CP6G)
    FNBPS=DFLOAT(NBPS)
    FNBS=DFLOAT(NBS)
    DPSS=((P07G-P06G)*T06G*26.966)/(P06G*BRPM*BRPM*518.7*GMU*FNBPS)
    DPSB=.8396-3.2323*(DABS(Q6G/(BRPM*FNBS)-.46875))**1.42327
    DPSB=DPSB*1.E-9
    ERR=DPSB-DPSS
    GC=11.661E-7/(BRPM*FNBS)+11.589E-5*VIM**.667/(BRPM*BRPM*FNBPS)
    GC=ERR/GC
    JV=JV+1
    WRITE(KO,204)  JV, GC
204 FORMAT(5X,'PASS NO.',I3,' THROUGH VELOCITY LOOP,  CORRECTION =',
   1  E12.5)
    WRITE(6,175)Q6G,BRPM,FNBS
175 FORMAT(1H0,3X,'Q6G=',E15.7,5X,'BRPM=',E15.7,5X,'FNBS=',E15.7)
    GC=0.0
    IF (DABS(GC) .LE. VLIM)  GO TO 502
    IF (JV .GE. NLIM) GO TO 503
    IF (GC .LT. 0.  .AND. Q6G/(BRPM*FNBS) .LT. .46875)  GO TO 504
506 CONTINUE
    VIM=VIM+GC
    VI=VIM*3.281
    GO TO 501
504 WRITE(KO,205)
205 FORMAT(50H**** BLOWERS ARE CHOKED - PROCESS NEXT CASE ******)
```

```
      GO TO 2
  503 WRITE(KO,203) GC
  203 FORMAT(52H**** FAILURE TO CONVERGE IN VELOCITY LOOP - ERROR = ,
     1  E12.5,6H******)
  502 CONTINUE
      T03G=T02G
      T04G=T02G
      T05G=T02G
      T09G=T08G
      T010G=T08G
      T011G=T01G
      BLPR=WG*.5*(CP6G+CP7G)*T06G*(BPR**((1.-2./(GAM6G+GAM7G))
     1  /ATAB)-1.)*778./550.
      BLPRM=BLPR*.7457
      DPI=4.317E-4*GI*GI*FI*DL(1)*DNP(1)/(ROLI*DDH(1))
      DPII=4.317E-4*GII*GII*FII*DL(2)*DNP(2)/(ROLII*DDH(2))
      DPIII=DPII
      DP=4.317E-4*G*G*F*DL(4)*DNP(3)/(ROL*DDH(4))
      ROA1=144.*PAT*AML/(1545.32*TA1)
      ROA2=ROA1
      LL=0
   37 Z1=ROA2
      PA2=PAT-GA*GA*((1.+DSIG(4)**2)*(ROA1/ROA2-1.)+
     1  AF*DALG(4)*DW(4)*ROA1/(.5*DSIG(4)*(ROA1+ROA2)))/
     2  (ROA1*2.*32.174*144.)
      ROA2=144.*PA2*AML/(1545.32*TA2)
      LL=LL+1
      Z3=ROA2-Z1
      IF  (DABS(Z3) .LT. ROLIM) GO TO 38
      IF  (LL .LE. NLIM)  GO TO 37
      WRITE(KO,401) Z3
  401 FORMAT(49H**** FAILURE TO CONVERGE IN AUX. DENSITY LOOP - *,
     1  'ERROR =',E12.5,6H******)
      GO TO 39
   38 WRITE(KO,202) LL, Z3
  202 FORMAT(10X,'TOTAL PASSES THROUGH AUX. DENSITY LOOP =',I3,
     1  ' - ERROR =',E12.5)
   39 PF=WA*CPA2*TA2*778./550.
      WRITE(6,10004)GAM2A,ATAB
10004 FORMAT(1HO,3X,'GAM2A=',E15.7,5X,'ATAB=',E15.7)
      PFM=.7457*PF
      R06G=.093178*P6G*GMU/T6G
      WCORR=60.*WG*DSQRT(1.4*GMU*518.7/(GAM6G*28.97*T06G))/R06G
      DO 99 KS=1,16
   99 SVR(KS)=BMT(KS)
      QDI=WI*1800.*(CP2+CP4)*(T4-T2)
      QDII=WII*1800.*(CP2+CP6)*(T6-T2)
      QDIII=QDII
      WRITE (6,10005)CP2,CP6,T6,T2,WII
10005 FORMAT(1HO,3X,'CP2=',E15.7,5X,'CP6='E15.7,5X,'T6='E15.7,5X,
     1'T2=',E15.7,5X,'WII=',E12.6)
```

```
      WRITE(6,10011)CP4,T4,WI
10011 FORMAT(1H0,3X,'CP4=',E15.7,5X,'T4=',E15.7,5X,'WI=',E12.6)
      GDA=W3*1800.*(CP3+CP1)*(T3-T1)
      WRITE(KO,20005)GDII,GDA
20005 FORMAT (1H0,3X,'GDII=',E12.6,5X,'GDA=',E12.6)
      CALL OUTPUT
      GO TO 2
   95 DO 96 KS=1,18
   96 SVR(KS)=BMT(KS)
      GO TO 10
   91 WRITE(KO,102)
  102 FORMAT(' SINGULAR MATRIX')
      GO TO 2
      END
```

```
      SUBROUTINE ENPUT
      IMPLICIT REAL*8 (A-H,O-Z)
      DIMENSION SVR(19)
      DIMENSION ESVR(18)
      COMMON /VAR/ T01G, T02G, T06G, T07G, T1, T2, T3, T4, T6, T8,
     A  T10, T14, T16, T18, T20, TA2, T08G, T7,
     B  T03G, T04G, T05G, T09G, T010G, T011G, T5, T9, T11,
     C  T12, T13, T15, T17, T19, TIG, T2G, T3G, T4G, T5G, T6G, T7G,
     D  T8G, T9G, T10G, T11G, TA1, EFFL, P01G, P02G, P03G, P04G, P05G,
     E  P06G, P07G, P08G, P09G, P010G, P011G, P1G, P2G, P3G, P4G, P5G,
     F  P6G, P7G, P8G, P9G, P10G, P11G, P(20), AC(20), VC(20), FM1,
     G  FM2, FM3, FM4, FM5, FM6, FM7, FM8, FM9, FM10, FM11, A(11),
     H  GAM1G, GAM2G, GAM3G, GAM4G, GAM5G, GAM6G, GAM7G, GAM8G, GAM9G,
     I  GAM10G, GAM11G, TGMI, TGMII, TMG3, TMA, GIMU, GIIMU, G3MU, AMU,
     1  PRGI,
     J  PRGII, PRG3, PRA, CPGI, CPGII, CPG3, CPA, TMI, TMII, TMIII, TM,
     1  ZIMU, ZIIMU, Z3MU, ZMU,
     K  PRI, PRII, PRIII, PR, CPI, CPII, CPIII, CP, GGI, GGII, GGIII,
     1GA, GI, GII, GIII, G, REGI,
     L  REGII, REG3, REA, REI, REII, REIII, RE, GFI, GFII, GFIII,
      COMMON/VARB/                                AF, FI, FII, F, GJI,
     M  GJII, GJIII, AJ, ZJI, ZJII, ZJIII, ZJ, HGI, HGII, HGIII, HA,
     1  HI, HII, HIII, H, CGI, CGII, CGIII,
     N  CA, CI, CII, CIII, C, UI, UII, UIII, U, AGI, AGII, AGIII, AA,
     1  TUNI, TUNII, TUNIII, TUN,
     O  TOWI, TOWII, TOW3, TOW, EPSI, EPSII, EPS3, EPSA, ESSI, ESSII,
     1  ESS3, ESS, WG,
     P  G6G, QCORR, BPR, ALT, PAT, PA2, RH, FN(4),      EFFLP, VI, VIM,
     Q  PIGA, H1M, CL1M, WT1M, DCM, BLPR, BLPRM, CPP, CPPM, PF, PFM,
     R  RO1, PLKW, WI, WII, WIII, WB, WM, WV1, WV2, WE, WS, WA, QP, GCM,
     S  GV, QV1, QV2, QE, QS, CF23, CF34, CF45, CF78, CF89, CF910,
      COMMON /VARC/CF111,      ATAP, H1, CL1, WT1, ACN(20), DC, DL(4),
     A  DH(4), DW(4), DDHG(4), DALG(4), DAFOA(4), DSIG(4), DDEL(4),
```

```
     B  DA(4), DK(3), DSL(4), DSI(4), DALF(4), DDH(4), CONV(16), DELM,
     C  ROLIM, PLIM, FG, TITLE(28), DP,  DPI, DPII, DPIII, PPR, PPRM,
     D  TA1F, RHP, TIGM, DKH(4), ETIG,  ET02G, ET06G, ET07G, ET1,
     E  ET2, ET3, ET4, ET6, ET8, ET10, ET14, ET16, ET18, ET20, ETA2,
     1  ET08G, ET7,
     F  EBPR, CWA, DNP(3), GDI, GDII, GDIII,
     1                                  GDA, EVIM, BRPM, VLIM, RQA1,
     G  RQA2,DAFAL(4),DSLL(4),AB(4)
      COMMON /IVAR/ NTAM, NDSGN, NCS, KI, KO, NLIM, NP(4), NFULL,
     1  NBS, NBPS, JCPRO
C
      EQUIVALENCE (ESVR(1), ETIG)
      EQUIVALENCE (SVR(1),T01G)
      NAMELIST/FPT/ NTAM, TA1F, PLKW, ETIG, ET02G, ET06G, ET07G, ET1,
     A  ET2, ET3, ET4, ET6, ETA2, ET14, ET16, ET8, ET10, ET18, ET20,
     B            EFFLP, WI, WII, WIII, WB, WM, WV1, WV2, WE, WS, CWA,
     C                   GP, GCM, GM, GV1, GV2, GE, GS, CF23, CF34,
     D  CF45, CF78, CF89, CF910, CF111,
     E               EVIM, ATAP, PIGA, M1M, CL1M, WT1M, FN, ACN, DCM,
     F                 DL, DH, DW, DDHG, DALG, DAFOA, DSIG, DDEL,
     G  DA, DKH, DSL, DSI, DALF, DDH, NP,
     H                  PAT, RHP, EBPR, A, CONV, DELM, NDSGN, NCS,
     I      NLIM, ROLIM, PLIM, FG, BRPM, VLIM, NBS, NBPS, JCPRO, RO1,
     J  DAFAL,DSLL, AB
C
      KI=5
      KO=6
      READ(KI,200) (TITLE(J),J=1,14)
      READ(KI,200) (TITLE(J),J=15,28)
  200 FORMAT(13A6,A2)
      READ(KI,FPT)
      TA1=TA1F+459.69
      TIG=TA1
      T02G=TA1+210.
      T06G=TA1+30.
      T07G=TA1+70.
      T1=TA1+20.
      T2=TA1+20.
      T3=TA1+40.
      T4=TA1+55.
      T6=TA1+30.
      T8=TA1+65.
      T10=TA1+65.
      T14=TA1+30.
      T16=TA1+75.
      T18=TA1+65.
      T20=TA1+65.
      TA2=TA1+30.
      T7=TA1+20.
      BPR=1.17
      VIM=120.
      DO 30 K=1,16
   30 IF (ESVR(K) .GT. 0.)  SVR(K)=ESVR(K)
```

```
      WRITE(6,10026)SVR(1),SVR(2),SVR(3),SVR(4),SVR(15),SVR(16),SVR(17),
     1SVR(18),SVR(19)
10026 FORMAT(1HO,3X,'SVR(1)=',E15.7,5X,'SVR(2)=',E15.7,5X,'SVR(3)=',E15.
     17,5X,'SVR(4)=',E15.7,//4X,'SVR(15)=',E15.7,5X,'SVR(16)=',E15.7,//
     25X,'SVR(17)=',E15.7,5X,'SVR(18)=',E15.7,5X,'SVR(19)=',E15.7)
      IF (EBPR .GT. 0.)  BPR=EBPR
      IF (EVIM .GT. 0.)  VIM=EVIM
      IF (NTAM .LT. 0)  CALL EXIT
      IF (NTAM .LE. 0)  GO TO 10
      DO 20 J=1,19
   20 SVR(J)=TA1
   10 CONTINUE
      PIG=PIGA*14.7
      RH=RHP*.01
      EFFL=EFFLP*.01
      VI=VIM*3.281
      DC=DCM*.03281
      H1=H1M*.03281
      WT1=WT1M*.03281
      CL1=CL1M*.03281
      CALL AIRP(TA1, PAT, TA1, RH, X, X, X, X, AML)
      ROA1=PAT*AML*.09317/TA1
      WA=ROA1*CWA*DSQRT(TA1/518.7)/60.
      DK(1) = DKH(1)/3600.
      DK(2) = DKH(2)/3600.
      DK(3) = DKH(4)/3600.
      DNP(1)=NP(1)
      DNP(2)=NP(2)
      DNP(3)=NP(4)
      A(1)=H1*CL1
      G6G=VI*A(1)*60.
      WRITE(KO,102)
  102 FORMAT('1')
      WRITE(KO,FPT)
  101 FORMAT(21X,14A6)
      WRITE(KO,101) TITLE
      RETURN
      END
```

```
      SUBROUTINE GASP(T, FN, GAM, CP, PR, UM, GMU )
      IMPLICIT REAL*8 (A-H,O-Z)
      DIMENSION FN(4), WM(4), TB(4), C(4), U(4), FK(4),
     1  G(4), X(4), CN(4), S(4)
C      1 = HE
C      2 = N2
C      3 = CO2
C      4 = CO
      DATA TB /4.215D0,77.4D0,194.66D0,81.5D0/
```

```
      DATA WM /4.00D0,28.016D0, 44.010D0, 28.010D0/ , R /1.98646D0/
C
      C(1) = 1.240E
C
      IF (T .LE. 650.)
     1  FK(1)=(.8+(T-475.)*(.97-.8)/175.)*.1
      IF (T .GT. 650.)
     1  FK(1)=(.97+(T-650.)*(1.13-.97)/200.)*.1
      FK(1)=FK(1)/3600.
C
      G(1)=1.6667
C
      U(1)=1.12+(T-400.)*(1.955-1.12)/500.
      U(1)=U(1)*1.E-5
C
C
      IF (T .LE. 600)
     1  C(2)=3.502+(T-400.)*(3.5065-3.502)/200.
      IF (T .GT. 600.  .AND.  T .LE. 800.)
     1  C(2)=3.5065+(T-600.)*(3.5315-3.5065)/200.
      IF (T .GT. 800.)
     1  C(2)=3.5315+(T-800.)*(3.559-3.5315)/100.
      C(2)=C(2)*R/WM(2)
C
      IF (T .LE. 650.)
     1  FK(2)=.925+(T-450.)*(1.265-.925)/200.
      IF (T .GT. 650.)
     1  FK(2)=1.265+(T-650.)*(1.573-1.265)/200.
      FK(2)=FK(2)*1.4E-2/3600.
C
      G(2)=1.4
      IF (T .GT. 600.)
     1  G(2)=1.4+(T-600.)*(1.391-1.4)/300.
C
      IF (T .LE. 550.)
     1  U(2)=.933+(T-450.)*(1.087-.933)/100.
      IF (T .GT. 550.  .AND.  T .LE. 725.)
     1  U(2)=1.087+(T-550.)*(1.33-1.087)/175.
      IF (T .GT. 725)
     1  U(2)=1.33+(T-725.)*(1.545-1.33)/175.
      U(2)=U(2)*1.1172E-5
C
C
      IF (T .LE. 600.)
     1  C(3)=4.195+(T-450.)*(4.653-4.195)/150.
      IF (T .GT. 600.  .AND.  T .LE. 750.)
     1  C(3)=4.653+(T-600.)*(5.045-4.653)/150.
      IF (T .GT. 750.)
     1  C(3)=5.045+(T-750.)*(5.365-5.045)/150.
      C(3)=C(3)*R/WM(3)
C
```

```
      IF (T .LE. 600.)
     1  FK(3)=.82+(T-425.)*(1.32-.82)/175.
      IF(T.LE.140.)FK(3)=5.714E-3
      IF (T .GT. 600.)
     1  FK(3)=1.32+(T-600.)*(2.12-1.32)/250.
      FK(3)=FK(3)*8.4075E-3/3600.
C
      IF (T .LE. 450.)
     1  G(3)=1.334+(T-400.)*(1.315-1.334)/50.
      IF (T .GT. 450.  .AND.  T .LE. 550.)
     1  G(3)=1.315+(T-450.)*(1.286-1.315)/100.
      IF (T .GT. 550.  .AND.  T .LE. 650.)
     1  G(3)=1.286+(T-550.)*(1.2645-1.286)/100.
      IF (T .GT. 650.  .AND.  T .LE. 750.)
     1  G(3)=1.2645+(T-650.)*(1.248-1.2645)/100.
      IF (T .GT. 750.  .AND.  T .LE. 850.)
     1  G(3)=1.248+(T-750.)*(1.235-1.248)/100.
      IF (T .GT. 850.)
     1  G(3)=1.235+(T-850.)*(1.2295-1.235)/50.
C
      IF (T .LE. 575.)
     1  U(3)=.9175+(T-450.)*(1.152-.9175)/125.
      IF (T .GT. 575.  .AND.  T .LE. 700.)
     1  U(3)=1.152+(T-575.)*(1.375-1.152)/125.
      IF (T .GT. 700.)
     1  U(3)=1.375+(T-700.)*(1.541-1.375)/100.
      U(3)=U(3)*9.2067E-6
C
      FT=FN(1)+FN(2)+FN(3)
      NGAS=3
      IF (FN(4) .LE. 0.)  GO TO 10
      FT=FT+FN(4)
      NGAS=4
C
      IF (T .LE. 540.)
     1  C(4)=3.503+(T-400.)*(3.506-3.503)/140.
      IF (T .GT. 540.  .AND.  T .LE. 630.)
     1  C(4)=3.506+(T-540.)*(3.513-3.506)/90.
      IF (T .GT. 630.  .AND.  T .LE. 720.)
     1  C(4)=3.513+(T-630.)*(3.529-3.513)/90.
      IF (T .GT. 720.  .AND.  T .LE. 810.)
     1  C(4)=3.529+(T-720.)*(3.552-3.529)/90.
      IF (T .GT. 810.)
     1  C(4)=3.552+(T-810.)*(3.583-3.552)/90.
      C(4)=C(4)*.0708989
C
      IF (T .LE. 540.)
     1  U(4)=.84+(T-400.)*(1.075-.84)/140.
      IF (T .GT. 540.  .AND.  T .LE. 720.)
     1  U(4)=1.075+(T-540.)*(1.34-1.075)/180.
      IF (T .GT. 720.)
     1  U(4)=1.34+(T-720.)*(1.575-1.34)/180.
      U(4)=U(4)*1.1132E-5
C
```

```
      IF (T .LE. 530.)
     1  G(4)=1.4
      IF (T .GT. 530.)
     1  G(4)=1.4+(T-530.)*(1.3885-1.4)/370.
C
      IF (T .LE. 540.)
     1  FK(4)=.825+(T-400.)*(1.087-.825)/140.
      IF (T .GT. 540.  .AND.  T .LE. 720.)
     1  FK(4)=1.087+(T-540.)*(1.385-1.087)/180.
      IF (T .GT. 720.)
     1  FK(4)=1.385+(T-720.)*(1.665-1.385)/180.
      FK(4)=FK(4)*.01342/3600.
C
C
   10 CP=0.
      DAM=0.
      GAM=0.
      UM=0.
      GMU=0.
      Z3=0.
      DO 11 I=1,NGAS
      S(I)=1.5*TB(I)*1.8
      X(I)=FN(I)/FT
   11 GMU=GMU+X(I)*WM(I)
      DO 50 I=1,NGAS
      CN(I)=X(I)*WM(I)/GMU
      CP=CP+CN(I)*C(I)
      GAM=CN(I)*C(I)+GAM
      DAM=CN(I)*C(I)/G(I)+DAM
      Z1=0.
      Z2=0.
      DO 30 J=1,NGAS
      IF (J .NE. I)  GO TO 12
      P=1.
      AM=1.
      GO TO 29
   12 D=X(J)/X(I)
      E=DSQRT(S(I)*S(J))
      UR=U(I)/U(J)
      WR1=DSQRT(8.*(1.+WM(I)/WM(J)))
      WR=(WM(J)/WM(I))**.25
      P=D*(1.+DSQRT(UR)*WR)**2/WR1
      AM=.25*D*(1.+DSQRT(UR*WR**3*(T+S(I))/(T+S(J))))**2*(T+E)/(T+S(I))
   29 Z1=Z1+P
      Z2=Z2+AM
   30 CONTINUE
      Z3=Z3+FK(I)/Z2
      UM=UM+U(I)/Z1
   50 CONTINUE
      GAM=GAM/DAM
      PR=CP*UM/Z3
      RETURN
      END
```

```
      SUBROUTINE MACH(DELM, NLIM, POG, GAM, FM, TOG, WG, GMU, A, PG,
     1 TG,FN,CP)
      IMPLICIT REAL*8 (A-H,O-Z)
      DIMENSION FN(4)
      DATA KO /6/
      I=0
   10 FMG=FM
      TG=1.+FMG*FMG*(GAM-1.)/2.
      WRITE(6,11)POG,TG,GAM
   11 FORMAT(1H0,3X,'POG=',E15.7,5X,'TG=',E15.7,5X,'GAM=',E15.7)
      PG=POG/TG**(GAM/(GAM-1.))
      TG=TOG/TG
      FM=WG*DSQRT(TG/(GAM*GMU))/(20.7774*PG*A)
      WRITE(6,12)PG,TG,FM
   12 FORMAT(1H0,3X,'PG=',E15.7,5X,'TG=',E15.7,5X,'FM=',E15.7)
      CALL GASP(TG,FN,GAM,CP,DUM,DUM,GMU)
      I=I+1
      FMG1=FMG-FM
      IF (DABS(FMG1) .LT. DELM)  RETURN
      IF (I .LT. NLIM) GO TO 10
      WRITE(KO,100) FMG1
  100 FORMAT('        FAILURE TO CONVERGE IN MACH NO. SUBROUTINE',
     1  ' - ERROR =',E12.5)
      RETURN
      END
```

```
      SUBROUTINE AIRP(TAMB, PAMB, T, RH, P, AMU, CPA, GAM, AML)
      IMPLICIT REAL*8 (A-H,O-Z)
      T2=DEXP(-38.09873+.1057402*TAMB-.674864E-4*TAMB*TAMB)
      WF=RH*18.016*T2/(28.966*(PAMB-T2))
      T2=T*T
      P=.5552+.134633E-2*T-.031E-4*T2+.20666E-8*T*T2
      AMU=1.E-5+.175E-7*(T-400.)
      CPA=.2421-.0015E-2*T+2.E-8*T2
      GAMA=CPA/(CPA-.0685545)
      CPW=.4509-.0054E-2*T+.0008E-4*T2
      GAMW=CPW/(CPW-.11022)
      A=WF*CPW
      B=(1.-WF)*CPA
      CPA=WF*CPW+(1.-WF)*CPA
      GAM=(A+B)/(A/GAMW+B/GAMA)
      AML=18.016*WF+28.966*(1.-WF)
      RETURN
      END
```

```
      SUBROUTINE LIQP(T, FG, UM, PR, CP)
      IMPLICIT REAL*8 (A-H,O-Z)
      C=T/1.8-273.
      F=FG*FG
      CP=1.-.465*FG+C*(.00115-.00105*(1.-FG)**3.0596)
      SF=1301./(998.33+8.1855*(C-20.)+.00585*(C-20.)**2)
      UM=DEXP(-3.01174+.49287*FG+(2.30654+1.18556*FG+.806*F)*SF)
      FK=137.-82.91667*FG+17.91667*F
      FK=1.*(FK+C*(106.-160.8833*FG+49.0833*F-FK)/100.)
      UM=0.014881
      PR = 1.0E3*UM*CP/FK
      UM=UM*.000672
      RETURN
      END




      SUBROUTINE SIMQ(A, B, N, KS)
      IMPLICIT REAL*8 (A-H,O-Z)
C
C     SIMQ SOLVES A SYSTEM OF LINEAR EQUATIONS  AX=B
C
C     INPUTS
C     A - MATRIX OF COEFFICIENTS STORED COLUMNWISE. DESTROYED IN
C         COMPUTATION.
C     B - VECTOR OF ORIGINAL CONSTANTS. DESTROYED IN COMPUTATION
C         SOLUTION IS RETURNED IN B
C     N - NUMBER OF EQUATIONS AND VARIABLES
C     KS - OUTPUT FLAG  0=NORMAL   1=SINGULAR SET OF EQUATIONS
C
      DIMENSION A(1), B(1)
C
C     FORWARD SOLUTION
C
      TOL=0.0
      KS=0
      JJ=-N
      DO 65 J=1,N
      JY=J+1
      JJ=JJ+N+1
      BIGA=0.0
      IT=JJ-J
      DO 30 I=J,N
C
C     SEARCH FOR MAXIMUM COEFFICIENT IN COLUMN
C
```

```
      IJ=IT+I
      IF (DABS(BIGA)-DABS(A(IJ))) 20,30,30
   20 BIGA=A(IJ)
      IMAX=I
   30 CONTINUE
C
C     TEST FOR PIVOT LESS THAN TOLERANCE (SINGULAR MATRIX)
C
      IF (DABS(BIGA)-TOL) 35, 35, 40
   35 KS=1
      RETURN
C
C     INTERCHANGE ROWS IF NECESSARY
C
   40 I1=J+N*(J-2)
      IT=IMAX-J
      DO 50 K=J,N
      I1=I1+N
      I2=I1+IT
      SAVE=A(I1)
      A(I1)=A(I2)
      A(I2)=SAVE
C
C     DIVIDE EQUATION BY LEADING COEFFICIENT
C
   50 A(I1)=A(I1)/BIGA
      SAVE=B(IMAX)
      B(IMAX)=B(J)
      B(J)=SAVE/BIGA
C
C     ELIMINATE NEXT VARIABLE
C
      IF (J-N) 55, 70, 55
   55 IQS=N*(J-1)
      DO 65 IX=JY,N
      IXJ=IQS+IX
      IT=J-IX
      DO 60 JX=JY,N
      IXJX=N*(JX-1)+IX
      JJX=IXJX+IT
   60 A(IXJX)=A(IXJX)-(A(IXJ)*A(JJX))
   65 B(IX)=B(IX)-(B(J)*A(IXJ))
C
C     BACK SOLUTION
C
   70 NY=N-1
      IT=N*N
      DO 80 J=1,NY
      IA=IT-J
      IB=N-J
```

```
      IC=N
      DO 80 K=1,J
      B(IB)=B(IB)-A(IA)*B(IC)
      IA=IA-N
   80 IC=IC-1
      RETURN
      END



      SUBROUTINE OUTPUT
      IMPLICIT REAL*8 (A-H,O-Z)
      DIMENSION QC(11), QCG(11), DPC(11), DPCR(11)
      DIMENSION VG(11), QG(11), PP(11), PD(11), ROG(11)
      COMMON /VAR/ T01G, T02G, T06G, T07G, T1, T2, T3, T4, T6, T8,
     A  T10, T14, T16, T18, T20, TA2, T08G, T7,
     B  T03G, T04G, T05G, T09G, T010G, T011G, T5, T9, T11,
     C  T12, T13, T15, T17, T19, T1G, T2G, T3G, T4G, T5G, T6G, T7G,
     D  T8G, T9G, T10G, T11G, TA1, EFFL, P01G, P02G, P03G, P04G, P05G,
     E  P06G, P07G, P08G, P09G, P010G, P011G, P1G, P2G, P3G, P4G, P5G,
     F  P6G, P7G, P8G, P9G, P10G, P11G, P(20), AC(20), VC(20), FM1,
     G  FM2, FM3, FM4, FM5, FM6, FM7, FM8, FM9, FM10, FM11, A(11),
     H  GAM1G, GAM2G, GAM3G, GAM4G, GAM5G, GAM6G, GAM7G, GAM8G, GAM9G,
     I  GAM10G, GAM11G, TGM1, TGM11, TGM3, TMA, G1MU, G11MU, G3MU, AMU,
     1  PRG1,
     J  PRG11, PRG3, PRA, CPG1, CPG11, CPG3, CPA, TM1, TM11, TM111, TM,
     1  Z1MU, Z11MU, Z3MU, ZMU,
     K  PR1, PR11, PR111, PR, CP1, CP11, CP111, CP, GG1, GG11, GG111,
     1GA, G1, G11, G111, G, REG1,
     L  REG11, REG3, REA, RE1, RE11, RE111, RE, GF1, GF11, GF111,
      COMMON/VARB/                                    AF, F1, F11, F, GJ1,
     M  GJ11, GJ111, AJ, ZJ1, ZJ11, ZJ111, ZJ, HG1, HG11, HG111, HA,
     1  H1, H11, H111, H, CG1, CG11, CG111,
     N  CA, C1, C11, C111, C, U1, U11, U111, U, AG1, AG11, AG111, AA,
     1  TUN1, TUN11, TUN111, TUN,
     O  TOW1, TOW11, TOW3, TOW, EPS1, EPS11, EPS3, EPSA, ESS1, ESS11,
     1  ESS3, ESS, WG,
     P  Q6G, QCORR, BPR, ALT, PAT, PA2, RH, FN(4),      EFFLP, V1, V1M,
     Q  P1GA, H1M, CL1M, WT1M, DCM, BLPR, BLPRM, CPP, CPPM, PF, PFM,
     R  R01, PLKW, W1, W11, W111, WB, WM, WV1, WV2, WE, WS, WA, QP, QCM,
     S  QM, QV1, QV2, QE, QS, CF23, CF34, CF45, CF78, CF89, CF910,
      COMMON /VARC/CF111,      ATAP, H1, CL1, WT1, ACN(20), DC, DL(4),
     A  DH(4), DW(4), DDHG(4), DALG(4), DAFOA(4), DSIG(4), DDEL(4),
     B  DA(4), DK(3), DSL(4), DSI(4), DALF(4), DDH(4), CONV(16), DELM,
     C  ROLIM, PLIM, FG, TITLE(28), DP,  DP1, DP11, DP111, PPR, PPRM,
     D  TA1F, RHP, TIGM, DKH(4), ETIG,  ET02G, ET06G, ET07G, ET1,
     E  ET2, ET3, ET4, ET6, ET8, ET10, ET14, ET16, ET18, ET20, ETA2,
     1  ET08G,ET7,
     F  EBPR, CWA, DNP(3), QD1, QD11, QD111,
     1                                  QDA, FVIM, BRPM, VLIM, ROA1,
     G  ROA2,DAFAL(4),DSLL(4),AB(4)
      COMMON/VARD/QC,QCG,CP2,CP6,W3,CP3,CP1,F111,TUN3
      COMMON /IVAR/ NTAM, NDSGN, NCS, K1, KO, NLIM, NP(4), NFULL,
     1  NBS, NBPS, JCPRO
```

```
      WRITE(KO,10023)WII,CP2,CP6,T6,T2,W3,CP3,CP1,T3,T1
10023 FORMAT (1HO,3X,'WII=',E12.6,5X,'CP2=',E15.7,5X,'CP6='E15.7,5X,
     1'T6=',E15.7,//4X,'T2=',E15.7,5X,'W3='E12.6,5X,'CP3=',E15.7,5X,
     2'CP1=',E15.7,//4X,'T3=',E15.7,5X,'T1=',E15.7)
      WRITE(KO,10029)GDII,GDA
10029 FORMAT (1HO,3X,'GDII=',E12.6,5X,'GDA=',E12.6)
      WRITE(KO,100)
      WRITE(KO,101) TITLE
      WRITE(KO,400)
  400 FORMAT('0     INPUT LIST'/' CAVITY * LASER SPECIFICATIONS'/
     1  '          DESCRIPTION',24X,' NAME    VALUE        UNITS')
      WRITE(KO,403) PIGA
  403 FORMAT('      INLET PRESSURE  ',12('. '),'PIGA  ',G12.6,'  ATM')
      WRITE(KO,404) H1M
  404 FORMAT('      INLET HEIGHT  ',13('. '),'H1M   ',G12.6,'  CM')
      WRITE(KO,405) WT1M
  405 FORMAT('      WIDTH IN FLOW DIRECTION ',8('. '),'WT1M  ',G12.6,
     1  '  CM')
      WRITE(KO,406) CL1M
  406 FORMAT('      LENGTH  ',16('. '),'CL1M  ',G12.6,'  CM')
      WRITE(KO,408) DCM
  408 FORMAT('      INLET HYDRAULIC DIAMETER  ',7('. '),'DCM   ',G12.6,
     1  '  CM')
      WRITE(KO,407) PLKW
  407 FORMAT('      LASER OUTPUT POWER  . . ',8('. '),'PLKW  ',G12.6,
     1  '  KW')
      WRITE(KO,401) EFFLP
  401 FORMAT('      LASER EFFICIENCY  ',11('. '),'EFFLP ',G12.6,
     1  '  PERCENT')
      WRITE(KO,409) NDSGN
  409 FORMAT('      DESIGN OPTION ',13('. '),'NDSGN ',I7,5X,'  -')
      IF (NDSGN .NE. 3) GO TO 50
      WRITE(KO,410) NCS
  410 FORMAT('      NUMBER OF AREAS (NDSGN=3) ',7('. '),'NCS   ',
     1  I7,5X,'  -')
      WRITE(KO,411) (ACN(K),K=1,NCS)
  411 FORMAT('      AREAS ',17('. '),'ACN   ',6(G12.6,1X),
     1  3(51X,6(G12.6,1X)))
      WRITE(KO,412)
  412 FORMAT(65X,'FT**2')
   50 WRITE(KO,413) FN
  413 FORMAT('      GAS MIXTURE ',14('. '),'FN    ',4F6.2,
     1  '  HE  TO  N2  TO  CO2  TO  CO')
      WRITE(KO,414)
  414 FORMAT('0INITIAL ESTIMATE OF STEADY STATE QUANTITIES',
     1  36X,'IF = 0.,USES')
      WRITE(KO,415) ETIG
  415 FORMAT('      GAS STATIC TEMPERATURE - STATION 1',3('. '),'ETIG  ',
     1  G12.6,'  DEG R',10X,'TA1 + 20.')
      WRITE(KO,416) ET02G
  416 FORMAT('      GAS TOTAL TEMPERATURE - STATION 2 ',3('. '),'ET02G ',
     1  G12.6,'  DEG R',10X,'TA1 + 210.')
      WRITE(KO,417) ET06G
```

```
  417 FORMAT('      GAS TOTAL TEMPERATURE - STATION 6 ',3('. '),'ET06G ',
     1  G12.6,'  DEG R',10X,'TA1 + 30.')
      WRITE(KO,418) ET07G
  418 FORMAT('      GAS TOTAL TEMPERATURE - STATION 7 ',3('. '),'ET07G ',
     1  G12.6,'  DEG R',10X,'TA1 + 70.')
      WRITE(KO,419) ET1
      WRITE(KO,420) ET2
      WRITE(KO,421) ET3
      WRITE(KO,422) ET4
      WRITE(KO,423) ET6
      WRITE(KO,424) ET8
      WRITE(KO,425) ET10
      WRITE(KO,426) ET14
      WRITE(KO,427) ET16
      WRITE(KO,428) ET18
      WRITE(KO,429) ET20
      WRITE(KO,1429) ET7
  419 FORMAT('      COOLANT TEMPERATURE - STATION  1  ',3('. '),'ET1   ',
     1  G12.6,'  DEG R',10X,'TA1 + 20.')
  420 FORMAT('      COOLANT TEMPERATURE - STATION  2  ',3('. '),'ET2   ',
     1  G12.6,'  DEG R',10X,'TA1 + 20.')
  421 FORMAT('      COOLANT TEMPERATURE - STATION  3  ',3('. '),'ET3   ',
     1  G12.6,'  DEG R',10X,'TA1 + 40.')
  422 FORMAT('      COOLANT TEMPERATURE - STATION  4  ',3('. '),'ET4   ',
     1  G12.6,'  DEG R',10X,'TA1 + 55.')
  423 FORMAT('      COOLANT TEMPERATURE - STATION  6  ',3('. '),'ET6   ',
     1  G12.6,'  DEG R',10X,'TA1 + 30.')
 1429 FORMAT('      COOLANT TEMPERATURE - STATION  7  ',3('. '),'ET7   ',
     1  G12.6,'  DEG R',10X,'TA1 + 20.')
  424 FORMAT('      COOLANT TEMPERATURE - STATION  8  ',3('. '),'ET8   ',
     1  G12.6,'  DEG R',10X,'TA1 + 65.')
  425 FORMAT('      COOLANT TEMPERATURE - STATION 10  ',3('. '),'ET10  ',
     1  G12.6,'  DEG R',10X,'TA1 + 65.')
  426 FORMAT('      COOLANT TEMPERATURE - STATION 14  ',3('. '),'ET14  ',
     1  G12.6,'  DEG R',10X,'TA1 + 30.')
  427 FORMAT('      COOLANT TEMPERATURE - STATION 16  ',3('. '),'ET16  ',
     1  G12.6,'  DEG R',10X,'TA1 + 75.')
  428 FORMAT('      COOLANT TEMPERATURE - STATION 18  ',3('. '),'ET18  ',
     1  G12.6,'  DEG R',10X,'TA1 + 65.')
  429 FORMAT('      COOLANT TEMPERATURE - STATION 20  ',3('. '),'ET20  ',
     1  G12.6,'  DEG R',10X,'TA1 + 65.')
      WRITE(KO,430) ETA2
  430 FORMAT('      AIR TEMPERATURE AFTER RADIATOR  ',4('. '),'ETA2  ',
     1  G12.6,'  DEG R',10X,'TA1 + 30.')
      WRITE(KO,431) EBPR
  431 FORMAT('      BLOWER PRESSURE RATIO ',9('. '),'EBPR  ',G12.6,
     1         '  -',14X,'1.17')
      WRITE(KO,402) EVIM
  402 FORMAT('      INLET VELOCITY  ',12('. '),'EVIM  ',G12.6,'  M/SEC',
     1  10X,'120.')
      WRITE(KO,432)
  432 FORMAT('0COOLING SYSTEM FLOWS')
      WRITE(KO,433) WI
  433 FORMAT('      HEAT EXCHANGER 1 (LIQUID) ',7('. '),'WI    ',
     1  G12.6,'  LB/SEC')
```

```
      WRITE(KO,434) WII
  434 FORMAT('      HEAT EXCHANGER 2 (LIQUID) ',7('. '),'WII    ',
     1  G12.6,'  LB/SEC')
      WRITE(KO,1000) WIII
 1000 FORMAT('      HEAT EXCHANGER 3 (LIQUID) ',7('. '),'WIII   ',
     1  G12.6,'  LB/SEC')
      WRITE(KO,435) WB
  435 FORMAT('      MIRROR BYPASS ',13('. '),'WB     ',
     1  G12.6,'  LB/SEC')
      WRITE(KO,436) WM
  436 FORMAT('      MIRROR  ',16('. '),'WM     ',
     1  G12.6,'  LB/SEC')
      WRITE(KO,437) WV1
  437 FORMAT('      VACUUM PUMP 1 ',13('. '),'WV1    ',
     1  G12.6,'  LB/SEC')
      WRITE(KO,438) WV2
  438 FORMAT('      VACUUM PUMP 2 ',13('. '),'WV2    ',
     1  G12.6,'  LB/SEC')
      WRITE(KO,439) WE
  439 FORMAT('      E-BEAM  ',16('. '),'WE     ',
     1  G12.6,'  LB/SEC')
      WRITE(KO,440) WS
  440 FORMAT('      SUSTAINER ',15('. '),'WS     ',
     1  G12.6,'  LB/SEC')
      WRITE(KO,441) CWA
  441 FORMAT('      CORRECTED FAN FLOW (AIR)  ',7('. '),'CWA    ',
     1  G12.6,'  CFM')
      WRITE(KO,445)
  445 FORMAT('0SPECIFICATIONS OF BLOWERS')
      WRITE(KO,442) ATAB
  442 FORMAT('      BLOWER POLYTROPIC EFFICIENCY  ',5('. '),'ATAB   ',
     1  G12.6,'  -')
      WRITE(KO,446) BRPM
  446 FORMAT('      BLOWER SPEED  ',13('. '),'BRPM   ',G12.6,'  RPM')
      WRITE(KO,447) NBS
  447 FORMAT('      NUMBER OF BLOWER SETS ',9('. '),'NBS    ',I6,6X,
     1  '  -')
      WRITE(KO,448) NBPS
  448 FORMAT('      NUMBER OF BLOWERS PER SET ',7('. '),'NBPS   ',
     1  I6,6X,'  -')
      WRITE(KO,543) VLIM
  543 FORMAT('      INLET VELOCITY TOLERANCE  ',7('. '),'VLIM   ',
     1  G12.6,'  M/SEC')
      WRITE(KO,444)
  444 FORMAT('0TUNNEL AREAS')
      WRITE(KO,443) A
  443 FORMAT('      STATION 1 TO STATION 11 ',8('. '),'A      ',
     1  6(1X,G12.3    )/50X,5(1X,G12.3    ),'FT**2')
      WRITE(KO,100)
      WRITE(KO,101) TITLE
      WRITE(KO,500)
  500 FORMAT('0     INPUT LIST (CONT.)')
      WRITE(KO,501)
  501 FORMAT('0HEAT EXCHANGER SPECIFICATIONS',22X,'EXCH 1',4X
     1  'EXCH 2',4X,     'EXCH 3',6X,     'RAD',     3X,'UNITS')
      WRITE(KO,502)
```

```
502 FORMAT(9X,'DESCRIPTION',25X,'NAME',5X,'(1)', 6X,'(2)', 6X,'(3)',
   1 7X,'(4)')
     WRITE(KO,503) DL
503 FORMAT('      CORE LENGTH (GAS) ',11('. '),'DL    ',
   1   4(2X,G12.3,2X),'FT')
     WRITE(KO,504) DH
504 FORMAT('      CORE HEIGHT ',14('. '),'DH    ',
   1   4(2X,G12.3,2X),'FT')
     WRITE(KO,505) DW
505 FORMAT('      CORE WIDTH (LIQUID) ',10('. '),'Dw    ',
   1   4(2X,G12.3,2X),'FT')
     WRITE(KO,506) DDHG
506 FORMAT('      HYDRAULIC DIAMETER (GAS)  ',7('. '),'DDHG ',
   1   4(2X,G12.3,2X),'FT')
     WRITE(KO,507) DALG
507 FORMAT('      SURFACE AREA / VOLUME (GAS) ',6('. '),'DALG ',
   1   4(2X,G12.3,2X),'1/FT')
     WRITE(KO,508) DAFOA
508 FORMAT('      FIN AREA / SURFACE AREA (GAS) ',5('. '),'DAFOA',
   1   4(2X,G12.3,2X),'-')
     WRITE(KO,509) DSIG
509 FORMAT('      FREE FLOW AREA / FACE AREA (GAS)  ',3('. '),'DSIG ',
   1   4(2X,G12.3,2X),'-')
     WRITE(KO,510) DDEL
510 FORMAT('      FIN THICKNESS (GAS) ',10('. '),'DDEL ',
   1   4(2X,G12.3,2X),'FT')
     WRITE(KO,511) DSL
511 FORMAT('      FIN LENGTH (GAS)  ',11('. '),'DSL   ',
   1   4(2X,G12.3,2X),'FT')
     WRITE(KO,516) DDH
516 FORMAT('      HYDRAULIC DIAMETER (LIQUID) ',6('. '),'DDH   ',
   1   4(2X,G12.3,2X),'FT')
     WRITE(KO,514) DALF
514 FORMAT('      SURFACE AREA / VOLUME (LIQUID)  ',4('. '),'DALF ',
   1   4(2X,G12.3,2X),'1/FT')
     WRITE(KO,550) DAFAL
550 FORMAT('      FIN AREA / SURFACE AREA (LIQUID)  ',3('. '),'DAFAL',
   1   4(2X,G12.3,2X),'-')
     WRITE(KO,515) DSI
515 FORMAT('      FREE FLOW AREA / FACE AREA (LIQUID) ',2('. '),
   1   'DSI  ',4(2X,G12.3,2X),'-')
     WRITE(KO,512) DA
512 FORMAT('      FIN THICKNESS (LIQUID)  ',8('. '),'DA    ',
   1   4(2X,G12.3,2X),'FT')
     WRITE(KO,551) DSLL
551 FORMAT('      FIN LENGTH (LIQUID)'',10('. '),'DSLL ',
   1   4(2X,G12.3,2X),'FT')
     WRITE(KO,552) AB
552 FORMAT('      PARTING PLATE THICKNESS ',8('. '),'AB    ',
   1   4(2X,G12.3,2X),'FT')
     WRITE(KO,541) NP
541 FORMAT('      NUMBER OF LIQUID PASSES ',8('. '),'NP    ',
   1   4(5X,I4,7X),'-')
     WRITE(KO,513) DKH
```

```
513 FORMAT('      FIN THERMAL CONDUCTIVITY  ',7('. '),'DKH  ',
   1  4(2X,G12.6,2X),'BTU/HR-FT-DEG R')
     WRITE(KO,517)
517 FORMAT('0HEAT INPUT RATES',39X,'VALUE      UNITS')
     WRITE(KO,518) QP
516 FORMAT('      PUMP  ',17('. '),'QP   ',
   1  2X,G12.6,2X,'BTU/SEC')
     WRITE(KO,519) QCM
519 FORMAT('      MIRROR CONTROL  ',12('. '),'QCM  ',
   1  2X,G12.6,2X,'BTU/SEC')
     WRITE(KO,520) QM
520 FORMAT('      MIRROR  ',16('. '),'QM   ',
   1  2X,G12.6,2X,'BTU/SEC')
     WRITE(KO,521) QV1
521 FORMAT('      VACUUM PUMP 1 ',13('. '),'QV1  ',
   1  2X,G12.6,2X,'BTU/SEC')
     WRITE(KO,522) QV2
522 FORMAT('      VACUUM PUMP 2 ',13('. '),'QV2  ',
   1  2X,G12.6,2X,'BTU/SEC')
     WRITE(KO,523) QE
523 FORMAT('      E-BEAM  ',16('. '),'QE   ',
   1  2X,G12.6,2X,'BTU/SEC')
     WRITE(KO,524) QS
524 FORMAT('      SUSTAINER ',15('. '),'QS   ',
   1  2X,G12.6,2X,'BTU/SEC')
     WRITE(KO,525)
525 FORMAT('0DIFFUSER LOSS COEFFICIENTS')
     WRITE(KO,526) CF23
     WRITE(KO,527) CF34
526 FORMAT('      STATION 2  TO  STATION 3  ',7('. '),'CF23 ',
   1  2X,G12.6,2X,'-')
     WRITE(KO,544) CF111
     WRITE(KO,531) CF910
     WRITE(KO,530) CF89
     WRITE(KO,529) CF78
     WRITE(KO,528) CF45
527 FORMAT('      STATION 3  TO  STATION 4  ',7('. '),'CF34 ',
   1  2X,G12.6,2X,'-')
528 FORMAT('      STATION 4  TO  STATION 5  ',7('. '),'CF45 ',
   1  2X,G12.6,2X,'-')
529 FORMAT('      STATION 7  TO  STATION 8  ',7('. '),'CF78 ',
   1  2X,G12.6,2X,'-')
530 FORMAT('      STATION 8  TO  STATION 9  ',7('. '),'CF89 ',
   1  2X,G12.6,2X,'-')
531 FORMAT('      STATION 9  TO  STATION 10 ',7('. '),'CF910',
   1  2X,G12.6,2X,'-')
544 FORMAT('      STATION 11 TO  STATION 1  ',7('. '),'CF111',
   1  2X,G12.6,2X,'-')
     WRITE(KO,532)
532 FORMAT('0AMBIENT CONDITIONS, DECISION VARIABLES, AND CONVERGENCE',
   1  ' TOLERANCES')
```

```
      WRITE(KO,533)  TA1F
  533 FORMAT('      AMBIENT TEMPERATURE ',10('. '),'TA1F ',2X,G12.6,2X,
     1  'DEG F')
      WRITE(KO,534) PAT
  534 FORMAT('      AMBIENT PRESSURE  ',11('. '),'PAT  ',2X,G12.6,2X,
     1  'PSIA')
      WRITE(KO,535) RHP
  535 FORMAT('      RELATIVE HUMIDITY ',11('. '),'RHP  ',2X,G12.6,2X,
     1  'PERCENT')
      WRITE(KO,542) FG
  542 FORMAT('      FRACTION OF GLYCOL IN COOLING LIQUID  . FG     ',
     1  G12.6, '  -')
      WRITE(KO,536) NLIM
  536 FORMAT('      MAXIMUM NUMBER OF LOOP CYCLES ',5('. '),'NLIM ',
     1  5X,I3,8X,'-')
      WRITE(KO,537) PLIM
  537 FORMAT('      PRESSURE TOLERANCE  ',10('. '),'PLIM ',2X,G12.6,2X,
     1  'PSIA')
      WRITE(KO,538) DELM
  538 FORMAT('      MACH NUMBER TOLERANCE ',9('. '),'DELM ',2X,G12.6,2X,
     1  '-')
      WRITE(KO,539) ROLIM
  539 FORMAT('      DENSITY TOLERANCE ',11('. '),'ROLIM',2X,G12.6,2X,
     1  'LE/FT**3')
      WRITE(KO,540) CONV
  540 FORMAT('      STATE VARIABLE TOLERANCES ',7('. '),'CONV ',
     1  5(2X,G12.3,1X),2(/50X,5(2X,G12.3,1X))/50X,2X,G12.3,2X,
     2  'DEG R')
      WRITE(KO,100)
  100 FORMAT('1')
      WRITE(KO,101) TITLE
  101 FORMAT(21X,14A6)
      CALL GASP(T1G, FN, GAM1G, Z, Z, Z, GMU)
      CALL GASP(T2G, FN, GAM2G, Z, Z, Z, GMU)
      CALL GASP(T3G, FN, GAM3G, Z, Z, Z, GMU)
      CALL GASP(T4G, FN, GAM4G, Z, Z, Z, GMU)
      CALL GASP(T5G, FN, GAM5G, Z, Z, Z, GMU)
      CALL GASP(T6G, FN, GAM6G, Z, Z, Z, GMU)
      CALL GASP(T7G, FN, GAM7G, Z, Z, Z, GMU)
      CALL GASP(T8G, FN ,GAM8G, Z, Z, Z, GMU)
      CALL GASP(T9G, FN ,GAM9G, Z, Z, Z, GMU)
      CALL GASP(T10G, FN, GAM10G, Z, Z, Z, GMU)
      CALL GASP(T11G, FN, GAM11G, Z, Z, Z, GMU)
      CON=32.174*1545.43/GMU
      VG(1)=FM1*DSQRT(GAM1G*CON*T1G)
      VG(2)=FM2*DSQRT(GAM2G*CON*T2G)
      VG(3)=FM3*DSQRT(GAM3G*CON*T3G)
      VG(4)=FM4*DSQRT(GAM4G*CON*T4G)
      VG(5)=FM5*DSQRT(GAM5G*CON*T5G)
      VG(6)=FM6*DSQRT(GAM6G*CON*T6G)
      VG(7)=FM7*DSQRT(GAM7G*CON*T7G)
      VG(8)=FM8*DSQRT(GAM8G*CON*T8G)
      VG(9)=FM9*DSQRT(GAM9G*CON*T9G)
      VG(10)=FM10*DSQRT(GAM10G*CON*T10G)
      VG(11)=FM11*DSQRT(GAM11G*CON*T11G)
      DO 28 K=1,11
   28 GG(K)=VG(K)*A(K)*60.
```

```
      WRITE(KO,102) ALT
  102 FORMAT('0  ALTITUDE  ',20('. '),1X,G12.6,' (K FT)')
      WRITE(KO,103) PAT
  103 FORMAT('   AMBIENT PRESSURE  ',16('. '),1X,G12.6,' (PSIA)')
      WRITE(KO,104) TA1F
  104 FORMAT('   AMBIENT TEMPERATURE ',15('. '),1X,G12.6,' (DEG F)')
      WRITE(KO,105) RHP
  105 FORMAT('   RELATIVE HUMIDITY ',16('. '),1X,G12.6,' (PERCENT)')
      WRITE(KO,107) PIGA
  107 FORMAT('   LASER INLET PRESSURE  ',14('. '),1X,G12.6,' (ATM)')
      TIGM=TIG/1.8
      WRITE(KO,108) TIGM
  108 FORMAT('   LASER INLET TEMPERATURE ',13('. '),1X,G12.6,' (DEG K)')
      Z=(T02G-T01G)/1.8
      WRITE(KO,142) Z
  142 FORMAT('   TEMPERATURE RISE ACROSS CAVITY  ',9('. '),1X,G12.6,
     1   ' (DEG K)')
      WRITE(KO,109) VIM
  109 FORMAT('   LASER INLET VELOCITY  ',14('. '),1X,G12.6,' (M/SEC)')
      WRITE(KO,110) PLKW
  110 FORMAT( '   LASER OUTPUT POWER . . ',13('. '),1X,G12.6,' (KW)')
      WRITE(KO,141) EFFLP
  141 FORMAT( '   LASER EFFICIENCY  ',16('. '),1X,G12.6,' (PERCENT)')
      WRITE(KO,114) WG
  114 FORMAT('    LASER GAS MASS FLOW RATE  ',12('. '),1X,G12.6,
     1   ' (LB/SEC)')
      WRITE(KO,115) Q6G
  115 FORMAT( '   VOLUME FLOW RATE AT BLOWER INLET  ',8('. '),1X,G12.6,
     1   ' (CFM)')
      WRITE(KO,116) QCORR
  116 FORMAT( '   CORRECTED VOLUME FLOW RATE AT BLOWER INLET  ',3('. '),
     1   1X,G12.6,' (CFM)')
      WRITE(KO,139) WA
  139 FORMAT( '   COOLING AIR FLOW RATE ',14('. '),1X,G12.6,
     1   ' (LB/SEC)')
      WRITE(KO,140) CWA
  140 FORMAT( '   COOLING AIR FLOW RATE ',14('. '),1X,G12.6,
     1   '(CFM)')
      WRITE(KO,117) BPR
  117 FORMAT( '   BLOWER PRESSURE RATIO ',14('. '),1X,G12.6,' (-)')
      WRITE(KO,111) BLPRM, BLPR
  111 FORMAT( '   BLOWER POWER REQUIRED ',14('. '),1X,G12.6,' (KW)',
     1   8X,G12.6,1X,' (HP)')
      WRITE(KO,112) PPRM, PPR
  112 FORMAT( '   COOLING PUMP POWER REQUIRED ',11('. '),1X,G12.6,
     1   ' (KW)',8X,G12.6,1X,' (HP)')
      WRITE(KO,113) PFM, PF
  113 FORMAT('    COOLING FAN POWER REQUIRED  ',11('. '),1X,G12.6,
     1   ' (KW)',8X,G12.6,1X,' (HP)')
      WRITE(KO,106) FN
  106 FORMAT('   LASER GAS MIXTURE ',15('. '),1X,F5.2,3(' TO',F5.2),2X,
     1   '(HE TO N2 TO CO2 TO CO)')
      WRITE(KO,143) GMU
  143 FORMAT('   MOLECULAR WEIGHT OF GAS   ',12('. '),1X,G12.6,
     1   ' (-)')
      WRITE(KO,118)
```

```
     1  'EXCH 2',      4X,'EXCH 3',      4X,'RAD',      4X,'UNITS')
  118 FORMAT('0',8X,'HEAT EXCHANGER VARIABLES',14X,'EXCH 1',3X,
     1  'EXCH 2',3X,      EXCH 3',5X,      RAD',5X,      'UNITS')
      WRITE(KO,119) QDI, QDII, QDIII, QDA
  119 FORMAT('   HEAT TRANSFER RATE  ',11('. '),2X,4(G12.2,3X),
     1  ' BTU/HR')
      WRITE(KO,120) DPI, DPII, DPIII, DP
  120 FORMAT('   LIQUID PRESSURE DROP  ',10('. '),2X,4(G12.2,3X),
     1  ' PSIA')
      WRITE(KO,121) NP
  121 FORMAT('   NUMBER OF LIQUID PASSES ',9('. '),2X,4(3X,I2,2X),' -')
      NFULL=0
      IF (NFULL .NE. 0)  RETURN
      WRITE(KO,122) TMI, TMII, TMIII, TM
  122 FORMAT('   MEAN TEMPERATURE ',9('.') ,'(LIQUID)',4('. '),2X,
     1  4(G12.2,3X),' DEG R')
      WRITE(KO,123) TGMI, TGMII, TGM3, TMA
  123 FORMAT(32X,'(GAS)',10X,4(G12.2,3X))
      WRITE(KO,124) ZIMU, ZIIMU, Z3MU, ZMU
  124 FORMAT('   VISCOSITY ',10('.'),'(LIQUID)',4('. '),2X,4(G12.2,3X),
     1  ' LB/FT-SEC')
      WRITE(KO,123) GIMU, GIIMU, G3MU, AMU
      WRITE(KO,125) PRI, PRII,PRIII,PR
  125 FORMAT('   PRANDTL NUMBER ',11('.'),'(LIQUID)',4('. '),2X,
     1  4(G12.2,3X),' -')
      WRITE(KO,123) PRGI, PRGII, PRG3, PRA
      WRITE(KO,126) CPI, CPII, CPIII, CP
  126 FORMAT('   SPECIFIC HEAT ',12('.'),'(LIQUID)',4('. '),2X,
     1  4(G12.2,3X),' BTU/LB-DEG R')
      WRITE(KO,123) CPGI, CPGII, CPG3, CPA
      WRITE(KO,127) GI, GII, GIII, G
  127 FORMAT('   MASS FLUX ',16('.'),'(LIQUID)',4('. '),2X,
     1  4(G12.2,3X),' LB/FT**2-SEC')
      WRITE(KO,123) GGI, GGII, GGIII, GA
      WRITE(KO,128) REI, REII, REIII, RE
  128 FORMAT('   REYNOLDS NUMBER ',10('.'),'(LIQUID)',4('. '),2X,
     1  4(G12.2,3X),' -')
      WRITE(KO,123) REGI, REGII, REG3, REA
      WRITE(KO,129) FI, FII, FIII, F
  129 FORMAT('   FRICTION FACTOR ',10('.'),'(LIQUID)',4('. '),2X,
     1  4(G12.2,3X),' -')
      WRITE(KO,123) GFI, GFII, GFIII, AF
      WRITE(KO,130) ZJI, ZJII, ZJIII, ZJ
  130 FORMAT('   HEAT TRANSFER FACTOR ',5('.'),'(LIQUID)',4('. '),2X,
     1  4(G12.2,3X),' -')
      WRITE(KO,123) GJI, GJII, GJIII, AJ
      WRITE(KO,131) HI, HII, HIII, H
  131 FORMAT('   HEAT TRANSFER COEF. ',6('.'),'(LIQUID)',4('. '),2X,
     1  4(G12.2,3X),' BTU/FT**2-SEC-DEG R')
      WRITE(KO,123) HGI, HGII, HGIII, HA
      WRITE(KO,132) CI, CII, CIII, C
  132 FORMAT('   FLUID CAPACITY RATE ',6('.'),'(LIQUID)',4('. '),2X,
```

```
     1  4(G12.2,3X),' BTU/SEC-DEG R')
        WRITE(KO,123) CGI, CGII, CGIII, CA
        WRITE(KO,133) UI, UII, UIII, U
  133 FORMAT('   OVERALL HEAT TRANSFER COEF. ',7('. '),2X,4(G12.2,3X),
     1  ' BTU/FT**2-SEC-DEG R')
        WRITE(KO,134) AGI, AGII, AGIII, AA
  134 FORMAT('   GAS HEAT TRANSFER SURFACE AREA  ',5('. '),2X,
     1  4(G12.2,3X),' FT**2')
        WRITE(KO,135) TUNI, TUNII, TUN3, TUN
  135 FORMAT('   NUMBER OF TRANSFER UNITS  ',8('. '),2X,
     1  4(G12.2,3X),' -')
        WRITE(KO,136) TOWI, TOWII, TOW3, TOW
  136 FORMAT('   CAP GAMMA ',16('. '),2X,4(G12.2,3X),' -')
        WRITE(KO,137) ESSI, ESSII, ESS3, ESS
  137 FORMAT('   SINGLE PASS EFFECTIVENESS ',8('. '),2X,
     1  4(G12.2,3X),' -')
        WRITE(KO,138) EPSI, EPSII, EPS3, EPSA
  138 FORMAT('   TOTAL EFFECTIVENESS ',11('. '),2X,
     1  4(G12.2,3X),' -')
        WRITE(KO,100)
        WRITE(KO,101) TITLE
        WRITE(KO,200)
  200 FORMAT('0',16X,'GAS FLOW SYSTEM VARIABLES BY STATION')
        WRITE(KO,201)
  201 FORMAT('0     STATION NUMBER',15X,'1', 3X,'2', 8X,'3', 8X,'4',
     1    3X,'5', 8X,'6'/34X,'7', 8X,'8', 8X,'9', 7X,'10', 7X,'11')
        WRITE(KO,204) P01G, P02G, P03G, P04G, P05G, P06G, P07G, P08G,
     1  P09G, P010G, P011G
  204 FORMAT('0     TOTAL PRESSURE       (PSIA)',
     1  6(1X,G12.3,1X)/31X,5(1X,G12.3,1X))
        WRITE(KO,203) PIG, P2G, P3G, P4G, P5G, P6G, P7G, P8G, P9G, P10G,
     1  P11G
  203 FORMAT('0     STATIC PRESSURE      (PSIA)',
     1  6(1X,G12.3,1X)/31X,5(1X,G12.3,1X))
        WRITE(KO,206) T01G, T02G, T03G, T04G, T05G, T06G, T07G, T08G,
     1  T09G, T010G, T011G
  206 FORMAT('0     TOTAL TEMP.          (DEG R)',
     1  6(1X,G12.3,1X)/31X,5(1X,G12.3,1X))
        WRITE(KO,205) TIG, T2G, T3G, T4G, T5G, T6G, T7G, T8G, T9G, T10G,
     1  T11G
  205 FORMAT('0     STATIC TEMPERATURE (DEG R)',
     1  6(1X,G12.3,1X)/31X,5(1X,G12.3,1X))
        WRITE(KO,207) FM1, FM2, FM3, FM4, FM5, FM6, FM7, FM8, FM9, FM10,
     1  FM11
  207 FORMAT('0     MACH NUMBER                (-)',
     1  6(1X,G12.3,1X)/31X,5(1X,G12.3,1X))
        WRITE(KO,208) VG
  208 FORMAT('0     VELOCITY             (FT/SEC)',
     1  6(1X,G12.3,1X)/31X,5(1X,G12.3,1X))
        WRITE(KO,209) GG
  209 FORMAT('0     VOL. FLOW RATE         (CFM)',
     1  6(1X,G12.3,1X)/31X,5(1X,G12.3,1X))
        Z=GMU*.093178
        ROG( 1)=PIG*Z/TIG
        ROG( 2)=P2G*Z/T2G
        ROG( 3)=P3G*Z/T3G
        ROG( 4)=P4G*Z/T4G
```

```
      ROG(5) = P5G*Z/T5G
      ROG( 6)=P6G*Z/T6G
      ROG( 7)=P7G*Z/T7G
      ROG( 8)=P8G*Z/T8G
      ROG(9) = P9G*Z/T9G
      ROG(10)=P10G*Z/T10G
      ROG(11)=P11G*Z/T11G
      WRITE(KO,220) ROG
  220 FORMAT('0     DENSITY          (LB/FT**3)',
     1  6(1X,G12.3,1X)/31X,5(1X,G12.3,1X))
      WRITE(KO,212) A
  212 FORMAT('0     AREA                  (FT**2)',
     1  6(1X,G12.3,1X)/31X,5(1X,G12.3,1X))
      WRITE(KO,213) GAMIG, GAM2G, GAM3G, GAM4G, GAM5G, GAM6G, GAM7G,
     1  GAM8G, GAM9G, GAM10G, GAM11G
  213 FORMAT('0     GAMMA                      (-)',
     1  6(1X,G12.3,1X)/31X,5(1X,G12.3,1X))
      PD(1) = (P01G-P02G)*27.7
      PD(2)=(P02G-P03G)*27.7
      PD(3)=(P03G-P04G)*27.7
      PD(4)=(P04G-P05G)*27.7
      PD(5)=(P05G-P06G)*27.7
      PD(6)=(P06G-P07G)*27.7
      PD(7)=(P07G-P08G)*27.7
      PD(8)=(P08G-P09G)*27.7
      PD(9)=(P09G-P010G)*27.7
      PD(10)=(P010G-P011G)*27.7
      PD(11)=(P011G-P01G)*27.7
      DO 27 K=1,11
   27 PP(K)=PD(K)/(27.7*P06G)
      WRITE(KO,210) PD
  210 FORMAT('0     PRESSURE DROP      (IN H2O)',6X,
     1  6(1X,G12.3,1X)/37X,5(1X,G12.3,1X))
      WRITE(KO,211) PP
  211 FORMAT('0     PRESSURE DROP / P06     (-)',6X,
     1  6(1X,G12.3,1X)/37X,5(1X,G12.3,1X))
      WRITE(KO,214)
  214 FORMAT('0',12X,'COOLING AIR VARIABLES')
      WRITE(KO,215)
  215 FORMAT('0     STATION NUMBER',18X,'1A',12X,'2A')
      WRITE(KO,216) PAT, PA2
  216 FORMAT('0     PRESSURE',12X,'(PSIA)',2(1X,G12.6,1X))
      WRITE(KO,217) TA1, TA2
  217 FORMAT('0     TEMPERATURE',8X,'(DEG R)',2(1X,G12.6,1X))
      WRITE(KO,218) ROA1, ROA2
  218 FORMAT('0     DENSITY',9X,'(LB/FT**3)',2(1X,G12.6,1X))
      DPPA=(PAT-PA2)*27.7
      WRITE(KO,219) DPPA
  219 FORMAT('0     PRESSURE DROP      (IN H2O)',7X,G12.6)
      WRITE(KO,100)
      WRITE(KO,101) TITLE
      WRITE(KO,300)
```

```
300 FORMAT('0',16X,'COOLING SYSTEM VARIABLES BY STATION')
    WRITE(KO,301)
301 FORMAT('0    STATION NUMBER',19X,'1',13X,'2',13X,'3',13X,'4',13X,
   1  '5',13X,'6',13X,'7'/38X,'8',13X,'9',12X,'10',12X,'11',12X,
   2  '12',12X,'13',12X,'14',/37X,'15',12X,'16',12X,'17',12X,'18',
   3  12X,'19',12X,'20')
    WRITE(KO,302) P
302 FORMAT('0    PRESSURE                (PSIA)',
   1  7(1X,G12.6,1X)/31X,7(1X,G12.6,1X)/31X,6(1X,G12.6,1X))
    WRITE(KO,303) T1, T2, T3, T4, T5, T6, T7, T8, T9, T10, T11, T12,
   1  T13, T14, T15, T16, T17, T18, T19, T20
303 FORMAT('0    TEMPERATURE             (DEG R)',
   1  7(1X,G12.6,1X)/31X,7(1X,G12.6,1X)/31X,6(1X,G12.6,1X))
    WRITE(KO,304) VC
304 FORMAT('0    VELOCITY              (FT/SEC)',
   1  7(1X,G12.6,1X)/31X,7(1X,G12.6,1X)/31X,6(1X,G12.6,1X))
    WRITE(KO,305) QC
305 FORMAT('0    VOL. FLOW RATE (FT**3/SEC)',
   1  7(1X,G12.6,1X)/31X,7(1X,G12.6,1X)/31X,6(1X,G12.6,1X))
    WRITE(KO,306) QCG
306 FORMAT('0    VOL. FLOW RATE   (GAL/MIN)',
   1  7(1X,G12.6,1X)/31X,7(1X,G12.6,1X)/31X,6(1X,G12.6,1X))
    WRITE(KO,307) DPC
    WRITE(KO,309) AC
309 FORMAT('0    AREA                    (FT**2)',
   1  7(1X,G12.6,1X)/31X,7(1X,G12.6,1X)/31X,6(1X,G12.6,1X))
307 FORMAT('0    PRESSURE DROP           (PSIA)',
   1  7(1X,G12.6,1X)/31X,7(1X,G12.6,1X)/31X,6(1X,G12.6,1X))
    WRITE(KO,308) DPCR
308 FORMAT('0    PRESSURE DROP / P1        (-)',
   1  7(1X,G12.6,1X)/31X,7(1X,G12.6,1X)/31X,6(1X,G12.6,1X))
    RETURN
    END
```

```
$FPT
NTAM    =                +0
TA1F    =   -.500000000000000000D+002
PLKw    =    .500000000000000000D+002
ETIG    =    .000000000000000000D+000
ET2G    =    .000000000000000000D+000
ET06G   =    .000000000000000000D+000
ET07G   =    .000000000000000000D+000
ET1     =    .000000000000000000D+000
ET2     =    .000000000000000000D+000
ET3     =    .000000000000000000D+000
ET4     =    .000000000000000000D+000
ET6     =    .000000000000000000D+000
ETA2    =    .000000000000000000D+000
ET14    =    .000000000000000000D+000
ET16    =    .000000000000000000D+000
ET8     =    .000000000000000000D+000
ET10    =    .000000000000000000D+000
ET18    =    .000000000000000000D+000
ET20    =    .000000000000000000D+000
EFFLP   =    .100000000000000000D+002
wI      =    .917399999999999999D+000
wII     =    .917399999999999999D+000
wIII    =    .917399999999999999D+000
wB      =    .500000000000000000D+000
wM      =    .908000000000000000D+000
wV1     =    .909999999999999999D-001
wV2     =    .813000000000000000D+000
WE      =    .908000000000000000D+000
wS      =    .454999999999999999D+001
CwA     =    .500000000000000000D+006
GP      =    .350000000000000000D+001
GCM     =    .950000000000000000D+000
GM      =    .472999999999999999D+001
GV1     =    .473000000000000000D+000
GV2     =    .425999999999999999D+001
GE      =    .472999999999999999D+001
GS      =    .000000000000000000D+000
CF23    =    .799999999999999999D-001
CF34    =    .150000000000000000D+000
CF45    =    .300000000000000000D-001
CF78    =    .150000000000000000D+000
CF89    =    .150000000000000000D+000
CF910   =    .300000000000000000D-001
CF111   =    .150000000000000000D+000
EVIM    =    .250000000000000000D+002
ATAP    =    .700000000000000000D+000
PIGA    =    .500000000000000000D+000
H1M     =    .500000000000000000D+001
CL1M    =    .400000000000000000D+002
WT1M    =    .500000000000000000D+001
```

AD-A068 547 ALABAMA UNIV IN HUNTSVILLE SCHOOL OF SCIENCE AND ENG--ETC F/G 20/5
INVESTIGATION OF TRANSIENT FLOW AND HEATING PROBLEMS CHARACTERI--ETC(U)
MAR 79 C C SHIH, G R KARR, J F PERKINS DAAK40-77-C-0161
UNCLASSIFIED UAH-RR-219 DRCPM-HEL-CR-79-8 NL

4 OF 4
AD
A068547

END
DATE
FILMED
6-79
DDC

```
FN      =   .3000000000000000000D+001, .2000000000000000000D+001,
            .5000000000000000000D+000, .3000000000000000000D+000
ACN     =   .0000000000000000000D+000, .0000000000000000000D+000,
            .0000000000000000000D+000, .0000000000000000000D+000,
            .0000000000000000000D+000, .0000000000000000000D+000,
            .0000000000000000000D+000, .0000000000000000000D+000,
            .0000000000000000000D+000, .0000000000000000000D+000,
            .0000000000000000000D+000, .0000000000000000000D+000,
            .0000000000000000000D+000, .0000000000000000000D+000,
            .0000000000000000000D+000, .0000000000000000000D+000,
            .0000000000000000000D+000, .0000000000000000000D+000,
            .0000000000000000000D+000, .0000000000000000000D+000,
            .0000000000000000000D+000, .0000000000000000000D+000
DCM     =   .3625999999999999999D+001
DL      =   .2000000000000000000D+001, .2000000000000000000D+001,
            .2000000000000000000D+001, .2231250000000000000D+001
DH      =   .6666666999999999999D+000, .6666666999999999999D+000,
            .6666666999999999999D+000, .1979291700000000000D+002
DW      =   .2000000000000000000D+001, .2000000000000000000D+001,
            .2000000000000000000D+001, .6041666999999999999D+000
DDHG    =   .2550000000000000000D-002, .2020000000000000000D-002,
            .2000000000000000000D-002, .7819999999999999998D-002
DALG    =   .2446060000000000000D+003, .2446060000000000000D+003,
            .2446060000000000000D+003, .5367599999999999999D+003
DAFCA   =   .8630000000000000000D+000, .8630000000000000000D+000,
            .8630000000000000000D+000, .8100000000000000000D+000
DSIG    =   .7698973899999999999D+000, .7698973899999999999D+000,
            .7698973899999999999D+000, .6583657999999999999D+000
DDEL    =   .4999999999999999999D-003, .4999999999999999999D-003,
            .4999999999999999999D-003, .4999999999999999999D-003
DA      =   .4999999999999999999D-003, .4999999999999999999D-003,
            .4999999999999999999D-003, .4999999999999999999D-003
DKH     =   .1000000000000000000D+003, .1000000000000000000D+003,
            .1000000000000000000D+003, .1000000000000000000D+003
DSL     =   .2265000000000000000D-001, .2265000000000000000D-001,
            .2265000000000000000D-001, .1045830000000000000D-001
DSI     =   .7271999999999999999D-001, .7271799999999999999D-001,
            .7271799999999999999D-001, .1332800000000000000D+000
DALF    =   .7271799999999999999D+002, .7271799999999999999D+002,
            .7271799999999999999D+002, .1332800000000000000D+003
DDH     =   .9999999999999999997D-003, .9999999999999999997D-003,
            .9999999999999999997D-003, .3999999999999999999D-002
NP      =        +1,                    +1,        +1,                  +4
PAT     =   .1469000000000000000D+002
RHP     =   .1000000000000000000D+003
EBPR    =   .0000000000000000000D+000
A       =   .2152992170000660520D+000, .0000000000000000000D+000,
            .5453999999999999999D+000, .5453999999999999999D+000,
            .5453999999999999999D+000, .3491000000000000000D+000,
            .5453999999999999999D+000, .5453999999999999999D+000,
            .5453999999999999999D+000, .5453999999999999999D+000,
            .4305564160000000000D+000
```

```
NLIM    =                +30
ROLIM   =          .999999999999999997D-003
PLIM    =          .999999999999999997D-003
PG      =          .000000000000000000D+000
SRPM    =          .112000000000000000D+005
VLIM    =          .500000000000000000D+000
NBS     =               +7
NBPS    =               +2
JCPRO   =               -1
R01     =          .415000000000000000D-002
DAFAL   =          .507999999999999999D+000, .507999999999999999D+000,
                   .507999999999999999D+000, .507999999999999999D+000
DSLL    =          .211667000000000000D-002, .211667000000000000D-002,
                   .211667000000000000D-002, .211667000000000000D-002
AB      =          .206330000000000000D-002, .206330000000000000D-002,
                   .206330000000000000D-002, .206330000000000000D-002
CONV    =          .500000000000000000D+000, .500000000000000000D+000,
                   .500000000000000000D+000, .500000000000000000D+000,
                   .500000000000000000D+000, .500000000000000000D+000,
                   .500000000000000000D+000, .500000000000000000D+000,
                   .500000000000000000D+000, .500000000000000000D+000,
                   .500000000000000000D+000, .500000000000000000D+000,
                   .500000000000000000D+000, .500000000000000000D+000
DELM    =          .999999999999999997D-003
NDSGN   =               +2
NCS     =               +1
```

INPUT LIST

CAVITY * LASER SPECIFICATIONS

DESCRIPTION	NAME	VALUE	UNITS
INLET PRESSURE	PIGA	.500000+000	ATM
INLET HEIGHT	H1M	.500000+001	CM
WIDTH IN FLOW DIRECTION	WT1M	.500000+001	CM
LENGTH	CL1M	.400000+002	CM
INLET HYDRAULIC DIAMETER	DCM	.862000+001	CM
LASER OUTPUT POWER	PLKW	.500000+002	KW
LASER EFFICIENCY	EFFLP	.100000+002	PERCENT
DESIGN OPTION	NDSGN	2	-
GAS MIXTURE	FN 3.00 2.00 .50 .50	HE TO N2 TO CO2 TO CO	

INITIAL ESTIMATE OF STEADY STATE QUANTITIES

				IF = 0.,USES
GAS STATIC TEMPERATURE - STATION 1	ETIG	.000000	DEG R	TA1 + 20.
GAS TOTAL TEMPERATURE - STATION 2	ET02G	.000000	DEG R	TA1 + 210.
GAS TOTAL TEMPERATURE - STATION 6	ET06G	.000000	DEG R	TA1 + 30.
GAS TOTAL TEMPERATURE - STATION 7	ET07G	.000000	DEG R	TA1 + 70.
COOLANT TEMPERATURE - STATION 1	ET1	.000000	DEG R	TA1 + 20.
COOLANT TEMPERATURE - STATION 2	ET2	.000000	DEG R	TA1 + 20.
COOLANT TEMPERATURE - STATION 3	ET3	.000000	DEG R	TA1 + 40.
COOLANT TEMPERATURE - STATION 4	ET4	.000000	DEG R	TA1 + 55.
COOLANT TEMPERATURE - STATION 6	ET6	.000000	DEG R	TA1 + 30.
COOLANT TEMPERATURE - STATION 8	ET8	.000000	DEG R	TA1 + 65.
COOLANT TEMPERATURE - STATION 10	ET10	.000000	DEG R	TA1 + 65.
COOLANT TEMPERATURE - STATION 14	ET14	.000000	DEG R	TA1 + 30.
COOLANT TEMPERATURE - STATION 16	ET16	.000000	DEG R	TA1 + 75.
COOLANT TEMPERATURE - STATION 18	ET18	.000000	DEG R	TA1 + 65.
COOLANT TEMPERATURE - STATION 20	ET20	.000000	DEG R	TA1 + 65.
COOLANT TEMPERATURE - STATION 7	ET7	.000000	DEG R	TA1 + 20.
AIR TEMPERATURE AFTER RADIATOR	ETA2	.000000	DEG R	TA1 + 30.
BLOWER PRESSURE RATIO	PEPR	.000000	-	1.17
INLET VELOCITY	LV1M	.250000+002	M/SEC	120.

COOLING SYSTEM FLOWS

HEAT EXCHANGER 1 (LIQUID)	WI	.917400+000	LB/SEC
HEAT EXCHANGER 2 (LIQUID)	WII	.917400+000	LB/SEC
HEAT EXCHANGER 3 (LIQUID)	WIII	.917400+000	LB/SEC
MIRROR BYPASS	WB	.500000+000	LB/SEC
MIRROR	WM	.908000+000	LB/SEC
VACUUM PUMP 1	WV1	.910000-001	LB/SEC
VACUUM PUMP 2	WV2	.818000+000	LB/SEC
E-BEAM	WE	.908000+000	LB/SEC
SUSTAINER	WS	.455000+001	LB/SEC
CORRECTED FAN FLOW (AIR)	CWA	.500000+006	CFM

SPECIFICATIONS OF BLOWERS

BLOWER POLYTROPIC EFFICIENCY	ATAB	.700000+000	-
BLOWER SPEED	BRPM	.112000+005	RPM
NUMBER OF BLOWER SETS	NBS	7	-
NUMBER OF BLOWERS PER SET	NBPS	2	-
INLET VELOCITY TOLERANCE	VLIM	.500000+000	M/SEC

TUNNEL AREAS

STATION 1 TO STATION 11 . . . . . A .215+000 .215+000 .545+000 .545+000 .545+000 .349+000
.545+000 .545+000 .545+000 .545+000 .431+000FT**2

INPUT LIST (CONT.)

HEAT EXCHANGER SPECIFICATIONS DESCRIPTION	NAME	EXCH 1 (1)	EXCH 2 (2)	EXCH 3 (3)	RAD (4)	UNITS
CORE LENGTH (GAS)	DL	.200+001	.200+001	.200+001	.228+001	FT
CORE HEIGHT	DH	.667+000	.667+000	.667+000	.198+002	FT
CORE WIDTH (LIQUID)	DW	.200+001	.200+001	.200+001	.200+001	FT
HYDRAULIC DIAMETER (GAS)	DDHG	.255-002	.202-002	.200-002	.782-002	FT
SURFACE AREA / VOLUME (GAS)	DALG	.245+003	.245+003	.245+003	.245+003	1/FT
FIN AREA / SURFACE AREA (GAS)	DAFOA	.863+000	.863+000	.863+000	.810+000	-
FREE FLOW AREA / FACE AREA (GAS)	DSIG	.770+000	.770+000	.770+000	.658+000	-
FIN THICKNESS (GAS)	DDEL	.500-003	.500-003	.500-003	.500-003	FT
FIN LENGTH (GAS)	DSL	.226-001	.226-001	.226-001	.105-001	FT
HYDRAULIC DIAMETER (LIQUID)	DDH	.100-002	.100-002	.100-002	.400-002	FT
SURFACE AREA / VOLUME (LIQUID)	DALF	.727+002	.727+002	.727+002	.133+003	1/FT
FIN AREA / SURFACE AREA (LIQUID)	DAFAL	.508+000	.508+000	.508+000	.508+000	-
FREE FLOW AREA / FACE AREA (LIQUID)	DSI	.727-001	.727-001	.727-001	.133+000	-
FIN THICKNESS (LIQUID)	DA	.500-003	.500-003	.500-003	.500-003	FT
FIN LENGTH (LIQUID)	DSLL	.212-002	.212-002	.212-002	.212-002	FT
PARTING PLATE THICKNESS	AB	.208-002	.208-002	.208-002	.208-002	FT
NUMBER OF LIQUID PASSES	NP	1	1	1	4	-
FIN THERMAL CONDUCTIVITY	DKH	.100000+003	.100000+003	.100000+003	.100000+003	BTU/HR-FT-DEG R

HEAT INPUT RATES		VALUE	UNITS
PUMP	QP	.350000+001	BTU/SEC
MIRROR CONTROL	QCM	.950000+000	BTU/SEC
MIRROR	QM	.473000+001	BTU/SEC
VACUUM PUMP 1	QV1	.473000+000	BTU/SEC
VACUUM PUMP 2	QV2	.426000+001	BTU/SEC
E-BEAM	QE	.473000+001	BTU/SEC
SUSTAINER	QS	.000000	BTU/SEC

DIFFUSER LOSS COEFFICIENTS			
STATION 2 TO STATION 3	CF23	.800000-001	-
STATION 3 TO STATION 4	CF34	.150000+000	-
STATION 11 TO STATION 1	CF111	.150000+000	-
STATION 9 TO STATION 10	CF910	.300000-001	-
STATION 8 TO STATION 9	CF89	.150000+000	-
STATION 7 TO STATION 8	CF78	.150000+000	-
STATION 4 TO STATION 5	CF45	.300000-001	-

AMBIENT CONDITIONS, DECISION VARIABLES, AND CONVERGENCE TOLERANCES

AMBIENT TEMPERATURE	TA1F	-.500000+002	DEG F
AMBIENT PRESSURE	PAT	.146900+002	PSIA
RELATIVE HUMIDITY	RHP	.100000+003	PERCENT
FRACTION OF GLYCOL IN COOLING LIQUID .	FG	.000000	-
MAXIMUM NUMBER OF LOOP CYCLES	NLIM	30	-
PRESSURE TOLERANCE	PLIM	.100000-002	PSIA
MACH NUMBER TOLERANCE	DELM	.100000-002	-
DENSITY TOLERANCE	ROLIM	.100000-002	LB/FT**3
STATE VARIABLE TOLERANCES	CONV	.500 .500 .500 .500 .500	
		.500 .500 .500 .500 .500	
		.500 .500 .500 .500 .500	
		.500 DEG R	

LASER TEST CASE

ALTITUDE	.000000	(K FT)	
AMBIENT PRESSURE	.146900+002	(PSIA)	
AMBIENT TEMPERATURE	-.500000+002	(DEG F)	
RELATIVE HUMIDITY	.100000+003	(PERCENT)	
LASER INLET PRESSURE	.500000+000	(ATM)	
LASER INLET TEMPERATURE	.227604+003	(DEG K)	
TEMPERATURE RISE ACROSS CAVITY	.120208+004	(DEG K)	
LASER INLET VELOCITY	.250000+002	(M/SEC)	
LASER OUTPUT POWER	.500000+002	(KW)	
LASER EFFICIENCY	.100000+002	(PERCENT)	
LASER GAS MASS FLOW RATE	.511910+000	(LB/SEC)	
VOLUME FLOW RATE AT BLOWER INLET	.114994+004	(CFM)	
CORRECTED VOLUME FLOW RATE AT BLOWER INLET . . .	.907787+003	(CFM)	
COOLING AIR FLOW RATE	.716645+003	(LB/SEC)	
COOLING AIR FLOW RATE	.500000+006	(CFM)	
BLOWER PRESSURE RATIO	.100362+001	(-)	
BLOWER POWER REQUIRED	.158944+000	(KW)	.213147+000 (HP)
COOLING PUMP POWER REQUIRED	.000000	(KW)	.000000 (HP)
COOLING FAN POWER REQUIRED	.746457+005	(KW)	.100101+006 (HP)
LASER GAS MIXTURE	3.00 TO 2.00 TO .50 TO .50		(HE TO N2 TO CO2 TO CO)
MOLECULAR WEIGHT OF GAS	.173403+002	(-)	

HEAT EXCHANGER VARIABLES		EXCH 1	EXCH 2	EXCH 3	RAD	UNITS
HEAT TRANSFER RATE		.15+007	.27+006	.27+006	.18+007	BTU/HR
LIQUID PRESSURE DROP		.00	.00	.00	.00	PSIA
NUMBER OF LIQUID PASSES		1	1	1	4	-
MEAN TEMPERATURE	(LIQUID)	.63+003	.45+003	.41+003	.44+003	DEG R
	(GAS)	.99+003	.41+003	.42+003	.43+003	
VISCOSITY	(LIQUID)	.10-004	.10-004	.10-004	.10-004	LB/FT-SEC
	(GAS)	.20-004	.10-004	.10-004	.11-004	
PRANDTL NUMBER	(LIQUID)	.94-001	.11+000	.12+000	.12+000	-
	(GAS)	.50+000	.43+000	.43+000	.72+000	
SPECIFIC HEAT	(LIQUID)	.10+001	.10+001	.10+001	.10+001	BTU/LB-DEG R
	(GAS)	.37+000	.35+000	.35+000	.24+000	
MASS FLUX	(LIQUID)	.95+001	.95+001	.95+001	.73+001	LB/FT**2-SEC
	(GAS)	.50+000	.50+000	.50+000	.24+002	
REYNOLDS NUMBER	(LIQUID)	.95+003	.95+003	.95+003	.29+004	-
	(GAS)	.63+002	.98+002	.98+002	.18+005	
FRICTION FACTOR	(LIQUID)	.00	.00	.00	.00	-
	(GAS)	.50-002	.41-001	.41-001	.30-001	
HEAT TRANSFER FACTOR	(LIQUID)	.11-001	.11-001	.11-001	.77-002	-
	(GAS)	.36-001	.36-001	.36-001	.55-002	
HEAT TRANSFER COEF.	(LIQUID)	.49+000	.43+000	.43+000	.24+000	BTU/FT**2-SEC-DEG R
	(GAS)	.10-001	.11-001	.11-001	.39-001	
FLUID CAPACITY RATE	(LIQUID)	.92+000	.92+000	.92+000	.96+001	BTU/SEC-DEG R
	(GAS)	.19+000	.18+000	.18+000	.17+003	
OVERALL HEAT TRANSFER COEF.		.81-002	.85-002	.85-002	.30-001	BTU/FT**2-SEC-DEG R
GAS HEAT TRANSFER SURFACE AREA		.65+003	.65+003	.65+003	.22+005	FT**2
NUMBER OF TRANSFER UNITS		.28+002	.31+002	.00	.68+002	-
CAP GAMMA		.10+001	.10+001	.10+001	.61+000	-
SINGLE PASS EFFECTIVENESS		.99+000	.99+000	.99+000	.10+001	-
TOTAL EFFECTIVENESS		.99+000	.99+000	.99+000	.10+001	-

GAS FLOW SYSTEM VARIABLES BY STATION

STATION NUMBER		1	2	3	4	5	6
		7	8	9	10	11	
TOTAL PRESSURE	(PSIA)	.737+001	.741+001	.740+001	.739+001	.739+001	.739+001
		.742+001	.740+001	.740+001	.740+001	.737+001	
STATIC PRESSURE	(PSIA)	.735+001	.727+001	.738+001	.737+001	.737+001	.739+001
		.742+001	.739+001	.739+001	.739+001	.737+001	
TOTAL TEMP.	(DEG R)	.410+003	.257+004	.257+004	.257+004	.257+004	.426+003
		.427+003	.413+003	.413+003	.413+003	.410+003	
STATIC TEMPERATURE	(DEG R)	.410+003	.256+004	.257+004	.257+004	.257+004	.426+003
		.427+003	.413+003	.413+003	.413+003	.410+003	
MACH NUMBER	(-)	.620-001	.164+000	.641-001	.642-001	.642-001	.388-001
		.248-001	.244-001	.244-001	.244-001	.310-001	
VELOCITY	(FT/SEC)	.820+002	.518+003	.203+003	.203+003	.203+003	.523+002
		.334+002	.324+002	.324+002	.324+002	.410+002	
VOL. FLOW RATE	(CFM)	.106+004	.670+004	.663+004	.663+004	.663+004	.110+004
		.109+004	.106+004	.106+004	.106+004	.106+004	
DENSITY	(LB/FT**3)	.290-001	.459-002	.463-002	.463-002	.463-002	.280-001
		.281-001	.289-001	.289-001	.289-001	.290-001	
AREA	(FT**2)	.215+000	.215+000	.545+000	.545+000	.545+000	.349+000
		.545+000	.545+000	.545+000	.545+000	.431+000	
GAMMA	(-)	.149+001	.135+001	.135+001	.135+001	.135+001	.149+001
		.149+001	.149+001	.149+001	.149+001	.149+001	
PRESSURE DROP	(IN H2O)	-.994+000	.297+000	.874-001	.171-001	-.675-001	-.741+000
		.692+000	.137-001	.273-002	.671+000	.218-001	
PRESSURE DROP / P06	(-)	-.485-002	.145-002	.427-003	.833-004	-.329-003	-.362-002
		.338-002	.667-004	.133-004	.328-002	.106-003	

COOLING AIR VARIABLES

STATION NUMBER		1A	2A
PRESSURE	(PSIA)	.146900+002	-.102425+001
TEMPERATURE	(DEG R)	.409690+003	.412585+003
DENSITY	(LB/FT**3)	.967795-001	-.670055-002
PRESSURE DROP	(IN H2O)	.435285+003	

APPENDIX E

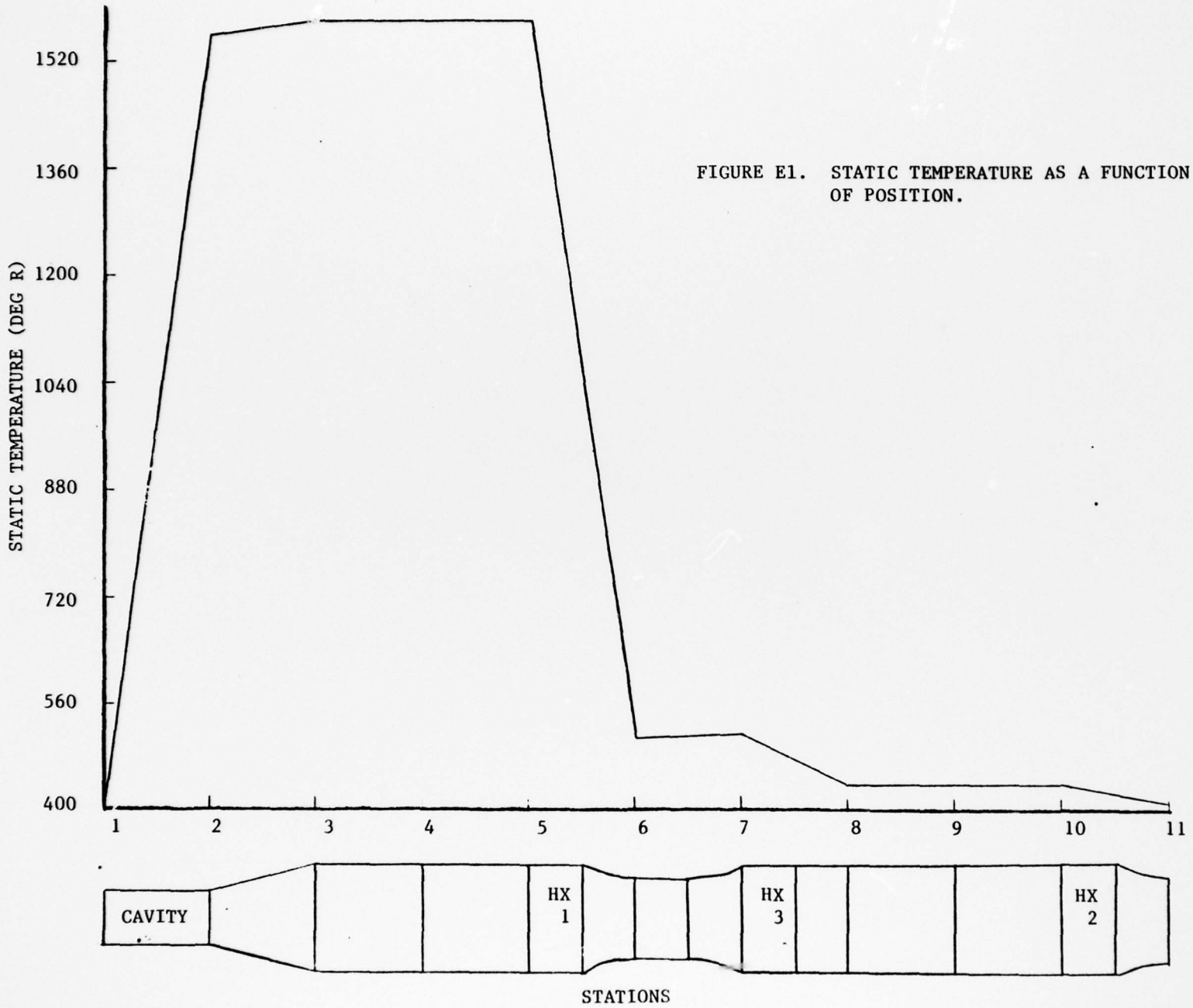

FIGURE E1. STATIC TEMPERATURE AS A FUNCTION OF POSITION.

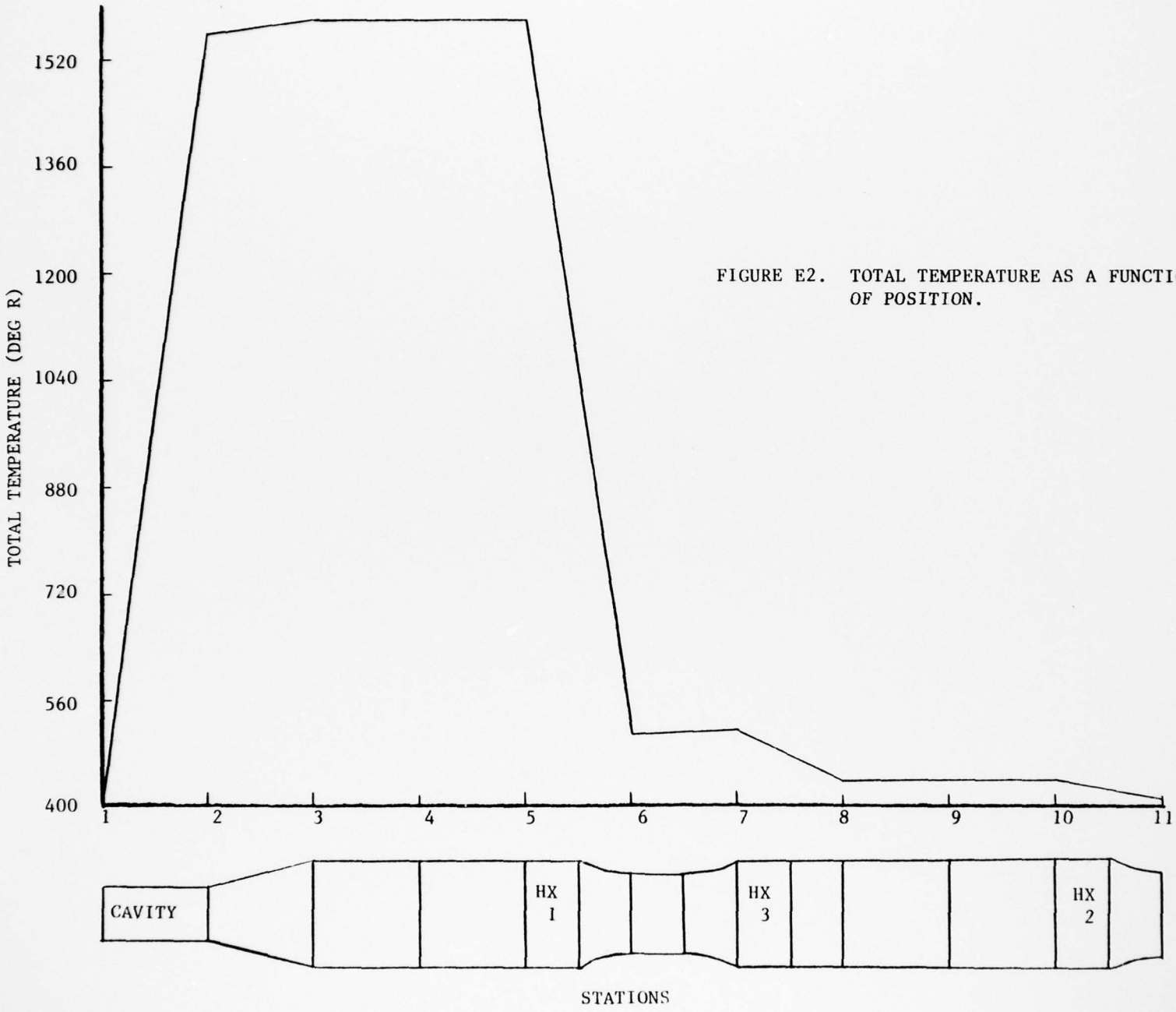

FIGURE E2. TOTAL TEMPERATURE AS A FUNCTION OF POSITION.

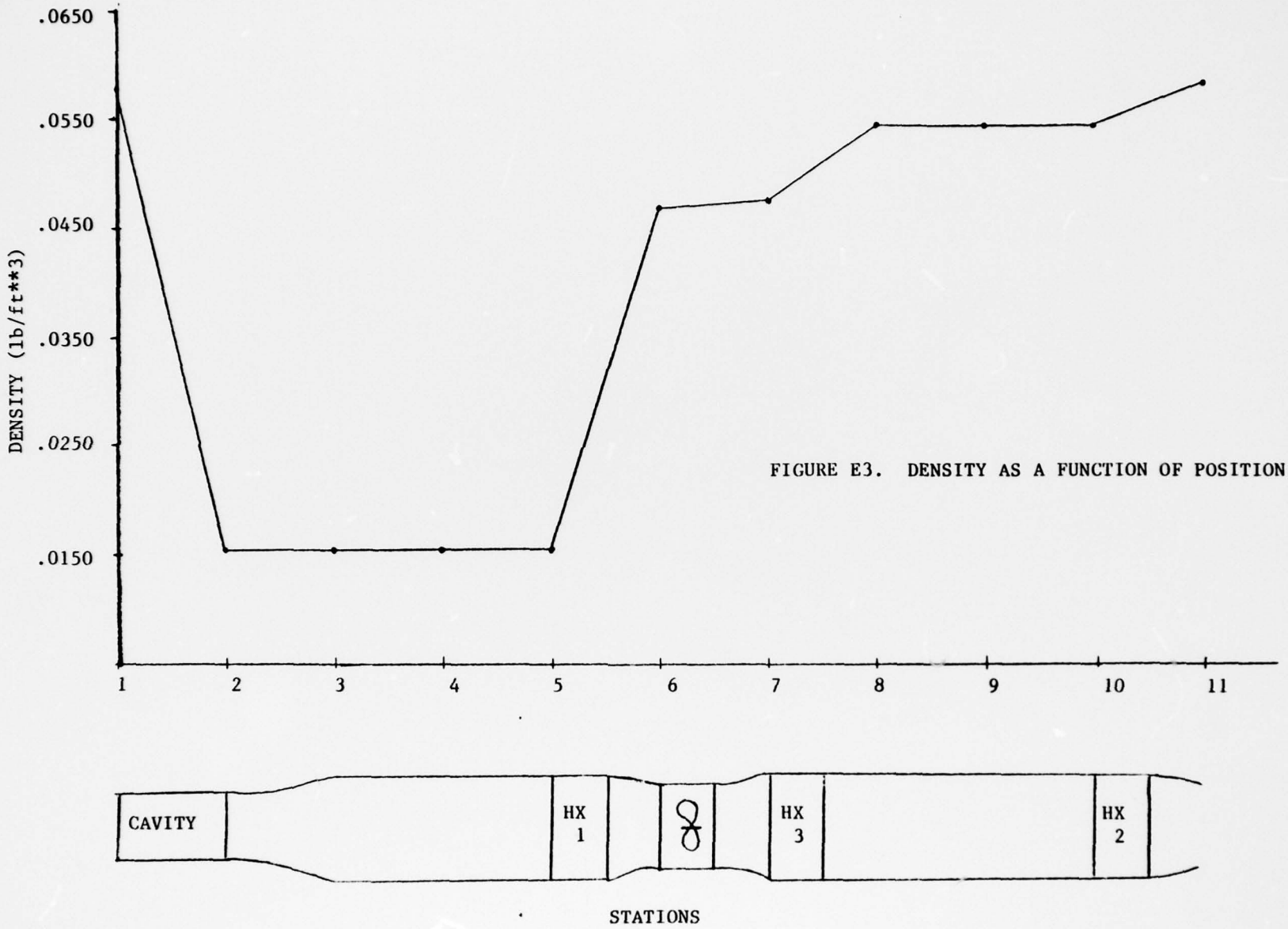

FIGURE E3. DENSITY AS A FUNCTION OF POSITION.

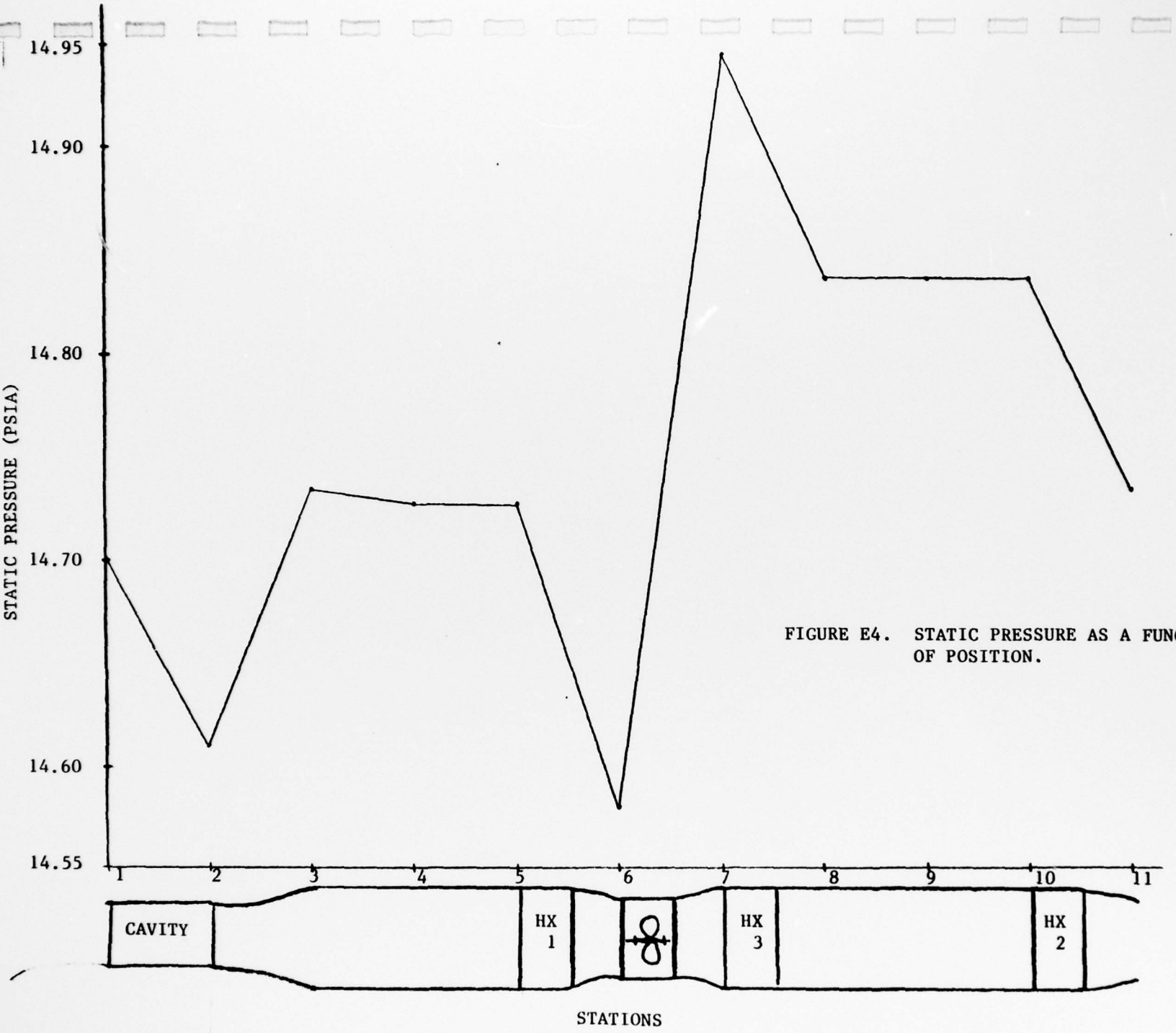

FIGURE E4. STATIC PRESSURE AS A FUNCTION OF POSITION.

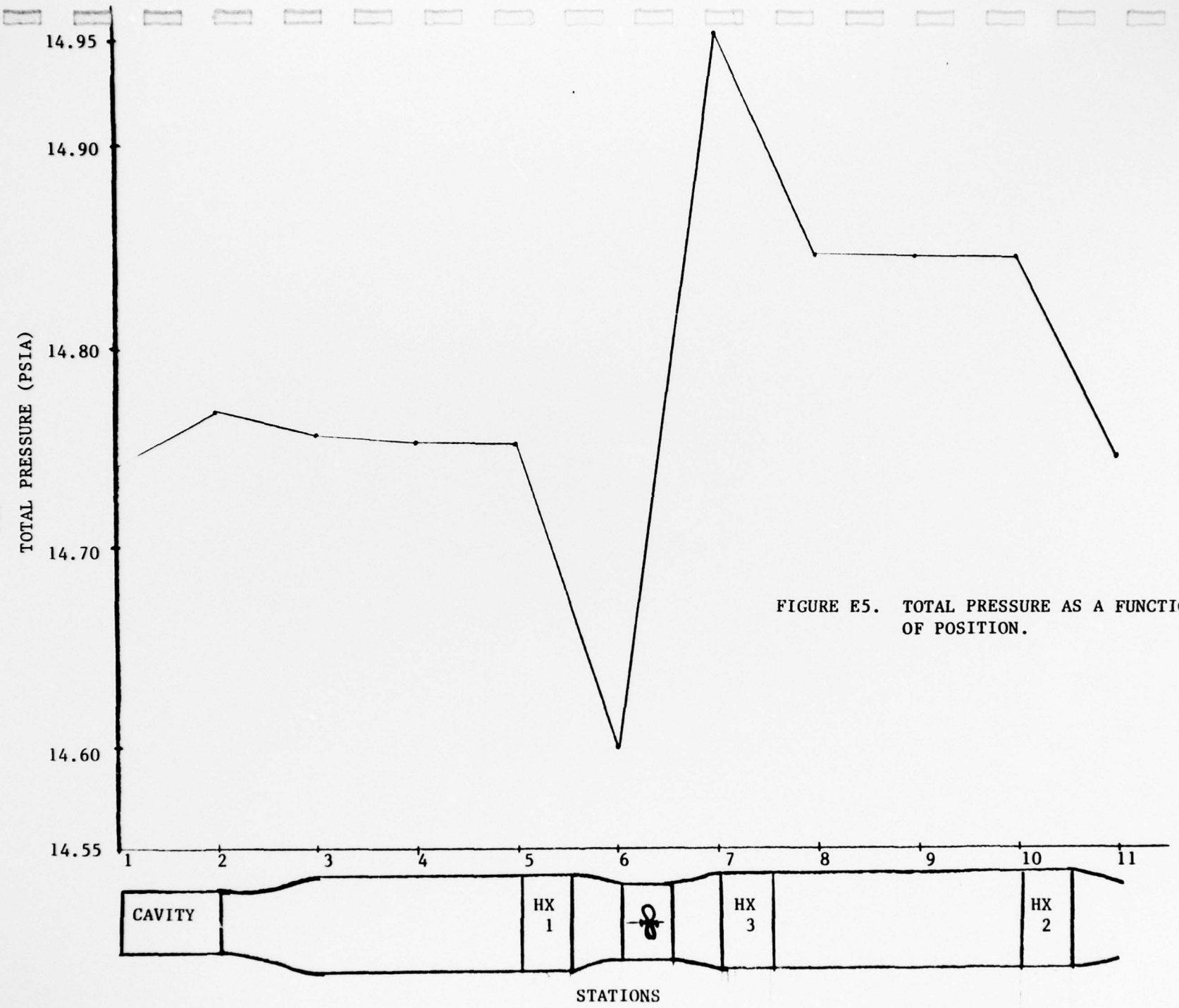

FIGURE E5. TOTAL PRESSURE AS A FUNCTION OF POSITION.

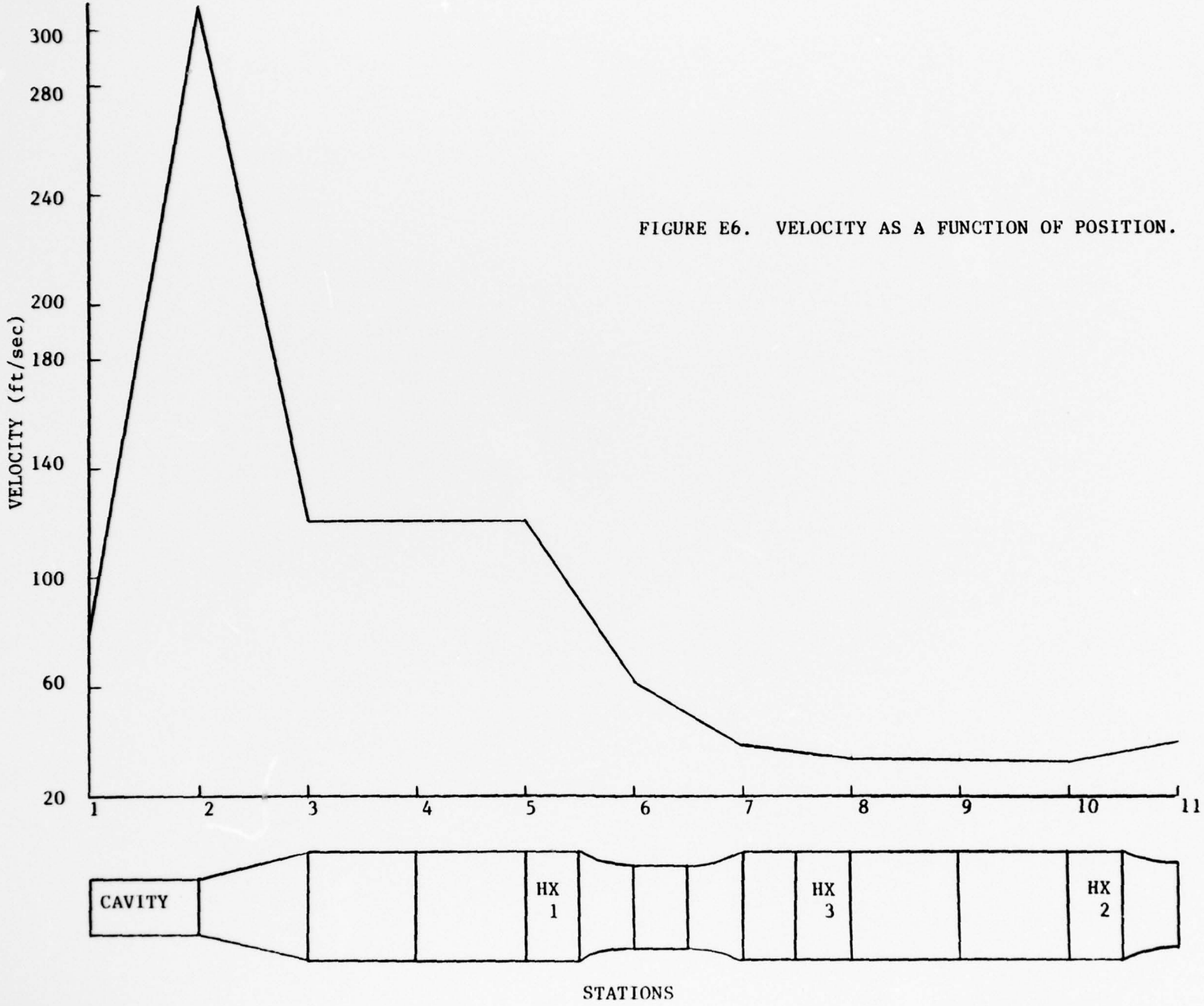

FIGURE E6. VELOCITY AS A FUNCTION OF POSITION.

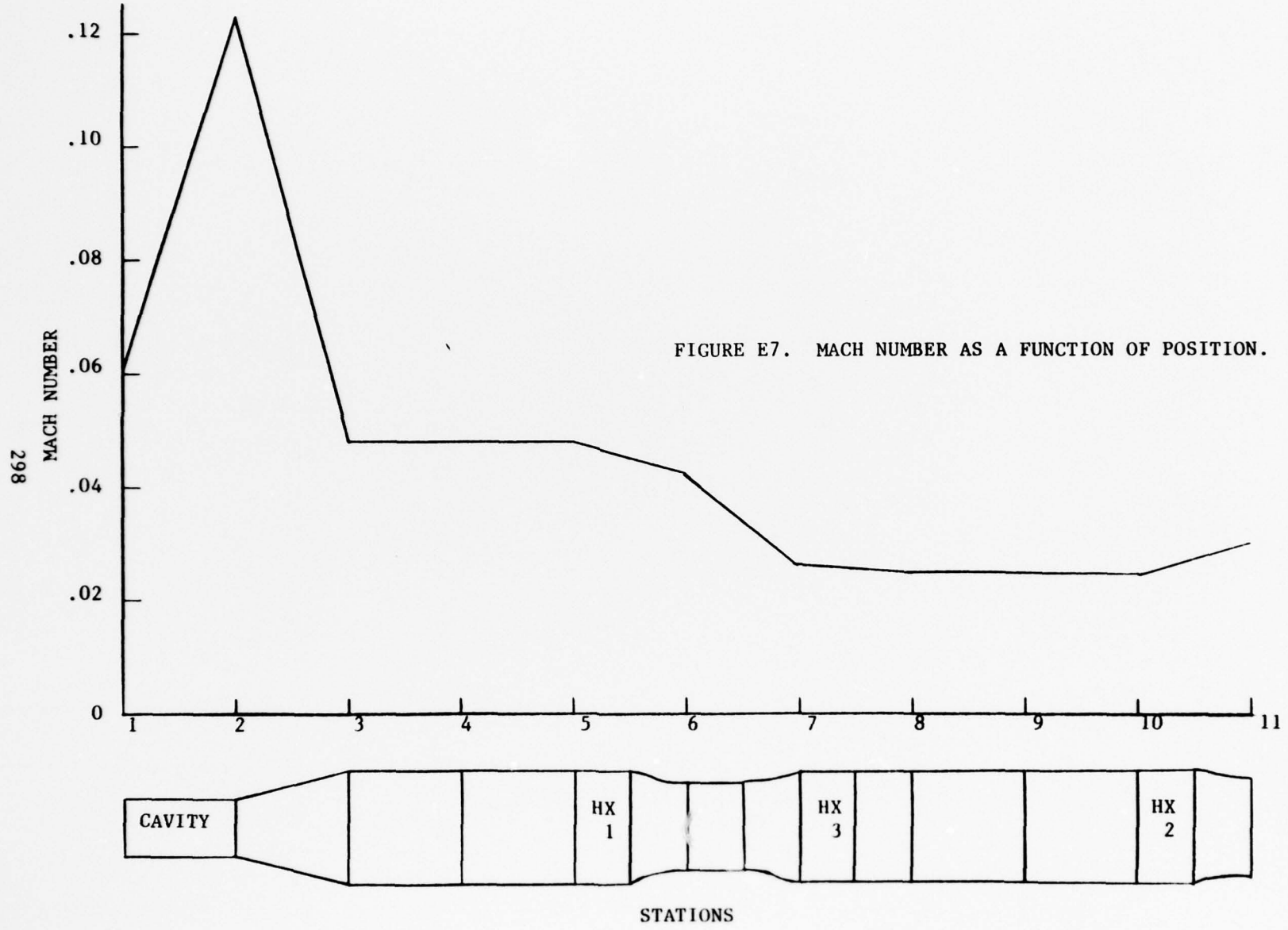

FIGURE E7. MACH NUMBER AS A FUNCTION OF POSITION.

DAAK40-77-C-0161
The Univ. of AL in Huntsville

REPORTS DISTRIBUTION LIST

		NUMBER OF COPIES
1.	Defense Advanced Research Projects Agency ATTN: Director, Laser Division 1400 Wilson Boulevard Arlington, VA 22209	1
2.	ODDR&E ATTN: Assistant Director (Space & Advanced Systems) The Pentagon Washington, DC 20301	1
3.	National Aeronautics and Space Administration Lewis Research Center ATTN: Dr. John W. Dunning, Jr. 21000 Brookpark Road Cleveland, OH 44135	1
4.	Defense Documentation Center Cameron Station Alexandria, VA 22314	2
5.	Department of the Army DCSRDA ATTN: DAMA-WSM-A (LTC Holmes) Washington, DC 20310	1
6.	Commander US Army Missile Research and Development Command ATTN: DRDMI-HSE (Dr. Werkheiser) Redstone Arsenal, AL 35809	5
7.	Commander US Army Missile Research and Development Command ATTN: DRCPM-HEL Redstone Arsenal, AL 35809	1
8.	Commander US Army Mobility Equipment R&D Command ATTN: AMXFB-EA (L. Amstutz) Fort Belvoir, VA 22060	1

NUMBER OF COPIES

9. Commander — 1
US Army Materiel Development and Readiness Command
ATTN: DRCRD-T (Dr. David Stefanye)
5001 Eisenhower Avenue
Alexandria, VA 22304

10. Commander — 1
US Army Electronics R&D Command
ATTN: DRSEL-CT-L (Dr. R. G. Buser)
Fort Monmouth, NJ 07703

11. CPT James G. Wilson — 1
Project Manager, High Energy Laser Project
US Naval Sea Systems Command
PMS 405
Washington, DC 20362

12. US Air Force Weapons Laboratory — 1
ATTN: COL Donald L. Lambertson (AR)
Kirtland AFB, NM 87117

13. US Air Force Aero Propulsion Laboratory — 1
ATTN: MAJ George Uhlig (AFAPL/NA)
Wright Patterson AFB, OH 45433

14. Dr. Walter Warren — 1
Aerospace Corporation
Post Office Box 92957
Los Angeles, CA 90009

15. Mr. A. Colin Stancliffe — 1
Airesearch Manufacturing Company
2525 West 190th Street
Torrance, CA 90503

16. Dr. Jack Daugherty — 2
AVCO-Everett Research Laboratory
2385 Revere Beach Parkway
Everett, MA 02149

17. Mr. Fred Tietzel (STOLAC) — 1
Battelle Columbus Laboratories
505 King Avenue
Columbus, OH 43201

NUMBER OF COPIES

18. Dr. Arthur N. Chester — 1
Hughes Research Laboratories
3011 Malibu Canyon Road
Malibu, CA 90265

19. Dr. Eugene Peressini (Bldg 6, MS/E-125) — 1
Hughes Aircraft Company
Centinela & Teale Streets
Culver City, CA 90230

20. Lawrence Livermore Laboratory — 1
ATTN: Dr. John Emmett
Post Office Box 808
Livermore, CA 94550

21. Dr. Keith Boyer (MS 530) — 1
Los Alamos Scientific Laboratories
Post Office Box 1663
Las Alamos, NM 87544

22. Mr. Peter H. Rose — 1
Mathematical Sciences Northwest, Inc.
4545 15th Avenue, NE
Seattle, WA 98105

23. Massachusetts Institute of Technology — 1
Lincoln Laboratories
ATTN: Dr. Rediker
Post Office Box 73
Lexington, MA 02173

24. Dr. Gerard Hasserjian — 1
Northrop Corporation
3401 West Broadway
Hawthorne, CA 90250

25. Mr. Marc T. Constantine — 1
Rocketdyne Division
Rockwell International Corporation
6637 Canoga Avenue
Canoga Park, CA 91304

NUMBER OF COPIES

26. Mr. Harvey Ford — 1
Science Applications, Inc.
6666 Powers Ferry Road, Suite 202
Atlanta, GA 30339

27. Mr. Alan F. Klein — 1
Systems, Science and Software
Post Office Box 1620
LaJolla, CA 92037

28. Mr. G. H. McLafferty — 1
United Aircraft Research Laboratory
400 Main Street
East Hartford, CT 06108

29. Mr. W. F. List — 1
Westinghouse Electric Corporation
Defense and Space Center
Friendship International Airport - Box 746
Baltimore, MD 21203